

AFAMRL-TR-80-52

(12)

LEVEL II

70



AD A110188

**EVALUATION OF A PROPOSED, MODIFIED  
F/FB-111 CREW SEAT AND RESTRAINT SYSTEM**

**JAMES W. BRINKLEY  
JAMES H. RADDIN, JR., LT COL, USAF, MC, FS  
BERNARD F. HEARON, MAJ, USAF, MC, FS  
LAWRENCE A. MCGOWAN, 1LT, USAF  
JOSEPH M. POWERS, CMSGT, USAF**

NOVEMBER 1981

**DTIC  
ELECTE  
S JAN 28 1982 D  
B**

DTIC FILE COPY

Approved for public release; distribution unlimited

**AIR FORCE AEROSPACE MEDICAL RESEARCH LABORATORY  
AEROSPACE MEDICAL DIVISION  
AIR FORCE SYSTEMS COMMAND  
WRIGHT-PATTERSON AIR FORCE BASE, OHIO 45433**

70

82 01 28 010

## NOTICES

When US Government drawings, specifications, or other data are used for any purpose other than a definitely related Government procurement operation, the Government thereby incurs no responsibility nor any obligation whatsoever, and the fact that the Government may have formulated, furnished, or in any way supplied the said drawings, specifications, or other data, is not to be regarded by implication or otherwise, as in any manner licensing the holder or any other person or corporation, or conveying any rights or permission to manufacture, use, or sell any patented invention that may in any way be related thereto.

Please do not request copies of this report from Air Force Aerospace Medical Research Laboratory. Additional copies may be purchased from:

National Technical Information Service  
5285 Port Royal Road  
Springfield, Virginia 22161

Federal Government agencies and their contractors registered with Defense Documentation Center should direct requests for copies of this report to:

Defense Documentation Center  
Cameron Station  
Alexandria, Virginia 22314

### TECHNICAL REVIEW AND APPROVAL AFAMRL-TR-80-52

The voluntary informed consent of the subjects used in this research was obtained as required by Air Force Regulation 169-3.

This report has been reviewed by the Office of Public Affairs (PA) and is releasable to the National Technical Information Service (NTIS). At NTIS, it will be available to the general public, including foreign nations.

This technical report has been reviewed and is approved for publication.

FOR THE COMMANDER



HENNING E. VON GIERKE  
Director  
Biodynamics and Bioengineering Division  
Air Force Aerospace Medical Research Laboratory

AIR FORCE/36780/31 December 1981 - 150

**Best  
Available  
Copy**

SECURITY CLASSIFICATION OF THIS PAGE (When Data Entered)

REPORT DOCUMENTATION PAGE		READ INSTRUCTIONS BEFORE COMPLETING FORM	
1. REPORT NUMBER AFAMRL-TR-80-52	2. GOVT ACCESSION NO. AD A110 188	3. RECIPIENT'S CATALOG NUMBER	
4. TITLE (and Subtitle)  EVALUATION OF A PROPOSED MODIFIED F/FB-111 CREW SEAT AND RESTRAINT SYSTEM		5. TYPE OF REPORT & PERIOD COVERED  Technical report	
		6. PERFORMING ORG. REPORT NUMBER	
7. AUTHOR(s) James W. Brinkley                      Lawrence A. McGowan James H. Raddin                      Joseph M. Powers Bernard F. Hearon		8. CONTRACT OR GRANT NUMBER(s)	
9. PERFORMING ORGANIZATION NAME AND ADDRESS Air Force Aerospace Medical Research Laboratory, Aerospace Medical Division, Air Force Systems Command, Wright-Patterson Air Force Base, OH 45433		10. PROGRAM ELEMENT, PROJECT, TASK AREA & WORK UNIT NUMBERS  62202F/7231/16/AA	
11. CONTROLLING OFFICE NAME AND ADDRESS		12. REPORT DATE November 1981	
		13. NUMBER OF PAGES 418	
14. MONITORING AGENCY NAME & ADDRESS (if different from Controlling Office)		15. SECURITY CLASS. (of this report)  UNCLASSIFIED	
		15a. DECLASSIFICATION/DOWNGRADING SCHEDULE	
16. DISTRIBUTION STATEMENT (of this Report)  Approved for public release; distribution unlimited			
17. DISTRIBUTION STATEMENT (of the abstract entered in Block 20, if different from Report)			
18. SUPPLEMENTARY NOTES			
19. KEY WORDS (Continue on reverse side if necessary and identify by block number)  Impact Protection                      Protective Equipment Crew Restraint                      Biomechanics Impact Tests Biodynamics			
20. ABSTRACT (Continue on reverse side if necessary and identify by block number) An extensive impact test program was conducted to evaluate a proposed F/FB-111 crew seat and restraint system redesign. A primary objective of the program was to determine whether the overall protection performance of the system might be degraded by the design changes which are intended to alleviate the current high spinal injury rate (34 percent). A total of 187 human impact tests were performed in the cardinal axes, including vertical (up to 10G, 8.1 m/sec), side-ward (up to 8G, 9.2 m/sec), and forward facing (up to 10G, 9.8 m/sec). (continued)			

DD FORM 1 JAN 73 1473

EDITION OF 1 NOV 65 IS OBSOLETE

SECURITY CLASSIFICATION OF THIS PAGE (When Data Entered)



(block 20 continued)

Subjects were exposed to similar impacts using different seat position adjustments to allow parametric analysis. Measured data included seat acceleration and velocity, head and chest translational acceleration components, triaxial forces acting on the seat pan and footrest, forces acting at the restraint harness attachments, and displacements of various body segments. In vertical impact tests, the forward position of the headrest appeared to cause increased forward acceleration of the head. Furthermore, small occupants can be positioned below the headrest in some seat positions. This situation is made possible because the seat pan vertical adjustment is independent of the headrest, and is made worse by removal of a portion of the lower headrest in the proposed modification. Vertical impact tests demonstrated increased head accelerations with higher shoulder harness angles. Analysis of restraint loads in sideward impacts showed that more of the lateral support is provided by the lap belt with higher shoulder harness angles. This indicates potentially degraded lateral support of the upper torso with the proposed modification.

## PREFACE

This report was prepared by the Biomechanical Protection Branch, Biodynamics and Bioengineering Division of the Air Force Aerospace Medical Research Laboratory. The research was accomplished in response to a request from the Life Support System Program Office of the Aeronautical Systems Division. Mr. Michael W. Higgins was the Program Manager for the Life Support System Program Office.

The test fixtures used during the experimental phase of the effort were designed and built by General Dynamics, Fort Worth Division. Mr. Andrew Shafer was the on-site engineering representative of General Dynamics during the test program.

The impact facilities and data collection equipment were operated by the Scientific Services Division of the Dynalectron Corporation under Air Force Contract F33615-79-C-0523. Mr. Harold F. Boedeker was the Engineering Supervisor for the Dynalectron Corporation.

Photographic support was provided by the 4950th Test Wing, Technical Photographic Division. Special acknowledgement is given to Mr. Paul Creiger for operation of the high speed motion picture cameras and to the many personnel who provided still photography coverage.

Anthropometric measurements of the test subjects were collected by Mr. Charles E. Clauser and Dr. Kenneth W. Kennedy of the Workload and Ergonomics Branch, Human Engineering Division of the Air Force Aerospace Medical Research Laboratory. The assessment of the anthropometric implications of the proposed modifications was based on measurements and analyses performed by Dr. Kennedy.

The authors wish to express their gratitude to the personnel of the Biomechanical Protection Branch who participated in the planning, preparation, and performance of the research program and in the preparation of this report. Special commendation is also given to the Air Force officers and airmen who volunteered to participate in the impact tests. The devotion, skills, and professionalism of the entire team of government and contractor personnel were vital to the successful and safe accomplishment of this evaluation.

Access	
NAIS	✓
DTIC	
Dist	
A	
DTIC COPY INSPECTED	

# TABLE OF CONTENTS

	Page
1 INTRODUCTION	8
A Background	9
B Program Objectives	16
2 TECHNICAL APPROACH	18
3 TEST ITEM	21
A Current Operational System	21
B Proposed Modifications	27
C Test Related Modifications	29
4 TEST EQUIPMENT, METHODS, AND FACILITIES	36
A Vertical Deceleration Tower	36
B Horizontal Deceleration Facility	36
C Experiment Control	38
D Electronic Instrumentation	48
E Medical Instrumentation	49
F Data Acquisition and Recording	49
G Photometric Instrumentation	49
H Anthropomorphic Dummy	50
I Engineering Safety	51
5 DATA ANALYSIS	52
A Electronic Data Reduction	52
B Photometric Data Processing and Analysis	52
6 HUMAN SUBJECTS	54
A Qualifications	54
B Subject Test Procedures	54
C Human Use Protocol	55
D Subject Anthropometry	56
7 CONDUCT OF TESTS	59
A Test Sequence	59
B Vertical Impact Tests	59
C Sideward Impact Tests	60
D Forward Facing Impact Tests	61
8 ANALYSIS AND RESULTS	63
A Vertical Impact Tests	63
B Sideward Impact Tests	66
C Forward Facing Impact Tests	69
D Medical Findings	74

# TABLE OF CONTENTS (cont)

	Page
9 DISCUSSION	80
A Comparison with Holloman AFB Data	80
B Subject Knee Injury	82
C Anthropometric Evaluation	87
D Back Injury Mechanism Implications	94
10 SUMMARY OF CONCLUSIONS	99
A Analysis of the F/FB-111 Seat and Restraint System	99
B AFAMRL Test Program	100
C Test Data Analysis	100
D Comparison AFAMRL Data - Holloman Data	101
E Anthropometric Analysis	101
F General Conclusions	101
APPENDIX A	
Data Acquisition Equipment and Methods	103
APPENDIX B	
Photometric Analysis Methods and Data	157
APPENDIX C	
Summary of Vertical Impact Test Data	195
APPENDIX D	
Summary of Lateral Impact Test Data	259
APPENDIX E	
Summary of Forward Facing Impact Test Data	350
REFERENCES	412

# LIST OF FIGURES

	Page
1 F/FB-111 Crew Escape Module	8
2 X, Y, and Z Axis Acceleration Measured at the Crew Module Center-of-Gravity During a Zero Altitude, Zero Airspeed Ejection Test	10
3 Dynamic Response Index Values Calculated from Qualification Ejection Test Data	11
4 X, Y, and Z Axis Acceleration Measured at the Crew Module Center-of-Gravity During a 270 KEAS Ejection Test	12
5 X, Y, and Z Axis Acceleration Measured at the Crew Module Center-of-Gravity During a 600 KEAS Ejection Test	13
6 Dynamic Response Index Values Calculated from Ground Impact Test Data	15
7 F/FB-111 Seat Installation on Crew Module Aft Bulkhead	21
8 Top View of Crew Module Cockpit Area	22
9 Side View of Crew Module Cockpit Area	22
10 F/FB-111 Crew Seat Design	23
11 F/FB-111 Restraint System	25
12 Proposed Crew Seat and Restraint System Configuration	28
13 The Horizontal Impact Test Fixture with Crew Seat	30
14 The Horizontal Impact Test Fixture with Rudder Pedal Support Structure	31
15 Rudder Pedal Installation	32
16 Test Fixture Showing Detail of the Vertical Seat Actuator Replacement Strut	33
17 Reflection Strap Attachment Points Shown During Static Test	35
18 AFAMRL Vertical Deceleration Tower and F/FB-111 Test Fixture Viewed from Below	37

# LIST OF FIGURES (cont)

	Page
19 Vertical Deceleration Tower Carriage and F/FB-111 Test Fixture with Volunteer Subject During Impact	38
20 Acceleration Profile Used During 8 G Vertical Tests	39
21 Acceleration Profile Used During 10 G Vertical Tests	40
22 AFAMRL Horizontal Deceleration Facility	41
23 Impact Sled Launch System	42
24 Top and Side View Drawings of the Hydraulic Decelerator	43
25 Hydraulic Decelerator with Top of Water Enclosure Removed	44
26 Test Fixture Mounted to Impact Carriage for X Axis Tests	45
27 Test Fixture Mounted to Impact Carriage for Y Axis Tests	45
28 Impact Profiles Used During the X Axis Test Series	46
29 Impact Profiles Used During the Y Axis Test Series	47
30 Examples of Tension-Time Curves Measured at the Crotch Strap End Fitting	73
31 Test Subject with Small Sitting Height with Head Braced Against Shoulder Straps	77
32 Test Subject After Shoulder Strap Haulback with the Harness Yoke Malpositioned	78
33 Test Subject After Shoulder Strap Haulback with the Harness Yoke Properly Positioned	79
34 Frame-by-Frame Displacement of Right Knee During Impact - Comparison of Tests 488 and 518.	84
35 Footrest Load Data in X Direction - Test 518	85
36 Combination of Anthropometric Values Which are Expected to Cause Negative Shoulder Strap Angles for Operational and Proposed Modified Systems	88

LIST OF FIGURES (cont)

	Page
37 Position of Helmet and Headrest when the Normal Helmet Contact Point is One Inch Above the Lower Edge of the Headrest	90
38 Relationship Between Helmet/Headrest Contact Point and Sitting Height, Sitting Height Percentile, and Seatback Angle	91
39 Weapons Systems Operator with His Seat Lowered for Radar Work	93

# LIST OF TABLES

	Page
1 Peak Acceleration Ranges Measured at the Seat Pan	14
2 Test Matrix for Vertical Impact Phase	18
3 Test Matrix for Sideward Impact Phase	19
4 Test Matrix for Forward Facing Test Phase	20
5 Summary of Inertia Reel Qualification Data	26
6 Summary of Inertia Reel Performance Test Data	29
7 Dummy Measurements	51
8 Subject Anthropometry Summary I	57
9 Subject Anthropometry Summary II	58
10 Group and Number of Subjects for Each Seat Position and Shoulder Strap Configuration in the Vertical Impact Test Phase	60
11 Number of Subjects for Each Seat Position and Shoulder Strap Configuration in the Lateral Impact Test Phase	61
12 Number of Subjects for Each Seat Position and Shoulder Strap Configuration in the Forward Facing Impact Test Phase	61
13 Summary of the Electronically Measured and Computed Data from the Vertical Impact Tests	64-65
14 Summary of the Statistically Significant Relationships from the Vertical Impact Tests	67
15 Summary of the Electronically Measured and Computed Data from the Sideward Impact Tests	68
16 Summary of the Electronically Measured and Computed Data from the Forward Facing Impact Tests	70
17 Summary of the Statistically Significant Relationships from the Forward Facing Impact Tests	72
18 Distribution of the Crotch Strap Load Characteristics	74
19 Frequency of Subjective Medical Findings	74
20 Frequency of Objective Medical Findings	75
21 Comparison of Holloman and AFAMRL Test Data	81



## Section 1

### INTRODUCTION

This report describes the results of a series of impact tests conducted to evaluate modifications to the crew seat and restraint system used in the F/FB-111 aircraft. The tests were requested by and conducted under the auspices of the Life Support System Program Office (ASD/AES) of the Aeronautical Systems Division of Air Force Systems Command, Wright-Patterson Air Force Base. ASD/AES is responsible for the research and development of appropriate measures to eliminate or reduce the high spinal injury rate currently being experienced as a result of operational use of the F/FB-111 emergency escape module. This responsibility is defined by the Air Force Systems Command Program Management Document R-P 6097 (3) P.E. 64212F/2229 entitled "F-111 Crew Restraint System Redesign".

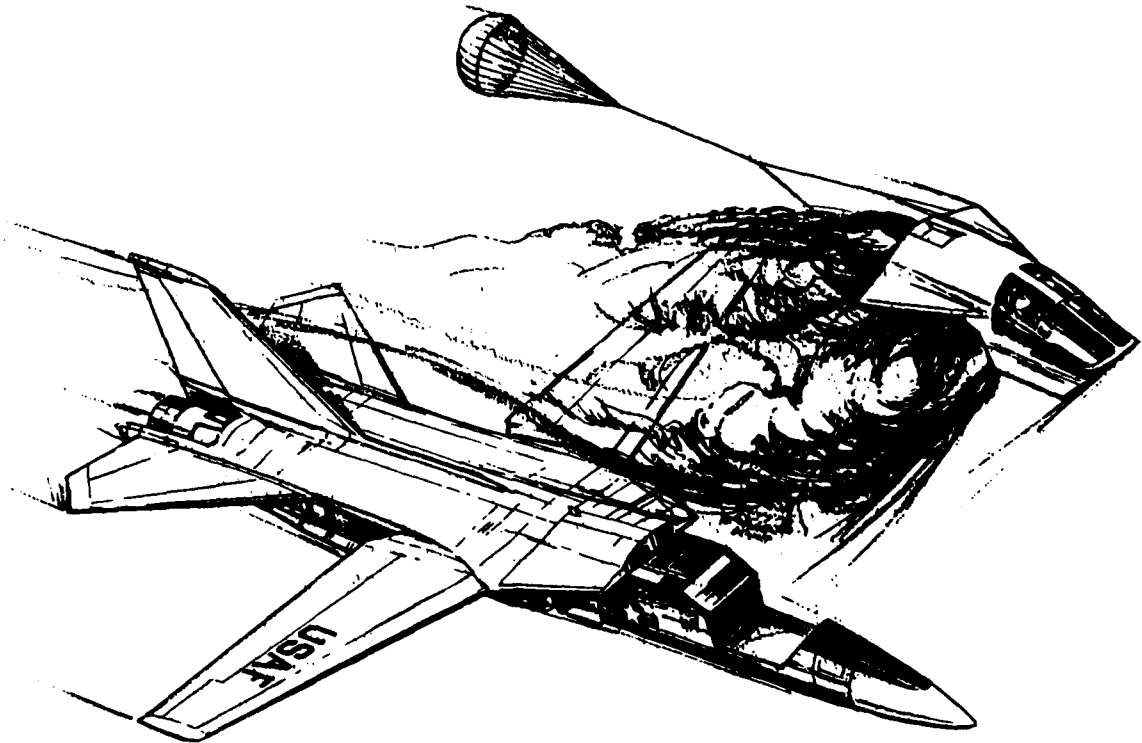


Figure 1. Crew Escape Module.

## A. BACKGROUND

The F-111 and FB-111 aircraft use an ejectable crew module to provide emergency escape for the aircrewmembers. The crew module is an integral portion of the aircraft fuselage prior to emergency escape. The module consists of the pressurized cockpit and the forward portion of the wing glove structure shown in Figure 1. When the escape sequence is initiated by either of the two crewmembers, the module is physically separated from the aircraft fuselage by a pyrotechnic system that explosively guillotines controls and cuts structural members that attach the module to the fuselage. The module is then thrust away from the fuselage by a solid propellant rocket motor. Aerodynamic stabilization and deceleration of the module is accomplished by the shape of the escape module, stabilization surfaces deployed from the module after separation from the fuselage, and a drogue parachute. After completion of the aerodynamic deceleration phase and achievement of a preselected altitude, the module is recovered using a single parachute. Ground or water landing impact is attenuated by gas-filled bags attached to the bottom of the crew module.

The acceleration environment that is associated with the use of the F/FB-111 crew escape module is complex. Within 2 to 10 milliseconds after a crewmember initiates the escape sequence, powered inertia reels retract the shoulder straps of the crew restraint systems. The retraction force varies as a function of the pre-ignition temperature of the propellant, the retraction distance, and the resistance to the retraction. Under nominal conditions the mean retraction force (measured using a rigid dummy) ranges from 153 lb to 258 lb for retraction distances of 2 inches and 13 inches respectively (Whitney *et al.*, 1970). The shoulder straps are nominally retracted in 0.16 to 0.34 sec. The crew module is severed from the aircraft fuselage and the ejection rocket is ignited approximately 0.39 sec after escape initiation. The ejection acceleration that is produced is a function of the aircraft flight conditions, i.e., airspeed, altitude and attitude, as well as crew module weight and pre-ignition temperature of the ejection rocket propellant.

The acceleration environment produced at low airspeeds is relatively mild. The rocket acceleration vector is applied up and forward through the center of gravity of the crew module at an angle of approximately 60 degrees with respect to the crew module waterline or floor. The acceleration at zero airspeed ranges from 8 to 12 G in the vertical ( $+G_z$ ) axis and 4.8 to 6 G in the longitudinal ( $+G_x$ ) axis of the module (Carney *et al.*, 1966; Hatcher, 1966). However, the major portion of the acceleration profile is preceded by a transient pulse as shown in Figure 2 (Hatcher, 1966). At zero airspeed, the transient pulse magnitude is approximately 16 G in the Z axis and 9.5 G in the X axis with a velocity change of about 7 to 10 ft/sec. The transient pulse has been attributed to the development of high pressure between the crew module and aircraft structure after the rocket is ignited. The pulse is not apparent in tests of the isolated rocket motor. The rocket produces a thrust of 27,200 lb at a pre-ignition temperature of 570° F, yielding a total impulse of 23,200 lb-sec (Atkins, 1971).

At higher airspeeds, where the aerodynamic forces become more predominant, the direction of the resultant acceleration vector shifts aft and the ejection acceleration magnitude increases. As the ejection speed increases the crew module also tends to pitch upward after severance from the aircraft fuselage. To counteract this motion and the high Z axis acceleration that is produced, a

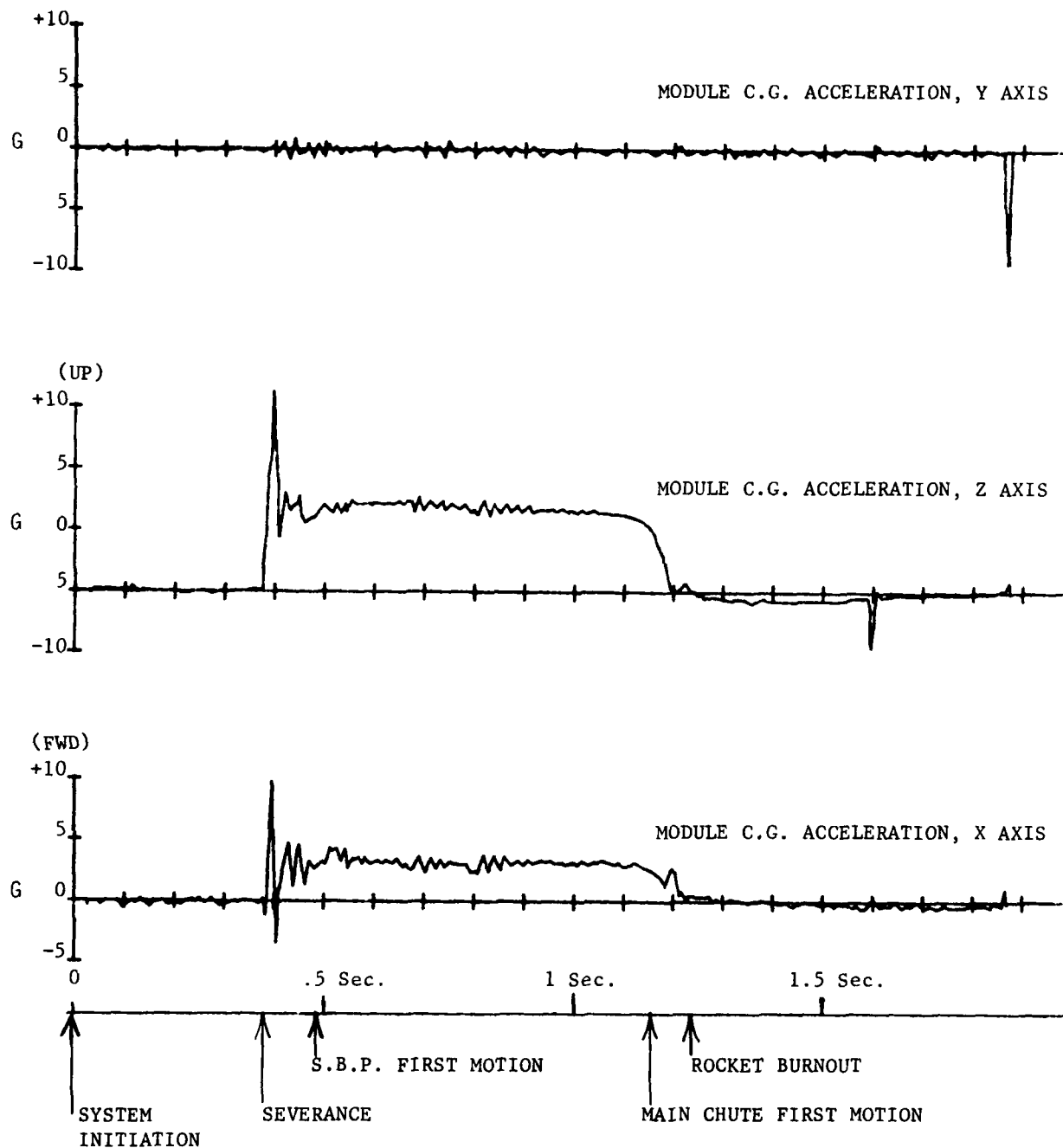


Figure 2. X, Y, and Z Axis Acceleration Measured at the Crew Module Center-of-Gravity During a Ground Level, Zero Airspeed Ejection Test.

secondary nozzle located at the top of the rocket motor is used above 300 knots. Opening of the secondary nozzle drops the primary nozzle thrust from 27,000 lb to 9,000 lb at 0.15 seconds from ejection initiation. The upper nozzle then produces a thrust approximately 7,000 lb yielding a resultant thrust of 14,550 lb (Atkins, 1971).

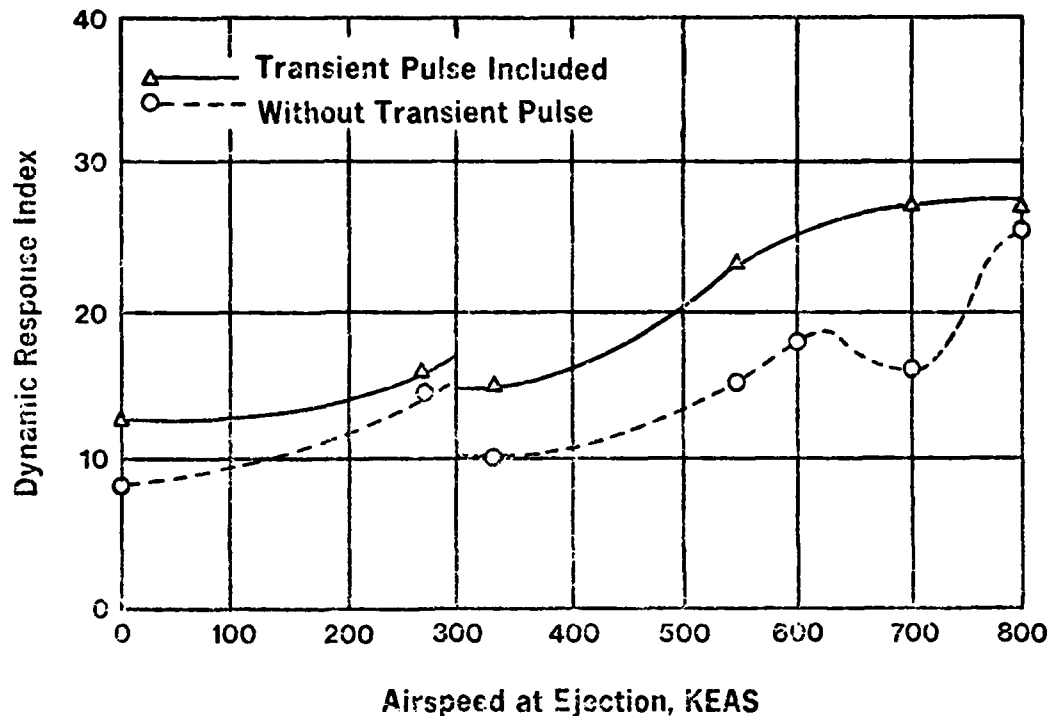


Figure 3. Dynamic Response Index Values Calculated From Qualification Ejection Test Data (Gossick *et al.*, 1968).

Although the secondary nozzle decreases the upward pitch motion, the Z axis accelerations continue to increase with airspeed. Figure 3 shows the relationship between airspeed and the Dynamic Response Index, a value calculated from the Z axis acceleration that is used to estimate the probability of spinal injury (Brinkley *et al.*, 1971). The data plotted in Figure 3 also shows the relationship between the effect of the transient pulse and airspeed in terms of the Dynamic Response Index. The amplitude of the transient pulse does not increase until airspeeds above 330 knots are achieved, and then it increases until, at 800 KEAS a value of 33 G in the Z axis and 10.5 G in the X axis was recorded (McCauley, 1966).

Figures 4 and 5 show linear acceleration data recorded during the ejection rocket burn phase of ejection tests accomplished at 270 and 600 KEAS. The accelerations were recorded at the center of gravity of the crew module during rocket sled ejection tests (Hefti, 1967; McCauley *et al.*, 1966). These data illustrate the relative magnitudes of the X, Y, and Z axes acceleration components. Note that the direction of the X axis acceleration reverses from

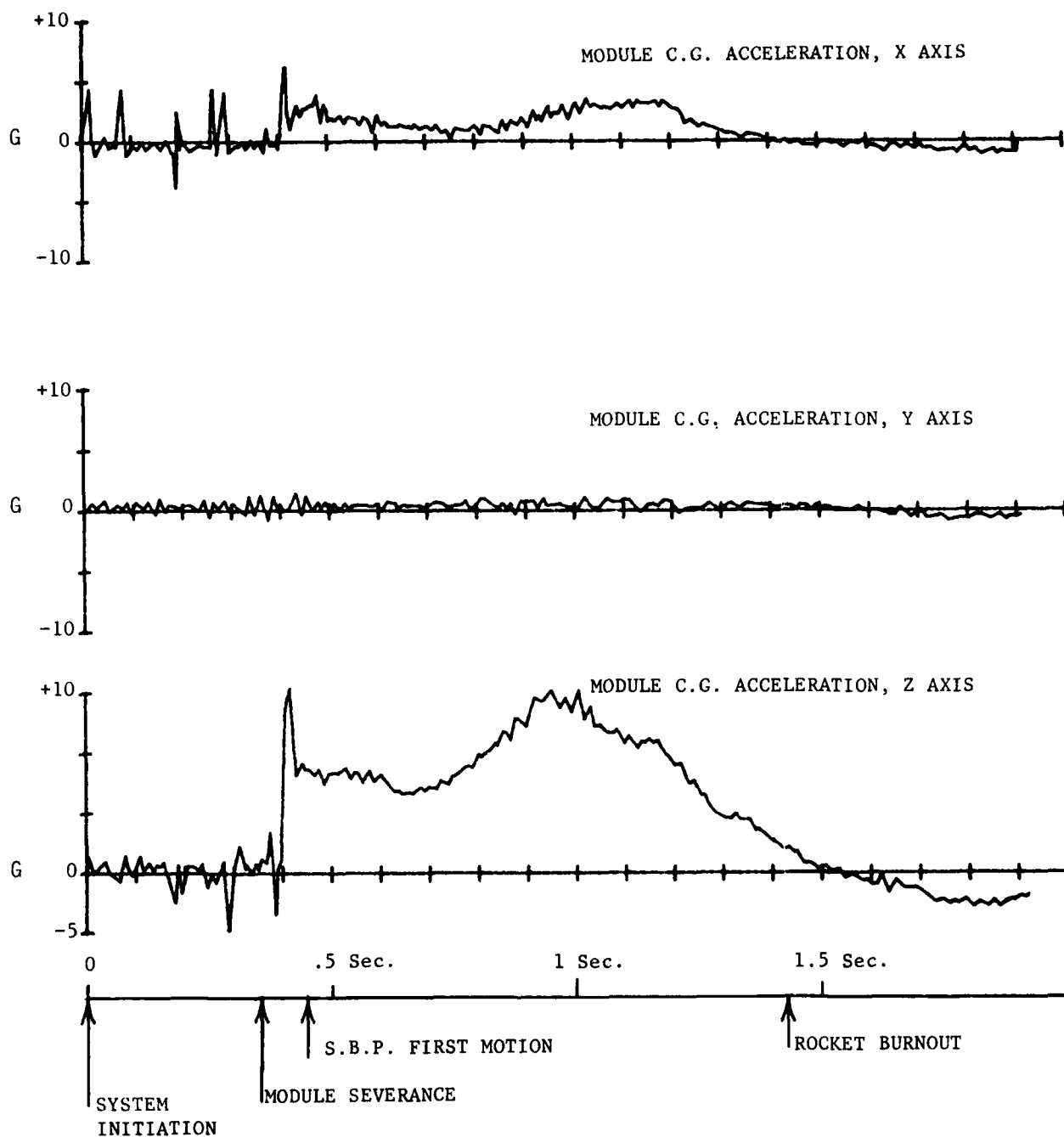


Figure 4. X, Y and Z Axis Acceleration Measured at the Crew Module Center-of-Gravity During a 270 KEAS Ejection Test.

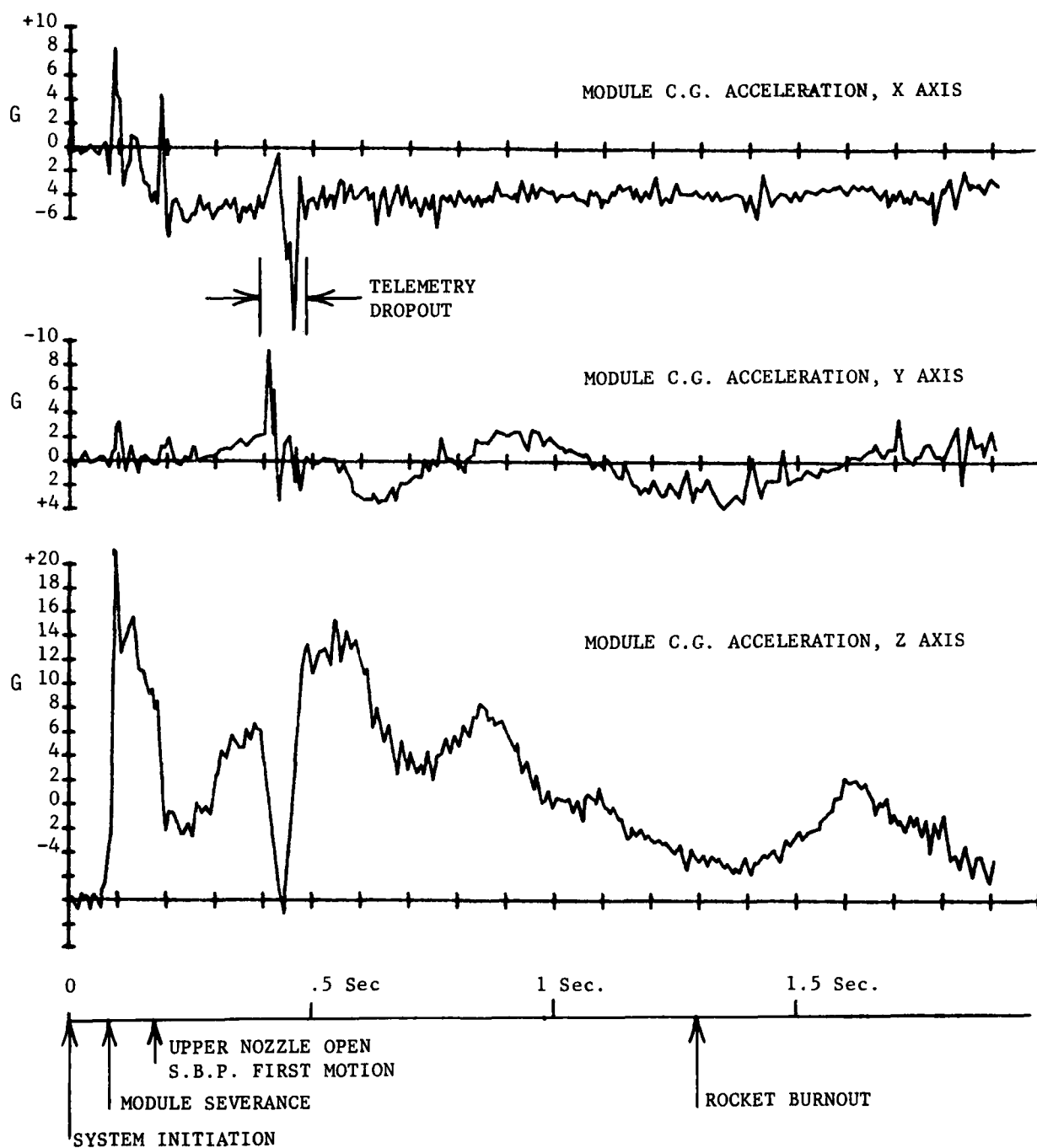


Figure 5. X, Y, and Z Axis Acceleration Measured at the Crew Module Center-of-Gravity During a 600 KEAS Ejection Test.

+G<sub>x</sub> at 270 KEAS to -G<sub>x</sub> at 600 KEAS. During the 270 KEAS test, the resultant acceleration vector direction (measured with respect to the crew module waterline) ranged from 66.9° (at the transient pulse) to a maximum of 78.9° at 0.967 sec, when the resultant was 15.3 G within the first one second after module severance. In contrast, the resultant acceleration vector direction ranged between 103° and 117° during the same period of time when the crew module was ejected at 600 KEAS. The change from +G<sub>x</sub> to -G<sub>x</sub> has been estimated to occur between 330 to 400 KEAS.

The drogue parachute is deployed 0.15 sec after rocket motor ignition. This parachute increases the aerodynamic drag of the crew module by approximately 50 percent. The drogue parachute is fully open within 0.6 to 1.1 sec depending upon airspeed and temperature.

The main recovery parachute is deployed within 1.03 to 4.39 sec below 15,000 ft depending upon the ejection airspeed. The initial parachute opening shock is applied along the longitudinal axis of the module. The opening shock at higher airspeeds, which is reduced by reefing the canopy, ranges from 1.4 to 7.5 G (maximum resultant acceleration) at velocities of 330 to 700 KEAS at 5,000 ft. Reefing line cutters disreef the parachute 2.5 sec after riser line stretch is reached. Seven seconds after deployment of the recovery parachute, an explosively activated device repositions the parachute bridle, allowing the crew module to be suspended in a level flight attitude prior to ground landing impact.

The nominal parachute descent rate is 31 ft/sec at 5,000 ft altitude. The maximum expected horizontal drift velocity is 43 ft/sec. This velocity will occur when the wind velocity is 20 knots combined with a parachute oscillation of 10 degrees. The air bag impact attenuator is most effective in reducing the vertical impact, but provides some attenuation of the horizontal movement at low to moderate drift rates. At higher drift rates the air bag shears from under the module and the impact energy is attenuated, albeit less effectively, by tumbling. Qualification tests of the impact attenuation system were conducted with impact velocities ranging from 33 to 44 ft/sec. Both ground (clay) and water impact conditions were studied. The data from the qualification tests are summarized in terms of the peak accelerations shown in Table 1 (Fricker, 1966).

TABLE 1. PEAK ACCELERATION RANGES MEASURED AT THE SEAT PAN

<u>Surface</u>	<u>Peak Acceleration (G) Ranges</u>		
	G <sub>x</sub>	G <sub>y</sub>	G <sub>z</sub>
Clay	9-15	2-16	16-21
Water	3-10	1-6	14-15

Aeromedical evaluation of the landing impact environment conducted during the crew module development and qualification test programs concluded that the probability of injury was higher than acceptable, i.e., greater than 5 percent but probably less than 20 percent under the most probable landing conditions (Gossick et al., 1968). Figure 6 summarizes all of the available landing

impact test data, including measurements made during air drops, ejection tests from a rocket propelled sled, and the previously mentioned qualification tests of the impact attenuation system. The severity of the landing impacts is expressed in terms of the Dynamic Response Index (Brinkley *et al.*, 1971). In the majority of the impacts plotted in Figure 6, the initial acceleration pulse was a Z axis component which was then followed by smaller magnitude accelerations in the X and Y axes.

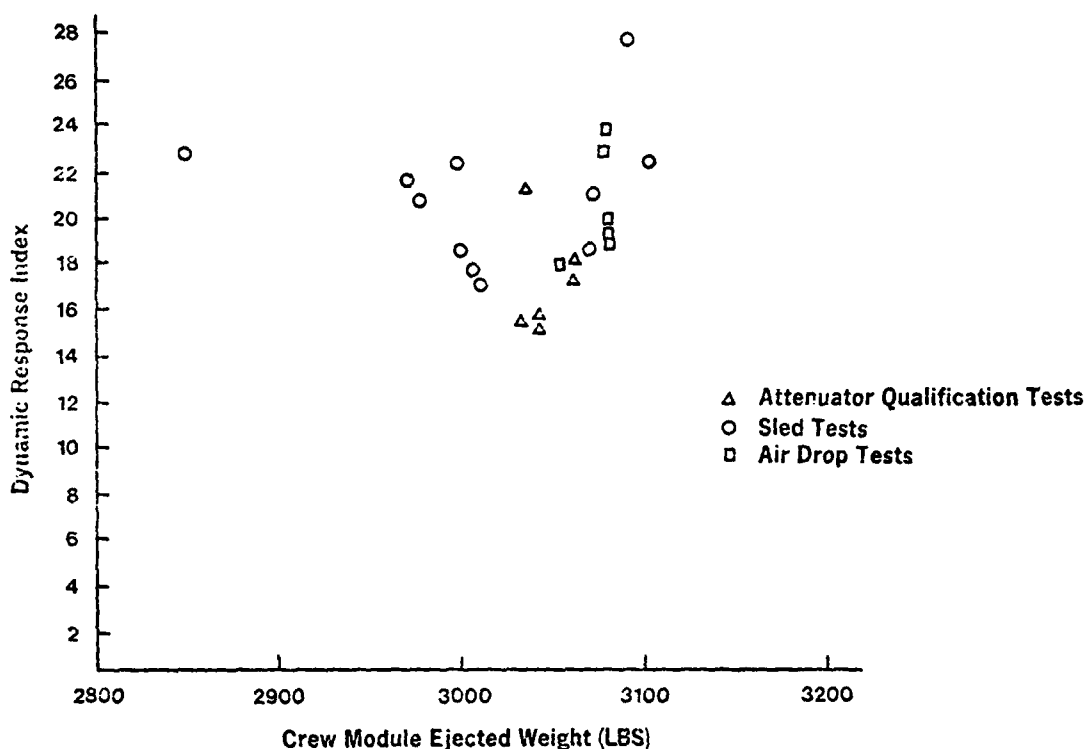


Figure 6. Dynamic Response Index Values Calculated From Ground Landing Impact Test Data (Gossick *et al.*, 1968).

Operational experience with the F/FB-111 crew escape module during the period of October 1967 to October 1979 has revealed a high spinal injury rate. Statistics available from the Air Force Inspection and Safety Center show that the spinal fracture rate for that period is 34 percent of survived ejections. Twelve spinal injury cases have been attributed to ejection force, 10 have been attributed to landing impact, and 5 have been related to both ejection and landing forces. The fractures that have occurred differ in type and location from those commonly observed in USAF ejection seats. The spinal fractures observed after F/FB-111 ejections have been found most frequently in the midthoracic region of the spinal column (Kazarian, 1977). The most frequent site of spinal fracture in ejection seat usage, when the aircraft canopy is jettisoned prior to escape, is the lower thoracic and upper lumbar spine.



An analysis of F/FB-111 operational ejection data and radiographs of the crewmembers conducted by Kazarian (1977) classified the spinal injuries under five headings, but summarized the vertebral fractures in terms of two modes of injury, i.e., the hyperflexion type and the hyperextension type. The hyperflexion injuries were defined as anterior wedge compression fractures resulting from acute flexion from the normal upper spinal curvature. The hyperextension type was defined in terms of reversal of the normal curvature of the spine that placed the anterior longitudinal ligament in tension. Two forms of hyperextension fractures were described: (1) hyperextension fractures without posterior vertebral centrum compression and (2) hyperextension fractures with posterior vertebral centrum compression. Kazarian reported that 18 of the 62 ejectees had incurred hyperextension spinal injuries and 14 had sustained hyperflexion fractures.

Kazarian theorized that the hyperextension injuries are due to the direction of force application of the powered inertia reel and that they occur during the powered inertia reel retraction phase of the ejection sequence. He also concluded that the hyperflexion injuries are due to the ineffectiveness of the upper torso harness and that they occur during ground landing impact. He related the observed spinal injuries to the adverse geometric reactions of the inertia reel and shoulder straps with the upper torso following ejection initiation. He suggested that the solution to the problem of F/FB-111 spinal injuries is elevation of the positions of the inertia reel and the shoulder strap anchor points above the crewmember's shoulder.

As a result of the observed injuries and the above mentioned recommendations, ASD/AES initiated a contract program with General Dynamics, Fort Worth Division (GD/FW), to investigate the feasibility of redesigning the F/FB-111 crew seat and restraint system to eliminate the downward shoulder strap angles. The contract program has been divided into three phases. The first phase was directed toward the development of design concepts (General Dynamics, 1978). The second phase, which is currently underway, is directed toward the design and testing of the revised crew seat and restraint system. The third phase of the program is intended to accomplish the fabrication of the modification kits and retrofit of the F/FB-111 fleet. The test program that is described within this report is the final effort under phase two.

## B. PROGRAM OBJECTIVES

The objectives of the crew seat and restraint system revision stated in the contract with General Dynamics are:

1. Eliminate the downward component of force on the spine caused by the shoulder straps.
2. Reduce rotation (down and forward) of the shoulders and back on ground impact.
3. Extend the seat back to provide support for the upper back during powered retraction.

The objectives of the test program described herein are summarized below.

1. The primary objectives are to assess the adequacy of the restraint system as an impact protection device, quantify the inertia reel strap

geometry for a range of subjects, and possibly uncover any areas in which the redesign may have decreased the restraint system performance.

2. The secondary objective is to study the rotation of the subjects' head and shoulders on impact using photometric data to further assess the performance of the redesigned seat and harness configuration.

The program is intended as a demonstration test rather than an exhaustive performance test. However, the efficacy of the redesigned configuration will be estimated by comparing inertial and kinematic responses of the test subjects within groups of seat adjustments and subject sizes, evaluating medical findings, evaluating subjective responses, and comparing test results with baseline data collected during previous tests of the current operational harness.

## Section 2

### TECHNICAL APPROACH

The experimental design was accomplished to demonstrate the redesigned crew seat and restraint system over its complete range of adjustments. The acceleration environments were selected because of the availability of baseline data and a desire to minimize the risks to the test subjects. The acceleration profiles that were used for the forward facing ( $-G_x$ ) and the sideward ( $+G_y$ ) impact tests were developed to approximate the acceleration profiles used in earlier tests of the F/FB-111 restraint system (Moss, 1968). Although vertical acceleration tests had not been accomplished in the earlier evaluation, these were considered to be crucial in the evaluation of the redesigned configuration in view of the large numbers of hyperflexion spinal injuries attributed to the inadequacy of the restraint during ground landing impact. The vertical ( $+G_z$ ) impact profile that was selected is one that has been extensively used by AFAMRL to evaluate other escape equipment with volunteer subjects.

At least two impact severity levels were used for each test series. The lower level was chosen to gain experience with the equipment being evaluated with minimal risk to the test subjects. The impact stress was then increased to the level where comparative data or experience were known to exist and the risk of injury was still acceptably low.

TABLE 2. TEST MATRIX FOR VERTICAL IMPACT PHASE

#### SHOULDER STRAP/SEAT POSITION

IMPACT LEVEL (G)	SHOULDER STRAP/SEAT POSITION				
	0°/90°	FD/90°	0°/103°	0°/110°	FD/110°
8			I, II		
10	I	I	I, II	II	II

The test matrix for the  $+G_z$  impact tests is shown in Table 2. Three seat back angles were explored. The 103° back angle (measured with respect to the crew module floor plane) was estimated to be the most likely to be used operationally. The 90° seat back position represents an extreme of adjustment; it was also considered a likely position to be selected by the aircraft weapons systems operator. The 110° seat back angle is near the other extreme and represents the position that might be used for comfort.

Two vertical adjustment positions were explored. In the first, the seat pan was elevated until the inertia reel straps were horizontal, i.e., zero degrees to the aircraft waterline. Negative strap angles were not explored since they had been theorized to predispose to spinal injuries and an experimental investigation of this factor would have required a more extensive test

program. The second position was one where the seat pan was adjusted to the lowest position, referred to as "full down". In the full down position, the inertia reel strap angle is a function of the mid-shoulder sitting height of each subject. The second position was considered less likely to be used than the first for the pilot, but apparently is used by the weapons systems operator. The 8 G trial or orientation tests were all accomplished in the 0°/103° shoulder strap/seat position cell of the matrix.

The test subjects were divided into two groups that were matched with respect to total body weight and mid-shoulder sitting height. The groups are designated in each cell of the matrix by Roman numeral I or II.

TABLE 3. TEST MATRIX FOR SIDEWARD IMPACT PHASE

		SHOULDER STRAP/SEAT POSITION		
		0°/90°	0°/103°	FD/103°
IMPACT LEVEL (G)	4	I	II	III
	6	I	II	III
	8	I,II,III	II,III	I,III

Table 3 provides the original test matrix for the +G<sub>y</sub> impact tests. Two seat back positions, which were judged to be of concern under sideward impact loading, were explored. The primary emphasis was placed on the position estimated to be most frequently used, the 103° position. Tests were conducted in all cells of the matrix. Three subject groups were established for this experimental design. The groups, designated by Roman numerals, were also matched according to body weight and mid-shoulder sitting height.

The -G<sub>x</sub> test matrix is shown in Table 4. As in the +G<sub>z</sub> test phase, all three seat back positions were explored. Emphasis was given to the 103° seat back position. No tests were scheduled for the cell: 8 G, FD/103°. The subjects were again tested by groups based on pairing according to total body weight and mid-shoulder sitting height.

Impact tests were performed under all conditions in the matrices using an anthropomorphic dummy prior to tests with volunteer subjects. As an additional safety precaution, a dummy test was performed each day prior to testing with human subjects.

TABLE 4. TEST MATRIX FOR FORWARD FACING IMPACT PHASE

		SHOULDER STRAP/SEAT POSITION			
		0°/90°	0°/103°	FD/103°	FD/110°
IMPACT LEVEL (G)	8	I	II		III
	10	I	I,II	II,III	III

The measured variables in each test included the shoulder strap geometry, the restraint preloads, the restraint forces during impact, the seat pan forces (horizontal and vertical), the foot bracing loads, acceleration of the subject's head and chest, acceleration of the impact carriage and seat pan, and the displacement of targets mounted on the subject's body segments.

The experimental matrix was designed to permit analysis of measured results by means of the Wilcoxon paired-replicate rank test. This test was used to establish statistically significant trends in test parameters from one test condition to another. Each experimentally measured parameter for each subject was compared to the same parameter for the same subject in a different test condition, thereby establishing a "pair difference". When a sufficient number of subjects' pair differences for a specific parameter changed in the same direction from one test condition to another, the trend was established as statistically significant by the Wilcoxon test. The 90% confidence level (assuming a two-tailed test) was the chosen level of significance in this study.

Severity indices (Gadd, 1966) were calculated as a means of comparatively evaluating body segment acceleration measurements. The severity index calculation was used to derive a parameter that is a function of the measured acceleration-time history, rather than a single value such as peak G. The index value was used for comparative purposes only; no exposure limit value was assigned to the chest or head acceleration severity indices.

### Section 3

#### TEST ITEM

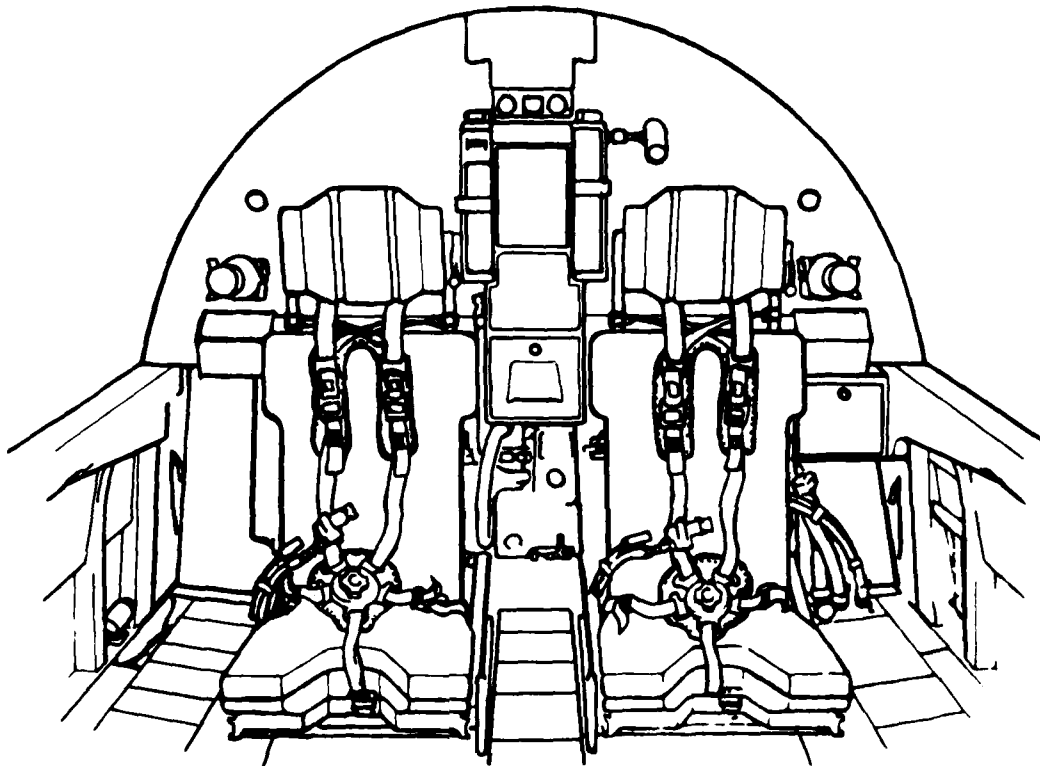


Figure 7. F/FB-111 Seat Installations on Crew Module Aft Bulkhead.

#### A. CURRENT OPERATIONAL SYSTEM

The F/FB-111 crew module contains two crew seats attached to the aft bulkhead of the cockpit structure as shown in Figure 7. The distance between the two seats is  $8 \frac{7}{8}$  inches. Instrument/control consoles are located between the seats and on the outboard side of each seat as shown in Figures 8 and 9. The ejection initiation handles are located on the center console. Small consoles are also positioned forward of the aircraft control columns between each crewmember's legs (see Figure 8). Rudder control pedals are located under the main instrument panel. These pedals may be adjusted over a fore-aft distance of 6 inches. Additional leg length accommodation is provided by horizontal adjustment of the seat pan.

The crew seat design shown in Figure 10 is unique to the F/FB-111 aircraft. The seat pan and the lower pivot point of the seat backrest can be adjusted in the aircraft longitudinal axis over a range of 5 inches in 1 inch increments. The vertical position of the seat pan and the lower backrest pivot are continuously adjustable over a range of 5 inches by an electro-mechanical

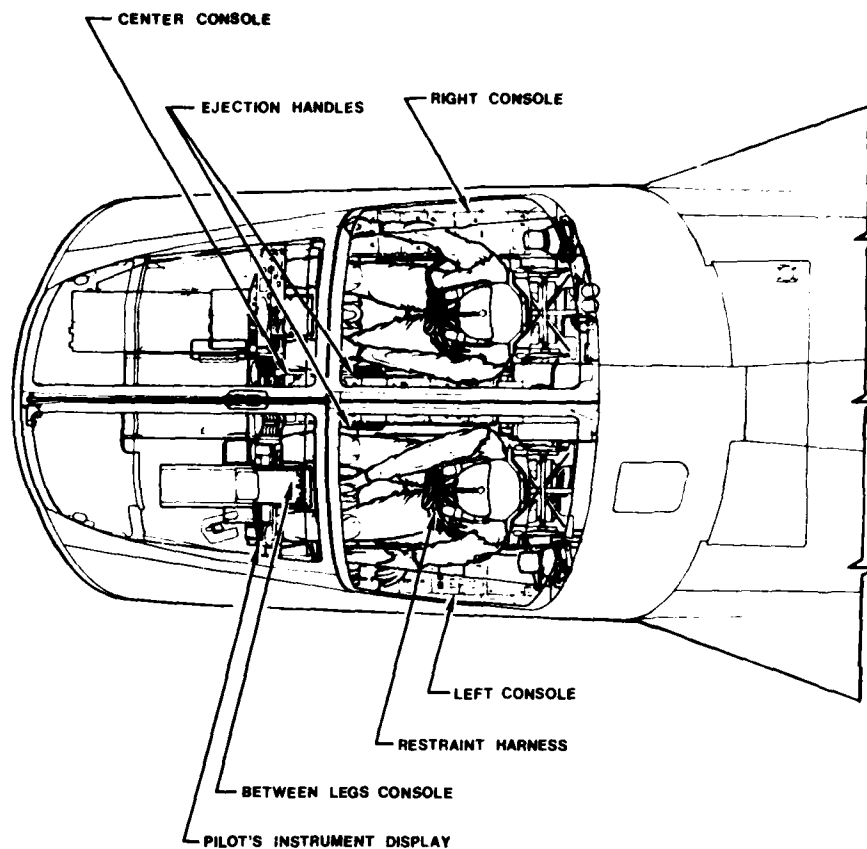


Figure 8. Top View of Crew Module Cockpit Area.

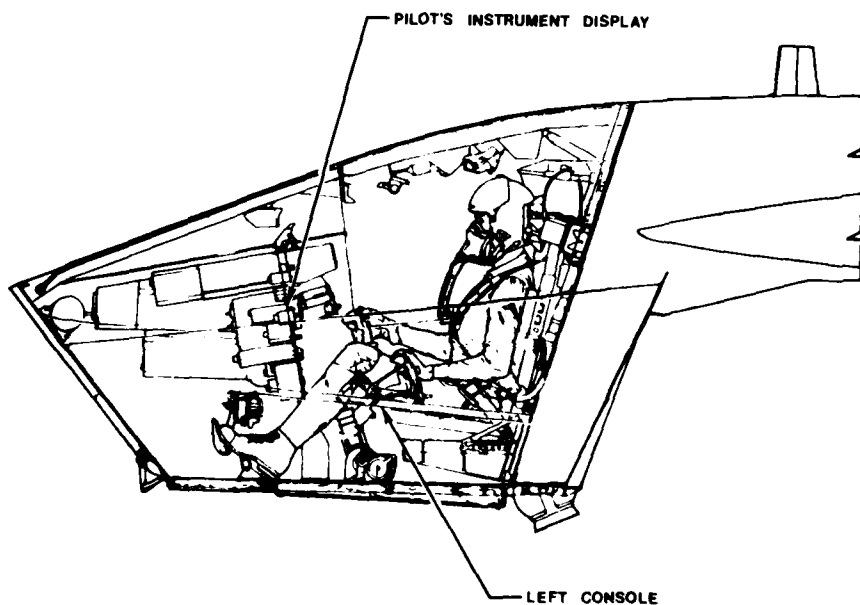


Figure 9. Side View of Crew Module Cockpit Area.

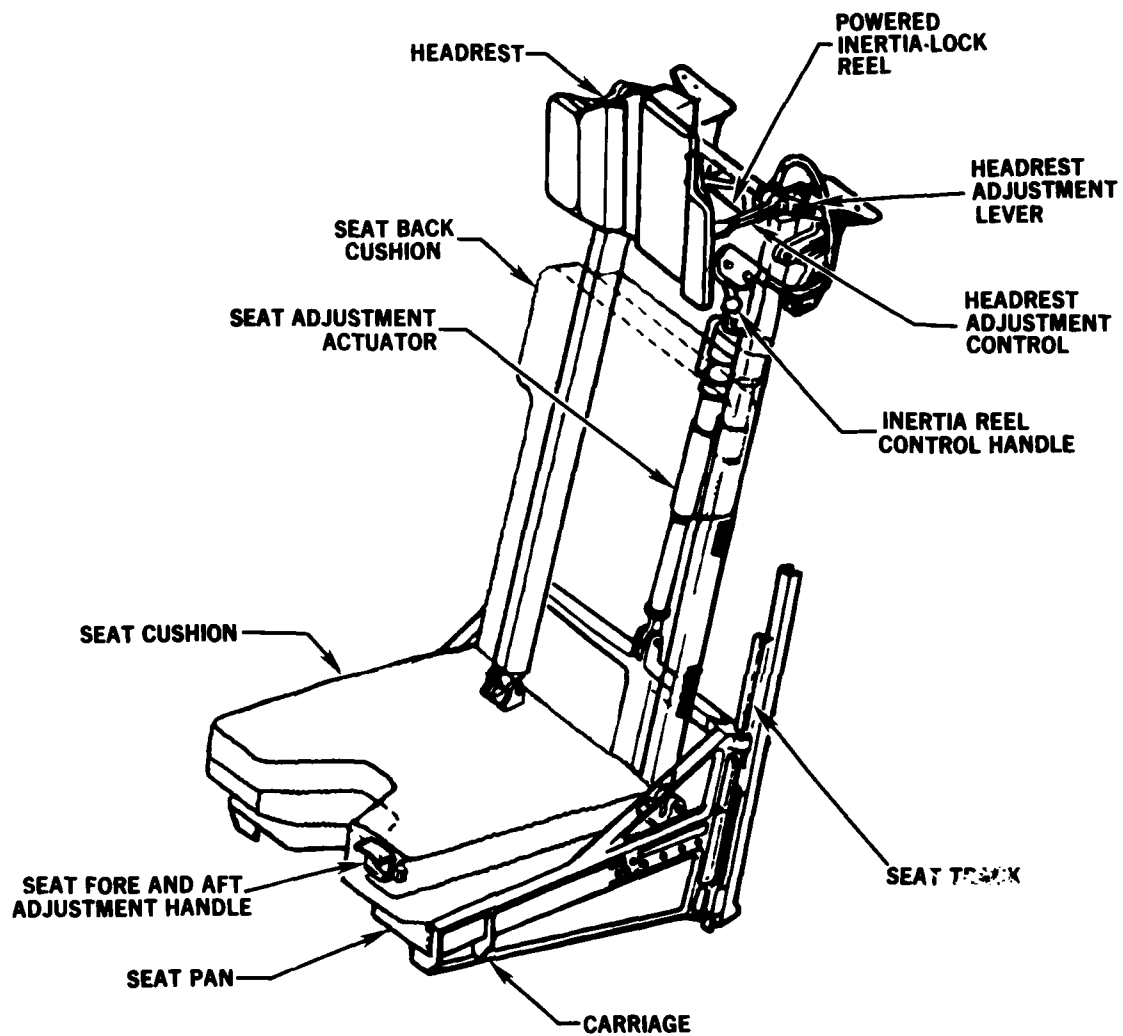


Figure 10. F/FB-111 Crew Seat Design.



actuator. The angle of the backrest is determined by the longitudinal and vertical position of the lower backrest pivot on the seat pan and the upper backrest pivot located on the support structure of the headrest. The headrest and the upper backrest pivot are adjustable, in 1 inch increments, over a longitudinal distance of 6 inches.

The set pan is constructed of a metal frame and fiberglass pan. The pan is shaped to provide a generalized buttocks contour. The seat pan cushion is made of two layers of plastic foam covered by stretchable fabric. The top layer of foam is a 1/2 inch thickness of 65.1 lb/ft<sup>3</sup> density plastic foam (B. F. Goodrich Koroseal M407). The lower layer, which is 2 inches thick, is composed of 1.6 lb/ft<sup>3</sup> density polyurethane foam (MIL-5-27332). The seat back cushion is constructed of the same 1.6 lb/ft<sup>3</sup> density polyurethane foam covered by stretchable knit nylon fabric. The helmet contact surfaces of the headrest are covered by 7/16 inch thick plastic foam (Uniroyal Ensolite, 6.28 to 8.5 lb/ft<sup>3</sup>).

The restraint system used in all operational F/FB-111 ejections since 1970 is the lap belt, shoulder strap and crotch strap configuration shown in Figure 11. The harness is attached to the crew seat at five points and to the inertia reel at two points. The shoulder strap geometry is unique in that the straps originate from the inertia reel, pass through the rollers attached to the shoulder strap yoke, and are attached to the top of the backrest on the opposite side of the seat. The intention of this cross-over geometry is to provide sideward impact protection. The lap belt is attached to the seat structure at the seat reference axis (the intersection of the plane of the seat back and the seat pan). The crotch strap (also referred to as the anchor strap or negative G strap) is attached to the front of the seat pan. The shoulder straps are attached to the shoulder strap yoke below the rollers above the chest strap adjustment buckles. The lap belt, crotch strap, and lower portion of the shoulder straps (chest straps) are constructed of 1 3/4 inch wide Terylene webbing. The shoulder straps attached to the inertia reel are 1 3/4 inches wide polyester webbing (Type I, MIL-W-25361).

The restraint system used in the F/FB-111 is not the system that was originally designed for this aircraft. The harness that is now operational is based on a design developed by the Royal Air Force Institute of Aviation Medicine (Reader, 1967). The harness was installed in the F/FB-111 aircraft in 1970, after the completion of development tests and evaluation. Demonstration impact tests were performed using prototypes of the harness (Moss, 1968). These tests were conducted on the Daisy Decelerator at Holloman AFB in 1968. The results of these tests indicated that the restraint system generally provided adequate restraint. However, the testing was limited in its scope. Extremes of subject size and seat adjustment were not evaluated. Furthermore, the acceleration vector orientations were limited to sideward (-G<sub>y</sub>) and forward facing (-G<sub>x</sub>) directions.

The inertia reel that is used to tighten the shoulder straps prior to ejection is a ballistically powered unit manufactured by Pacific Scientific Company (PSCO P/N 0103147-75). The reel is mounted to the aircraft bulkhead below the headrest support frame and maintains this fixed position during seat or headrest adjustments. The reel is powered by a pyrotechnic gas generator that is fired within 0.01 sec after manual ejection initiation. The reel is

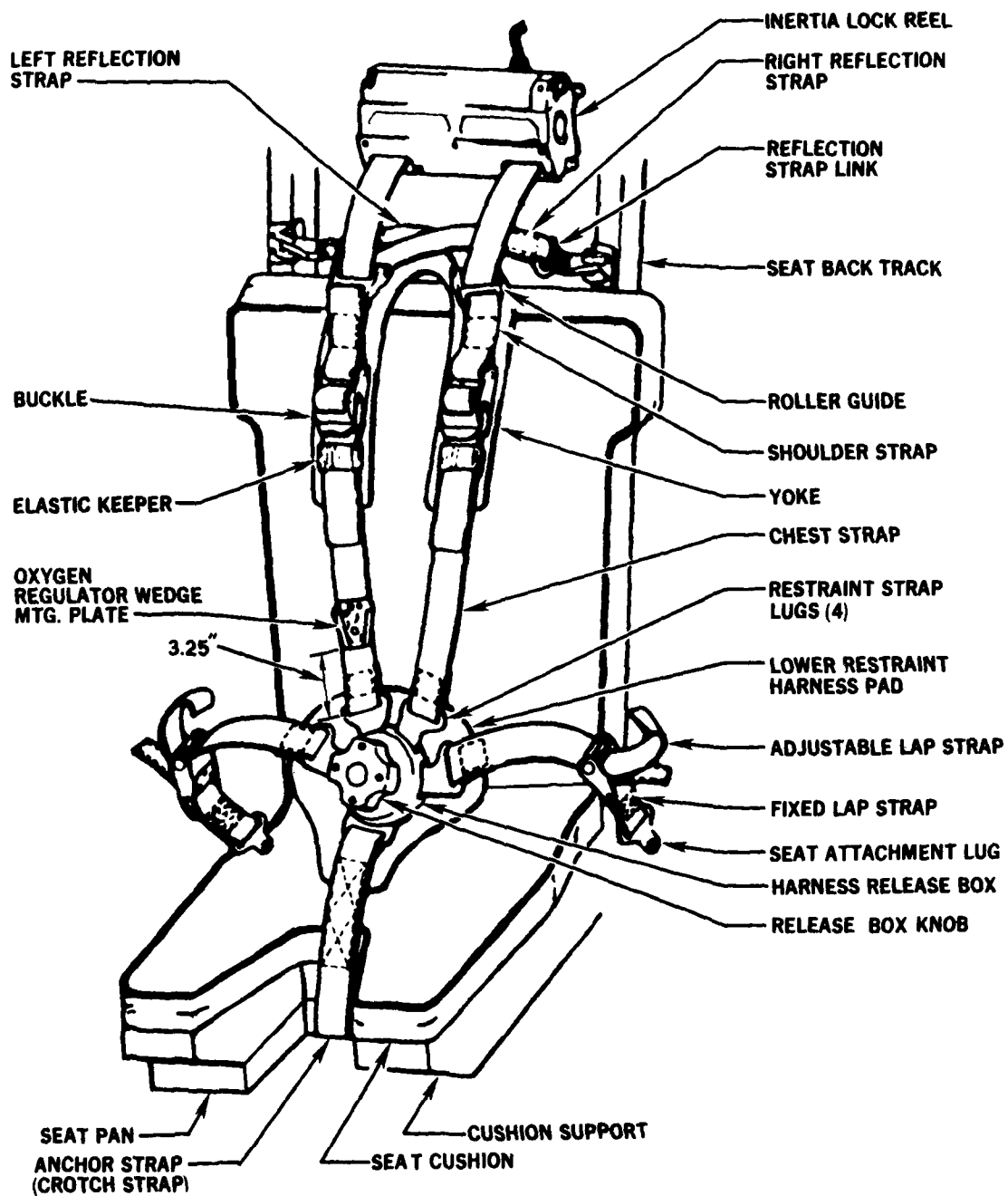


Figure 11. F/FB-111 Restraint System.

automatically locked during firing. The data collected during the original qualification tests of the reel (Whitney et al., 1970) are summarized in Table 5.

TABLE 5

SUMMARY OF INERTIA REEL QUALIFICATION TEST DATA

NUMBER TESTED	TEMP. (°F)	DISTANCE (Inches)	TIME (Sec)	VELOCITY (Ft/Sec)	PEAK LOAD (Lb)	RESIDUAL (Lb)
17	+200	10	$\bar{x} = 0.162$ $s = .013$	$\bar{x} = 6.51$ $s = .506$	$\bar{x} = 227$ $s = 32.51$	$\bar{x} = 77.2$ $s = 14.91$
2	+200	2	$\bar{x} = 0.265$ $s = .021$	$\bar{x} = 3.25$ $s = .354$	$\bar{x} = 180$ $s = 14.14$	$\bar{x} = 38.0$ $s = 4.24$
17	- 65	13	$\bar{x} = 0.254$ $s = .020$	$\bar{x} = 4.68$ $s = .574$	$\bar{x} = 258$ $s = 26.99$	$\bar{x} = 46.6$ $s = 13.02$
3	- 65	2	$\bar{x} = 0.270$ $s = .030$	$\bar{x} = 2.23$ $s = .208$	$\bar{x} = 153$ $s = 40.42$	$\bar{x} = 93.7$ $s = 11.06$

$\bar{x}$  = sample mean

s = standard deviation

Peak Load = maximum shoulder strap force during first one second with duration of 0.1 second.

Residual = maximum shoulder strap force one minute after firing reel.

These tests were conducted using a test apparatus that included a rigid torso simulator. The tests conducted at 200° F were accomplished with the torso set to simulate the 95th percentile body size and a 100 lb opposing force was applied to the shoulder straps. The -65° F/13 inch retraction tests were conducted with the torso simulating 5th percentile properties and no external opposing force was applied. The -65° F/2 inch retractions were done with the same initial conditions as the 200° F test series.

The F/FB-111 crew seat and restraint harness deviates from current USAF seat and restraint design criteria in several major aspects. First, the position of the tie-down points of the shoulder straps can be below the mid-shoulder height of the 95th percentile crewmember. Attachment of the reflection (or cross-over) straps at a point that is 24.09 inches above the seat reference axis assures that these two tie-down points will be at or below the mid-shoulder sitting height of approximately 90% of the flying population. Since the seat pan can be vertically adjusted with respect to the fixed position of

the inertia reel straps (fuselage station 263.25 and waterline 200.75), the tie-down points created by the inertia reel can also be located below the mid-shoulder height of 75 percent of the flying population. Second, the headrest is mounted forward of the seat backrest and causes the plane of contact of the back of the flight helmet to protrude as much as 2 1/4 inches forward of the seat back plane. This headrest position was dictated by a USN requirement to provide head support to maintain over-the-nose vision during carrier launches. The current USAF design specification for capsule emergency escape systems (MIL-C-25969B, 1970) indicates that the headrest should be located 1 inch aft of the plane of the seat back.

#### B. PROPOSED MODIFICATIONS

The General Dynamics Corporation has redesigned the crew seat and restraint system under Contract No. F33657-78-C-0651, with the Life Support System Program Office. General Dynamics first conducted a feasibility study to determine approaches to improve the crew seat and restraint system. A redesigned crew seat and restraint configuration was then selected for testing in June 1978 (ASD TWX 131630Z). The proposed redesign consists of:

1. Rerouting the inertia reel straps to raise the shoulder strap tie-down point of the inertia reel.
2. Moving the cross-over strap attachment points up to the headrest support frame.
3. Extension of the height of the backrest.

The redesigned configuration is shown in Figure 12. Rerouting of the inertia reel straps is accomplished by two sets of rollers that are attached to the inertia reel assembly. These rollers increase by 1.9 inches the height of the points through which the retraction loads are applied to the crewmember and through which a portion of the inertial loads of the human body are carried during acceleration of the crew module throughout the escape sequence. The reflection strap attachments are mounted to points at waterline 203.2 within the headrest support frame and move fore and aft when the headrest position is adjusted.

The backrest extension increases the height of the backrest at the center and each side by 2 1/4 inches. Each side of the seat back extension is recessed by 1 1/4 inches to clear the inertia reel straps when the seat is adjusted to its upper limit. A section of the contact surface at the bottom of the headrest has also been removed to provide clearance for the shoulder straps. This reduces the height of the headrest support surface from 9.0 to 6.34 inches.

The restraint harness assembly is not changed in the proposed modification.

Table 6 summarizes the data obtained from inertia reel tests accomplished with the modified shoulder strap routing and attachment arrangement (Whitney, 1979). These tests differed from the earlier tests of the inertia reel in several respects. First, the 200° F tests were accomplished with a 5th percentile simulated torso and the -65° F tests used a 95th percentile torso with an opposing force of 100 lb. Second, tests were not accomplished at 2 inch retraction distances. The retraction time at -65° F was much slower ( $\bar{x}$  = 0.338 sec versus 0.254 sec) and the peak load was lower ( $\bar{x}$  = 179 lbs versus 258 lbs). The difference in performance has been attributed to a change in the inertia reel gas



Figure 12. Proposed Crew Seat and Restraint System Modifications.

generator as well as the change in the harness configuration and test procedures.

TABLE 6

SUMMARY OF INERTIA REEL PERFORMANCE TEST DATA

NUMBER TESTED	TEMP. (°F)	DISTANCE (Inches)	TIME (Sec)	VELOCITY (Ft/Sec)	PEAK LOAD (Lb)	RESIDUAL (Lb)
4	+200	10	$\bar{x} = 0.170$	$\bar{x} = 6.38$	$\bar{x} = 231$	$\bar{x} = 89.3$
			$s = 0.008$	$s = 0.457$	$s = 18.80$	$s = 9.777$
4	- 65	13	$\bar{x} = 0.338$	$\bar{x} = 3.60$	$\bar{x} = 179$	$\bar{x} = 53.0^*$
			$s = 0.034$	$s = 0.424$	$s = 26.69$	$s = 15.13$

\*n = 3. Residual loads invalid on one test due to misrigging of reel.

C. TEST RELATED MODIFICATIONS

The impact test program was accomplished using two crew seats salvaged from an F-111 aircraft. The seats were modified by GD/FW to represent the proposed redesigned configuration. Test fixtures necessary to mount the seats on the test facilities were designed and built by GD/FW. The horizontal impact test fixture is shown in Figure 13. Rudder control pedals and foot load measuring equipment were supported by the structure shown in Figures 14 and 15. The vertical impact test fixture is identical in layout of equipment, but the structural design of the seat support frame differs as required to mate with the AFAMRL Vertical Deceleration Tower and carry vertical loads. The orientation of the load cells within the foot load measuring assembly also change between vertical and horizontal test fixtures.

Variations from the actual aircraft installation were:

1. The side, center, and "between the legs" consoles were not simulated.
2. The instrument panel was not simulated.
3. The seat support frame of the test fixture prevented movement of the headrest to the most aft adjustment increment.
4. The vertical seat adjustment actuator was not used in the vertical impact tests. The actuator was replaced by the strut shown in Figure 16. Vertical adjustment is thereby limited to 1 inch increments but covers the 5 inch range provided by the operational configuration.
5. The addition of transducers to measure loads within the restraint harness.
6. Instrumentation of the seat pan to measure vertical and horizontal loads.
7. During the  $-G_x$  impact tests, a 1 inch thick layer of Ensolite plastic foam was added to the helmet contact surface of the headrest. Since the subjects did not wear flight helmets during this phase of the test program, the

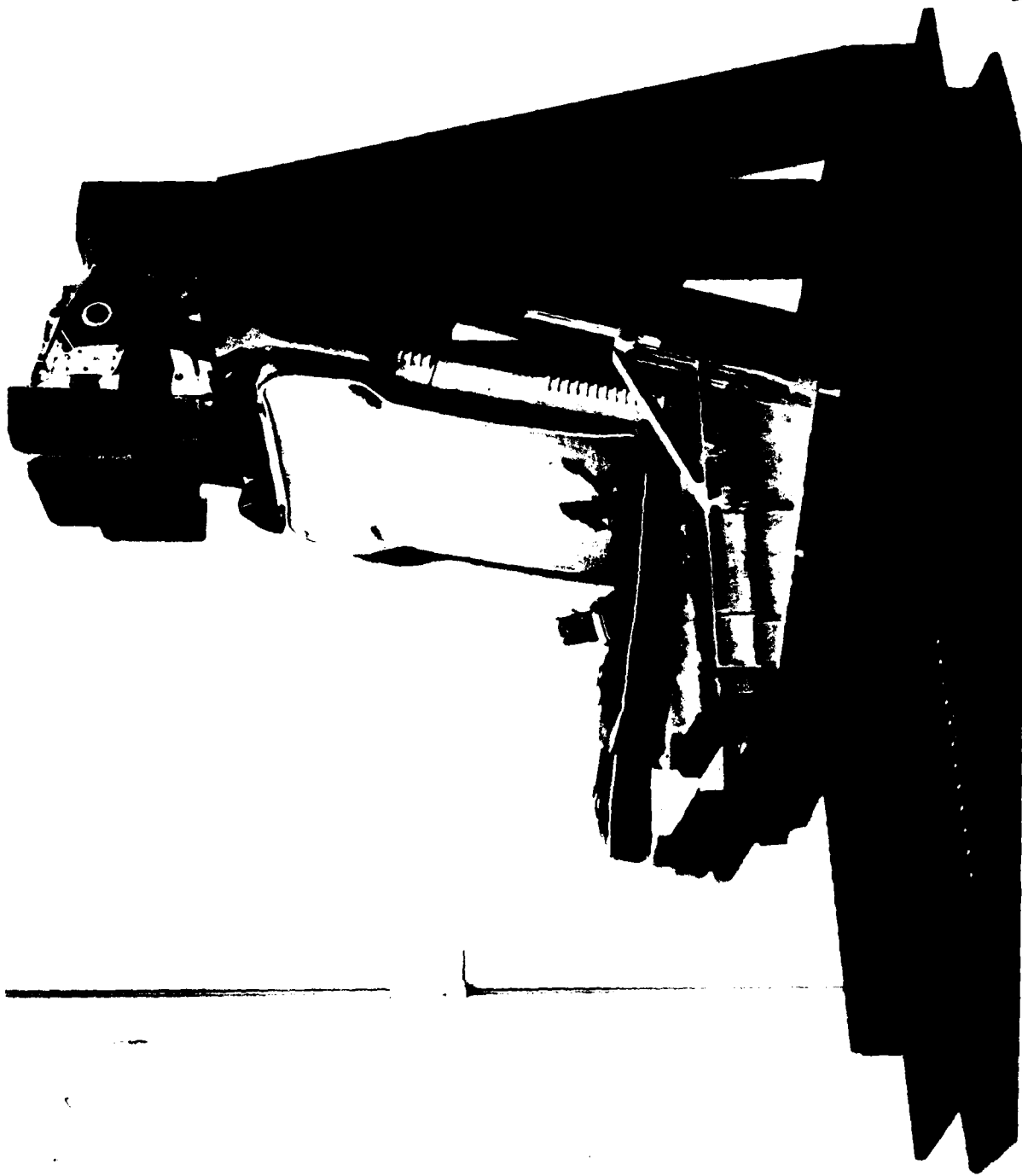


Figure 13. The Horizontal Impact Test Fixture with the Crew Seat.

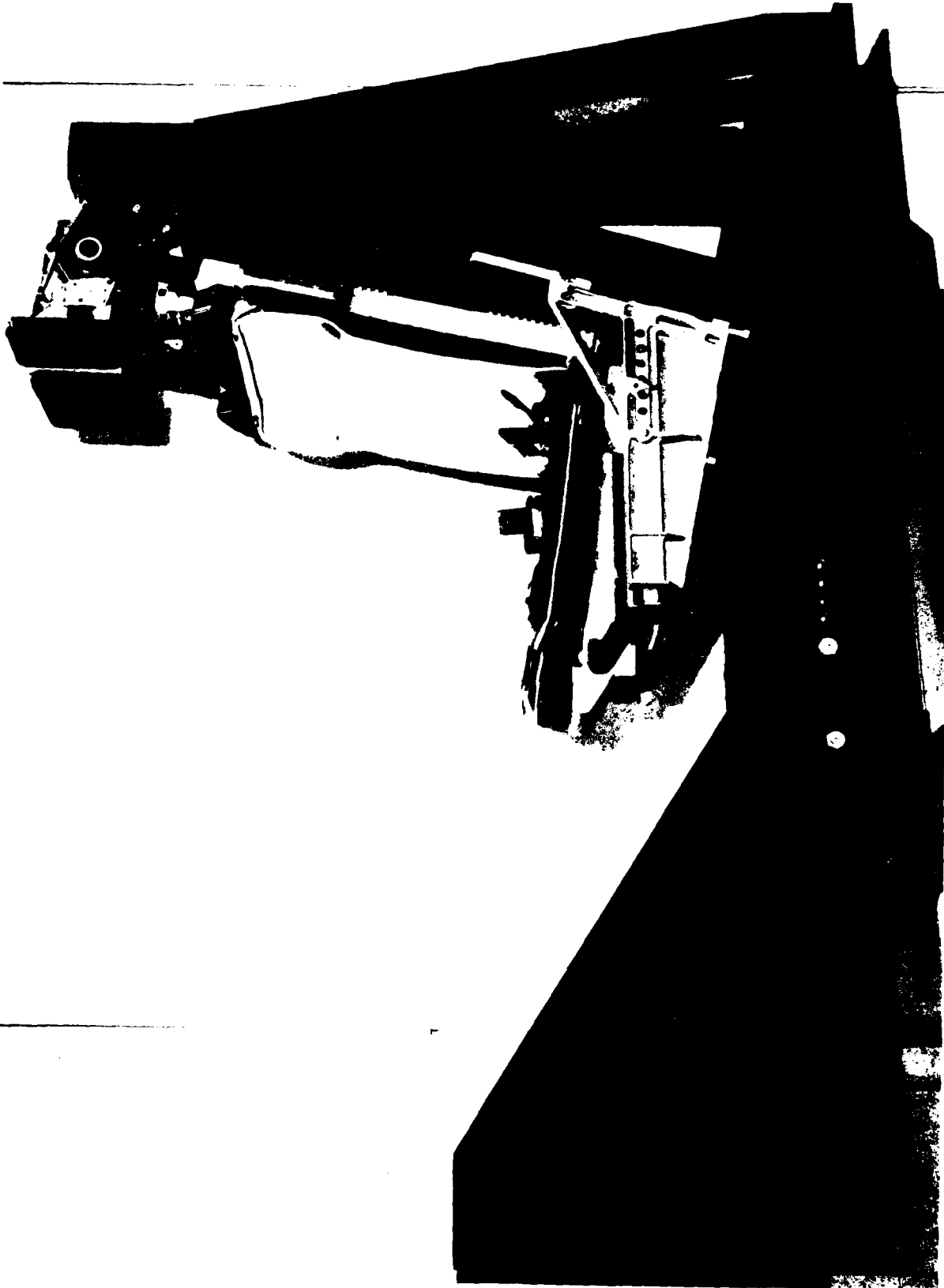


Figure 14. The Horizontal Impact Test Fixture with Rudder Pedal Support Structure.



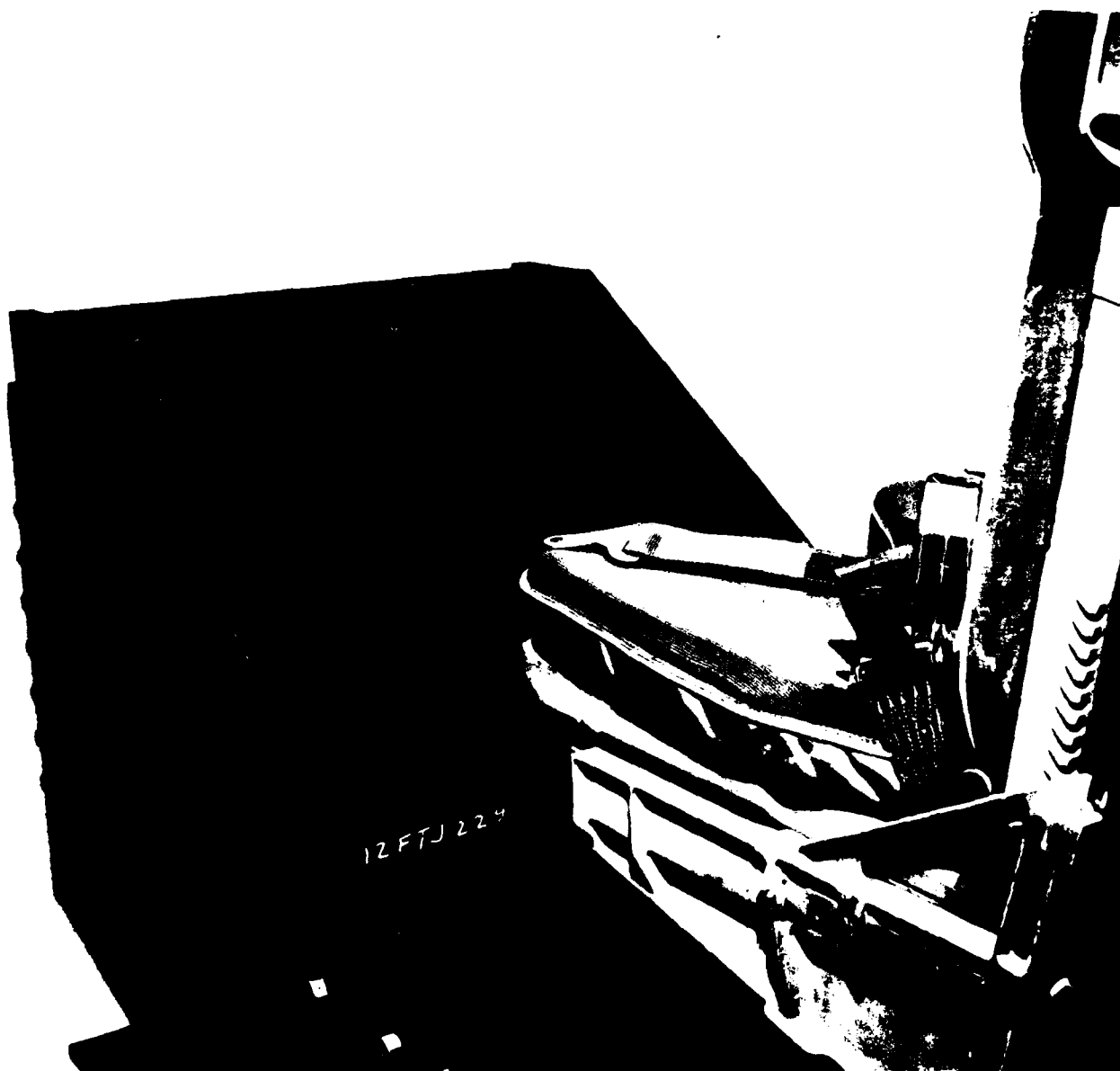


Figure 15. Rudder Pedal Installation.

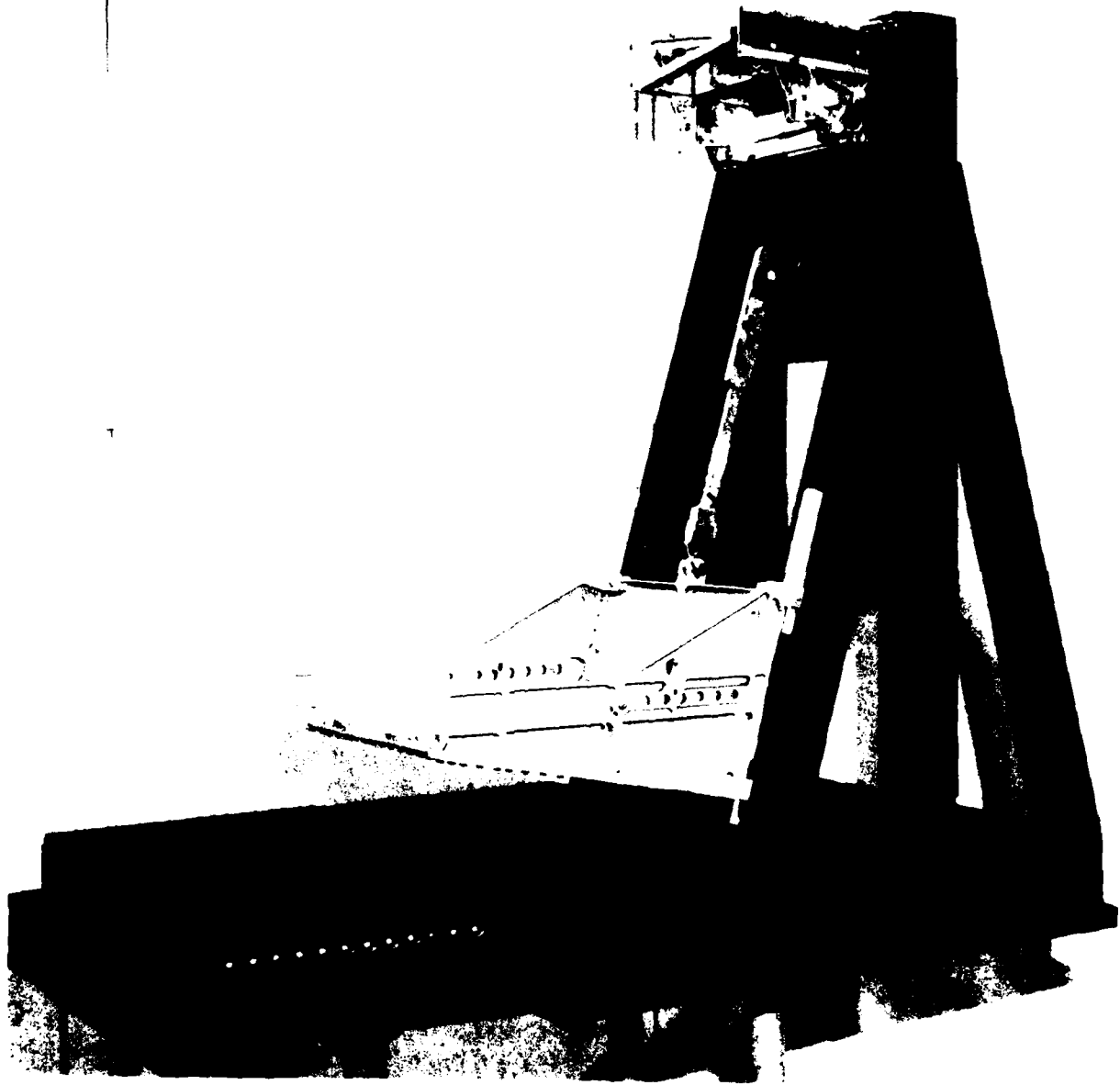


Figure 16. Test Fixture Showing Detail of Vertical Seat Actuator Replacement Strut.

additional foam assured that the subject's head would be in the same initial position as it would have been if a flight helmet had been worn.

Of these variations, only the absence of the consoles was found to have any known influence on the test results and this influence was restricted to the sideward impact tests.

Instrumentation of the restraint harness and seat pan was accomplished without altering the interface between the body support/restraint and the test subjects. Forces were measured at each strap of the harness by the use of strain gages applied to the metal end fittings of the lap belt, reflection straps, and the crotch strap. LeBow gages were used on the inertia reel straps. Three load cells and two mechanical links with strain gages were mounted within the seat pan structure without altering the outer shape of the seat pan configuration.

The support structure for the reflection strap attachments was provided with two sets of mounting holes for the attachment of the reflection straps. These attachment points are located 2 1/16 inches and 3 1/2 inches from the plane of symmetry of the crew seat. Either set of holes was considered to be a feasible mounting site for the final production hardware. It was estimated that the outermost mounting sites would provide slightly better protection during sideward impact and the inner set would (1) reduce the possibility of interference of the reflection straps with the crewmember's helmet in lower seat positions and (2) reduce medial loading of the crewmember's shoulders and neck. Conceivably, the attachments of the reflection straps could also be fastened at a central point on the support.

The reflection straps were attached to the inner set of mounting holes throughout the impact test program. Figure 17, a photograph taken during a static load test at GD/FW, shows the location of these points. These holes are about 3 3/16 inches closer to the plane of symmetry of the seat than the pivot points of the attachments to the backrest of the configuration that is currently operational. The holes are also aft of the current attachment points by approximately 0 to 5 5/8 inches depending on the adjustment position of the headrest/seat back pivot.

The restraint system was pretensioned prior to the impact test. The pretest load was 20  $\pm$  5 lb measured in each side of the lap belt. The total load acting at each shoulder strap roller guide was set to this same value by measuring the load in the right and left inertia reel straps. This measure was a little more than one-half of the total force applied at the roller guide. The resulting preload in the shoulder straps is lower than the load expected in operational use, but the test program requires the imposition of preloads on the subject for long periods of time before impact compared to the pre-ejection sequence. Therefore, application of operational loads was not considered practical without an inertia reel. Previous tests of similar F-111 harnesses in England and at Holloman AFB indicated subjective complaints with pretensions of 50 pounds per strap and greater. Previous experience at AFAMRL indicated that significant variations in restraint performance occur as a function of pretension primarily in the range below 20 pounds. With the pretensions applied in this program, adequate pretension was felt to be assured at impact since the track friction prior to brake contact applies a further preload of approximately 0.3 G. In vertical tests, a similar preload was anticipated as the seat cushion was unloaded during the drop.

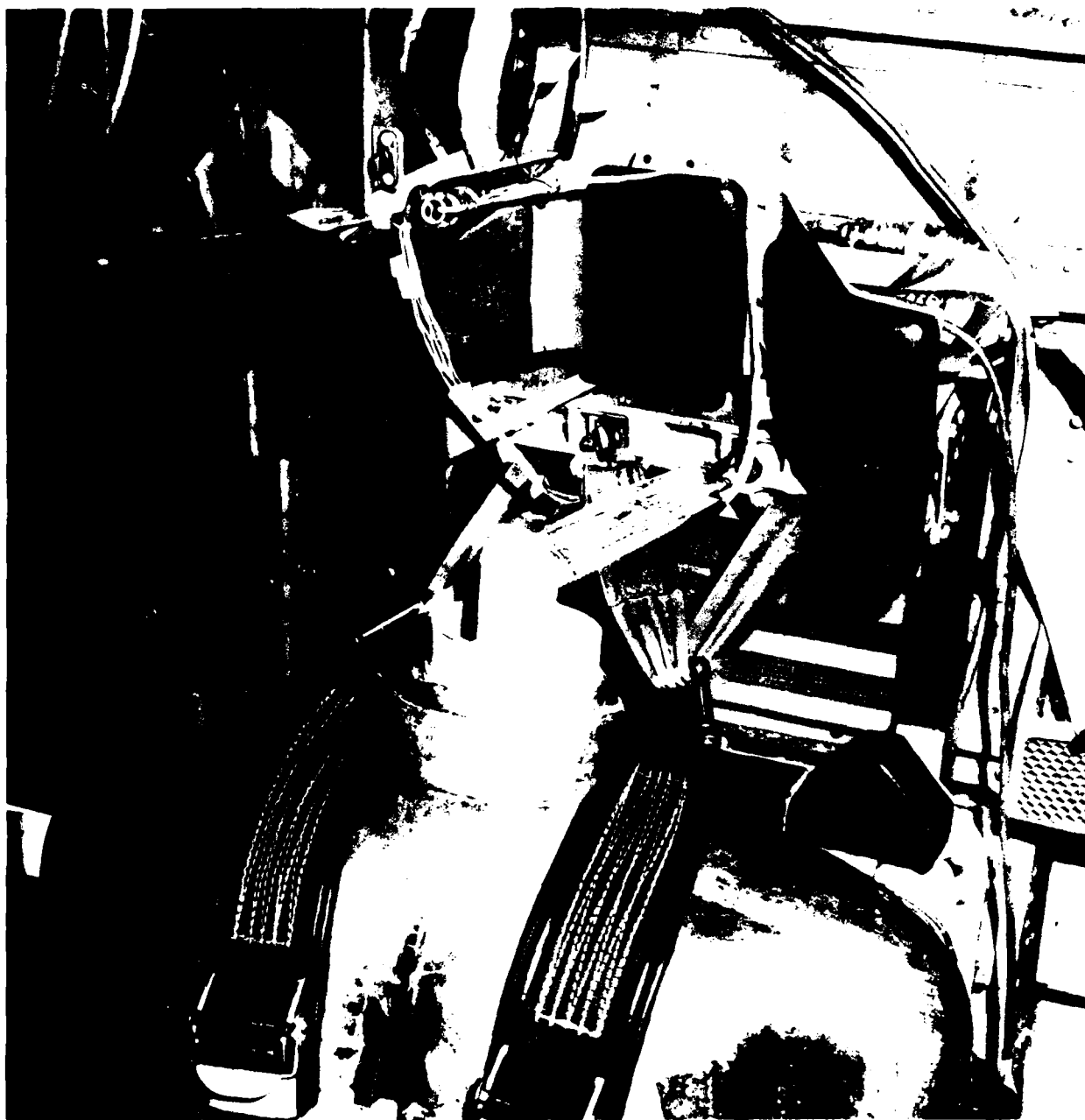


Figure 17. Reflection Strap Attachment Points Shown During Static Tests.

## Section 4

### TEST EQUIPMENT, METHODS AND FACILITIES

#### A. VERTICAL DECELERATION TOWER

The AFAMRL Vertical Deceleration (VDT) Tower and the crew seat test fixture, shown in Figures 18 and 19, were used for the vertical impact test phase. The test facility consists of a 60 ft high steel tower, which supports a guide rail system, an impact carriage, a hydraulic deceleration device, and a test control and safety system. The impact carriage that is used to carry the test specimen can be raised to a height of up to 42 ft prior to release. After release, the carriage free falls until a plunger attached to the carriage enters a water-filled cylinder mounted at the base of the tower. The deceleration profile that is produced as the plunger displaces the water in the cylinder is a function of the free fall distance, the carriage and test specimen mass, the shape of the plunger, and the diameter of the cylinder orifice.

Figures 20 and 21 show typical sled acceleration data recorded during the Z-axis tests. The 10 G test level mean acceleration for the entire vertical test series was 10.46 G with an estimated standard deviation of 0.22.

#### B. HORIZONTAL DECELERATOR FACILITY

The AFAMRL Horizontal Decelerator (HD), shown in Figure 22, was used for the sideward and forward facing impact tests. The facility consists of the launch system, a track, an impact sled, a hydraulic decelerator, and the safety and control system.

The launch system, which is used to accelerate the impact sled, is shown in Figure 23. Prior to initiation of testing, energy is stored in a flywheel that is driven by an electric motor. During a launch, the flywheel is coupled to a reel by an electronically controlled hydraulic clutch. Fabric tape, attached to the reel and a shuttle sled, is wound onto the reel to accelerate the shuttle sled which pushes the impact sled toward the Hydraulic Decelerator. The acceleration phase of the launch occurs for a distance of 73 to 75 ft. The impact sled then separates from the shuttle sled and coasts approximately 135 ft to the impact area. During the coast, phase the sled velocity is measured and controlled by an active velocity control system described later in this report.

The hydraulic decelerator, shown in Figure 24, is a horizontal cylinder bored within a series of steel blocks. The cylinder blocks are mounted within a water containment enclosure. At the point of impact, a 5 ft piston attached to the impact sled punctures a polyethylene retaining membrane and forces the water within the cylinder through orifices in the cylinder wall. In Figure 25, the top of the water enclosure has been removed to show the positions of the orifice plugs that surround the cylinder block. The deceleration profile is controlled by varying the diameter of the orifices.

Figures 26 and 27 show the fixtures mounted to the impact sled for the X and Y axes test phases. The maximum sled acceleration profiles used in the X and Y axes tests are shown in Figures 28 and 29.



Figure 18. AFAMRL Vertical Deceleration Tower and F/FB-111 Test Fixture Viewed from Below.

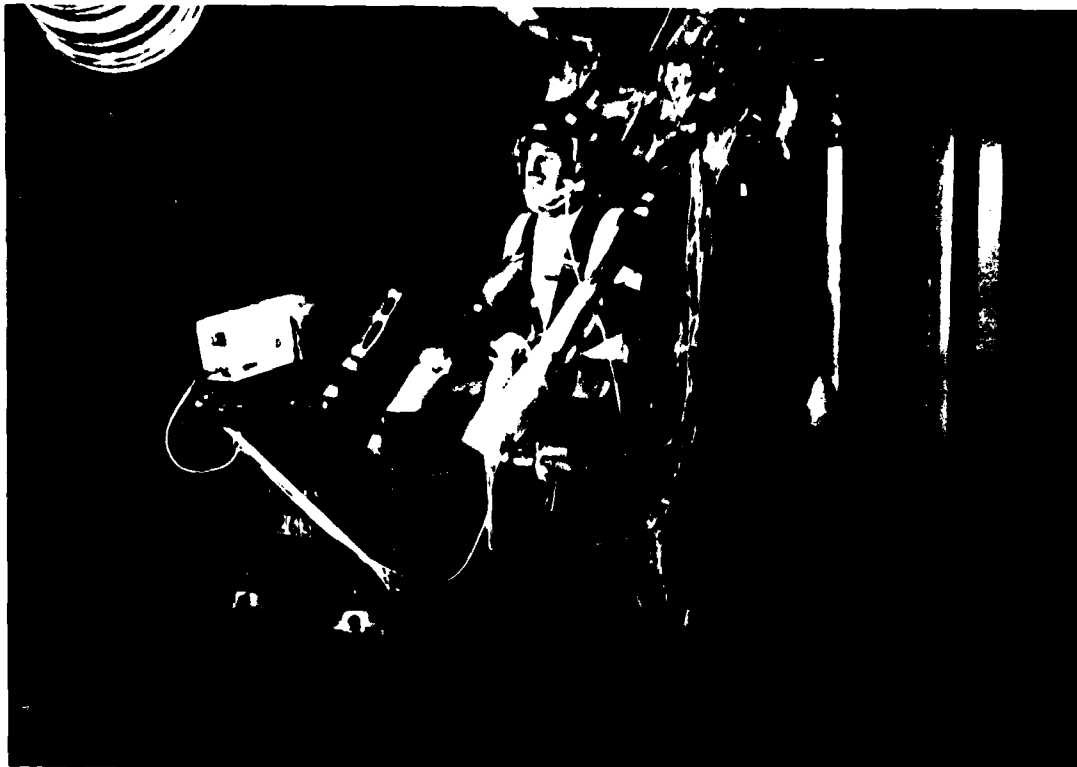


Figure 19. Vertical Deceleration Tower Carriage and F/FB-111 Test Fixture with Volunteer Subject During Impact.

All tests accomplished on the Horizontal Decelerator Facility are initiated and controlled by a master safety and control system. This system monitors the status of the critical launch system components, sled velocity, the data acquisition systems, and test area security. The system provides automatic test abort, if the equipment status is unacceptable or if the subject, medical monitor, safety officer, or deceleration area technician release hand-held switches.

#### C. EXPERIMENT CONTROL

Reproducing impact conditions during tests conducted in the low velocity range on the HD requires that a special velocity control system be used (Juhasz *et al.*, 1980). This system reduces the likelihood that the test subjects will be exposed to excessive impact velocities and accelerations. The control system assures a predictable velocity profile during a sled run by activating the sled mounted brake hardware whenever an instantaneous actual velocity exceeds the instantaneous model velocity stored in a PDP-11/34 computer. Each test is initiated with a slightly overspeed launch to assure that the actual velocity profile during a sled run never falls below the model velocity profile stored in the computer. Otherwise, convergence of the two would require increasing the sled velocity which is not possible with brakes as actuators. Upon entering the deceleration phase of a test, the sled trips a switch which starts the computer control program. At each control window of 320 msec duration, the program

UDT CARRIAGE ACCELERATION Z-AXIS

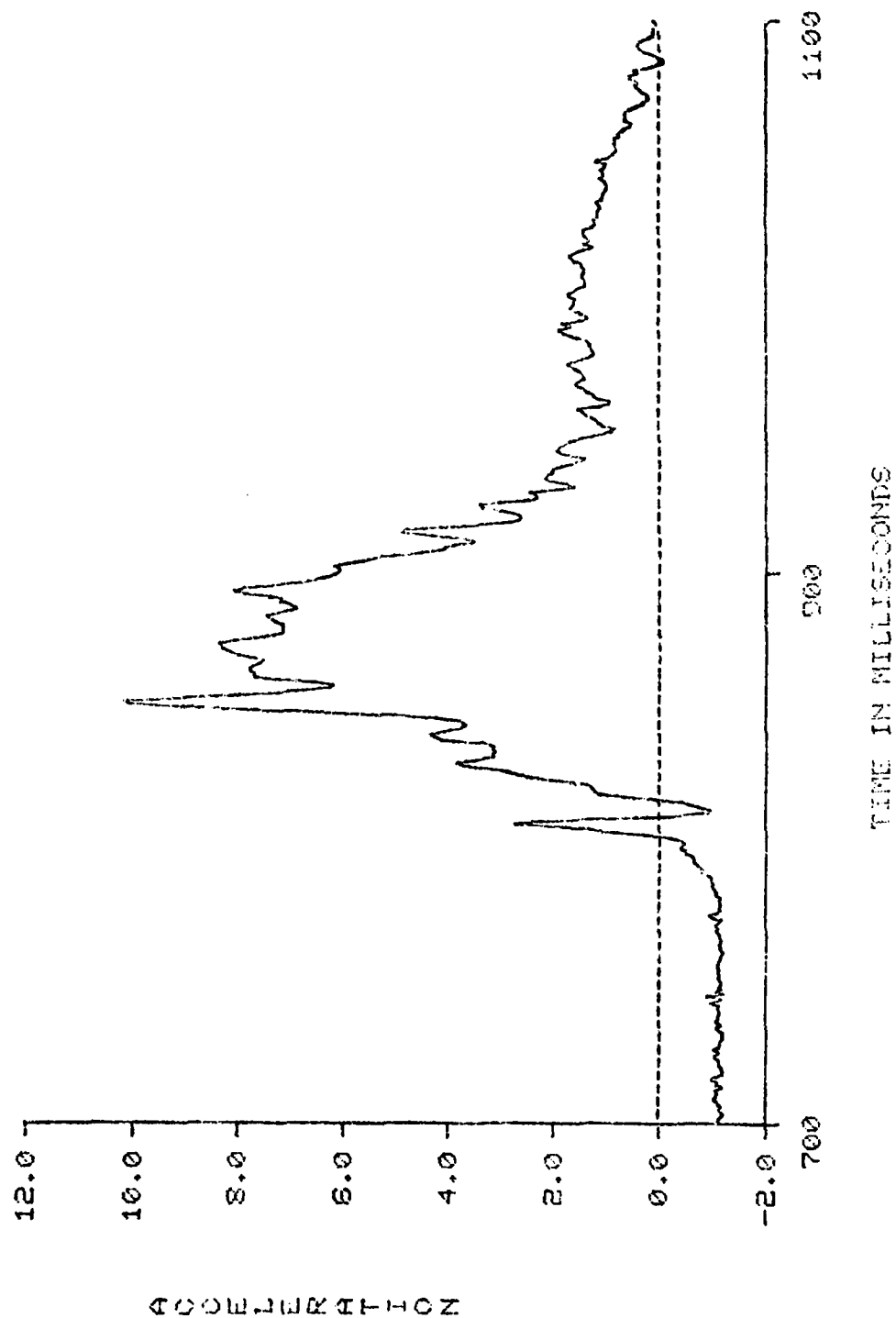


Figure 20. Acceleration Profile Used During 8 G Vertical Tests.



# UDT CARRIAGE ACCELERATION Z-AXIS

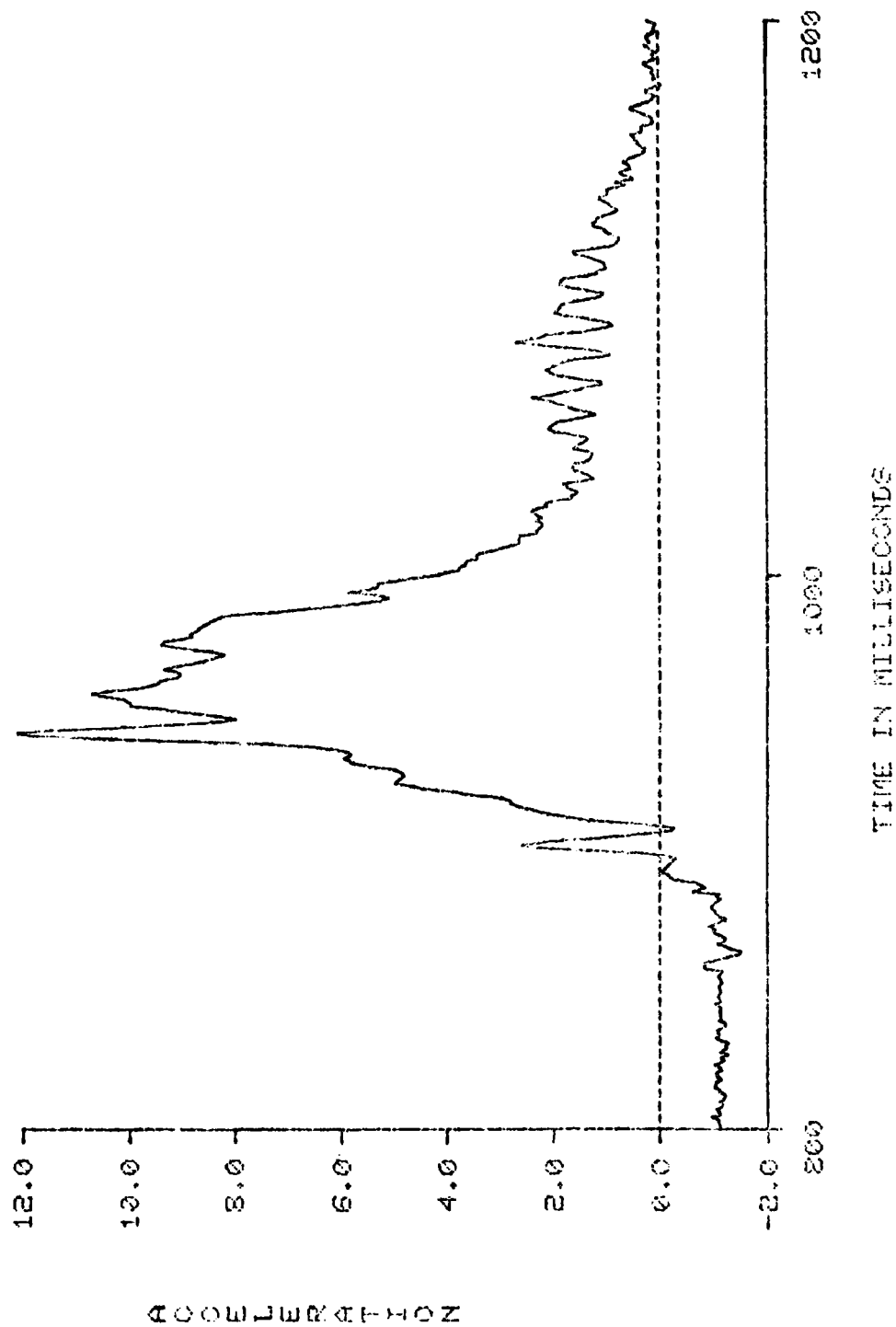


Figure 21. Acceleration Profile Used During 10 G Vertical Tests.

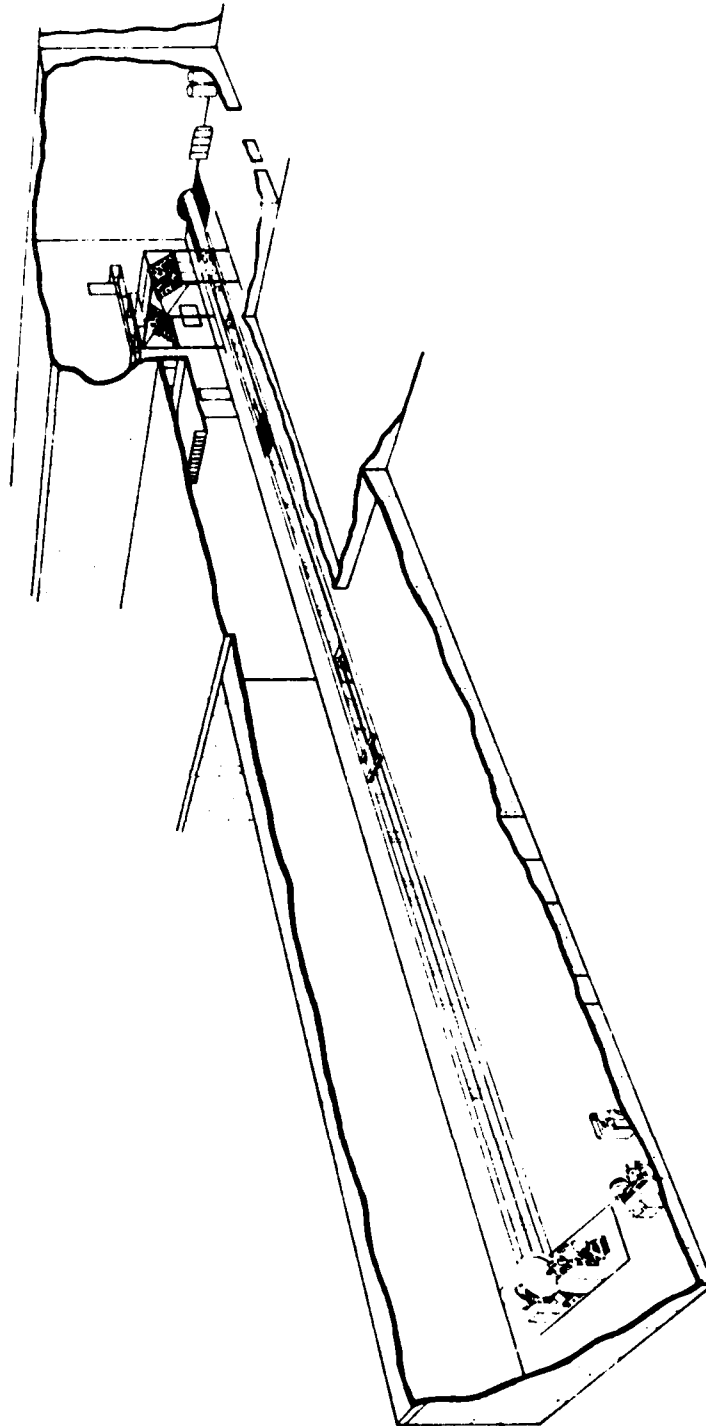
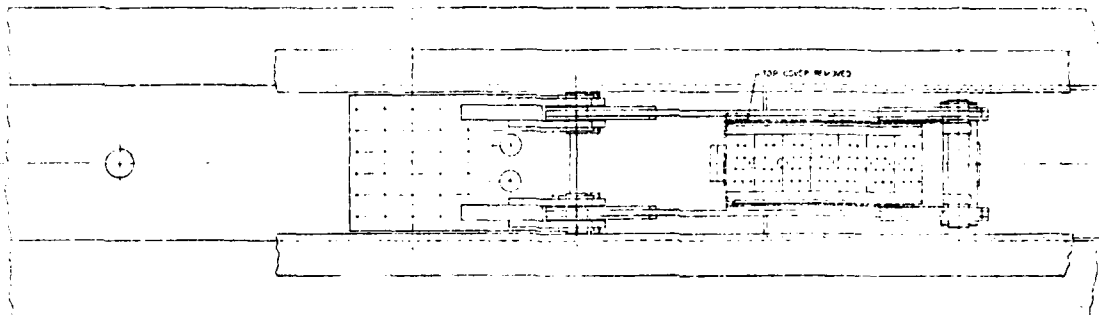


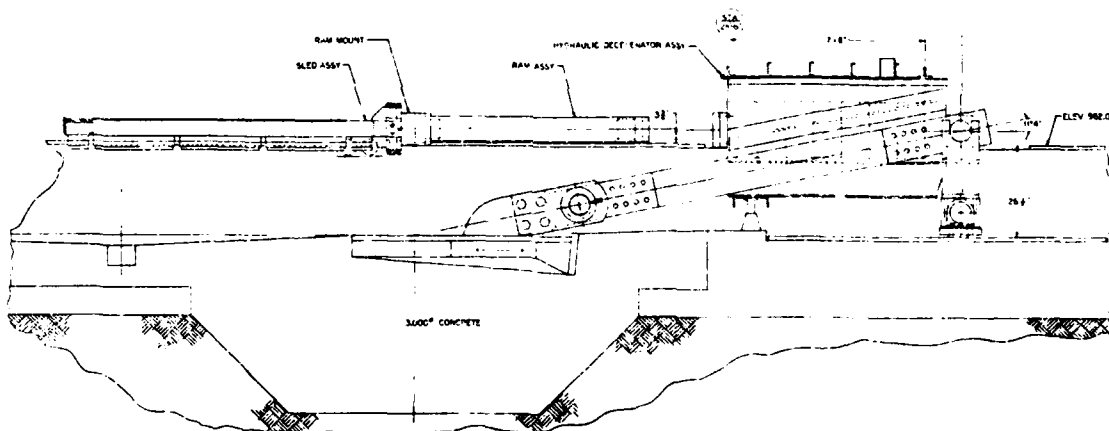
Figure 22. AFAMRL Horizontal Decelerator Facility.



Figure 23. Impact Sled Launch System.



Top View



Side View

Figure 24. Top and Side View Drawings of the Hydraulic Decelerator.

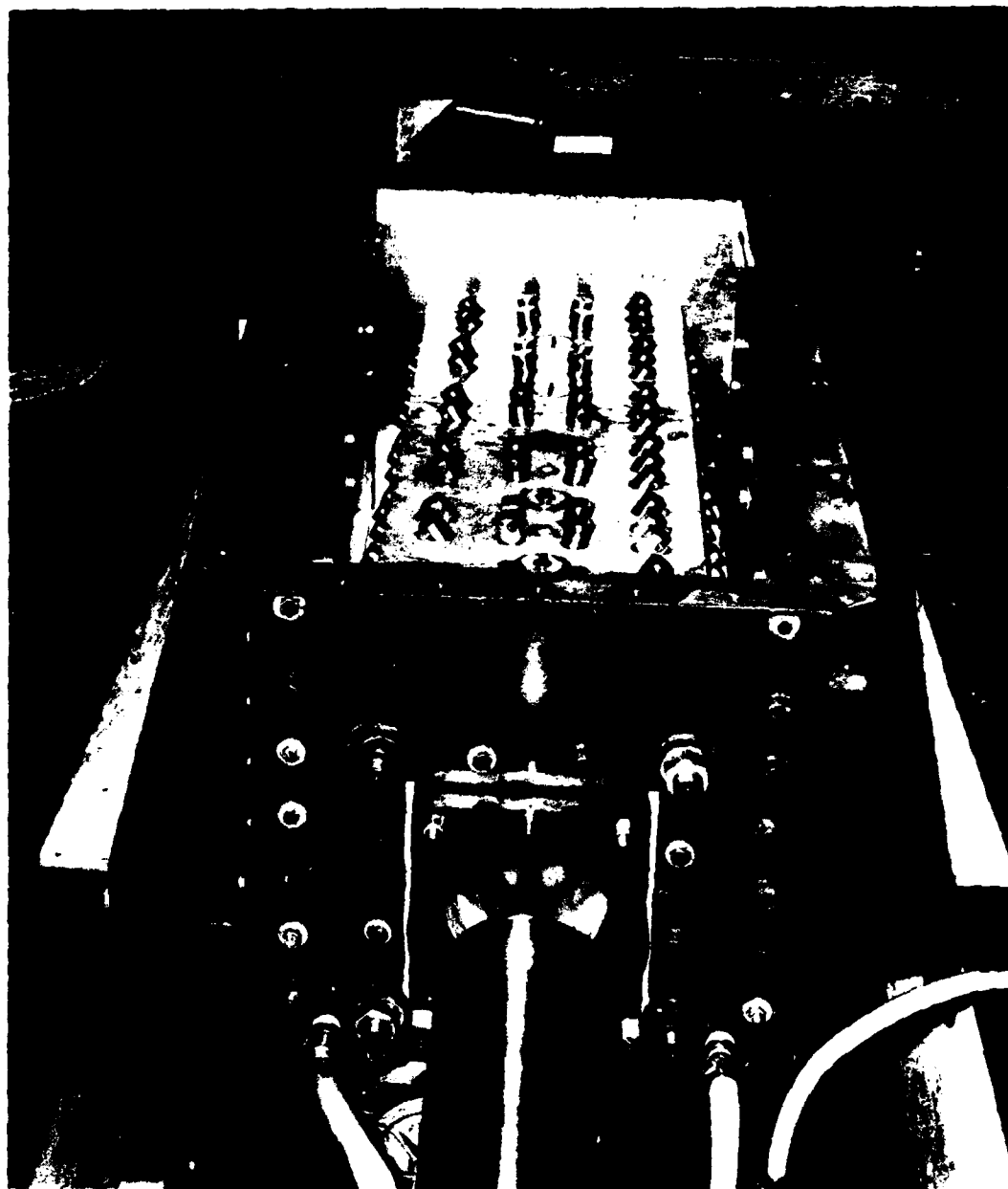


Figure 25. Hydraulic Decelerator with Top of Water Enclosure Removed.



Figure 26. Test Fixture Mounted on the Impact Carriage for the X Axis Tests.

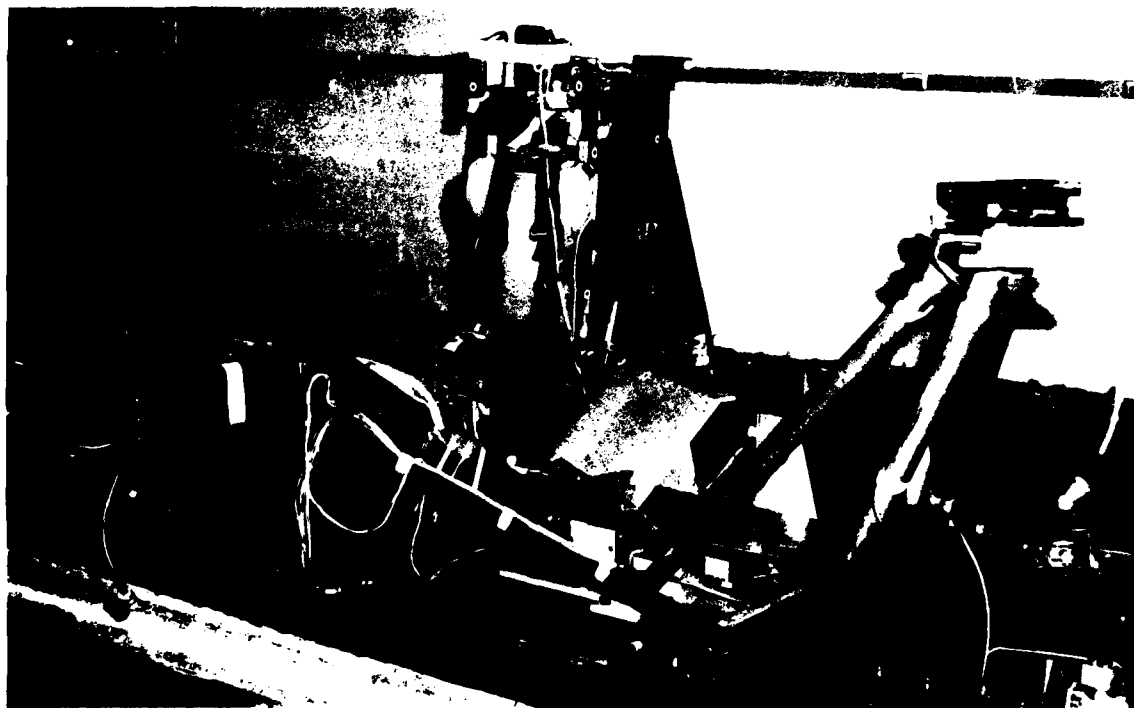


Figure 27. Test Fixture Mounted on the Impact Carriage for the Y Axis Tests.

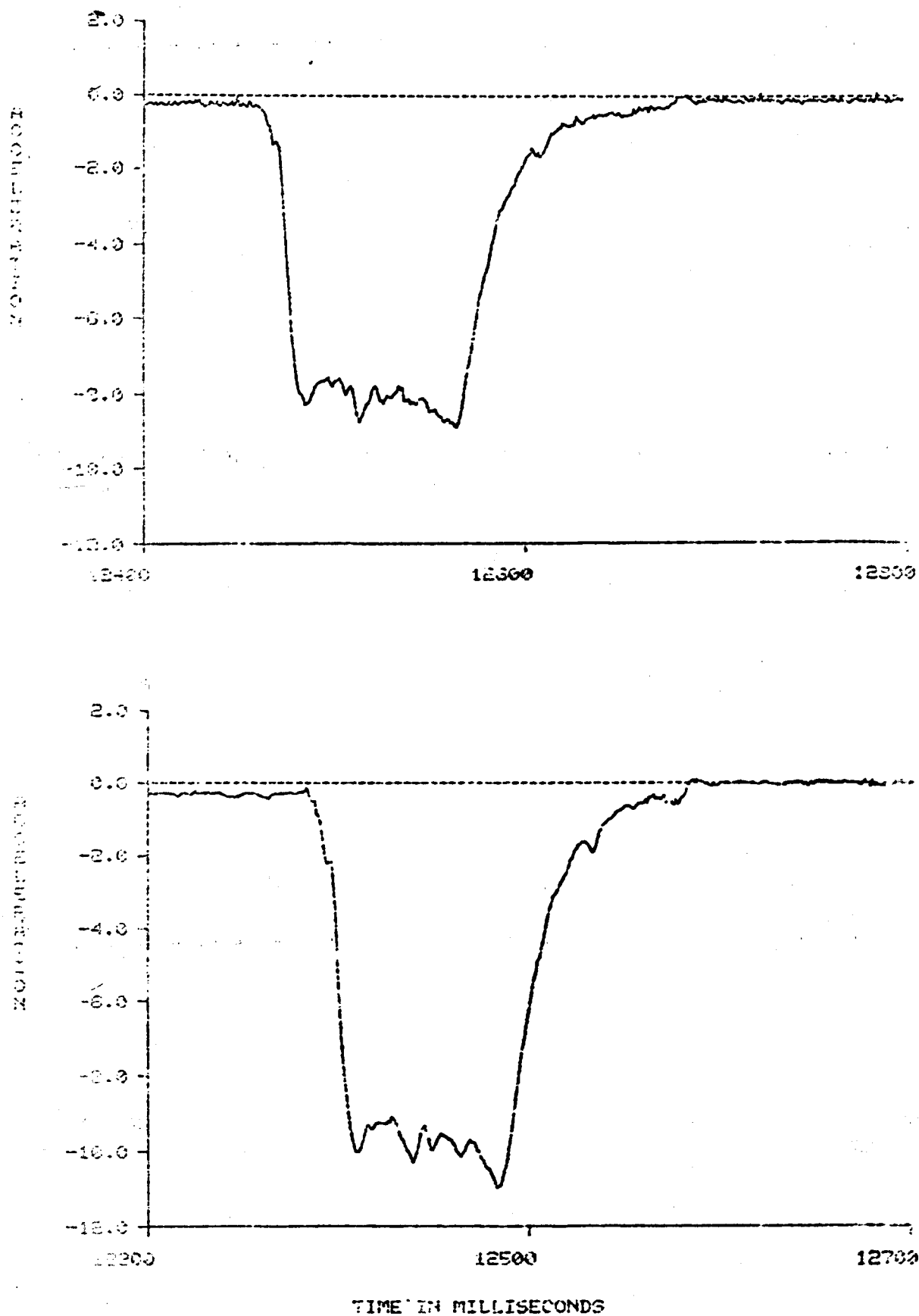


Figure 28. Impact Profiles Used During the X Axis Test Series.

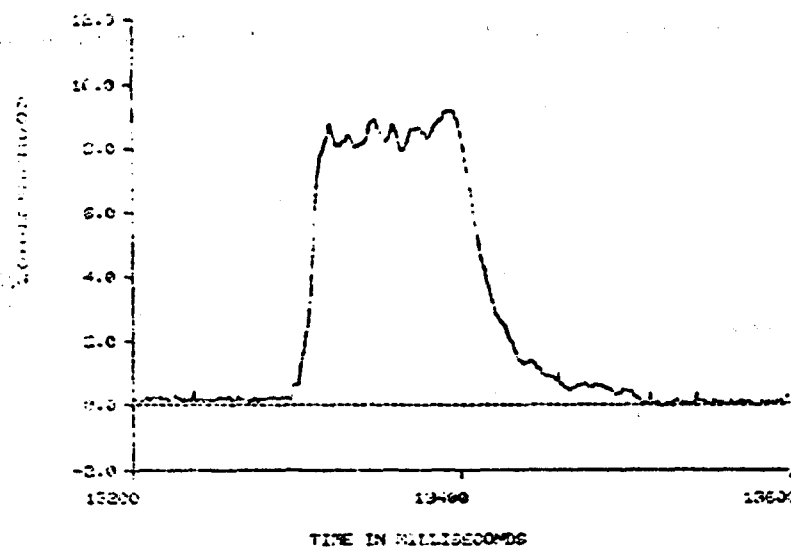
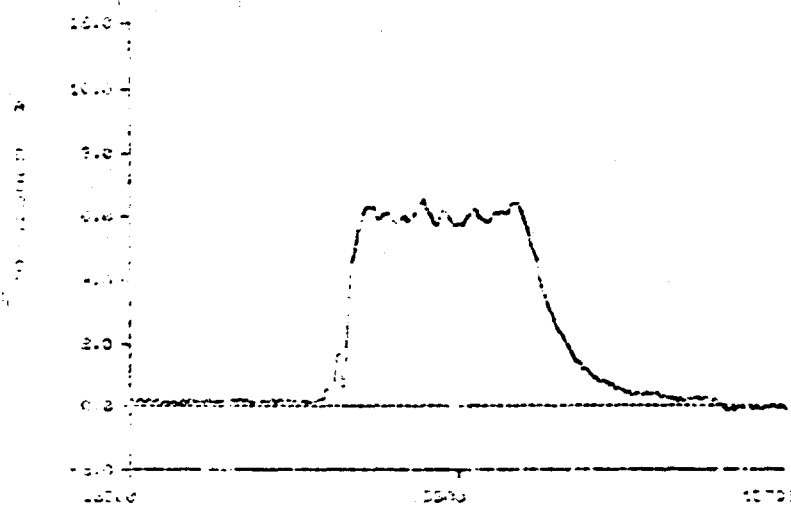
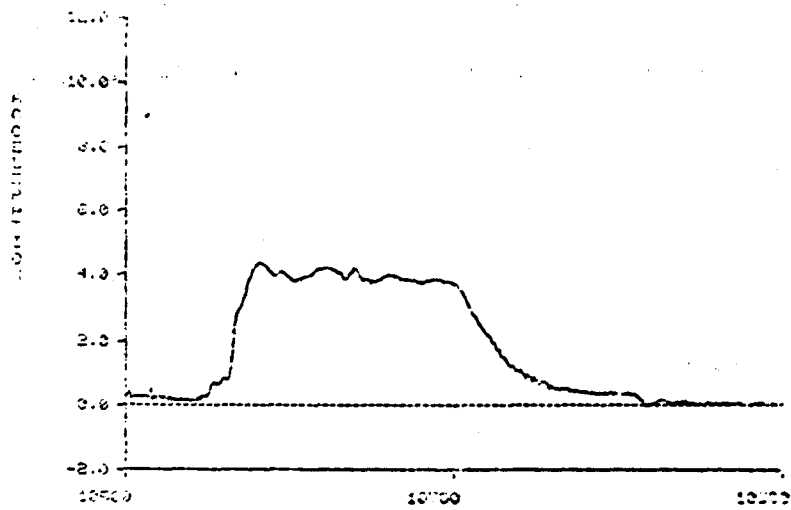


Figure 29. Impact Profiles Used During the Y Axis Test Series.

Best Available Copy



calculates the velocity error as the difference between the instantaneous actual velocity and instantaneous model velocity. Then the computer outputs a five volt signal to the brake hardware for a time proportional to the velocity error. The signal excites the solenoids of two control valves, which apply nitrogen gas at 280 psi to activate the two brake units on the sled.

The predictability of sled impact velocities was improved with this control system. More than nineteen sled tests at each test level (4, 6, 8, and 10 G) were conducted, with and without the operation of the velocity control system, to demonstrate the reliability of the system. For sled tests without the control brake system, the velocity of impact had a standard deviation of 3.51 ft/sec at a desired 4 G level of sled impact. With the control brake system, the standard deviation of the impact velocity for a 4 G impact sled test was reduced to 0.75 ft/sec, improving the predictability of sled impact velocity by a factor of 4.7 for a 4 G impact test.

#### D. ELECTRONIC INSTRUMENTATION

Electronic data collected during the three test phases included sled acceleration and velocity, test fixture loads and acceleration, subject head and chest acceleration, harness loads and electrocardiograms. Detailed descriptions of the instrumentation, electronic data processing equipment, mounting procedures, and calibration techniques are provided within Appendix A. The following information summarizes the electronic instrumentation that was used to acquire the test data.

Sled acceleration was measured using three miniature, piezoresistive accelerometers mounted to the structure of the VDT carriage and the HD sled. Vertical velocity of the carriage was determined at the point of impact. The velocity of the HD sled was computed from displacement data collected throughout the launch, coast, and impact phases of the X and Y axes tests.

The test fixture was instrumented to measure the acceleration transmitted to the subject and the inertial forces reacted into the seat, restraint, and footrest by the subject. Triaxial acceleration was measured on the seat pan structure to quantify the acceleration input. The seat pan structure included three load cells and three load links to measure the vertical and horizontal forces reacted through the structure. Inertial forces were measured in the restraint system by using strain gages bonded to the seat attachment hardware or Lebow belt load cells. Leg bracing forces were measured by three triaxial load cells that were incorporated within the rudder pedal support structure.

Triaxial accelerometer arrays were used to measure acceleration on the head and chest of each subject. The chest accelerometer package was held tightly against the subject's sternum by a Velcro chest strap. The subject's head accelerometers were mounted on a dental bite block, which was held in the subject's mouth during the test. A few veteran panel members used permanent metal bite plates which had been fabricated at the Dental Clinic. For most subjects, however, a temporary, disposable bite block made of Optosil was fabricated prior to each test. This technique has proven to be not only a safe means of providing intraoral/dental protection during impact, but also an effective way of eliminating movement of the accelerometer package relative to the subject's head during impact. Comparisons between data obtained with the metal bite plate and

the Optosil bite block have shown no difference in the quality of the measurements.

#### E. MEDICAL INSTRUMENTATION

The medical instrumentation for each impact exposure in this program was standardized as follows. Three stick-on EKG electrodes were placed on the subject, one on the upper posterior aspect of each arm and a third on the right lateral chest, sixth intercostal space, mid-axillary line. The snap-on lead from each of these electrodes was plugged into a telemetry transmitter, which in turn was strapped to the left upper extremity of the subject. Continuous remote transmission of a single lead EKG to a portable EKG machine located at trackside was assured prior to each impact. Sitting and standing EKG's were obtained immediately pre-impact and post-impact and a continuous tracing was obtained during test countdown and impact. If the medical monitor observed a significant relative decrease in pretest heart rate, indicative of vasovagal pre-syncope, or a pretest arrhythmia, he was able to abort the impact. Coincident with EKG recording, pretest and post-test sitting and standing blood pressure determinations were made for each subject by the medical technician using a sphygmomanometer. These pressures were recorded on the appropriate EKG tracing.

#### F. DATA ACQUISITION AND RECORDING

Both data acquisition/processing and control requirements were satisfied by utilizing the Automatic Data Acquisition System (ADACS), which has the capability of sampling 48 data channels at a rate of 1000 samples/second/channel. For the F-111 test program, analog signal data were taken from 38 data channels. The on-board portion of the ADACS amplifies, filters, and encodes the analog data samples from all 48 channels into a digital format (pulse code modulated) which is then transmitted via an umbilical cable to a word formatter. The word formatter reformats the serial data into parallel data which are then routed to the PDP-11/34 computer for storage, analysis, and control. For details on this system, see Appendix A.

#### G. PHOTOMETRIC INSTRUMENTATION

The movements of the subject's helmet, head, and other specific body segments were recorded by photographing the motion of fiducial markers attached to these sites. High speed, 16 mm Milliken cameras, Teledyne model number DBM 45, were used in all test phases. These cameras were operated at a speed of 500 frames per second with a shutter opening of 140°. Two cameras were mounted on the impact sled or carriage and the third camera was mounted on a fixed structure within the laboratory area.

During the vertical impact test phase, one camera was mounted to the side of the test fixture so that the camera axis was perpendicular to the midsagittal plane of the test subject. A second on-board camera was mounted on the footrest structure to provide a front view of the subject. The third camera was mounted to a structural beam of the building and provided a frontal - left oblique view of the impact carriage throughout the deceleration stroke.

The Y axis impact tests were accomplished with one on-board camera mounted to the footrest structure and a second camera mounted to provide a frontal - left oblique view of the subject as shown in Figure 27. The third camera was mounted

to the top of the hydraulic decelerator enclosure to view the left side of the subject. This camera was also used during the forward facing tests to provide a frontal view of the subject.

The on-board camera mounts that were used in the X axis tests are shown in Figure 26. One on-board camera documented the subject's motion in the mid-sagittal plane and the second camera was located to provide a frontal - left oblique view.

Timing reference marks were recorded on the 16 mm film once every 0.01 second. These reference marks were synchronized with the electronic instrumentation recordings.

The fiducial markers that were attached to the subjects and the test fixture consisted of a one-half inch diameter black spot printed on a one inch diameter white target. The locations of the markers were different in each test phase, but generally followed the guidelines provided in the Federal Motor Vehicle Safety Standard No. 208 (U.S. Department of Transportation, 1972). More complete descriptions of the fiducial marker locations as well as the photometric instrumentation system are provided in Appendices A and B.

A video camera was also used to document the tests. This camera and the recorder used with it are capable of recording motion at a rate of 120 frames per second with an effective shutter speed of 10 microseconds or less. Use of this system allowed the investigators to evaluate the kinematic response of each subject immediately after each test. This system is described in Appendix A.

Photographs of the test subject and equipment configuration were taken prior to each test. Items of special interest were photographed as required.

#### H. ANTHROPOMORPHIC DUMMY

The test dummy used for this program was an Alderson Research Laboratories, Inc., model VIP-95, serial number 124. This dummy is designed to represent a 95th percentile adult male. The dummy was originally built for  $-G_x$  automotive crash testing, and was based on specifications furnished to Alderson by the National Highway Traffic Safety Administration. The dummy is not designed to produce meaningful response dynamics in vertical or lateral impact. In forward facing ( $-G_x$ ) impact, the dummy is designed to reproduce head-neck response of cadavers. Head-neck dynamic response of the dummy was not relied upon in any direction. Instead, the dummy was used to determine structural integrity of the test apparatus and for comparison with previous dummy results to establish equivalency for predictions of human safety.

Prior to testing, the dummy's joints were adjusted to a nominal one G value in accordance with the Federal Motor Vehicle Safety Standard No. 208 (U.S. Department of Transportation, 1972).

On one occasion during lateral testing, the head and neck assembly separated from the shoulder area. This was attributed (by the manufacturer) to the fact that the dummy was not designed for lateral impact testing. Modifications were made to strengthen the head and neck area on the basis of discussion with

Alderson Research Laboratories. The modifications consisted of installing two additional bolts in the lateral plane of the neck attachment to the shoulders.

TABLE 7. DUMMY MEASUREMENTS

Weight	208 lb.
Sitting Height	38.5 in.
Hip Breadth, Sitting	16.1 in.
Hip Circumference, Sitting	46.5 in.
Waist Circumference, Sitting	42.0 in.
Chest Depth	10.6 in.
Chest Circumference	43.5 in.

An additional problem was encountered during the lateral impact tests. The impact displaced the left leg laterally enough to cause a tear in the dummy's "skin" at the leg/torso junction. This problem was resolved by placing a strap around both legs, causing both legs to move together.

#### I. ENGINEERING SAFETY

The reliability and safety of the test equipment and facilities were evaluated analytically and experimentally prior to the initiation of the tests with volunteer subjects. General Dynamics performed stress analyses of the test fixtures used for the vertical and horizontal impact tests. Acceptable margins of safety were demonstrated for all load bearing elements by means of static load tests (Shaffer, 1979). The test fixtures were then dynamically tested on the AFAMRL Vertical Deceleration Tower and the Horizontal Decelerator Facility at 150 percent of the impact levels for volunteer subjects in each of the planned test configurations.

An independent safety review was accomplished by a committee chaired by the AFAMRL Safety Officer. The Engineering Safety Review Committee surveyed each of the test facilities to determine their operational procedures, maintenance, potential failure modes, failure risks, operational history, and demonstrated reliability in accordance with the Aerospace Medical Research Laboratory Regulation 127-1 (1976). Final approval for the commencement of tests was granted by HQ USAF/SG, in accordance with Air Force Regulation 169-3 (1979), after review of the findings of the Engineering Safety Review Committee and recommendations of the AFAMRL Human Use Review Committee.

## Section 5

### DATA ANALYSIS

#### A. ELECTRONIC DATA REDUCTION AND ANALYSIS

Data from each test was reduced in a standardized format associated with each impact direction. Examples of reduced electronic data may be reviewed in Appendices C thru E. Computed summaries provide relevant maxima and minima from a total of 38 recorded signals. Relevant sums, vector resultants, severity indices, and times were also computed. Shoulder strap sums are the maximum value of the sum of the two inertia reel straps and the two reflection strap measurements. The sums of the measured forces are also the maximum values of continuously summed measurements. Scaled plots of selected signals and computed resultants were produced. Time integrals of sled acceleration signals were compared with signals from velocity transducers. Inspection of the sample products in the appendices will serve to demonstrate the approach.

In order to investigate the effects of varying the seat adjustments through the wide range available in the F/FB-111, sufficient tests were performed to allow parametric analysis, particularly in the  $-G_x$  and  $G_z$  phases of the test program. Selected channels were analyzed by means of the Wilcoxon paired-replicate rank test to determine statistical significance (Wilcoxon *et al.*, 1964). This statistical test utilizes pairs of impact tests in which the same subject is subjected to the same impact in two different seat positions. As a control, test parameters such as sled acceleration were similarly analyzed to assure that the comparisons were not biased.

#### B. PHOTOMETRIC DATA PROCESSING AND ANALYSIS

The test subject's kinematic motion was derived by an analysis of the 16 mm high-speed films. The reduction method used for the Vertical Deceleration Tower tests required the films of the side on-board camera only. The subject's fiducials on these films were electronically tracked with a PDS Model 200 Photo Digitizing System (PDS), which includes an Automatic Film Reader (AFR), an electronic scanning camera, and a DGC NOVA 3/12 computer.

The AFR is manually initialized by designating the targets of interest with a cursor in the first frame of data. Targets on subsequent frames are automatically scanned, acquired, and identified, and their X and Y coordinates are recorded. If a target was obscured, or otherwise lost during the reduction of data from the vertical impact tests, its position was manually tracked or estimated. During reduction of the  $-G_x$  and  $+G_y$  test data, the obscured targets were assigned zero values, leaving gaps in the data. The gaps were later closed by linear interpolation using a computer program referred to as SLED. Up to twelve targets within one film frame could be automatically scanned at a rate of  $\frac{1}{4}$  frame per second. The AFR also extracted digital timing information from the timing marks on the films.

The frame-by-frame digitized position coordinates of the fiducials were processed by the NOVA computer and stored on magnetic tape. This digital data, along with the data from the Photo Anthropometric Sheets, was used by a computer program that computed and plotted the actual displacements, velocities, and accelerations of the fiducials of interest.

The photometric data analysis procedure for the horizontal impact test films provided the data from both on-board cameras to a second computer program. The computer program interpolated the best-fit position of the fiducials viewed simultaneously by the two cameras.

Not all of the tests were selected for processing, because of the schedule limitations of the evaluation program. Films of small, medium and large-sized subjects were chosen from each element of the corresponding test matrix. This allowed comparison of subjects grouped by size.

Existing photo analysis software was modified to suit the F-111 test conditions. (See Appendix B for a full description of changes.) A computer program, TOWER, was written and used to analyze the data from the vertical ( $+G_z$ ) tests. Motion of the fiducials was assumed to be planar, as observed by the side camera. Program SLED was written and used to analyze the film data from the horizontal ( $+G_y$ ,  $-G_x$ ) tests. It was designed to take time synchronized digital data from two camera views and solve for the most likely points of intercept for up to six pairs of rays in a three dimensional rectilinear coordinate system. This program required the output of another computer program, POOCH, which derived the precise location and orientation of the cameras by optimizing the surveyed coordinates of the cameras relative to up to ten reference points.

Camera vibrations and film reading errors led to noise in fiducial position coordinates. To minimize these effects, the digital position data was converted from the time domain to the frequency domain by Fast Fourier Transforms (FFTs). Then, assuming that the human responses would be represented by lower frequencies, the FFT terms were truncated to eliminate frequencies above 30 Hertz. Frequency spectra were plotted to demonstrate this smoothing.

Photometric analysis provided plots of displacement, velocity, and acceleration versus time for each fiducial. Errors in precisely quantifying fiducial displacements were due to (1) inaccuracies in measuring initial target displacements relative to the test fixture, (2) camera vibration, and (3) film reading errors.

Section 6  
HUMAN SUBJECTS

A. QUALIFICATIONS

All subjects who participated in impact experiments during the evaluation of the proposed modified F/FB-111 crewseat and restraint system were members of the AFAMRL Impact Acceleration Stress Panel, which is composed of volunteer active duty Air Force members whose primary duties do not involve participation as subjects. A total of 23 subjects were utilized during this program. There were no special technical qualifications or training requirements for subjects, but all subjects were qualified to participate only after successfully completing an intensive medical screening evaluation. This evaluation was directed by the panel physician and consisted of medical history screening, physical examination, visual acuity, audiometry, blood pressure, routine laboratory examinations (blood work and urinalysis), standard 12-lead EKG, pulmonary function tests, electroencephalogram, treadmill exercise stress test, and x-rays, including chest, skull, and complete spine films. The x-rays were reviewed by the panel physician in consultation with a radiologist (and orthopedic surgeon, as necessary) to assure elimination of individuals with disqualifying radiographic findings. Female subjects had a negative pregnancy test documented and underwent a pelvic exam by a gynecologist, to assure there were no gynecologic contraindications to their participation. Relevant abnormalities in any part of the medical evaluation led to elimination or specialty consultation and further examinations as required. Annual re-qualification of panel members was accomplished with a limited medical evaluation, including a physical examination and other relevant medical tests.

Informed consent was provided by all subjects on an ongoing basis during the test program. Prior to each phase of testing, subjects received a thorough briefing on the experimental procedures and potential medical risks pertinent to that particular test axis. The subjects signed a witnessed consent form attesting to the fact that a detailed briefing was received and summarizing its content. The medical investigator continued to stress that any subject was free to withdraw at any time for any reason.

B. SUBJECT TEST PROCEDURES

Prior to every impact exposure, each subject underwent a brief medical history and physical examination. Particular attention was directed toward detecting any new neck or back symptoms, new medications, abnormalities of recent sleep patterns, or recent overindulgence in food or alcoholic beverages. No subject was exposed if symptoms were present which may have obscured detection of test-related injury or which may have indicated predisposition to such injury.

All subjects wore orange cut-off underwear designed to allow mounting of camera targets and instrumentation. Male subjects wore athletic supporters and some wore protective cups during  $-G_x$  exposures. Female subjects wore two-piece bathing suit tops and appropriate undergarments. All subjects were instructed to void prior to entering the test area.

Other pretest procedures included placing stick-on EKG electrodes and camera targets on subjects, obtaining standing and sitting blood pressures, and assuring adequate remote recording of an EKG (single lead) telemetry package. Subjects wore USAF HGU-26P flight helmets for  $G_z$  and  $G_y$  tests. The flight helmet was not worn during the  $-G_x$  tests since it was previously established that the additional mass of the helmet might provoke neck strain at the impact test level.

The subject was provided with a finger-operated microswitch which was connected to the impact facility such that the facility would not operate unless the switch was depressed. Similar switch controls were provided to the physician monitor, the safety monitor, and the water brake technician during  $G_y$  and  $-G_x$  testing. Agreement of all these individuals was necessary for the test to proceed.

The subjects were instructed to brace for the impact by pressing their helmets against the headrest, hands against anterior thighs at or near the knees, and feet against the footrest. This body position is shown in Figure 19.

During testing, an ambulance and crew were alerted and standing by within one-half mile of the test facility. In addition, emergency medical equipment was arranged in the test area for use by the physician monitor in the event of an emergency. This equipment included a defibrillator, oxygen equipment, intubation equipment, IV solutions and equipment, appropriate emergency drugs, backboard, harness cutters and bandages.

A physician monitor, who was responsible for assuring subject safety during testing, was present for each test and reserved the right to cancel any test at any time for any reason. Such reasons may have included a recent history of neck or back strain, pretest pre-syncope, pretest arrhythmia, poor bracing posture just prior to impact or any other condition of the subject, equipment, or procedure which was deemed by the monitor to place the subject at undue risk.

Following the impact exposure, the physician monitor assured that the subject was uninjured. Post-test blood pressures and EKG (single lead) were obtained and a brief post-test physical examination was accomplished. The subject was then provided with contacts to obtain later medical care as required or to ask questions relating to his participation. Impact exposures for each subject occurred no more frequently than once in any five-day period.

#### C. HUMAN USE PROTOCOL

The "Protocol for the Demonstration and Evaluation of the Modified F/FB-111 Crewmember Restraint System" described the details of human subject participation in this research effort, as outlined in the above paragraphs. After a thorough review of all biodynamic human impact test data, including data obtained in tests of the operational F/FB-111 restraint system at Holloman AFB, a medical risk analysis of the proposed impact tests was prepared and was presented in this protocol. Potential adverse effects were categorized as either anticipated, clinically inconsequential effects or very low probability effects of some clinical consequence. The overall risk to



human subjects was judged to be acceptable when compared to the potential benefit of minimizing F/FB-111 crewmember morbidity and mortality. Finally, the protocol indicated that all human tests would be conducted within human tolerance levels, below the operational envelope and only after an analysis of dummy test data. Furthermore, testing would begin at a benign (orientation) G level and would then proceed to the test G level.

The protocol, AFAMRL Protocol #79-06, was presented for review and approval to the AFAMRL Human Use Review Committee (HURC) on 9 April 1979. This committee is composed of physicians, safety engineers, a legal consultant, a chaplain, and civilian research scientists. It reviews all protocols at AFAMRL in which human experimentation is proposed. The HURC approved this protocol and the AFAMRL Commander concurred with this approval on 10 April 1979. The protocol was then forwarded to the Office of the Air Force Surgeon General where, as SGO File #R79-2, it was reviewed and approved on 9 May 1979.

Vertical ( $G_z$ ) dummy test data were presented to the HURC on 19 June 1979 and committee approval to initiate  $G_z$  testing was obtained. On 7 August 1979, lateral ( $G_y$ ) dummy test data were presented to the HURC and approval to initiate  $G_y$  testing was obtained. On 25 September 1979, a subject sustained a ligamentous knee injury during an 8 G lateral impact and lateral testing was suspended. A report of the investigation of this injury was presented to the HURC on 11 October 1979, at which time approval to initiate  $-G_x$  testing was obtained after presenting fore-aft ( $-G_x$ ) dummy test data. Finally, when suggested modifications to the test fixture resulted in continued questions regarding knee injury potential in  $G_y$ , the investigators' decision to cancel any further lateral testing was announced to the HURC on 27 November 1979.

#### D. SUBJECT ANTHROPOMETRY

Table 8 is a summary of the most pertinent anthropometric dimensions of each test subject. These dimensions were used to match the subject groups used in the experimental design. The mean and standard deviation computed from each set of dimensions compare favorably with the mean and standard deviation of the dimensions obtained from an anthropometric survey of USAF personnel conducted in 1967. Forty-nine anthropometric measurements were obtained from all but five subjects. The mean and range of eighteen of the test measurements are listed in Table 9.

TABLE 8. SUBJECT ANTHROPOMETRY SUMMARY I

SUBJECT NUMBER	WEIGHT (lb)	STATURE (in)	SITTING HEIGHT (in)	MID-SHOULDER SITTING HEIGHT (in)
D1	203	74.0	40.0	28.0
E1	186	73.0	38.3	26.8
F2	159	67.0	37.4	26.2
F3	167	69.0	36.4	26.0
G2	117	63.0	33.3	23.1
H2	175	70.7	37.0	25.9
J1	157	70.3	37.4	25.4
J2	203	73.0	38.7	27.0
M2	162	66.1	35.1	24.0
M5	171	73.0	39.0	27.2
M6	163	68.0	37.0	26.0
M7	133	66.0	34.4	24.0
M8	185	72.0	37.1	25.5
M9	167	71.0	39.0	27.0
M10	140	66.0	36.1	25.0
O1	174	73.0	39.2	27.0
P2	163	71.1	38.0	27.0
R1	201	71.0	38.4	26.2
S3	167	70.0	37.0	26.0
S4	159	68.0	37.0	25.0
S5	165	70.0	34.4	24.6
W1	155	73.4	37.8	25.3
MEAN	167	69.9	37.2	25.8
STANDARD DEV.	21.1	2.97	1.71	1.21

TABLE 9. SUBJECT ANTHROPOMETRY SUMMARY II

	N	Mean	Standard Deviation	Range
Weight	18	163	21.1	117 - 203
Stature	18	69.5	3.19	62.8 - 73.6
Cervicale Height	18	59.5	2.87	54.4 - 63.1
Trochanteric Height	18	35.9	2.00	32.3 - 38.6
Tibiale Height	18	17.7	0.97	15.8 - 19.5
Chest Circumference	18	36.0	1.84	35.3 - 42.4
Waist Circumference	18	33.3	2.45	29.6 - 39.0
Buttock Circumference	18	38.1	2.20	35.0 - 42.9
Acromion-Radiale Length	18	12.9	0.66	11.7 - 13.7
Radiale-Stylian Length	18	10.4	0.69	8.5 - 11.3
Sitting Height	18	37.2	1.68	33.3 - 39.7
Mid-Shoulder Height	18	25.7	1.28	23.1 - 28.0
Buttock-Knee Length	18	23.8	1.03	21.9 - 25.4
Knee Height, Sitting	18	21.5	1.29	18.7 - 23.5
Head Length	18	7.8	0.23	7.4 - 8.1
Head Breadth	17	6.1	0.49	5.6 - 6.5
Head Circumference	18	22.4	0.61	21.5 - 23.6
Hip Breadth, Sitting	18	14.4	0.83	12.4 - 15.7

## Section 7

### CONDUCT OF TESTS

#### A. TEST SEQUENCE

The test parameters for each test were provided to the test personnel at the beginning of each day of testing. The first test of each day was done with an anthropomorphic dummy using the equipment configuration and test level planned for the first human test of the day. If no abnormalities were detected, the test personnel proceeded with preparations for the tests with volunteer subjects.

High speed motion picture cameras were loaded and mounted on the test fixture. The seat pan, headrest, and footrest were adjusted to the appropriate configuration based upon the test plan and the anthropometry of the individual test subject. The accelerometer packages were then oriented in their respective reference planes and reference values were sampled using the data acquisition system.

During the preparation of the test fixture and instrumentation, the subject received a pretest medical examination and the accelerometer mouthpiece was individually fitted. The chest accelerometers were strapped to the subject prior to seating the subject. After the subject was seated, the restraint harness was fitted using the procedure described in the F/FB-111 Technical Order. The positions of the photographic fiducials and the restraint angles were then measured.

The lap belts were tightened to  $20 \pm 5$  lb and the shoulder straps were preloaded to yield a force of  $14 \pm 5$  lb in the inertia reel straps.

The final pretest sequence consisted of the acquisition of photographs of the test subject and equipment configuration, measurement of blood pressure, evaluation of the electrocardiograph recording, and final safety checks of the facility.

After completion of each test, the subject's blood pressure was obtained, the subject was released from the restraint harness, and specific test measurements were reviewed.

#### B. VERTICAL IMPACT TESTS

Prior to the commencement of tests with volunteer subjects, a series of tests were performed with an anthropomorphic dummy. Two tests on the 14th and 15th of June 1979 established the drop height and other parameters of the 10 G test level. A 15 G structural proof test was completed on 18 June 1979. One dummy test in each of the five seat configurations was accomplished on the 18th and 19th of June 1979. These tests verified the dynamic ranges of the measurements and provided preliminary data for the AFAMRL/HURC evaluation. Throughout the  $G_z$  phase, 23 additional dummy tests were completed to provide an additional degree of safety in the facility operation. One additional dummy test (Test No. 256) was accomplished on 18 July 1979 to establish tare loads.

The two groups of volunteer subjects were tested in three seat configurations as originally planned. The total number of subjects tested in each cell of the experimental matrix is shown in Table 10. The first +G<sub>z</sub> test with a volunteer subject was accomplished on 21 June 1979, and the final +G<sub>z</sub> test was completed on 27 July 1979.

TABLE 10. GROUP AND NUMBER OF SUBJECTS FOR EACH SEAT POSITION AND SHOULDER STRAP CONFIGURATION IN THE VERTICAL IMPACT TEST PHASE

	0°	Max*
90°	I - 10	I - 9
103°	I - 10	
110°	II - 10	
	II - 9	I - 6

\*Maximum positive angle in full down seat position.

#### C. SIDEWARD (G<sub>y</sub>) IMPACT TESTS

Sideward impact tests with a dummy subject were initiated on 23 July 1979 and were successfully completed on 2 August 1979 after a series of 16 tests. These tests established facility operating characteristics.

The first fully instrumented dummy tests were started on 2 August 1979 to furnish data for the HURC review. These consisted of at least one test in each of the required seat configurations and at each of the impact test levels.

A 12 G proof test was completed on 6 August 1979 and the tare load test for the lateral configuration was accomplished on 27 November 1979. A series of dummy tests, conducted during the period from 9 to 16 August 1979, consisted of 39 tests to prove the reliability of the sled velocity control system. Change of a proximity sensor, used to activate the trim brake program, generated a requirement for an additional 6 reliability tests on 29 August 1979.

As mentioned previously, one dummy test was conducted each test day prior to using human subjects to verify system operation. In addition, one test was completed on 27 November 1979, after simulated side and between-the-legs consoles had been installed on the test fixture. A total of 76 dummy tests were accomplished during the sideward impact phase of the program.

Tests with human subjects started on 17 August 1979. The 6 G level was reached on 30 August 1979 and the 8 G tests started on 5 September 1979. The sideward impact phase was discontinued on 25 September 1979 following a subject knee injury. The numbers of human tests in each cell of the experimental matrix are given in Table 11.

An error was made in setting the preload of the left shoulder strap during the sideward tests. The electronic system that was used to sample the preload was incorrectly programmed and, therefore, the preload values of the strap were twice as high as intended. The error did not affect the accuracy of the loads measured during the impact tests. Furthermore, tests conducted with dummy subjects have determined that differences in the preload values did not influence the peak loads measured during impact.

TABLE 11. NUMBER OF SUBJECTS FOR EACH SEAT POSITION AND SHOULDER STRAP CONFIGURATION IN THE SIDEWARD IMPACT TEST PHASE

	0°	Max*
90°	5	0
103°	7	8

\*Maximum positive angle in full down seat position.

#### D. FORWARD FACING IMPACT TESTS

Since the impact profiles had been established during the sideward impact test phase, no additional profile tests were required prior to the start of the forward facing test phase. A 15 G structural proof test was completed on 2 October 1979 and a tare load test was completed on 18 October 1979.

An initial dummy test series was accomplished on 2 October 1979. This series consisted of at least one test in each required seat configuration and at each impact level. These data were used during the HURC review. Again, one dummy test was conducted each test day prior to using human subjects to verify system operation. Twenty-two dummy tests were completed during the forward facing impact test phase.

Forward facing impact tests with volunteers started on 11 October 1979 and were completed on 13 November 1979. The numbers of human tests completed in each cell of the experimental matrix are given in Table 12.

TABLE 12. NUMBER OF SUBJECTS FOR EACH SEAT POSITION AND SHOULDER STRAP CONFIGURATION IN THE FORWARD FACING IMPACT TEST PHASE

	0°	Max*
90°	10	0
103°	15	11
110°	0	2

\*Maximum positive angle in full down seat position.

During forward facing tests prior to Test No. 584, the right and left lap belt and left shoulder strap preloads were erroneously set at twice the intended preload values. This error did not affect the accuracy of the loads measured during the impact tests.

## Section 8

### ANALYSIS AND RESULTS

#### A. VERTICAL IMPACT TESTS

The results of the  $+G_z$  tests are summarized in Table 13. Measurements from each test in this series as well as typical analog data sets from each cell of the experimental design matrix are presented in Appendix C. All accelerations and loadings were considered to be well within human tolerance. Several significant correlations were observed which will be discussed in the following paragraphs. Some observed variations, though statistically significant at the chosen 90% confidence level, may not be of a magnitude to cause concern at the levels tested. However, they demonstrate trends which may have potential significance in higher level operational impacts. They certainly indicate that restraint system performance varies with the chosen seat adjustment and with crewmember size.

The peak resultant acceleration measured on the chest decreases significantly with seat back angle variation from  $90^\circ$  (vertical) to  $103^\circ$  (back  $13^\circ$ ). The change in the peak resultant chest acceleration is statistically significant while the change in chest Severity Index (SI) is not. A further decrease might be expected as the angle is moved to  $110^\circ$ , but this decrease is not consistent and is not statistically significant in the current sample. These findings are consistent with the interpretation that a damping of the anterior chest acceleration takes place as the subject's upper torso is supported more by the seat back and less by axial loading of the spine into the seat pan.

The X axis acceleration of the head increases significantly with seat back angle variation from  $103^\circ$  to  $90^\circ$ . The increase is also significant from  $110^\circ$  to  $103^\circ$ . In addition, the Z axis acceleration of the head increases from  $110^\circ$  to  $103^\circ$ . These findings are consistent with the interpretation that the head receives more support in the  $+G_z$  direction as the seat is reclined. The findings also highlight a potential area of concern, since the location of the headrest well forward of the seat back plane appears to cause increased forward and down rotation of the head in  $+G_z$  impact. Examination of the data indicates that the forward pitching of the head and neck occurs later than the initial  $+G_z$  response.

Lap belt loads decrease significantly as the seat back angle is varied from  $90^\circ$  to  $103^\circ$ . However, they increase again from  $103^\circ$  to  $110^\circ$ . These findings are consistent with the interpretation that the forward reaction of the upper torso seen in the belt at  $90^\circ$  is decreased at  $103^\circ$ , but that further reclining to  $110^\circ$  may produce a forward submarining tendency of the subject's pelvis, with the  $110^\circ$  seat back acting as an inclined plane. This interpretation, however, is not borne out by the seat X load link data.

The vertical component of the loads measured in the seat pan decrease significantly as the seat back angle is varied from  $90^\circ$  to  $103^\circ$ , and decrease further from  $103^\circ$  to  $110^\circ$ . These findings are consistent with the interpretation that more upper torso load is reacted into the reclined seat back. The implication is that axial loading of the lower spine is decreased in vertical impact with a reclined seat. This implication is not unexpected.



**Table 13 Summary of Electronically Measured and Computed Data  
from the Vertical Impact Tests**

	GROUP I			GROUP II		
	0	90	103	0	103	110
Shoulder Harness Angle	Mean	s	Mean	s	Mean	s
Seatback Angle	10.4	0.19	10.5	0.26	10.6	0.28
Sled Z (G)	10.5	0.09	10.7	0.28	-24.9	1.15
Sled Velocity (ft/sec)	17.8	2.2	16.3	1.9	11.0	0.68
Seat Z (G)	32.1	4.2	30.4	6.3	17.2	2.1
Chest Resultant	4.97	1.3	3.89	1.7	31.8	5.9
Chest SI					4.19	0.6
Head X (G)	12.8	1.7	12.6	1.3	13.6	0.8
Head Y (G)	13.2	1.6	12.9	1.3	13.7	0.9
Head Z (G)	23.2	3.5	22.0	2.5	24.0	1.7
Head Resultant (G)	189	35	185	26	175	36
Head SI	1.12	0.18	1.11	0.26	1.07	0.20
Shoulder Sum (1b)	168	45	150	39	145	41
Shoulder Sum/wt	1.00	0.29	0.89	0.25	0.89	0.21
Lap Belt Sum (1b)	230	49	258	34	245	53
Lap Belt Sum/wt	1874	179	1797	168	1767	296
*Seat Link X Sum (1b)	11.04	0.72	10.61	0.74	10.76	0.75
*Seat Pan Z Sum (1b)	11.12	0.71	10.72	0.75	10.87	0.75
*Seat Force/wt	-462	143	-460	130	-472	143
*Footrest X Sum (1b)	919	94	858	114	918	98
*Footrest Z Sum (1b)	1012	129	962	145	993	136
*Resultant Foot Force (1b)						

\* Includes Tare Loads

**Table 13 Summary of Electronically Measured and Computed Data  
from the Vertical Impact Tests (Continued).**

	GROUP III			GROUP IV		
	0°		MAX 90°	0°		MAX 110°
	Mean	s		Mean	s	
Shoulder Harness Angle						
Seatback Angle						
Sled Z (G)	10.4	0.21	10.4	10.4	0.26	10.8
Sled Velocity (ft/sec)				-24.4	0.44	-24.5
Seat Z (G)	10.5	0.10	10.6	10.8	0.34	11.1
Chest Resultant (G)	17.8	2.4	17.9	17.3	2.4	16.1
Chest SI	31.9	4.4	30.6	30.6	4.7	26.9
Head X (G)	5.04	1.3	4.36	3.11	0.8	2.38
Head Y (G)						
Head Z (G)	13.1	1.5	14.3	13.2	0.4	13.7
Head Resultant (G)	13.4	1.6	14.6	13.4	0.4	14.0
Head SI	23.6	3.4	28.2	23.1	1.4	23.4
Shoulder Sum (1b)	189	37	191	192	37	144
Shoulder Sum/wt	1.08	0.14	1.11	1.15	0.21	0.89
Lap Belt Sum (1b)	168	48	165	169	44	174
Lap Belt Sum/wt	0.97	0.29	0.99	1.01	0.22	1.05
*Seat Link X Sum (1b)	237	48	258	236	62	221
*Seat Pan Z Sum (1b)	1906	156	1853	1665	261	1675
*Seat Pan Z Sum/wt	10.97	0.73	10.67	9.98	0.55	10.02
*Seat Force/wt	11.06	0.72	10.75	10.07	0.56	10.12
*Footrest X Sum (1b)	-479	140	-574	-463	127	-477
*Footrest Z Sum (1b)	922	100	982	967	93	959
*Resultant Foot Force (1b)	1022	133	1121	1056	127	1038

\* Includes Tare Loads

The resultant acceleration of the head and the head Severity Index (Gadd, 1966), values are significantly increased as the seat vertical position is lowered from a relatively high position (producing a horizontal shoulder harness span to the structural attachment) to a full down position (producing the greatest positive shoulder harness angle). This increase occurs with the seat back in the 90° position but not at 110°. Furthermore, the increase can be attributed to the Z component of head acceleration since Z was significantly increased while X was not. In other words, in the 90° seat position, downward head acceleration is more severe in vertical impact when the shoulder harness angle increases from 0° to a relatively large positive value. This indicates that, from the standpoint of head acceleration, the restraint performance in vertical impact may be degraded by the proposed modification which raises the shoulder harness attachment points considerably beyond currently accepted design practice. This effect is not seen when the seat is fully reclined, in which position a portion of vertical support is provided through the seat back. In the more erect positions, forward location of the headrest may be a contributing factor as well, but, if so, the increased shoulder harness angle makes the effect more pronounced.

A statistically significant change in shoulder harness loads was observed between the two vertical adjustments tested with the 110° seat back position. However, this difference was between maximum values which occurred during the free fall period (i.e., pre-impact values). The differences in shoulder harness load measured during impact were not statistically significant.

Footrest X component, Z component, and resultant loads were also significantly increased as the 90° seat was lowered to the full down positions. This is consistent with the interpretation that a portion of the inertial loading from the lower extremities was transferred from the seat pan to the footrest. This occurs because, as the seat pan is lowered with respect to the fixed footrest, a smaller portion of the thigh is supported by the seat pan.

A summary of the observed correlations from the Wilcoxon analysis of pair differences is presented in Table 14. When the difference is statistically significant, the highest set of values within each pair is designated by the shaded area; the arrow designates the direction of the trend. The results are discussed in Section 9.

#### B. SIDEWARD IMPACT TESTS

The results of the +G<sub>y</sub> tests are summarized in Table 15. Maximum values of each measurement taken during the sideward impact test series as well as typical analog data sets from each cell of the experimental design matrix are also presented in Appendix D. All accelerations and loadings were considered to be well within human tolerance. This remains true in spite of the occurrence of a significant knee injury in an 8 G<sub>y</sub> test. This subject injury is discussed in detail in Section 9B. The injury led to the cessation of lateral testing before sufficient data could be obtained to allow statistically meaningful comparison of paired exposures using the Wilcoxon test. Therefore, these results are reported primarily as anecdotal observations. Nevertheless, several trends appeared to be sufficiently consistent in these data to allow tentative conclusions to be drawn. Since these conclusions agree with expected physical behavior based on restraint system design principles, it is

**Table 14 Summary of the Statistically Significant Relationships  
from the Vertical Impact Tests**

Shoulder Harness Angle Seatback Angle	0° 90°	0° 103°	0° 103°	0° 110°	0° 90°	MAX 90°	0° 110°	MAX 110°
Chest Resultant Acceleration	↑	↓	↓	↓	↑	↓	↓	↓
Head X Acceleration					↑	↓	↓	↓
Head Z Acceleration					↑	↓	↓	↓
Head Resultant Acceleration					↑	↓	↓	↓
Head Severity Index					↑	↓	↓	↓
Total Shoulder Harness Load		↓	↓	↓	↑	↓	↓	↓
Total Lap Belt Load	↑	↓	↓	↓	↑	↓	↓	↓
Seat Pan X Force					↑	↓	↓	↓
Seat Pan Z Force					↑	↓	↓	↓
Seat Pan Total Force					↑	↓	↓	↓
Footrest X Force					↑	↓	↓	↓
Footrest Z Force					↑	↓	↓	↓
Footrest Total Force					↑	↓	↓	↓

**Table 15** Summary of the Electronically Measured and Computed Data  
from the Sideward Impact Tests

	0 90		0 103		MAX 103	
	Mean	s	Mean	s	Mean	s
Shoulder Harness Angle						
Seatback Angle						
	n=5		n=7		n=8	
Sled Y (G)	8.50	0.51	8.28	0.26	8.18	0.33
Sled Velocity (ft/sec)	29.7	1.2	29.2	0.51	29.5	0.55
Seat Y	8.92	0.40	9.27	0.17	9.34	0.22
Chest Resultant (G)	13.2	1.3	12.5	1.3	13.5	2.1
Chest SI	27.4	5.7	24.5	3.0	28.3	3.7
Head X (G)	-9.23	1.5	-8.35	1.1	-8.74	1.4
Head Y (G)	9.14	0.81	9.64	1.3	9.55	1.7
Head Z (G)	-7.47	1.8	-6.28	3.2	-4.66	1.3
Head Resultant (G)	14.1	2.1	13.6	1.8	13.0	1.1
Head SI	46.0	13	44.7	7.8	42.0	6.3
Shoulder Refl (Left) (lb)	70.3	21	76.7	18	90.8	9.1
Shoulder Refl (Right) (lb)	126	21	124	18	118	32
Shoulder Reel (Left) (lb)	103	35	117	17	163	25
Shoulder Reel (Right) (lb)	227	69	206	28	184	62
Shoulder Sum (lb)	495	110	484	74	523	104
Shoulder Sum/wt	3.04	0.66	2.92	0.20	3.07	0.50
Lap Belt (Left) (lb)	254	74	357	117	399	117
Lap Belt (Right) (lb)	344	101	421	88	510	103
Lap Belt Sum (lb)	560	146	725	165	830	168
Lap Belt Sum/wt	3.40	0.58	4.34	0.44	4.95	1.2
Seat Link X (Left) (lb)	-140	77	95.7	33	70.0	44
Seat Link X (Right) (lb)	42.7	26	121	21	164	32
Seat Link X Sum (lb)	126	70	81.4	95	201	53
Seat Link Y (lb)	309	33	296	10	300	32
Seat Pan Z Sum (lb)	940	285	857	192	895	127
Seat Pan Z Sum/wt	5.59	0.79	5.13	0.55	5.30	0.67
Resultant Seat Force (lb)	989	275	903	169	945	110
Resultant Seat Force/wt	5.91	0.71	5.43	0.42	5.60	0.65
Foot X Preload (lb)	-481	73	-563	116	-642	254
Foot Z Preload (lb)	188	33	233	37	214	58
Resultant Foot Force (lb)	847	47	898	77	965	193
Crotch Strap (lb)	601	163	817	125	1030	156

N.B. - Subject groups are not identical. Results cannot be directly compared.

anticipated that they would be statistically supported at the chosen 90% confidence level if additional data could have been collected.

The shoulder harness loads follow an interesting pattern in the +G<sub>y</sub> tests. With the horizontal (0°) shoulder harness angle, both the inertia reel strap and the reflection strap on the left show increasing loads as the seat back is reclined from 90° to 103°, and a greater increase as the shoulder harness angle is raised to maximum at a seat back angle of 103°. This could possibly be explained by a difference in subject size among the groups, since the subjects who had completed the sideward impact series did not provide the anthropometrically paired groups that had been originally planned. However, the inertia reel strap and the reflection strap loads on the right decrease in those situations where the strap loads on the left increase. If the increased harness loads on the left resulted from a subject size variation between groups, we would have expected that harness loads on the right would have increased as well. Since the +G<sub>y</sub> impact throws the subject to his left, these findings raise the question of degraded lateral support as the seat is reclined, and particularly as the shoulder harness angle is raised.

This degradation appears to be further confirmed when lap belt and crotch strap loads are examined. Total lap belt loads increase in the same way that the left shoulder harness loads increase (greater as the seat is reclined and greater as the shoulder harness angle is raised). The effect is, if anything, more notable when the lap loads are normalized with respect to subject weight, tending to discredit subject size variation as an explanation. The same variation is seen again in a more striking manner in the crotch strap loads which average 601 pounds peak at 0° shoulder harness/90° seat back, increase to 817 pounds at 0°/103°, and increase further to 1030 pounds at maximum/103°. The differences between these means is greater than one standard deviation in all cases. Taken together, these findings are consistent with the proposition that the lateral support of the upper torso is degraded as the shoulder harness angle is raised from 0°, with the result that a greater degree of lateral support loads are transferred through the body to the lap belt and crotch strap.

These results are discussed further in Section 9.

#### C. FORWARD FACING IMPACT TESTS

The results of the -G<sub>x</sub> tests are summarized in Table 16. Maximum values of each measurement recorded or computed from the forward facing impact tests as well as typical data sets from each seat configuration are presented in Appendix E. All accelerations and loadings were considered to be well within human tolerance. Several significant correlations were observed which will be discussed in the following paragraphs.

The peak resultant acceleration measured on the chest decreased significantly as the seat back angle was varied from 90° to 103° with shoulder harness at 0°. This parameter decreased further as the shoulder harness angle was raised from 0° to maximum by lowering the seat at a fixed seat back angle of 103°. These results are consistent with the interpretation that a damping of the anterior chest acceleration occurs as the effective shoulder harness angle is raised, possibly allowing greater forward displacement of the chest.

**Table 16 Summary of the Electronically Measured and Computed Data  
from the Forward Facing Impact Tests**

	GROUP I				GROUP II			
	0°		103°		0°		103°	
	Mean	s	Mean	s	Mean	s	Mean	s
Shoulder Harness Angle								
Seatback Angle								
Sled X (G)	-9.13	0.27	-9.26	0.32	-9.21	0.46	-9.29	0.32
Sled Velocity (ft/sec)	+31.4	0.35	+31.7	0.61	+31.6	0.78	+31.5	0.33
Seat X (G)	-10.8	0.45	-10.8	0.49	-10.6	0.49	-10.8	0.33
Chest Resultant (G)	13.5	1.4	11.7	0.95	12.1	0.99	11.8	1.0
Chest SI	28.5	2.2	27.7	3.6	28.0	2.8	27.1	1.4
Head X (G)	-9.1	1.2	-9.1	0.9	-9.7	1.3	-9.0	1.5
Head Y (G)	2.0	1.0	1.9	0.9	1.7	1.5	1.4	1.3
Head Z (G)	-4.6	4.0	-4.7	4.0	-5.9	2.2	-4.7	1.4
Head Resultant (G)	10.5	1.4	10.7	1.2	11.3	1.7	10.0	1.5
Head SI	24.0	6.2	22.6	5.2	26.5	7.6	22.1	6.0
Shoulder Refl (Left) (1b)	104	21	112	21	115	20	124	15
Shoulder Refl (Right) (1b)	123	22	129	20	138	25	168	18
Shoulder Reel (Left) (1b)	183	33	192	36	192	34	202	29
Shoulder Reel (Right) (1b)	201	37	200	29	219	32	234	31
Shoulder Sum (1b)	604	104	626	101	657	96	719	80
Shoulder Sum/wt	3.79	0.38	3.96	0.33	4.05	0.45	4.32	0.70
Lap Belt (Left) (1b)	260	53	287	54	315	89	317	78
Lap Belt (Right) (1b)	255	71	286	46	315	87	288	74
Lap Belt Sum (1b)	510	120	566	99	623	173	600	152
Lap Belt Sum/wt	3.24	0.85	3.66	1.02	3.92	1.38	3.74	1.24
*Seat Link X (Left) (1b)	-206	27	-246	31	-257	47	-247	60
*Seat Link X (Right) (1b)	-177	13	-211	32	-215	38	-195	41
*Seat Link X Sum (1b)	-357	35	-436	65	-450	88	-431	107
*Seat Link Y (1b)	58.7	13	54.7	10	55.3	9	76.7	8
*Seat Pan Z Sum (1b)	589	98	670	113	706	158	583	171
*Seat Pan Z Sum/wt	3.69	0.45	4.25	0.68	4.40	1.1	3.54	0.74
*Resultant Seat Force (1b)	648	97	744	131	777	181	640	185
*Resultant Seat Force/wt	4.07	0.49	4.71	0.75	4.84	1.27	3.90	0.86
Foot X Preload (1b)	-596	221	-566	219	-493	236	-556	246
Foot Z Preload (1b)	237	75	220	85	198	100	205	73
Resultant Foot Preload (1b)	643	230	608	233	532	255	594	254
*Resultant Foot Force (1b)	1403	254	1363	272	1349	310	1374	283

\* Includes Tare Loads

The peak resultant head acceleration and the magnitude of the Z component of the acceleration of the head decreased significantly at the 103° seat back angle, when the shoulder harness angle was raised from 0° to maximum. This is consistent with the interpretation that less forward rotation of the head occurs in -G<sub>x</sub> impacts as the shoulder harness angle is raised. This finding is also consistent with the lower peak resultant chest acceleration described above. The head effect would probably be less significant at higher impact levels where voluntary neck muscles provide a relatively smaller effect.

Shoulder harness loads tended to increase as the seat back angle was varied from 90° to 103° with a 0° shoulder harness angle. The loads increased further as the 103° seat was lowered to raise the shoulder harness angle from 0° to maximum. With reclining seat back angle, the increase was statistically significant in the left reflection strap. With increased shoulder harness angle, the increase was statistically significant in the right reflection strap and in the total shoulder harness load. In both comparisons, however, the tendency to increase was consistent in all shoulder straps and totals (with the exception of a one pound reversal of this trend in the right inertia reel strap). The inertia reel straps appeared to carry slightly higher loads than the reflection straps. These findings are consistent with an analysis of the physical properties of the configuration, since tension produced in a strap is greater for a force applied perpendicularly with the strap fixed at both ends than it is for the same force applied as tension in the direction of the strap.

Total seat pan force, as well as the X and Z components, increased significantly as the seat back angle was reclined from 90° to 103° with a 0° shoulder harness angle. Interestingly, these same values decreased significantly as the 103° seat was lowered to produce a maximum shoulder harness angle. (The Y component, though very small, did show a significant increase in the second comparison, the physical significance of which is doubtful.) These findings are consistent with the interpretation that a reclined initial position produces a greater reaction of upper torso forces into the seat pan, both in X and Z.

A summary of the observed statistically significant differences obtained from the Wilcoxon analysis is presented in Table 17.

The crotch strap was a special case in the -G<sub>x</sub> tests. The tension-time curve for this restraint system component appeared to produce three characteristic curves, designated negative, neutral, and positive. Examples are shown in Figure 30. The distribution of the occurrence of each curve in the -G<sub>x</sub> tests is presented in Table 18. Since no groin symptomatology was reported in the -G<sub>x</sub> tests, and since crotch strap loading increased in the same configurations which showed increased shoulder harness loads, it could be theorized that the crotch strap tension was related to shoulder harness loads being carried to the lower seat structure, rather than being related to direct loading of the groin. This finding is consistent with the crotch strap effectively performing its intended function in the -G<sub>x</sub> tests.

These results are discussed further in Section 9.



**Table 17 Summary of the Statistically Significant Relationships  
from the Forward Facing Impact Tests**

	0° 90°	0° 103°	0° 103°	MAX 103°
Shoulder Harness Angle				
Seatback Angle				
Chest Resultant Acceleration		←		←
Head Z Acceleration				←
Head Resultant Acceleration				←
L Shoulder Reflection Strap	→			
R Shoulder Reflection Strap			→	
Total Shoulder Strap Load			→	
Seat Pan X Force	→			←
Seat Pan Y Force			→	
Seat Pan Z Force	→			←
Seat Pan Total Force	→			←

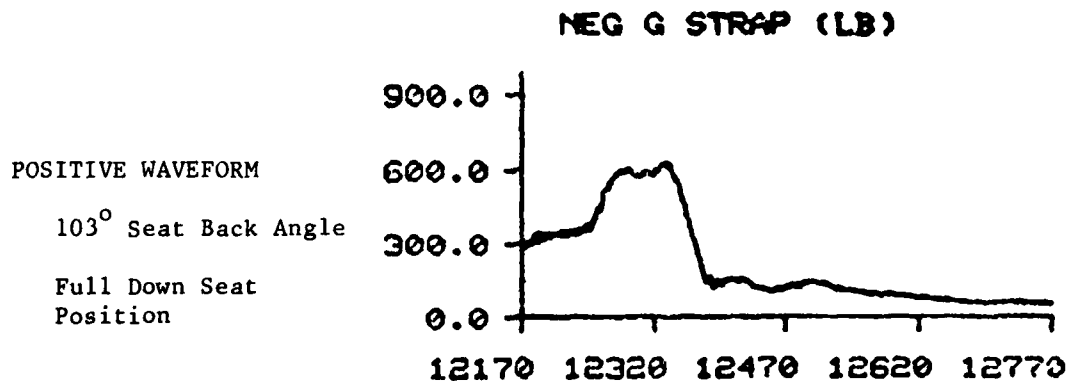
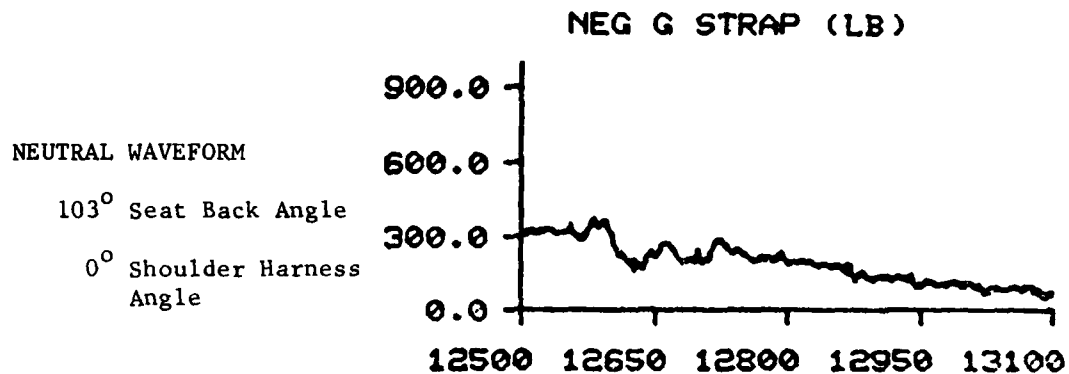
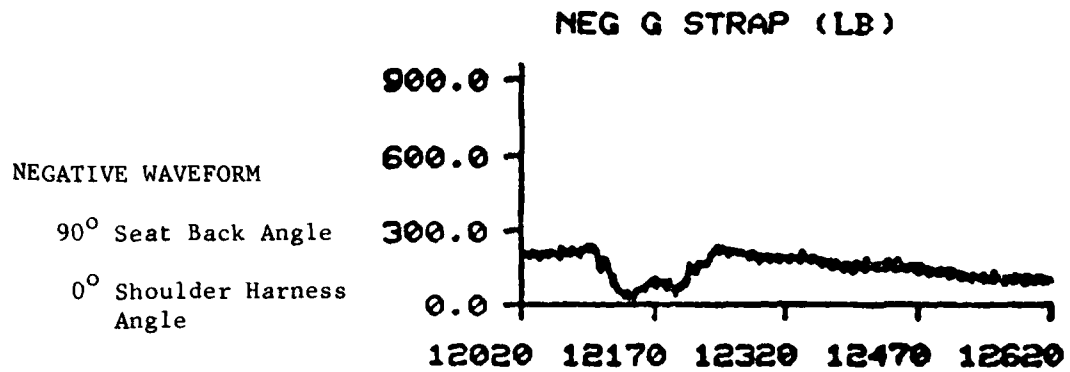


Figure 30. Examples of Tension-Time Curves Measured at the Crotch Strap End Fitting. Subject M-2.

TABLE 18. DISTRIBUTION OF THE CROTCH STRAP LOAD CHARACTERISTICS

Seat Configuration is indicated by Seat Back Angle/Shoulder Harness Angle			
	90°/0°	103°/0°	103/Max*
Negative Waveform	7	5	1
Neutral Waveform	1	11	2
Positive Waveform	1	0	7

\*Maximum positive angle in full down seat position.

#### D. MEDICAL FINDINGS

The following is a summary of the medical findings obtained during the evaluation of the proposed, modified F/FB-111 crewmember restraint system. These data were derived primarily from a review of the Impact Data Sheets which were prepared by the medical monitor following each impact exposure and which documented pretest and post-test histories and physical examinations. Although two physicians accomplished most (greater than 90%) of the medical monitoring during this program, five physicians in all participated in the monitoring and were responsible for the following data.

TABLE 19. FREQUENCY OF SUBJECTIVE MEDICAL FINDINGS

	+G <sub>z</sub>	+G <sub>y</sub>	-G <sub>x</sub>
Pretest Paresthesia	5	0	1
Pain at Shoulder Harness	0	13	0
Back Pain			
Cervical	2	3	3
Thoracic	1	3	0
Lumbar	3	0	0

The pretest phase, prior to actual impact exposure, was a variable period of time (approximately 10-20 minutes) during which pretest measurements were made and the harness straps were adjusted. In general, the majority of subjects during this period of time complained of harness tightness, particularly in the shoulder straps. On six occasions during this pretest period (see Table 19), the shoulder straps were sufficiently tight to produce upper extremity paresthesias, presumably on the basis of venous congestion. In one subject, this paresthesia occurred on three successive exposures and resulted in a persistent mild paresthesia of the hand in the ulnar distribution, which has improved since completion of the test program. In general, however, these paresthesias resolved within seconds after the harness was released following the impact.

Table 19 also lists the reports of pain on impact and indicates an increased frequency of such reports during G<sub>y</sub> testing. Pain in the region in contact with the shoulder harness was noted during 13 (thirteen) G<sub>y</sub> impacts at both the 6 and 8 G peak levels. On 11 occasions, this pain was localized to the left shoulder.

Pain in the vertebral and paravertebral regions on impact occurred in a total of 15 tests with a distribution as shown in Table 19. Two of the three occurrences of cervical discomfort in the  $-G_x$  impact tests were attributed to the shoulder harness yoke. The thoracic discomfort in the  $G_y$  impact tests occurred primarily in the T<sub>5</sub>-T<sub>6</sub> region. There was no clinical correlation with any of these occurrences of pain, the majority of which were considered fleeting discomforts, resolving immediately post-impact.

TABLE 20. FREQUENCY OF OBJECTIVE MEDICAL FINDINGS

	$+G_z$	$+G_y$	$-G_x$
Venous Congestion	3	0	0
Petechiae	1	0	0
Abrasions	0	10	0
Contusions	0	4	1
Muscle Strains	2	1	2
Ligamentous Injury	0	1	0

In the pretest phase during harness adjustment, one subject developed venous congestion of the upper extremities without paresthesia on three occasions (see Table 20). This resolved immediately after harness release post-impact. One subject was noted to have proximal upper extremity and axillary petechiae post-impact, also presumably on the basis of venous congestion. Minor abrasions were sustained on 10 occasions, all during  $G_y$  testing at 6 and 8 G levels. Five of these were abrasions of the right upper medial thigh and were attributed to contact with the crotch strap during the impact. Two of these five events were sufficiently severe to produce minor contusions of the right upper medial thigh. Three abrasions and one contusion were attributed to the shoulder harness. Erythema of regions in contact with the restraint harness occurred in the majority of subjects (particularly in fair-skinned subjects), but this was generally not recorded on the Impact Data Sheet and is not reported among the objective medical findings.

Five muscle strains involving the cervical (3) and thoracic (2) paravertebral muscles were reported during post-test physical examinations. These were evidenced by persistent, post-test, localized pain and/or tenderness, muscle spasm, or mild thoracic scoliosis. However, the true frequency of minor muscle strains, particularly in the  $G_y$  test series, is probably significantly greater than reflected in Table 20. Minor muscle soreness, primarily involving the paracervical muscles, was often not noted by subjects until several hours or longer post-impact. All muscle strains responded well to routine conservative care (rest and local heat).

The subjective and objective medical findings described above are considered to be of no clinical consequence. However, during an 8 G sideward impact, a female subject incurred a ligamentous knee injury requiring surgical correction. This injury involved disruption of the mid-substance of the right anterior cruciate ligament and stretching of the right medial collateral ligament. Further details of this injury and its implications are found elsewhere in this report. (See Section 9B.)

A few subjects noted that they were more comfortable in the 110° seat back angle position than in either the 103° or 90° position. One subject also noted that, in the 110°/full down seat position, the hands-on-knees bracing posture was more easily accomplished during -G<sub>x</sub> testing. However, from the medical monitor's point of view, head displacements were greater for subjects in the 110° seat position than for those in the 103° position, and much greater than for those in the 90° position during -G<sub>x</sub> tests.

The relationship between subject size and seat position was critical in several tests wherein a seat position change was necessary to accommodate the subject. Subjects small in stature, in the full down seat position, at times were not able to reach and to brace against the headrest with their heads. In this circumstance, in the +G<sub>z</sub> test series, the helmeted subjects were instructed to push their heads back against the shoulder straps, as shown in Figure 31. Since this type of bracing was not believed to be critical in this axis, no change in seat position was necessary. However, when this circumstance occurred in -G<sub>x</sub> tests, the seat position was changed to enable the smaller subject to reach the headrest and thereby to brace effectively. On the other hand, subjects large in stature at times could not be accommodated in the 110°/full down seat position for -G<sub>x</sub> tests, due to preloading into the crotch strap and/or the extraordinary length of their lower extremities. The seat position for these subjects was changed to obviate these problems.

Attempts were made to utilize hard cup groin protectors for male subjects during +G<sub>y</sub> and -G<sub>x</sub> tests. This was not successful for the sideward tests due to the occurrence of a mild superficial abrasion and discomfort of the right upper medial thigh, which was attributed to the cup, on the first lateral test. The device was not utilized in +G<sub>y</sub> tests thereafter. The hard cup protector was initially used by all male subjects during the -G<sub>x</sub> tests to afford protection from possible crotch strap loading. As this potential problem was not demonstrated in the early -G<sub>x</sub> tests, the protector was made optional to subjects, and most elected not to utilize it in the later tests. No significant problems were encountered when the cup was not used. Some subjects expressed the belief that the presence of a protector created a preloading into the crotch strap, particularly in the 110°/full down seat position. When this circumstance was encountered, the cup was removed. If preloading continued to be a problem, then the seat position was changed.

Adjusting and readjusting the F/FB-111 restraint harness on subjects during this program led to the discovery that a critical maladjustment of the harness was possible. If a subject was seated leaning slightly forward (with his shoulders and head away from the seat back and headrest, respectively) prior to harness adjustment, then he could not voluntarily achieve a fully upright posture (with shoulders and head firmly against the seat back and headrest, respectively) following adjustment of the shoulder harness straps. This limitation to free aft movement of the subject's neck and shoulders was due to the shoulder harness yoke, the position of which is determined by the chest strap adjustment relative to the release box, which is, in turn, fixed relative to the seat pan by the crotch strap.

In the operational environment, unless extraordinary care is taken by the crewmember when adjusting the chest straps of the shoulder harness, the harness yoke may be adjusted downward against the crewmember's shoulders and posterior neck, while he is leaning slightly forward. If the harness is maladjusted in



Figure 31. Test Subject with Small Sitting Height with Head Braced Against the Shoulder Straps.



Figure 32. Test Subject After Shoulder Strap Haulback with the Harness Yoke Malpositioned.

this manner, a crewmember cannot assume the recommended pre-ejection body position and, when ejection is initiated, the harness yoke will impose a downward load on the crewmember as the inertia reel straps are retracted. Thus, when he adjusts the chest straps, a crewmember must be seated with his shoulders firmly against the seat back and his head against the headrest. This will prevent the imposition of a potentially injurious postero-inferior load on the vertebral column during haulback, which may compromise the crewmember's tolerance of loads subsequently imposed during ejection and landing impact.

Of course, no human tests were conducted in the maladjusted configuration. However, this position was found to be possible for all subjects but one (exception due to small stature) and was photographically documented for all subjects. Figures 32 and 33 show a subject, after simulated harness haulback, in the maladjusted and properly adjusted positions, respectively. The maladjusted position may be easily achieved by crewmembers as in, for example, the case in which the crewmember flexes his head in order to visualize the harness during adjustment. We believe that this finding is of great significance, in that harness maladjustment, as described above, provides a heretofore unrecognized mechanism of spinal injury in F/FB-111 ejectees. This finding and its implications are discussed in further detail in Section 9C.

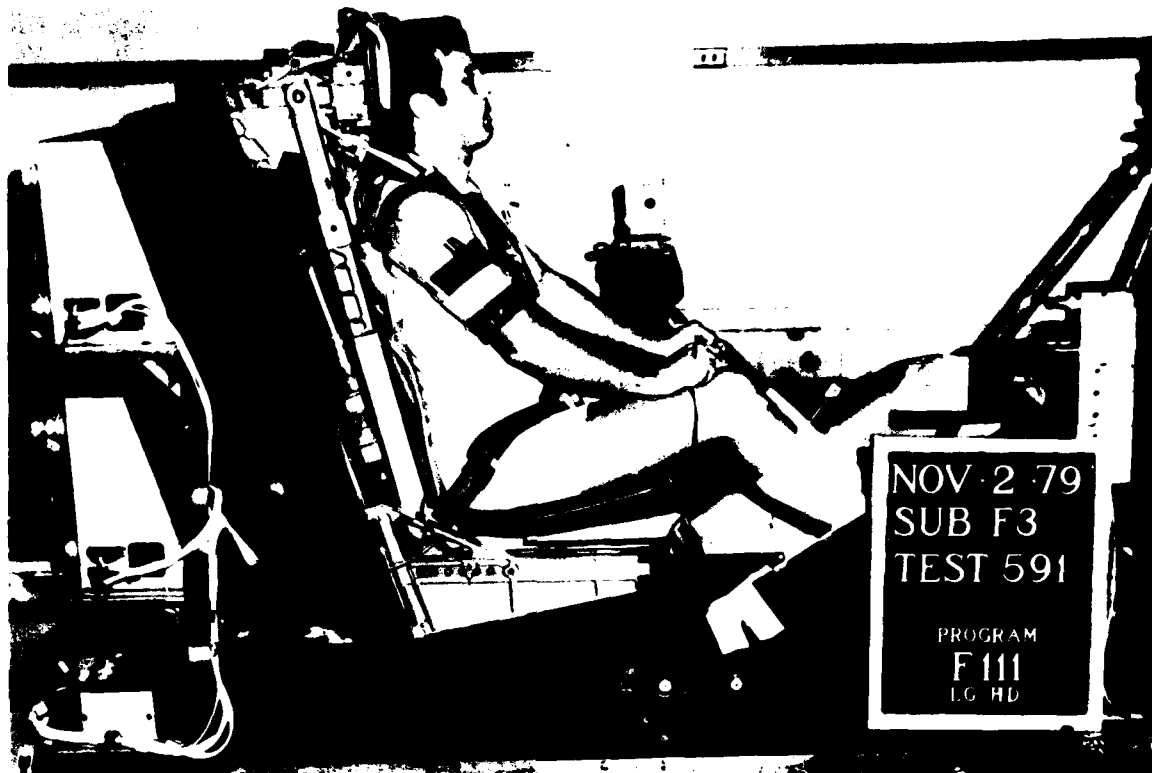


Figure 33. Test Subject After Shoulder Strap Haulback with the Harness Yoke Properly Positioned.

Subject attrition during this test program was not unusual. Twenty-three subjects of the AFAMRL Impact Acceleration Stress Panel participated in this test program. Fifteen of those subjects remained as panel members following program completion. Four subjects left the panel due to new duty assignments and permanent changes of station. One subject voluntarily withdrew from the test program following a muscle strain incurred during a 10  $G_z$  test. Another subject was eliminated from participation by the impact panel physician due to a significantly anomalous biodynamic response to a 6  $G_y$  test. A third subject was also eliminated from further participation by the impact panel physician when he was found to have incurred a back injury, unrelated to his participation as an impact subject. This injury, attributed to strenuous physical exercise, was clinically diagnosed as protrusion of the L<sub>4</sub>-L<sub>5</sub> intervertebral disc with left-sided L<sub>5</sub> radiculopathy and resolved with conservative treatment. Finally, a fourth subject incurred a ligamentous injury of the right knee. (See Section 9B.)

In summary, excepting the test in which the knee injury occurred, these impact tests were very well tolerated by all subjects. The increased frequency of significant subjective and objective medical findings in the  $G_y$  test series (as indicated in Tables 19 and 20) supports our overall impression that the effects of the impact environment in the  $G_y$  tests were more severe than the effects of the + $G_z$  or - $G_x$  environments.



## Section 9

### DISCUSSION

#### A. COMPARISON WITH HOLLOMAN AFB DATA

Sixteen human impact tests were performed in March 1968, at Holloman AFB, New Mexico (Moss, 1968) to evaluate a prototype of the restraint harness currently used in the F/FB-111. These tests were accomplished using a boilerplate version of the F/FB-111 seat. The headrest and inertia reel straps were individually adjustable in the vertical direction. The seat back angle was 103° aft of the aircraft waterline. Various vertical seat adjustments were chosen for these tests depending on subject size. It is unclear what the shoulder harness angles were for each test. It is clear, however, that the restraint harness configuration at Holloman was intended to duplicate the currently operational configuration. Therefore, a comparison was made between the results of the Holloman tests of the current operational harness and the results of the tests of the proposed modification to the F/FB-111 harness described within this report. An attempt was made to elucidate performance changes which could be attributed to the modification.

Results from the eight forward facing Holloman tests are compared with mean results from all 33 experimental level forward facing tests at AFAMRL in the left half of Table 21. It should be noted that the sled velocities and accelerations at AFAMRL were significantly lower, on average, than the velocities and accelerations at Holloman. This is borne out in the lap belt load differences. However, the loads in the shoulder harness reflection straps appear closer than expected to the Holloman data, indicating a different function of the reflection straps in their modified location. Furthermore, the peak resultant acceleration measured on the subjects' chests during the AFAMRL tests was relatively close to the Holloman value, but indicated a greater amplification of the chest acceleration with respect to the impact sled acceleration for the proposed harness modification.

Results from the eight sideward impact tests conducted at Holloman AFB are compared with mean results from all 20 experimental level sideward impact tests at AFAMRL in the right half of Table 21. It should be noted that the sled accelerations and velocities for the lateral tests are more comparable between programs than in the forward facing direction. However, the Holloman tests were conducted in the -G<sub>y</sub> or "eyeballs right" direction while the AFAMRL tests were in the +G<sub>y</sub> or "eyeballs left" direction. Therefore, some transposition is necessary when comparing strap loads. The most striking difference is found when comparing lap and reflection strap loads. Lap loads appear to be reasonable, with the greatest loads being found in the belt half that the subject displaces away from in the impact (i.e., left greater than right for "eyeballs right", right greater than left for "eyeballs left"). The comparison changes for the shoulder harness loads, particularly in the reflection straps. In the Holloman tests, the subject tended to displace to the right in the seat, but this was effectively resisted by the right reflection strap which was attached to the left portion of the seat. This strap shows the highest loads (404 pounds) with a portion of this load seen in the right reel strap. The reflection strap of the modified system appears to be unable to perform its intended function, for the anchor point has been located higher and more medially. Thus, in the AFAMRL tests with the modification, the subject tends to displace to the

**Table 21 Comparison of Holloman and AFAMRL Test Data**

Forward Facing Impact Tests			Sideward Impact Tests		
$-G_x$		$-G_x$	$-G_y$		$+G_y$
Holloman	AFAMRL	Holloman	AFAMRL		
Mean	s	Mean	s	Mean	s
8		16		8	17
8		33		8	20
68.9	2.6	69.6	3.2	69.3	1.8
154	24	163.8	21.6	157	14.7
35.7	1.2	37.2	1.7	35.4	0.7
38.2	3.2	31.5	0.5	32	0.5
13.1	2.1	9.2	0.3	9.6	0.4
13.9		12.3	1.4	13.3	13.1
286	60	193	32	151	34
318	79	215	37	266	52
169	64	114	20	37	20
185	51	143	28	404	46
579	144	297	71	508	104
564	145	283	75	294	71
310	120	-	-	698	51
					</

left. If the reflection straps had been in their former, lower and more out-board positions, the left reflection strap would presumably have carried similarly high loads in providing lateral restraint. Instead, it carries the lowest loads (81 pounds). The results of this variation in the impact dynamics appear to be:

1. Greater amplification of the chest acceleration with respect to the impact sled acceleration.
2. Greater total lap belt load application than expected, since a greater proportion of the lateral torso restraint is now provided by the lap belt.
3. Greater crotch strap loads as the subject apparently suffers greater displacement relative to the seat.

In summary, the AFAMRL test results indicate a different function of the reflection straps, particularly in their function as lateral restraint devices, when they are relocated as proposed. The differences are seen in strap loads and in resultant subject severity measures such as chest resultant acceleration. (Since no head acceleration measures were made at Holloman, head response comparisons could not be performed.) The lateral restraint degradation that is apparent from this comparison adds further evidence to the indications of lateral restraint degradation which appeared in the lateral parametric comparisons at AFAMRL relating to shoulder harness angle (see Section 8B.).

#### B. SUBJECT KNEE INJURY

On 25 September 1979, a female subject incurred a right knee ligamentous injury during a routine lateral impact at the AFAMRL Horizontal Decelerator Facility. The impact test occurred as programmed and all equipment functioned normally. Impact peak G was 7.96 with an average value of 7.36 and a velocity change of 29.8 ft/sec. Programmed values for this test were 8.0 G peak with a velocity change of 30 ft/sec. Fifty-nine other lateral impact tests (nineteen tests at 8 G) were completed during this test program with no untoward effects and absolutely no knee symptomatology. The injured subject had previously experienced uneventful lateral impacts at 4 and 6 G.

The subject's response to impact appeared to be normal, until she indicated pain in the right knee immediately post-impact. Although she was able to weight-bear immediately post-injury, buckling of the right knee with walking prompted an immediate orthopedic consultation at the USAF Medical Center, Wright-Patterson AFB. There the subject was found to have a clinically unstable right knee and she was, therefore, admitted to the Medical Center for surgical correction of her ligamentous knee injury. On 27 September 1979, under general anesthesia, x-rays of the right knee under valgus stress revealed significant medial widening of the joint space, and thus an arthrotomy was performed. The subject was found to have significant stretching of the medial collateral ligament (MCL) with intraligamentous disruption of the anterior cruciate ligament (ACL). These ligaments were repaired and the subject was placed in a long leg cast. Four months post-injury, the subject had an excellent surgical result as demonstrated by a minimal (3-4 mm) anterior draw sign of the right knee on physical exam. She was progressing well in her right lower extremity physical therapy rehabilitation program and she was ambulating with the aid of a knee brace.

A review of the high-speed films of the test in question (Test No. 518) qualitatively revealed little difference in the motion of the right knee when compared with right knee motion in other similar tests. However, tracking the displacement of the right knee on a frame-by-frame basis, plotting this displacement for the test in question, and comparing other pertinent tests revealed a significant quantitative difference between right knee displacement in Test No. 518 and that displacement in other comparable tests (such as Test No. 488). As shown in Figure 34, there is a significant downward component to the displacement of the right knee during Test No. 518, and, near full medial excursion, the right knee motion is momentarily suspended. This is believed to be the point of ligament failure.

As in all tests done during this program, the subject was bracing prior to impact. This bracing technique consisted of the subject pressing her helmeted head back against the headrest, her hands against her knees, and her feet against the footrest. A free body analysis of the right knee at impact revealed the following forces to be operative: (1) the lateral inertial force of the knee and leg displacing to the left, reacting against the restrained pelvis proximally and the footrest distally, (2) the internal forces of the contracting muscles of the right lower extremity, and (3) the force of the right upper extremity on the knee due to bracing. The latter two forces were examined indirectly by an analysis of foot load data.

A review of the foot load data obtained during lateral testing showed that the typical preload in X (load in X direction prior to impact) for most subjects due to bracing was between 300 and 500 pounds. However, some subjects had significantly greater preloads in X, in the range of 750 to 1000 pounds. In Test No. 518, the preload in X was significantly greater than usual (approximately 900 pounds). An abrupt unloading in X occurred between 156 and 170 msec into the impact, and is believed to be the point of ligament failure. (See Figure 35.) Note that this corresponds temporally to the presumed point of ligament failure derived from photometric data.

The role of the hands-on-knees bracing posture was further investigated by utilizing the photometric data and tracing the path of the subject's right hand during impact. As can be seen in Figure 34, this path followed a downward trajectory. However, the subject's right hand was no longer in contact with her right knee at 140 msec into the impact (see Figure 35), a full 16 msec prior to unloading in X. Therefore, it was concluded that the bracing force of the subject's right upper extremity on her right lower extremity was negligible and did not play a role in the injury.

The subject's anthropometry was an additional factor that was considered. Compared to the typical USAF female, her height (5'10") is greater than 99th percentile, her sitting height is 75th percentile, and her buttock-to-knee length is greater than 99th percentile (and greater than the 95th percentile compared to USAF males). This extraordinary buttock-to-knee length may have played a significant role in her injury, as this distance represents the moment arm of the subject's right knee as it rotated about the pelvis. Possible factors contributing to this subject's injury, therefore, include (1) the subject's extraordinary anthropometry, (2) the subject's particular bracing mode, and (3) the seat position, which placed the subject's knees in 40° of flexion.

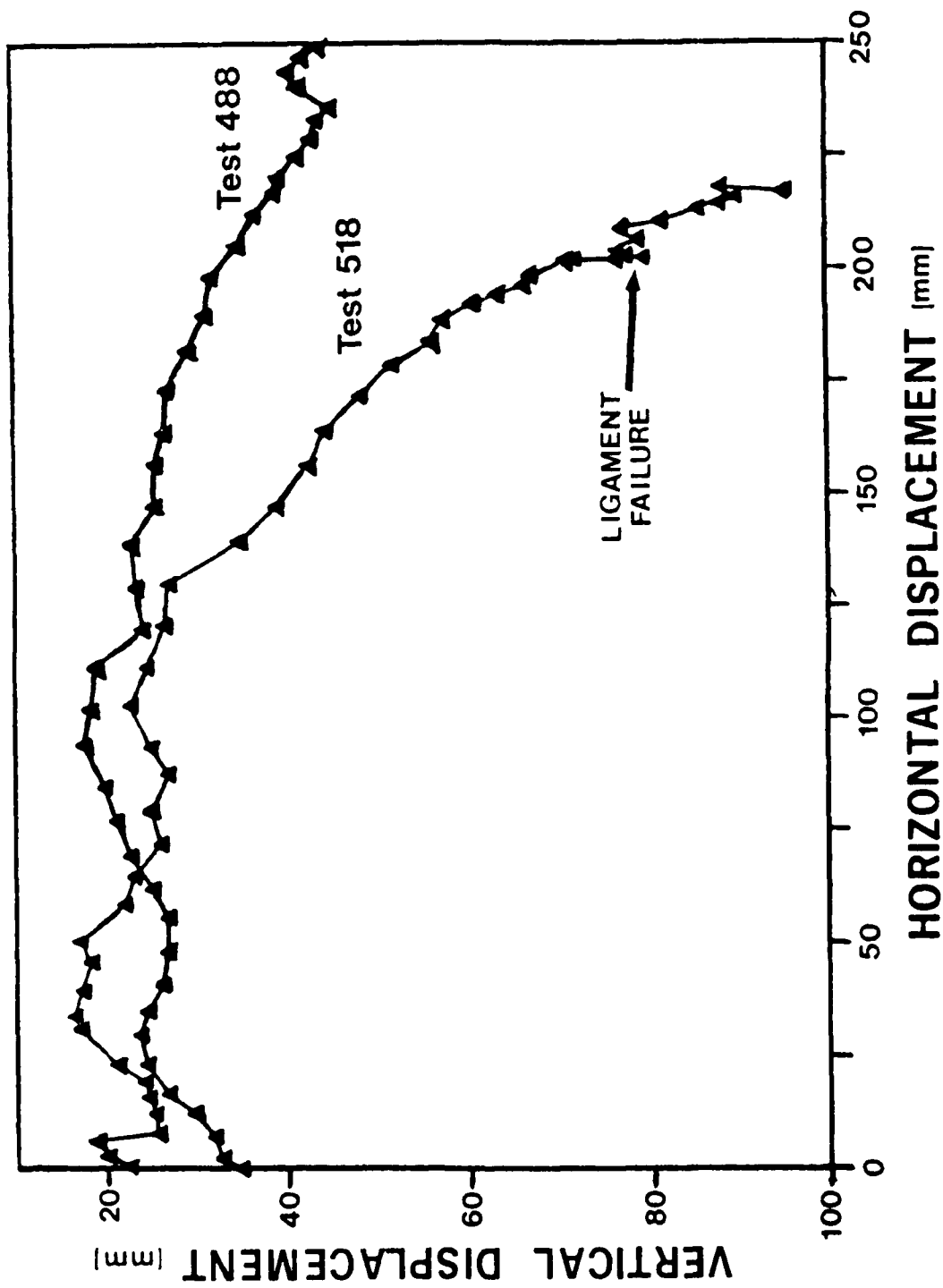


Figure 34. Frame-by-Frame Displacement of Right Knee During Impact - Comparison of Tests 488 and 518.

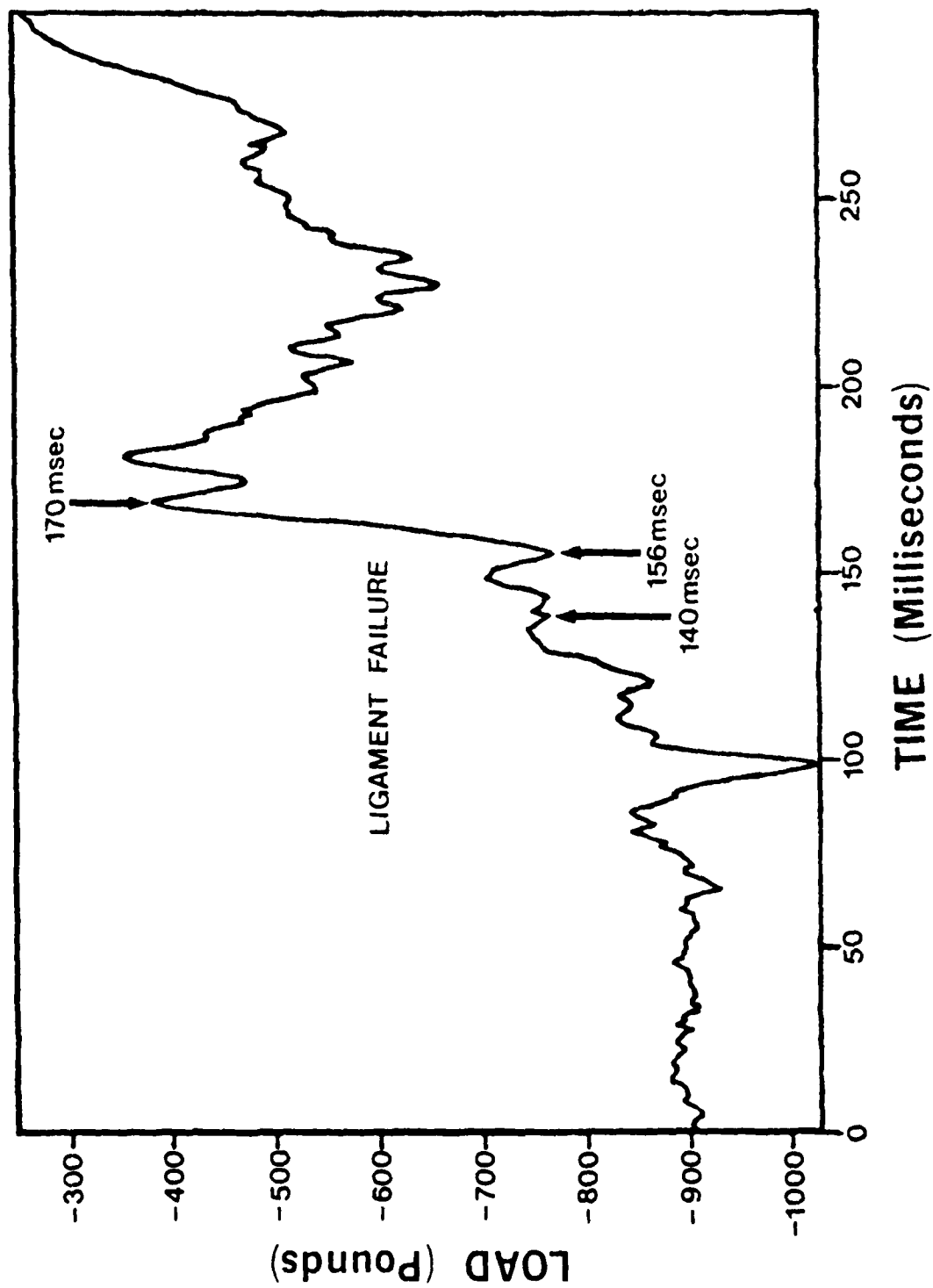


Figure 35. Footrest Load Data in X Direction - Test 518.

The type of inertial loading experienced during these lateral tests produced a valgus stress at the right knee and external rotation of the tibia on the femur. Furthermore, it is likely that the extraordinary degree of pre-impact bracing, which to some extent was protective against MCL injury (Pope et al., 1979), established the subject's right foot in a fixed position throughout the impact. Rapid deceleration and twisting of the knee (external or internal rotation of the tibia on the femur) during complete or partial weight-bearing (foot position fixed) is certainly a well-recognized mechanism of ACL injury (Feagin, 1979; Kennedy et al., 1974; McMaster et al., 1974). This appears to be the mechanism of injury which was operative in this case.

Grood et al. (1978) have indicated that the most common ligamentous knee injury which occurs in young individuals and during rapid loading of the knee is an intraligamentous (rather than bone avulsion) injury. The type of ACL injury sustained in this case corresponds to these observations.

At 40° of knee flexion, the ACL is lax (Kennedy et al., 1977) and therefore its energy absorbing capacity is nil. As the right knee was displaced medially during impact, after the muscles of the right lower extremity absorbed as much energy as they were able, it became necessary for the ACL to absorb energy, but it was in a poor position to do so. Therefore, ligament failure occurred.

Limitation of female (as compared to male) hip adduction on the basis of differences between male and female pelvic geometry may have a role in this injury mechanism, though this role has yet to be defined. Also, the role of ligamentous laxity, as possibly being indicative of predisposition to ligamentous injury, remains unclear.

This injury was reported through official Air Force channels and a committee appointed by the AFAMRL Commander was established to conduct an independent investigation of the injury. A criticism of the committee was that the test fixture utilized was unlike the operational seat in that the test fixture had no between-the-legs console which may have provided some lateral support for the lower extremities in the lateral impact environment. In response to this criticism, a mock-up of the console was fabricated and placed on the test fixture. However, after a medical risk analysis of this new test fixture, it was felt that the injury potential for the lower extremities could have been significantly increased, rather than decreased. Therefore, lateral testing, which had been suspended following this knee injury, was not resumed.

After an analysis of the above data, it appears that this injury occurred in a completely unforeseeable fashion. Certainly an analysis of the data of this subject's previous 4 and 6 G lateral impacts was not, in any sense, predictive of this injury. Several contributing factors (outlined above), each in itself of minimal consequence, apparently acted together in a synergistic fashion to create an environment in which the injury occurred. This injury, therefore, represents the realization of an extremely rare risk in lateral impact testing.

The following implications from this injury analysis are drawn.

1. Recognizing that the F/FB-111 crew seat and restraint system was designed for individuals having 5th to 95th percentile stature and/or sitting height, an increased injury potential may exist when this equipment is utilized by disproportionate individuals with extraordinary anthropometry, i.e., individuals with certain extraordinary body dimensions not reflected in stature or sitting height. However, this injury is not specific to the F/FB-111 crew seat and restraint system.
2. Future lateral impact testing must be conducted only after the question of support of the lower extremities has been adequately addressed.
3. Crewmember bracing modes preparative for ground landing impact following ejection require further biodynamic investigation.

#### C. ANTHROPOMETRIC EVALUATION

During the preliminary and critical design reviews of the proposed crew seat and restraint system redesign configuration held at General Dynamics, the mock-up of the proposed system was noted to permit the shoulder strap angle to be as much as  $-90^\circ$  with respect to the aircraft waterline. This condition was found when individuals who have large mid-shoulder sitting heights raised the seat pan to a level at which their flight helmet was one inch from contact with the inner surface of the aircraft canopy. Since this finding represented a failure of the proposed system configuration to meet one of the specific objectives of the redesign effort, ASD/AES requested that AFAMRL conduct an anthropometric evaluation of the design to determine the extent of the deficiency. This effort was accomplished by Dr. Kennedy (AFAMRL/HEG) and documented in a letter to BBP dated 3 October 1979. It was found that the critical anthropometric dimensions that determine the shoulder strap angles in the F/FB-111 cockpit are sitting height and mid-shoulder sitting height. Negative shoulder strap angles were found to be expected with the combination of anthropometric values shown in Figure 36. The area where the anthropometric values are estimated to cause negative shoulder strap (both inertia reel and reflection straps) angles with the redesigned configuration is shaded by crossed diagonal lines. This figure also shows the area, shaded by diagonal lines, where the anthropometric values will cause negative inertia reel strap angles when the current operational harness is used. The influence of the reflection strap angle could not be quantified for the operational harness. On the basis of these anthropometric data, it was estimated that the proposed redesign would allow negative shoulder strap angles for 13% of the flight crewmembers. In contrast, the current operational harness allows an estimated 34% of the flight crewmembers to have negative inertia reel strap angles.

A second potential problem observed during the mock-up review was that the removal of the lower portion of the headrest might compromise the degree of head support provided to crewmembers with short sitting heights. The elimination of 2.66 inches from the lower portion of the headrest was necessary to provide clearance for the elevated reflection and inertia reel straps. This feature of the proposed redesign proved to be a significant problem during the impact test program as previously described in Section 8D of this report.



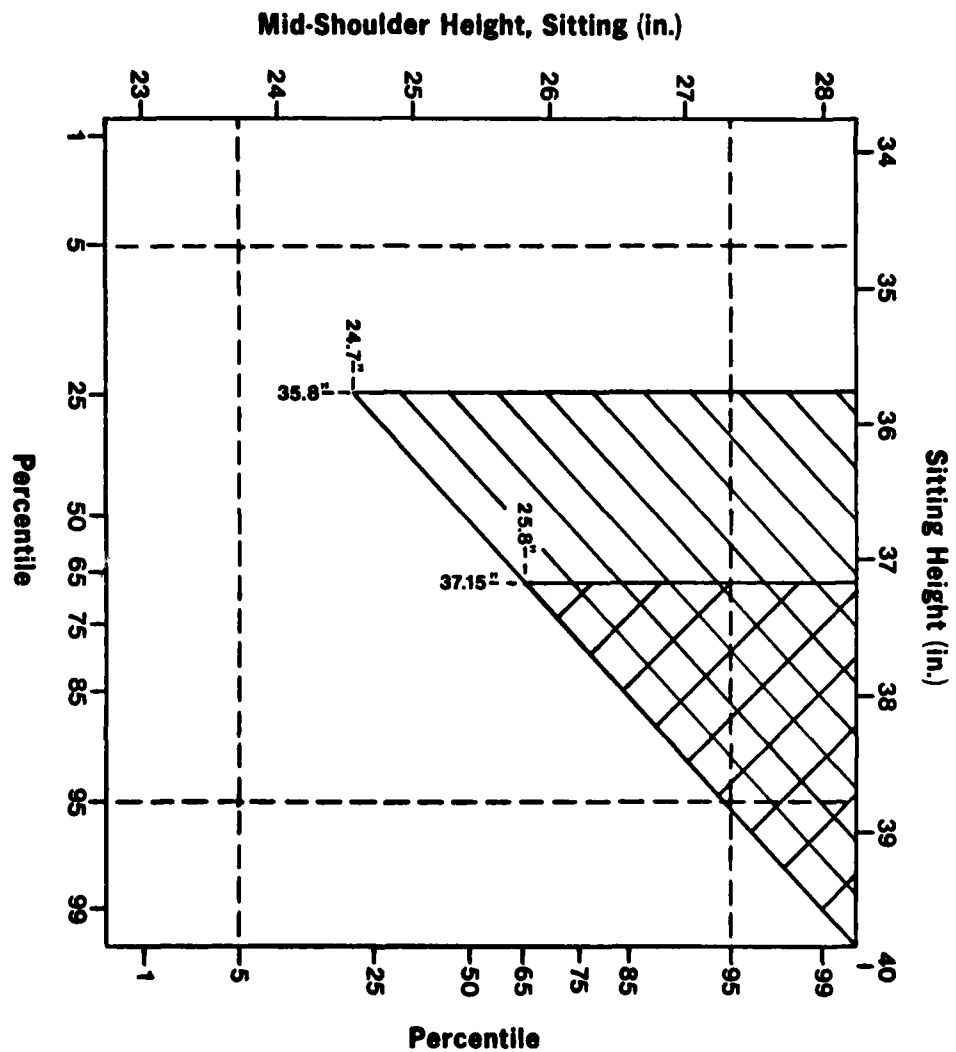


Figure 36. Combination of Anthropometric Values Which Are Expected to Cause Negative Inertia Reel Strap Angles for the Current Operational Restraint and the Proposed Modification to the Crew Seat and Restraint System.

A further anthropometric study was accomplished to provide an estimate of the extent to which the headrest modification would compromise head and neck protection. The study was conducted using the crew seat and restraint system prototype used in the horizontal impact tests. The study was accomplished with the seat back set at the three positions studied during the impact tests, i.e., 90°, 103°, and 110°. The seat pan positions studied were: (1) the lowest position of vertical adjustment, (2) seat pan raised until the helmet contact point was on the lower edge of the headrest, and (3) seat pan raised until the normal helmet contact point was one inch above the lower edge of the headrest as shown in Figure 37. Only the third position would provide any degree of head support during impact exposures where the head and neck would be driven rearward and downward. Photometric data collected during this program showed that the average vertical displacement of the subject's head exceeded one inch.

The data from the anthropometric study show that if the seat pan is in the lowest position, 38 percent of the flying population would not have even marginal head support (helmet contact point one inch above headrest edge) with the seat back at the 90° position, 75 percent would not have adequate support if the seat back were reclined to 103°, and 94 percent would not have adequate support if the seat back were reclined to 110°. This relationship is shown in Figure 38. This figure also shows the position of the lower edge of the headrest and the normal helmet contact point with and without the headrest modification. Note that the current operational configuration does not provide adequate head support for a portion of the flying population, if the seat pan is in the lowest position. Figure 38 can be used to determine the distance the seat occupant must raise his seat to obtain head support. This is accomplished by using the individual's sitting height and measuring the distance from that level up to the level of desired helmet contact. For example, an individual with a sitting height of 34.7 inches (5th percentile) must raise the seat pan 2.7 inches to place the helmet contact point on the lower limit line when the seat back is inclined to 103°, and 4 inches when the seat back is inclined to 110°. Unfortunately, restoration of the lower portion of the headrest is not feasible, since it would force the shoulder straps to be deflected downward, around the lower edge of the headrest, and then upward to the crewmember's shoulders just as in the current operational configuration. In this condition, the retraction force of the inertia reel would be reduced by friction and the mechanical pulley effect of bending the strap around the headrest structure.

The headrest was originally designed to maintain the pilot's eye near the cockpit design eye point during aircraft carrier launch to assure adequate over-the-nose vision. Therefore, the helmet contact point is up to 2 1/4 inches forward of the plane of the seat back rather than in the same plane or one inch aft as is the case of USAF ejection seat design practice. As a result of this problem, an individual's neck will be adversely flexed forward prior to ejection and ground landing impact. This preflexed position of the head and neck creates an additional moment acting on the spinal column to cause down and forward rotation of the upper torso during ground impact and ejection. The fact that the headrest is so far forward of the seat back also aggravates the problem created by removing the lower portion of the headrest. When the impact load causes the helmet to move downward from the headrest, the helmet will impact the shoulder straps.

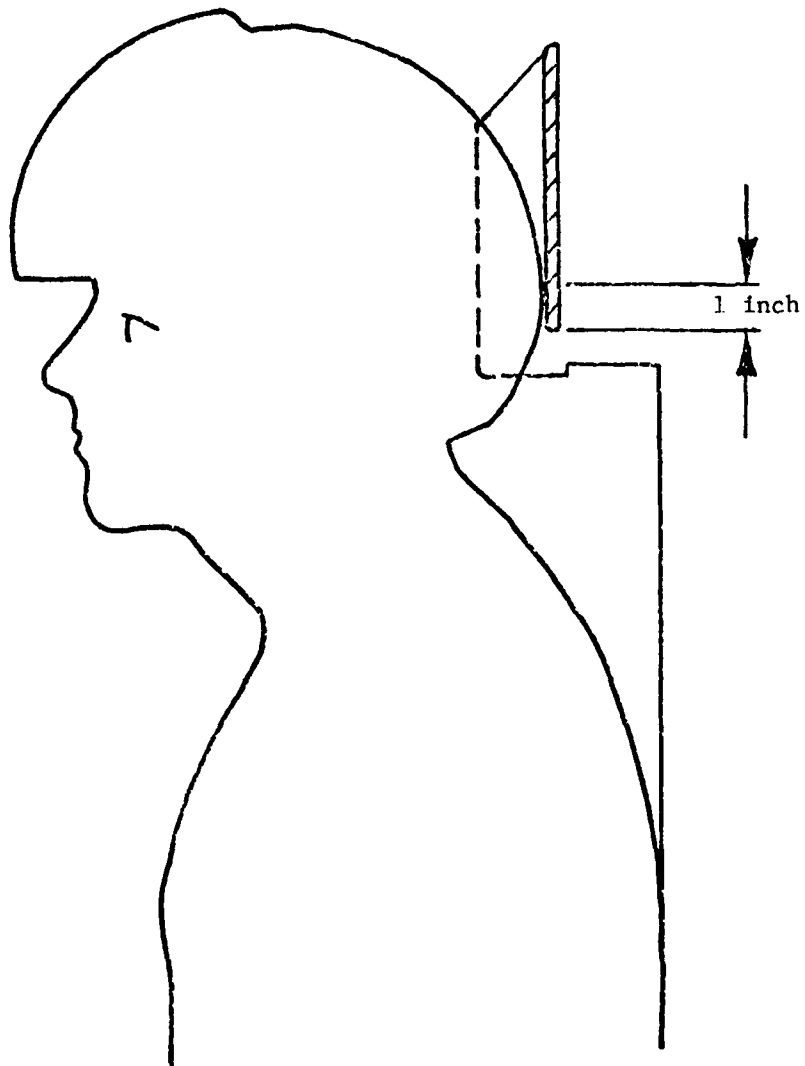


Figure 37. Position of Helmet and Headrest when the Normal Helmet Contact Point is One Inch Above the Lower Edge of the Headrest.

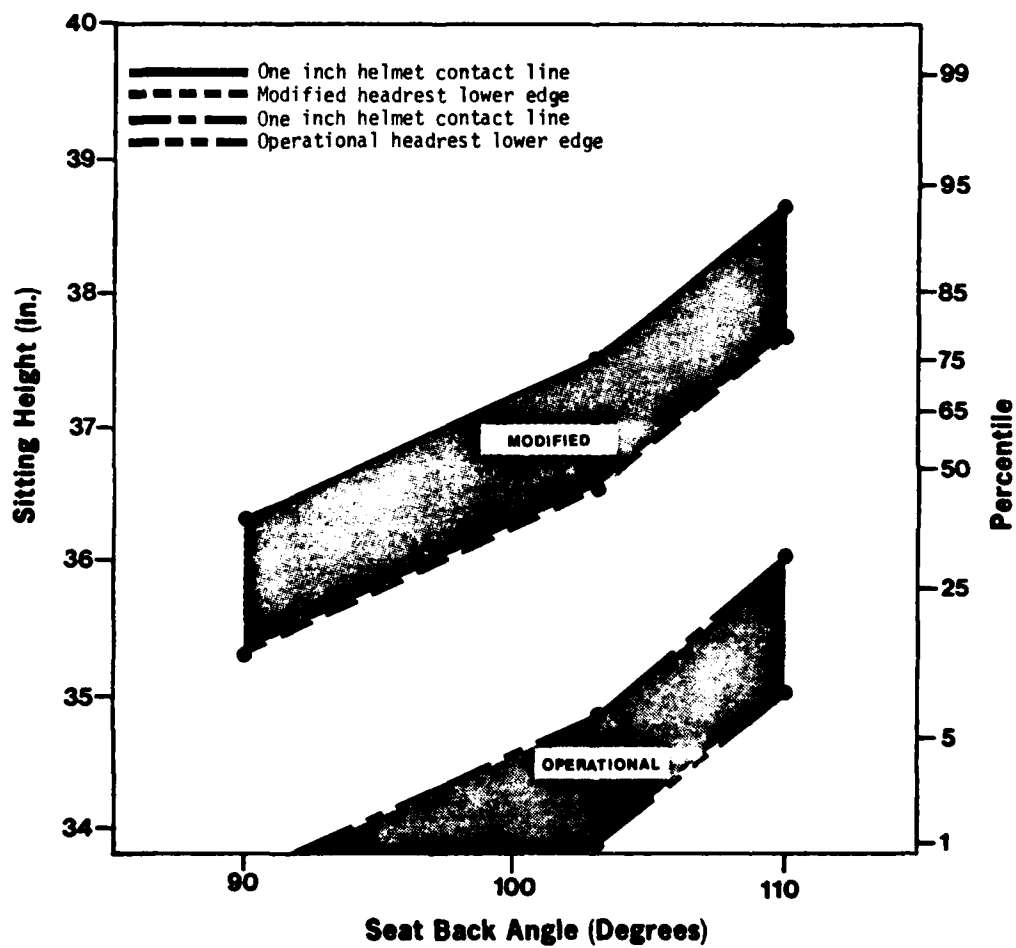


Figure 38. Relationship Between Helmet/Headrest Contact Point and Sitting Height, Sitting Height Percentile, and Seat Back Angle.

From the standpoint of crew size accommodation, the proposed redesign of the F/FB-111 crew seat and restraint system is deficient in two respects. First, it fails to eliminate the possibility that the crewmembers will operate with negative shoulder strap angles. The angles of the inertia reel straps of the current operational restraint and the proposed redesign configuration provide a point of comparison, albeit a limited one. (The complex geometry of the operational reflection strap defies simple characterization.) The inertia reel strap angles range from  $-20^{\circ}$  to  $22^{\circ}$  in the operational system and from  $-9^{\circ}$  to  $+39^{\circ}$  in the proposed system.<sup>1</sup> The reflection strap angles of the proposed modification range from  $-5^{\circ}$  to  $+38^{\circ}$ . Second, the removal of the lower portion of the headrest has degraded the impact protection capabilities of the crew seat configuration. Although it has never been advisable for personnel with small sitting heights to operate with the seat pan in the full down position, crewmembers have not been adequately advised to avoid this position.

The removal of the lower portion of the headrest is an inherent part of the redesign approach. The removal is necessary to provide clearance for the higher position of the shoulder straps. Although this problem was generally recognized as a result of mockup reviews, the extent of the problem was not quantified prior to the commencement of this experimental evaluation. As previously mentioned some subjects were not tested with the seat pan in the full down position because of this problem. Figure 39 shows a crewmember seated in a flight simulator during the mock-up review at Mountain Home AFB (Final Report, TAC Project 79G-019T, 1979). The crewmember was described as a small weapons systems operator with his seat lowered for radar work. The proposed change in the headrest causes further deterioration in system performance. Further redesign should be seriously considered. If the proposed headrest is incorporated without further redesign, all crewmembers must be warned of the hazard.

- 
1. The maximum negative shoulder strap angle occurs when: the seat pan is in the highest vertical position possible with one inch clearance between the occupant's helmet and the aircraft canopy, and the occupant's sitting height is 37.2 inches and mid-shoulder sitting height is 27.3 inches (both 95th percentile dimensions). The headrest of the operational system does not permit the inertia reel strap to have a negative angle more than  $8^{\circ}$  without contact with the strap. As the strap deflects beyond this point, the strap is bent around the headrest structure thereby reducing the retraction force applied to the occupant. The maximum positive angle occurs when the seat pan is moved to the lowest vertical position, the seat back angle is fully reclined, and the occupant has a mid-shoulder sitting height of 23.7 inches (5th percentile).



Figure 39. Weapons Systems Operator with His Seat Lowered for Radar Work.

#### D. BACK INJURY MECHANISM IMPLICATIONS

The back injury mechanism assessment (Kazarian, 1977), which served as the basis for the modification program, theorized that back injuries in the use of the F/FB-111 emergency escape system resulted from the presence of negative shoulder harness angles. These angles occur when the aft attachment point of the shoulder harness is below the level at which the shoulder harness passes over the crewmember's shoulder. For the harness currently in operational use, determination of the value of this angle is a complex question since each strap from the inertia reel passes forward to the shoulder, around a roller and then aft and across to attach to the contralateral upper seat back structure, as previously shown in Figure 11. Quantification of the angle of the reflection strap depends on whether it is defined as the angle between the strap and its vertical projection on a horizontal plane or as the angle between the strap's horizontal projection on a sagittal plane and the waterline. The proposed modification raises both posterior attachment points. It also moves the attachment point of the reflection strap posteriorly and medially, since it utilizes the headrest structure rather than the seat structure. The difficulty in defining the angle remains. The angles reported in this test program are in accordance with the first definition stated above.

For some crewmembers, the result of the proposed modification would be to change the shoulder harness angle from near  $0^{\circ}$  to a larger positive angle. This has now been experimentally shown to be associated with degraded lateral and vertical impact protection. For other crewmembers, the modification may raise the angle from a negative angle to near zero. The effect of this variation is difficult to assess, since no tests were performed in the current series with a significant negative shoulder strap angle. The performance of such tests was avoided, since the premise on which the proposed modification is based was that the negative shoulder strap angle is the primary restraint system design factor causing the excessive spinal injury rate. On the other hand, positive angles with the seat in the full down position were, in general, not extreme. Shoulder harness angles that were recorded during the tests ranged from  $-1^{\circ}$  to  $33.5^{\circ}$ . The vertical travel from full down to the position producing a  $0^{\circ}$  shoulder harness angle was not great for large subjects. The mean angle for  $0^{\circ}$  tests was  $2.59^{\circ}$ , with a standard deviation of  $2.97^{\circ}$ , and a range of  $16.5^{\circ}$ . The large range is due to the fact that some small subjects did not reach  $0^{\circ}$  even with the seat full up. The mean angle for all full down tests was  $23.6^{\circ}$  with a standard deviation of  $7.02^{\circ}$ , and a range of  $28.75^{\circ}$ . The mean tended to increase with seat position as the seat was reclined from  $90^{\circ}$  to  $103^{\circ}$  or  $110^{\circ}$ . It should be further noted that reclining the seat from  $90^{\circ}$  with the shoulder harness angle maintained at  $0^{\circ}$  with respect to the waterline, effectively raises the shoulder harness angle with respect to the spine. The larger range and standard deviation in the full down case is due to the fact that some large subjects did not develop large positive angles in the full down position since they were already in the lower range of seat travel at zero degrees.

These considerations lead to the conclusion that the body restraint and support deficiencies observed in this study will apply more to crewmembers having small to medium mid-shoulder sitting heights and/or crewmembers flying in the right seat position and having a tendency to use lower seat position adjustments. The improvement or degradation for crewmembers having medium to large mid-shoulder

sitting heights cannot be clearly established, since negative shoulder harness angles were not utilized with human subjects. This prevented the performance of human tests using the operational harness with negative and zero shoulder harness angles as required to complete the comparison. It must be recognized, therefore, that assessments of the relative effectiveness of the proposed modification are based on a partial experimental data base. This must be coupled with reasonable assumptions about the performance of the currently operational system derived from cautious examination of the previous Holloman AFB tests results and the official accident data base as compiled at the Air Force Inspection and Safety Center, Norton AFB.

The limitations of the data base for the assessment of the proposed modification are, in the opinion of the investigators, more important in the evaluation of the vertical impact protection provided by the proposed modification, since no experimental comparison could be made with the operational system. Furthermore, comparison with impact tests of conventional restraint systems proved of no value, because these restraints have not been tested using the unorthodox seat configuration of the F/FB-111. Therefore, after a more detailed review of existing F/FB-111 accident data, completion of an experimental risk analysis, and approval of human use protocols, the investigators intend to conduct a series of vertical impact tests of the operational restraint system and a conventional lap belt/shoulder harness to complete the data base.

In spite of the difficulties noted above, certain conclusions can still be drawn which expand the back injury mechanism assessment previously available. Experimental experience with the test item had led to a deeper appreciation for the complexity of the problem. The insights gained in assessing the proposed modification can also be applied to develop an understanding of effective mechanisms in the currently operational system.

The F/FB-111 system departs markedly, in several important areas, from conventional restraint and body support design philosophy. These areas have been previously identified in this report: the use of the shoulder harness yoke, the use of the crossing reflection straps, the potential for imposition of negative shoulder harness angles, the location of the headrest well forward of the seat back plane, and the wide latitude for seat geometry adjustment, including the independent motion of the seat with respect to the headrest. These variations from conventional design practice that are present in the current operational system have not been eliminated in the proposed modification. Therefore, findings derived from the modified system may be cautiously applied to the operational system if the differences are considered.

The apparent intent of the crossing reflection straps, in concert with the shoulder harness yoke assembly, is to provide lateral restraint during ground landing impact. In the first place, the available experimental data base indicates that lateral restraining forces are best applied by means of body support plates rather than by harness restraint. In the second place, this technique apparently imposes unconventional loads on the crewmember which have not been adequately addressed in previous analyses. The primary intention of the modification is based on eliminating downward loads applied by the shoulder straps by raising both inertia reel and reflection strap tie-down positions. However, the reflection straps produce a medial load as well, since the force at



each shoulder roller is the resultant of the nominally aft-directed inertia reel strap and the aft and medially-directed reflection strap. The medial component would be even greater in the operational harness. The effect of the forces is to pull the shoulders toward each other posteriorly in a manner similar to a figure 8 clavicle strap.

Such forces may be deleterious in at least two ways. First, they correlate well with the clinically observed anterior parasternal and sterno-clavicular symptomatology observed in the F/FB-111 ejectees. Secondly, these forces tend to rotate the scapulae medially, forming a potential fulcrum which may act in the genesis of the hyperextension injuries theorized by Kazarian (1977).

A further problem in this lateral restraint technique relates to the yoke, as previously described in Section 8D. If the yoke is adjusted too tightly, or if it is adjusted while the spine is moderately flexed, the yoke will provide a downward load on the crewmember during retraction, even with positive shoulder harness angles. In fact, in the extreme case, the yoke may prevent torso erection altogether, since the yoke can cause the distance from the seat pan to the upper spine to be less than required for an erect torso against the seat back. If full retraction takes place, spinal injury is likely to result, probably by means of a hyperflexion mechanism. If retraction is not complete, the crewmember will be held in a non-optimum position for ground impact, predisposing to injury, the type probably depending on the relative magnitude of  $G_y$ ,  $G_z$ , and whether the component in the X axis is positive or negative.

A further imposition of non-optimum position for ground landing occurs as a result of the headrest position forward of the seat back plane. This is more pronounced for seat back angles close to  $90^\circ$ . The  $+G_z$  test data indicates greater hyperflexion for the  $90^\circ$  seat back angle and for more positive shoulder harness angles. If the headrest were further aft, then the head could be allowed to achieve a more erect position and  $+G_z$  acceleration would produce less forward and down head rotation.

The unusual design approach in this system, with many sources of adverse loading, makes it difficult to assign a simple cause and effect mechanism for spine injury. It would be particularly surprising to find that at least three dissimilar types of spinal injuries experienced in such a thoroughly unconventional system could be remedied by the simple expedient of partially correcting negative shoulder harness angles.

If the premise is accepted that negative angles may increase injury potential and should therefore be removed, we would expect that the proposed modification would lead to decreased injuries, particularly in large crewmembers. However, the current test results indicate that lateral impact protection is degraded, according to several criteria, as the shoulder harness angle is raised from  $0^\circ$  to the relatively large positive angles in the modified configuration. Furthermore, the results of the vertical impact tests showed that the tendency for hyperflexion of the head and neck is increased as the seat pan is lowered and the harness angle is increased. Assuming that the proposed modification and the operational harness are equivalent for  $0^\circ$  shoulder harness angles, this raises the question of new injury potential from the modification, particularly in smaller crewmembers. (The improvement or degradation of lateral, vertical, and fore-aft protection with variation from negative to  $0^\circ$  shoulder harness angle remains unknown.) In order to rationally assess the

trade-off between potential for decreased injury and potential for increased injury from the modification, it would be necessary to experimentally quantify actual injury rates in the two configurations at operational impact levels. This, of course, cannot be done. We are left with the problem of estimating the trade-off with insufficient data. From an aeromedical point of view, however, we have the following information:

1. Negative shoulder harness angles, in this harness, have been theorized to lead to back injury.

2. Positive shoulder harness angles, during the experimental program, have led to measurably degraded performance in lateral and vertical impact tests, when compared to a horizontal shoulder harness.

3. Experience with this harness during the experimental program has led to the identification of plausible additional/alternate mechanisms for the operational injuries that would not be addressed by eliminating negative shoulder harness angles alone.

4. The F/FB-111 seat and restraint system departs radically from proven design practice in a number of areas. These areas include, for example, headrest location well forward of the seat back plane, independent vertical motion of the seat with respect to the headrest and shoulder harness attachment, medially deviated resultant force applied by the shoulder harnesses, and a shoulder harness yoke device allowing adjustment which may restrict erection of the torso during retraction.

5. The F/FB-111 crew module acceleration and force differ radically from that of an open ejection seat, but does not differ radically from impact accelerations and forces which have been extensively studied experimentally. Areas of difference include, for example, absence of windblast and an arbitrary acceleration direction imposed on the seated occupant during ground landing impact.

Conclusions which appear evident from an examination of the above considerations and the available information base are as follows:

1. It would be surprising to find comparable restraint performance between the F/FB-111 system and an open ejection seat system, since both the restraint designs and the acceleration-force environments differ radically.

2. Since the wealth of experimental human impact experience more closely characterizes the F/FB-111 environment than that of an open ejection seat, it would seem most reasonable to consider proven design practice in order to further improve this system (e.g., conventional seat belt - double shoulder harness with deployed side body support plates). This would of course involve a more extensive redesign and retrofit effort than is associated with the proposed modification.

3. If the above solution is not practical at this late date, limited modifications to the existing harness system will be problematic at best, since the trade-offs remain uncertain. Negative shoulder harness angles represent only one of the many deviations from proven design practice. Their elimination should probably be pursued, but only as a part of a hardware (and,

if necessary, procedural) modification program, which attempts to address the other mechanisms by which undesirable forces may be placed on the crewmember and the attendant problems which may be unintentionally produced by the modification.

The objective of this test program has been not to verify that the proposed modification would be effective in decreasing injury, but rather to determine if the restraint performance would be potentially degraded by its incorporation. Such degradation has been measured. However, the extensive effort devoted to this test program has led to the accomplishment of more than the objective. Much has been learned as the dynamics of this restraint system have been studied with human subjects. New insights have resulted. The findings and conclusions go beyond the stated objectives, but they are nevertheless derived from the planned testing and are considered relevant to the requirements which led to this test program.

## Section 10

### SUMMARY OF CONCLUSIONS

A. THE FOLLOWING OBSERVATIONS AND CONCLUSIONS WERE REACHED AS A RESULT OF THE ANALYSIS OF THE F/FB-111 SEAT AND RESTRAINT SYSTEM REQUIRED IN ASSOCIATION WITH THE CURRENT TEST PROGRAM.

1. The acceleration stress which would be imposed on a conventionally restrained aircrewman in an F/FB-111 crew module is sufficient, both at high speed ejection and at ground landing impact, to cause a significant spinal injury rate. (Section 1A.) It is different from the acceleration stress imposed by all other operational escape systems.
2. Accident data from October 1967 to October 1979 has revealed a spinal fracture rate of 34% of survived ejections. (Section 1A.)
3. Dr. Kazarian has suggested that the operational injuries may be significantly reduced by elevating all posterior attachments for the shoulder harnesses, since he theorized that the high injury rate is partly caused by the negative shoulder harness angles. He also suggested adding an extension to the upper seat back structure. (Section 1A.)
4. General Dynamics, under contract to ASD/AES, has developed a proposed modification to the seat design, incorporating Kazarian's suggestions. The stated objectives of the contract effort (Section 1A) are:
  - (a) Eliminate the downward component of force on the spine caused by the shoulder straps during retraction/ejection and ground landing impact.
  - (b) Reduce rotation (down and forward) of the shoulders and back on ground impact.
  - (c) Extend the seat back to provide support for the upper back during powered retraction.
5. Because of redesign constraints (including cost), the redesign continues to incorporate a variety of deviations from conventional design practice, including a shoulder harness yoke assembly which may restrict torso erection and produce downward spinal loads, a cross-over reflection strap arrangement which produces a medial-posterior resultant load at each shoulder, a headrest assembly which may orient the head well forward of the seat back plane, and a geometrical seat adjustment capability which may place some crewmembers in awkward positions. (Sections 3B, 9C, and 9D.)
6. The analysis of these deviations has led to the identification of additional potential and plausible injury mechanisms not involving negative shoulder harness angles. (Section 9D.)
7. The AFAMRL test program reported herein was designed to assess whether the proposed modification might otherwise degrade crew protection. The assessment was to be based on analysis of data from vertical (+G<sub>z</sub>), sideward (+G<sub>y</sub>), and forward facing (-G<sub>x</sub>) impact tests and comparison with tests of the operational harness conducted years ago at Holloman AFB before installation of the operational harness into the crew module. No AFAMRL tests were to be conducted with the operational harness or with negative shoulder harness angles to

assess the alleged benefits to be expected from the design objectives, presented in paragraph 4 above.

B. THE FOLLOWING FACTS SUMMARIZE THE AFAMRL TEST PROGRAM.

1. Tests were conducted in such a way that effects of varying seat back angles and shoulder harness angles could be elucidated. The seat back angles tested were  $90^{\circ}$ ,  $103^{\circ}$ , and  $110^{\circ}$  from horizontal. Shoulder harness angles that occurred during the tests ranged from  $-1^{\circ}$  to  $33.5^{\circ}$ . (Section 2.)

2. The test item was provided by General Dynamics with additional instrumentation supplied by AFAMRL. (Section 3B.)

3. Subjects (male and female) were qualified and utilized in accordance with applicable human use regulations. (Section 6.)

4. The Vertical Deceleration Tower and the Horizontal Decelerator Facility were utilized to provide nominal experimental  $+G_z$  impacts of 10 G (30 ft/sec),  $+G_y$  impacts of 8 G (30 ft/sec) and  $-G_x$  impacts of 10 G (32 ft/sec). (Sections 4A and 4B.)

5. Relevant accelerations, forces, and loads were measured electronically. Appropriate physiological data were obtained. High speed cameras documented subject motion. (Sections 4D, 4E, 4F, and 4G.)

6. The Wilcoxon paired-replicate rank test was used to assess the statistical significance of the results. (Section 5A.)

7. Human subject tests took place between 21 June and 13 November 1979. A total of 187 tests were performed with the volunteer subjects. Seventy-three of these tests were vertical impacts, 60 were sideward impacts, and 54 were accomplished with forward facing impact orientations. (Section 7.)

8. The sideward impact test program was discontinued following an injury to a female subject. This resulted in an incomplete sideward impact test set. (Section 9B.)

C. THE FOLLOWING OBSERVATIONS AND CONCLUSIONS WERE DERIVED FROM THE TEST DATA ANALYSIS.

1. All forces, loads, and accelerations measured at these impact levels were considered to be well within human tolerance, in spite of the unexpected occurrence of a serious knee injury during an 8 G sideward impact test. (Sections 8 and 9B.)

2. Chest acceleration measured during vertical impact tests decreases as the seat is reclined, apparently due to increasing support from the seat back. (Section 8A.)

3. Head X acceleration in  $+G_z$  impact tests increases as the seat is erected. This increase would presumably be less if the headrest did not position the head so far forward. (Section 8A.)

4. Head acceleration in  $+G_z$  impact tests increases, particularly in the Z axis, as the seat pan is lowered and the shoulder harness angle is increased. (Section 8A.)

5. The shoulder harness loads measured in sideward impact tests (where the subject's inertial response was leftward) appear to increase on the left and decrease on the right, as the seat reclines and/or as the shoulder harness angles are increased. The lap belt and crotch strap loads increase as well. Since reaction of the subject was to the left into the harness, these results indicate less adequate sideward restraint with a reclined seat and/or when the seat pan is in a lower position and the shoulder harness angles are large. (Section 8B.)

6. X axis testing demonstrated physically consistent and reasonable results. No evidence of degraded performance was noted; however, there was also no evidence of improved performance. (Section 8C.)

7. The knee injury of the female subject indicated potential for unexpected injuries with subjects having unusual anthropometric proportions and/or variations in bracing. (Section 9B.)

D. THE FOLLOWING CONCLUSIONS RESULT FROM COMPARISON OF AFAMRL DATA ON THE PROPOSED MODIFICATION WITH TEST DATA ON THE OPERATIONAL SYSTEM COLLECTED AT HOLLOMAN AFB.

1. The modified reflection straps appear to carry greater loads in  $-G_x$  impact. (Section 9A.)

2. The modified reflection straps appear to carry lower loads in  $+G_y$  impact, consistent with degraded sideward restraint. (Section 9A.)

E. THE FOLLOWING CONCLUSIONS DERIVE FROM THE ANTHROPOMETRIC ANALYSIS.

1. Negative shoulder strap angles are still possible when the modified harness is used, although the possibility of negative shoulder harness angles has been reduced from 34% of the flying population to 13%. (Section 9C.)

2. The modified headrest degrades head support when the seat is in the lower range of vertical seat adjustment. (Section 9C.)

F. THE FOLLOWING ARE GENERAL CONCLUSIONS.

1. Trends appear in experimental test data which indicate potentially degraded impact protection for some crewmembers in the F/FB-111 system modified as proposed.

2. The accelerations imposed on the F/FB-111 capsule during high speed escape and ground landing impact can be expected to injure a significant number of aircrewmembers, even with optimum restraint.

3. A major reduction of the spinal injury rate as a result of incorporating the proposed modification appear problematic since:

(a) The data indicate that the tendency for hyperflexion of the head and neck during vertical acceleration is increased when the shoulder strap angle is a large positive value.

(b) Several plausible injury mechanisms remain in the modified system, even with positive shoulder harness angles.

(c) The modification continues to allow negative shoulder harness angles for a significant number of crewmembers who are seated in operationally likely seat positions.

(d) Head support is reduced or eliminated for a significant number of crewmembers when the seat is in the lower vertical adjustment range.

4. Significant reduction of the spinal injury rate appears achievable only by a combination of three approaches:

(a) Conduct further experimental research to: (1) determine the relative efficacy of the current operational crew seat and restraint system, the proposed modification, and a more conventional restraint system; (2) better define the phase of the escape sequence and the etiology of the spinal injuries that have been observed; and (3) generically investigate the relationships between protection system design factors (such as headrest position, shoulder strap angle, pre-impact body positioning/bracing, and anthropometric variations) and the human body impact responses that are related to spinal injury potential.

(b) Application of proven design principles to the F/FB-111 crew seat and restraint system, involving a more extensive modification than currently proposed.

(c) Decreasing the acceleration stress imposed by high speed escape and, in particular, the high impact loads experienced during ground landing impact in the F/FB-111 crew module.

APPENDIX A  
DATA ACQUISITION EQUIPMENT AND METHODS

Prepared by  
Harold F. Boedeker  
Greg A. Buckingham

Dynalelectron Corporation  
Scientific Services Division

Prepared under  
Contract F33615-79-C-0523

INTRODUCTION

Under Contract F33615-79-C-0523, Dynalelectron was requested by the Air Force Aerospace Medical Research Laboratory/Biomechanical Protection Branch to instrument a test fixture fabricated by General Dynamics Corporation and collect data under test conditions for the F/FB-111 Crew Seat and Restraint Harness Redesign evaluation program. The testing was conducted in three axes of acceleration on the Horizontal Deceleration and Vertical Deceleration Tower Test Facilities located at the Air Force Aerospace Medical Research Laboratory, Building 824, Area B, Wright-Patterson Air Force Base. The following is a discussion of the equipment and procedures used in acquiring and processing data to describe the kinematic and inertial responses of the human body. Installation and sensor specifications along with operating principles and data acquisition techniques are discussed.



## DATA MEASUREMENT DEVICES

### ACCELEROMETERS

Twelve accelerometers were installed on the test fixture. These accelerometers were configured in groups of three to create triaxial measurement packages. Each package was mounted to measure accelerations in the X, Y, and Z axes. Figure A - 1 shows the coordinate system utilized for the testing and the corresponding output polarity for an applied acceleration.

The accelerometer package used to measure head accelerations was designed for use inside the subject's mouth. It consisted of three Endevco Model 2264 accelerometers mounted to a plastic block and covered with medical grade silicone rubber sealant. This created a small electrically isolated package approximately 9/16 x 9/16 x 1 inch with three cables exiting one end. The accelerometer package was mounted to a special dental bite block that was custom fitted to each subject. When assembled, the unit weighed approximately 50 grams. The specifications of the accelerometers used in the package are shown in Figure A - 2. During dummy runs the dental bite block was not used and the package was mounted to a bracket at the approximate center of the dummy's head.

The chest accelerometer package consisted of three Endevco Model 2264 accelerometers mounted on an aluminum block  $\frac{1}{2} \times \frac{1}{2} \times \frac{1}{2}$  inch. This block was inserted into an aluminum protective shield to which was attached a length of Velcro<sup>®</sup> fastener strap. In use the package was placed over the subject's sternum and was held in place by fastening the Velcro<sup>®</sup> strap.

The sled (carriage) accelerometer package consisted of two Endevco Model 2264 and one Endevco Model 2262. These accelerometers were rigidly fastened to the test sled or carriage to measure the acceleration vectors. The package was oriented such that the Model 2262 transducer measured the primary acceleration and the Model 2264's measured the secondary axes. The specifications for these accelerometers are shown in Figures A - 2 and A - 3.

#### HARNESS INSTRUMENTATION

The harness instrumentation consisted of seven load measuring transducers located at the seven points the harness attached to the seat. The harness, seat, and test fixture are shown in Figure A - 4. Two types of transducers were used in measuring harness loads. Five of the transducers were strain gage bridges bonded to the restraint harness hardware end fittings. The remaining two were automotive belt load measuring cells (see note 1). All of the transducers produced a positive output when placed under tension in accordance with the AFAMRL/BBP coordinate system.

The five strain gage transducers were of three types as shown in Figure A - 5. Each unit had four strain gages attached and wired as a four arm active bridge. Figure A - 5 shows the wiring diagram of the units using 350 ohm resistive gages (Micro Measurements EA-06-125BZ-350). The two reflection strap units are pictured in Figure A - 6, also the lap and crotch strap units are pictured in Figure A - 7. The two automotive belt load cells were placed to measure inertia reel strap loads as shown in Figure A - 6. These units are Lebow Model 3419 automotive belt force cells. The specifications are shown in Figure A - 8.

#### SEAT PAN INSTRUMENTATION

The seat pan instrumentation consisted of nine transducers measuring force and acceleration. Acceleration measurements were made

Note 1) One harness cell was originally a belt load type device and was replaced by a strain gage device. See Section "Z Axis".

using Endevco Model 2264 accelerometers mounted on a plastic block at the approximate center of the seat pan assembly. These accelerometers were oriented along with X, Y, and Z coordinate axes according to the AFAMRL/BBP coordinate system (Reference Figure A - 1). The specifications are contained in Figure A - 2.

The load measurements were made utilizing two types of force transducers to fit the physical size limitations of the seat pan. Z axis load measurements were taken using Strainert Flat Load Cells Model FL2.5U2SPKT. Three of the cells were used in a three point mounting configuration as shown in Figure A - 9. The X axis and Y axis loads were measured using devices built specifically for this application by General Dynamics. These load links were instrumented with resistive strain gages as shown in Figure A - 10. Each load link has four resistive arms with 2 arms active. The end of each unit was mounted with swivel balls to eliminate cross-axis forces in the measurements. All of the force transducer outputs were wired to correspond with the coordinate system shown in Figure A - 11.

#### FOOT REST INSTRUMENTATION

The foot rest assembly was instrumented with three GSE load cells Model T-10952C. These load cells were mounted between the foot pedal support and the test fixture to measure applied foot loads. The load cell orientation was changed between the vertical and horizontal tests. Figure A - 13 shows the two orientations and the drawings of Figure A - 12 show the load cell location for the two configurations. Each cell measured triaxial loads. The cells were capable of measuring 2500 lb in the Z axis and 500 lb in the X and Y axes.

#### Z AXIS (VERTICAL IMPACT)

The seat geometry drawing in Figure A - 14 shows the polarity of the various output signals. Included in the drawings are the dimensions of each fixed load cell and the variables introduced by the seat

height and seat pan adjustments. The crotch strap load was measured using a Lebow belt tension gage in place of the strain gages on the harness. The Digital Instrumentation Requirements sheet of Figure A - 15 contains the pertinent data for all of the transducers used in the  $G_z$  test program.

#### Y AXIS (SIDEWARD IMPACT)

During the Y axis test program three different transducers were used to measure the crotch strap load. The program commenced using the Lebow belt cell which was replaced by a strain gage harness buckle. This first harness strain gage unit was damaged during testing and replaced with another strain gaged cell. The sled Y accelerometer was an Endevco Model 2260 used in the primary axis of testing as the sled reference. The drawings of Figure A - 16 illustrate the seat geometry for the Y axis testing as well as the seat pan adjustment and the harness geometry. The Digital Instrumentation Requirements sheets of Figure A - 17 contain the pertinent data for all of the transducers used in the sideward test program.

#### X AXIS (FORWARD IMPACT)

The Endevco Model 2260A sled X accelerometer which was in use at the start of the X axis program became unstable and was replaced by an Endevco Model 2262 accelerometer. The seat geometry drawings shown in Figure A - 18 contain the load cell dimension locations and the seat pan adjustment references. The Digital Instrumentation Requirements sheet of Figure A - 19 contains the pertinent data for all of the transducers used in the X axis test program.

#### CALIBRATION

Strainsert Load Cells were calibrated on a periodic basis at the Precision Measurement Equipment Laboratories (PMEL), Wright-Patterson Air Force Base. The PMEL returns each device with a certificate providing current sensitivity and linearity data.

Accelerometers, strain gaged belts, and Lebow belt load cells were calibrated at the AFAMRL/BBP Laboratory. These calibrations were performed prior to and upon the completion of each phase of the test program. Calibration of each test accelerometer was performed to determine sensitivity, phase, and frequency characteristics by using the reciprocity method. This method utilizes a shaker table to physically vibrate the test and standard accelerometers simultaneously for comparison of the outputs.

Test accelerometer sensitivity was obtained by comparing the output at 100Hz and 40G to the output of a laboratory standard accelerometer which is calibrated yearly to standards traceable to the National Bureau of Standards. The frequency response and phase characteristic of each accelerometer was obtained using a random noise generator to drive the shaker assembly and analyzing the output data by Fourier Analysis via the PDP 11/15 and Time Data unit. Accelerometer natural frequency and dampening factor are also derived and computed from this information.

Belt load cells and strain gage cells were calibrated under tension load on a special test fixture. The sensitivity and linearity of each device was obtained by comparing its output to that of the "standard" load cell mounted to the test fixture. The "standard" load cells are also calibrated on a yearly basis by standards traceable to the National Bureau of Standards. Factory calibration data for the GSE Triaxial Load Cells were used for this test program.

All calibration records are maintained on file for reference. The pre and post test calibration data for the "in-house" calibrated devices for each of the three phases of the test program are shown in the Table of Figure A - 20.

## ACCELEROMETER COORDINATE SYSTEM

### ACCELERATION

Accelerometers will be oriented and wired to provide an output corresponding to the applied acceleration. Use this table as a reference:

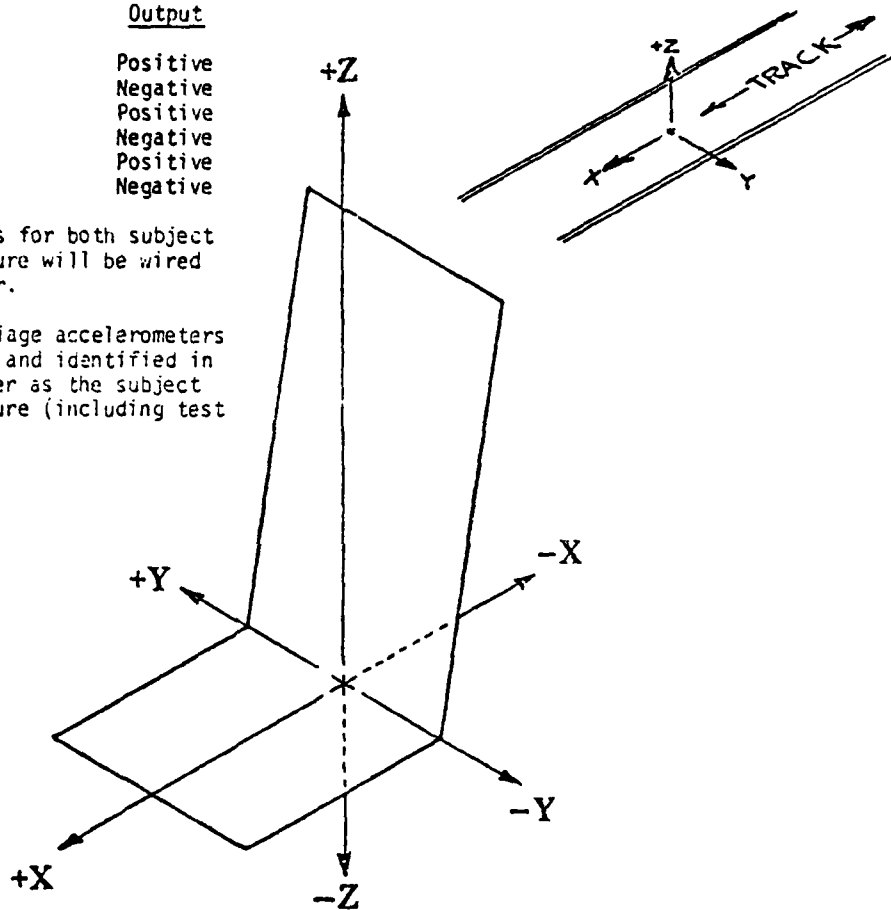
Acceleration	Output
+Gx	Positive
-Gx	Negative
+Gy	Positive
-Gy	Negative
+Gz	Positive
-Gz	Negative

Accelerometers for both subject and test fixture will be wired in this manner.

Sled and carriage accelerometers will be wired and identified in the same manner as the subject and test fixture (including test profiles).

### BARE SLED AND MACHINE TESTS

Accelerometers will be oriented to provide outputs to agree with track coordinate system with polarities as noted in test log.



## AMRL BBP COORDINATE SYSTEM ( Left Hand Rule )

Figure A - 1

# MODEL 2264-200

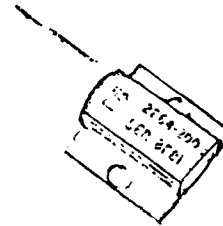
±200 g  
One gram

## MINIATURE PIEZORESISTIVE ACCELEROMETER

The Model 2264-200 is a very low mass, piezoresistive accelerometer designed for modal studies, flutter testing and similar applications requiring good low frequency response and minimum mass loading.

With only a small amount of damping, the Model 2264-200 has no phase shift over its useful frequency range of steady state to 1200 Hz. Protection against overranging results from the high environmental rating of ±1000 g peak. The accelerometer can be operated over a temperature range of 0°F to 150°F (−18°C to 66°C).

The 2264-200 utilizes Piezite® Element Type P-11 gages in a half bridge circuit providing a low impedance nominal output of 500 mV full scale at 10 Volts dc excitation.



### SPECIFICATIONS FOR MODEL 2264-200 ACCELEROMETER

#### DYNAMIC

RANGE ..... −200 g to +200 g  
SENSITIVITY (at rated excitation)<sup>1</sup> ..... 2.5 mV/g, nominal; 2.0 mV/g, minimum  
MOUNTED RESONANCE  
FREQUENCY ..... 1700 Hz, nominal  
AMPLIFICATION FACTOR, Q ..... 10, maximum, at resonance and 75°F  
FREQUENCY RESPONSE<sup>2</sup>  
(reference 100 Hz) ..... ±10% max., 0 to 1200 Hz  
at +75°F (24°C)  
TRANSVERSE SENSITIVITY ..... 3% maximum  
LINEARITY AND HYSTERESIS<sup>3</sup> ..... ±2% of reading, maximum, 0 to 150 g;  
±2.5% of reading, maximum, 0 to 200 g.  
THERMAL SENSITIVITY SHIFT ..... ±40 mV max., at 0°F and 150°F  
(−18°C and 66°C), ref. 75°F (24°C)  
WARMUP TIME ..... 1 minute

#### ELECTRICAL

EXCITATION<sup>4</sup> ..... 10.0 V dc  
RESISTANCE PER ARM<sup>5</sup> ..... 1700Ω ± 20%, at +75°F (24°C)  
ZERO MEASURAND OUTPUT ..... ±50 mV dc max., at +75°F  
THERMAL ZERO SHIFT ..... ±40 mV max., at 0°F and 150°F  
(−18°C and 66°C)  
INSULATION RESISTANCE<sup>6</sup> ..... 10M Ω minimum at 100 V dc

#### ENVIRONMENTAL

##### ACCELERATION LIMIT<sup>7</sup> (in any direction)

Static: ±1000 g.  
Sinusoidal: ±1000 g pk.  
Shock: ±1000 g pk, 1.5 millisecond duration or longer.  
CAUTION: Keep protective sleeve on accelerometer until ready to use.

##### TEMPERATURE

Operating: 0°F to 150°F (−18°C to 66°C)  
Non-Operating: −65°F to 200°F (−54°C to 93°C)

##### HUMIDITY ALTITUDE

Epoxy Sealed  
Not Affected

#### NOTES

- <sup>1</sup>Measured with steady state acceleration.
- <sup>2</sup>In shock measurements, minimum pulse duration for half sine or triangular pulses should exceed 1.5 milliseconds to avoid excessive high frequency ringing. (See Endevco Piezoresistive Accelerometer Manual.)
- <sup>3</sup>Unit is calibrated at 10.0 V dc. Lower excitation voltages may be used but should be specified at time of order. Use ENDEVCO's Model 4220 Power Supply, or Model 4470 Signal Conditioning as excitation source.
- <sup>4</sup>Due to self heating of the piezoresistive elements, the measured resistance is sensitive to the applied voltage.
- <sup>5</sup>Measured between all leads tied together and shield or case.

Figure A - 2- ACCELEROMETER SPECIFICATION

2262A-200  
2262CA-200

Damped, Overload Stops

PIEZORESISTIVE  
ACCELEROMETERS



SPECIFICATIONS FOR MODEL

2262A-200 and 2262CA-200 ACCELEROMETERS

DYNAMIC

RANGE

-200 g to 200 g

OVERRANGE LIMITING

±300 to ±1 200 g

SENSITIVITY

2.5 mV/g typical  
(1.2 mV/g typical)

2 mV/g minimum  
(1 mV/g minimum)

MOUNTED NATURAL FREQUENCY (AT 75°F)

7 000 Hz typical

FREQUENCY RESPONSE

±5% maximum 0 to 3 000 Hz  
at 75°F, -35°F/10°; typical at  
0/200°F and 3 000 Hz

DAMPING RATIO

0.7 typical

TRANSVERSE SENSITIVITY

3% maximum

THERMAL SENSITIVITY SHIFT

LINEARITY AND HYSTERESIS

±2% of reading, maximum,  
to 200 g

ELECTRICAL

EXCITATION

10.00 Vdc

INPUT RESISTANCE (AT 75°F)

1 800 Ω typical  
(1 000 Ω typical)

OUTPUT RESISTANCE (AT 75°F)

1 200 Ω typical  
(1 000 Ω typical)

INSULATION RESISTANCE

100 GΩ minimum

ZERO MEASURAND OUTPUT

±25 mV maximum

ENVIRONMENTAL

ACCELERATION LIMITS  
(in any direction)

0°F to +200°F

Static 2 000 g  
Sinusoidal 1 000 g pk  
Shock 2 000 g half sine pulse

TEMPERATURE

Compensated 0°F to +200°F (-18°C to +93°C)  
Nonoperating -20°F to +220°F (-29°C to +104°C)

HUMIDITY

Sealed by glass to metal fusion and welding.

Figure A - 3- ACCELEROMETER SPECIFICATION



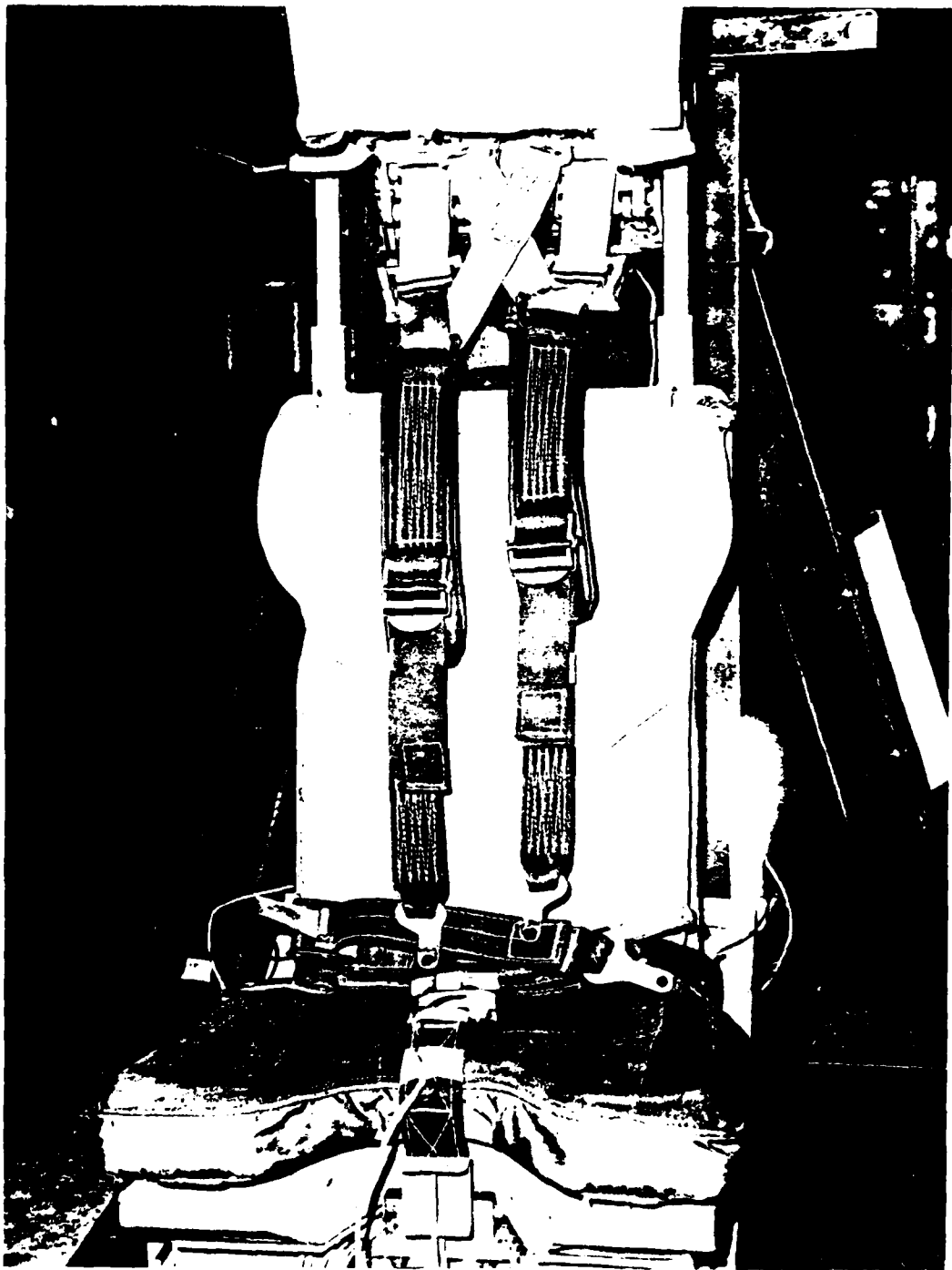
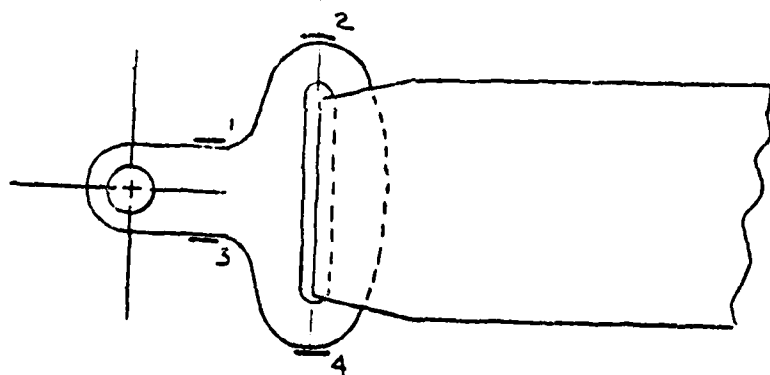
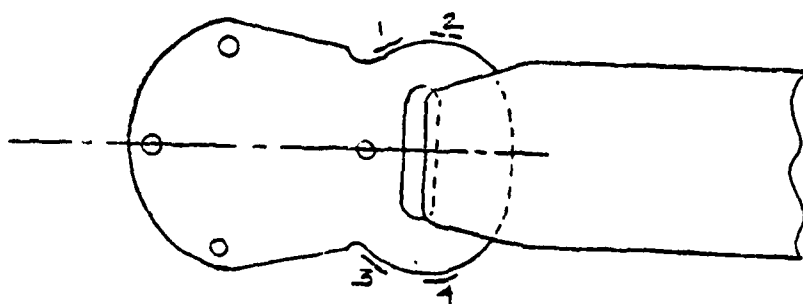


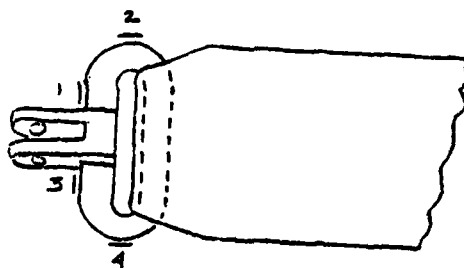
Figure A - 4- HARNESS ASSEMBLY



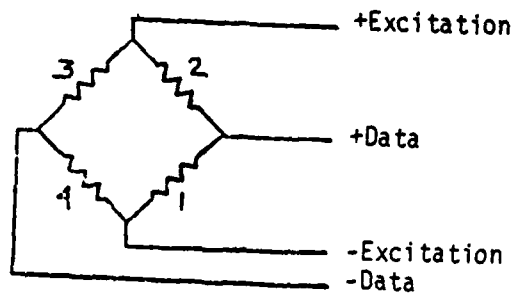
Right & Left  
Lap Attachment



Crotch  
Strap



Right & Left  
Reflection



Notes:  
\*Strain Gages are  
Micro-Measurements  
Model EA-06-125BZ-350

\*All units wired  
identical  
\*All 4 arms active

Figure A - 5- HARNESS INSTRUMENTATION



Figure A - 6- HARNESS INSTRUMENTATION

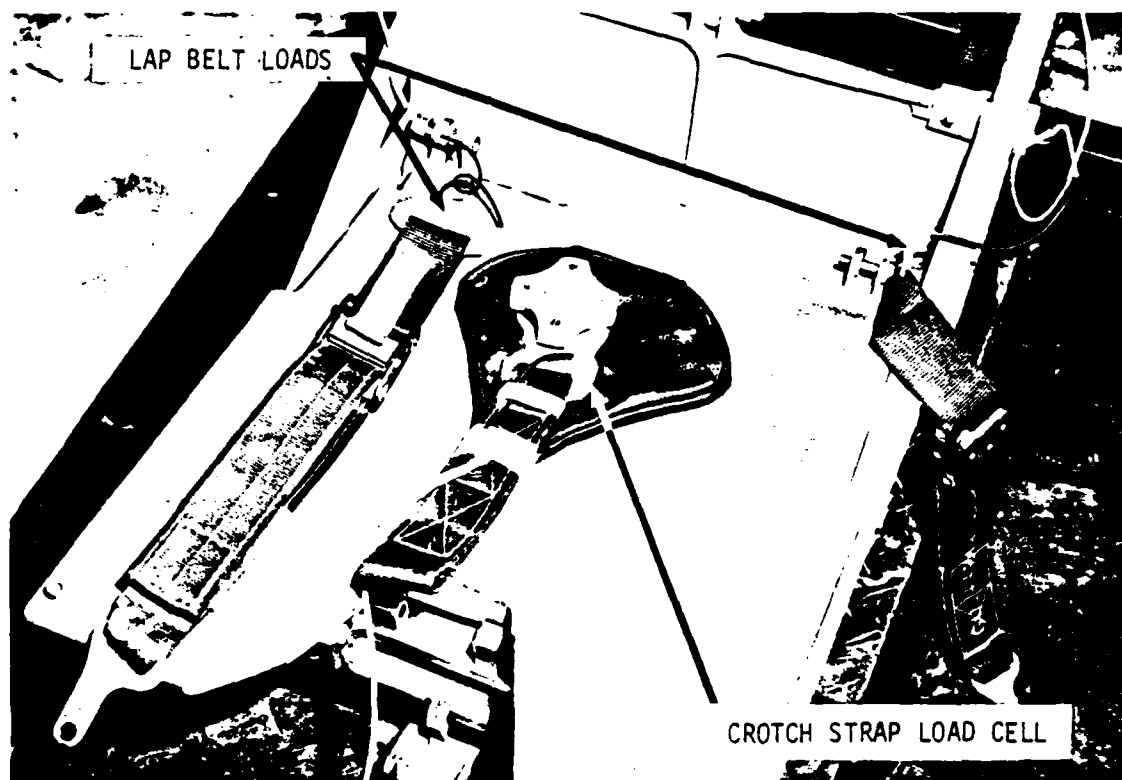
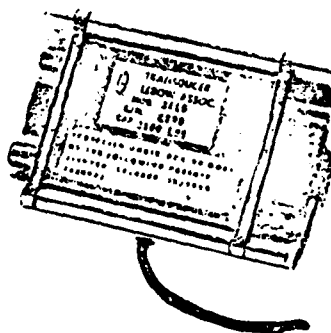


Figure A - 7- HARNESS INSTRUMENTATION

# AUTOMOTIVE LOAD CELLS



Model 3419  
Capacity Available  
3500 lbs.

## SPECIFICATIONS

Output at rated capacity: millivolts per volt, nominal	$\pm 2$
Nonlinearity: of rated output	$\pm 2\%$
Hysteresis: of rated output	$\pm 4\%$
Repeatability: of rated output	$\pm 1.0\%$
Zero balance: of rated output	$\pm 2\%$
Bridge resistance: ohms nominal	350
Temperature range, compensated: °F	+ 30 to + 150
Temperature range, useable: °F	- 65 to + 200
Temperature effect on output: of reading per °F	$\pm 0.003\%$
Temperature effect on zero: of rated output per °F	$\pm 0.003\%$
Overload rating, safe: of rated capacity	150%
Excitation voltage, maximum: volts DC or AC rms	20
Insulation resistance, bridge/case: megohms at 50 VDC	1000
Belt thickness: (maximum) inches	0.10
Belt width: (maximum) inches	2.00
Weight: in ounces	8
Available capacities: pounds	3500

Figure A - 8- LEBOW BELT LOAD CELL

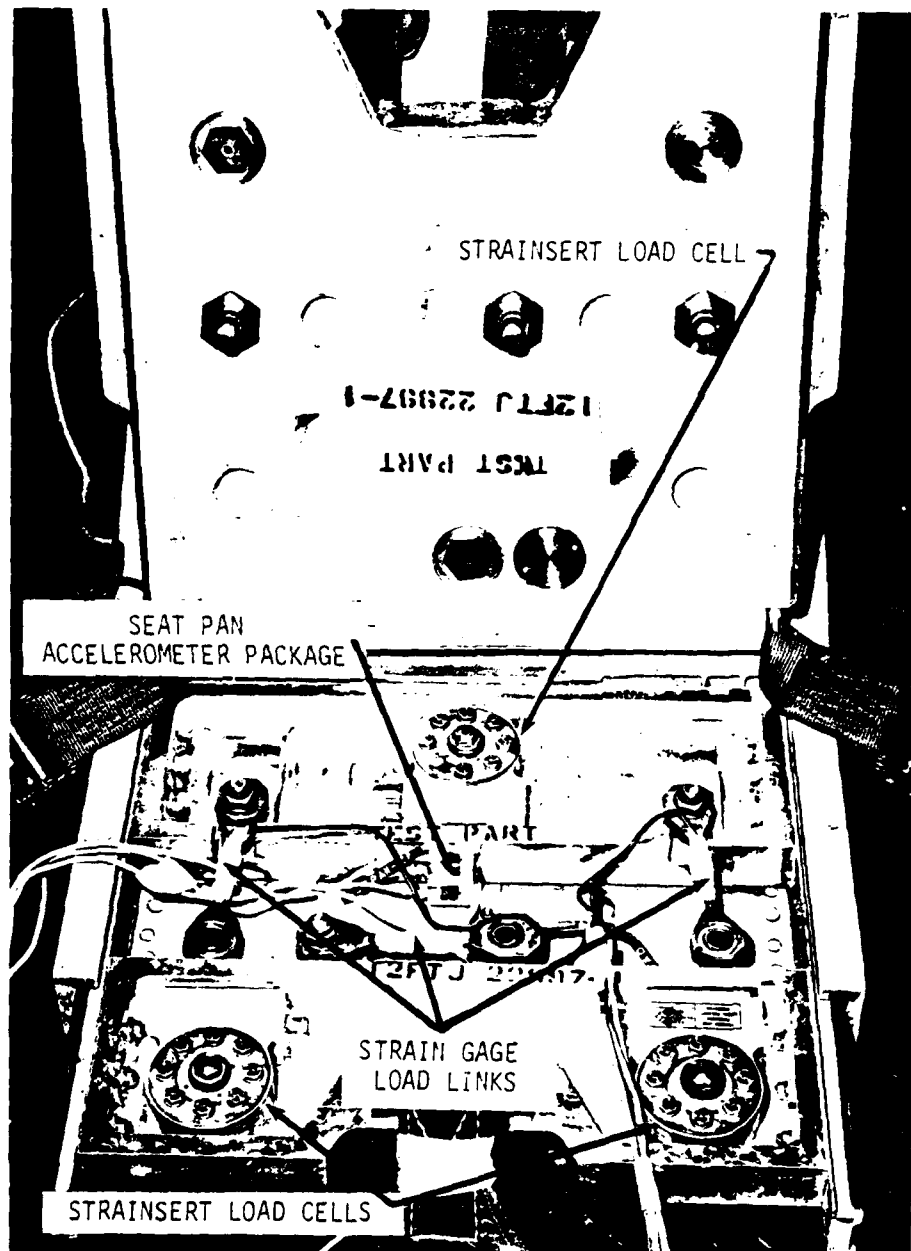
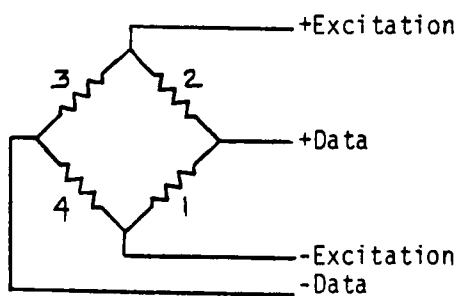
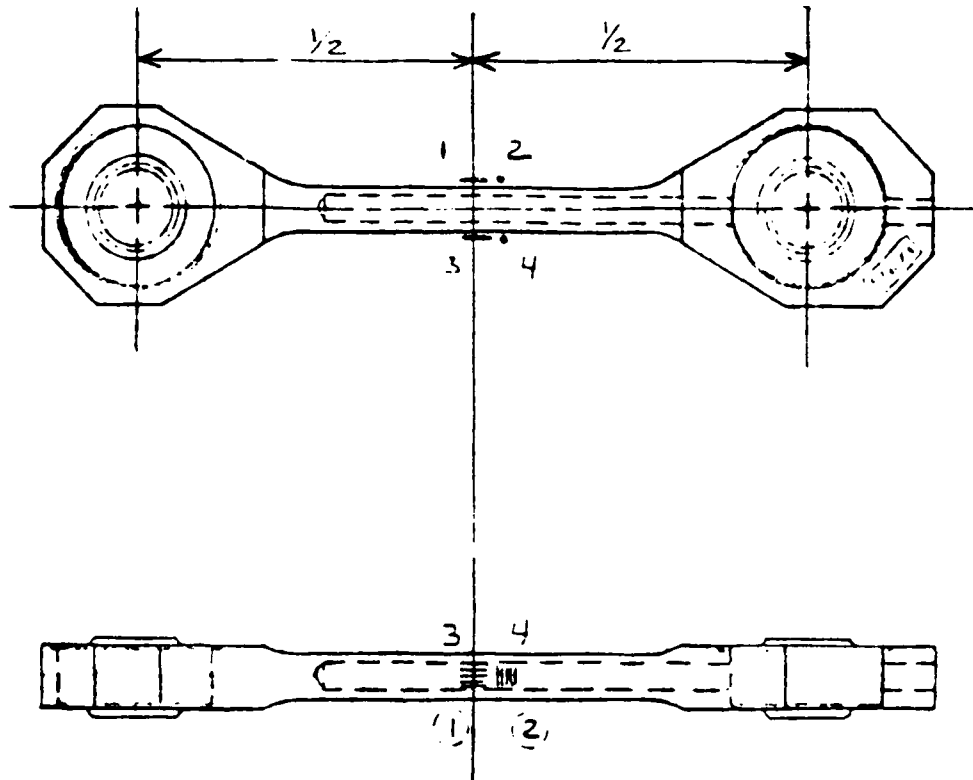


Figure A - 9 - SEAT PAN ASSEMBLY



Full Bridge with 2 arms active

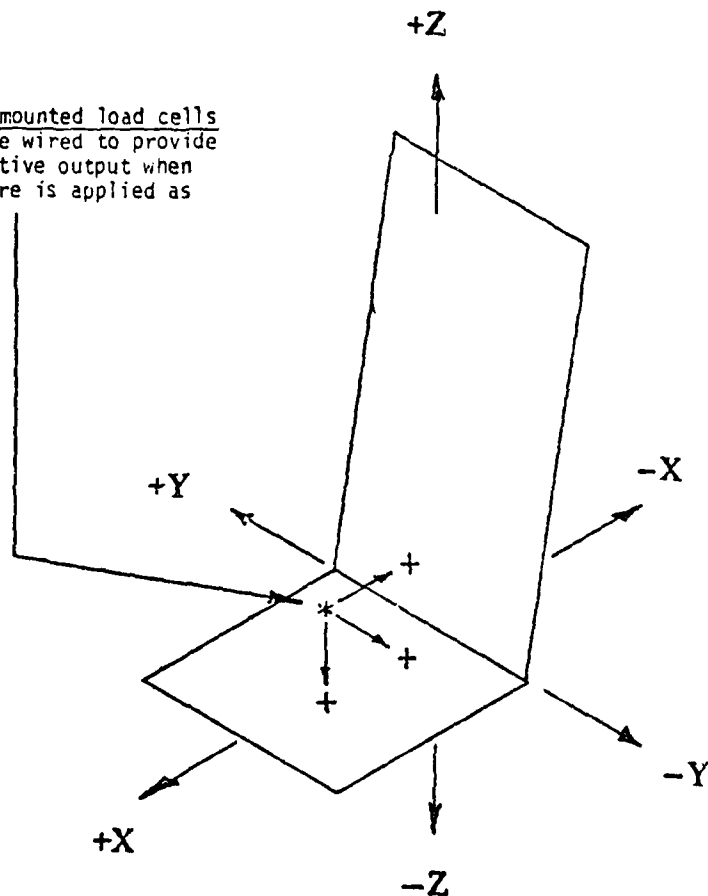
Strain Gages are MicroMeasurements  
Model EA-06-062TJ-350

Figure A - 10- SEAT PAN LOAD LINK

## LOAD CELL COORDINATE SYSTEM

Swivel mount and Lebow belt  
load cells will be wired to  
provide a positive output  
when the belt is pulled.

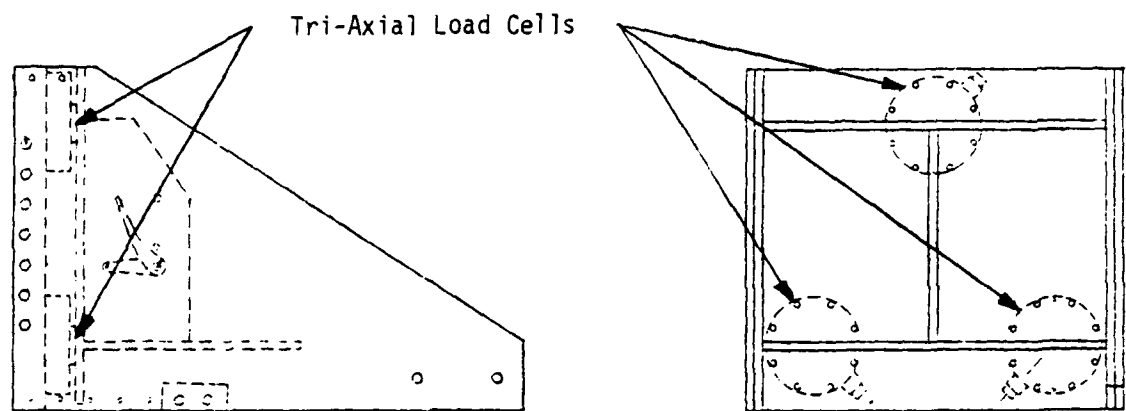
Fixed mounted load cells  
will be wired to provide  
a positive output when  
pressure is applied as  
shown.



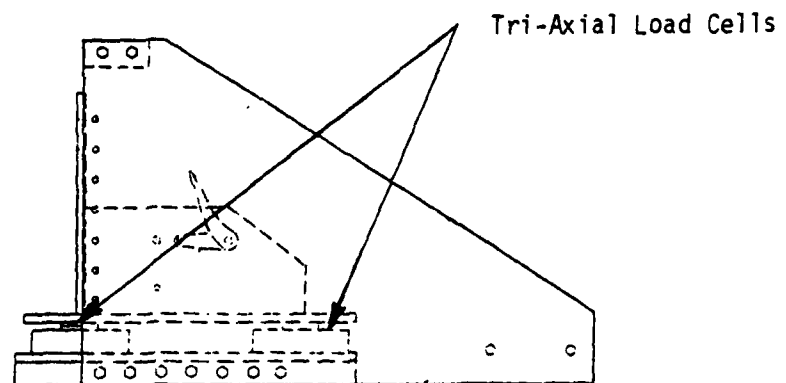
## AMRL BBP COORDINATE SYSTEM ( Left Hand Rule )

Figure A - 11





Horizontal Test Configuration



Vertical Test Configuration

Figure A - 12- FOOT REST LOAD CELL LOCATIONS

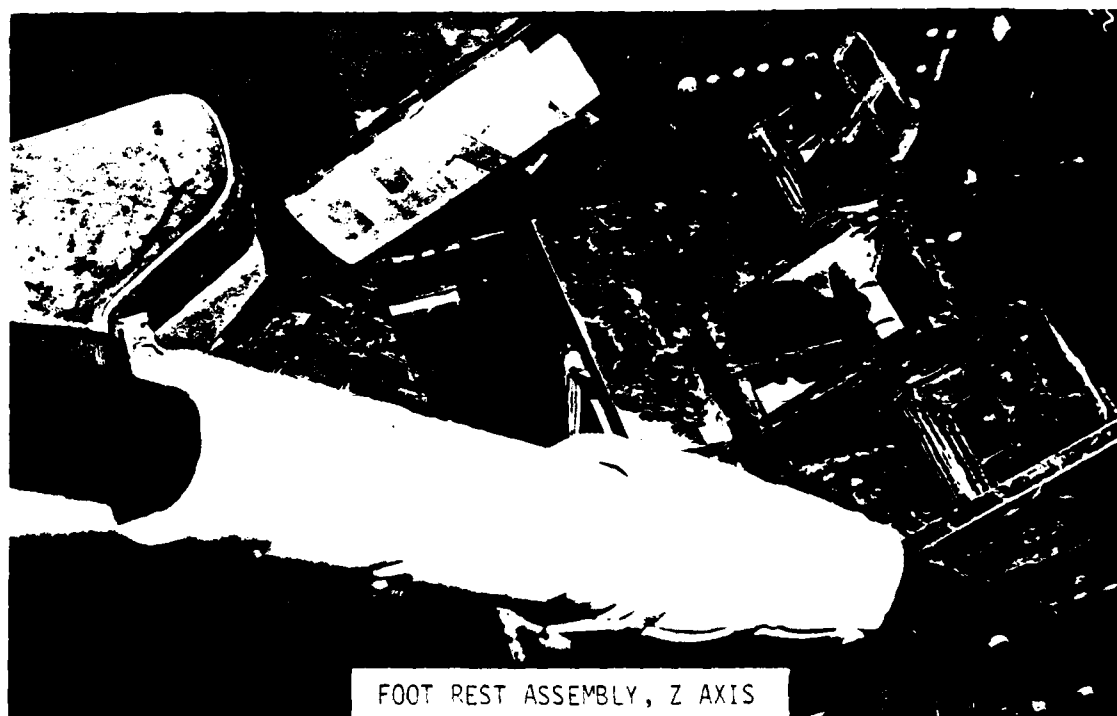
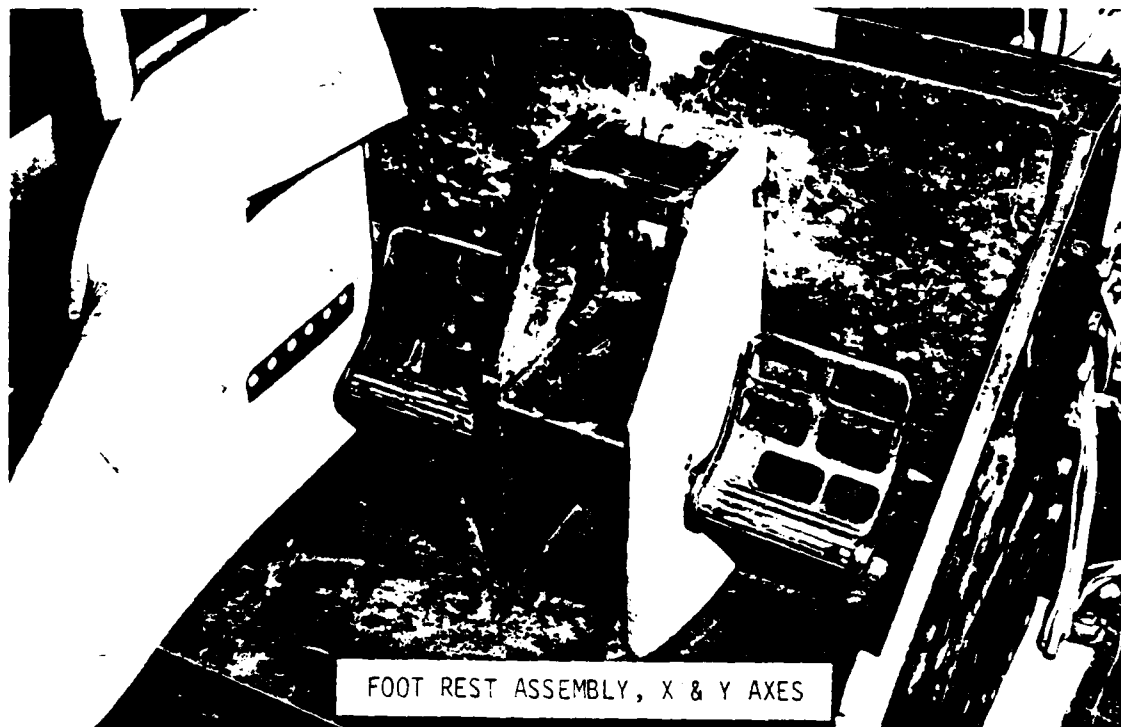
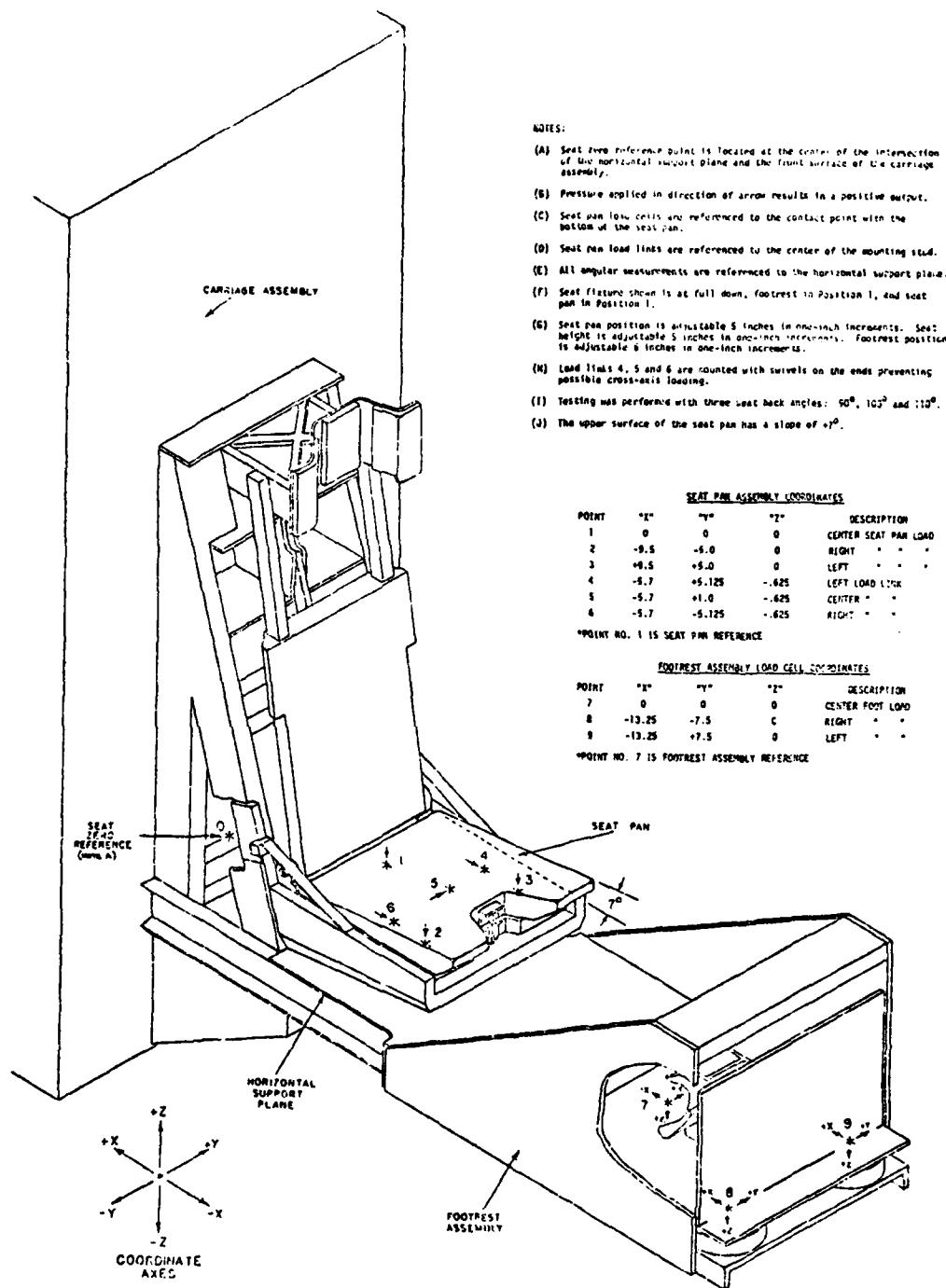


Figure A - 13- FOOT REST CONFIGURATIONS



F-III +G<sub>z</sub> Program Seat Geometry

Figure A - 14a

"X" AND "Z" AXIS COORDINATES W/ SEAT PAN REFERENCE POINT  
FOR ALL VALUES OF SEAT HEIGHT AND SEAT PAN POSITION

SEAT HEIGHT	"X" AXIS SEAT PAN POSITION						"Z" AXIS
	1	2	3	4	5	6	AVG
	1	2	3	4	5	6	AVG
1	-16.50	-17.50	-18.50	-19.50	-20.50	-21.50	-19.17
2	-16.50	-17.50	-18.50	-19.50	-20.50	-21.50	-19.17
3	-17.07	-18.07	-19.07	-20.07	-21.07	-22.07	-19.50
4	-17.35	-18.35	-19.35	-20.35	-21.35	-22.35	-19.68
5	-17.63	-18.63	-19.63	-20.63	-21.63	-22.63	-19.85
6	-17.92	-18.92	-19.92	-20.92	-21.92	-22.92	-20.03

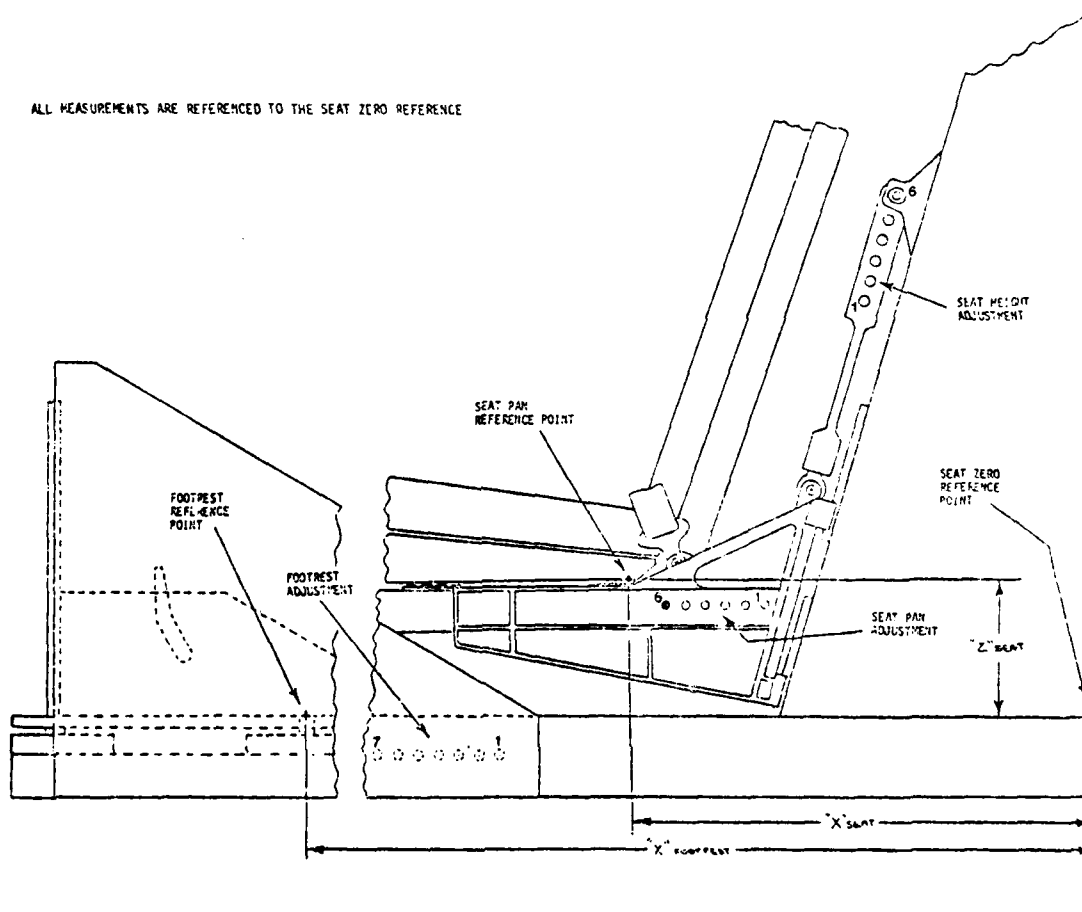
"Y" AXIS COORDINATES ARE -0 FOR ALL CONDITIONS

"X" AXIS COORDINATES W/ FOOTREST REFERENCE POINT  
FOR ALL VALUES OF FOOTREST POSITION

"X" AXIS FOOTREST POSITION						
1	2	3	4	5	6	7
-46.0	-47.0	-48.0	-49.0	-50.0	-51.0	-52.0

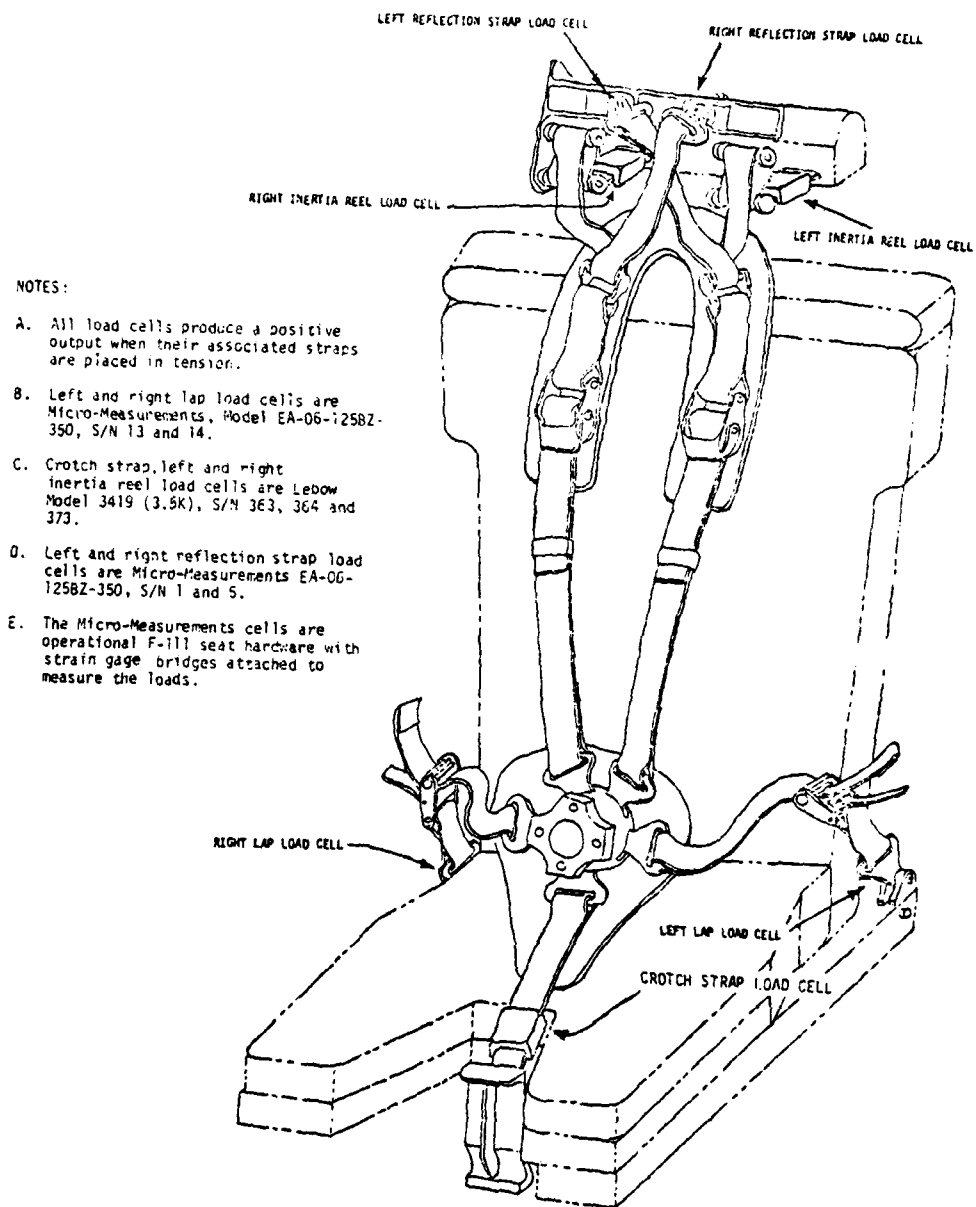
"Y" AND "Z" AXIS MEASUREMENTS ARE -0 FOR ALL CONDITIONS

ALL MEASUREMENTS ARE REFERENCED TO THE SEAT ZERO REFERENCE



F-III +G<sub>z</sub> Program Seat Geometry

Figure A - 14b



F-111 +G<sub>z</sub> Harness Instrumentation  
Figure A - 14c

DIGITAL INSTRUMENTATION REQUIREMENTS														
DYNALLECTRON CORPORATION														
PROGRAM F-111 GZ														
FACILITY VERTICAL ACCELERATION TOWER														
DATE 14 Jun 79 THRU 27 Jul 79														
RUN 177 THRU 276														
DATA CHANNEL	DATA POINT	POINTER MAG & TYPE	S/M	POINTER SENS	RECITE V CHAN	FILTER SERIES	AMP GAIN	SAMPLE RATE	F.S. SENS	FILTER HZ	POINTER ZERO RANGE	BRIDGE BALANCE RESISTORS	BRIDGE COMPLETION RESISTORS	SPECIAL NOTATIONS
1	Carriage Z	Endevco 2262A-200	FR37	5.612 mv/g	10.00	60	25	1K	17.82 g	120	2.640 +5.0 -0.0	1.3M into ground	-	Balance represents +1 g offset
2	Head X	Endevco 2264-200	B180	2.694 mv/g	10.00	60	50	1K	18.56	120	2.50 +5.0 -0.0	400K ideal + into ground	2 resistors @ 1.95K	
3	Head Y	"	BQ42	2.747 mv/g	10.00	60	100	1K	9.10	120	2.50 +5.0 -0.0	1.35M into ground	-	
4	Head Z	"	2051	2.556 mv/g	10.00	60	25	1K	39.12	120	2.564 +5.0 -0.0	145K ideal into ground	-	
5	Chest X	Endevco 2264-150	8C26	2.754 mv/g	10.00	60	50	1K	18.16 g	120	2.50 +5.0 -0.0	1.2M into ground	-	
6	Chest Y	"	8813	2.395 mv/g	10.00	60	100	1K	10.44 g	120	2.50 +5.0 -0.0	304K into ground	-	
7	Chest Z	"	2A20	2.579 mv/g	10.00	60	25	1K	38.78 g	120	2.565 +5.0 -0.0	153K ideal into ground	-	Balance represents +1 g offset
8	Left Leg	Micro-Me EA-06-12587-350	15	14.91 uv/lb	10.00	60	201	1K	334.2 lb	120	2.50 +5.0 -0.0	40.5K into ground	-	
9	Right Leg	"	14	13.57 uv/lb	10.00	60	201	1K	916.6 lb	120	2.50 +5.0 -0.0	42.8K into ground	-	
10	H-5 Strap	Lebow 3419 (3.5K)	373	7.912 uv/lb	10.00	60	402	1K	786.0 lb	120	2.50 +5.0 -0.0	-	-	Tests 177 - 185 negative output
11	Left Seat Pan	Strainert FL2.50-25RPT	3294-3	7.995 uv/lb	10.00	60	201	1K	1556 lb	120	2.50 +5.0 -0.0	-	-	
12	Right Seat Pan	"	3294-4	8.000 uv/lb	10.00	60	201	1K	1555 lb	120	2.50 +5.0 -0.0	-	-	
13	Center Seat Pan	"	3294-6	8.049 uv/lb	10.00	60	201	1K	1545 lb	120	2.50 +5.0 -0.0	890K into ground	-	
14	Left Perfect. Strap	Micro-Me EA-06-12587-350	02-5	29.30 uv/lb	10.00	60	100	1K	853.2 lb	120	2.50 +5.0 -0.0	27.2K into ground	-	

Δ NEGATIVE "G" STRAP ALSO KNOWN AS CROTCH STRAP

NOTE: Test 178 - No data required

PAGE 1 OF 3

NOTE: Test 178 - No data required

Δ NEGATIVE - G STRAP ALSO KNOWN AS CROUCH STRAP

Figure A - 15a

VMM

DIGITAL INSTRUMENTATION REQUIREMENTS										DYNAL ELECTRON CORPORATION				
PROGRAM F-111 GZ		DATE 14 Jun 79		THRU 27 Jul 79		PUN 177		THRU 276		FILTER Hz	REDUCE ZERO RANGE	BRIDGE BALANCE RESISTORS	BRIDGE COMPLETION RESISTORS	SPECIAL NOTATIONS
FACILITY	VERTICAL ACCELERATION TOWER	DATA POINT	SENSOR MFG & TYPE	S/N	SENSOR SENS	EXCITE V	CHAM	FILTER SERIES	AMP GAIN	AMP S/N	SAMPLE DATE	F.S. SENSE 2.5 Volt		
15	Right Reflect. Strip	15	Micro-Hg EA-08-350	01-1	25.90 uv/lb	10.00	15	60	100	28	1K	965.3 lb	60.6K - Into ground	
16	Left Inertia Reel Strip (1.5K)	16	Lebow 3419	363	8.025 uv/lb	10.00	16	60	402	6	1K	774.9 lb	-	
17	Right Inertia Reel Strip	17	"	364	7.390 uv/lb	10.00	17	60	402	5	1K	841.5 lb	-	
18	Left Load Link	18	Micro-Hg EA-08-064 TJ-350	001	10.92 uv/lb	10.00	18	60	402	11	1K	569.5 lb	106.7K - Into ground	
19	Right Load Link	19	"	002	10.17 uv/lb	10.00	19	60	402	4	1K	611.5 lb	55K + Into ground	
20	Left Foot Load X	20	GSE T-10952C	001	28.00 uv/lb	10.00	20	60	100	15	1K	892.9 lb	-	
21	Left Foot Load Y	21	"	001	28.02 uv/lb	10.00	21	60	100	3	1K	892.2 lb	-	
22	Left Foot Load Z	22	"	001	16.94 uv/lb	10.00	22	60	50	26	1K	2952 lb	-	
23	Right Foot Load A	23	"	002	28.30 uv/lb	10.00	23	60	100	1	1K	883.4 lb	-	
24	Right Foot Load Y	24	"	002	28.02 uv/lb	10.00	24	60	100	10	1K	892.2 lb	-	
25	Right Foot Load Z	25	"	002	16.69 uv/lb	10.00	25	60	50	23	1K	2996 lb	-	
26	Center Foot Load X	26	"	003	27.74 uv/lb	10.00	26	60	100	6	1K	901.2 lb	-	
27	Center Foot Load Y	27	"	003	27.94 uv/lb	10.00	27	60	100	26	1K	894.8 lb	-	
28	Center Foot Load Z	28	"	003	16.59 uv/lb	10.00	28	60	50	6	1K	3014 lb	-	

Figure A - 15b

DIGITAL INSTRUMENTATION REQUIREMENTS														
PROGRAM F-111 G2		DATE 14 Jun 79		THRU 27 Jul 79		DYNALLECTRON CORPORATION								
FACILITY VERTICAL DECELERATION LOWER		RUN 177		THRU 276										
DATA CHANNEL	DATA POINT	DOUCER MFG & TYPE	S/N	DOUCER SENS	ERGIE V LIAM	FILTER SERIES	AMP GAIN S/N	SAMPLE RATE	F S SENS	FILTER HZ	DOUCER ZERO RANGE	BRIDGE BALANCE RESISTORS	BRIDGE COMPLETION RESISTORS	SPECIAL NOTATIONS
29	Velocity	Globe 226672			29	60	17	15	48.33 cps	120	2.5	45.0	-	Attenuated 30:1
30	Carriage X	Endevco 2264-200	0749	*2.545 mv/g	10.00	60	1	15	19.65 g	120	2.5	45.0 + into ground	1.471K	Vel(FPS) = 1.611x30 Volts (but 2.5)
31	Carriage Y	-	8V56	2.803 mv/g	10.00	60	22	5	17.84 g	120	2.5	45.0 + into ground	1.65K	*Test 177-203 Accel. S/N 8x10, Sens. 2.558 mv/g
32	Seat Pan X	-	8M12	3.174 mv/g	10.00	60	4	12	15.75 g	120	2.5	45.0 + into ground	1.65K	
33	Seat Pan Y	-	8V41	3.316 mv/g	10.00	60	25	24	15.08 g	120	2.5	45.0 + into ground	1.471K	
34	Seat Pan Z	-	8M63	2.782 mv/g	10.00	60	20	9	17.97 g	120	2.639	135K	-	
35	Carriage Load	Micro-Me 2A-06-062	004	10.35 wv/lb	10.00	60	402	2	600.9 lb	120	2.50	243K + into ground	-	
48	5 Volt E/c.	-			48	180	14	-	5 Volt	120	0.0	45.0	-	
47	2.5 Volt Bias				47	180	3	-	2.5 Volt	360	0.0	45.0	-	Test 179 and subsequent

\*NOTE: Tests 177 - 185 Vel. output positive

PAGE 3 OF 3

\*NOTE: Tests 177 - 185 Vel. output positive



# SEAT PAN ASSEMBLY COORDINATES

Point	"X"	"Y"	"Z"	Description
1	0	0	0	CENTER SEAT PAN LOAD
2	+0.5	+0.0	0	RIGHT SEAT PAN LOAD
3	+0.5	-5.0	0	LEFT SEAT PAN LOAD
4	+0.7	-5.125	-0.625	LEFT LOAD LINK
5	+0.7	-1.0	-0.625	CENTER LOAD LINK
6	+0.7	+6.125	-0.625	RIGHT LOAD LINK

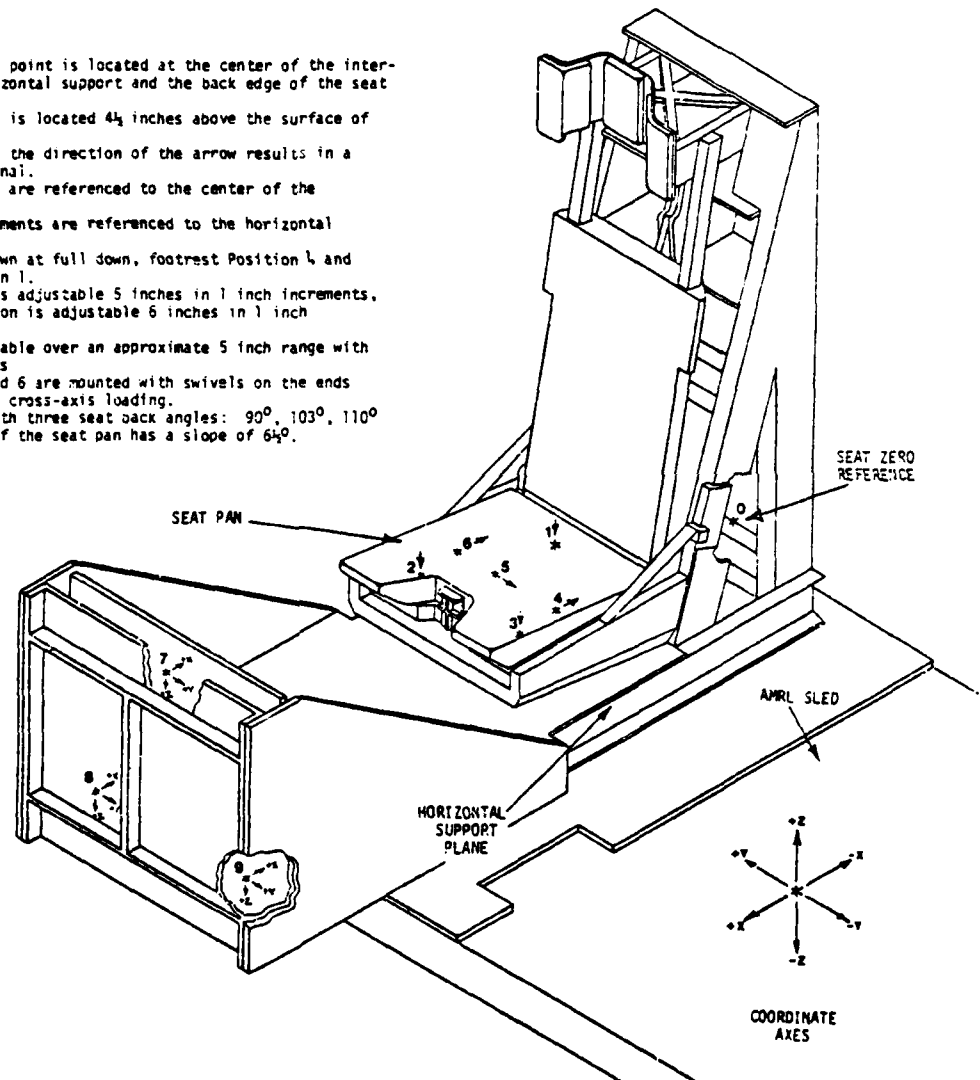
\*No. 1 IS SEAT PAN REFERENCE POINT

# FOOTREST ASSEMBLY LOAD CELL COORDINATES

Point	"X"	"Y"	"Z"	Description
7	0	0	0	CENTER FOOT LOAD
8	0	-47.5	-13.25	RIGHT FOOT LOAD
9	0	-47.5	-13.25	LEFT FOOT LOAD

\*Point No. 7 IS THE FOOTREST ASSEMBLY REFERENCE

- Seat zero reference point is located at the center of the intersection of the horizontal support and the back edge of the seat frame.
- Seat zero reference is located 4 1/4 inches above the surface of the AMRL Sled.
- Pressure applied in the direction of the arrow results in a positive output signal.
- Seat pan load links are referenced to the center of the mounting stud.
- All angular measurements are referenced to the horizontal support plane.
- Seat fixture is shown at full down, footrest Position 1, and seat pan is Position 1.
- Seat Pan position is adjustable 5 inches in 1 inch increments, and Footrest position is adjustable 6 inches in 1 inch increments.
- Seat height is variable over an approximate 5 inch range with no fixed stop points.
- Load Links 4, 5, and 6 are mounted with swivels on the ends preventing possible cross-axis loading.
- Testing was done with three seat back angles: 90°, 103°, 110°.
- The upper surface of the seat pan has a slope of 6 1/4°.



## **+G<sub>y</sub> Seat Geometry**

Figure A - 16a

"X" AND "Z" AXIS COORDINATES OF SEAT PAN REFERENCE POINT FOR  
MINIMUM AND MAXIMUM SEAT HEIGHT ADJUSTMENT AND ALL VARIABLES  
OF SEAT PAN POSITION

SEAT HEIGHT	Full Up	SEAT PAN POSITION "X" AXIS						"Z" AXIS DIMENSION	Full Down
		1	2	3	4	5	6		
		+18.5	+17.5	+18.5	+19.5	+20.5	+21.5	+11.44	Full Up
		+17.92	+18.92	+19.92	+20.92	+21.92	+22.92	+6.65	Full Down

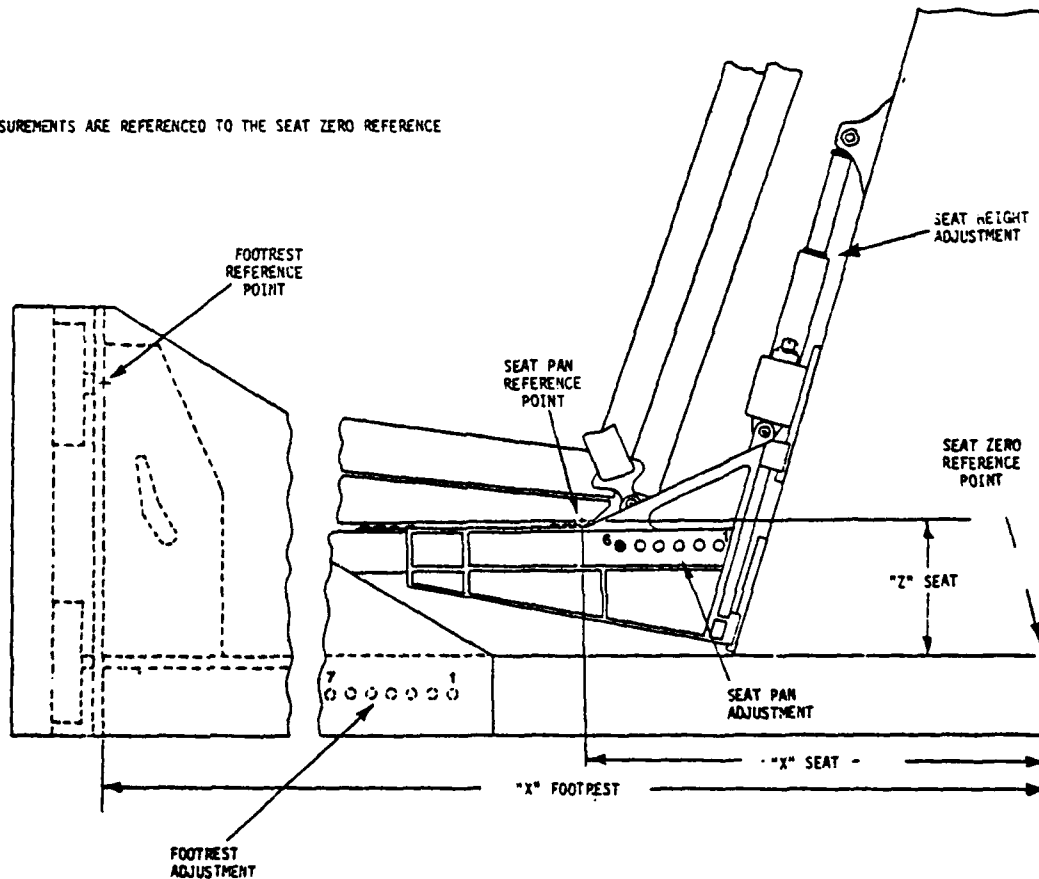
"X" AXIS DIMENSION IS 20 INCHES FOR ALL CONDITIONS

SEAT PAN IS CONTINUOUSLY VARIABLE IN THE "Z" AXIS BETWEEN  
THE TOP AND BOTTOM POINTS.

"X" AXIS COORDINATES OF FOOTREST ASSEMBLY  
REFERENCE POINT FOR ALL VARIABLES OF FOOTREST POSITION

	FOOTREST POSITION					
	1	2	3	4	5	6
"X"	+56.0	+57.0	+58.0	+59.0	+60.0	+61.0
"Y"	20	20	20	20	20	20
"Z"	+13.25	+13.25	+13.25	+13.25	+13.25	+13.25

ALL MEASUREMENTS ARE REFERENCED TO THE SEAT ZERO REFERENCE

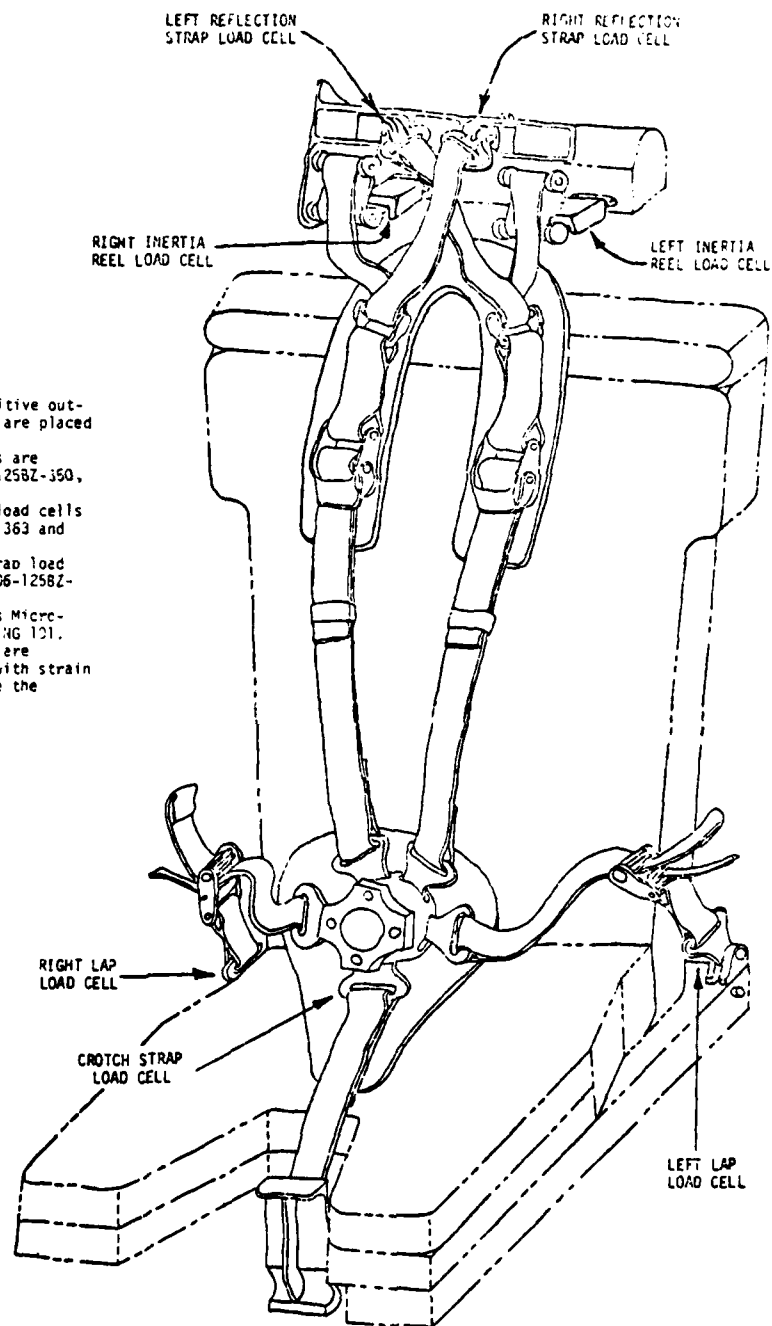


## +G<sub>y</sub> Seat Geometry

Figure A - 16b

NOTES:

- A All load cells produce a positive output when their associated straps are placed in tension.
- B Left and right lap load cells are Micro-Measurements, Model EA-06-1258Z-350, S/N 13 and 14.
- C Left and Right inertia reel load cells are Lebow Model 3419 (3.5K), S/N 363 and 364.
- D Left and right reflection strap load cells are Micro-Measurements EA-06-1258Z-350, S/N 1 and 5.
- E Crotch strap load cell is Micro-Measurements EA-06-1258Z-35, S/N HG 121.
- F The Micro-Measurements cells are operational F-111 seat hardware with strain gage bridges attached to measure the loads.



## +G<sub>y</sub> Harness Geometry

Figure A - 16c

PROGRAM F-111  
 FACILITY 100 G LAUNCH  
 DATE 1 Aug. 79 THRU 25 Sept. 79  
 RUN 323 THRU 521

DIGITAL INSTRUMENTATION REQUIREMENTS  
 DYNALECTRON CORPORATION

DATA CHANNEL	DATA POINT	EXCITE MFG. & TYPE	S/N	EXCITE V	FILTER SERIES	AMP GAIN	S/N	SAMPLE RATE	F.S. SENS. FORMAT	FILTER HZ	EXCITE ZERO RANGE	BRIDGE BALANCE RESISTORS	BRIDGE COMPLETION REGISTERS	SPECIAL NOTATIONS
1	SEED Y	Endevco 2260-250	RF47	10.00	50	100	9	1K	19.86 g	120	2.50	15.0	--	
2	HEAD X	Endevco 2264-200	BH80	10.00	60	25	13	1K	37.12 g	120	2.50	170K into Gnd	2	
3	HEAD Y	"	BQ42	10.00	60	25	3	1K	36.40 g	120	2.50	120K into Gnd	--	
4	HEAD Z	"	BQ51	10.00	60	25	27	1K	39.12 g	120	2.50	145K into Gnd	--	
5	CHEST X	Endevco 2264-150	BC26	10.00	60	50	14	1K	18.16 g	120	2.50	1.2M into Gnd	--	Test 373-417 AMP Gain @100 F.S. = 9.078
6	CHEST Y	"	BQ13	10.00	60	50	10	1K	20.88 g	120	2.50	304K into Gnd	--	
7	CHEST Z	"	2A20	10.00	60	100	2	1K	9.694 g	120	2.76	153K into Gnd	--	
8	LEFT LAP	Micro-Peel 22-36-125	*16	10.00	60	201	6	1K	224.2 lb	120	2.50	40.5K into Gnd	--	*Test 373-426 SN-15 @14.91 uV/lb F.S. = 834.2
9	RIGHT LAP	"	14	10.00	60	201	6	1K	916.6 lb	120	2.50	42.8K into Gnd	--	
10	U-C STRAP	Micro-Peel 22-36-125	*143377	10.00	60	402	7	1K	*3308 lb	120	2.50	--	--	*Test 373-354 SN-373 Load @336 lb F.S. 07.912 uV/lb
11	LEFT STRAP	Micro-Peel 22-36-125	3294-3	10.00	60	201	35	1K	1556 lb	120	2.50	--	--	Test 355-426 no inst. this point**
12	RIGHT STRAP	"	3294-4	10.00	60	201	32	1K	1555 lb	120	2.50	--	--	Compression made Test 373-354 - no Sens. Change
13	SEAT F41	"	3294-6	10.00	60	201	15	1K	1545 lb	120	2.50	890K into Gnd	--	
14	SEAT F42	"	*02-4	10.00	60	100	12	1K	*833.4 lb	120	2.50	36.3K into Gnd	--	*Test 373-355 Full Scale @12.5 lb @4.2

\*\* Test 427-430 SN-142111  
 Test 429 Seat Pan Modification Made - right seat load and center seat load have hold down bolts attached to seat.  
 Test 456 H-B Strap strain gage damaged SN144111 Sens. 321 uV/lb F.S. 19374  
 Test 459 H-B Strap strain gage installed SN143377 Sens. 1.86 uV/lb F.S. 3308  
 \*\* NEGATIVE 4.5194V ALSO READ ON RS CROUCH STRAP  
 Test 389 New Full Scale for Left & Right Reflect Straps. See Special Notations  
 812.5 lb  
 PAGE 1 OF 3

\*\* Test 327-426 SN 146211  
 Test 229 Seat Pan Modification Made - right seat load and center seat load have hold down bolts attached to seat.  
 Test 456 H-G Strap strain gage damaged SN144111 Sens. .321 uV/lb F.S. 19374  
 Test 452 H-G Strap strain gage installed SN143377 Sens. 1.86 uV/lb F.S. 3308  
 Δ NEGATIVE TO STRAP ALSO KNOWN AS CRACK STRAP

Figure A - 17a

DIGITAL INSTRUMENTATION REQUIREMENTS										DYNALLECTRON CORPORATION				
PROGRAM		DATE		THRU		THRU		THRU						
F-111 G		1 Aug 79		1 Aug 79		1 Aug 79		1 Aug 79						
FACILITY		LGM G LAUNCH		RUN		373		THRU		521				
DATA CHANNEL	DATA POINT	SENSOR MFG & TYPE	S/N	SENSOR SENS	FACITE V CHAN	FILTER SERIES	AMP S/N	FORMATE	F.S. SENS	FILTER HZ	SENSOR ZERO RANGE	BRIDGE BALANCE RESISTORS	BRIDGE COMPLETION RESISTORS	SPECIAL NOTATIONS
23	LEFT FOOT * LOAD Z	GSE 7-10952C	002	28.30 uV/lb	10.00 23	60	100	1K	883.4 lb	120	2.50 +5.0 -0.0	--	--	Actual X used in Z Axis
24	LEFT FOOT * LOAD Y	"	002	28.02 uV/lb	10.00 24	60	50	1K	1784 lb	120	2.50 +5.0 -0.0	--	--	
25	LEFT FOOT * LOAD X	"	002	16.69 uV/lb	10.00 25	60	201	1K	715.2 lb	120	2.50 +5.0 -0.0	--	--	Actual Z used in X Axis
20	RIGHT FOOT * LOAD Z	"	001	28.00 uV/lb	10.00 20	60	100	1K	892.9 lb	120	2.50 +5.0 -0.0	--	--	Actual X used in Z Axis
21	RIGHT FOOT * LOAD Y	"	001	28.22 uV/lb	10.00 21	60	50	1K	1784 lb	120	2.50 +5.0 -0.0	--	--	
22	RIGHT FOOT * LOAD X	"	001	16.94 uV/lb	10.00 22	60	201	1K	714.2 lb	120	2.50 +5.0 -0.0	--	--	Actual Z used in X Axis
26	ENTER FOOT * LOAD Z	"	003	27.74 uV/lb	10.00 26	60	100	1K	911.2 lb	120	2.50 +5.0 -0.0	--	--	Actual X used in Z Axis
27	ENTER FOOT * LOAD Y	"	003	27.94 uV/lb	10.00 27	60	50	1K	1790 lb	120	2.50 +5.0 -0.0	--	--	
28	ENTER FOOT * LOAD X	"	003	16.59 uV/lb	10.00 28	60	201	1K	749.7 lb	120	2.50 +5.0 -0.0	--	--	Actual Z used in X Axis
21-27	ENTER				--	1000	1	1K	--	2000	2.50 +5.0 -0.0	--	--	Test 428-429 No Event
33	11 START				5.00	37	21	1	--		0.0 +5.0 -0.0			Located just after shuttle separates Test 429 and subsequent
33	22 START				5.00	38	1				0.0 +5.0 -0.0			Located just prior to water brake Test 429 and subsequent

\*NOTE Foot Load Cell usage as indicated in special notations.

PAGE 3 OF 3

Figure A - 17b

1/8/79

DIGITAL INSTRUMENTATION REQUIREMENTS										DYNAL ELECTRON CORPORATION				
PROGRAM		F-111		DATE 1 Aug 79		THRU 25 Sept 79		THRU 373						
FACILITY		LOW G LAUNCH		RUN		THRU		521						
DATA CHANNEL	DATA POINT	TOUCHER MFG & TYPE	S/N	TOUCHER SENS	EXCITE V CHAN	FILTER SERIES	AMP GAIN S/N	SAMPLE RATE	F.S. SENS	FILTER HZ	TOUCHER ZERO RANGE	BRIDGE BALANCE RESISTORS	BRIDGE COMPLETION RESISTORS	SPECIAL NOTATIONS
15	PELLET REFLECTION STRAP LEFT	Micro-Meas EA-06-125 BL-350 Letom	01-1	25.90 uV/lb	10.00	60	402 29	1K	240.1 lb	120	2.50 15.0 -0.0	60.6K -into Gnd	--	Test 373-388 Full Scale = 965.2 lb, g = 100
16	INERTIA STRAP LEFT	3419-3.5K	363	8.025 uV/lb	10.00	60	402 24	1K	774.9 lb	120	2.50 15.0 -0.0	--	--	
17	INERTIA STRAP LEFT	"	364	7.390 uV/lb	10.00	60	402 11	1K	841.5 lb	120	2.50 15.0 -0.0	--	--	
18	LOAD LINK LEFT	Micro-Meas EA-06-062 TL-350	001	10.92 uV/lb	10.00	60	402 19	1K	563.4 lb	120	2.50 15.0 -0.0	106K -into Gnd	--	
19	LOAD LINK LEFT	"	002	10.17 uV/lb	10.00	60	402 28	1K	611.5 lb	120	2.50 15.0 -0.0	55K -into Gnd	--	
29	VELOCITY	Globe Inc 22A672		2020 Volts/FPS 10.25 "inches"	--	60	1 17	1K	*77.26 Ft/Sec	120	2.50 15.0 -0.0	--	--	Test 373-439 F.S. = 71.87 FPS -2089 Volt FPS Sens. Atten. 1/30 x 5 Gain Test 440 and subsequent atten. 36.252
36	SLID X	Endevco 2264-200	B749	2.545 mV/g	10.00	60	100 26	1K	9.323 g	120	2.50 15.0 -0.0	2M -into Gnd	1.65K	
31	SLID Z	"	B756	2.803 mV/g	10.00	60	100 22	1K	8.319 g	120	2.78 15.0 -0.0	1.3K -into Gnd	"	
32	SLID Y	"	BH12	*4.726 mV/g	10.00	60	100 4	1K	5.290 g	120	2.50 15.0 -0.0	131K -into Gnd	"	*Bias Jumper not used in connector
35	SEAT BELT Y	"	BV41	*4.853 mV/g	10.00	60	50 25	1K	10.30 g	120	2.50 15.0 -0.0	61K -into Gnd	1.471K	*Bias Jumper not used in connector
34	SEAT BELT Z	"	BN63	2.782 mV/g	10.00	60	100 20	1K	3.366 g	120	2.78 15.0 -0.0	135K -into Gnd	"	
35	SEAT BELT LINK	Micro-Meas EA-06-062 TL-350	004	10.35 uV/lb	10.00	60	201 26	1K	1212 lb	120	2.50 15.0 -0.0	243K -into Gnd	--	
47	2.5 VOLT					190	1 3	1K	2.5 Volt	360	2.50 15.0 -0.0	--	--	
49	5 VOLT EXC.					180	1 14	1K	5 Volt	360	0.0 15.0 -0.0	--	--	

Figure A - 17c

# SEAT PAN ASSEMBLY COORDINATES

Point	"X"	"Y"	"Z"
1	0	0	0
2	+9.5	+5.0	0
3	+9.5	-5.0	0
4	+5.7	-5.125	-.625
5	+5.7	-1.0	-.625
6	+5.7	+5.125	-.625

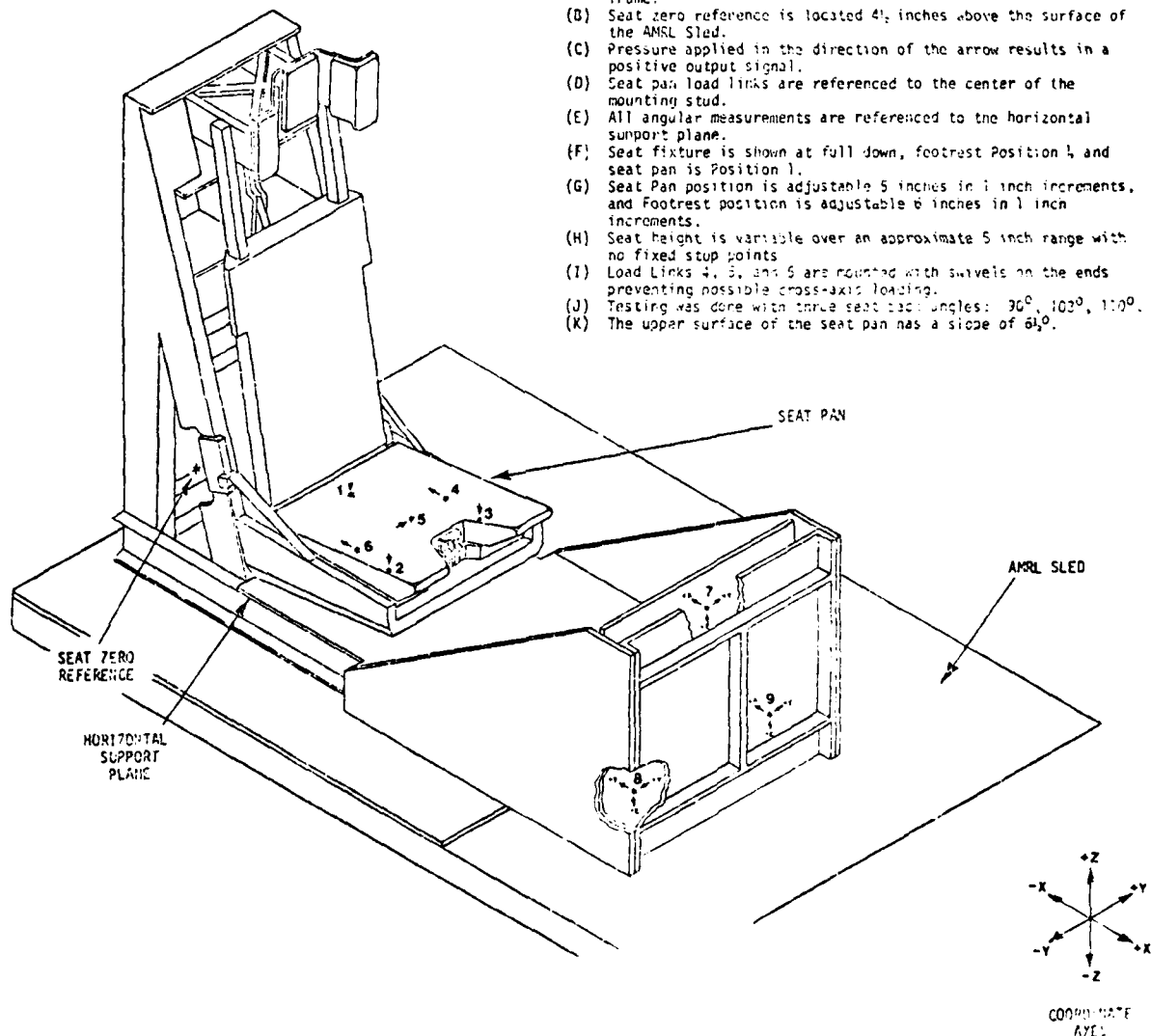
\*No. 1 IS SEAT PAN REFERENCE POINT

# FOOTREST ASSEMBLY LOAD CELL COORDINATES

Point	"X"	"Y"	"Z"	Description
7	0	0	0	CENTER FOOT LOAD
8	0	+7.5	-13.25	RIGHT FOOT LOAD
9	0	-7.5	-13.25	LEFT FOOT LOAD

\*Point No. 7 IS THE FOOTREST ASSEMBLY REFERENCE

- (A) Seat zero reference point is located at the center of the intersection of the horizontal support and the back edge of the seat frame.
- (B) Seat zero reference is located 4 1/2 inches above the surface of the AMSL Sled.
- (C) Pressure applied in the direction of the arrow results in a positive output signal.
- (D) Seat pan load links are referenced to the center of the mounting stud.
- (E) All angular measurements are referenced to the horizontal support plane.
- (F) Seat fixture is shown at full down, footrest Position 4, and seat pan is Position 1.
- (G) Seat Pan position is adjustable 5 inches in 1 inch increments, and Footrest position is adjustable 6 inches in 1 inch increments.
- (H) Seat height is variable over an approximate 5 inch range with no fixed stop points.
- (I) Load Links 4, 5, and 6 are mounted with swivels on the ends preventing possible cross-axis loading.
- (J) Testing was done with three seat back angles: 90°, 103°, 110°.
- (K) The upper surface of the seat pan has a slope of 6 1/2°.



-G<sub>x</sub> Seat Geometry  
Figure A - 18a

\*X\* AND \*Y\* AXIS COORDINATES OF SEAT PAN REFERENCE POINT, FOR MINIMUM AND MAXIMUM SEAT HEIGHT ADJUSTMENT AND ALL VARIANTS OF SEAT PAN POSITION

	SEAT PAN POSITION *X* AXIS						*Y* AXIS DIMENSION	
	1	2	3	4	5	6		
SEAT HEIGHT Full Up	+16.5	+17.5	+18.5	+19.5	+20.5	+21.5	+11.34	Full Up
SEAT HEIGHT Full Down	+17.92	+18.92	+19.92	+20.92	+21.92	+22.92	+6.53	Full Down

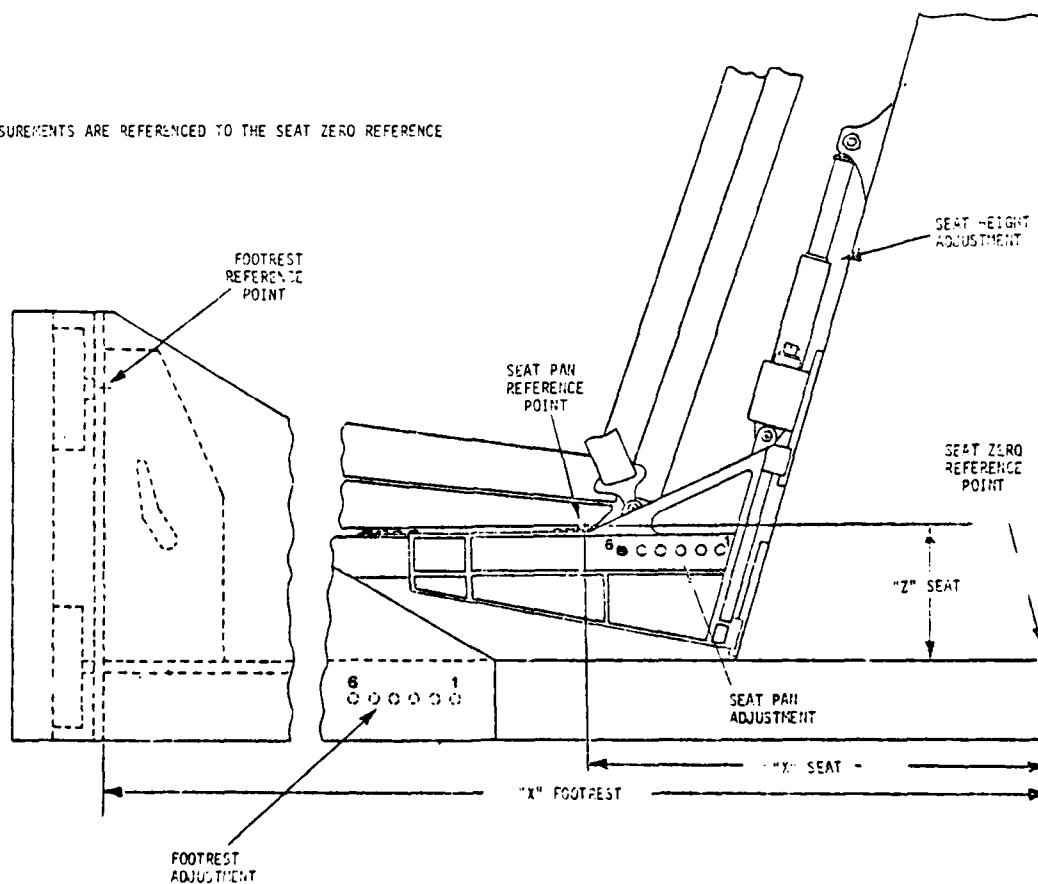
\*Y\* AXIS DIMENSION IS 10 INCHES FOR ALL CONDITIONS

\*SEAT PAN IS CONTINUOUSLY VARIABLE IN THE \*Z\* AXIS BETWEEN THE TOP AND BOTTOM POINTS

\*Z\* AXIS COORDINATES OF FOOTREST AND SEAT PAN REFERENCE POINTS FOR SEAT HEIGHT ADJUSTMENT

	FOOTREST POSITION					
	1	2	3	4	5	6
*X*	+50.0	+51.0	+52.0	+53.0	+54.0	+55.0
*Y*	50	50	50	50	50	50
*Z*	+13.25	+12.25	+13.25	+12.25	+13.25	+12.25

ALL MEASUREMENTS ARE REFERENCED TO THE SEAT ZERO REFERENCE



## -G<sub>x</sub> Seat Geometry

Figure A - 18b



## DIGITAL INSTRUMENTATION REQUIREMENTS

PROGRAM E-1116 DATE 28 SEPT. 79 THRU 13 NOV. 79  
 FACILITY 104 G LAMICH RUN 522 THRU 601

DATA CHANNEL	CATA POINT	REDUCER MFG. & TYPE	S/N	REDUCER SEAS	EXCITE V	FILTER SERIES	AMP GAIN	SAMPLE RATE	F.S. SENS	POKER ZERO RANGE	BRIDGE BALANCE RESISTORS	BRIDGE COMPLETION RESISTORS	SPECIAL NOTATIONS
1	Site Y	Endevco 2264-200	8149	2.545 mV/g	10.00	60	100	1K	2.5 Volt	2.50	2M	2 Resistors	
2	Head X	Endevco 2264-200	8180	2.694 mV/g	10.00	60	25	1K	37.12 g	2.50	170K		
3	Head Y	"	3042	2.747 mV/g	10.00	60	50	1K	18.20 g	2.50	120K	"	
4	Head Z	"	8051	2.556 mV/g	10.00	60	25	1K	39.12 g	2.56	145K	"	
5	Chest X	Endevco 2264-150	8C26	2.754 mV/g	10.00	60	50	1K	18.16 g	2.50	1.2M	"	
6	Chest Y	"	2313	2.395 mV/g	10.00	60	100	1K	10.44 g	2.50	304K	"	
7	Chest Z	"	2A20	2.579 mV/g	10.00	60	50	1K	19.39 g	2.76	153K	"	
8	Left Lap	Micro-Meas EA-06-125	14	15.06 mV/lb.	10.00	60	100	1K	1657 lb.	2.50	40.5K		
9	Right Lap	"	14	13.57 mV/lb.	10.00	60	100	1K	1842 lb.	2.50	42.8K		
10	H-G Strain	"	143377	1.88 mV/lb.	10.00	60	402	1K		2.50			
11	Left Seat Pan 2	Strainmeter 2.5u-25 RPT	3294-3	7.955 mV/lb.	10.00	60	201	1K	3208 lb.	2.50			
12	Right Seat Pan 2	"	3294-4	8.000 mV/lb.	10.00	60	201	1K	1556 lb.	2.50			
13	Center Seat Pan 2	"	3294-6	8.049 mV/lb.	10.00	60	201	1K	1555 lb.	2.50	890K		Load Cell Placed in Config. using Tension Cal.
14	Left Seat Pan 2	Strainmeter 2.5u-25 RPT	02-4	29.82 mV/lb.	10.00	60	100	1K	1545 lb.	2.50	36.3K		

Δ NEGATIVE-G STRAP ALSO KNOWN AS CROTCH STRAP

NOTE: Test 522 only: Sled Y Chan. 36  
Sled X Chan. i

PAGE 1 OF 3

Figure A - 19a

DIGITAL INSTRUMENTATION REQUIREMENTS										DYNAELECTRON CORPORATION				
PROGRAM		F-111 G <sub>4</sub>		DATE 28 Sept. 79		THRU 13 Nov. 79		THRU 603						
FACILITY		LOW G LAUNCH		RUN 522		THRU 603								
DATA CHANNEL	DATA POINT	EXCITER	EXCITER S/N	EXCITER TYPE	EXCITER S/N	EXCITER TYPE	EXCITER S/N	EXCITER TYPE	EXCITER S/N	EXCITER TYPE	EXCITER S/N	EXCITER TYPE	EXCITER S/N	EXCITER TYPE
15	Right Foot Load X	25.90 uW/lb	001	EA-06-115 01-1	60	29	5	1K	1	480.2 lb	120	2.50	60.6K	Actual X used in Z axis
16	Left Foot Load X	8.025 uW/lb	363	EA-06-115 01-1	60	24	13	1K	1	774.9 lb	120	2.50	106K	Actual X used in Z axis
17	Right Foot Load X	7.390 uW/lb	364	EA-06-115 01-1	60	11	5	1K	1	841.5 lb	120	2.50	55K	Actual X used in Z axis
18	Left Foot Load X	10.92 uW/lb	001	EA-06-115 01-1	60	19	4	1K	1	1139 lb	120	2.50	106K	Actual X used in Z axis
19	Right Foot Load X	10.17 uW/lb	002	EA-06-115 01-1	60	28	9	1K	1	1223 lb	120	2.50	55K	Actual X used in Z axis
20	Left Foot Load X	28.00 uW/lb	001	EA-06-115 01-1	60	34	15	1K	1	892.9 lb	120	2.50	106K	Actual X used in Z axis
21	Right Foot Load X	28.02 uW/lb	001	EA-06-115 01-1	60	33	7	1K	1	443.9 lb	120	2.50	55K	Actual X used in Z axis
22	Left Foot Load X	16.94 uW/lb	001	EA-06-115 01-1	60	18	22	1K	1	1476 lb	120	2.50	106K	Actual X used in Z axis
23	Right Foot Load X	28.30 uW/lb	002	EA-06-115 01-1	60	30	1	1K	1	883.4 lb	120	2.50	55K	Actual X used in Z axis
24	Left Foot Load X	28.02 uW/lb	002	EA-06-115 01-1	60	23	4	1K	1	443.9 lb	120	2.50	106K	Actual X used in Z axis
25	Right Foot Load X	16.69 uW/lb	002	EA-06-115 01-1	60	25	19	1K	1	1498 lb	120	2.50	55K	Actual X used in Z axis
26	Left Foot Load X	27.74 uW/lb	003	EA-06-115 01-1	60	36	6	1K	1	901.2 lb	120	2.50	106K	Actual X used in Z axis
27	Right Foot Load X	27.94 uW/lb	003	EA-06-115 01-1	60	21	10	1K	1	445.2 lb	120	2.50	55K	Actual X used in Z axis
28	Left Foot Load X	16.59 uW/lb	003	EA-06-115 01-1	60	28	31	1K	1	1507 lb	120	2.50	106K	Actual X used in Z axis

\* NOTE Foot Load Cell usage as indicated in special notations

PAGE 2 OF 3

Figure A - 19b

DIGITAL INSTRUMENTATION REQUIREMENTS														DYNAL ELECTRON CORPORATION			
PROGRAM		E-111 G <sub>2</sub>		DATE		28 SEPT. 79		THRU		13 NOV. 79							
FACILITY		L-16 LAUNCH		RUN		522		THRU		603							
DATA CHANNEL	DATA POINT	SENSOR MFG & TYPE	S/N	SENSOR SENS	EXCITE V	FILTER SERIES	S/M	AMP GAIN	S/M	SAMPLE RATE	FORMAT	F.S. SENS - 2.5 Volts	FILTER #2	BRIDGE ZERO RANGE	BRIDGE BALANCE RESISTORS	BRIDGE COMPLETION RESISTORS	SPECIAL NOTATIONS
29	Velocity	Globe Ind 22672		* 2020 Volts/FPS 10.25 mV/g	--	60	17	1	--	1K	1	77.26 ft	120	2.50	+5.0 -0.0		*Attenuator Set @ 6.242 = .03236 Volts/FPS
31	Slid Z	Endevco 2264-200	BV56	2.803 mV/g	10.00	60	22	100	2	1K	1	8.919 g	120	2.78	+5.0 -0.0	1.34 Resistors into Gnd	
32	Seat Pan X	"	BV12	*4.728 mV/g	10.00	60	4	50	28	1K	1	10.58 g	120	*3.50	+5.0 -0.0	131K into Gnd	*Test 522-530 Xducer Zero @ 2.50 *Bias Jumper not used in Connector
33	Seat Pan Y	"	BV41	*4.853 mV/g	10.00	60	25	50	24	1K	1	10.30 g	120	2.50	+5.0 -0.0	61K into Gnd	*Bias Jumper not used in Connector
34	Seat Pan Z	"	BV63	2.782 mV/g	10.00	60	20	100	4	1K	1	8.986 g	120	2.78	+5.0 -0.0	135K into Gnd	
35	Center Load Link X	Micro-Meas EA-06-062 1.1-350	004	10.35 uV/lb	10.00	60	26	402	9	1K	1	600.9 lb	120	2.50	+5.0 -0.0	82K into Gnd	
36	Slid Y	Endevco 2262A-200	*FR37	5.674 mV/g	10.00	60	26	25	7	1K	1	*17.62 g	120	2.50	+5.0 -0.0	--	*Test 522-530 S/N R647 @ 1.259 mV/g @ 100 Gain (F.S. 19.86 g) Patch event out to Channel 1 via Slid Data Positive Signal - Low to High
37	Point				--	1000	21	1	--	1K	1	--	2000	2.50	+5.0 -0.0	--	Located just after shuttle separates
38	Slid				5.00	37	1	1	--	1K	1	--	--	0.0	+5.0 -0.0	--	Located just prior to water brake
39	T2 Start				5.00	38	1	1	--	1K	1	--	--	0.0	+5.0 -0.0	--	
47	2.5 Volt Bias				--	39	3	1	--	1K	1	2.5 Volt	360	2.50	+5.0 -0.0	--	
48	5 Volt E.C.				5.00	47	14	1	--	1K	1	5 Volt	360	0.0	+5.0 -0.0	--	

PAGE 3 OF 3

Figure A - 19c

PROGRAM F-111 GY DATE 14 Dec 1979  
 LOW G LAUNCH FACILITY RUN NO'S 522-603

DATA POINT	TRANSDUCER MFG & MODEL	S/N	PRE CAL		POST CAL		% CHANGE	COMMENTS
			DATE	SENS mV/g	DATE	SENS mV/g		
Sled X	Endevco 2260-250-10	RF47	26 Mar 79	1.259	15 Oct 79	--	--	Calibration check showed defective erratic open
Sled X	Endevco 2262A-200	FR37	15 Oct 79	5.674	12 Dec 79	5.656	0.8	Test 539 and subsequent
Sled Y	Endevco 2264-200	BX49	28 June 79	2.545	12 Dec 79	2.566	0.8	
Sled Z	Endevco 2264-200	BV56	24 May 79	2.803	12 Dec 79	2.820	0.6	
Head X	Endevco 2264-200	BN80	30 Apr 79	2.694	12 Dec 79	2.326	-13.8	Accelerometer showed noise spikes above 20g; F <sub>N</sub> shifted from 4.6 to 4.2 KHz
Head Y	Endevco 2264-200	BQ42	30 Apr 79	2.747	12 Dec 79	2.721	-0.9	
Head Z	Endevco 2264-200	BQ51	30 Apr 79	2.556	12 Dec 79	2.557	0	
Chest X	Endevco 2264-150	BC26	30 Apr 79	2.754	11 Dec 79	2.788	1.2	
Chest Y	Endevco 2264-150	BB13	30 Apr 79	2.395	11 Dec 79	2.411	0.7	
Chest Z	Endevco 2264-150	2A20	30 Apr 79	2.579	12 Dec 79	2.592	0.5	
Seat Pan X	Endevco 2264-200	PM12	24 May 79	3.174	13 Dec 79	3.170	-0.1	
Seat Pan Y	Endevco 2264-200	BV41	24 May 79	3.316	13 Dec 79	3.280	-1.1	
Seat Pan Z	Endevco 2264-200	BN63	8 Mar 79	2.732	13 Dec 79	2.807	0.9	

Figure A - 20a

PROGRAM F-111 GY DATE 14 December, 1979  
 LOW G LAUNCH FACILITY RUN NO'S 522-603

DATA POINT	TRANSDUCER SEC & MODEL	S/N	PRE CAL		POST CAL		% CHANGE	COMMENTS
			DATE	SENS uV/lb	DATE	SENS uV/lb		
Left Lap	MM EA-06-1258Z-350	16	5 June 79	15.09	14 Dec 79	14.94	-1.0	
Right Lap	MM EA-06-1258Z-350	14	5 June 79	13.57	14 Dec 79	13.78	1.5	
N-G Strap	MM EA-06-1258Z-350	143377	4 Sept 79	1.88	17 Dec 79	2.175	15.7	
Left Inert Reel	Lebow 3419-3.5K	363	1 June 79	8.025	17 Dec 79	7.80	-2.8	
Right Inert Reel	Lebow 3419-3.5K	364	1 June 79	7.390	17 Dec 79	7.35	-0.5	
Left Reflect	MM EA-06-1258Z-350	02-4	2 May 79	29.82	17 Dec 79	27.94	-6.3	Initially calibrated prior to belt having been sewn to buckle
Right Reflect	MM EA-06-1258Z-350	01-1	2 May 79	25.90	17 Dec 79	24.30	-6.1	
Left Load Link	MM EA-06-062-TJ-350	001	1 June 79	10.92	14 Dec 79	10.94	0.2	
Right Load Link	MM EA-06-062-TJ-350	002	1 June 79	10.17	14 Dec 79	10.24	0.7	
Cen Load Link	MM EA-06-062-TJ-350	004	1 June 79	10.35	14 Dec 79	10.53	1.7	

MM - Micro Measurements Strain Gauge

Figure A - 20b

PROGRAM F-111 + Gy

DATE 14 Dec. 1979

LOW G LAUNCH FACILITY RUN NO'S 373-521

DATA POINT	TRANSDUCER MFG & MODEL	S/N	PRE CAL		POST CAL		% CHANGE	COMMENTS
			DATE	SENS mV/g	DATE	SENS mV/g		
Sted X	Endevco 2264-200	BX49	28 Jun 79	2.545	12 Dec 79	2.566	0.8	Calibration Check Showed Defective Erratic Open.
Sted Y	Endevco 2260-250-10 RF47		26 Mar 79	1.259	15 Oct 79	--	--	
Sted Z	Endevco 2264-200	BV56	24 Mar 79	2.803	12 Dec 79	2.820	0.6	
Head X	Endevco 2264-200	BN80	30 Apr 79	2.694	12 Dec 79	2.326	-13.8	Accelerometer Showed Noise Spikes above 20g; F <sub>N</sub> Shifted from 4.6KHz to 4.2 KHz
Head Y	Endevco 2264-200	BQ42	30 Apr 79	2.747	12 Dec 79	2.721	-0.9	
Head Z	Endevco 2264-200	BQ51	30 Apr 79	2.556	12 Dec 79	2.557	0	
Chest X	Endevco 2264-150	BC26	30 Apr 79	2.754	11 Dec 79	2.788	1.2	
Chest Y	Endevco 2264-150	BB13	30 Apr 79	2.395	11 Dec 79	2.411	0.7	
Chest Z	Endevco 2264-150	2A20	30 Apr 79	2.579	12 Dec 79	2.592	0.5	
Seat Par. X	Endevco 2264-200	BV12	24 May 79	3.171	13 Dec 79	3.170	0.1	
Seat Par. Y	Endevco 2264-200	BV41	24 May 79	3.316	13 Dec 79	3.230	-1.1	
Seat Par. Z	Endevco 2264-200	BN63	8 Mar 79	2.782	13 Dec 79	2.807	0.9	

Figure A - 20c

PROGRAM F-111 + Gy DATE 14 December 1979  
 LOW G LAUNCH FACILITY RUN NO'S 373-521

DATA POINT	TRANSDUCER MFG & MODEL	S/N	PRE CAL		POST CAL		% CHANGE	COMMENTS
			DATE	SENS uV/lb.	DATE	SENS uV/lb.		
Left Lap	MM EA-06-1258Z-350	15	5 Jun 79	14.91	18 Dec 79	14.06	-5.7	Buckle deformation noted during testing
Left Lap	MM EA-06-1258Z-350	16	5 Jun 79	15.09	14 Dec 79	14.94	-1.0	
Right Lap	MM EA-06-1258Z-350	14	5 Jun 79	13.57	14 Dec 79	13.78	1.5	
N-G Strap	Lebow 3419-3.5K	373	13 Jun 79	7.912	18 Dec 79	8.16	3.1	Test 373 - 384 Only
N-G Strap	MM EA-06-1258Z-350	144111	16 Aug 79	.321	--	--	--	Test 427 - 456 Only - Damaged
L. Inert Reel	Lebow 3419-3.5K	363	1 Jun 79	8.025	17 Dec 79	7.80	-2.8	
R. Inert Reel	Lebow 3419-3.5K	364	1 Jun 79	7.390	17 Dec 79	7.35	-0.5	
L. Reflect	MM EA-06-1258Z-350	02-5	16 May 79	29.10	28 Aug 79	28.04	*-4.3	Test 375 - 427 Only
L. Reflect	MM EA-06-1258Z-350	02-4	2 May 79	29.10	27 Aug 79	27.94	*-4.0	Test 471 and 500 Only
L. Reflect	MM EA-06-1258Z-350	02-6	3 May 79	30.77	11 Sept 79	29.45	*-4.5	Test 428 - 470 Only
R. Reflect	MM EA-06-1258Z-350	01-1	2 May 79	25.90	17 Dec 79	24.30	*-6.1	
L. Load Link	MM EA-06-062-TJ-350	001	1 Jun 79	10.92	14 Dec 79	10.94	0.2	
R. Load Link	MM EA-06-062-TJ-350	002	5 Jun 79	10.17	14 Dec 79	10.24	0.7	
C. Load Link	MM EA-06-062-TJ-350	004	5 Jun 79	10.35	14 Dec 79	10.53	1.7	
N-G Strap	MM EA-06-1258Z-350	143377	4 Sept 79	1.88	17 Dec 79	2.175	15.7	

\* Calibrated Prior to Belt Having  
 Been Sewn on Buckle

MM - Micro Measurements Strain Gauge

Figure A - 20d

PROGRAM F-111 + G2 DATE 14 Dec. 1979

VERTICAL DROP TOWER FACILITY RUN NO'S 177-276

DATA POINT	TRANSDUCER MFG & MODEL	S/N	PRE CAL		POST CAL		% CHANGE	COMMENTS
			DATE	SENS mV/g	DATE	SENS mV/g		
Carriage X	Endevco 2264-200	BW10	24 May 79	2.558	9 Nov 79	2.582	0.9	
Carriage Y	Endevco 2264-200	BV56	24 May 79	2.803	12 Dec 79	2.820	0.6	
Carriage Z	Endevco 2262A-200	FR37	10 May 79	5.612	15 Oct 79	5.674	1.1	
Head X	Endevco 2264-200	BT80	30 Apr 79	2.694	12 Dec 79	2.526	-13.8	Accelerometer showed noise spikes above 20g; F <sub>0</sub> shifted from 4.6 to 4.2 KHz
Head Y	Endevco 2264-200	BQ42	30 Apr 79	2.777	12 Dec 79	2.771	0	
Head Z	Endevco 2264-200	BQ51	30 Apr 79	2.556	12 Dec 79	2.557	0	
Chest X	Endevco 2264-150	BC26	30 Apr 79	2.754	11 Dec 79	2.788	1.2	
Chest Y	Endevco 2264-150	BB13	30 Apr 79	2.395	11 Dec 79	2.411	0.7	
Chest Z	Endevco 2264-150	2A20	30 Apr 79	2.579	12 Dec 79	2.592	0.5	
Seat Pan X	Endevco 2264-200	BW12	24 May 79	3.174	13 Dec 79	3.170	-0.1	
Seat Pan Y	Endevco 2264-200	BV41	24 May 79	3.316	13 Dec 79	3.280	-1.1	
Seat Pan Z	Endevco 2264-200	BN63	8 Mar 79	2.782	13 Dec 79	2.807	0.9	

Figure A - 20e



PROGRAM F-111 + GZ

DATE 14 December, 1979

## VERTICAL DROP TOWER FACILITY RUN NO'S 177-276

DATA POINT	TRANSDUCER NEG & MODEL	S/N	PRE CAL		POST CAL		% CHANGE	COMMENTS
			DATE	SENS UV/IN	DATE	SENS UV/IN		
Left Lap	M-M EA-06-1258Z-350	15	5 June 79	14.91	13 Dec 79	14.06	1.7	Buckle deformation noted during testing
Right Lap	M-M EA-06-1258Z-350	14	5 June 79	13.15	14 Dec 79	13.78	1.5	
M-C Strap	Lebow 3419	373	1 June 79	7.912	18 Dec 79	8.16	3.1	Initially calibrated prior to belt having been sewn to buckle
L. Inert Reel	Lebow 3419	363	1 June 79	8.025	17 Dec 79	7.80	-2.8	
R. Inert Reel	Lebow 3419	364	1 June 79	7.390	17 Dec 79	7.35	-0.5	
L. Reflec.	M-M EA-06-1258Z-350	02-5	16 May 79	29.30	28 Aug 79	28.04	-4.3	
R. Reflec	M-M EA-06-1258Z-350	01-1	2 May 79	25.90	17 Dec 79	24.30	-6.1	
L. Load Link	M-M EA-06-062TJ-350	001	1 June 79	10.92	14 Dec 79	10.94	0.2	
R. Load Link	M-M EA-06-062TJ-350	002	5 June 79	10.17	14 Dec 79	10.24	0.7	
C. Load Link	M-M EA-06-062TJ-350	004	5 June 79	10.35	14 Dec 79	10.53	1.7	

MM - Micro Measurements Strain Gauge

Figure A - 20f

## AUTOMATIC DATA ACQUISITION AND CONTROL SYSTEM

### SLED-BORNE DATA ACQUISITION SYSTEM

Figure A-21 shows the block diagram of the Sled-Borne Data Acquisition (SBDA) System. This system consists of four parts: the power conditioner, the signal conditioner, the encoder and the junction box. The power conditioner receives a 28 vdc, 4A power source and provides several regulated supplies. They are the +15 and -12 vdc (0.8A) supply for the signal conditioners, the 5 vdc and the 10 vdc bridge excitation voltages (1.2A total), and the 2.5 vdc signal output bias voltage (0.1A). The original 28 vdc source also powers the pulse code modulator (PCM) encoder.

The signal conditioner consists of 48 signal modules. Each module is capable of processing a sensor (transducer) signal which can be a voltage generating source or a bridge-type sensor. If a bridge-type sensor is used, the bridge excitation voltage is selectable from the 5V or the 10V source. The bridge (half or full bridge) can be completed and balanced by connecting external resistors to the module input connector.

The signal conditioning module has two sections. The amplifier section has seven programmable gains to cover the input signal dynamic ranges from 50 MV to 5 V. The filter section has four programmable frequencies according to the SAE recommended classes 60, 180, 600, and 1000. There are three external connectors for each signal module. The input connector connects a signal source or a bridge, the balance resistors, the bridge completion resistors, the strapping of excitation voltage, and the reference offset. The gain plug selects one of the seven amplifier gains and the filter frequency plug selects one of the four filter classes.

The 48 channel data signals are time multiplexed via an encoder which digitizes the 48 analog data sources into 48 11-bit digital words. Two additional 11-bit synchronization (sync) words are added to the data frame. The 50-word frame was then sampled at a rate of 1000 samples/second. This serial digital data along with three additional synchronization pulse trains (bit sync, word sync, and frame sync) are connected to the computer room by four twisted pairs incorporated into a drag cable. They pass through a junction box to the digital computer interface to allow recording and processing.

#### PDP 11-34 DATA COLLECTION AND STORAGE

The PDP 11-34 minicomputer is the main control for all electronic data collection and storage functions. The block diagram of Figure A-22 shows the processor and its related equipment. All data transfer in the data collection system is under software control by the central processor unit. Serial data is constantly being received by the data formatter unit from the sled data encoder. This data is converted by the data formatter from serial to parallel for input via a buffered data channel to computer memory for storage on disk. Finally, the data is transferred from disk to magnetic tape for permanent storage following the test event.

#### QUICK LOOK INERTIAL DATA

After each test, the data was sampled and checked. This check was made using the Single Channel Analysis (SCAN) routine for the PDP 11-34 processor. This routine allows the operator to access and plot up to 2000 points of data for any of the 48 data channels. The SCAN program can process vertical or horizontal deceleration data under operator control. The operator selects the channel to be processed and enters its location description as well as the start and stop points to be processed. A maximum of 2000 milliseconds or 2000 data points may be accessed for each plot. The program converts the raw data into the appropriate units of measure and calculates the minimum and maximum values during the sample interval. If the sample is acceleration data, the velocity will also

be calculated using an integration process. An added optional feature is a digital smoothing routine which can smooth the data to remove any excess high frequency component that may be present.

#### TIMING REFERENCE - INERTIAL DATA

A 100 Hertz timing reference was an integral part of the Data Acquisition System. Figure A-23 shows the timing signal wave shape. This 100 Hertz signal was initiated when the sled passed over a detector located approximately 10 feet from the waterbrake. One hundred and twenty milliseconds after this timing signal, a second signal, marking the beginning of the impact event, was generated and provided a temporal reference for electronic and photometric data.



Figure A-21 - SLED BORNE EQUIPMENT

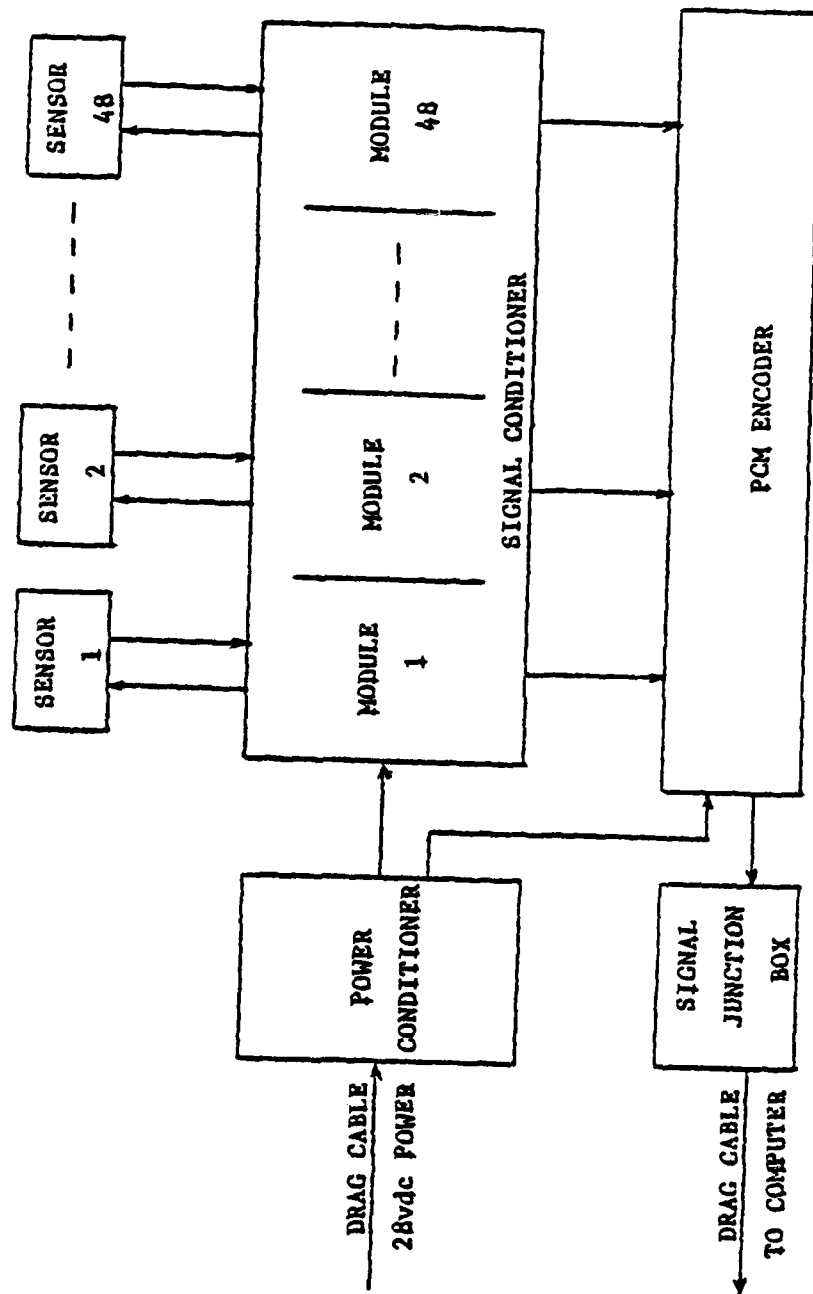


Figure A-22 - Sled Borne Data Acquisition System

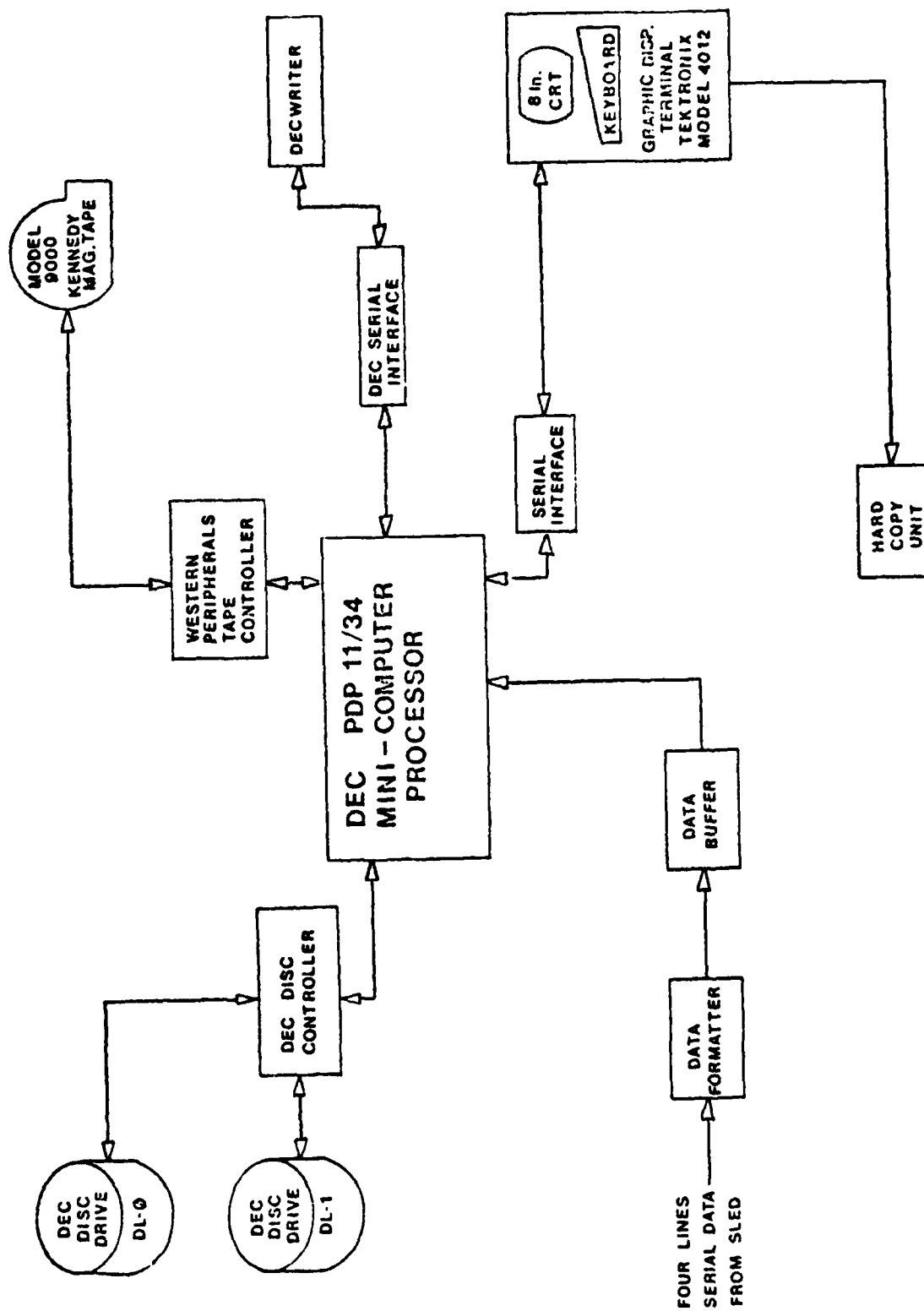


Figure A-23 - Central Data Acquisition and Storage System

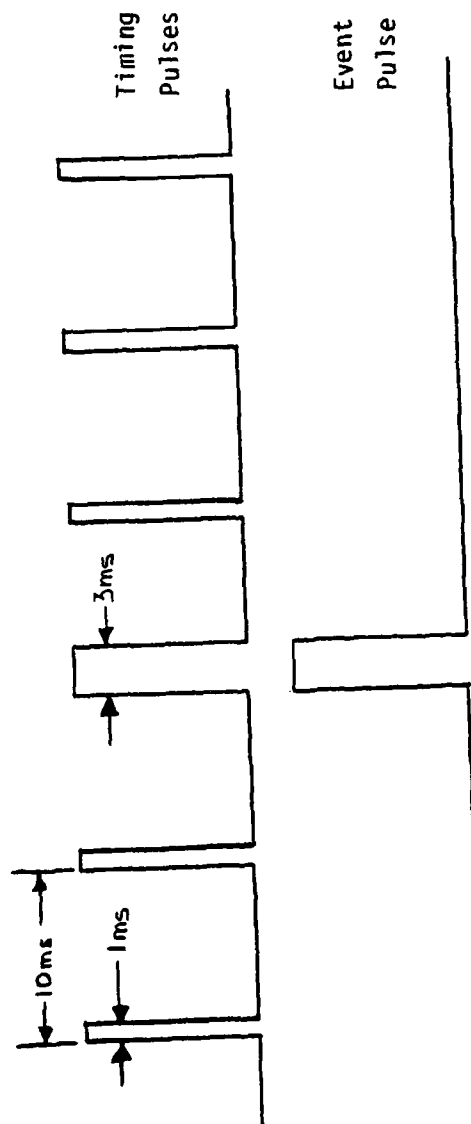


Figure A-24 - Timing Signals (Inertial Data)



## KINEMATIC DATA ACQUISITION SYSTEM

### HIGH SPEED CAMERAS AND CONTROL

Kinematic data were acquired through the use of high speed 16mm cameras operating at a rate of 500 frames per second. The cameras were Teledyne Milliken Model DBM45 pin registered units which were capable of withstanding 25 G. Two cameras were mounted on the test sled or carriage and one camera was mounted off the sled or carriage. During a test the cameras were started and stopped automatically by the Camera and Lighting Control Station which is part of the impact facility safety and control system. The cameras were started at a preset time in the test sequence and run for a period of 8 seconds.

### AUTOMATIC FILM READER

The AFR subsystem was developed by Photo Digitizing Systems, Inc. It automatically extracts photo data, digitizes it and records it on magnetic tape. The subsystem consists of:

- Film motion analyzer with 16mm projection head
- Electronic scanning camera
- Control unit
- Alphanumeric Cathode Ray Tube (CRT)
- Line printer
- Magnetic tape transport

The film reader recognizes quadrant or circular fiducial targets. It automatically tracks targets and extracts data for up to ten targets per film frame at a minimum rate of one-half film frame per second. Film may be processed through the reader manually or automatically. Figure A-25 is a block diagram of the Automatic Film Reader System (AFR).

The X-Y coordinate position of each target on each film frame is input to the computer and recorded on magnetic tape.

A NOVA 3/12 computer controls the AFR which contains 16k 16-bit words of core memory, a CRT terminal, and a magnetic tape transport with suitable interface. In addition, a parallel data link is provided between the NOVA 3/12 and the PDP 11/34.

An alphanumeric CRT (DGC 6052) automatically displays the AFR control information. The CRT display and its keyboard function are used as separate devices. The keyboard is a transmit-only device and the display is a receive-only device but has the additional capability of transmitting cursor position information on program request.

A hard copy device, LA36 Decwriter II, provides hard copies of the information presented on the 6052 CRT. The LA36 is medium-sized interaction terminal with a low-speed impact printer and a standard ASCII keyboard consisting of alphanumeric characters and non-printing system control codes.

Either the Decwriter or the 6052 CRT output may be assigned to the PDP 11/34A. Programs can also be established which can "download" from the disc on the PDP 11/34A to the NOVA, or digital film data can be loaded on the PDP 11/34A for processing or disc storage.

#### QUICK LOOK KINEMATIC DATA

The Instar (Instant Analytical Replay) System is a high-performance video recorder and display device designed for the analysis of high speed motion. It is a compact, portable, fully transistorized instrument that combines the long recording capacity and instant replay features of video tape. Each system records 120 frames/second with an effective shutter speed of 10 $\mu$ s or less and will playback all recordings in real time, stop action, reverse slow motion, and variable slow motion (2%-15% of real time). Each of the frames is sequential and non-interlaced.

Instar incorporates two cameras and a special effects generator for the added flexibility of split screen. The simultaneous display of two events offers the precise evaluation of three dimensional problems

or the referencing of one physical event to an instrument (i.e., digital clock or oscilloscope). Other features include:

- End of tape sensing
- Foolproof logic control sequences
- Dynamic braking
- Interscene blanking
- Video logic signal processing modules

The Instar System was utilized to record each impact event. This video tape was available for review by the test conductor and/or medical monitor immediately after the impact event.

#### TIMING REFERENCE - KINEMATIC DATA

The high-speed cameras utilized a light-emitting diode driver, LM Dearing Model 2/3/3R, to place a mark on the film, thereby establishing a time reference. This mark (a red bar) was generated once every 10 milliseconds for a duration of 1 millisecond and was initiated when the sled passed a detector mounted approximately 10 feet in front of the waterbrake. These photo timing pulses were generated at the same time as the electronic timing pulses, thus providing temporal correlation between the two signals. A special event flash was used to mark the film frame at the start of the impact event. This flash consisted of an electronic photo flash which was actuated by the electronic event signal. Figure A-26 shows the film, flash, and timing bars.

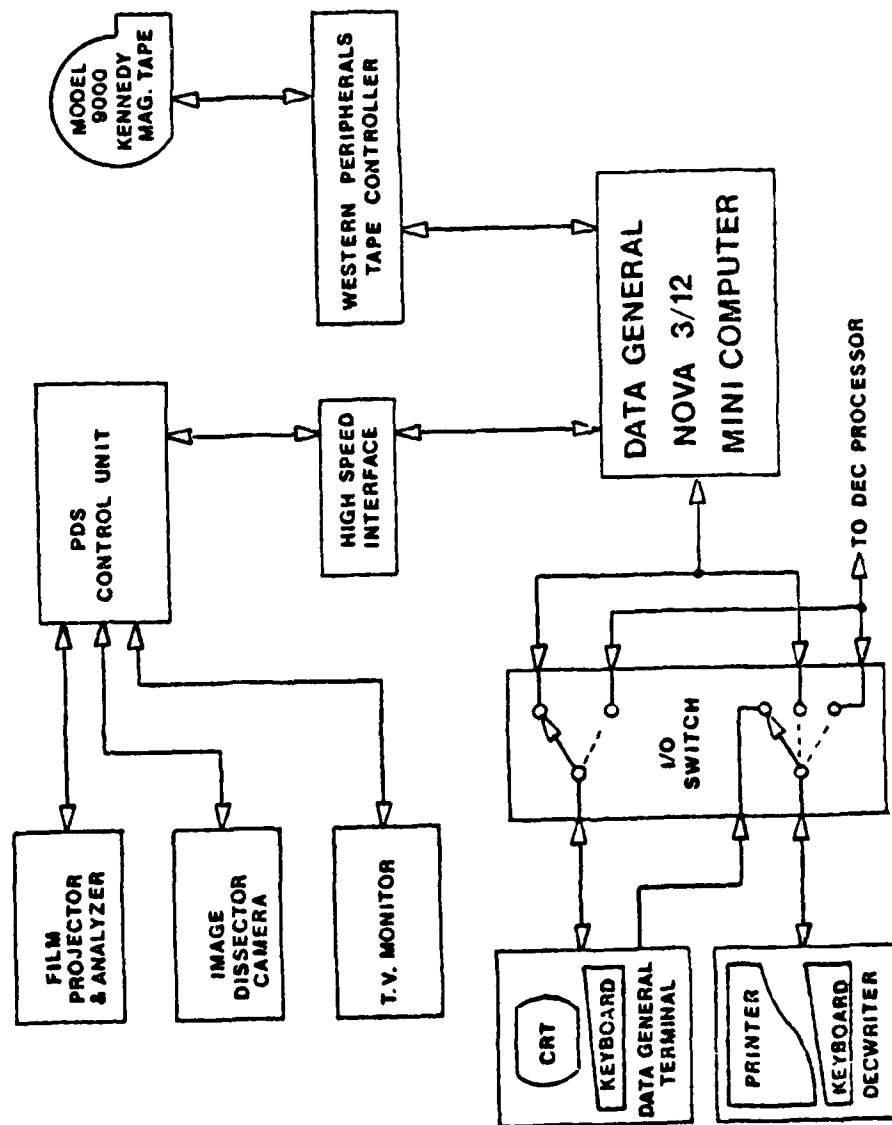


Figure A-25 - Automatic Film Reader System

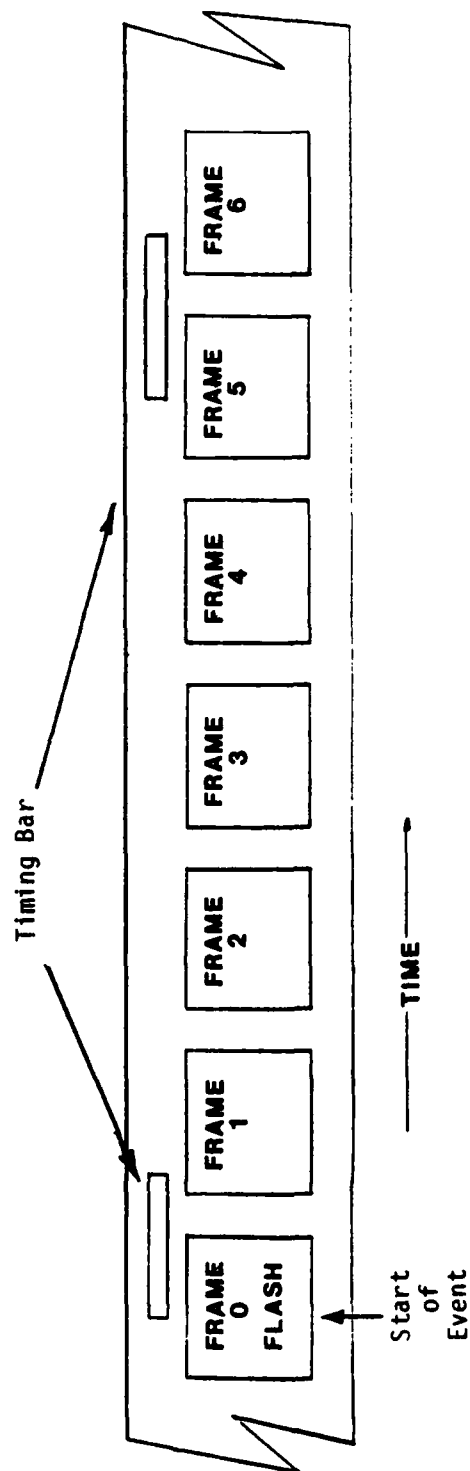


Figure A-26 - Timing Reference (Photo Data)

## APPENDIX B

### PHOTOMETRIC ANALYSIS METHODS

#### INTRODUCTION

The objective of photometric analysis was to analyze the motions of photometric targets (fiducials) attached to the test subject in order to describe the body's dynamic response to impact. This appendix describes the reduction methods and software used to derive this information.

Complete reduction of a test film involved target position digitization and computer plotting of positions, velocities, and accelerations of each fiducial. These plots and the results of the electronic data were used to describe test subject motion.

The F-111 photometric analysis was accomplished using an automatic film reading system. Photoanalysis software had been previously developed under a contract with the University of Dayton Research Institute (UDRI). This software was used in the present study, but changes were required to suit specific needs.

The analysis techniques are described in five sections. The first describes the test set-up on both the Vertical Deceleration Tower (VDT) and the Horizontal Decelerator (HD) impact facilities. The next section explains the film analysis equipment and methods. The last three sections briefly describe the three software programs developed to reduce the digitized film data. The programs are called TOWER, POOCH, and SLED. They were written in Fortran IV language suitable for use on the Control Data Corporation (CDC) CYBER 74 computer system. The final section of this appendix contains conclusions and recommendations.

#### TEST CONDITIONS

Testing was divided into three phases. The first phase was conducted on the VDT and consisted of 73 vertical ( $+G_z$ ) impacts. High speed motion pictures were recorded with two on-board cameras and one off-board camera. (See Figure B - 1.) The second and third phases ( $+G_y$  and  $-G_x$ , respectively) were conducted on the HD facility. There were a total of 60 lateral tests and 54 fore-aft tests in these phases. High speed motion pictures were recorded with two on-board cameras and one off-board camera. (See Figure B - 2.)

Guidelines for placing targets on the subjects and the test fixture were obtained from SAE J138, "Film Analysis Guide for Dynamic Studies of Test Subjects". Fiducials were affixed to each subject as shown in Figures B - 3, B - 4, and B - 5.

Before an impact test, each target's relative position was documented on a Photo Anthropometric Data Sheet. A portion of the data recorded on these sheets for the vertical test phase included the Y axis distance from the right shoulder target to the opposite shoulder and the Y axis distance from the

cheek target to the nose. This information was required for input into the  $+G_z$  film analysis routine.

The photo anthropometric data recorded before the  $+G_y$  and  $-G_x$  tests were not required for the film analysis routines. These data were used to check the initial target positions derived from the film analyses.

Reference targets affixed to the test fixture were accurately surveyed for each test phase. These stationary targets were needed as orientation for the moving targets and also enabled the camera's vibrations to be identified within the data. For the  $+G_z$  phase, one target was used as a stationary reference point. By computing the distance from this reference point to each target on the subject for each frame of film, errors due to vibration of the camera support were reduced. The error in the actual positions of the targets was at most  $\pm 0.5$  inches. However, the error in net displacements was at most  $\pm 0.15$  inches. Errors in velocities and accelerations were not estimated.

In the  $+G_y$  and  $-G_x$  phases, several targets were used for reference to check the accuracy of the SLED computer program. The program located these points to within 0.4 inches of their actual surveyed positions. Errors in the raw test data due to film reading and camera vibrations were reduced in a smoothing routine which will be described later. Errors in the net displacements were of the same magnitude as for the  $+G_z$  tests.

The set of test films selected for digital processing was chosen to provide a representative sample from all the tests at the maximum impact level for each phase. The subjects were exposed in different seat configurations according to the experimental design. Three films of each configuration were chosen to provide data on a small, a medium, and a large subject.

#### FILM ANALYSIS

The 16 mm high speed films were analyzed using an automatic film reader that digitized the fiducial positions frame-by-frame. These digital data were then used with computer programs to provide descriptions of target motions.

The Automatic Film Reader (AFR) is part of a Photo Digitizing Systems model 200 processor. This system also consists of an electronic scanning camera and a Data General Corporation (DGC) Nova 3/12 computer. The semiautomatic AFR is manually initialized by selecting, with a cursor, the targets of interest in the first frame of data. Targets on subsequent frames are automatically scanned, acquired, and identified and their X and Y coordinates are digitized by the Nova computer. The digitized data are then stored on magnetic tape.

A target was manually tracked if it was partially obscured or otherwise lost by the AFR. Up to twelve targets within one film frame can be automatically scanned at a rate of  $\frac{1}{2}$  frame per second. The rate of manual tracking is about one frame per minute depending on the number of targets. The X and Y coordinate resolution specified by the manufacturer of the AFR is 0.025% of the major film dimension.

The PDS is also capable of tracking timing bars (t-bars) on the edge of the film. The centers of the t-bars are located and a film speed is calculated at every frame with a timing bar. Frames between the t-bars are assigned the film speed computed from the previous t-bar. These film speeds are digitized, as are the target position data for each frame. When read into the computer analysis program, the film speeds are used to assign a discrete time to each frame.

Specific photo reduction procedures were written to instruct the operator of the AFR. The test films were selected as previously described. For the  $+G_z$  tests, only the side camera films were needed for analysis. For the  $+G_y$  and  $-G_x$  tests, both on-board camera films were needed for analysis.

The targets to be tracked for each test phase were identified on a Camera Fiducial Requirements Sheet. The AFR operator previewed the films to determine if each target was observable throughout the impact. If a target was obscured, its position was either estimated by the operator, if possible, or assigned a value of zero.

The operator listed each processed film in a log book. This log documented the targets that were tracked, the number of frames processed, and the number of frames between the event flash (or first timing bar if there was no flash) and the first tracked frame. Sufficient frames were tracked to characterize the subject's impact response. This number varied between 75 and 150 frames.

The operator also logged the presence of the event flash and timing bars. The event flash was missing on seven  $+G_z$  tests. All other tests had an event flash. If there was no event flash, the resulting data could not be precisely synchronized with the electronic data. If there were no timing bars on the film, the data were processed using the gross estimate of a constant film speed of 500 frames per second.

In AMRL-TR-78-94, UDRI has documented computer analysis routines that were used to process film data from past impact studies at AFAMRL/BBP. The three programs developed were named HIFPD, POOCH, and SLED. The programs contain the fundamental algorithms required to reduce the data. However, special modifications of the programs were required to handle the films processed in this study. These modifications, described in the next section, included the renaming of targets and a new algorithm for smoothing the raw position data.

#### PROGRAM TOWER

The program that evolved from UDRI's HIFPD was named program TOWER. This was the routine used to reduce the test film data from the side camera on the  $+G_z$  impacts. The program is supplied with program control parameters, the digital coordinates of the fiducials from the PDS, and the pretest measurements of the targets' initial positions. The resulting output consists of tabulations and plots of the frame-by-frame positions, velocities, and accelerations of up to eight targets. In addition, the angular velocity and angular acceleration between two head targets are computed and plotted.



The following sections present a general description of the main program and all subroutines, except the CALCOMP routines, which make up the standard CDC plotting package. The focus of the following sections will be on the differences between TOWER and UDRI's HIFPD (Graf et al., 1978).

One of the major differences between TOWER and HIFPD arose from the orientation of the on-board side camera on the VDT. The camera's optical axis was inclined at a positive angle of seven and one-half degrees with respect to the horizontal. Therefore, the film image was no longer planar motion normal to the optical axis. HIFPD could only be used with film data from a camera whose optical axis was normal to the plane of motion.

Rather than analytically model and program the analysis routine to take into account this novel camera orientation, an empirical approach was used instead. A premeasured gridboard was photographed at two distances from the side camera. The board was marked in inches and had fiducials applied at intersections of its vertical and horizontal lines. The resulting grid films were put on the AFR and the fiducials were tracked. The reader's film image coordinates allowed an empirical equation to be developed that transformed the three known quantities (target distance along +Y axis from zero reference on the F-111 seat and target's horizontal and vertical film image coordinates) into the two unknown quantities (the target's X and Z coordinates relative to the zero reference of the F-111 seat).

Since target motion was assumed to be planar, each target's measured Y coordinate was considered to be constant. The time-varying X and Z coordinates, therefore, as well as the fixed Y coordinate, completely determined a target's motion. These coordinates were plotted to show position in the X-Z plane. First and second time derivatives were plotted to show velocity and acceleration. The transformation from image coordinates to scene coordinates, which was solved from the grid films, was accurate to within  $\pm 0.5$  inches.

Another difference between TOWER and HIFPD was the determination of film speed and time scale. In HIFPD, the film speed was calculated from the ratio of the number of frames read to the total elapsed time (found by counting the timing bars and multiplying by 0.01 seconds). This resulted in a constant average film speed.

However, high speed camera motors, such as those used in this study, generally do not run at constant speed. To account for this, the PDS software calculated the film speed from every pair of adjacent timing bars. A target's coordinates during the four or five frames between timing bars was assigned a time based on a film speed computed from the two timing bars enclosed in that particular interval. Therefore, the time dependent calculations were made on the premise that film speed was the same for all frames within a pair of timing bars. The PDS software computed the film speed, S, in frames per second as follows:

$$S = \frac{(L_2 - L_1 + M \times NL)}{(N \times NL)} \times R$$

where  $L_1$  is the vertical coordinate (in AFR units) of the center of the first timing bar;  $L_2$  is the vertical coordinate (in AFR units) of the center of the second timing bar; M is the number of frames skipped between the pair of

timing bars (including the frame of the second t-bar); N is the number of timing bars between the first and second, including the second (in this case,  $N = 1$ , always); NL is the vertical dimension (in AFR units) of one frame of film; and R is the known frequency of the timing bars (in this case,  $R = 100$  Hz). In Program TOWER, the time displacement then was given by  $t \text{ (sec)} = 1/S$ . (Note: If only every i-th frame of film is tracked, where  $i \geq 1$ , then incorrect speeds, which are integer multiples of the true speeds, may be generated.)

The flash frame's time was assigned zero on all films. If no event flash occurred during the test, the photo data could not be referenced to time zero. In this event, the film data's time base was initialized at the first t-bar, which usually appeared about nine frames after the start of the event. Finally, if for some reason no timing bars were marked on the film, then the film speed was assumed to be 500 frames per second for the time calculations.

As in HIFPD, the program TOWER contained an algorithm to reduce the effect of camera vibration in the target position data. The effect of camera vibration on the data was visualized by plotting the position of the seat reference target. High frequency vibration of this "stationary" target was due to the lack of rigidity in the camera mount and framing variations in the camera. In order to eliminate this "noise" from the data, the seat reference target's position on each frame of film was compared to its position on the initial frame. The difference between these two values in the X and Z directions was subtracted out of all of the moving target data. Then, the data were transformed into scene coordinates with the formula described earlier.

The position data were then filtered. In HIFPD, a subroutine was used that smoothed the X and Z axes data with a moving, eleven point, quadratic least square fit. TOWER employed a superior smoothing subroutine. The data were transformed from the time domain to the frequency domain by taking discrete or Fast Fourier Transforms (FFT's). Plots of amplitude versus frequency for several target's displacement data showed that noise occurred at frequencies higher than those expected for the relevant data. Most of this noise was eliminated simply by dropping off high frequency terms from the Fourier representation. The chosen cut-off frequency was 20 Hz.

After the data were filtered, they were converted back to the time domain by an inverse FFT. Then, TOWER printed the frame-by-frame position data and CALPLOT routines were employed to plot the resultant data. A composite plot was drawn that included each target's path in the X-Z plane throughout the impact. (See sample plots.)

Computing velocities and accelerations was a simple matter in the frequency domain. This was accomplished with subroutine DERIV by taking each target's X and Z time histories, computing their FFT, and then multiplying each term by the coefficient of their corresponding angular frequency followed by computation of the inverse FFT. This was done twice if the second derivative was needed for acceleration. When  $dx/dt$ ,  $dz/dt$ ,  $d^2x/dt^2$ , and  $d^2z/dt^2$  were found in the time domain, resultant velocities and accelerations were computed by  $vel^2 = (dx/dt)^2 + (dz/dt)^2$  and  $acc^2 = (d^2x/dt^2)^2 + (d^2z/dt^2)^2$ .

By computing the angle between two head targets (as done in program HIFPD), program TOWER derived the angular velocities and accelerations of a pair of head targets with the same DERIV subroutine. These data were also printed and plotted.

The accuracy of the filtering and differentiating routines was verified using an analytical sine wave. First, the filter routine was checked with raw target data. These data were filtered at 120 Hz and the output was verified. Then, to check the FFT representation, sample points from five cycles of a sine wave were input, transformed to the frequency domain, transformed back to the time domain, and output. The output was identical to the input. Similarly, the differentiation routine was verified using a sampled sine wave. The output was verified to be the corresponding sampled cosine wave.

TOWER utilized punched cards and magnetic tape as data sources. The punched cards were coded with program control variables and test parameters. The magnetic tape was coded with the digitized film frame position data. The typical procedure was to process a series of tests on the CDC computer in a batch type operation. Below is a description of the punch card input.

<u>Column</u>	<u>Format</u>	<u>Name</u>	<u>Description</u>
<u>Card Number 1</u>			
1-10	A10	Title (1)	Test date
11-20	A10	Title (2)	Test number
21-30	A10	Title (3)	F-111 (test program)
31-40	A10	Title (4)	G <sub>z</sub> (test phase)
41-50	A10	Title (5)	Subject identification
51-60	A10	Title (6)	Impact level (G's)
61-70	A10	Title (7)	Seat configuration
<u>Card Number 2</u>			
1-5	I5	NF	Number of frames tracked for this test.
6-10	I5	NTR	Number of targets tracked.
11-15	I5	ILASH	Equals zero when flash present; equals 1 when flash not present.
16-20	I5	INFR	Number of frames between event flash and first processed frame.
21-25	I5	IPC	Flag controlling plots: 0 - plot data, 1 - omit plots.
26-30	I5	IPR	Flag controlling printout: 0 - print data; 1 - omit all data.
31-35	I5	IPL	Flag controlling linear velocity and acceleration printout: 0 - print and plot; 1 - print only; 2 - omit all data.
36-40	I5	IPA	Flag controlling angular velocity and acceleration printout: 0 - print and plot; 1 - print only; 2 - omit all data.
41-50	2(I5)	JD, JR	First and last frame numbers of data to be plotted.
51-55	I5	IFILE	File location of test data on mag tape.

<u>Column</u>	<u>Format</u>	<u>Name</u>	<u>Description</u>
<u>Card Number 3</u>			
1-40	NTR(I5)	IDT(I), I = 1, NTR	Target name identification list. <sup>1</sup>
<u>Card Number 4</u>			
1-40	NTR(I5)	JDT(I) I = 1, NTR	Target location on magnetic tape.
<u>Card Number 5</u>			
1-10	F10.4	DT	Flag indicating presence of t-bar: 0.0 - no t-bar; 1.0 - t-bar tracked.
11-80	NTR (F10.4)	D(IDT(I)) I = 1, NTR	Constant Y coordinates of each target.

Output from TOWER consists of printouts and plots. The first printout is the title and test parameter summary page. Then the X and Z raw data (corrected for camera vibration) are listed in AFR counts, frame-by-frame, for each target. The data are then transformed to scene coordinates and filtered to minimize noise. Then the minimum and maximum displacements are printed for each target, as well as the means and standard deviations of the difference between smoothed and unsmoothed data. These data are then printed, frame-by-frame, giving the time (in seconds) and the X and Z coordinates in inches. Plots are made of the targets' X and Z positions with respect to time, resulting in a composite picture of all the targets' paths in the X-Z plane. Velocity and acceleration of each target are then printed, frame-by-frame, and plotted along the time scale. Similarly, angular velocities and accelerations from pairs of head targets are printed and plotted.

All of the VDT tests were previewed to select a representative sample. The total number of films processed was eighteen.

---

<sup>1</sup> The following list defines target names corresponding to target identification numbers.

<u>ID Code</u>	<u>Target Name</u>
1	Seat reference
2	Upper helmet
3	Middle helmet
4	Lower helmet
5	Shoulder
6	Elbow
7	Cheek
8	Nose

The form of program TOWER has not yet been finalized. Comment statements need revision and unused codes remaining from HIFPD should be deleted. Actually, there is still much to be accomplished to refine the program to improve its generality of application, ease of operation, and error analysis. However, TOWER satisfied the basic requirements for determining position and resultant velocity and acceleration (both linear and angular) of selected targets in the vertical portion of the test program.

#### PROGRAM POOCH

Program POOCH was developed by UDRI to accurately determine the location and orientation of a camera with respect to a coordinate system. The resulting position information was then input to program SLED - a program similar to TOWER regarding form and content of output. However, SLED reduced film data from two cameras rather than one. A brief description of program POOCH will be given here, but for a complete description see AMRL-TR-78-94.

The idea behind POOCH is relatively simple. To obtain the necessary input data, the coordinates of a number of points rigidly affixed to the sled were accurately measured. Their film frame image coordinates were then read with the AFR for each camera. With this information and rough estimates of camera position and focal length, program POOCH accurately determined the camera's location and orientation.

POOCH derived a complete description of camera position, including the location of the camera focal point ( $xx, yy, zz$ ), the focal length ( $ff$ ), the azimuth angle ( $th$ ), the elevation angle ( $ph$ ) of the camera optical axis, and the angle ( $\alpha$ ) by which the camera is rotated. The ( $xx, yy, zz$ ) coordinates were with respect to a right-handed, mutually orthogonal, XYZ coordinate system, whose origin was at the established zero reference point on the test fixture. The program operated in a right-handed coordinate system, which was the mirror image of the usual left-handed biodynamic coordinate system. The focal length of the camera was considered to be the product of the true camera focal length and magnification of the film frame reader. The unit vector along the optical axis ( $fn$ ) was normal to the film frame. The mutually orthogonal film frame axes were defined as  $p$  and  $q$  in POOCH. Unit vectors  $i$  and  $j$  were directed along the positive  $p$  and  $q$  axes, respectively. The  $p$  and  $q$  axes were horizontal and vertical with respect to the film frame. The unit vectors  $fn, i$ , and  $j$  formed a mutually orthogonal right-handed set. The azimuth and elevation angles of the camera's optical axis were easily found if the components of  $fn$  were found with respect the XYZ system. (See Figure B - 6.) The last of the seven unknowns is the tilt angle,  $\alpha$ , of the camera from the horizontal about its optical axis. The tilt angle was not used in the analysis and the cameras were assumed to have a tilt angle of zero.

The way in which POOCH derived these unknowns is explicitly described in AMRL-TR-78-94. Essentially, the unknowns were derived from scene and film image coordinates of five or more reference points on the test fixture. For the horizontal testing, the F-111 fixture was targeted with fiducials at fourteen different points. These points were accurately surveyed ( $\pm 0.2$  inches) and approximately five were tracked for each data set provided to POOCH. The first part of the data provided to POOCH consisted of rough estimates of  $ff$ ,

xx, yy, zz, as well as two generous bounds on ff called fp and fq. The complete input list is described below in punch card format.

<u>Column</u>	<u>Format</u>	<u>Name</u>	<u>Description</u>
<u>Card Number 1</u>			
1-30	3(F10.5)	XX,YY,ZZ	The X, Y, and Z coordinates of the estimated camera position (in feet).
31-40	F10.5	FF	The nominal focal length of the camera (in inches) times the magnification of the AFR.
41-60	2(F10.5)	XSR	A factor intended to account for distortion when present; 0.0 was used in all runs.
71-75	I(5)	N	The number of image points and associated object points.
<u>Card Number 2</u>			
1-20	2(F10.5)	P(1),Q(1)	The horizontal and vertical coordinates of the image of the first reference point.
21-50	3(F10.5)	X(1),Y(1) Z(1)	The X, Y, and Z coordinates of the first reference point.
<u>Card Number 3</u>			
(Same as Card Number 2, but for second reference point.)			
<u>Card Number N + 1</u>			
(Between five and ten reference points are input.)			

The working output from POOCH consisted of check values for the reference points which indicated the precision of the solution. The values which completely defined the camera location were listed. These included the three components of the camera position vector, renamed ra, rb, and rc; the azimuth (th), elevation (ph), and magnitude of ff; and the azimuth and elevation of i (thi and phi, respectively). This set of eight values was punched on cards and input to program SLED.

## PROGRAM SLED

Program SLED performed the analysis of the  $+G_y$  and  $-G_x$  photo data from two on-board cameras on the horizontal impact sled. The results of the analysis took the form of listings and plots of the positions, velocities, and accelerations of chosen fiducials. An overview of the program operation will be given below. SLED used a different approach in solving for each target's positions. A two ray solution technique was used and is briefly described in the next section. The linear and angular velocities and accelerations were derived using the same techniques as described in the program TOWER review. Additional details can be found in AMRL-TR-78-94. The following describes the modifications made to the original SLED program developed by UDRI.

The two on-board cameras were designated Camera A and Camera B. To completely define Camera A, three components of its position vector,  $r_{aa}$ ,  $r_{ab}$ , and  $r_{ac}$  were input as well as the azimuth,  $\theta_{ia}$ , and the elevation, and the magnitude of  $\mathbf{r}_a$  which were  $\theta_{ia}$ ,  $\phi_{ia}$ , and  $r_a$ . In addition, the azimuth,  $\theta_{ia}$ , and the elevation,  $\phi_{ia}$ , of the horizontal film frame unit vector,  $\mathbf{a}_i$ , were input. For Camera B, the analogous quantities were, in the same order,  $r_{ba}$ ,  $r_{bb}$ ,  $r_{bc}$ ,  $\theta_{ib}$ ,  $\phi_{ib}$ ,  $\theta_{ib}$ , and  $\phi_{ib}$ . These values were determined using program POOCH. Input from magnetic tapes consisted of the film frame coordinates of the targets' paths throughout the impact.

Briefly, SLED solved for target positions as follows. First, the two sets of camera data were time synchronized. A subroutine found that pair of film frames from each camera whose times bracketed a specific time. Another subroutine then drew a pair of rays from the camera's focal point to one of the moving targets in these two successive film frames and interpolated the target's position at the intermediate time. Then, this was accomplished for the second camera and a position was picked that was the best fit between the two cameras. Each target was tracked in this manner.

Program SLED was modified for the F-111 program to analyze those fiducials of interest. Modifications related to the calculation of frame times, the filtering of noise, and the handling of discontinuities in the input data.

Frame times were calculated as described for program TOWER. Film speeds were calculated from every adjacent pair of timing marks (t-bars). Frame times were assigned assuming the film speed was constant between adjacent t-bars.

Filtering was accomplished with the FFT technique described earlier for program TOWER. Discrete data were transformed to the frequency domain and filtered. Differentiation was accomplished easily to derive velocity and acceleration before transformation back to the time domain for output.

A new algorithm was added to SLED to handle discontinuities in the target data. During the film reading stage, when a target was obscured, its position was assigned zero coordinates. The discontinuity algorithm searched for this gap in the data and then interpolated target position by fitting a straight line between the endpoints of the gap. In this way, spikes in the velocity and acceleration output were prevented.

To verify program SLED and its modifications, a test run was made to demonstrate that the program gave the proper position coordinates of the stationary reference targets. The filtering and differentiation subroutines had already been verified for program TOWER.

SLED was input with data on punched cards and magnetic tapes. The punched cards provided the cameras' position data, the actual position coordinates of up to ten reference targets, and the program control variables. The magnetic data was coded with the digitized film frame position data. The typical procedure was to process a series of tests on the CDC computer in a batch operation. Below is a description of the punched card input.

<u>Column</u>	<u>Format</u>	<u>Name</u>	<u>Description</u>
<u>Card Number 1</u>			
1-10	A10	Title (1)	Test number
11-20	A10	Title (2)	Test date
21-30	A10	Title (3)	F-111 (Test program)
31-40	A10	Title (4)	+G <sub>y</sub> or -G <sub>x</sub> (Test phase)
41-50	A10	Title (5)	Subject identification
51-60	A10	Title (6)	Impact level (G's)
61-70	A10	Title (7)	Seat configuration
<u>Card Number 2</u>			
1-5	I5	IPR	Flag controlling printout: 1 - printout data; 0 - omit printout.
6-10	I5	IPA	Flag controlling angular velocity and acceleration printout: 0 - print and plot; 1 - print only; 2 - plot only.
11-15	I5	IPF	Flag controlling FIND, SOLVE and CORR printout: 0 - omit printout; 1 - print data.
16-20	I5	IPD	0 - G <sub>y</sub> test; 1 - G <sub>x</sub> test.
21-25	I5	NFA	Number of frames read from Camera A.
26-30	I5	NFB	Number of frames read from Camera B.
31-35	I5	IFT	0 - omit FFT filtering; 1 - filter data.
<u>Card Number 3</u>			
1-30	3(F10.3)	RAA,RAB RAC	Camera A position coordinates (feet).
31-40	F10.3	FA	Camera A focal length (feet times AFR magnification).



<u>Column</u>	<u>Format</u>	<u>Name</u>	<u>Description</u>
<u>Card Number 4</u>			
1-20	2(F10.3)	THA,PHA	Camera A optical axis azimuth and elevation (radians).
21-30	F10.3	GA	Camera A tilt angle. Not presently used.
31-50	2(F10.3)	THIA, PHIA	Azimuth and elevation of Camera A film frame $\bar{i}$ vector (radians).
<u>Card Number 5</u>			
1-30	3(F10.3)	RBA,RBB RBC	Camera B position coordinate (feet).
31-40	F10.3	FB	Camera B focal length (feet x 20).
<u>Card Number 6</u>			
1-20	2(F10.3)	THB,PHB	Camera B optical axis azimuth and elevation (radians).
21-30	F10.3	GB	Camera B tilt angle. Not presently used.
31-40	2(F10.3)	THIB, PHIB	Azimuth and elevation of Camera B film frame $\bar{i}$ vector (radians).
<u>Card Number 7</u>			
1-2	I2	NM	Number of moving targets tracked.
3-4	I2	NOA	Number of reference (object) targets tracked by Camera A.
5-6	I2	NOB	Number of reference targets tracked by Camera B.
7-8	I2	NFX	Total number of reference targets whose position coordinates are read in.
9-20	6(12)	JMT(I) I = 1,6	Positions of moving targets on magnetic tape.
<u>Card Number 8</u>			
1-18	6(I3)	JOA(I) I = 1,NOA	Positions of Camera A reference targets on magnetic tape.
<u>Card Number 9</u>			
1-18	6(I3)	JOB(I) I = 1,NOB	Positions of Camera B reference targets on magnetic tape.
<u>Card Number 10</u>			
1-30	3(F10.5)	XX(1), YY(1), ZZ(1)	Position coordinates of reference targets (feet).

<u>Column</u>	<u>Format</u>	<u>Name</u>	<u>Description</u>
<u>Card Number 9 NFX</u>			
1-30	3(F10.5)	XX(NFX), YY(NFX), ZZ(NFX)	Position coordinates of reference targets (feet).

Output from SLED consisted of printouts and plots. The initial printout consisted of the input data, including the raw position data of the moving targets frame-by-frame. Then, the moving target coordinates in the actual scene were obtained and printed out in 2 msec time steps. A composite plot (X versus Z) was made of this data. More printout was then generated showing the maximum and minimum positions, velocities, and accelerations. Then, the velocities and accelerations for each target were printed frame-by-frame and corresponding plots were generated.

With the  $-G_x$  test films, it was possible to derive angular accelerations between two head targets since their motions were planar. This same technique was used in TOWER for the  $+G_z$  test films. The  $+G_y$  tests presented a more complicated problem, however, since the motion of the targets was not planar. Therefore, angular velocity and acceleration were not computed for any of the lateral tests.

The philosophy in choosing tests to process was the same as that applied in choosing the sample from the  $+G_z$  test phase. The films were first previewed to eliminate those that could not be processed. Then, the tests were grouped according to the experimental test matrix of that particular test phase. From the tests of each element of the matrix, three tests were selected involving a small, a medium, and a large subject. From the  $+G_y$  tests, there were three test conditions of interest, each corresponding to a matrix element. These were tests at 8 G's in seat configurations of  $90^\circ/0^\circ$ ,  $103^\circ/0^\circ$ , and  $103^\circ/FD$ . Three pairs of test films (from two on-board cameras) were chosen from each of these three types of tests. Thus, nine tests were analyzed for the lateral phase of testing. In the  $-G_x$  phase, the same seat configurations were used, but at an impact level of 10 G's. Nine of these tests were also analyzed.

Program SLED, like TOWER, should be made applicable to a broader range of test environments and could be modified to improve the presentation of the data. However, SLED satisfied the basic requirements for producing position, velocity, and acceleration of the targets in this study.

## CONCLUSION

The photometric analysis accomplished the basic requirements of describing the subject's kinematic response to impact. The software was adequate, but it could be improved. Specifically, these improvements should include generality of application, ease of operation, and evaluation of accuracy.

For the future, it is desirable to evaluate kinematic motions more accurately using not only photometric data, but also electronic data derived from inertial sensors. The velocity and acceleration transducers that sense the motions of particular points on the subject and impact vehicle can be analyzed in conjunction with the photo data. Through an optimal estimation process, it should be possible to derive total response more accurately. This goal is beyond the scope of the current test program, but with improved techniques and instrumentation (such as angular accelerometers), the goal is achievable and will be pursued in future programs.

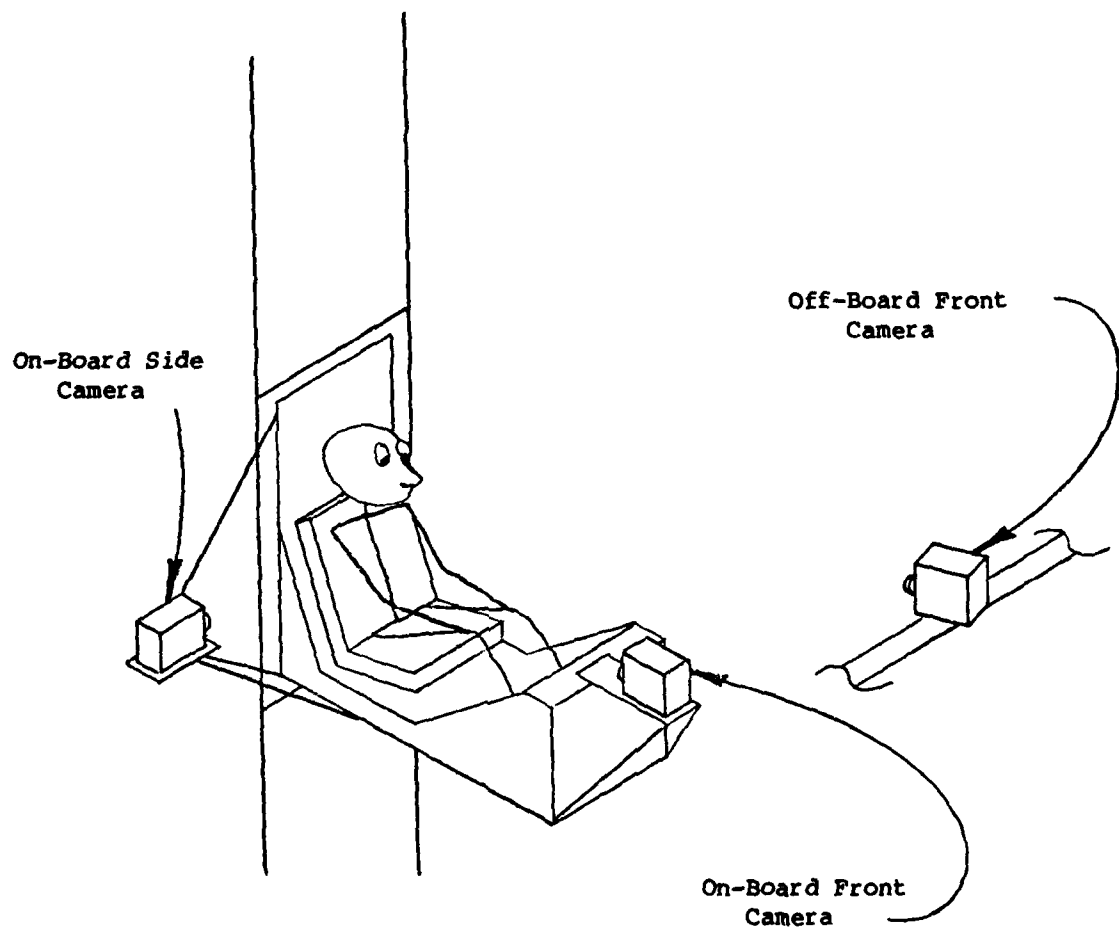
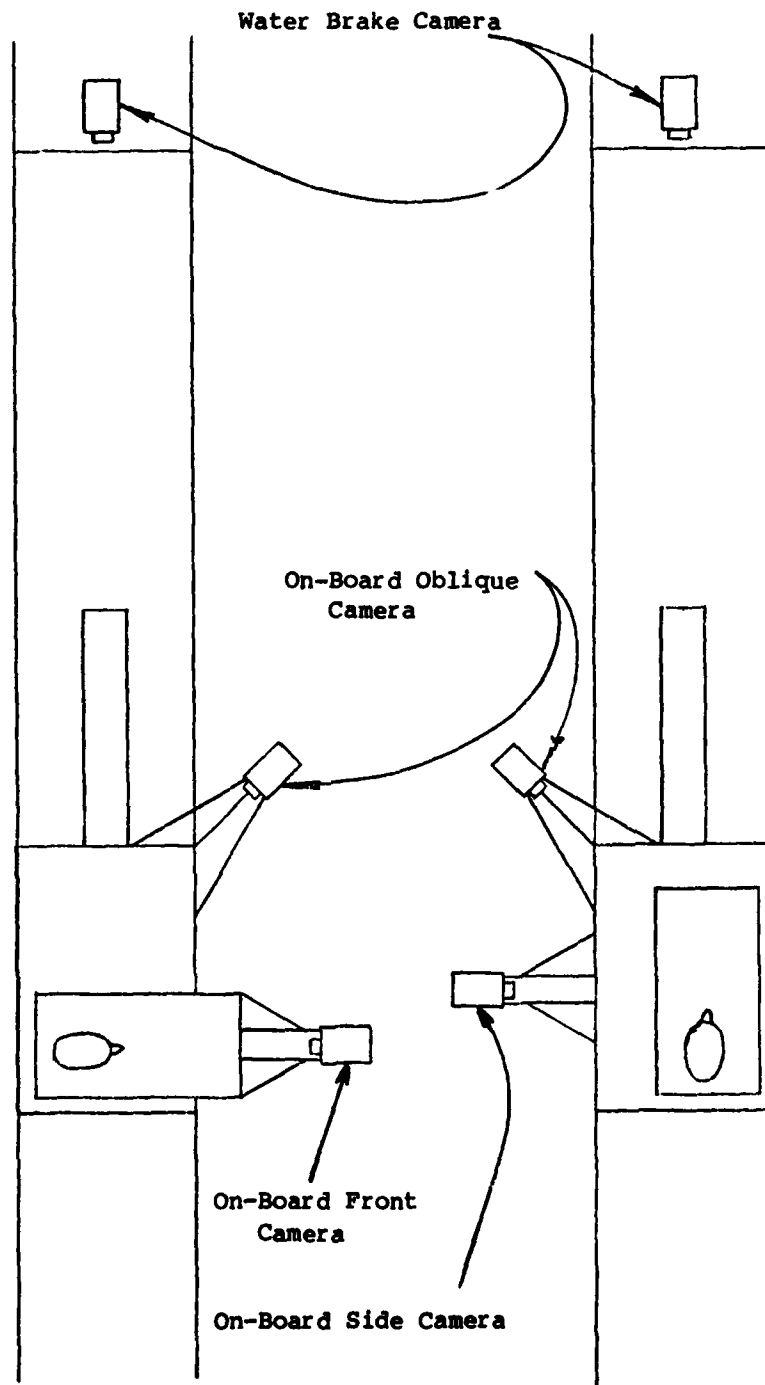


Figure B - 1. Camera Locations for the +G<sub>z</sub> Tests.



+G<sub>y</sub> Tests                      -G<sub>x</sub> Tests

Figure B - 2. Camera Locations During Tests Conducted on the Horizontal Decelerator.



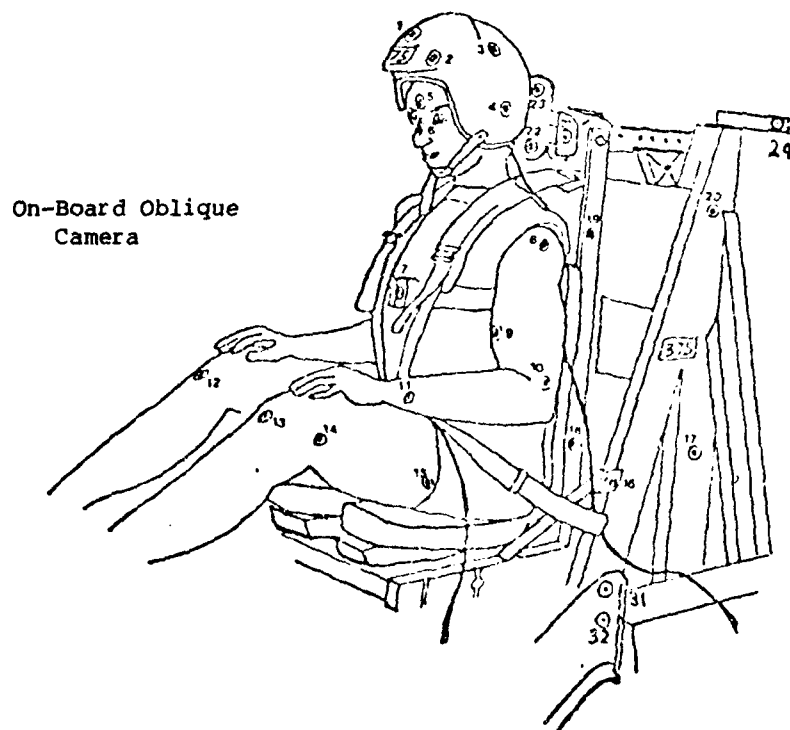
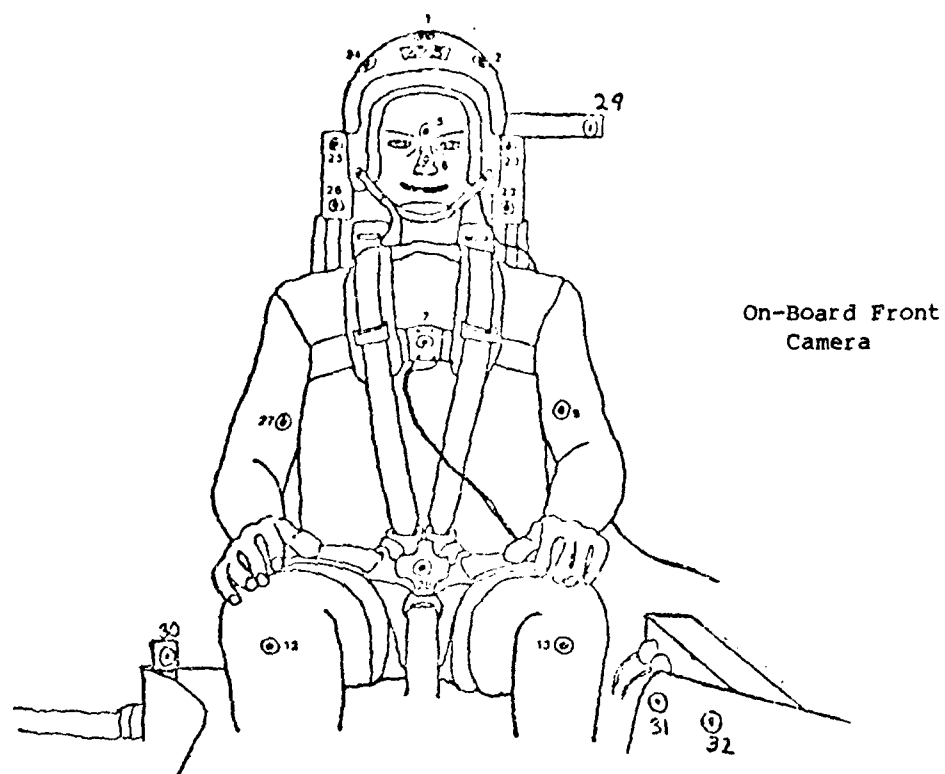
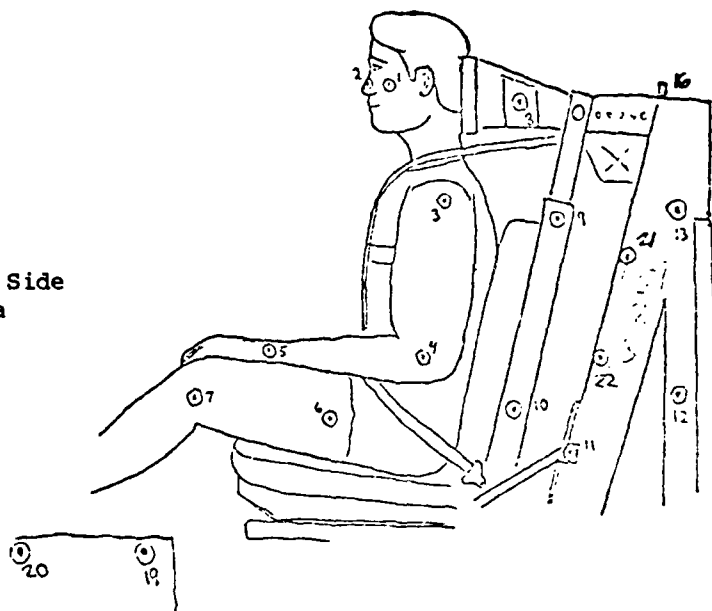


Figure B - 4. Fiducial Locations for +G<sub>y</sub> Tests.

On-Board Side  
Camera



On-Board Oblique  
Camera

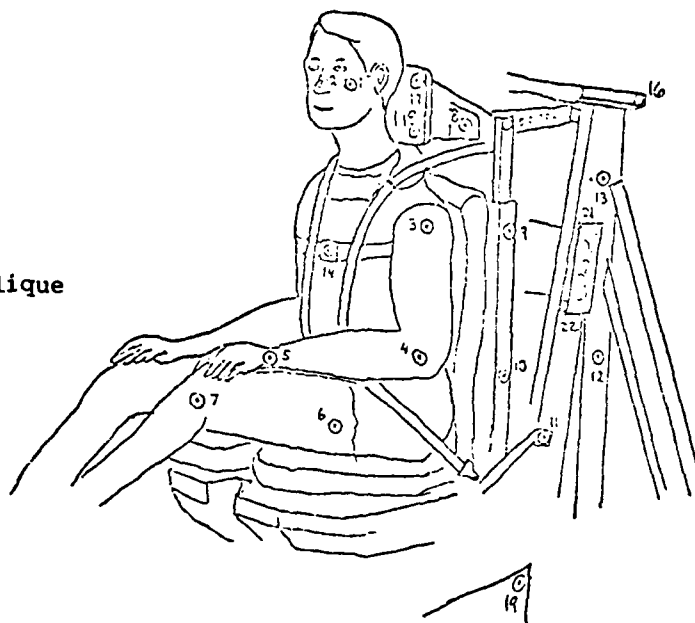


Figure B - 5. Fiducial Locations for  $-G_x$  Tests.



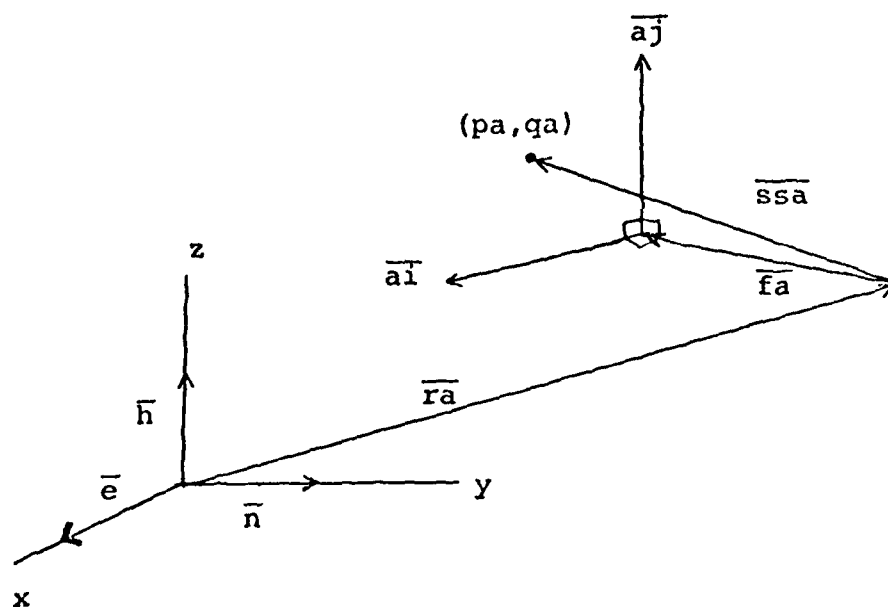
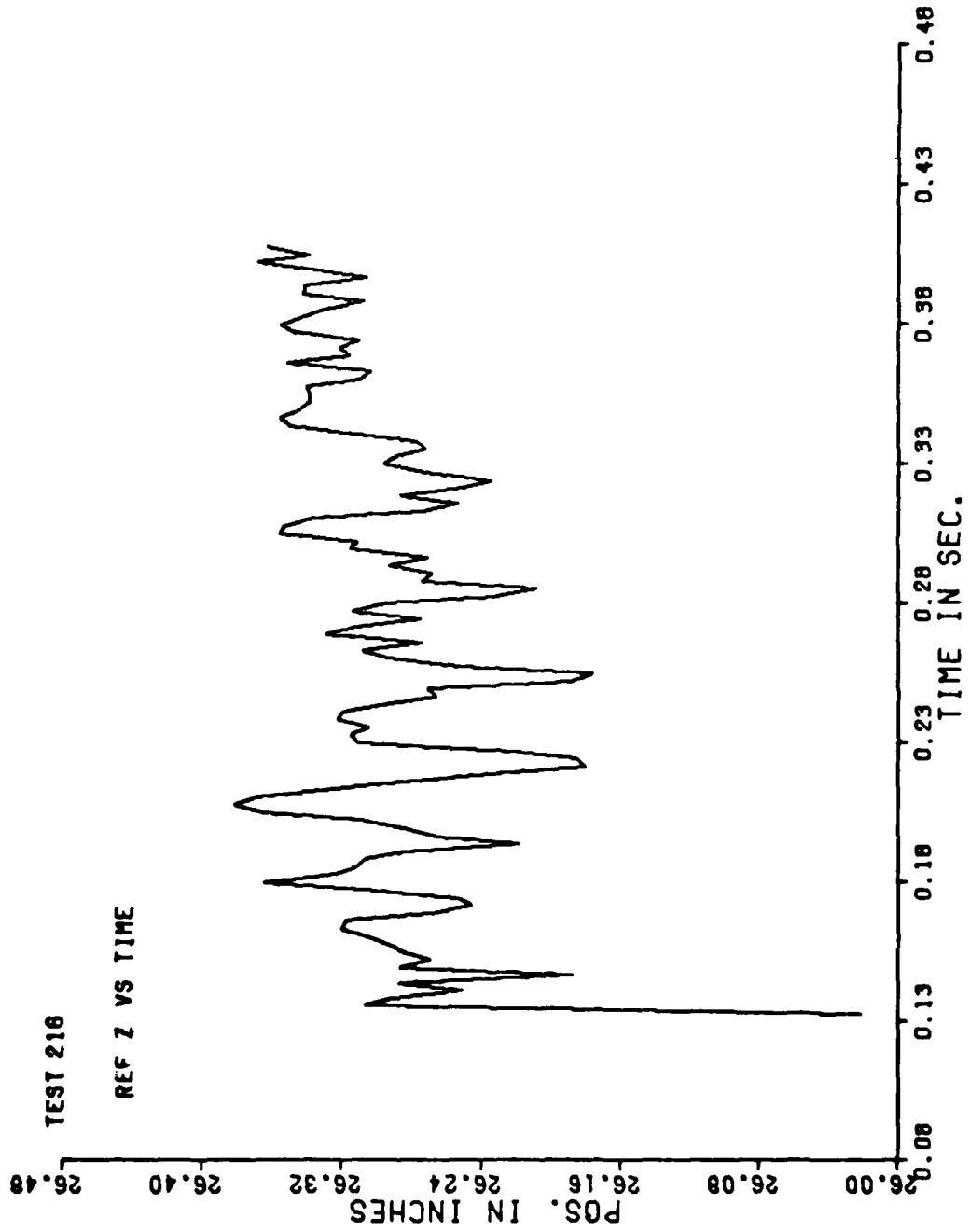
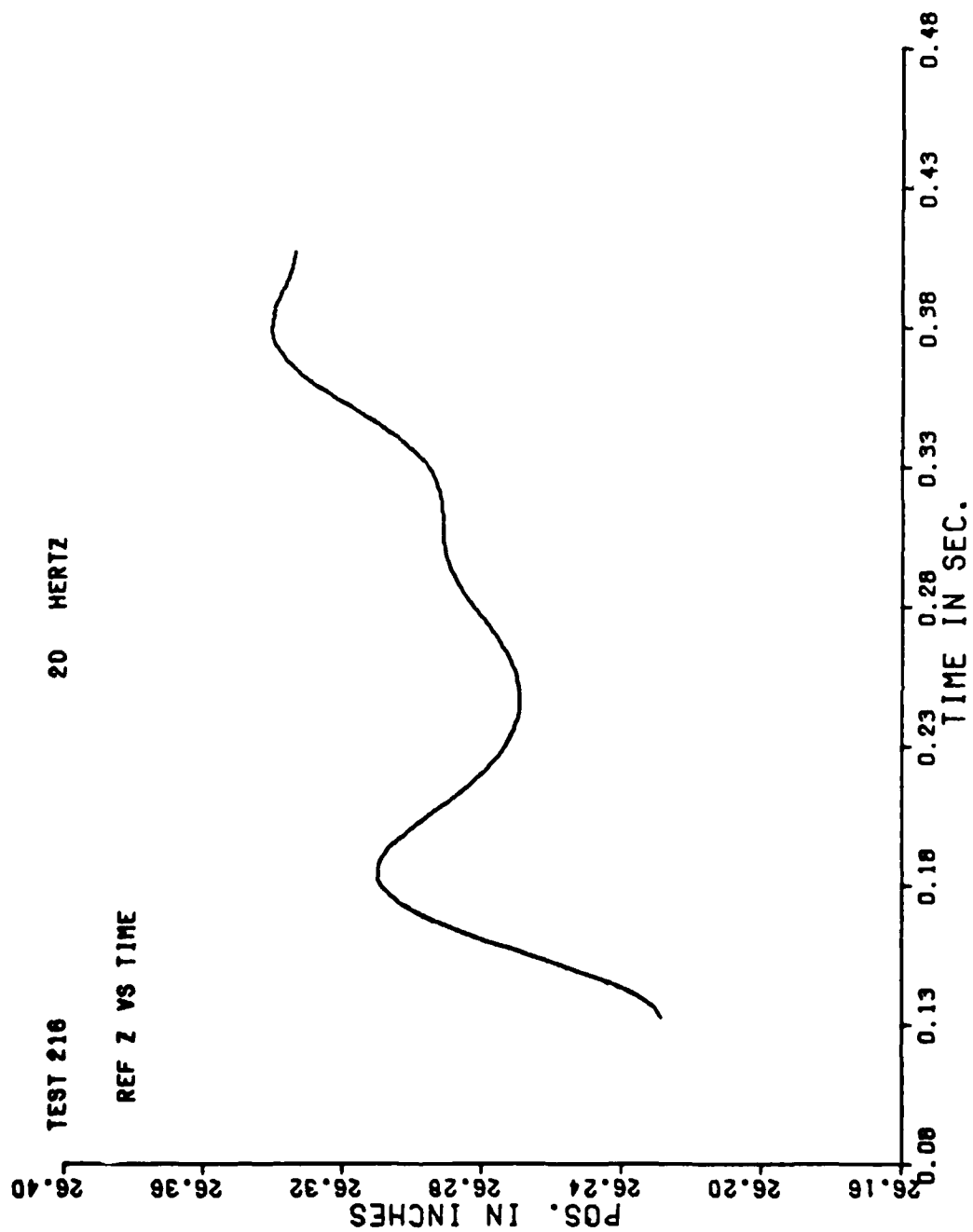
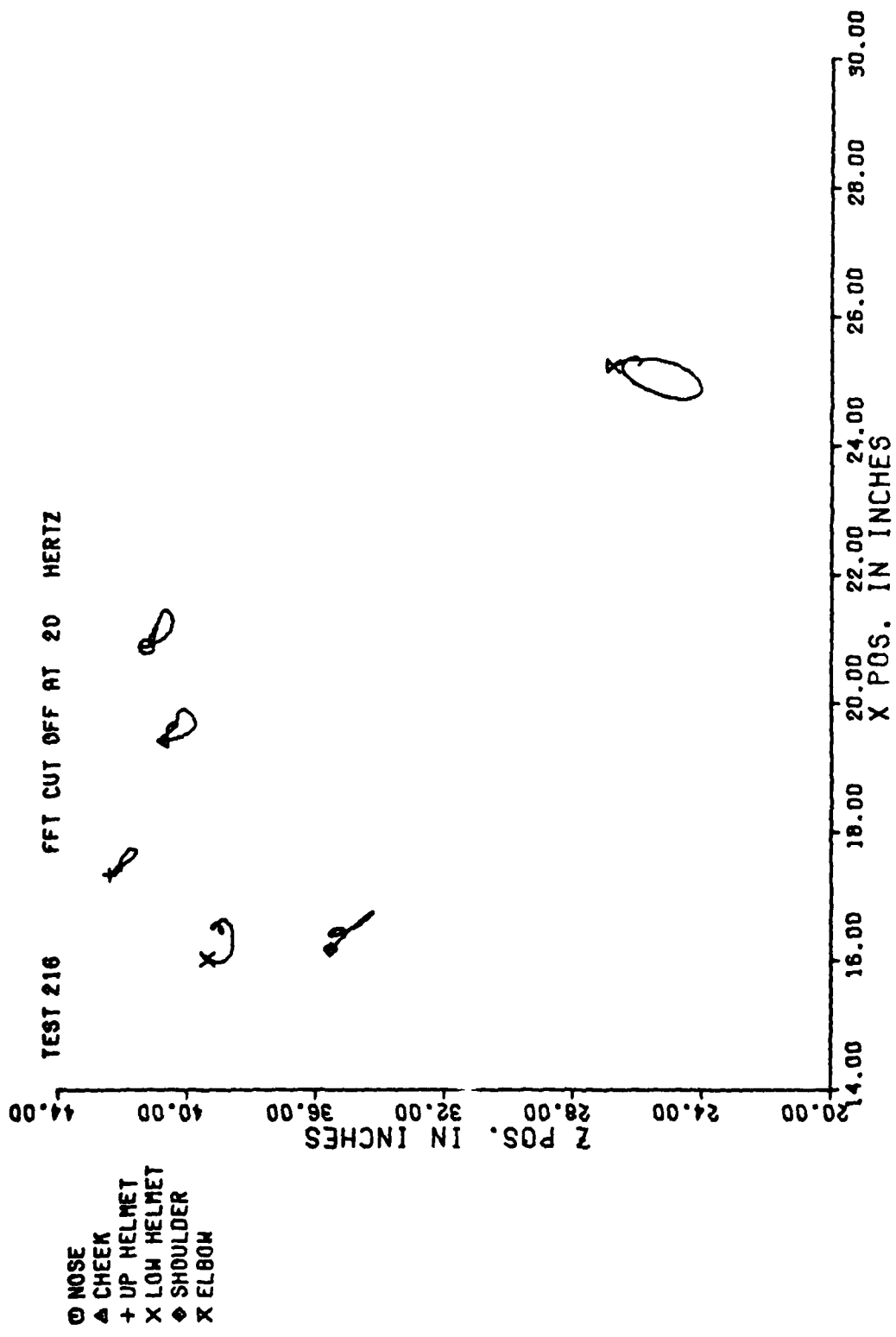


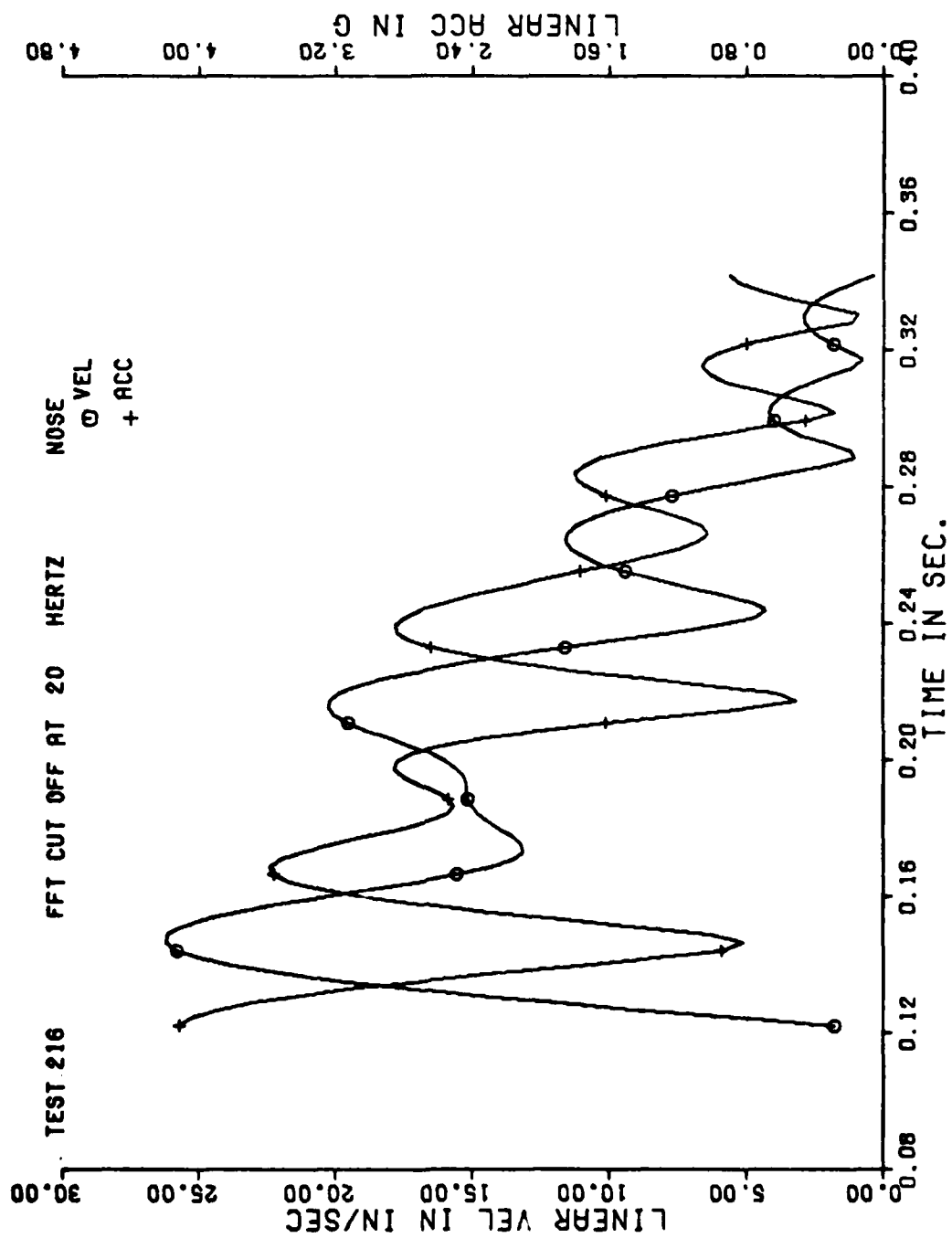
Figure B - 6. Coordinate System Used During Photometric Data Processing.

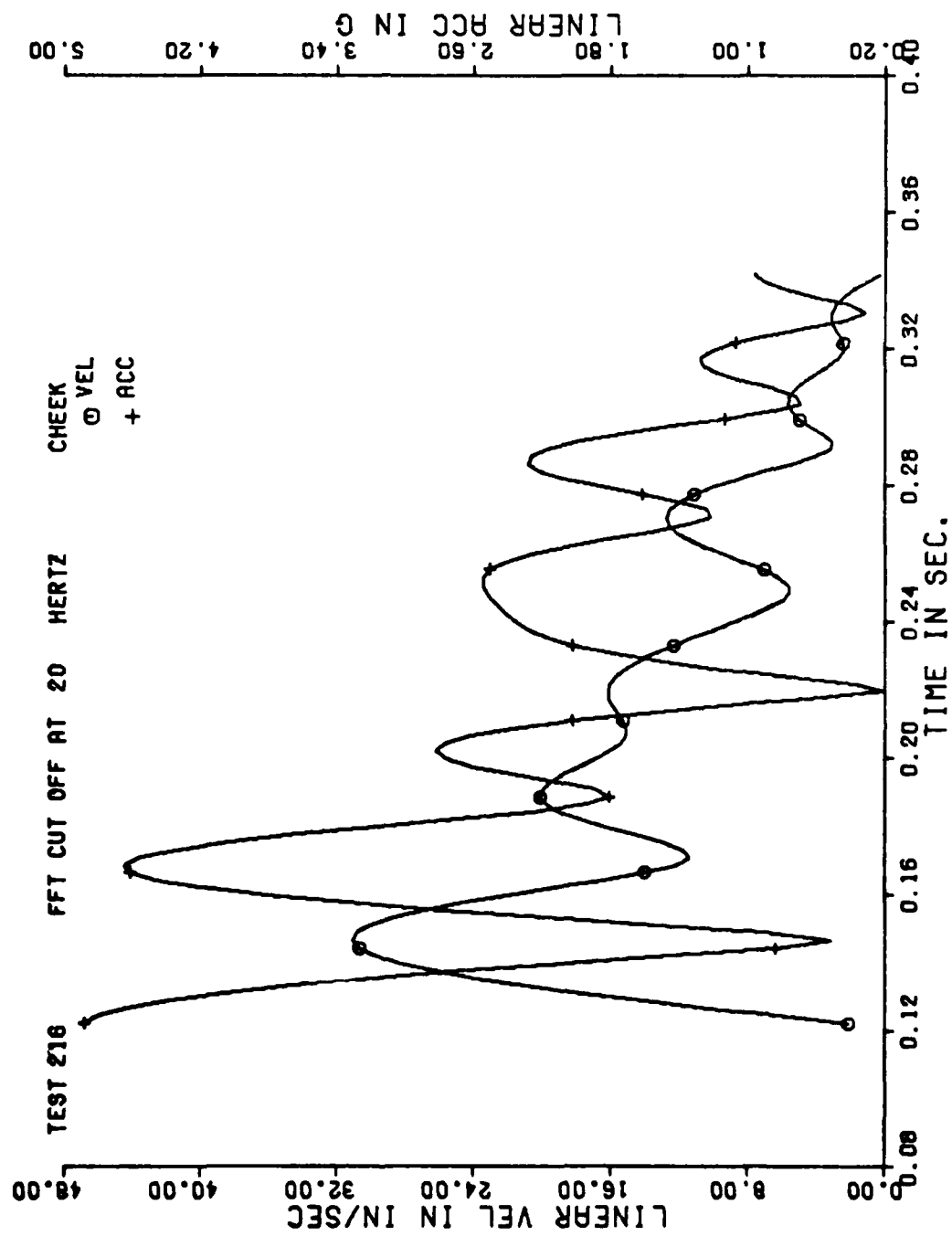
TYPICAL GRAPHIC DATA FROM PROGRAM TOWER

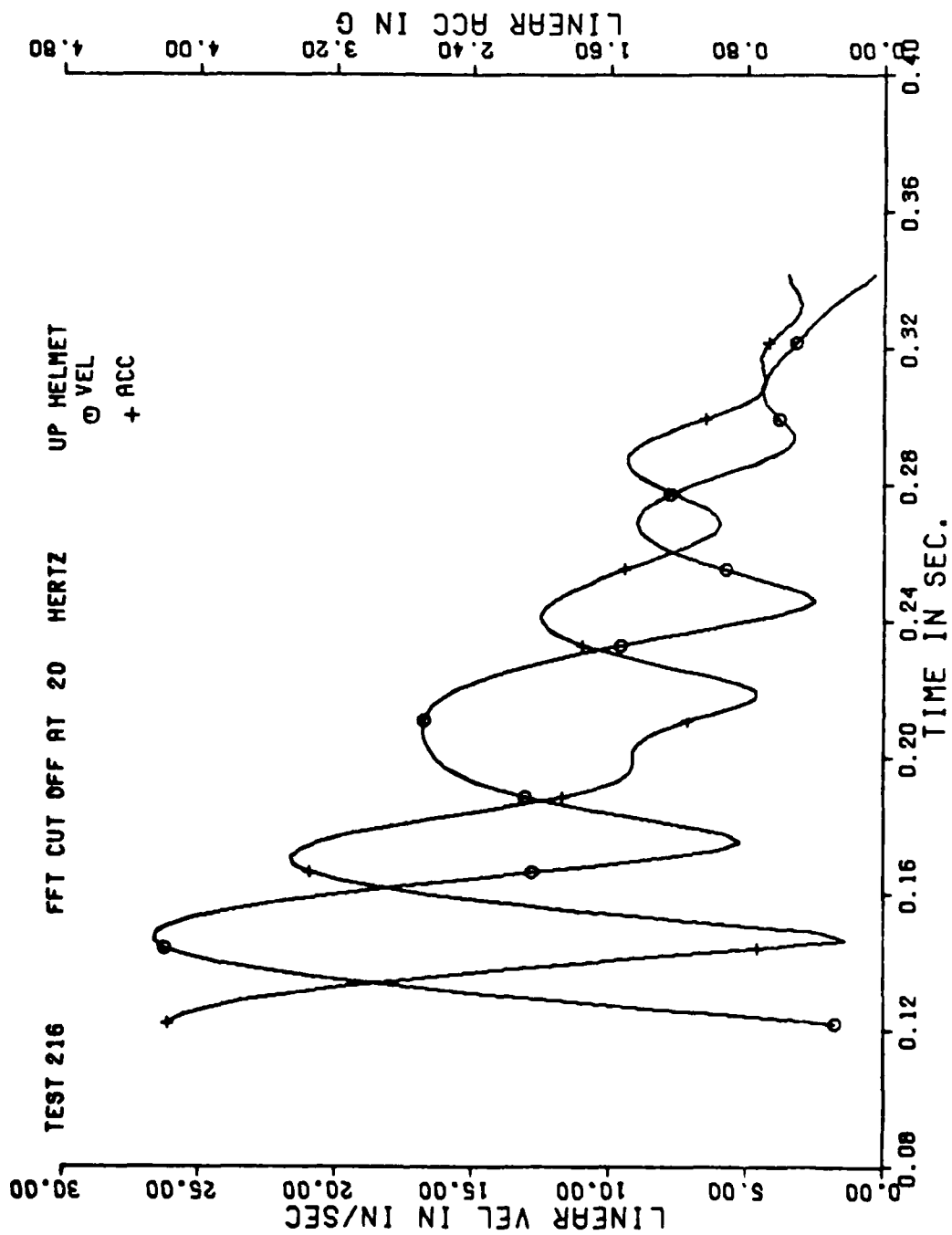


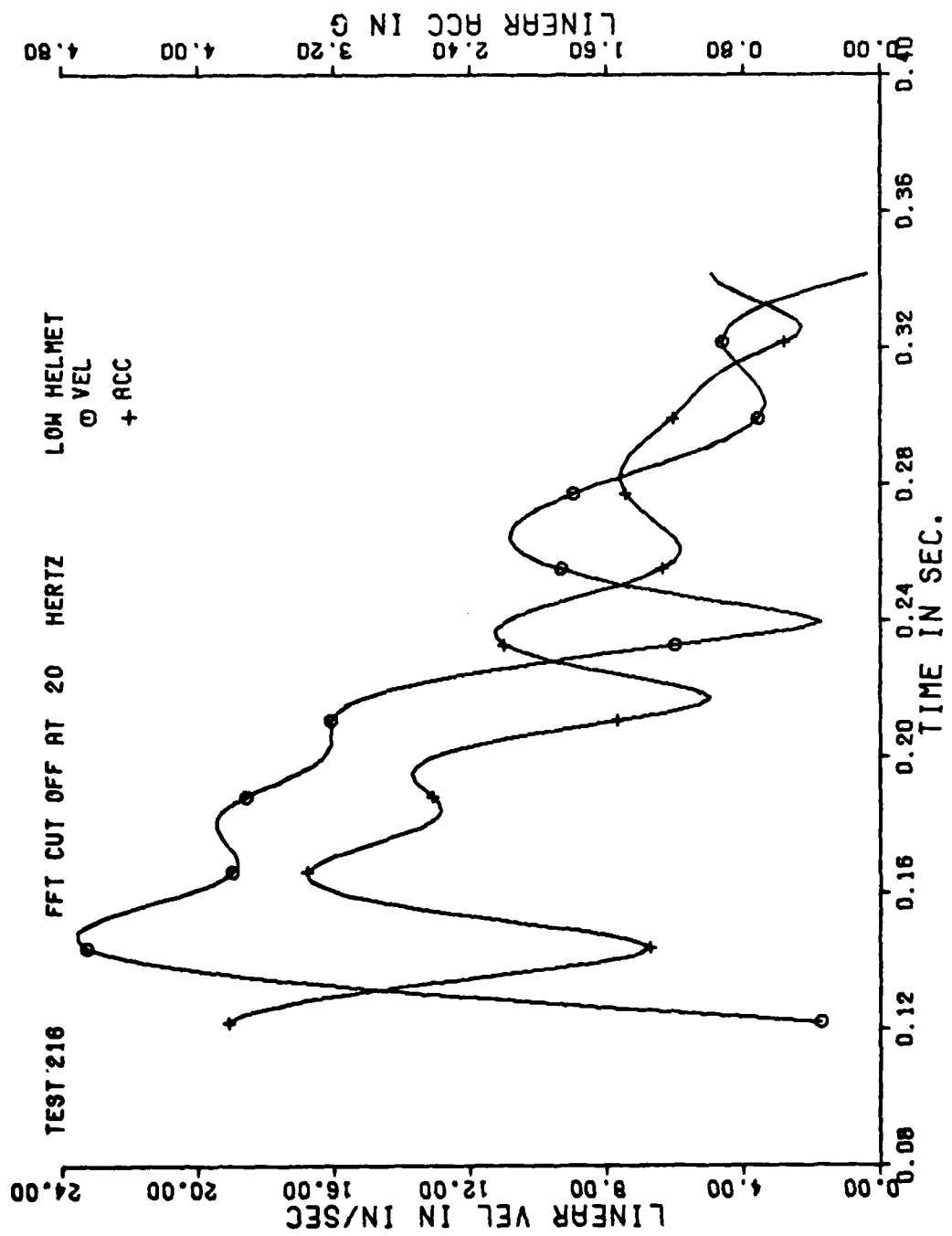




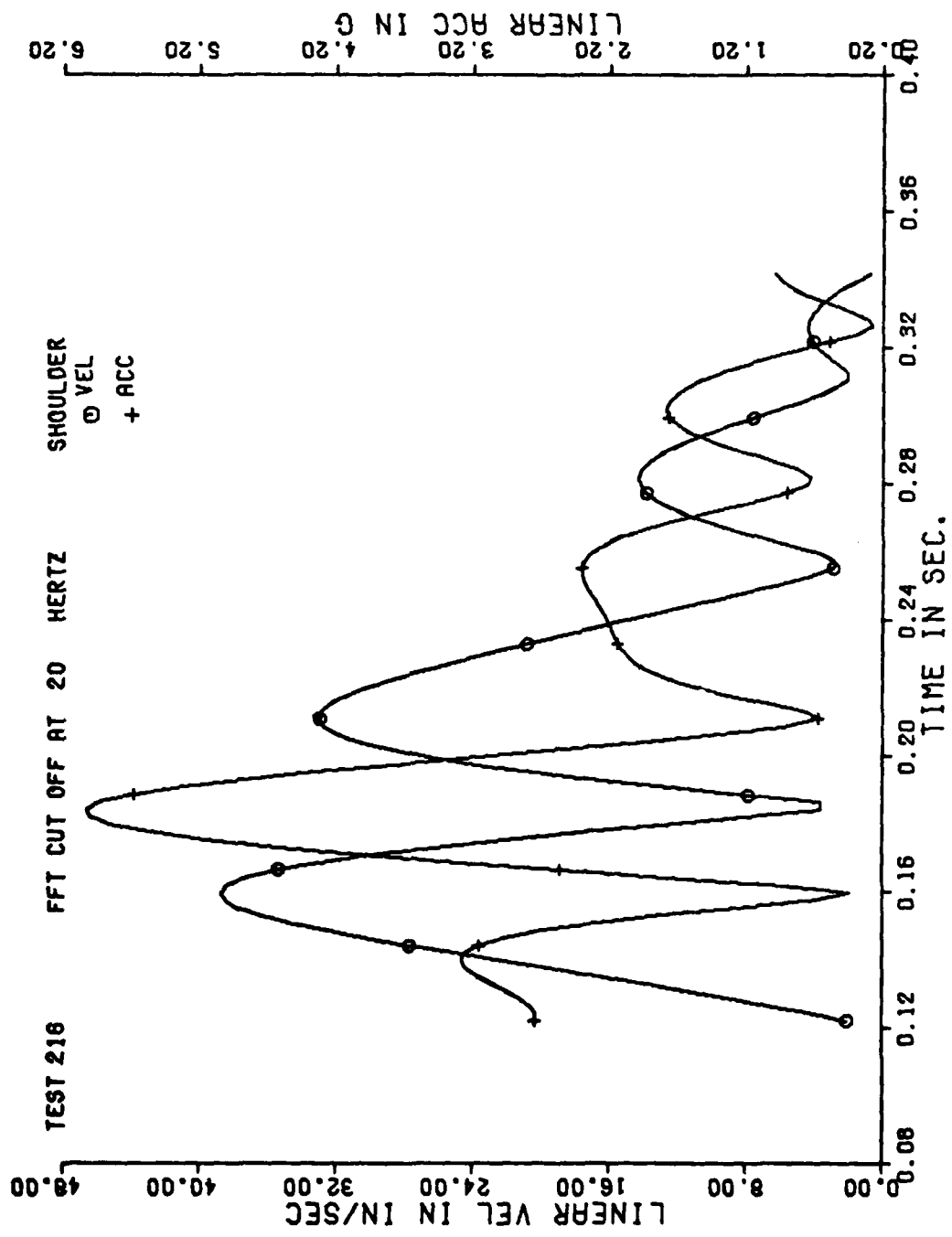


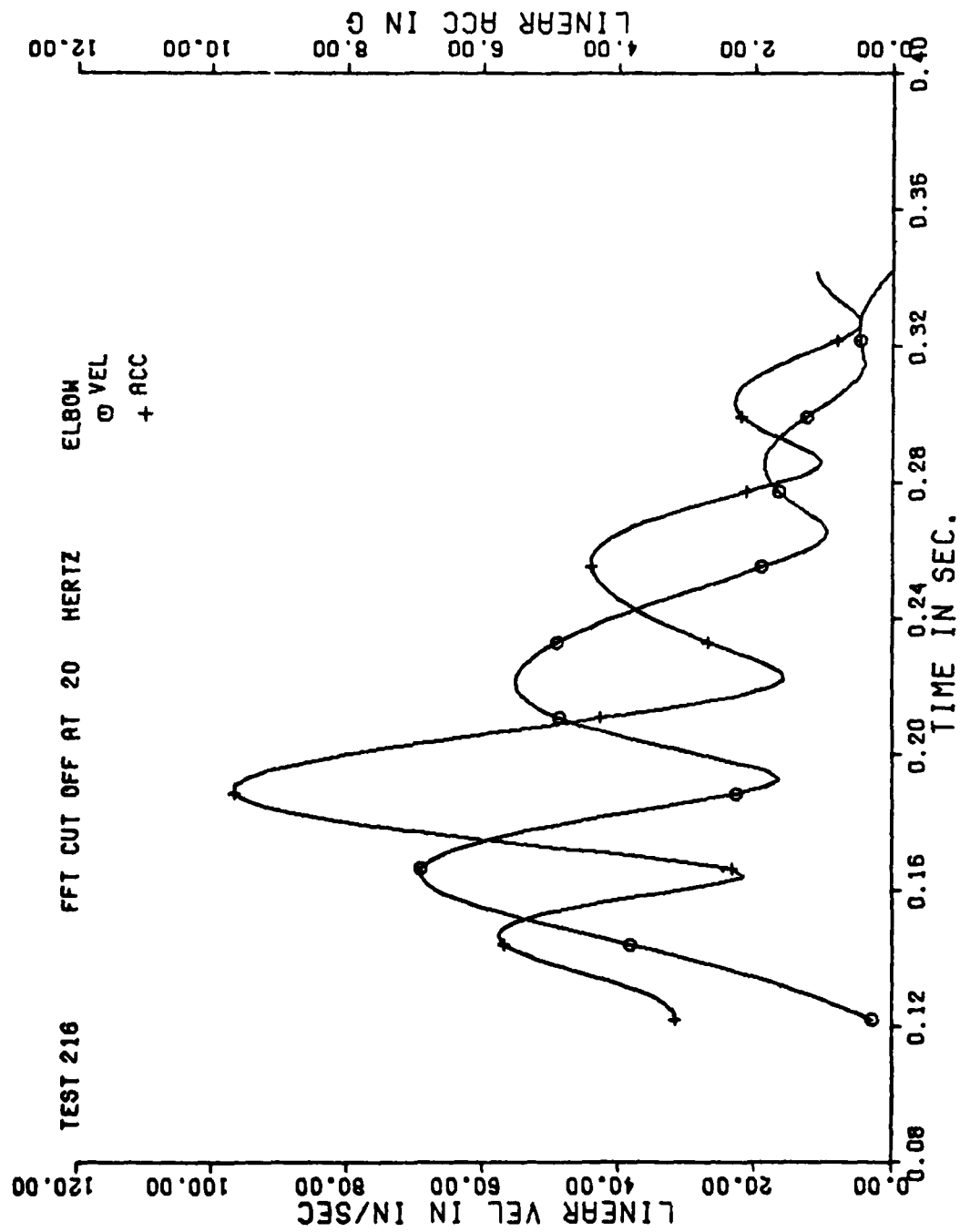


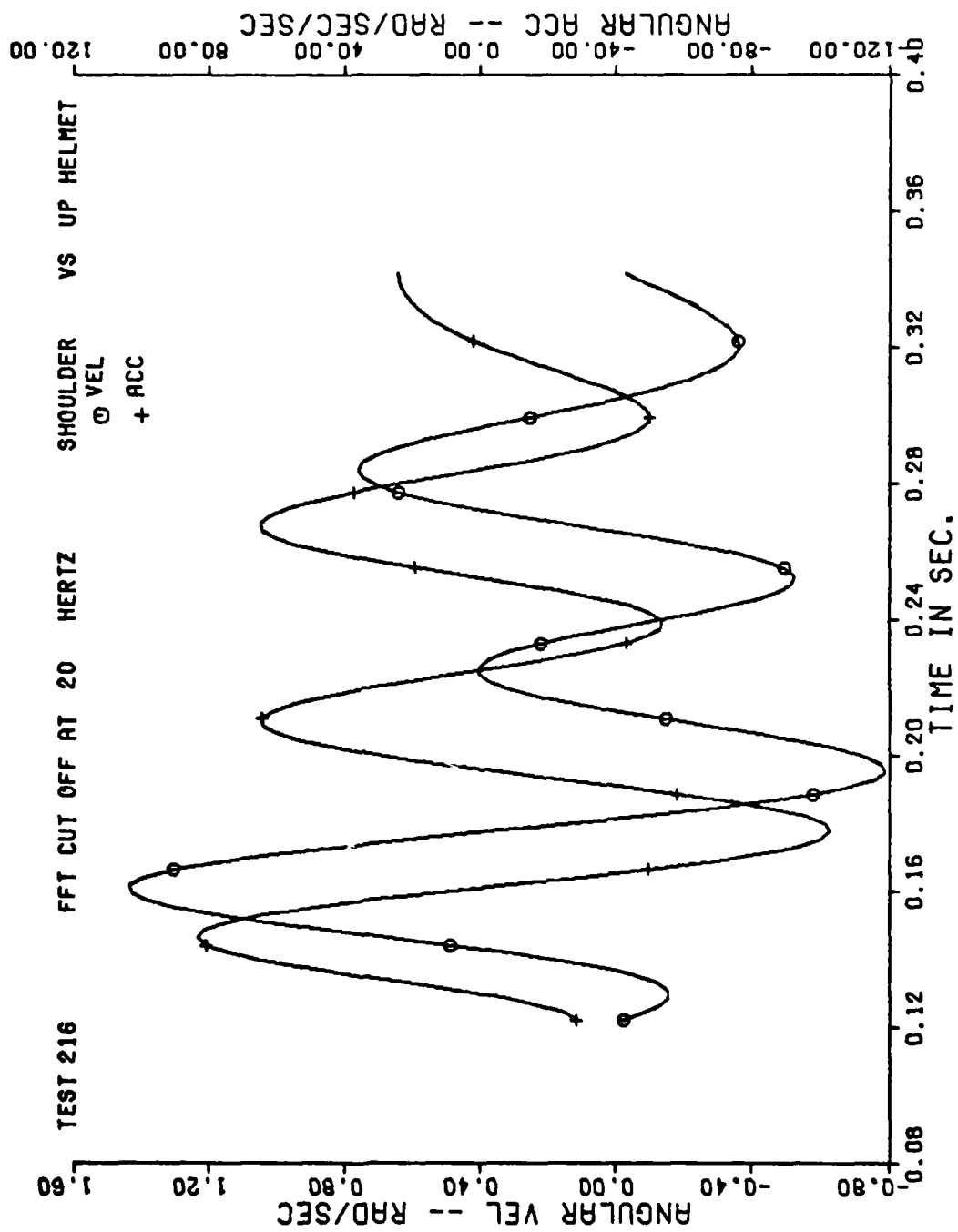


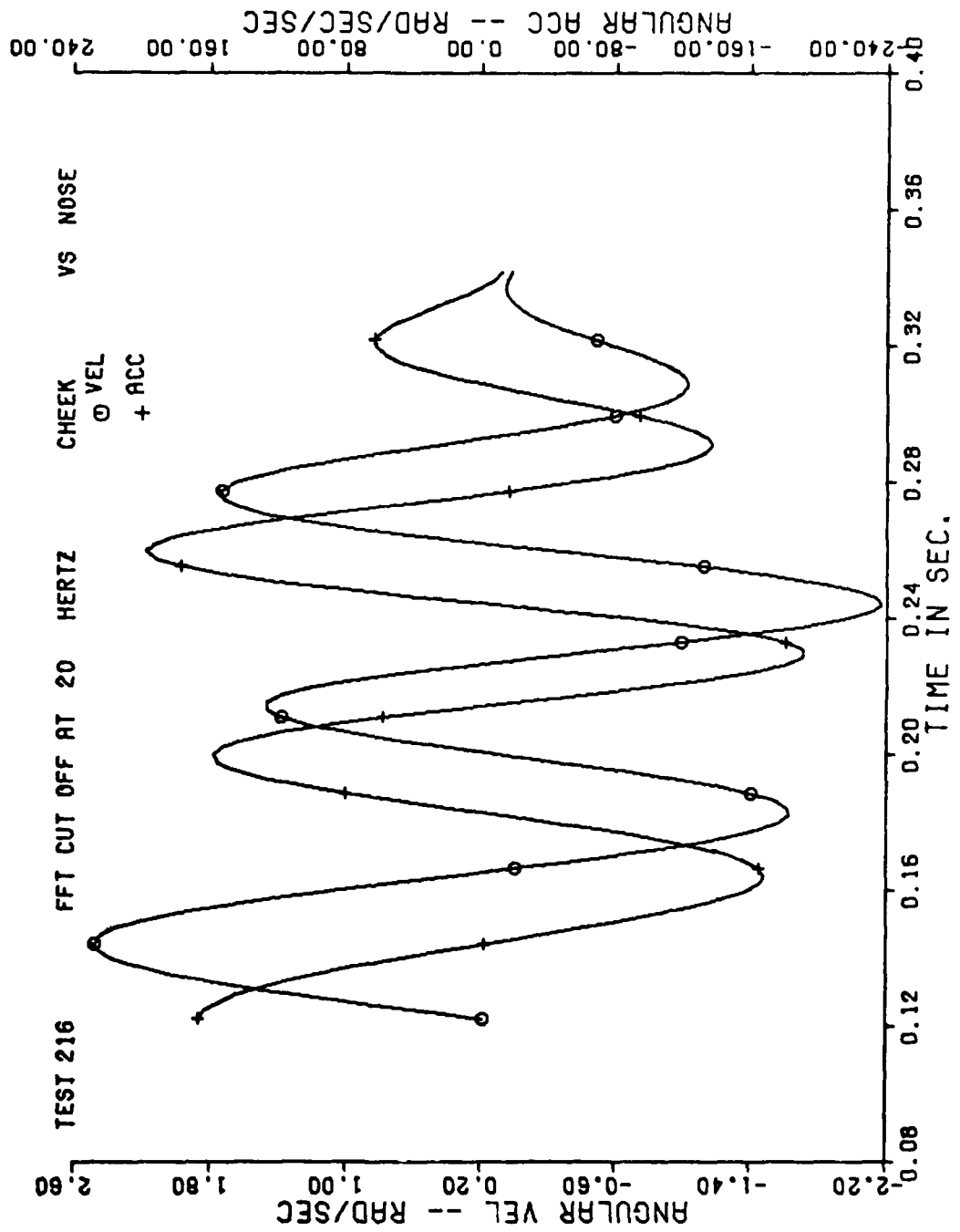


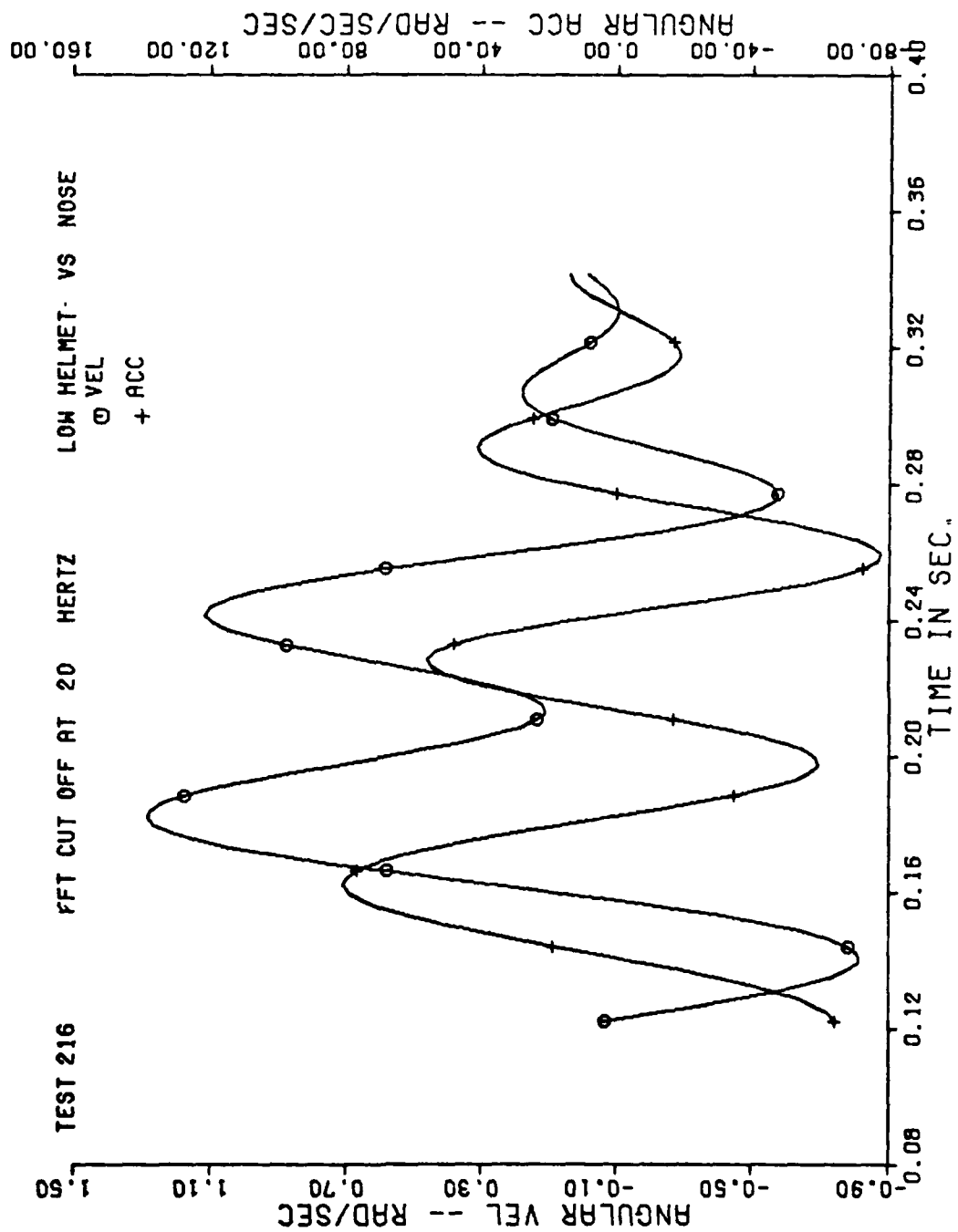




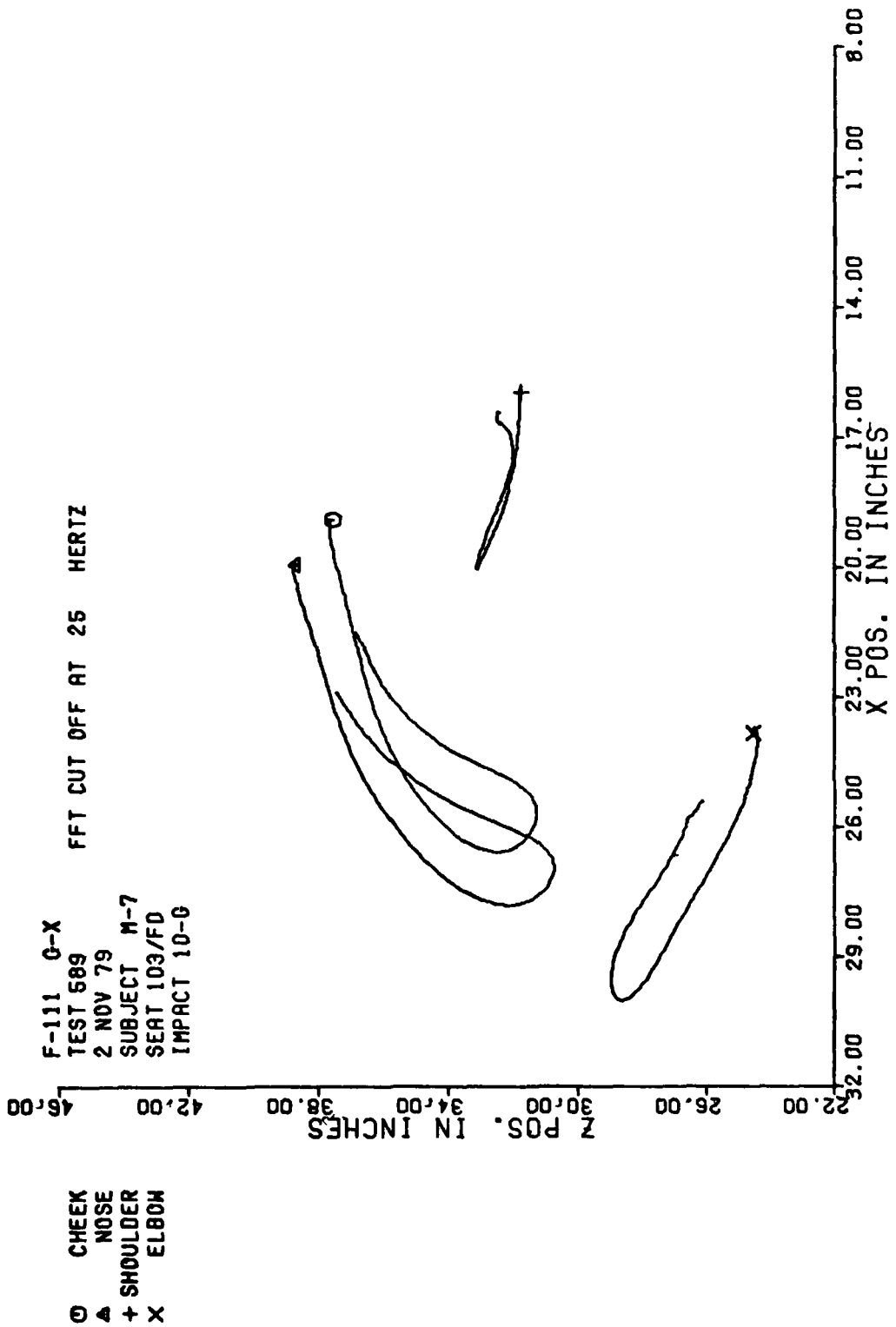


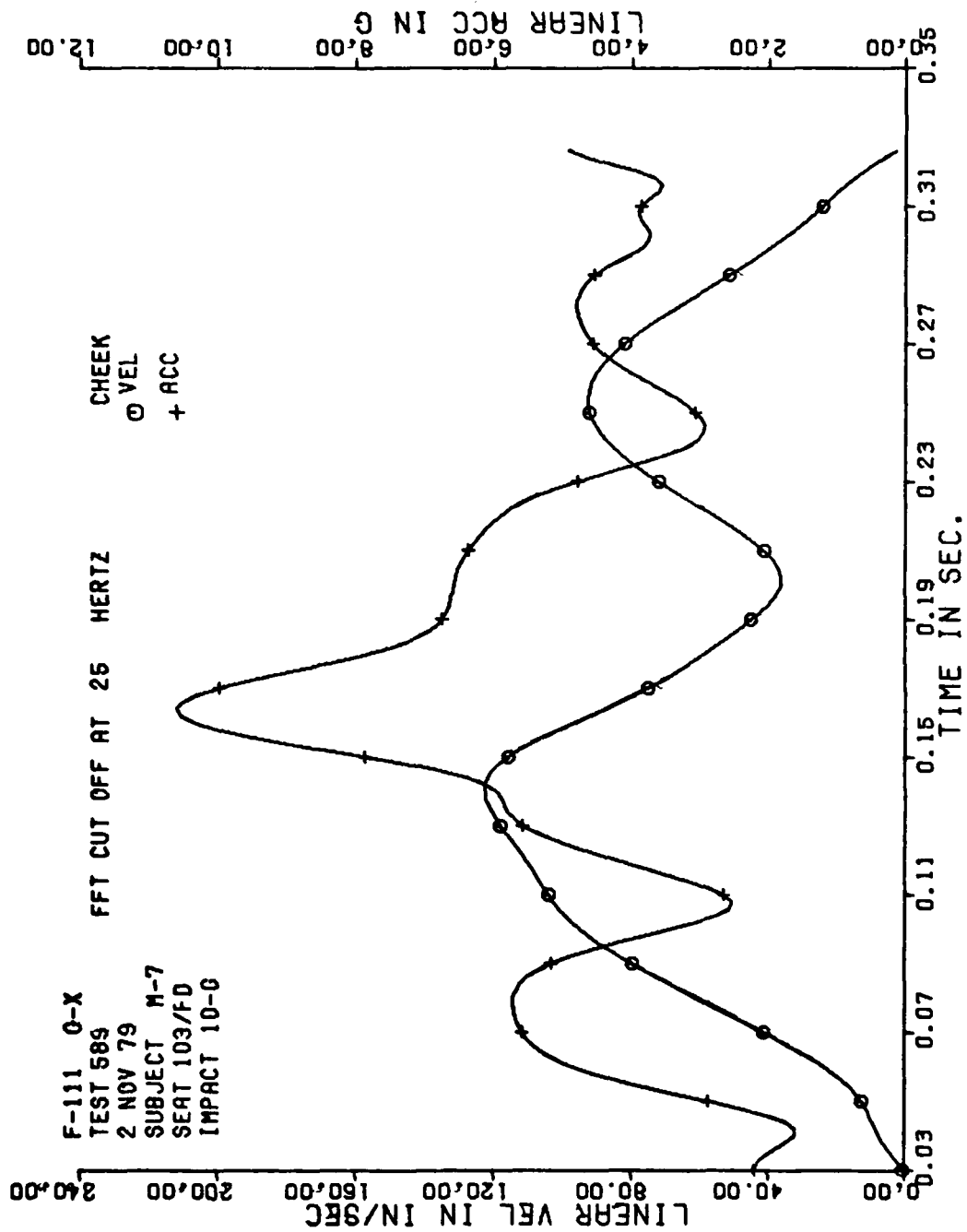


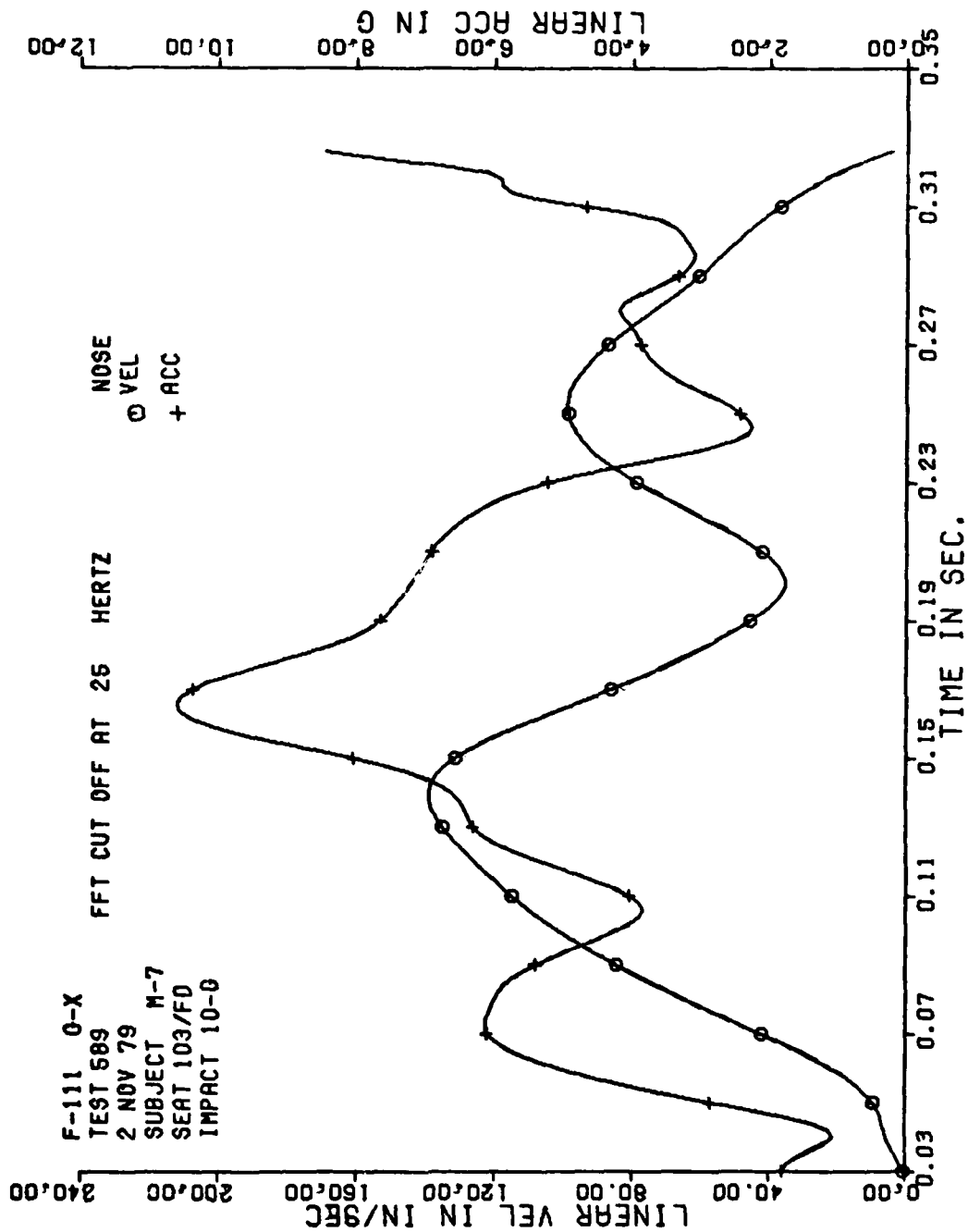




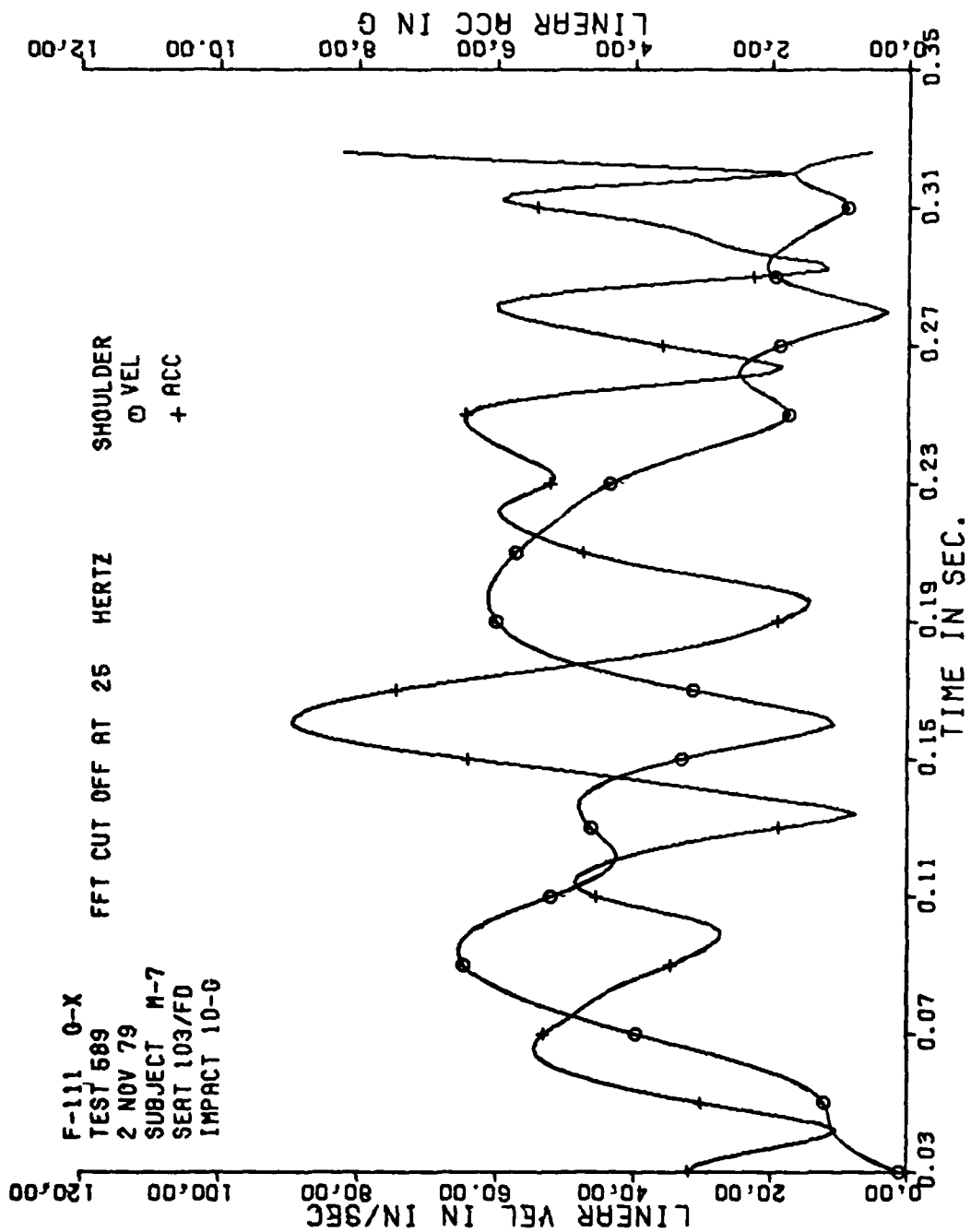
TYPICAL GRAPHIC DATA FROM PROGRAM SLED

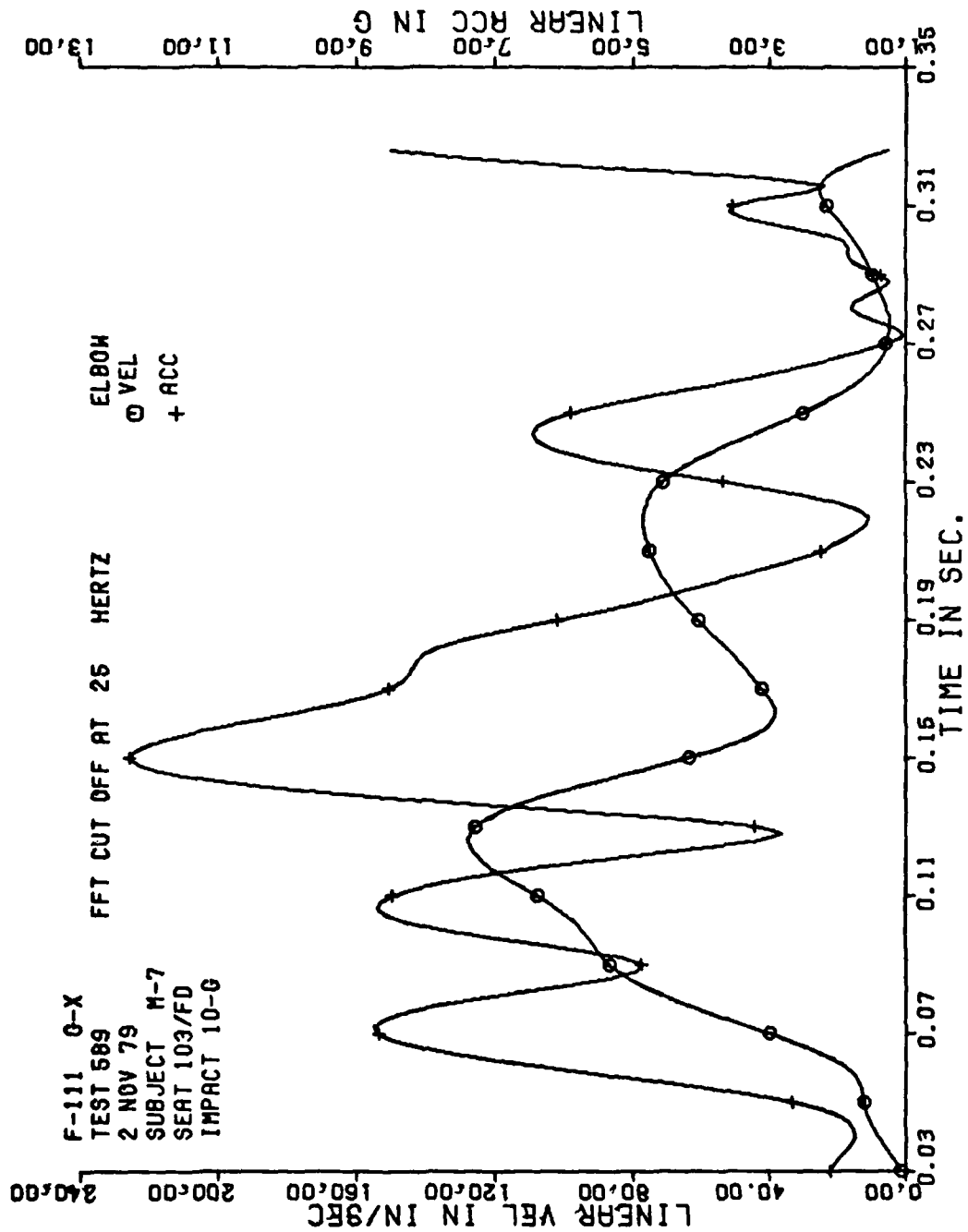


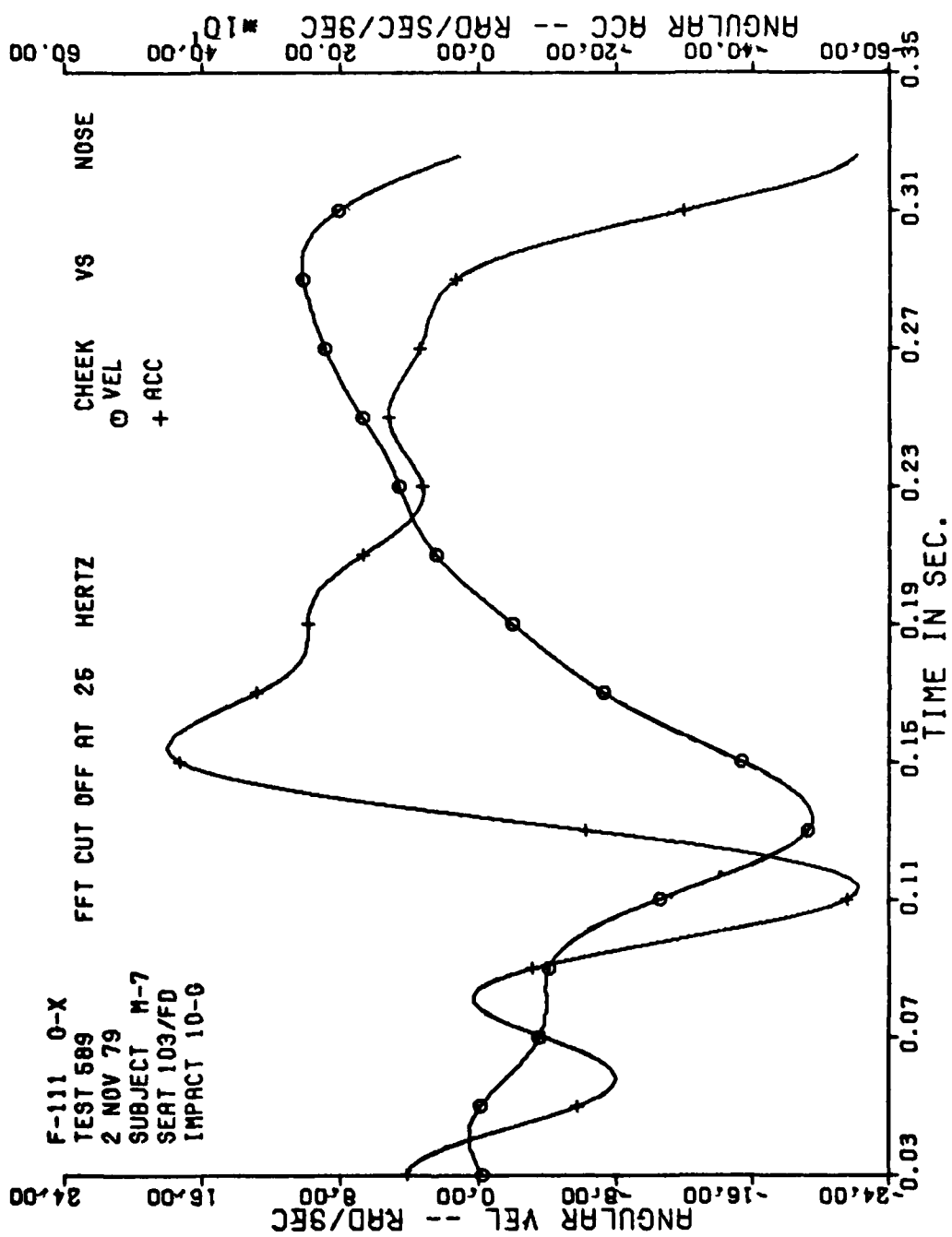












## APPENDIX C

### SUMMARY OF VERTICAL IMPACT TEST DATA

This appendix contains tables that list the maximum values of the measured forces, loads, accelerations, severity indices, and velocities measured during each vertical impact test with a volunteer subject. Also included is one set of data plots for each six cells of the test matrix used in the +G<sub>z</sub> phase. The test conditions are summarized as follows:

1. 8G, 0° shoulder strap, 103° seat back angle.
2. 10G, 0° shoulder strap, 103° seat back angle.
3. 10G, 0° shoulder strap, 90° seat back angle.
4. 10G, 0° shoulder strap, 110° seat back angle.
5. 10G, (FD) maximum shoulder strap angle, 90° seat back angle.
6. 10G, (FD) maximum shoulder strap angle, 110° seat back angle.

A complete data package has been submitted to ASD/AES and a complete data package will be maintained by AFAMRL/BBP until this work unit is retired. The experimental results will eventually be recorded within a permanent data bank at AFAMRL.

The sample data plots were selected based on the subject who had the most measured responses which fell within one-half standard deviation of the mean of the measured responses of all of the subjects.

P-111 8G<sub>z</sub> TEST SUMMARY TABLE (CONFIGURATION 0/103)

TEST #	187	188	189	190	192	193	194	196	199	200
Subject ID	R-1	S-3	W-1	O-1	F-2	M-9	J-2	M-6	M-8	M-10
Subject Weight	197	163	158	175.5	156	167	210	163	184	145
Carriage Z	8.24	7.58	8.74	7.74	8.94	8.81	8.36	8.60	8.38	7.85
Carriage Velocity	-23.6	-23.9	-23.8	-23.6	-23.6	-23.7	-23.7	-23.4	-23.3	-23.5
Seat Z	7.64	7.91	8.77	8.07	8.94	8.88	8.60	8.60	8.44	8.53
Chest X	-5.71	-3.2	-3.41	-1.85	-2.57	-2.5	-5.29	-4.61	-4.49	-2.87
Chest Y	1.69	1.08	1.36	-1.27	1.36	.74	-1.66	.96	-1.25	.85
Chest Z	10.3	12.6	13.5	15.6	14	10.8	16.1	11.4	12.7	11.5
Chest Res	11.7	12.9	13.9	15.7	14.2	11	16.7	11.9	13	11.6
Chest SI	15	20.3	23.5	24.6	18.3	12.1	29.8	15.1	22.7	19.8
Head X	-3.64	2.75	3.06	-3.62	2	2.7	2.6	2.89	3.92	3.46
Head Y	2.65	-2.03	-2.58	-2.68	-2.3	-2.0	-1.99	-2.13	-2.07	-2.09
Head Z	11.6	11.3	10.4	11.5	11	10.2	10.5	9.82	9.17	9.69
Head Res	12.4	11.4	10.6	11.5	11.2	10.3	10.8	9.92	10	10
Head SI	28.9	16.1	16.9	16.1	15.8	19.5	16.2	19.6	17.1	13.5
Shoulder Sum	144.2	87.1	97.0	82.3	86.7	104.5	155.2	170.1	144.3	104.3
Shoulder Sum/Wt	.73	.53	.61	.47	.56	.63	.74	1.04	.78	.72
Lap Belt Sum	105.2	65.8	171.6	94.5	115.1	124.8	111.2	158	108	110.7
Lap Sum/Wt	.53	.4	1.09	.54	.74	.75	.53	.97	.59	.76
Seat Link X	200.8	193.6	161.6	274.6	191.7	238.7	309.5	196.2	214.9	162.8
Seat Link Y	57.4	39	48.8	-57	57.2	73.9	50.8	53.4	45.5	31
Seat Pan Z	1495	1523	1147	1571	1254	1509	1688	1406	1554	1237
Seat Z/Wt	7.59	9.35	7.26	8.95	8.04	9.04	8.04	8.62	8.45	8.53
Res Seat Force	1508	1535	1157	1595	1268	1528	1716	1418	1569	1247
Seat Force/Wt	7.66	9.41	7.33	9.09	8.13	9.15	8.17	8.70	8.53	8.60
Foot Rest X	-447.6	-244.3	-420.3	-429.6	-405.5	-293.8	-489.8	-330.3	-484.4	-216.2
Foot Rest Y	-55.4	-45.9	-63.3	-54.7	58.8	-50.1	-65	-59.5	-48.5	51.5
Foot Rest Z	827.2	656.5	855.5	794.9	769.8	687.2	923	705.3	793.9	633.1
Res Foot Force	908.8	699.2	913.9	892.1	824.3	729.1	1030	764.8	921.6	661.7

P-111 8G<sub>z</sub> TEST SUMMARY TABLE (CONFIGURATION O/103)

TEST #	201	203	205	206	207	211	215	226	229	MEAN	STANDARD DEVIATION
Subject ID	S-5	M-7	G-2	M-5	D-1	S-4	E-1	H-2	J-1		
Subject Wt	170	135	121.5	170	187	152	190	178	158	167.37	21.47
Carriage Z	8.38	9.96	8.59	8.45	8.53	8.79	8.64	8.49	8.61	8.51	.50
Carriage Vel	23.4	-23.3	-23.2	-23.4	-23.4	-22.8	-22.3	-22.1	-22.4	-23.28	.52
Seat Z	8.36	9.94	8.95	8.50	8.42	9.05	8.85	8.93	8.58	8.63	.49
Chest X	-4.18	-3.95	-3.65	-2.30	-3.22	-4.51	-5.1	-4.99	-2.74	-3.78	1.18
Chest Y	1.04	-1.03	1.16	-1.06	.52	-1.57	1.2	1.22	.82	.33	1.17
Chest Z	11.8	11	10.8	13.2	12.7	11.8	12.6	13.2	11.8	12.49	1.55
Chest Res	12.3	11.2	11	13.2	13.1	12	13	13.9	12.1	12.86	1.53
Chest SI	14.3	17.3	15.9	20.6	21.1	21	16.3	19.0	17.9	19.19	4.20
Head X	2.85	-3.43	2.36	3.71	2.68	5.1	3.98	2.47	2.33	2.01	2.58
Head Y	-2.05	-2.11	-2.19	-2.58	-1.93	-1.73	-2.52	-2.65	-1.12	-1.90	1.16
Head Z	10.6	8.93	10.2	11.9	9.84	11.1	9.44	11.0	9.61	10.41	.86
Head Res	10.7	9.57	10.4	12.1	9.90	11.1	9.56	11.1	9.67	10.64	.84
Head SI	15.4	12.8	15.3	18.6	13.9	19.7	13.4	14.8	12.5	16.11	3.61
Shoulder Sum	93.6	164.5	127.9	120.2	123.1	154.2	204.2	118.9	152.3	128.14	33.62
Shoulder Sum/Wt	.55	1.22	1.05	.71	.66	1.02	1.08	.67	.96	.78	.22
Lap Belt Sum	66.6	145	79.7	124.4	94.7	120.2	146	125.8	162.3	117.35	30.18
Lap Sum/Wt	.39	1.07	.66	.73	.51	.79	.77	.71	1.03	.71	.21
Seat Link X	178.8	187.5	123.9	146.6	269.9	179.9	272.7	295.3	182.9	209.57	52.55
Seat Link Y	37	-65.4	-22.2	32.0	-44.4	-33.8	43.8	-58.8	-50.2	12.53	48.78
Seat Pan Z	1576	1322	1022	1244	1780	1292	1564	1611	1245	1423.16	201.31
Seat Z/Wt	9.27	9.79	8.41	7.32	9.52	8.5	8.23	9.05	7.88	8.52	.73
Res Seat For	1586	1334	1030	1252	1799	1303	1587	1639	1258	1438.37	205.96
Seat Force/Wt	9.33	9.88	8.47	7.37	9.62	8.57	8.36	9.21	7.96	8.61	.73
Foot Rest X	-413.2	-115.8	-207.1	-679	-411.5	-347.5	-425	-298	-533.1	-378.05	131.21
Foot Rest Y	-62.6	-64.8	63.1	53.9	-57.3	-45.3	-73.2	-66.5	60.7	-46.04	36.85
Foot Rest Z	738.3	731.3	639	852.8	840.0	692.1	773.6	658.7	808.9	762.16	92.69
Res Ft Force	838.7	732.9	644.8	1048	882.0	759.0	855.6	713.1	921.6	828.48	117.17

F-111 LOG<sub>2</sub> TEST SUMMARY TABLE (CONFIGURATION 0/90)

TEST #	221	228	230	235	239	249	259	260	262	263
Subject ID	J-2	M-9	M-2	S-3	O-1	M-8	R-1	M-10	J-1	M-7
Subject Wt	210	168	166	163	174	182	205	145	159	136
Carriage Z	10.8	10.3	10.3	10.0	10.5	10.5	10.2	10.4	10.4	10.4
Carriage Vel	-28.1	-29.3	-25.0	-23.3	-24.0	-24.4	-24.5	-24.7	-24.7	24.9
Seat Z	10.6	10.6	10.5	10.3	10.6	10.6	10.5	10.6	10.5	10.5
Chest X	-4.45	4.43	2.26	2.45	4.26	-2.76	-6.14	2.69	2.04	4.37
Chest Y	-2.11	1.12	-0.99	1.49	-1.36	-1.80	1.76	1.49	1.41	1.25
Chest Z	17.8	14.2	16.9	18.3	20.3	18.9	17.6	20.6	13.6	17.8
Chest Res	17.9	14.5	17.0	18.3	20.3	19.1	18.4	20.6	13.7	17.9
Chest SI	36.7	27.3	33.0	35.0	36.9	31.3	30.3	32.8	23.4	34.2
Head X	3.93	3.16	7.13	3.47	4.77	5.04	6.67	5.71	5.19	-5.13
Head Y	-2.01	-1.88	-2.08	-0.96	-3.99	-3.00	-2.18	2.63	-1.60	-2.85
Head Z	12.0	11.4	10.6	14.5	15.1	14.0	14.2	13.1	12.6	10.3
Head Res	12.3	11.7	10.8	14.5	15.2	14.6	14.8	14.0	12.7	11.4
Head SI	19.5	19.0	23.3	22.3	28.2	27.8	24.9	26.3	21.3	19.2
Shoulder Sum	254	218	167	161	164	166	221	143	202	197
Shoulder Sum/Wt	1.21	1.30	1.01	0.99	0.94	0.91	1.08	0.99	1.27	1.45
Lap Belt Sum	157	219	164	133	139	96.9	224	140	236	171
Lap Sum/Wt	0.75	1.31	0.99	0.82	-0.80	0.53	1.09	0.97	1.48	1.26
Seat Link X	336	235	246	207	272	174	251	201	209	171
Seat Link Y	50.5	60.8	51.3	-44.0	50.9	-59.8	48.0	-47.3	-65.7	44.1
Seat Pan Z	2212	1980	1809	1934	1757	1992	2085	1639	1848	1583
Seat Z/Wt	10.1	11.8	10.9	11.9	10.1	10.9	10.2	11.3	11.6	11.6
Res Seat Force	2138	1994	1825	1945	1777	2000	2099	1651	1859	1591
Seat Force/Wt	10.2	11.9	11.0	11.9	10.2	11.0	10.2	11.4	11.7	11.7
Foot Rest X	-635	-355	-327	-475	-534	-681	-564	-271	-471	-310
Foot Rest Y	-56.3	76.3	-85.4	65.9	55.7	-77.5	-69.0	-49.7	57.9	68.8
Foot Rest Z	1081	801	833	924	997	1017	966	815	863	891
Res Foot Force	1186	857	879	1041	1112	1173	1110	855	968	936

F-111 LOG<sub>2</sub> TEST SUMMARY TABLE (CONFIGURATION 0/90)

TEST #	MEAN	STANDARD DEVIATION
Subject Wt	170.8	23.45
Carriage Z	10.38	.21
Carriage Vel	-25.29	1.88
Seat Z	10.53	.09
Chest X	.92	3.89
Chest Y	.23	1.58
Chest Z	17.6	2.28
Chest Res	17.77	2.23
Chest SI	32.1	4.21
Head X	3.99	3.45
Head Y	-1.79	1.76
Head Z	12.78	1.68
Head Res	13.2	1.6
Head SI	23.19	3.52
Shoulder Sum	189.3	34.74
Shoulder Sum/Wt	1.12	.18
Lap Belt Sum	167.99	45.23
Lap Sum/Wt	1.0	.29
Seat Link X	230.2	49.61
Seat Link Y	8.88	54.77
Seat Pan Z	1873.9	179.02
Seat Z/Wt	11.04	.71
Res Seat Force	1887.9	181.22
Seat Force/Wt	11.12	.71
Foot Rest X	-462.3	142.59
Foot Rest Y	-1.33	70.74
Foot Rest Z	918.8	94.41
Res Foot Force	1011.7	129.41



F-111 10G<sub>z</sub> TEST SUMMARY TABLE (CONFIGURATION FD/90)

TEST #	238	245	250	258	269	270	271	274	275	MEAN	STANDARD DEVIATION
Subject ID	M-9	J-2	M-2	S-3	O-1	R-1	M-10	M-8	J-1		
Subject Wt	169	211	156	163	175	202	144	182.5	159	173.5	21.85
Carriage Z	10.5	10.4	10.3	10.3	10.5	10.4	10.4	10.4	10.4	10.4	.07
Seat Z	10.8	10.3	10.8	10.6	10.8	10.5	10.6	10.6	10.4	10.6	.18
Chest X	3.1	-2.1	-2.5	-3.7	-2.1	-7.1	-4.1	-3.5	-4.3	-2.92	2.73
Chest Y	-2.1	-2.4	1.3	1.6	.9	1.2	1.3	2.2	2.6	.53	1.85
Chest Z	16	16	16.2	21.9	20.8	18	13.5	15.5	20.6	17.61	2.88
Chest Res	16.1	16.2	16.2	22	20.9	19.1	14	15.8	21	17.92	2.86
Chest SI	24.4	28.7	25.7	33.9	34.1	35.6	25.3	26.9	37.4	30.22	5.01
Head X	4	4.6	4.6	5.5	.1	7	4.4	3.7	5.4	4.37	1.88
Head Y	.6	-1.1	0	-2.1	-7	-2.1	-2.9	-3.1	-2.6	-1.44	1.4
Head Z	12.5	12.2	12.4	15.2	14.9	15.4	13.3	15.7	18	14.4	1.94
Head Res	12.6	12.4	12.5	15.5	15.2	16.2	13.9	15	18.4	14.63	2.0
Head SI	22.3	19.9	21.2	27.5	36.4	38.8	31.3	24.5	32	28.21	6.81
Shoulder	226.1	272.3	149.3	175.1	182.1	181.7	202.6	158.7	168.9	170.8	38.19
Shoulder/Wt	1.3	1.3	1	1.1	1	.9	1.4	.9	1.1	1.11	.18
Lap Belt	191.8	156.3	193.4	152.4	126.6	185.7	218.2	114.6	165	167.11	33.53
Lap Belt/Wt	1.1	.7	1.2	.9	.7	.9	1.5	.6	1	.96	.28
Seat Link X	249	341	256.6	238.4	315.2	253.1	189	248.1	230.7	257.9	45.08
Seat Link Y	-29.3	76.3	61.2	-61.9	-108.2	50.3	21.3	-65.8	-33.6	-9.97	64.72
Seat Pan Z	1858	2239	1701	1878	1871	2064	1230	1973	1861	1852.8	278.43
Seat Pan Z/Wt	11	10.6	10.9	11.5	10.7	10.2	8.5	10.8	11.7	10.6	.93
Res Seat For	1874	2264	1718	1893	1898	2080	1244	1988	1875	1870.4	280.5
Seat Force/Wt	11.1	10.7	11	11.6	10.8	10.3	8.6	10.9	11.8	10.76	.93
Foot Rest X	-439.6	-762.1	-445.3	-524.6	-528.3	-643.8	-508.8	-712.8	-599.2	-573.8	113.8
Foot Rest Y	-60.1	-73	-58.8	-39.5	-35.2	39.3	81.4	-54.6	68	-14.72	60.23
Foot Rest Z	911.7	1071	921	916.5	992.5	1044	1011	1047	925.5	982.2	64.31
Res Foot For	968	1313	998.4	1046	1078	1198	1034	1252	1104	1110.2	118.7
Carriage Vel	-23.2	-23.9	-24.8	-24.7	-24.5	-25.3	-24.9	-24.0	-24.9	-24.57	.64

F-111 LOG<sub>2</sub> TEST SUMMARY TABLE (CONFIGURATION 0/103)

TEST #	197	198	202	208	210	212	213	216	217	219	220
Subject ID	R-1	M-2	O-1	W-1	M-9	J-2	F-2	D-1	M-6	G-2	S-5
Subject Wt	198	158	176	155	169	210.5	159	199	163	118	171
Carriage Z	10.8	10.1	10.2	10.5	10.6	10.6	10.6	10.9	10.7	10.9	10.8
Seat Z	10.7	10.7	10.4	10.5	10.9	10.6	10.9	11	11.2	11.1	10.7
Chest X	-7.9	-3.3	-6.3	-5.3	-2.96	-4.68	-3.21	-3.93	-5.69	-6.24	-7.66
Chest Y	.7	-1.4	1.4	1.4	1.33	-1.78	1.77	1.69	-1.09	-2.21	-3.61
Chest Z	13.6	15.3	17.9	20.1	15.1	17.7	17.9	17.6	17	15.9	18
Chest Res	15.7	15.5	18.5	20.5	15.2	17.8	18	18	17.9	16	19
Chest SI	29.1	30.3	34	41.6	24.5	38.7	32.9	33.4	34.2	23.8	36.4
Head X	5	6.3	2.5	3.31	4.79	4.63	4.29	5.15	4.59	4.05	4.12
Head Y	-6	-4	-1	-2.85	-1.49	-2.02	-2.35	-1.98	-2.13	-2.29	-1.49
Head Z	12.8	10.4	13.8	14.3	11.7	11.8	12.8	14	14.3	13.3	13.8
Head Res	12.9	10.5	14	14.6	11.7	11.9	12.9	14.3	14.4	13.6	13.8
Head SI	22.3	19.3	23.5	25.6	17.5	21.4	24	24.3	26.1	24.5	23.1
Shoulder	204.4	209.4	150.1	127.2	206.3	161.3	193.9	189.5	212.2	118.6	139.3
Shoulder/Wt	1	1.3	.9	.82	1.22	.77	1.22	.95	1.3	1.01	.82
Lap Belt	149.2	159.5	137.6	129.5	180.2	172	179.2	121.8	194.2	98.5	111.9
Lap Belt/Wt	.8	1	.8	.84	1.06	.82	1.13	.61	1.19	.83	.66
Seat Link X	277.6	260	270.6	217.5	217.6	341.5	220.5	305.7	276.9	196.7	223.7
Seat Link Y	50.3	-29.7	-64.4	-49.4	-50.8	58.7	43.8	60.8	-92.2	-59.7	48
Seat Pan Z	1822	1677	1778	1478	1815	2079	1605	2279	1873	1364	1944
Seat Pan Z/Wt	9.2	10.6	10.1	9.53	10.7	9.88	10.1	11.5	11.5	11.6	11.4
Res Seat For	1843	1696	1799	1494	1828	2107	1619	2299	1895	1378	1957
Seat Force/Wt	9.3	10.7	10.2	9.64	10.8	10	10.2	11.6	11.6	11.7	11.5
Foot Rest X	-626.7	-402.6	-494	-458.4	561.6	-563.6	-398.1	-574.8	-407.1	-263.5	-460.7
Foot Rest Y	-51.2	59.7	69.9	-9.2	-76.1	-71.2	-74.5	55.3	-51.4	69.1	-52
Foot Rest Z	968.7	878.5	975.2	915	723.2	989.5	864.6	1005	855.4	789.5	911.3
Res Foot Rest	1154	968.7	1073	1019	902.9	1130	925.7	1093	889.2	806.2	992.7
Carriage Vel	-26.4	-26.4	-26.3	-26.2	-25.9	-25.3	-24.7	-25.2	-25.1	-25.5	-25.3

F-111 10G<sub>Z</sub> TEST SUMMARY TABLE (CONFIGURATION O/103)

TEST #	223	224	225	231	233	242	243	244	248	MEAN	STANDARD DEVIATION
Subject ID	M-7	S-4	S-3	M-8	E-1	H-2	M-5	M-10	J-1		
Subject Wt	136	152.5	163	187	189.5	180	170	145	163	168.13	22.28
Carriage Z	10.8	10.7	10.6	10.1	10	10.4	10.4	10.5	10.5	10.54	.27
Seat Z	11.2	11.2	11.1	10.5	10.4	10.7	10.5	10.6	10.5	10.77	.28
Chest X	-2.76	-4.68	-3.79	-8.69	-4.37	-4.94	-1.4	-2.88	-4.53	-4.77	1.89
Chest Y	-1.58	-2.16	1.07	-1.74	2.44	2.05	1.63	2.77	1.33	.20	1.91
Chest Z	13.8	14.5	14.6	17.9	16.4	17.7	14	17	14.1	16.28	1.82
Chest Res	14	14.6	14.9	19.8	16.5	18.2	14.2	17.2	14.7	16.81	1.94
Chest SI	20.1	33	26.8	41.5	28	31	23.3	31.6	28.5	31.14	5.86
Head X	-4.61	3.32	-2.78	3.67	4.9	5.18	4	4.95	4.24	3.58	2.64
Head Y	-3.03	-1.63	-1.7	-1.95	-2.88	-2.63	-2.58	-1.25	-2	-1.91	.73
Head Z	11.6	12.5	13.6	14.6	12.6	16	14.8	13.7	12.1	13.23	1.33
Head Res	12.5	12.6	13.8	14.9	12.7	16.2	14.9	14.2	12.3	13.44	1.34
Head SI	22.1	21.3	20.8	26	21.6	18.7	25.4	25.2	22.1	23.24	2.62
Shoulder	226.4	202.6	173.8	162.7	190.8	152.5	203.6	164.8	186.5	178.9	30.45
Shoulder/Wt	1.67	1.33	1.07	.87	1.01	.85	1.2	1.14	1.14	1.08	.23
Lap Belt	120.2	121.2	140.7	80.6	214.6	152.1	133.8	136.9	225.9	142.98	52.73
Lap Belt/Wt	.88	.8	.86	.43	1.13	.85	.79	.94	1.39	.89	.22
Seat Link X	271.1	217.6	250.8	254.8	344.6	333.4	189.2	248.1	234.7	257.63	45.99
Seat Link Y	-62.7	-78.3	47.1	45.7	67.2	-67.6	41.7	-60	-59.4	-10.82	58.72
Seat Pan Z	1586	1568	1867	2043	2052	2042	1745	1606	1693	1795.8	231.52
Seat Pan Z/Wt	11.7	10.5	11.5	10.9	10.8	11.3	10.3	11.1	10.4	10.72	.73
Res Seat For	1608	1584	1884	2058	2069.17	2081	1755	1626	1709	1814.45	233.9
Seat Force/Wt	11.8	10.4	11.6	11	11	11.5	10.3	11.2	10.5	10.83	.74
Foot Rest X	-198.2	-421	-427.5	-479.5	-480.5	-473.4	-784.7	-310	-534.6	-466.03	129.08
Foot Rest Y	-107.9	51.6	-57.6	-66.8	-78.7	82.2	-73.1	-85.7	72.2	-23.91	69.06
Foot Rest Z	633.8	826	846.7	845.8	985.5	895.9	1020	814.5	907.3	882.57	97.89
Res Foot Rest	661.4	885.3	889.8	965.7	1065	966.1	1257	857.8	1016	975.93	134.2
Carriage Vel	-24.9	-25.3	-24.8	-24.7	-22.2	-24.5	-24	-24	-24.1	-25.05	1.01

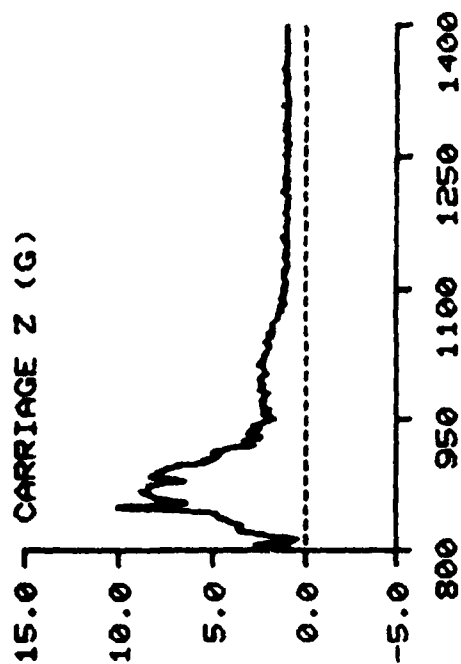
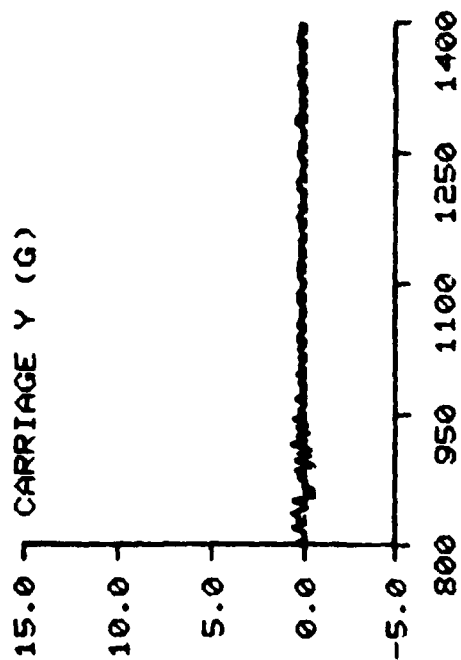
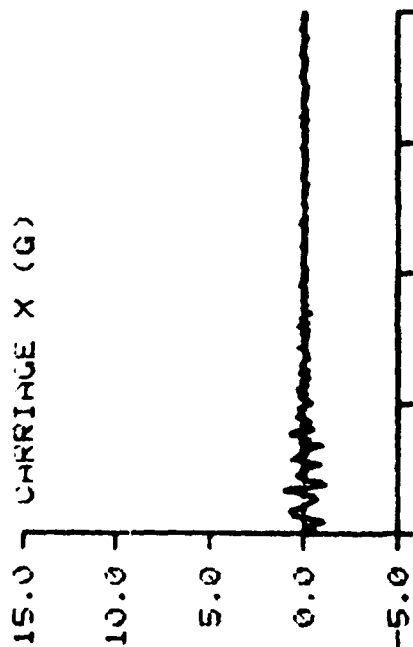
F-111 LOG<sub>2</sub> TEST SUMMARY TABLE (CONFIGURATION 0/110)

TEST #	218	234	240	247	252	254	255	272	236	MEAN	STANDARD DEVIATION
Subject ID	F-2	G-2	S-4	D-1	E-1	M-6	M-5	W-1	S-5	S	
Subject Wt	155	119.5	152.5	200	188	163	172	155	173	164.2	23.16
Carriage Z	10.6	10.2	10.5	10.2	10.5	10.4	10.7	10.4	10.1	10.4	.20
Carriage Vel	-25.1	-24.4	-24.2	-24	-24.6	-24.4	-24.7	-24.9	-23.9	-24.47	.40
Seat Z	11.2	10.5	10.8	10.9	10.9	10.9	11.1	10.6	10.3	10.8	.29
Chest X	-5.02	-6.96	-5.11	-5.6	-5.96	-5.2	-2.78	-4.12	-8.81	-5.51	1.7
Chest Y	2.33	-1.62	-1.48	2.92	1.77	-1.16	1.25	1.46	-4.33	.13	2.39
Chest Z	19	16	12.8	15.1	15.7	15.2	14.1	13	19.1	15.56	2.27
Chest Res	19.6	16.2	13.4	16.2	16.4	16	14.3	13.5	20.9	16.28	2.56
Chest SI	35.7	33.1	25.8	26.4	28.6	24.5	24.7	22.5	35.3	28.51	4.97
Head X	3.25	2.56	4.89	2.03	4.28	-2.02	2.86	3.5	3.69	2.78	2.0
Head Y	-2.14	-1.54	-2.11	-2.62	-2.78	-1.89	-2.54	-2.91	-1.83	-2.26	.47
Head Z	13.4	12.7	12.4	13.4	12.7	12.5	13.5	12.5	13.4	12.94	.47
Head Res	13.4	12.8	12.9	13.5	12.9	12.6	13.6	13.1	13.8	13.18	.41
Head SI	23.7	20.9	26.7	23.4	22.2	21.4	23.3	24	25.1	23.41	1.8
Shoulder Sum	234.2	135.7	195.7	177.4	232.3	192.9	192.4	200.1	177.5	193.33	29.29
Shoulder/Wt	1.51	1.14	1.28	.89	1.24	1.18	1.12	1.29	1.03	1.19	.18
Lap Belt	209.7	112.9	206.1	171.4	228.6	179.7	155.8	216.3	134.2	179.41	39.53
Lap Belt/Wt	1.35	.95	1.35	.86	1.22	1.10	.91	1.4	.78	1.10	.24
Seat Link X	242.7	202.1	219.7	233.8	353.1	220.1	177.6	198.8	208.6	228.5	50.58
Seat Link Y	-93.5	-64.2	55.3	-63.3	-73.7	54.9	-85.3	-81.8	-91.4	-49.22	60.09
Seat Pan Z	1431	1298	1590	1987	1863	1704	1649	1240	1760	1613.56	251.39
Seat Pan Z/Wt	9.23	10.9	10.4	9.94	9.91	10.5	9.59	8	10.2	9.85	.85
Res Seat For	1453	1315	1605	2000	1897	1717	1660	1256	1775	1630.89	252.17
Seat Force/Wt	9.38	11	10.5	10	10.1	10.5	9.65	8.1	10.3	9.95	.84
Foot Rest X	-490.1	-229.2	-409	-523.4	-473.4	-448.6	-611.4	-510.1	-453.3	-460.9	104.03
Foot Rest Y	-50.1	63.3	-59.2	-65	-89.1	95.1	-62.3	80.7	85.1	-1.17	78.15
Foot Rest Z	922.6	800	783.6	1034	1030	836.2	1036	1010	980.5	936.99	104.73
Res Foot For	1006	826.5	883.5	1151	1108	925.8	1169	1133	1077	1025.5	134.2

F-111 LOG<sub>2</sub> TEST SUMMARY TABLE (CONFIGURATION FD/110)

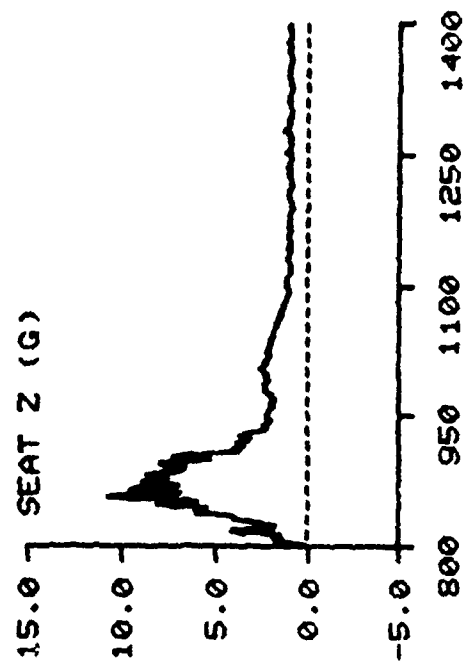
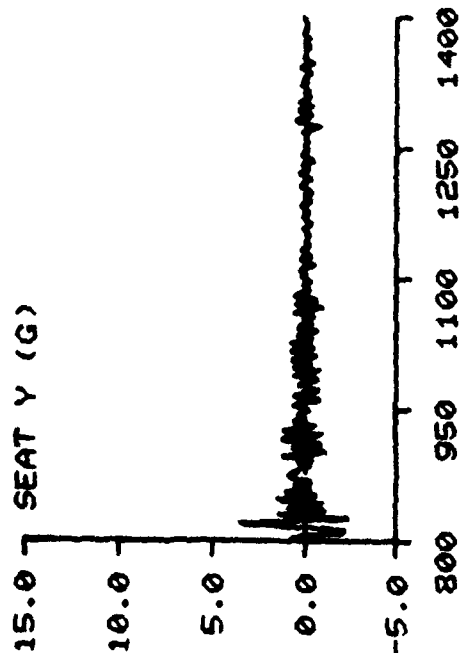
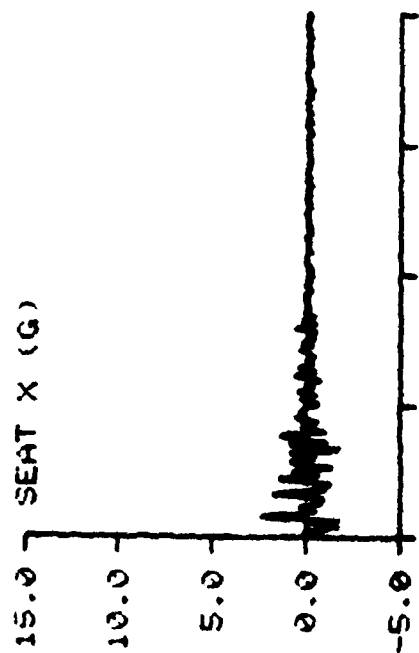
TEST #	241	253	265	266	267	276	MEAN	STANDARD DEVIATION
Subject ID	F-2	S-5	E-1	D-1	G-2	M-5		
Subject Wt	153	173	191.5	201	120	172	168.4	29.02
Carriage Z	10.4	10.7	10.6	10.5	10.5	10.3	10.5	.14
Carriage Vel	-23.8	-24.4	-24.3	-24.6	-24.8	-25.2	-24.52	.48
Seat Z	11.1	11.3	11.2	11.1	11.1	10.7	11.08	.20
Chest X	-4.99	-9.12	-5.84	-6.21	-6.07	-4.35	-6.1	1.64
Chest Y	1.53	1.85	1.43	2.90	-1.39	1.98	1.38	1.46
Chest Z	18.4	15	14.6	16.1	13.2	13.2	15.08	1.97
Chest Res	19.0	17	15.5	17.4	14.1	13.8	16.13	2.03
Chest SI	35.7	25.6	28.9	31.1	20	20.2	26.92	6.22
Head X	-2.93	-1.68	3.39	1.84	3	3.94	1.26	2.87
Head Y	-2.07	-1.82	-2.74	-2.14	-1.53	-1.62	-.56	2.13
Head Z	13.5	13.2	13.2	13.2	14	15.1	13.7	.75
Head Res	13.8	13.3	13.3	13.3	14.3	15.5	13.92	.87
Head SI	20.8	21.6	22.7	20.4	25	30	23.42	3.62
Shoulder Sum	169.1	132.7	145.2	97.9	143.5	174.4	143.8	27.6
Shoulder Sum/Wt	1.11	.77	.76	.49	1.2	1.01	.89	.26
Lap Belt Sum	208.7	182.9	198.9	138.9	122.3	192	173.95	35.02
Lap Belt Sum/Wt	1.36	1.06	1.04	.69	1.02	1.12	1.05	.22
Seat Link X	223.8	198.1	317	226.5	179.8	217.6	228.5	51.27
Seat Link Y	-64.5	-69.6	-65.8	-59.3	-55.4	-62	-62.77	5.02
Seat Pan Z	1389	1690	1911	1988	1415	1655	1674.7	246.5
Seat Z/Wt	9.08	9.77	9.98	9.89	11.8	9.62	10.02	.93
Res Seat Force	1408	1701	1939	2002	1426	1668	1690.8	248.9
Seat Force/Wt	9.2	9.83	10.1	9.96	11.9	9.7	10.12	.93
Foot Rest X	-566	-476.3	-435.8	-499.9	-370.1	-515.9	-477.3	67.95
Foot Rest Y	-87.6	-65.9	-68	-63.1	61.5	-52	-45.85	53.84
Foot Rest Z	948.5	981.2	978	1018	830.2	995.6	958.6	66.89
Res Foot Force	1046	1059	1048	1097	867.6	1111	1038.1	87.69

F-111 TEST NO: 205 SUBJECT ID: G-2



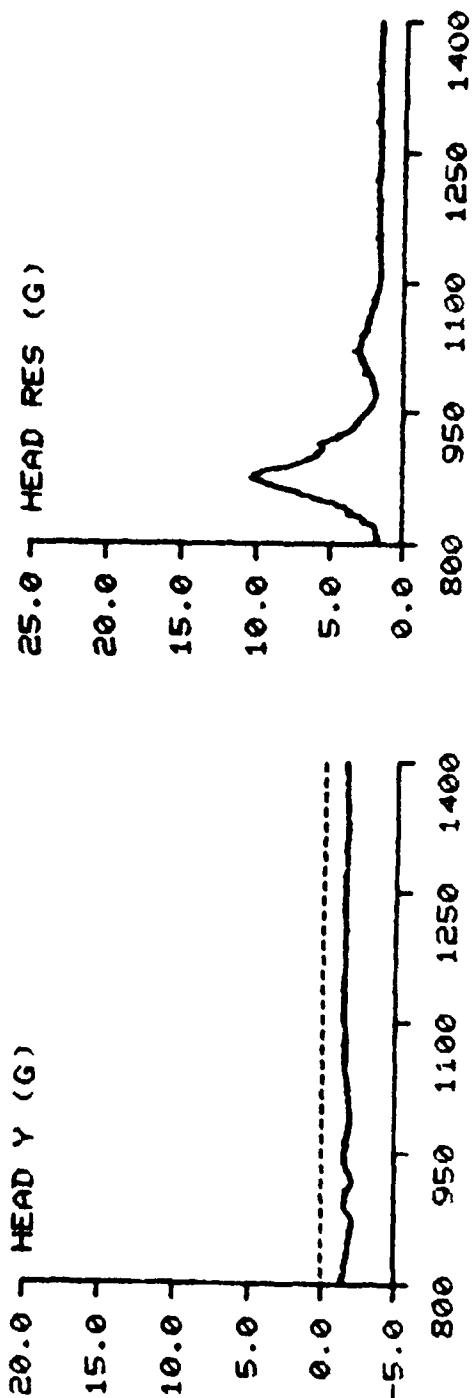
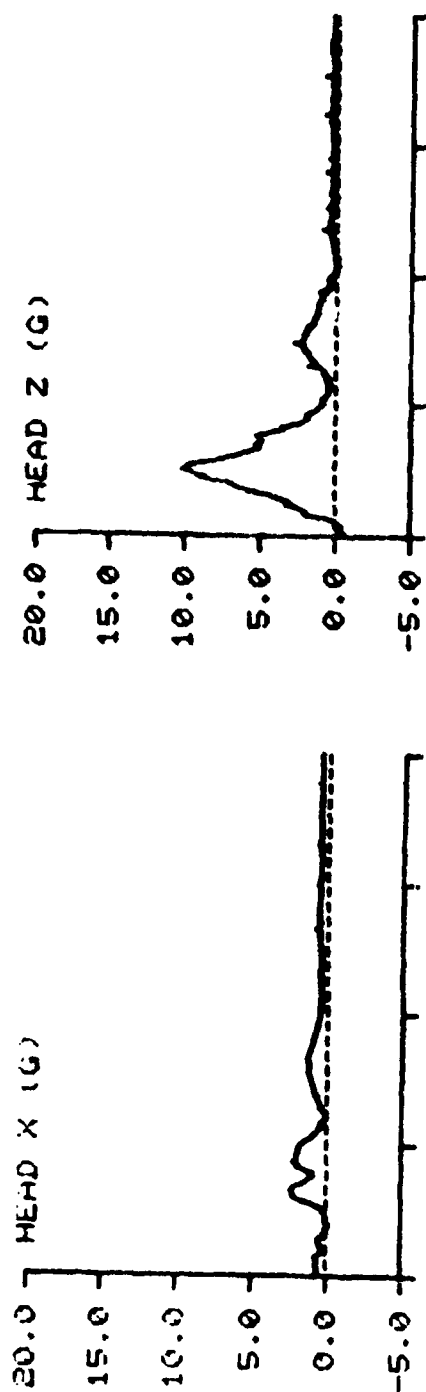
TIME IN MILLISECONDS

F-111 TEST NO: 205 SUBJECT ID: G-2



TIME IN MILLISECONDS

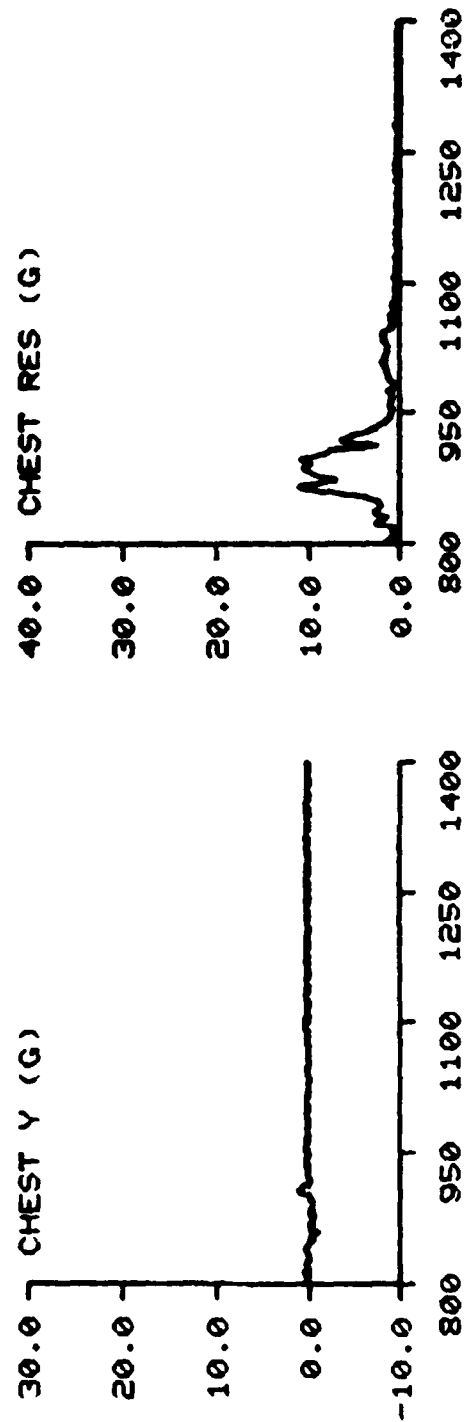
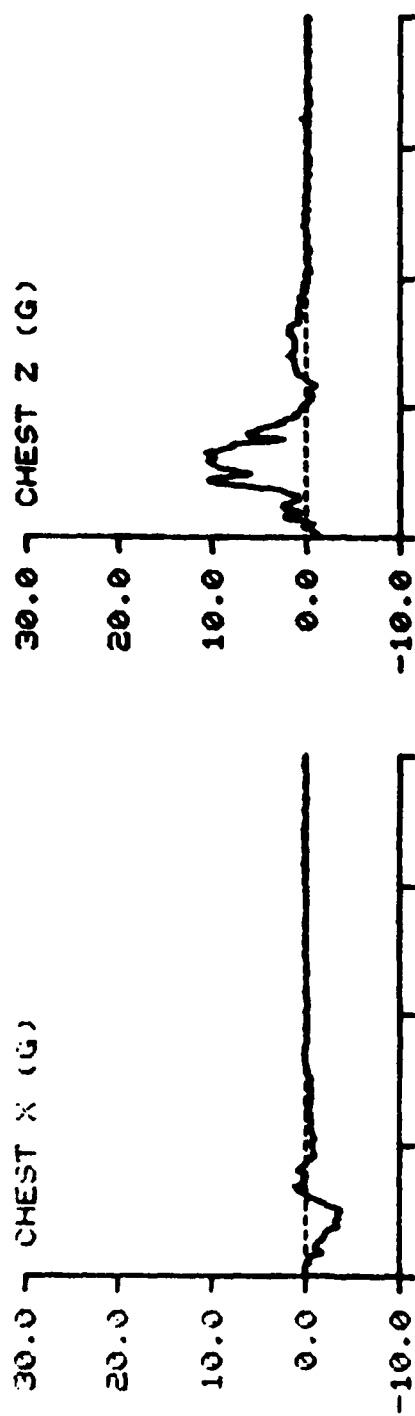
F-111      TEST NO: 205      SUBJECT ID: G-2



TIME IN MILLISECONDS

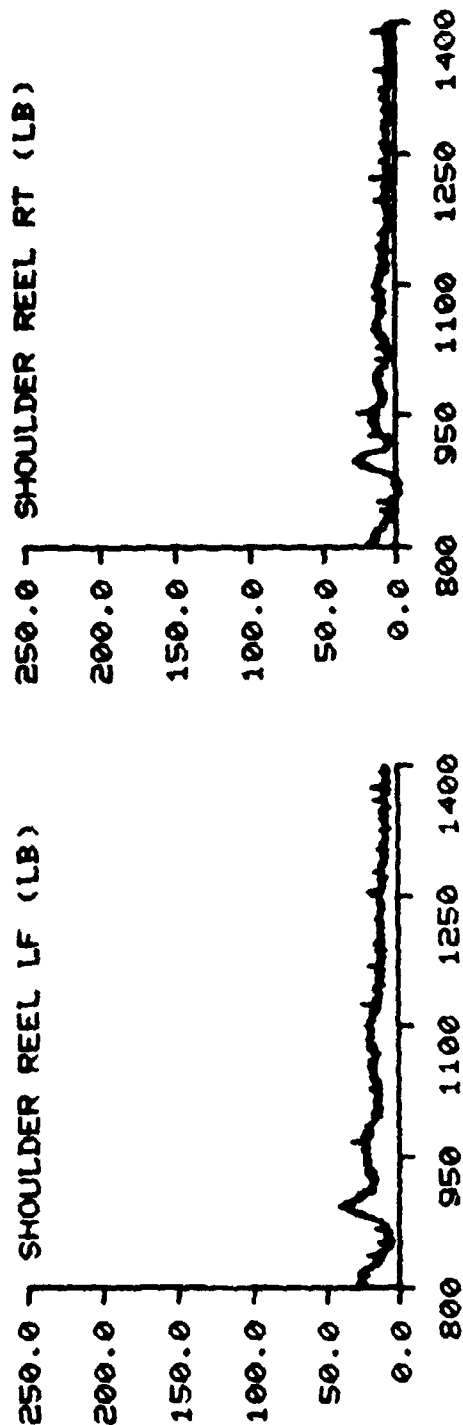
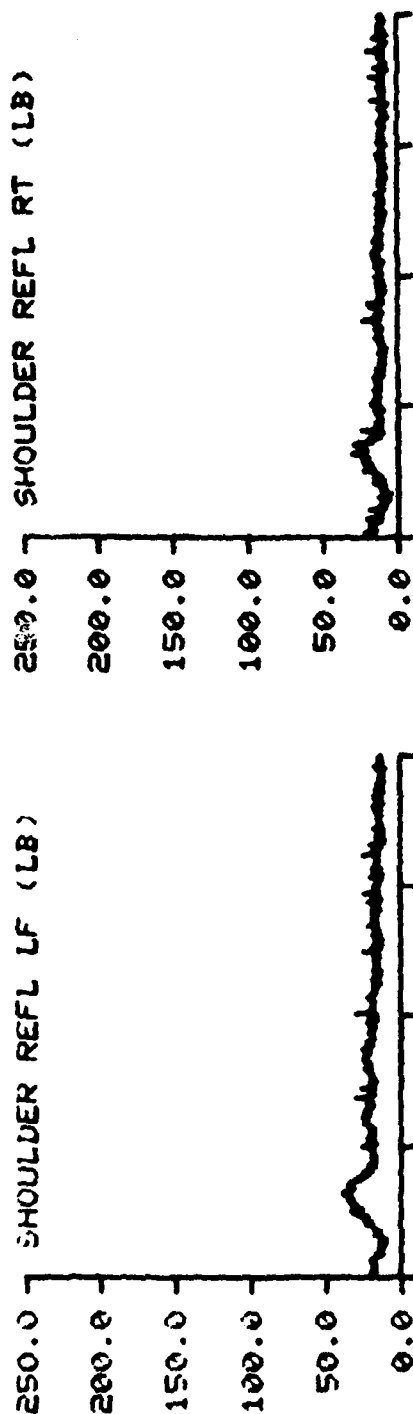


F-111      TEST NO: 205      SUBJECT ID: G-2



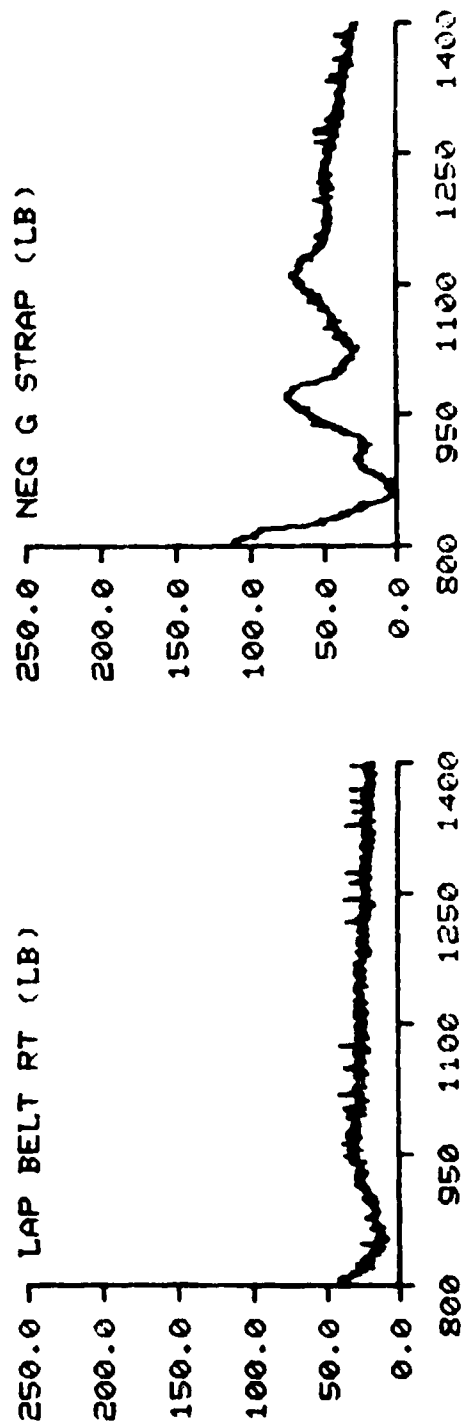
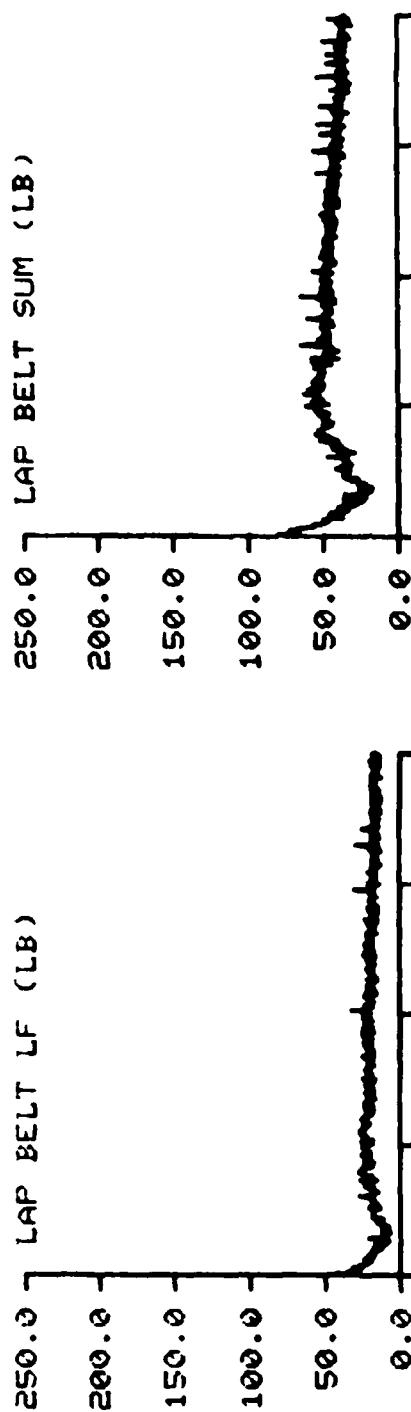
TIME IN MILLISECONDS

F-111 TEST NO: 205 SUBJECT ID: G-2



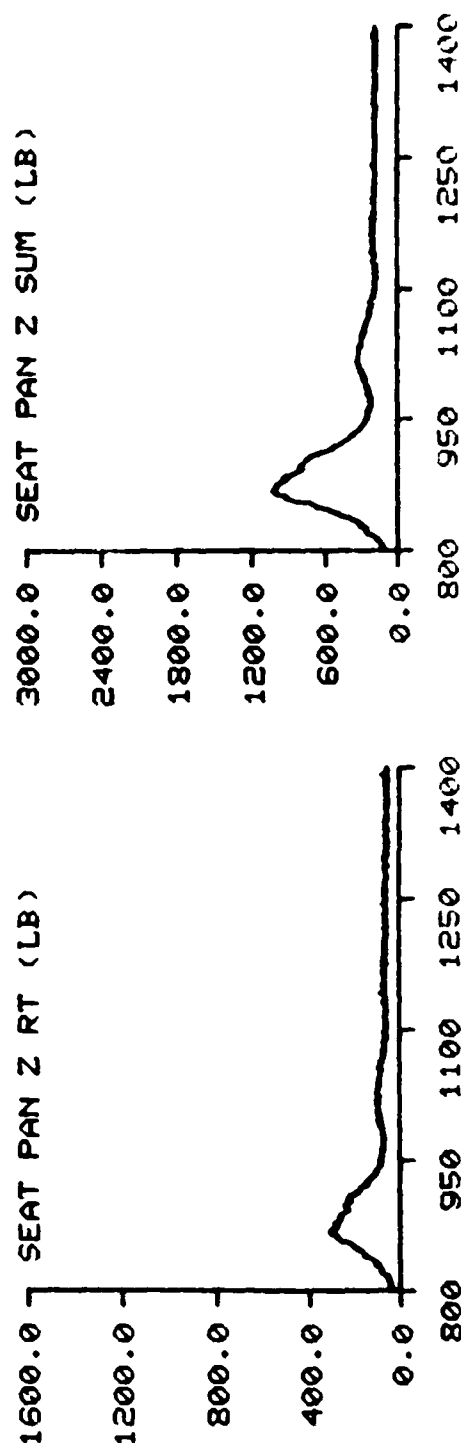
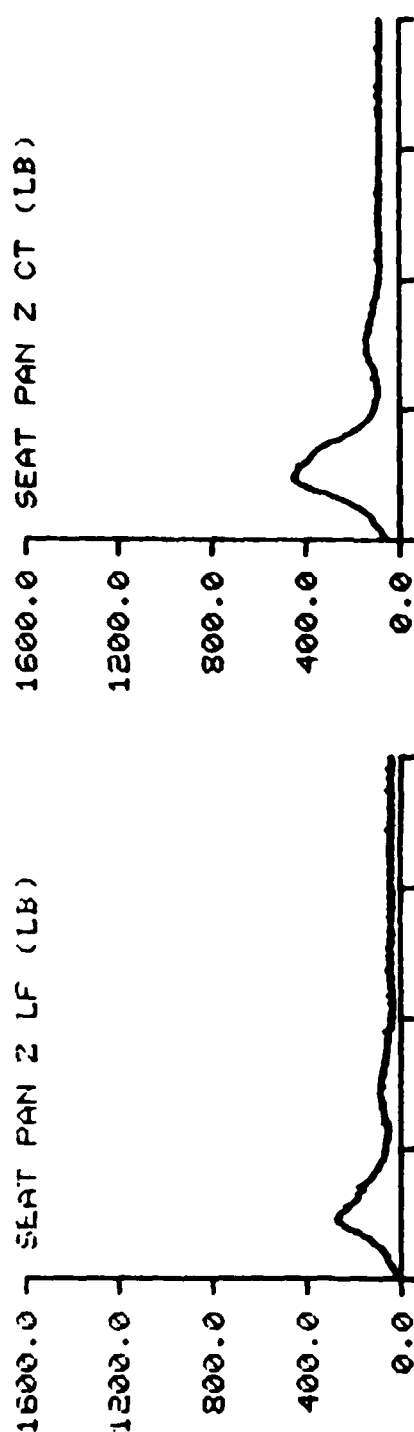
TIME IN MILLISECONDS

F-111 TEST NO: 205 SUBJECT ID: G-2



TIME IN MILLISECONDS

F-111      TEST NO: 205      SUBJECT ID: G-2

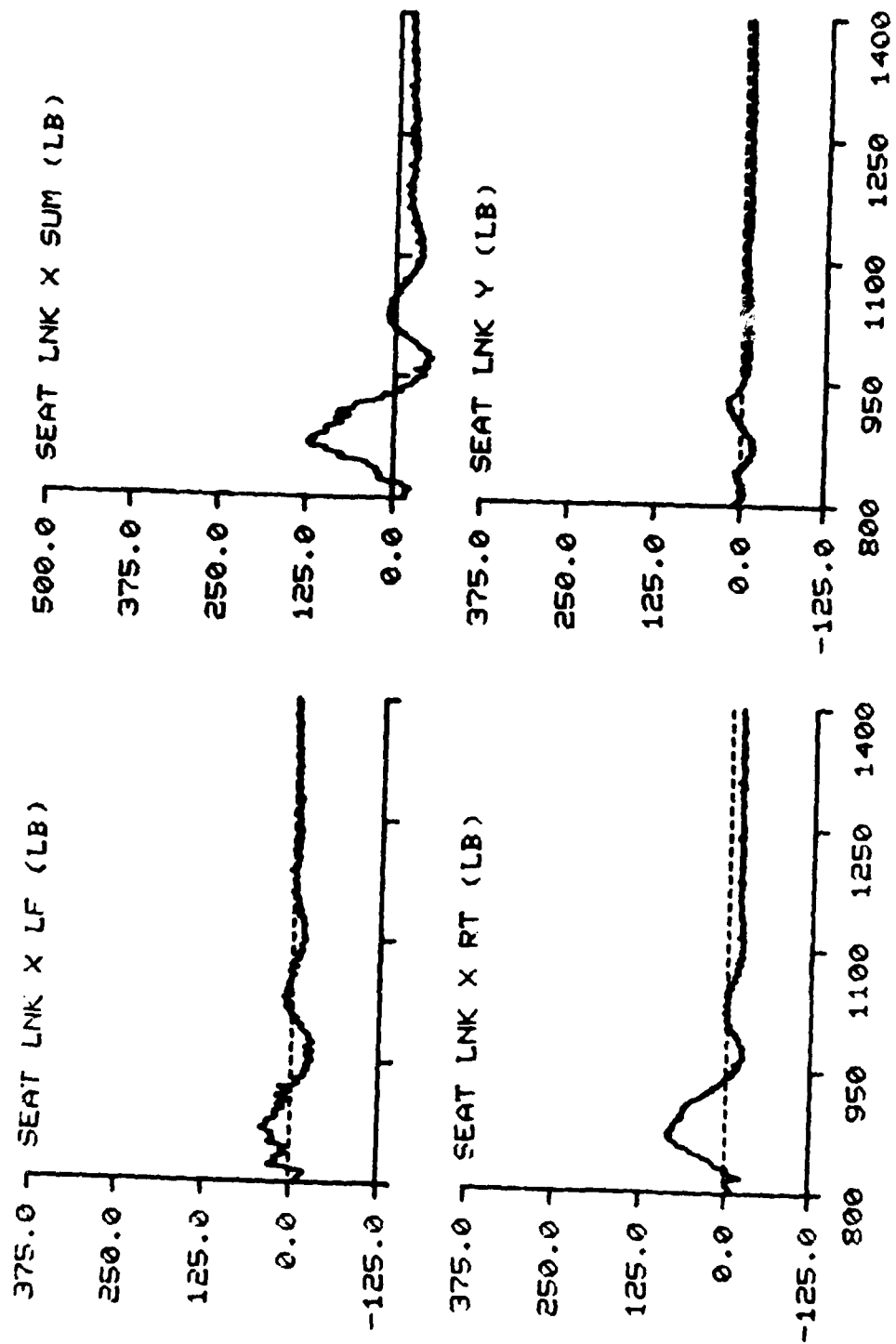


TIME IN MILLISECONDS

F-111

TEST NO: 205

SUBJECT ID: G-2

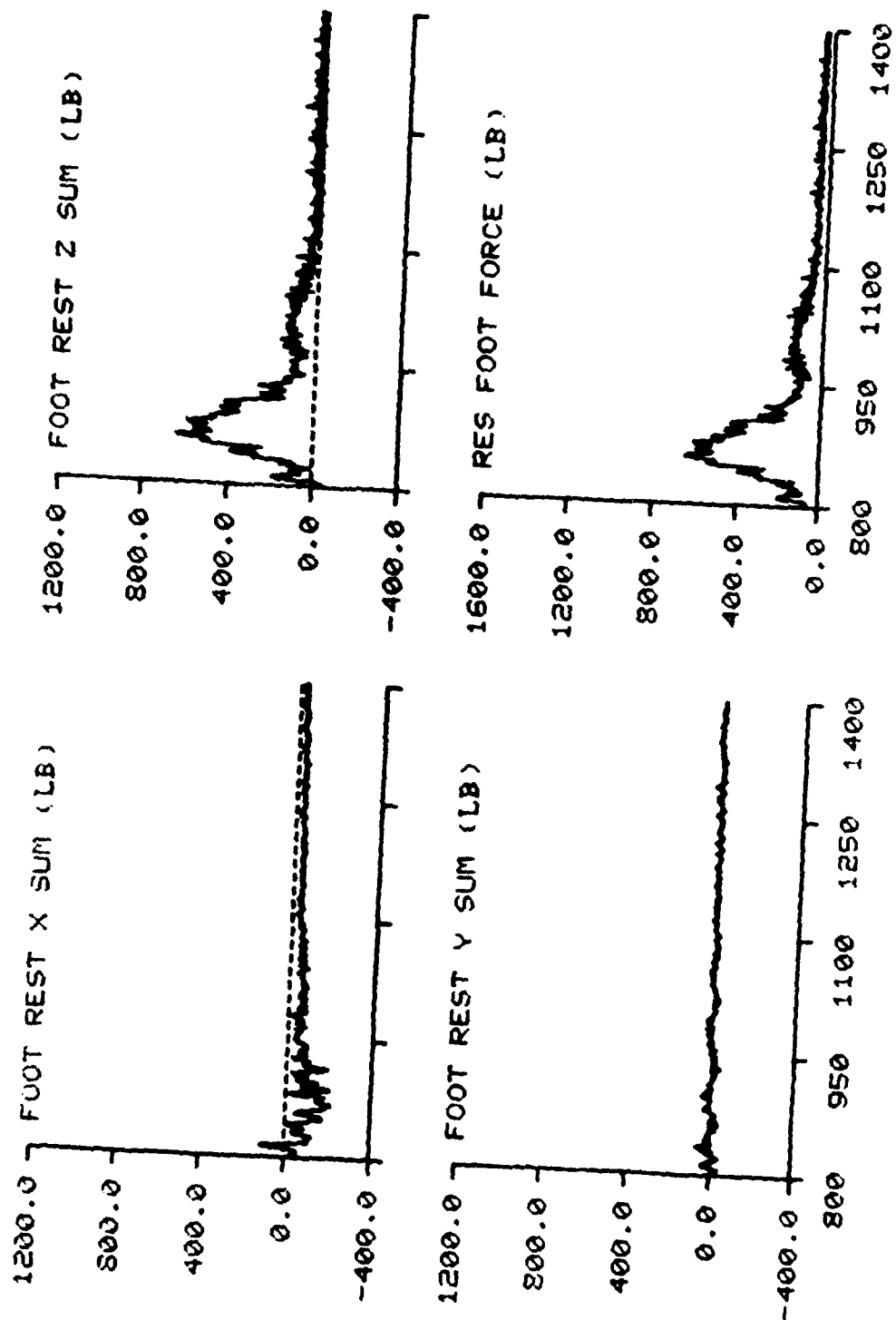


TIME IN MILLISECONDS

F-111

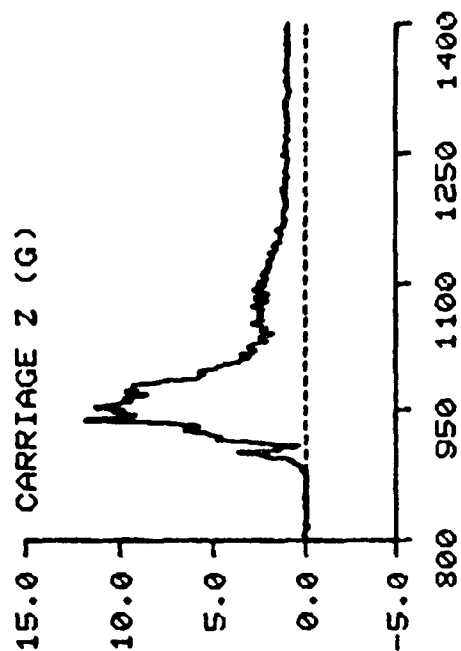
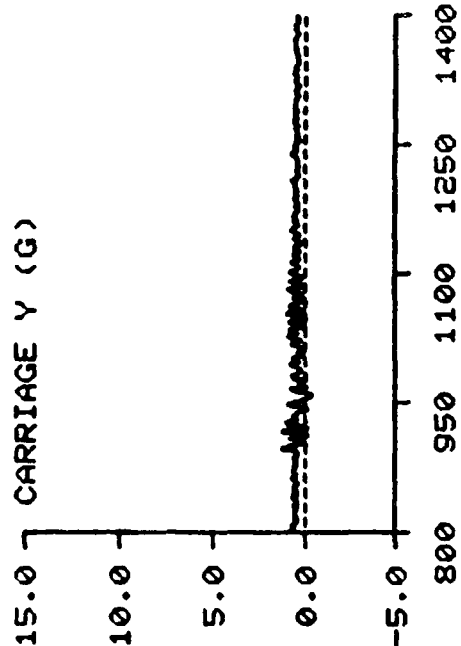
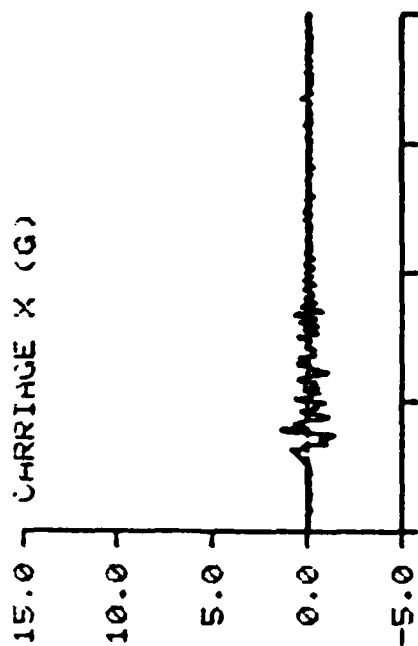
TEST NO: 205

SUBJECT ID: G-2



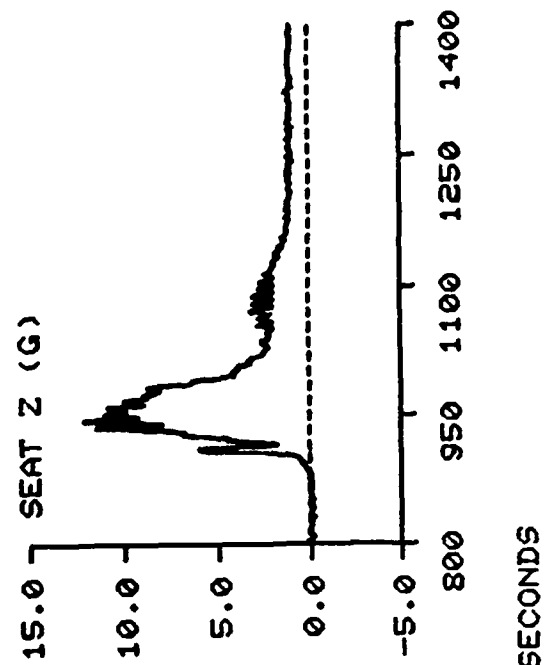
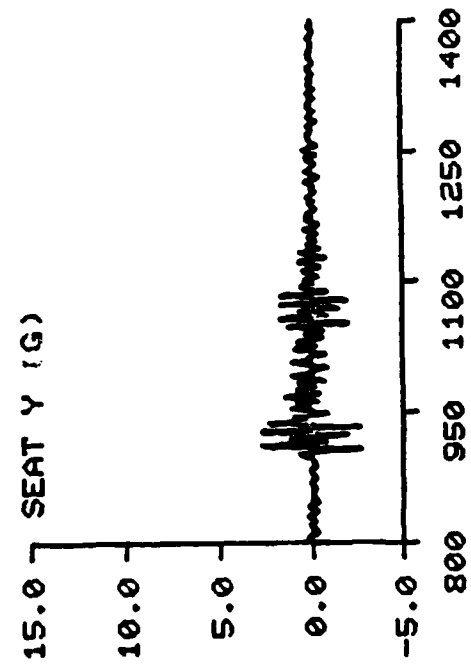
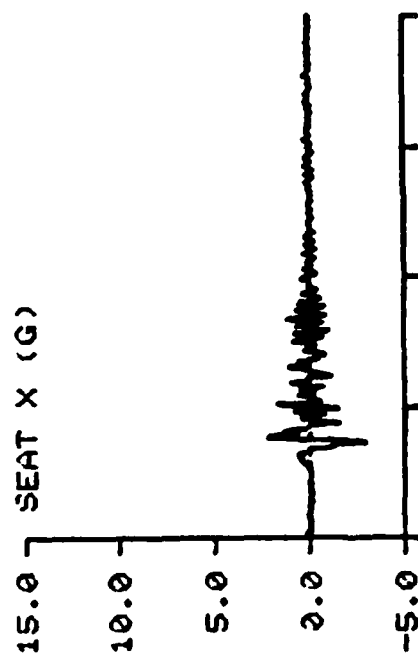
TIME IN MILLISECONDS

F-111      TEST NO: 244      SUBJECT ID: M-10



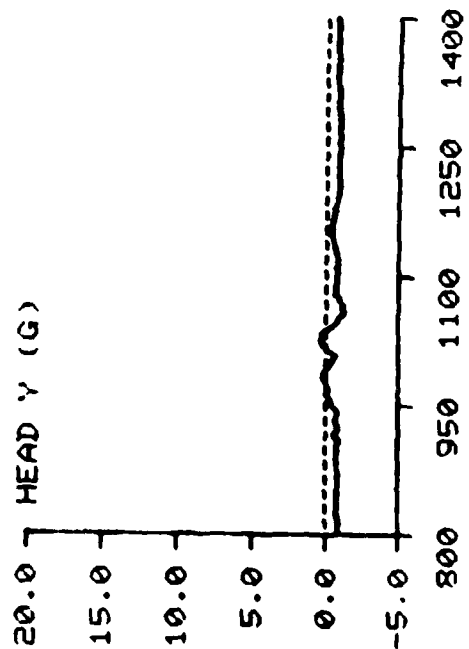
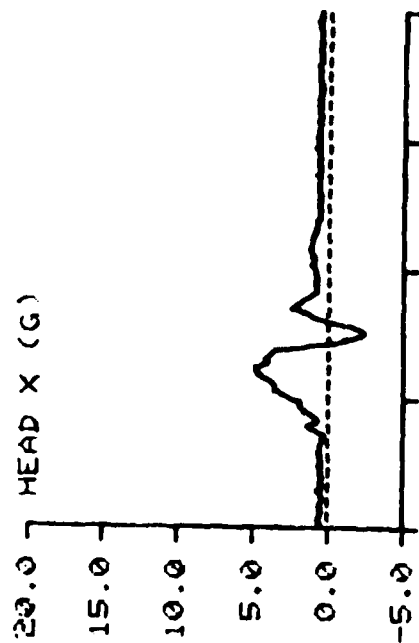
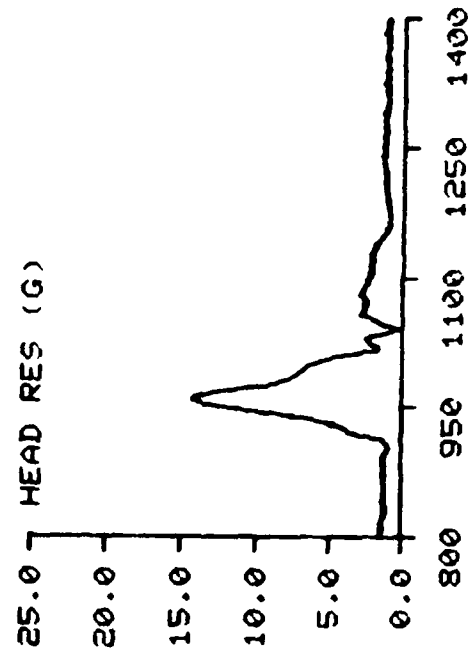
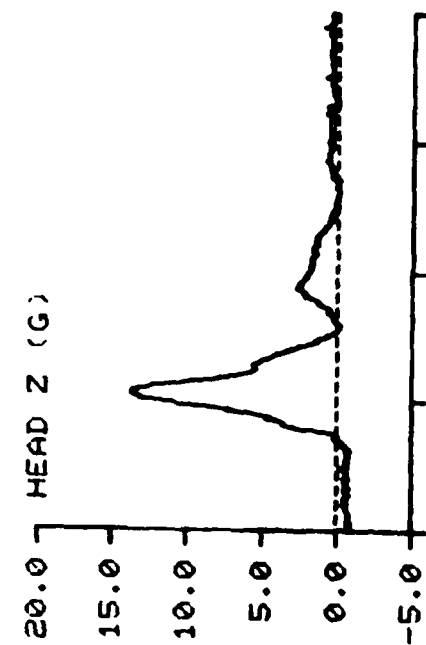
TIME IN MILLISECONDS

F-111      TEST NO: 244      SUBJECT ID: M-10



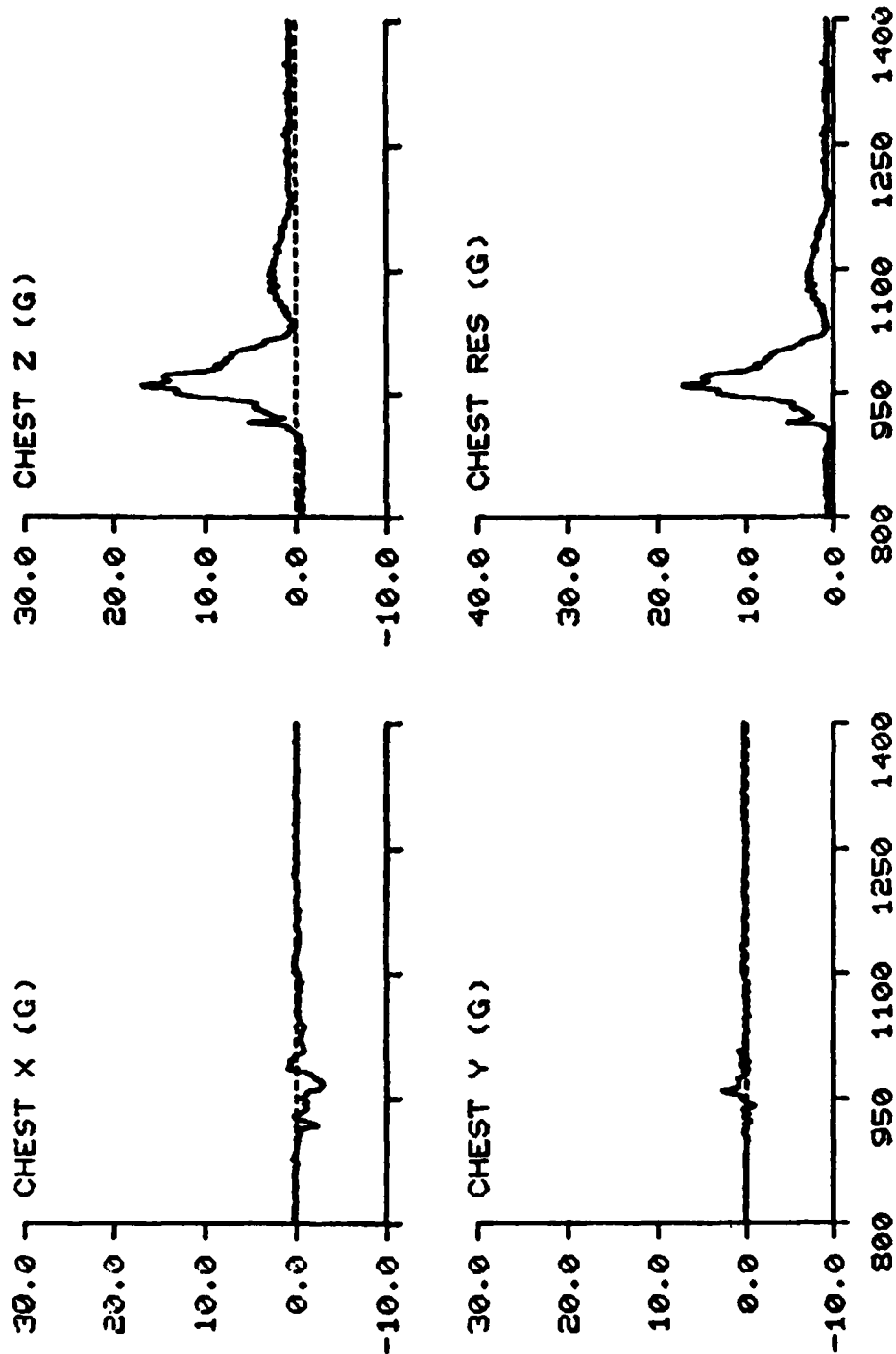


F-111      TEST NO: 244      SUBJECT ID: M-10



TIME IN MILLISECONDS

F-111      TEST NO: 244      SUBJECT ID: M-10

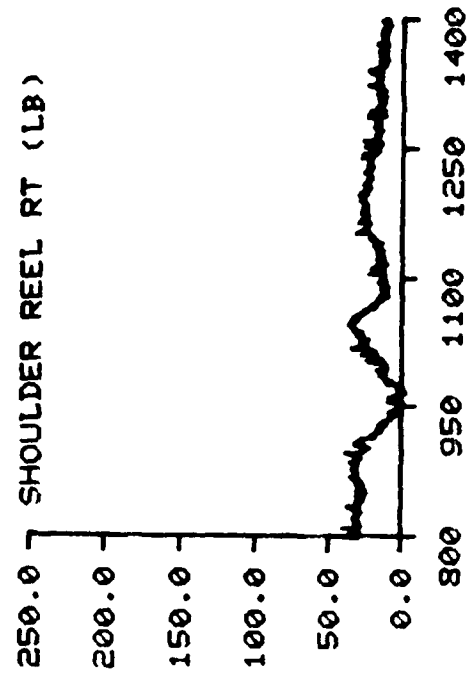
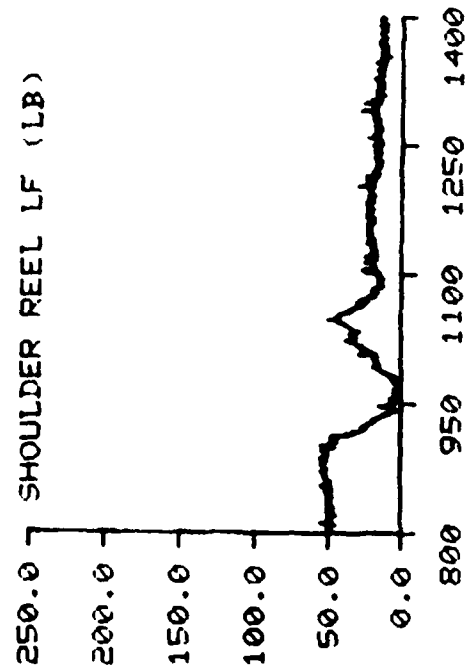
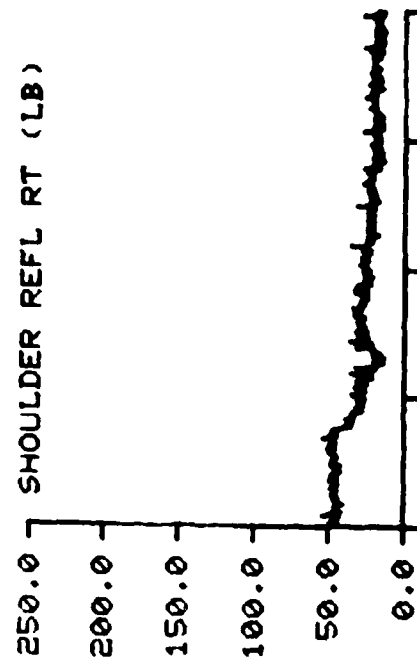
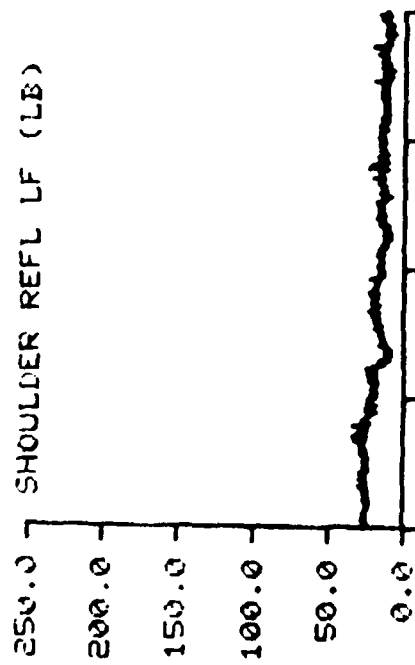


TIME IN MILLISECONDS

F-111

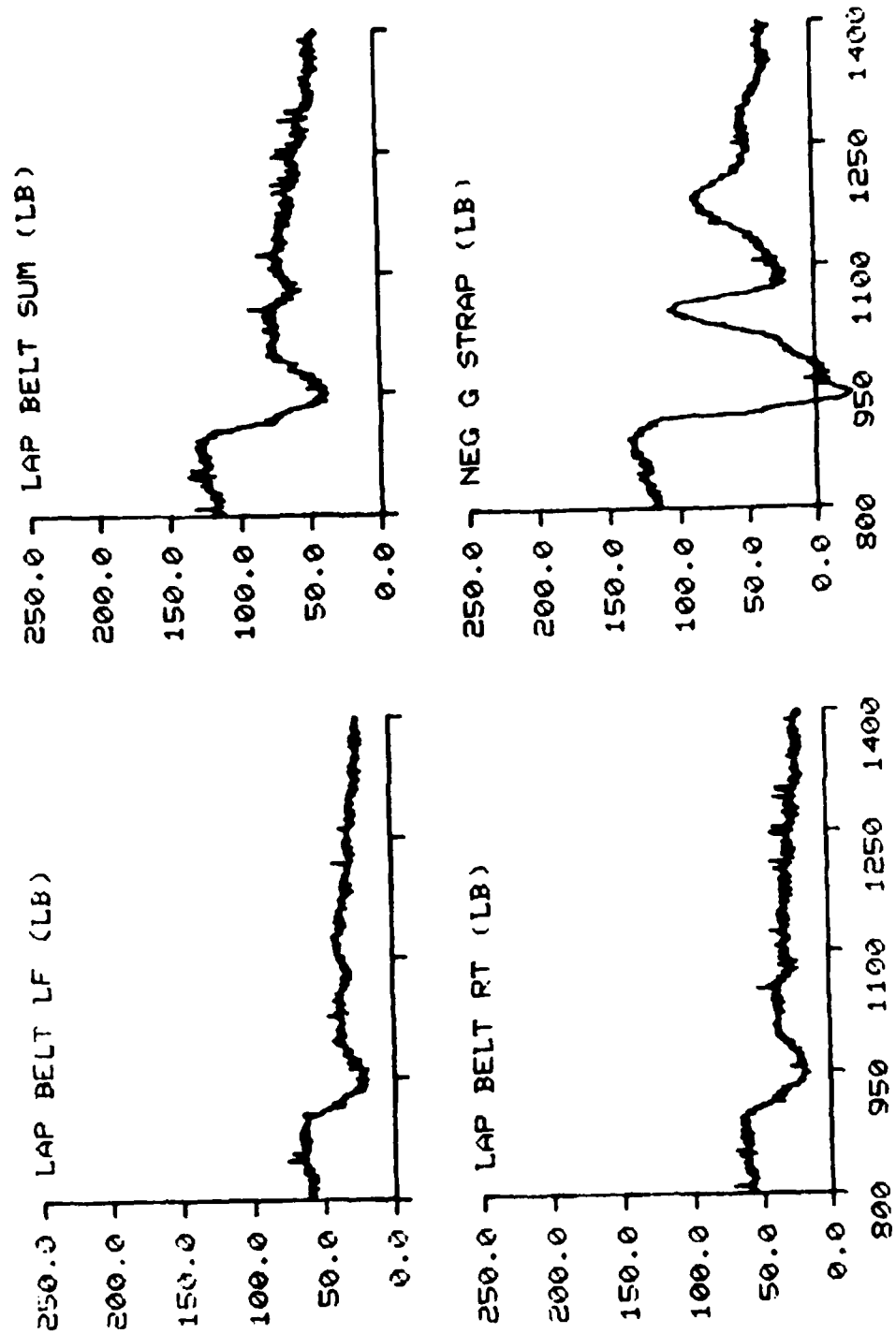
TEST NO: 244

SUBJECT ID: M-10



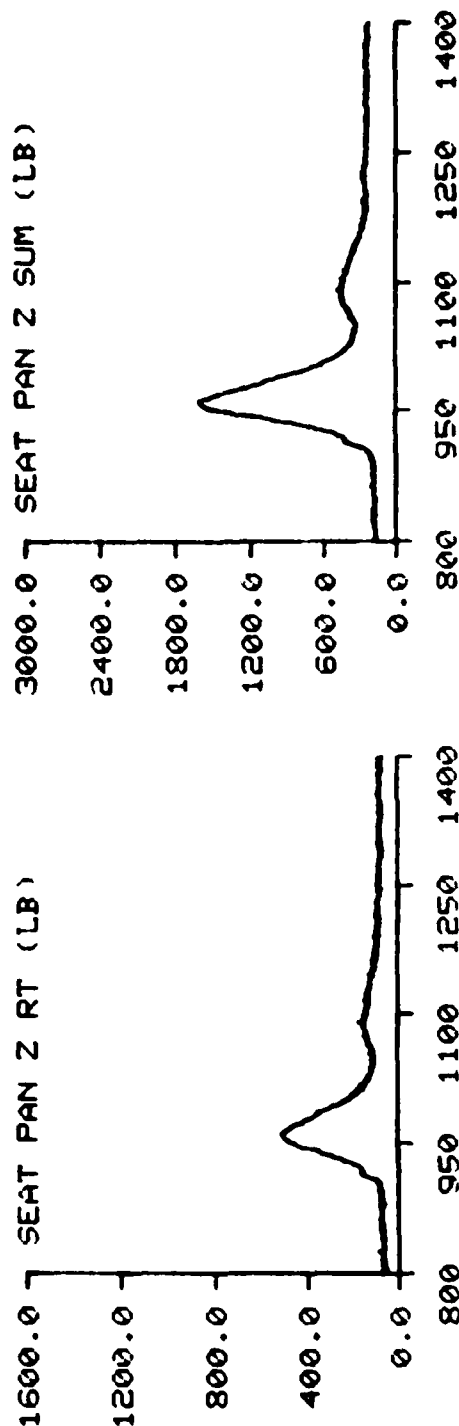
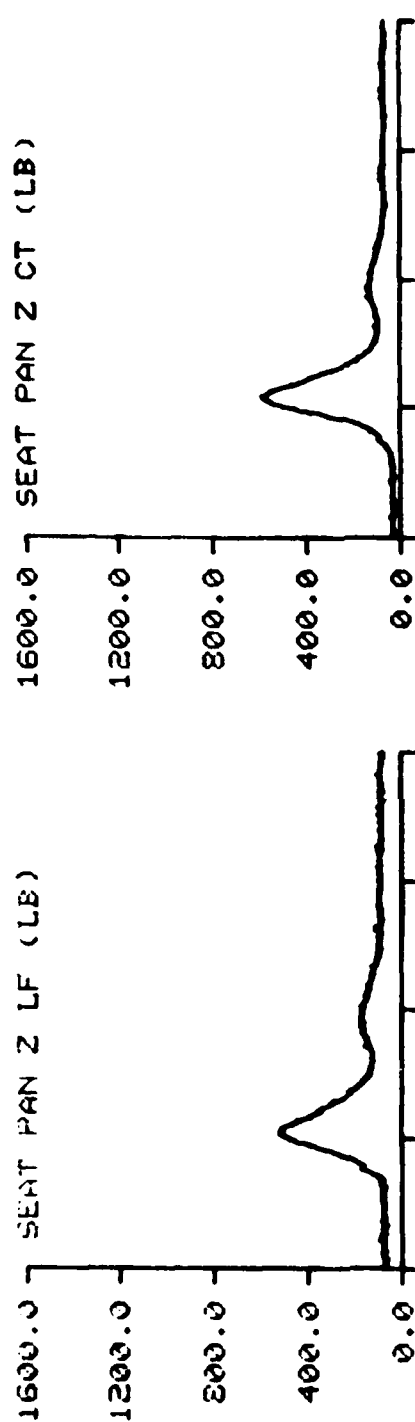
TIME IN MILLISECONDS

F-111      TEST NO: 244      SUBJECT ID: M-10

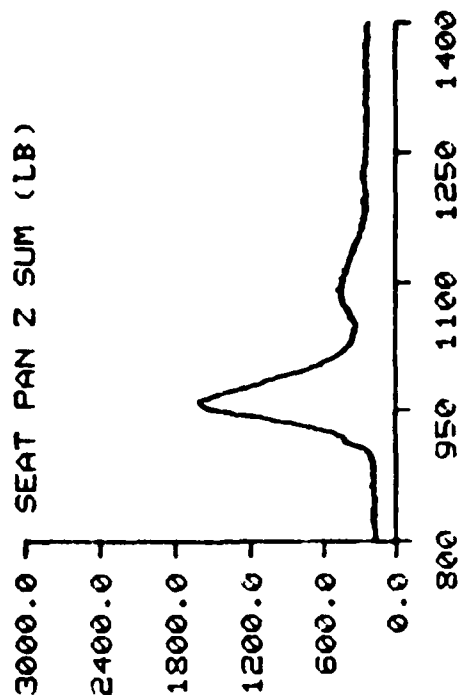


TIME IN MILLISECONDS

F-111      TEST NO: 244      SUBJECT ID: M-10

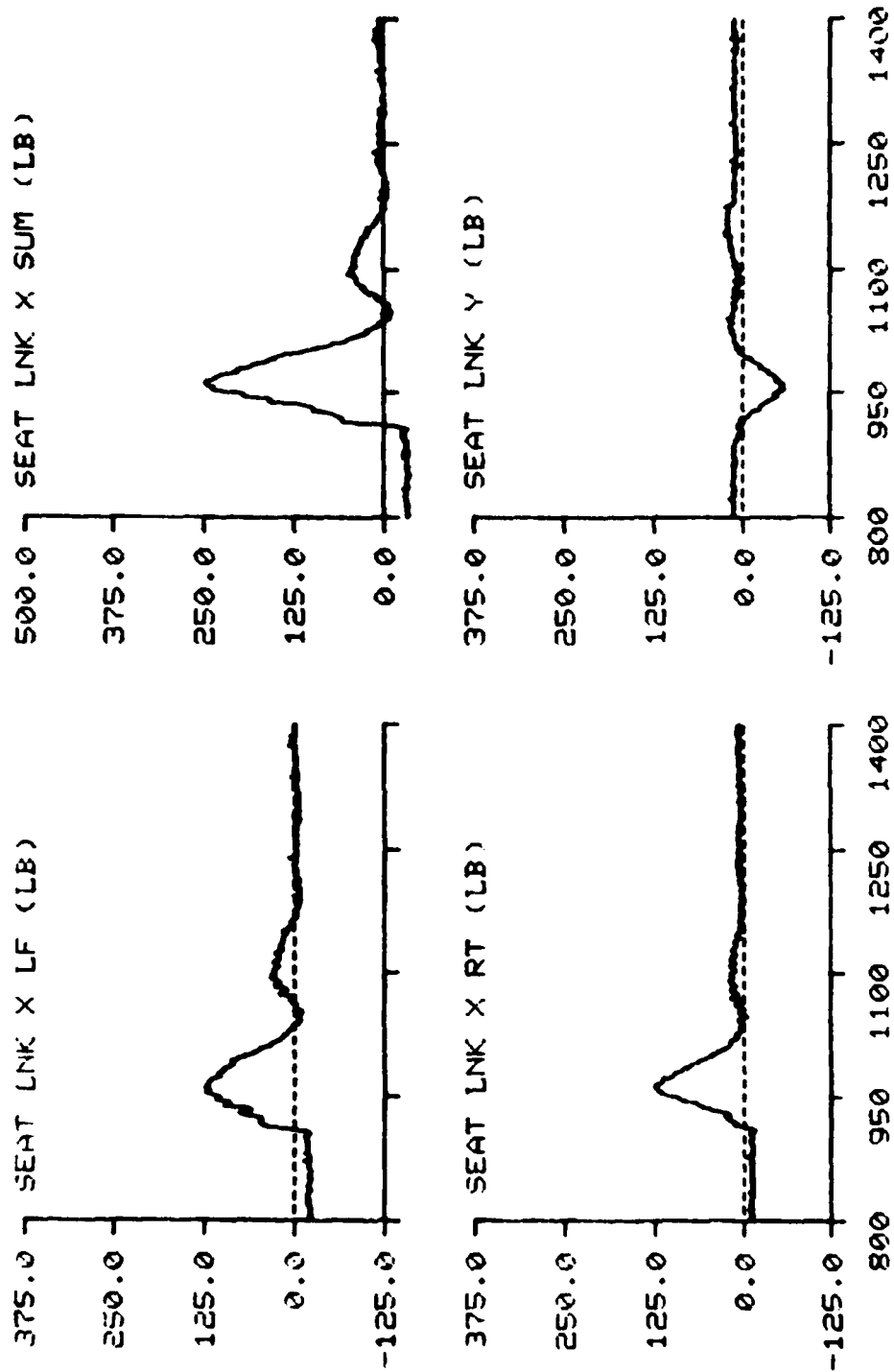


SEAT PAN Z CT (LB)



TIME IN MILLISECONDS

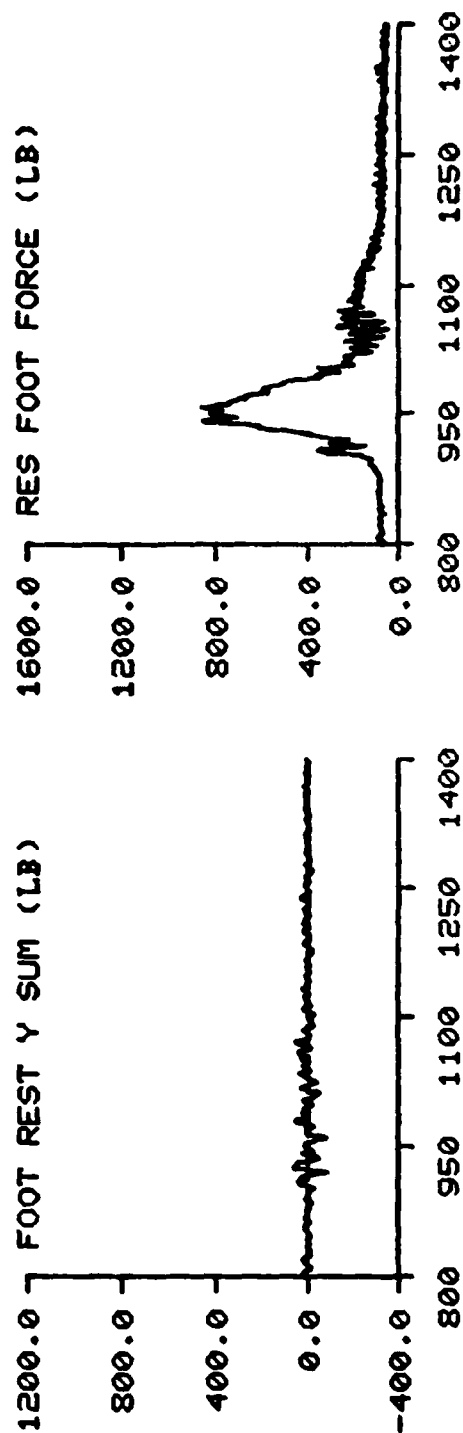
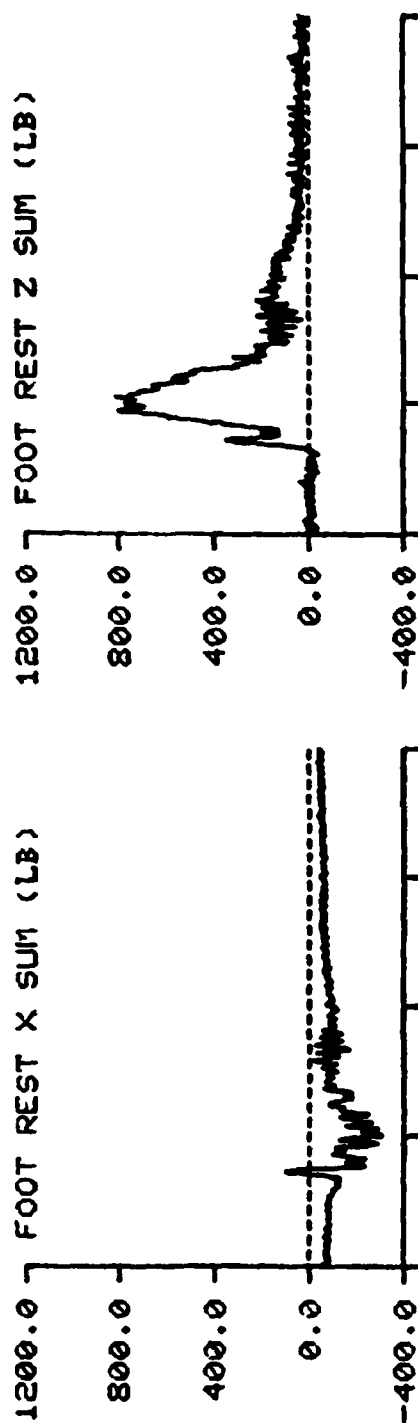
F-111 TEST NO: 244 SUBJECT ID: M-10



F-111

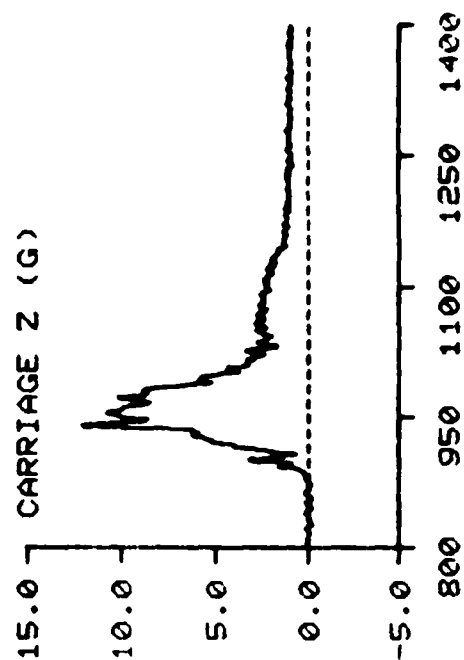
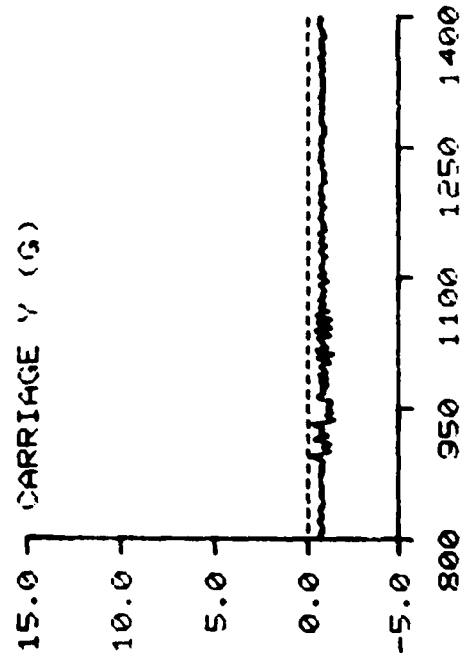
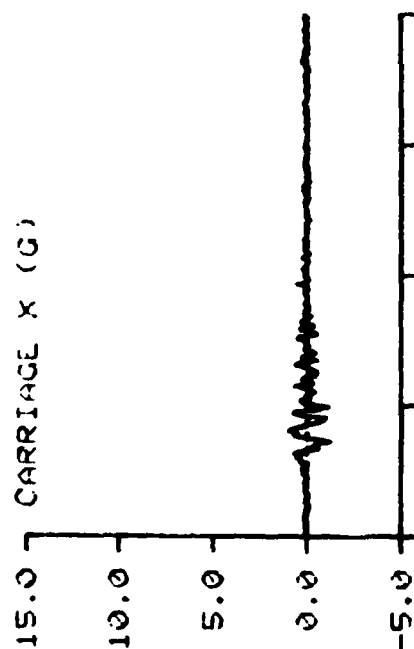
TEST NO: 244

SUBJECT ID: M-10



TIME IN MILLISECONDS

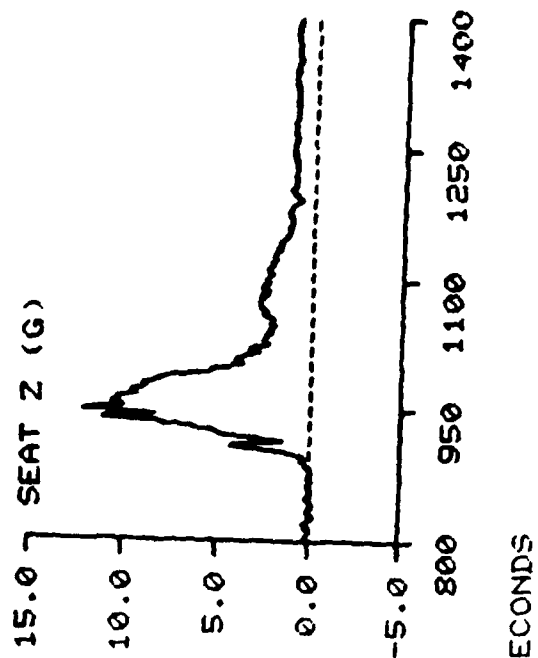
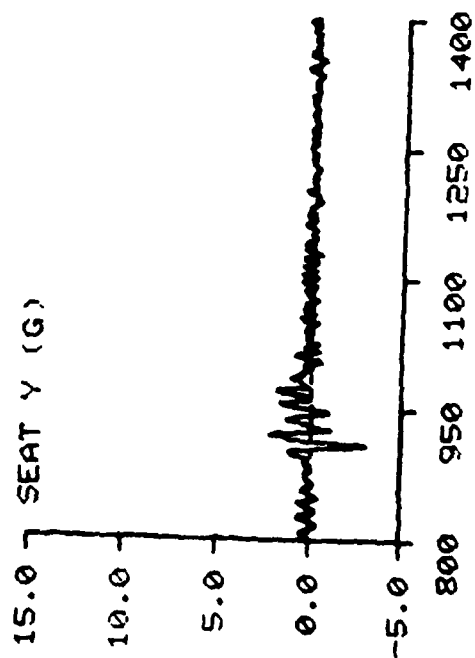
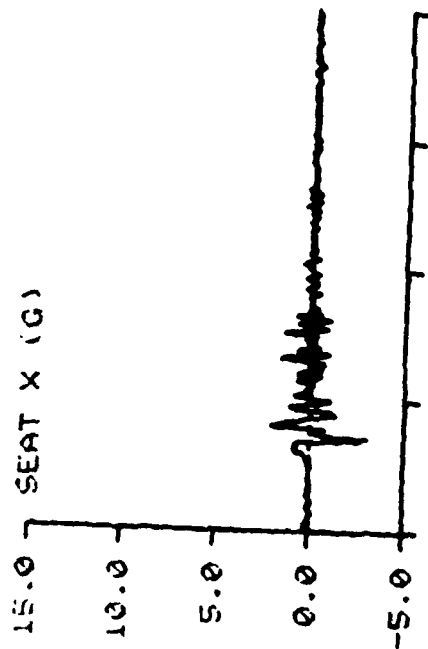
F-111 TEST NO: 252 SUBJECT ID: E-1



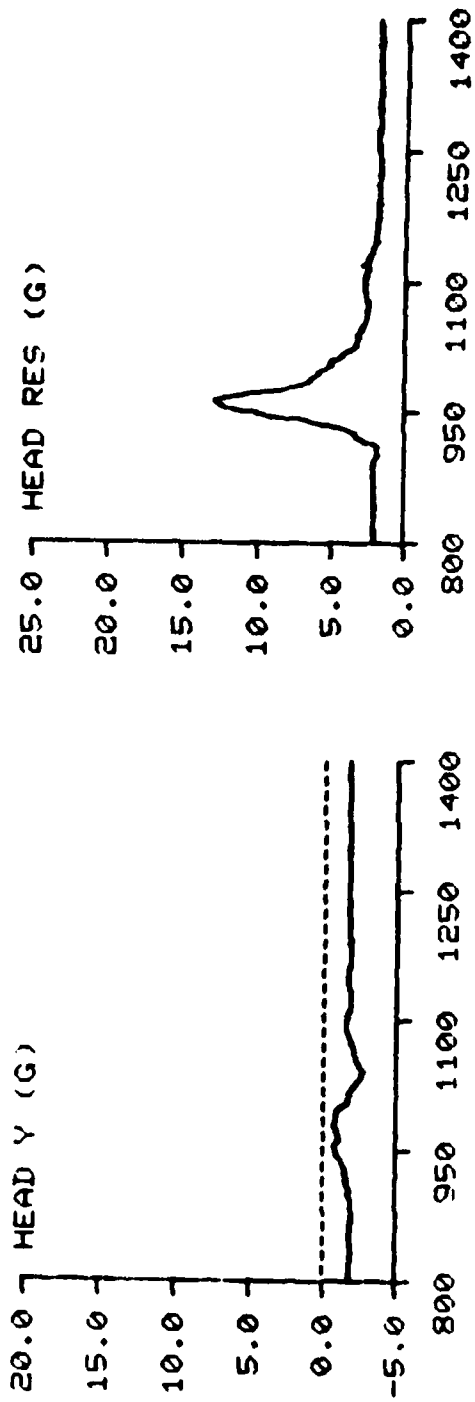
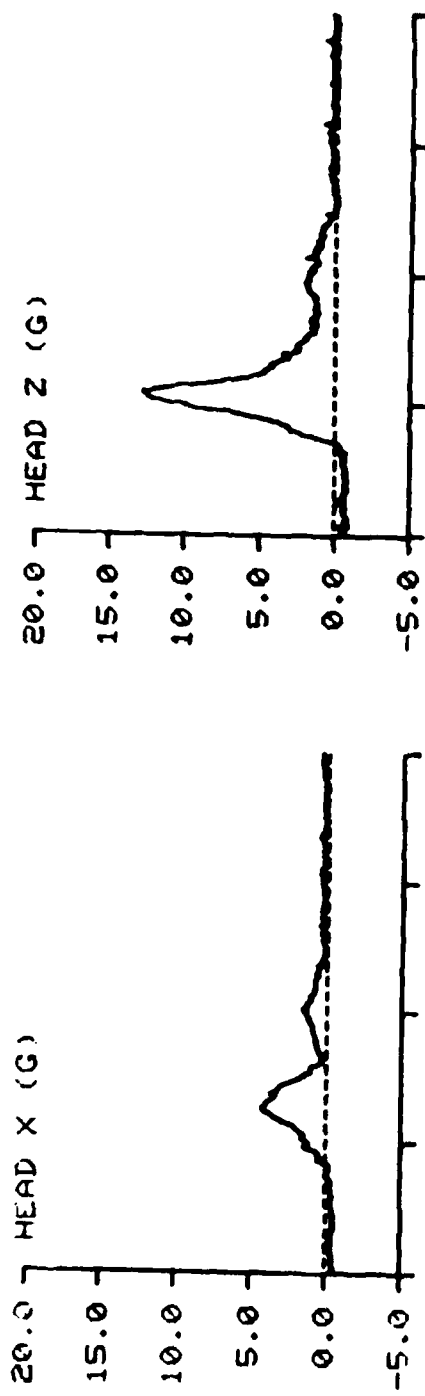
TIME IN MILLISECONDS



F-111 TEST NO: 252 SUBJECT ID: E-1



F-111 TEST NO: 252 SUBJECT ID: E-1



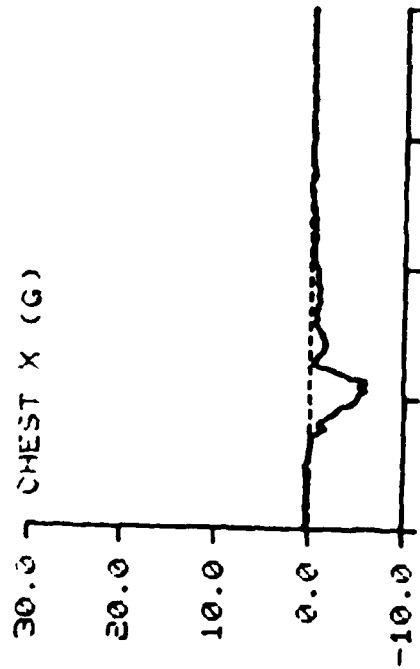
TIME IN MILLISECONDS

F-111

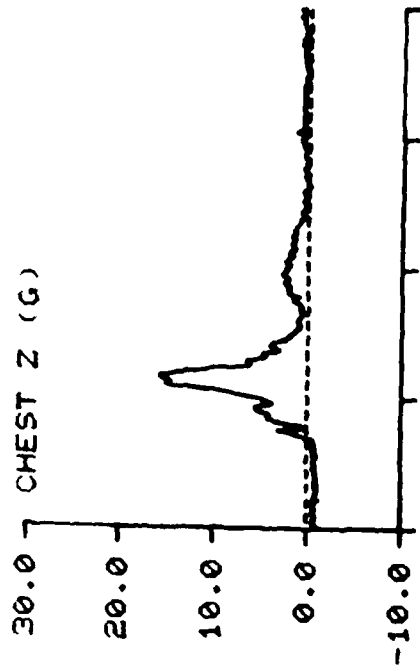
TEST NO: 252

SUBJECT ID: E-1

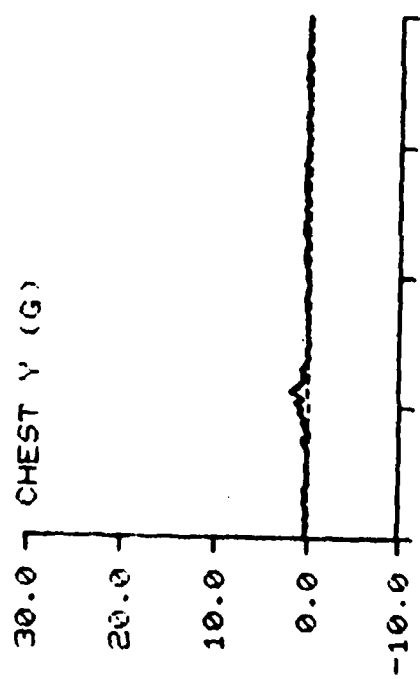
CHEST X (G)



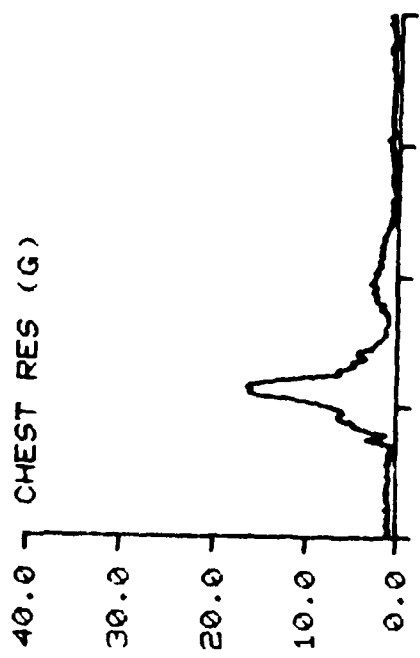
CHEST Z (G)



CHEST Y (G)



CHEST RES (G)

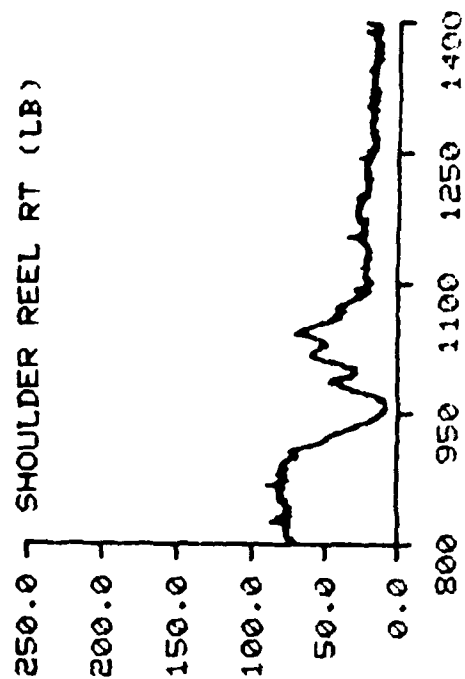
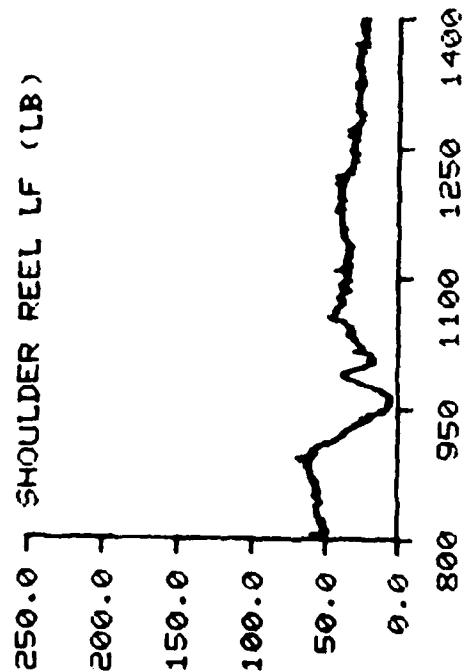
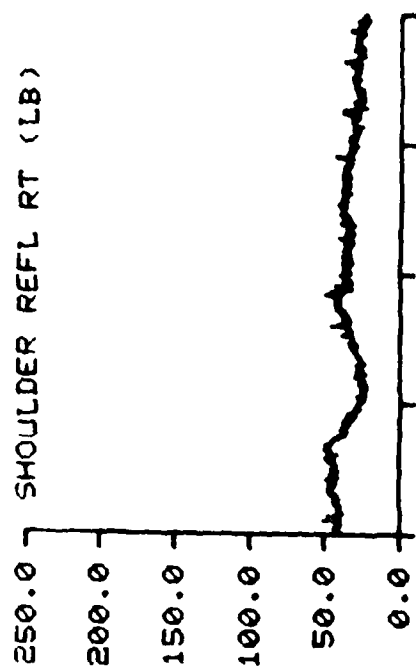
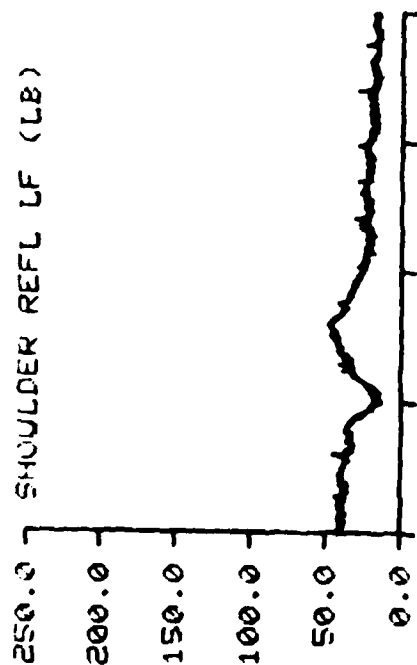


TIME IN MILLISECONDS

F-111

TEST NO: 252

SUBJECT ID: E-1

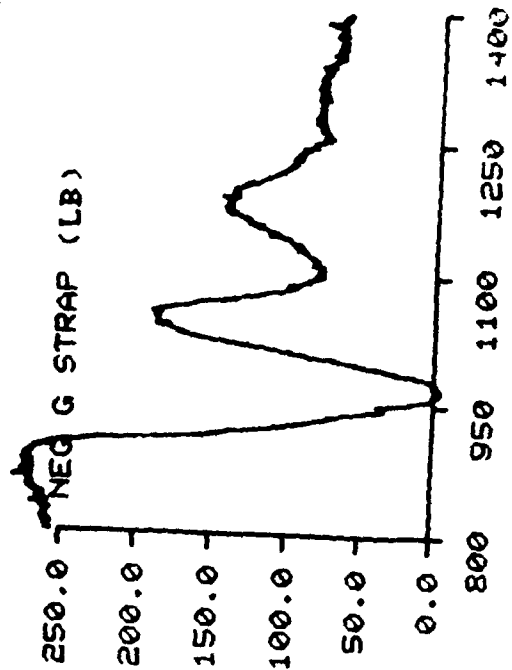
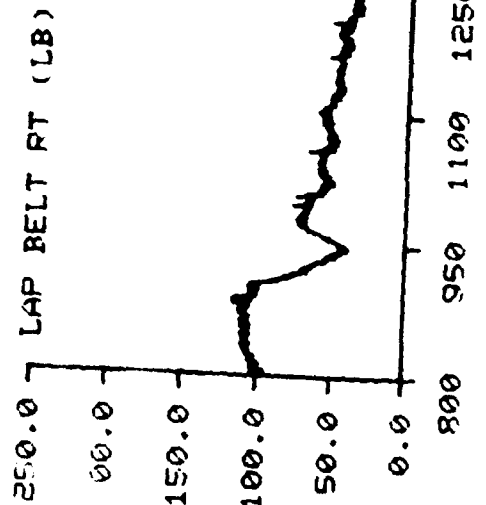
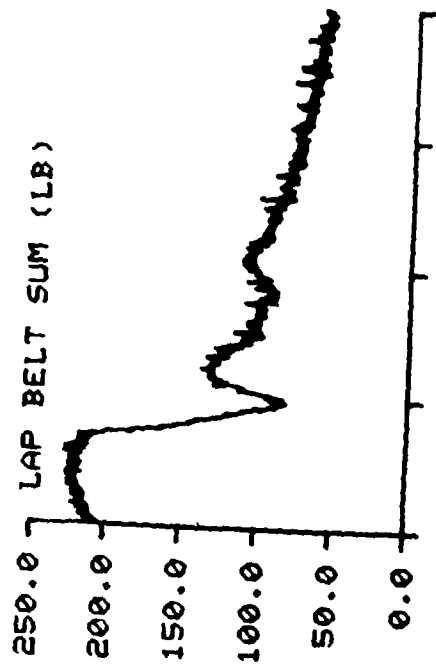
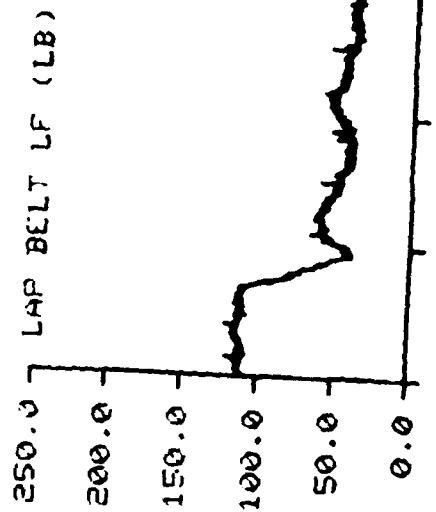


TIME IN MILLISECONDS

F-111

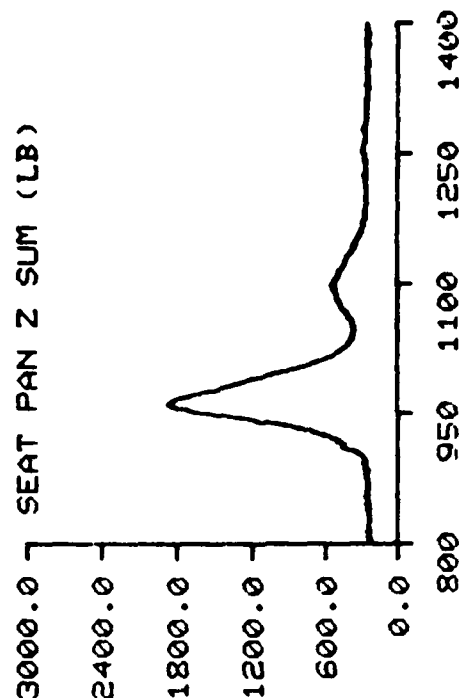
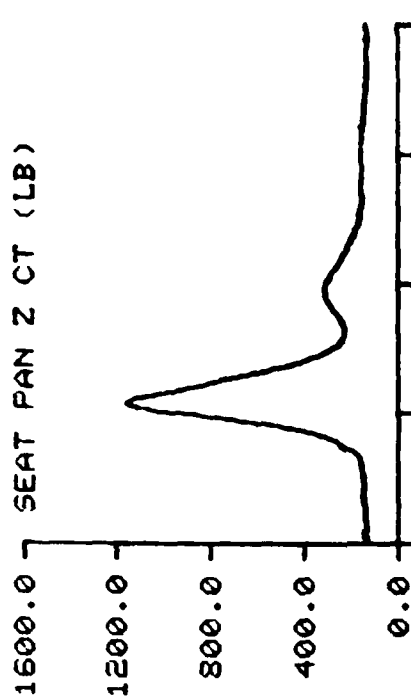
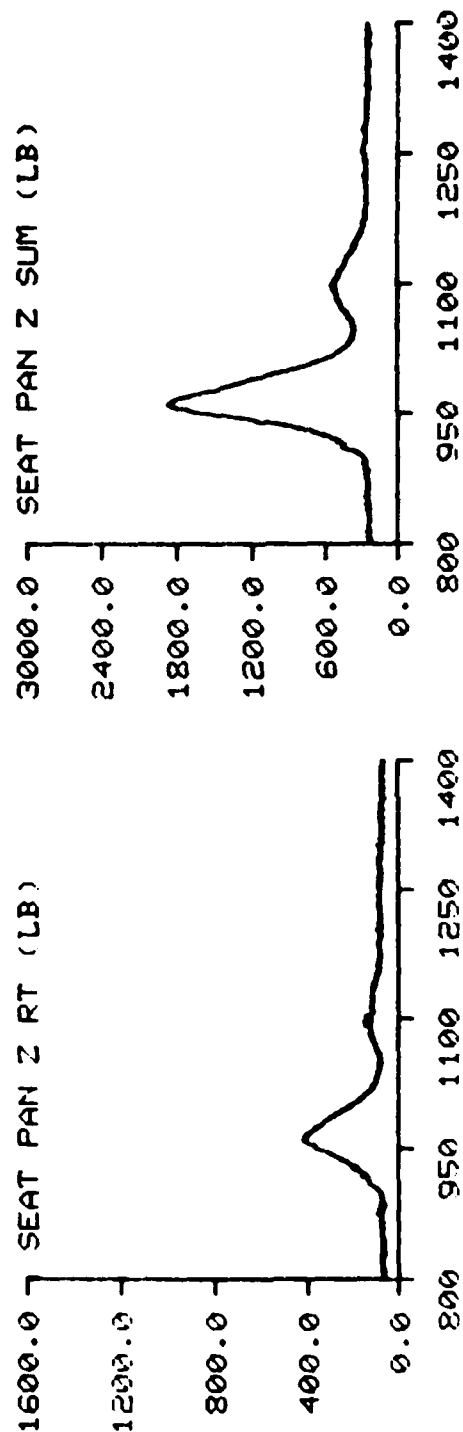
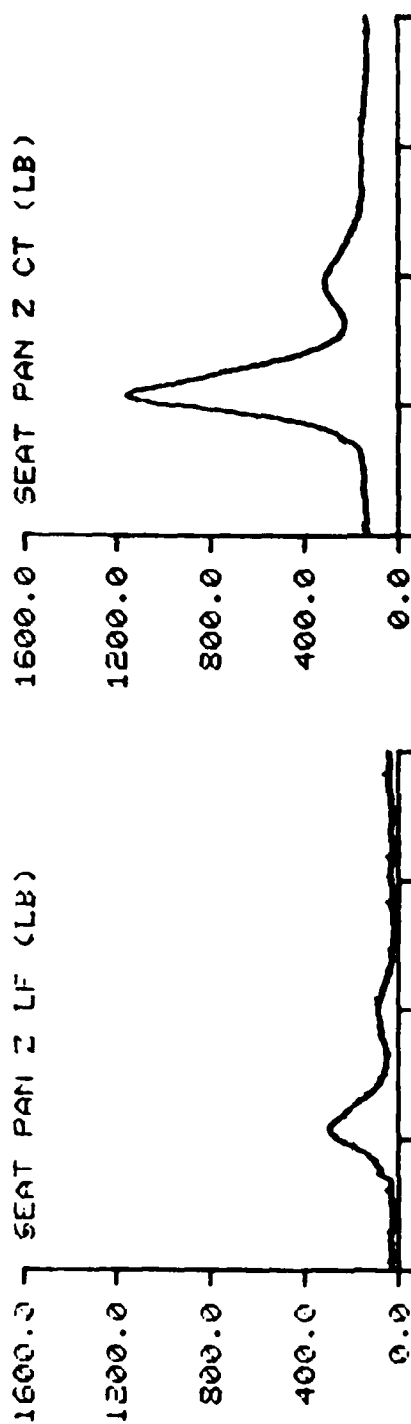
TEST NO: 252

SUBJECT ID: E-1



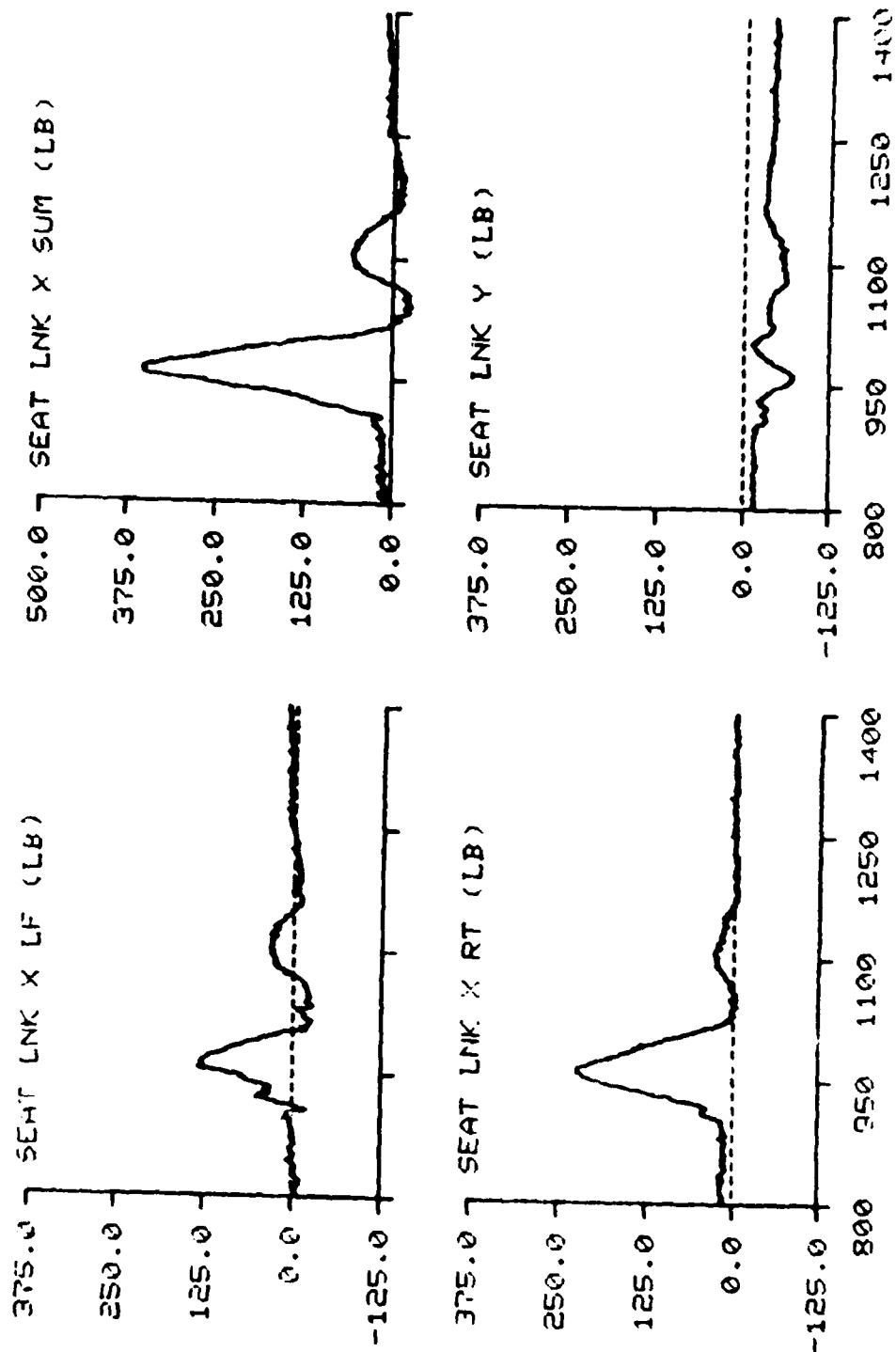
TIME IN MILLISECONDS

F-111 TEST NO: 252 SUBJECT ID: E-1



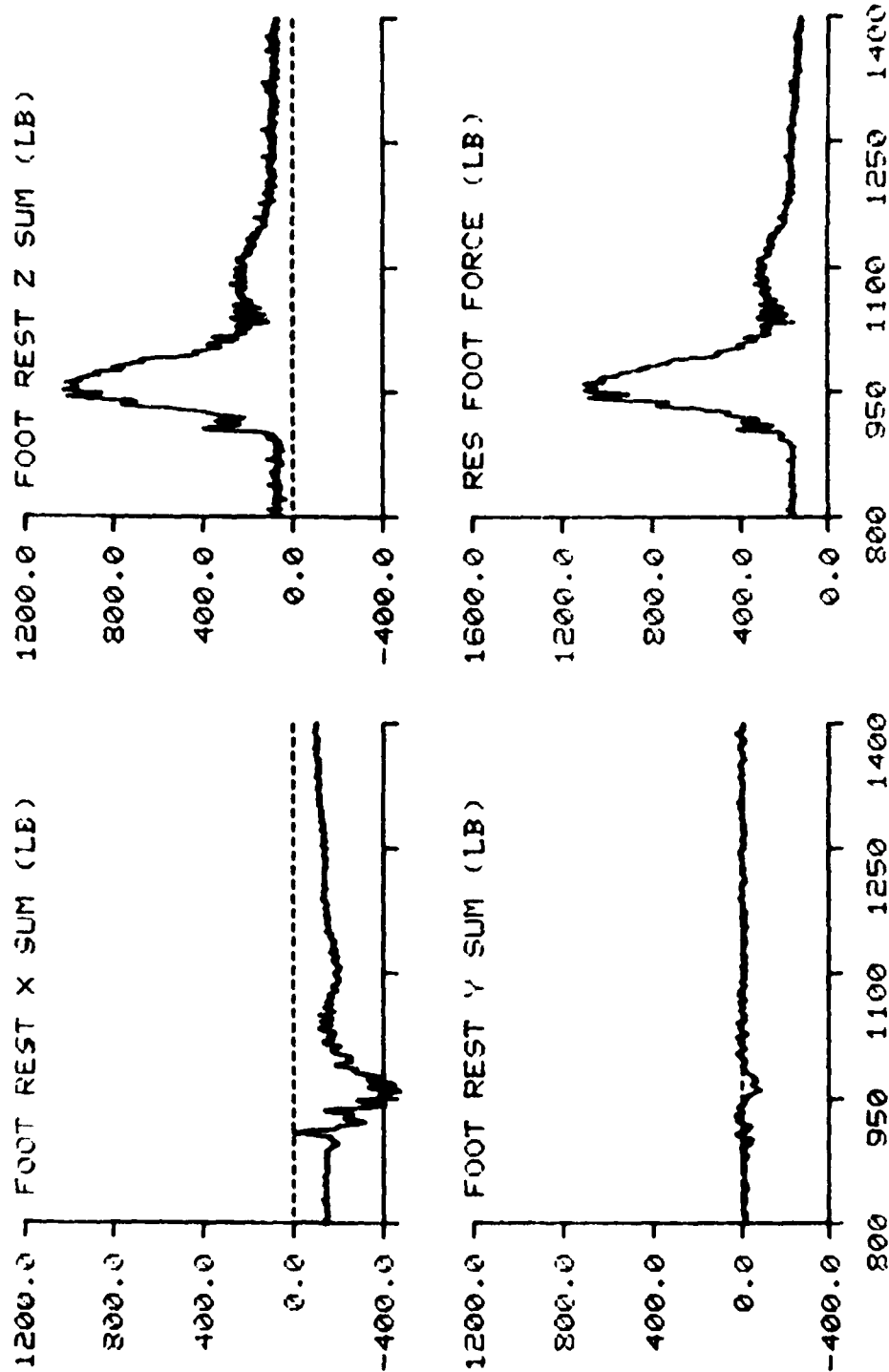
TIME IN MILLISECONDS

F-111 TEST NO: 252 SUBJECT ID: E-1



TIME IN MILLISECONDS

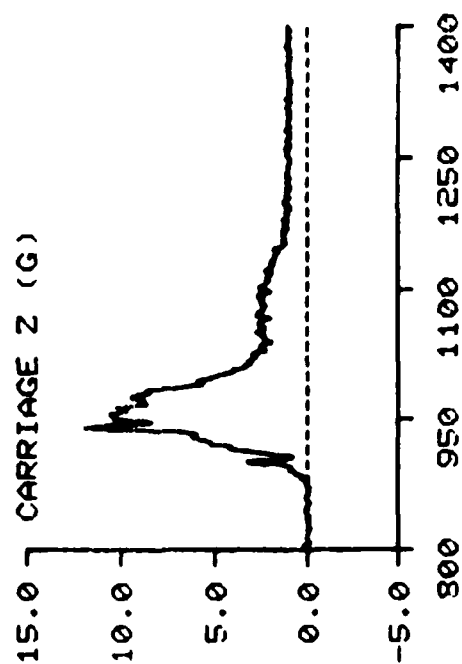
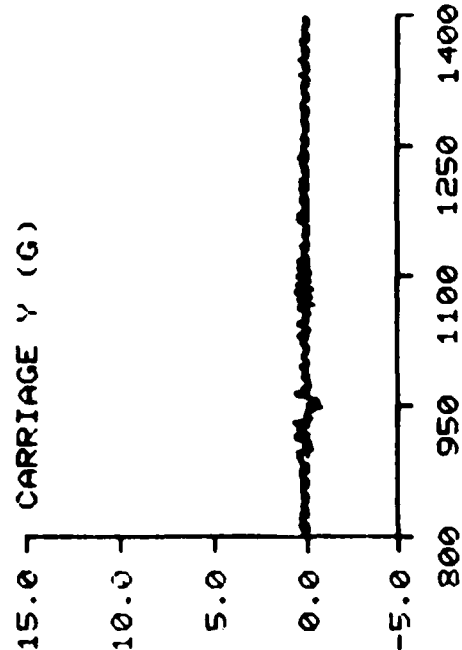
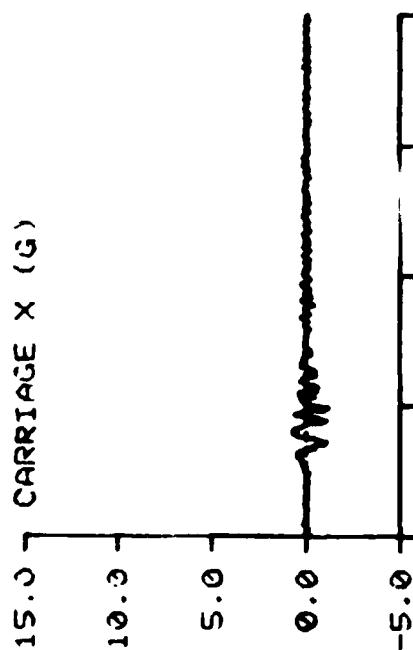
F-111 TEST NO: 252 SUBJECT ID: E-1



TIME IN MILLISECONDS

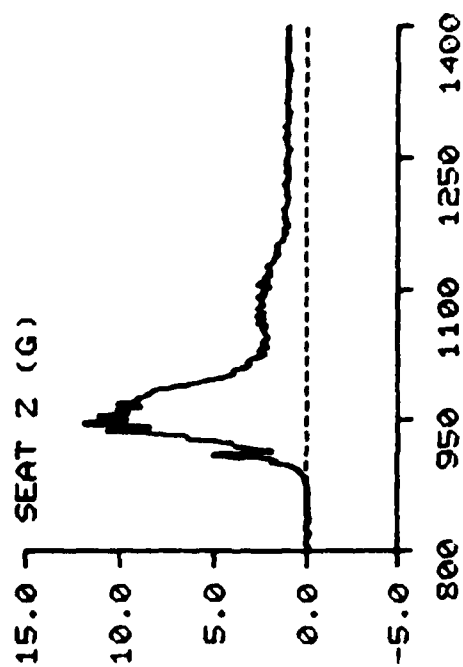
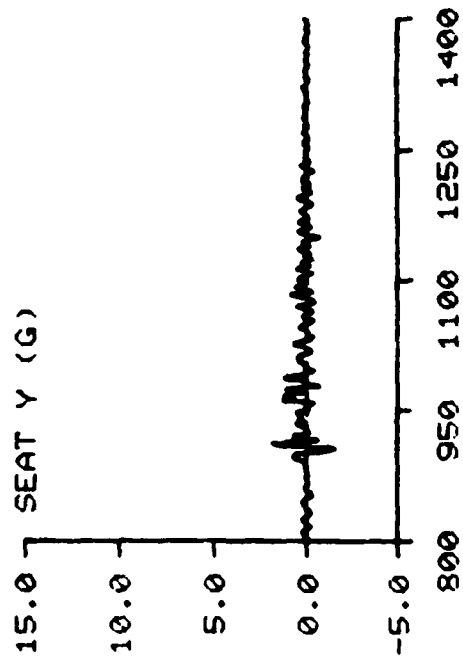
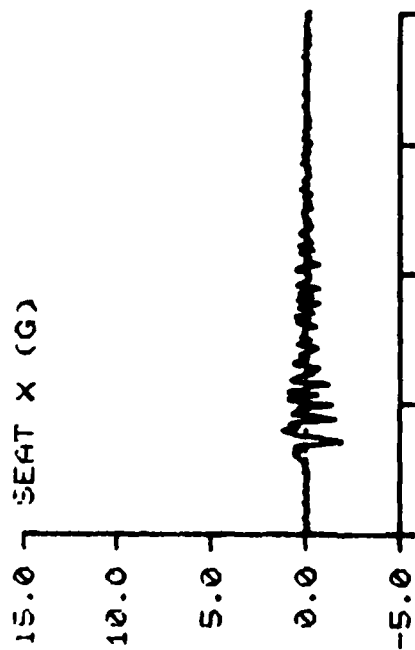


F-111 TEST NO: 260 SUBJECT ID: M-10



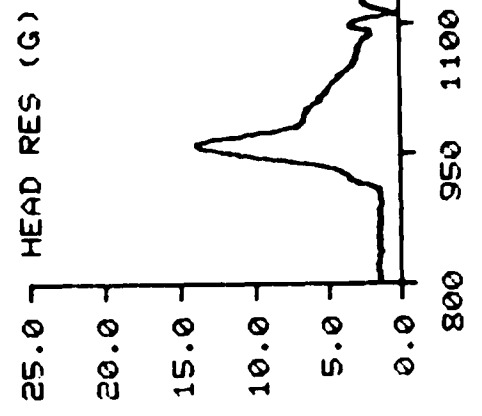
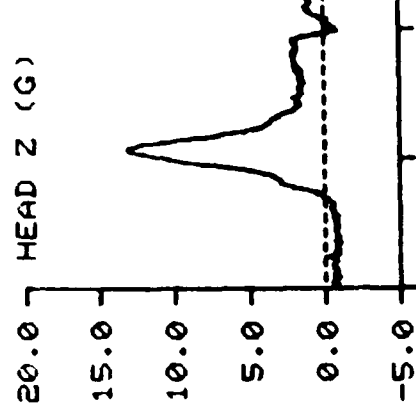
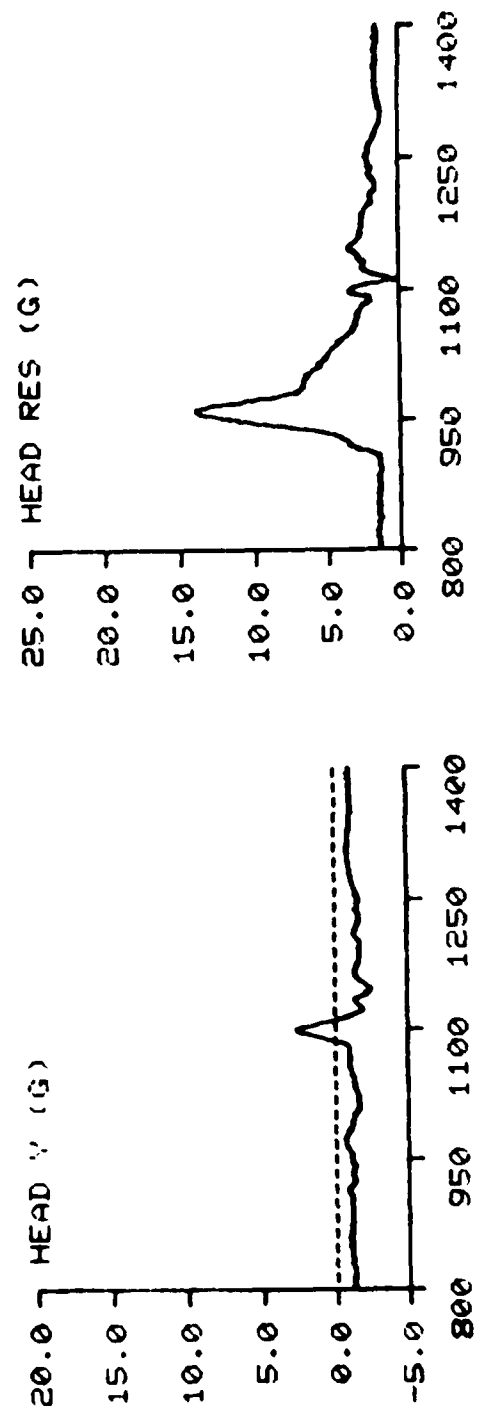
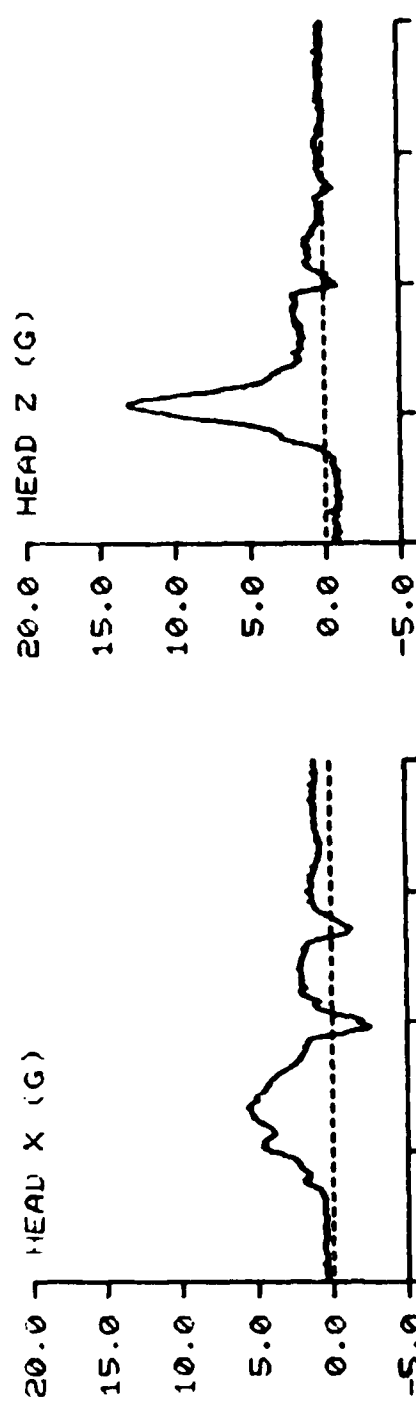
TIME IN MILLISECONDS

F-111 TEST NO: 260 SUBJECT ID: M-10



TIME IN MILLISECONDS

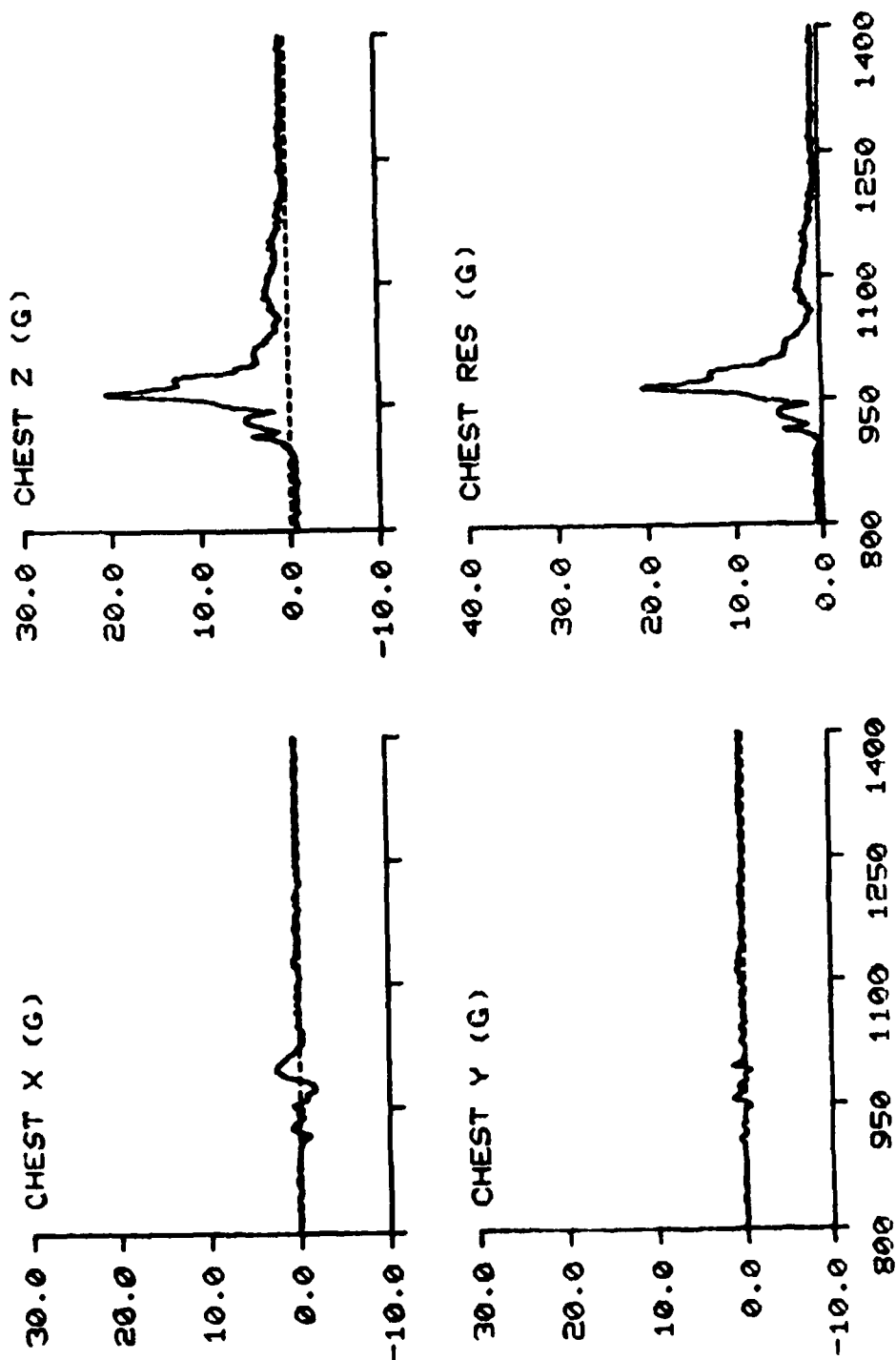
F-111      TEST NO: 260      SUBJECT ID: M-10



TIME IN MILLISECONDS

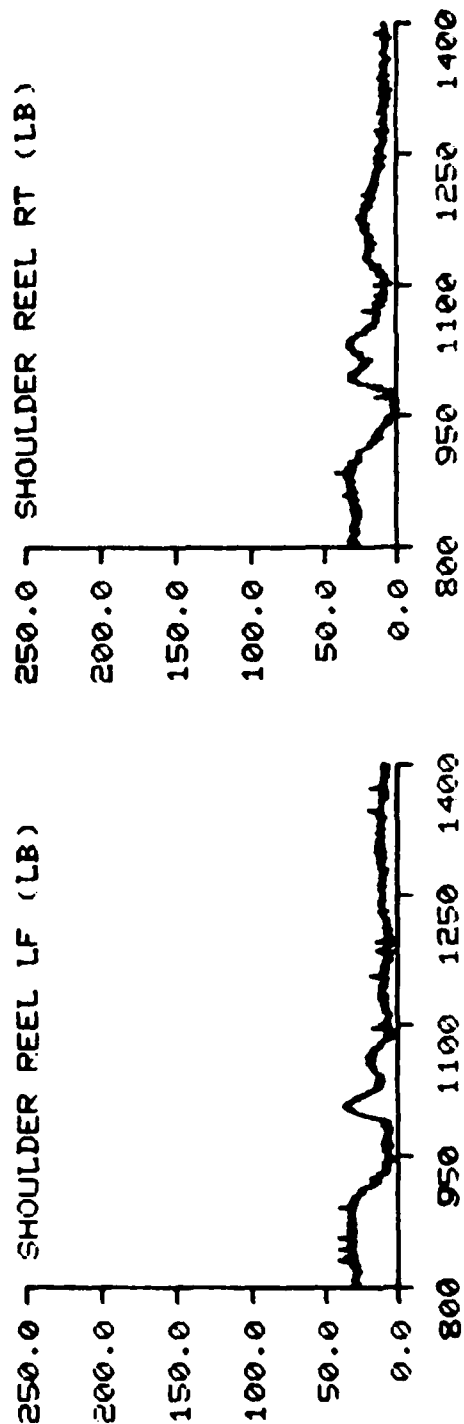
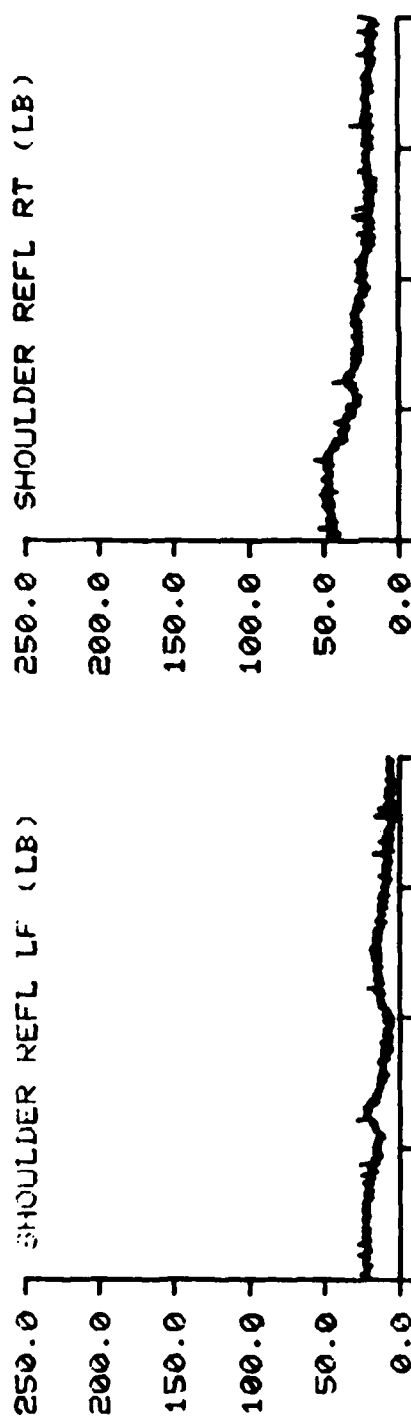
SUBJECT ID: M-10

F-111 TEST NO: 260



TIME IN MILLISECONDS

F-111      TEST NO: 260      SUBJECT ID: M-10



TIME IN MILLISECONDS

F-111

TEST NO: 260

SUBJECT ID: M-10

LAP BELT LF (LB)

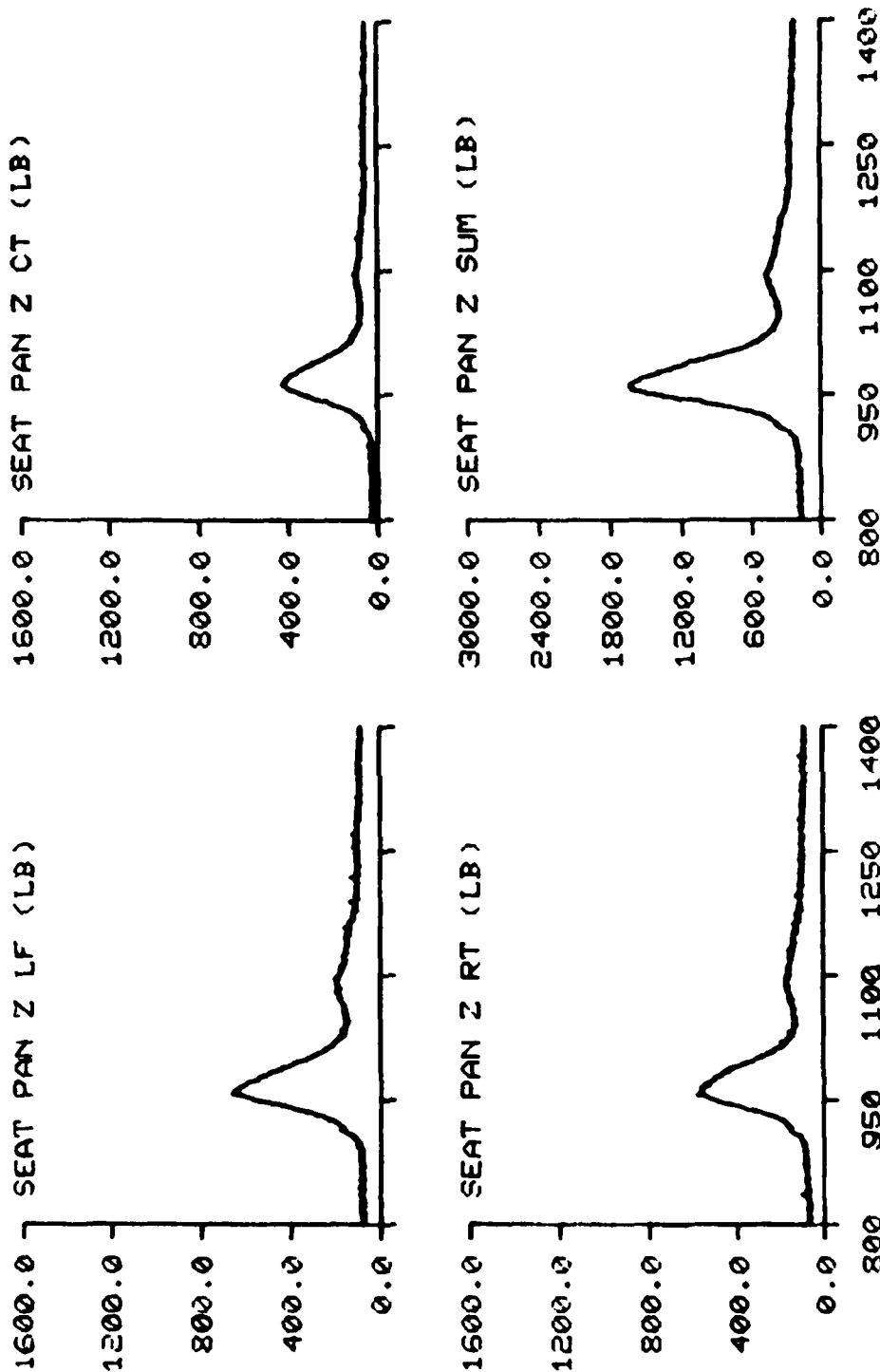
LAP BELT SUM (LB)

LAP BELT RT (LB)

NEG G STRAP (LB)

TIME IN MILLISECONDS

F-111      TEST NO: 260      SUBJECT ID: M-10

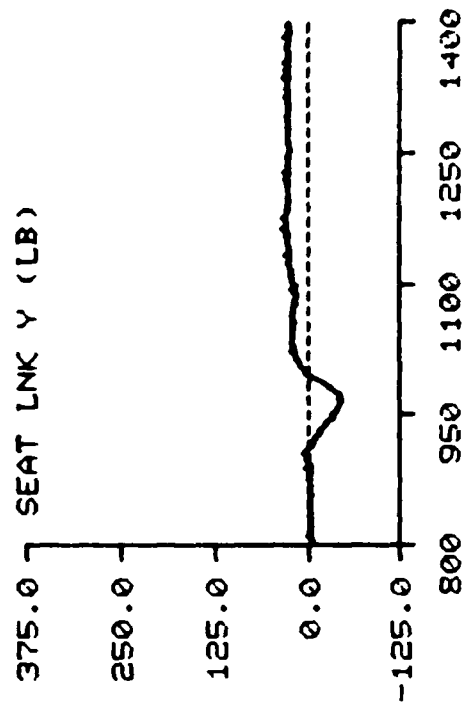
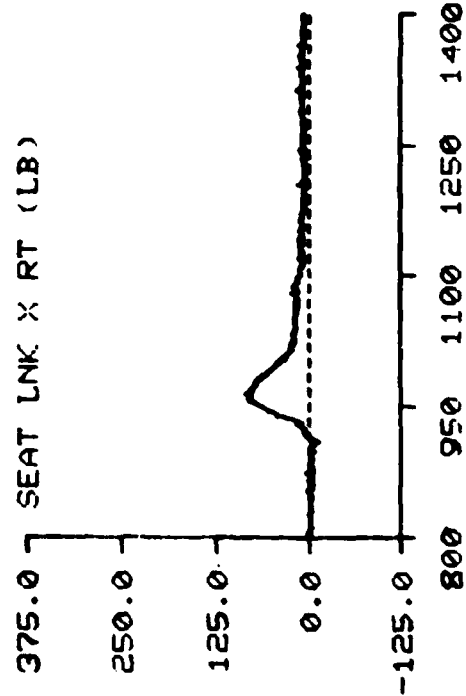
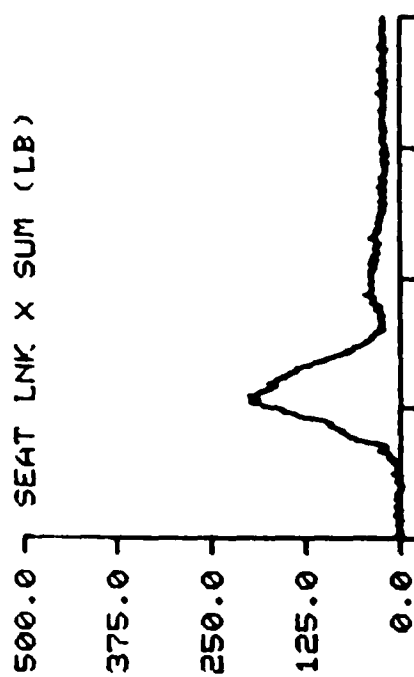
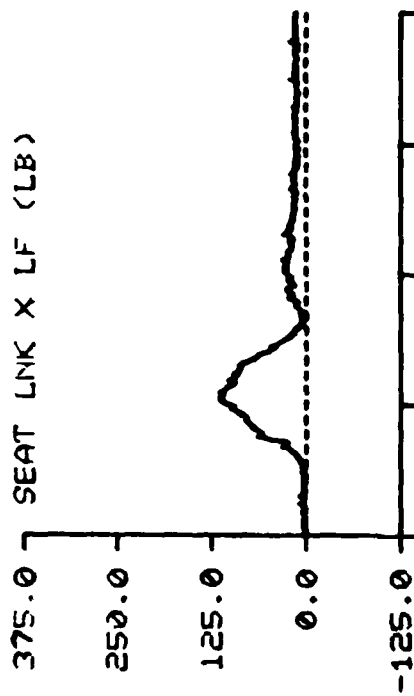


TIME IN MILLISECONDS

F-111

TEST NO: 260

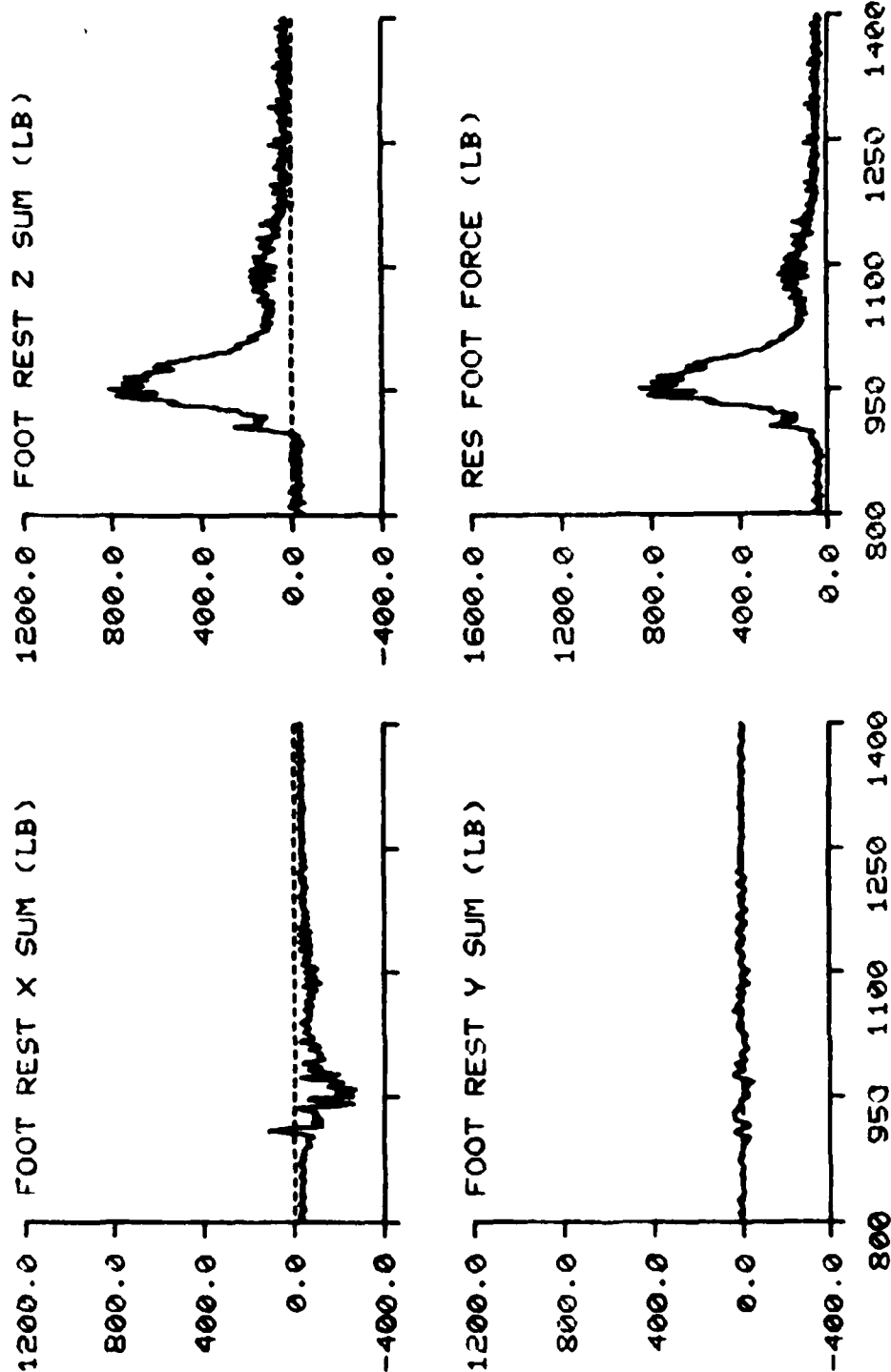
SUBJECT ID: M-10



TIME IN MILLISECONDS

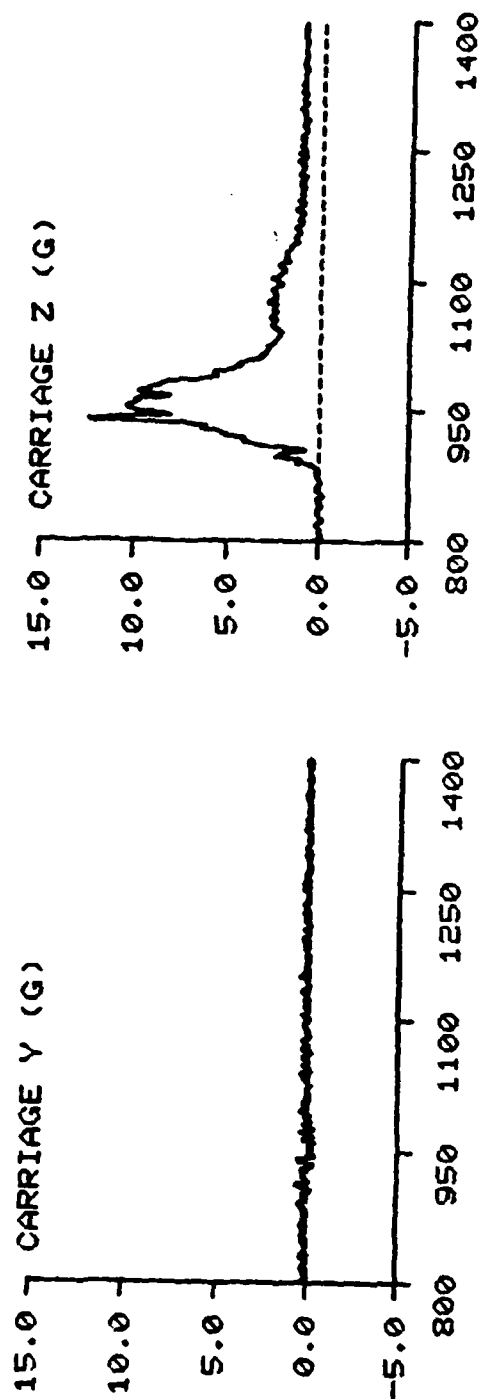
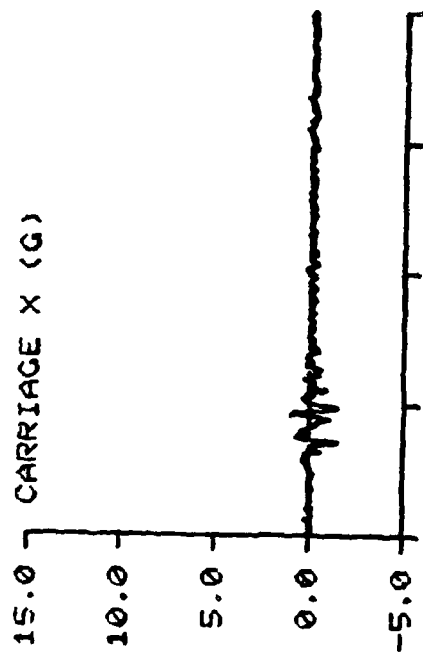


F-111      TEST NO: 260      SUBJECT ID: 11-10

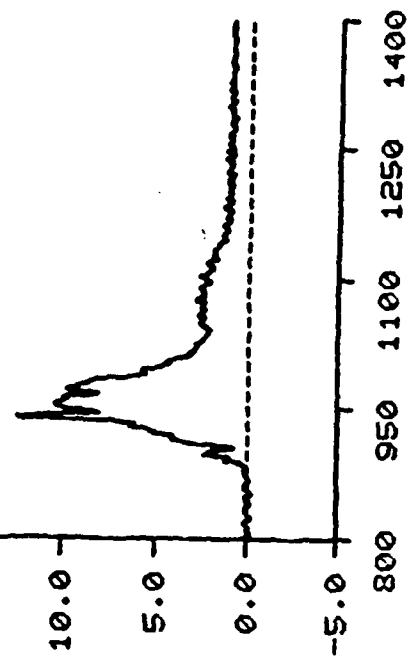


TIME IN MILLISECONDS

F-111      TEST NO: 265      SUBJECT ID: E-1

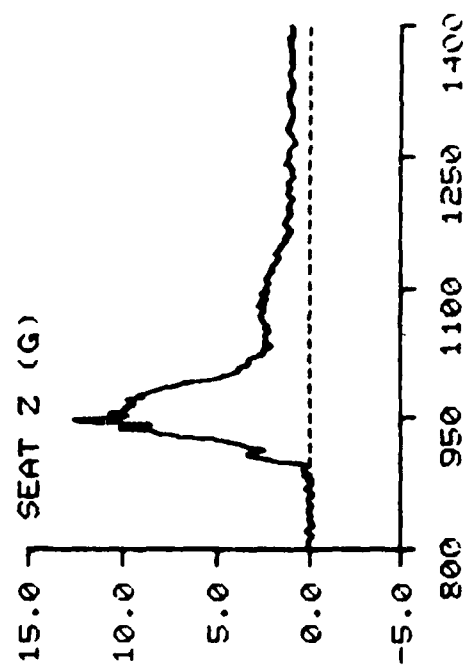
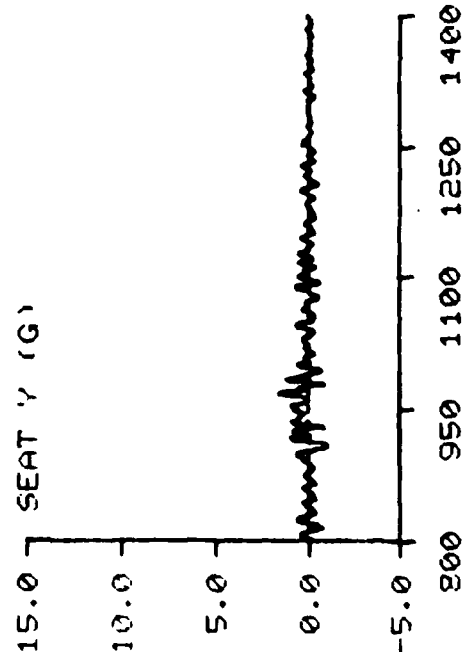
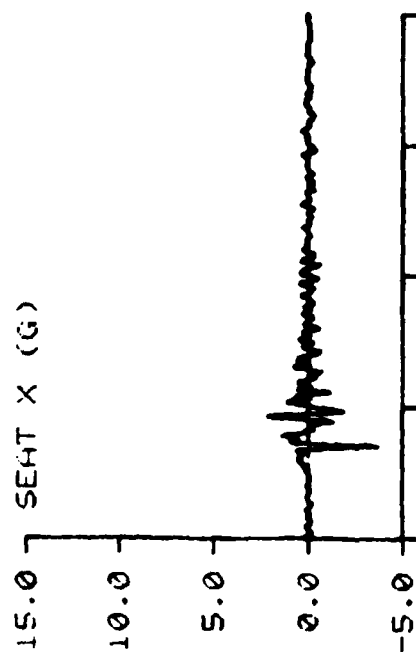


CARRIAGE Z (G)



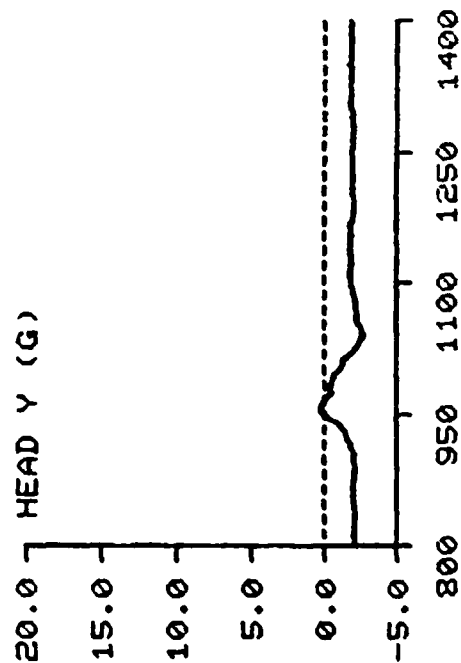
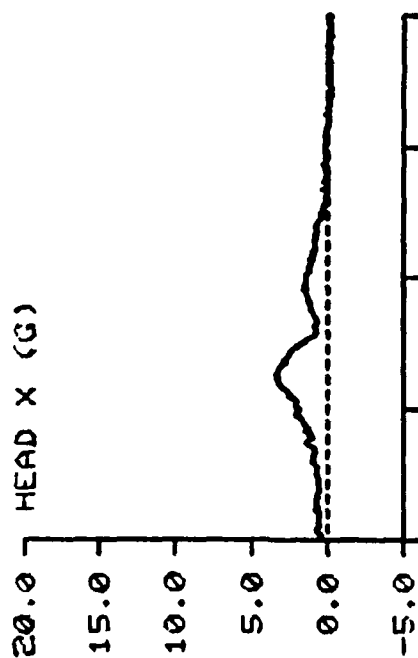
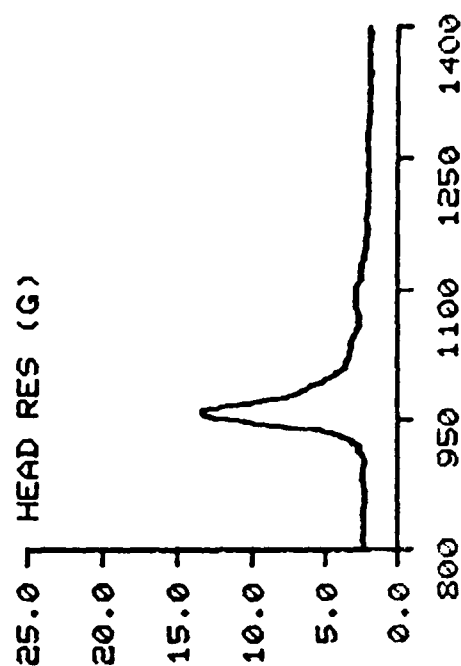
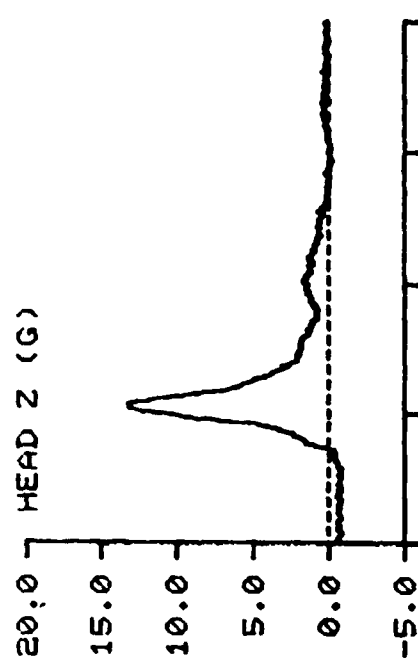
TIME IN MILLISECONDS

F-111      TEST NO: 265      SUBJECT ID: E-1



TIME IN MILLISECONDS

F-111      TEST NO: 265      SUBJECT ID: E-1

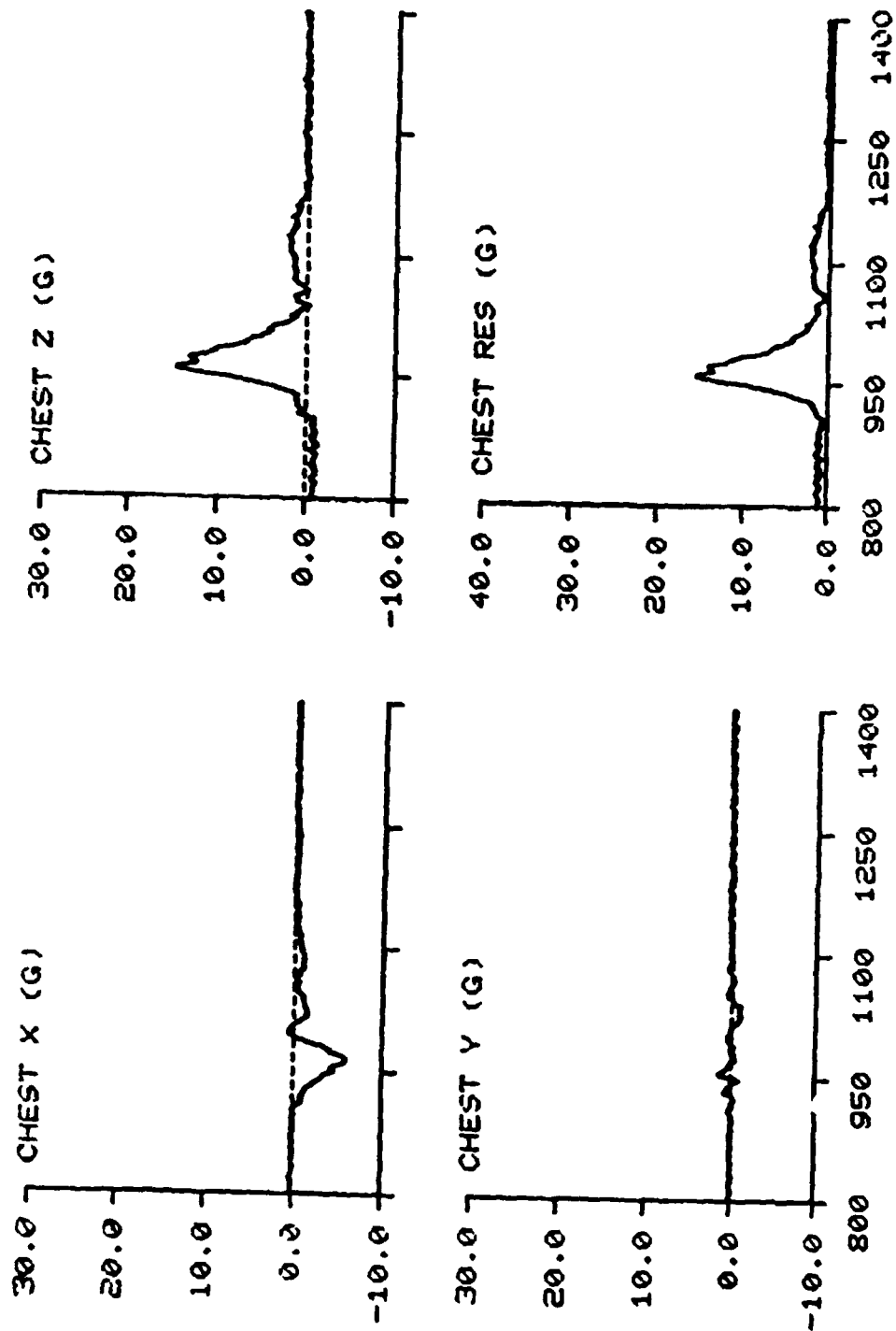


TIME IN MILLISECONDS

F-111

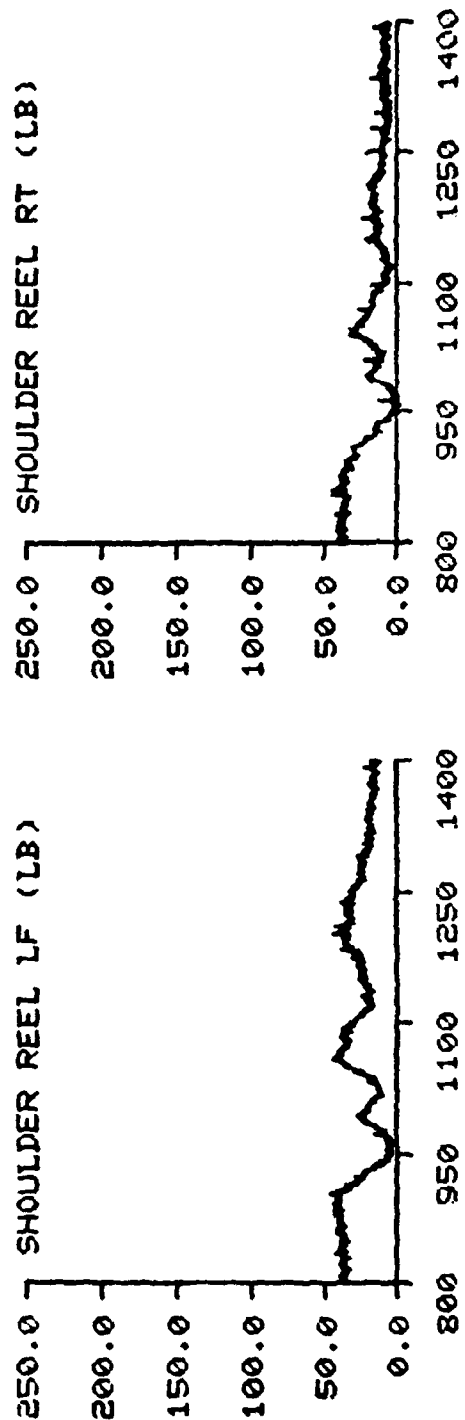
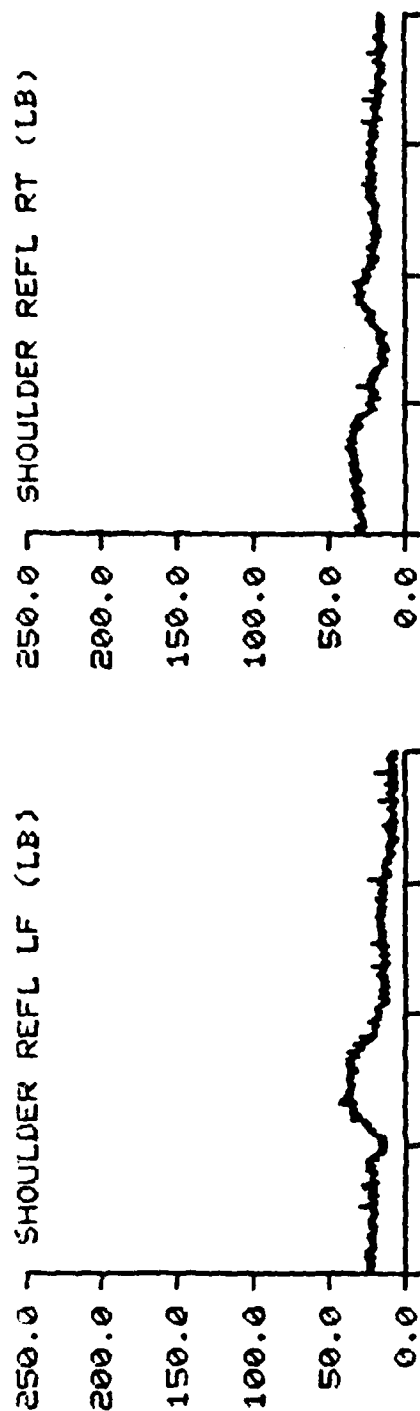
TEST NO: 265

SUBJECT ID: E-1



TIME IN MILLISECONDS

F-111 TEST NO: 265 SUBJECT ID: E-1



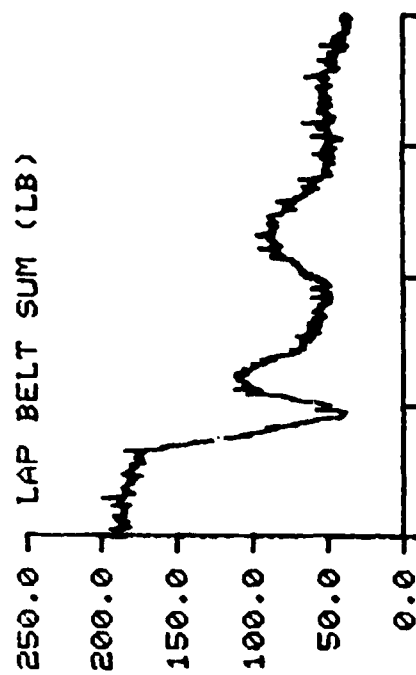
TIME IN MILLISECONDS

F-111

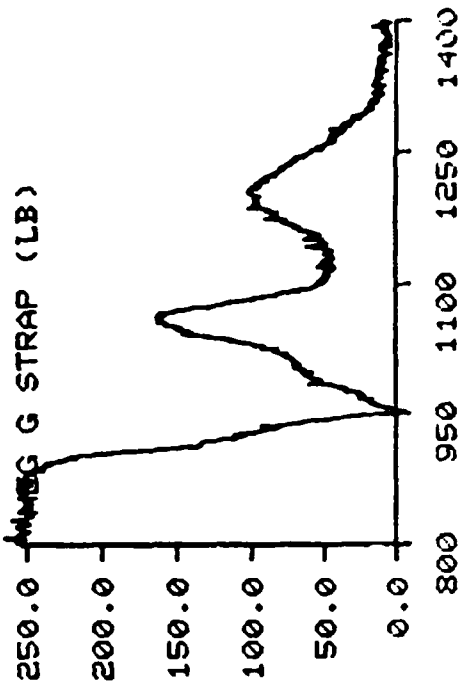
TEST NO: 265

SUBJECT ID: E-1

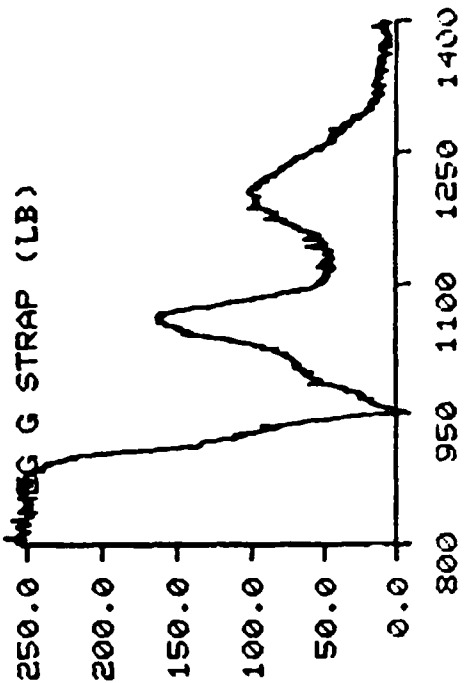
LAP BELT LF (LB)



LAP BELT RT (LB)

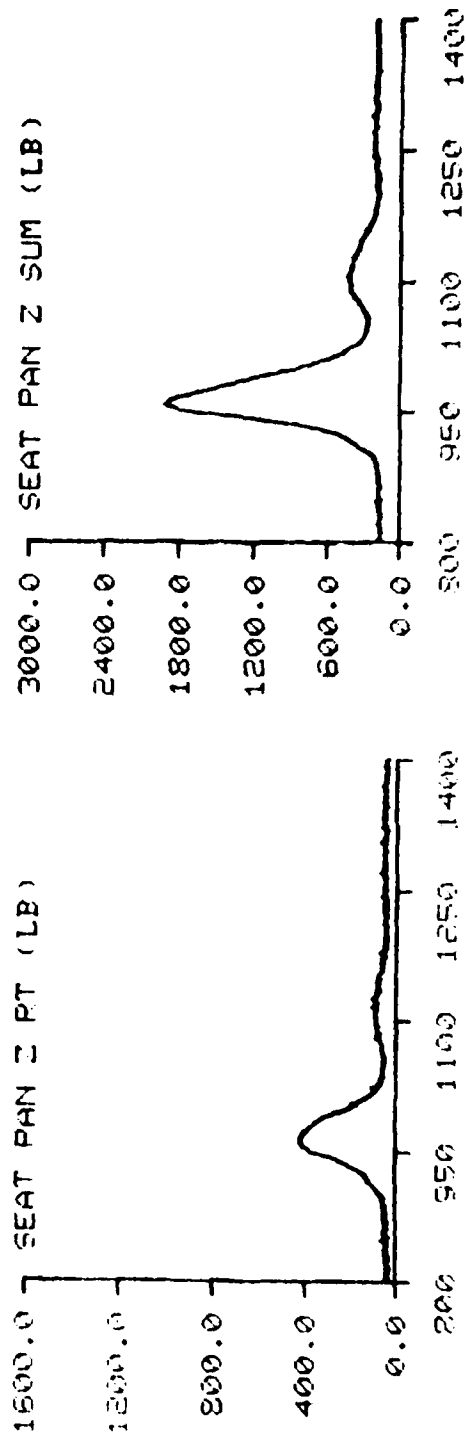
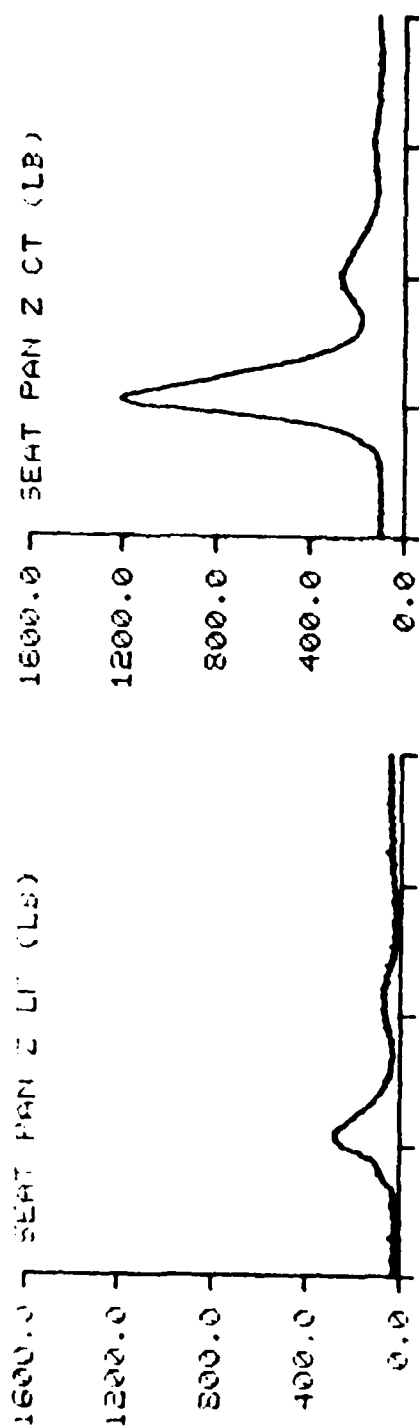


WING G STRAP (LB)



TIME IN MILLISECONDS

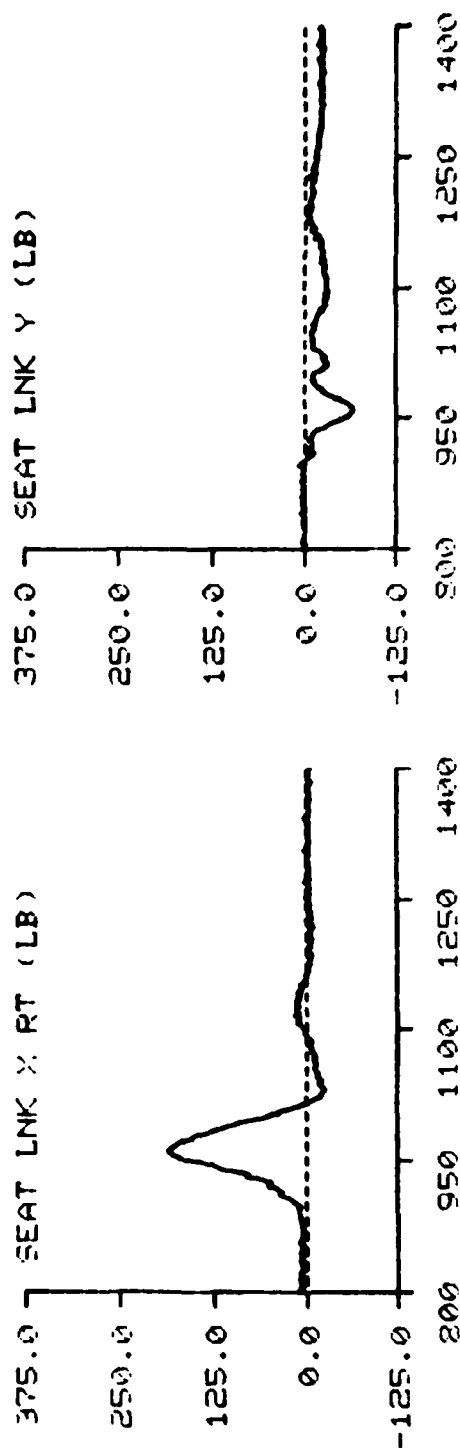
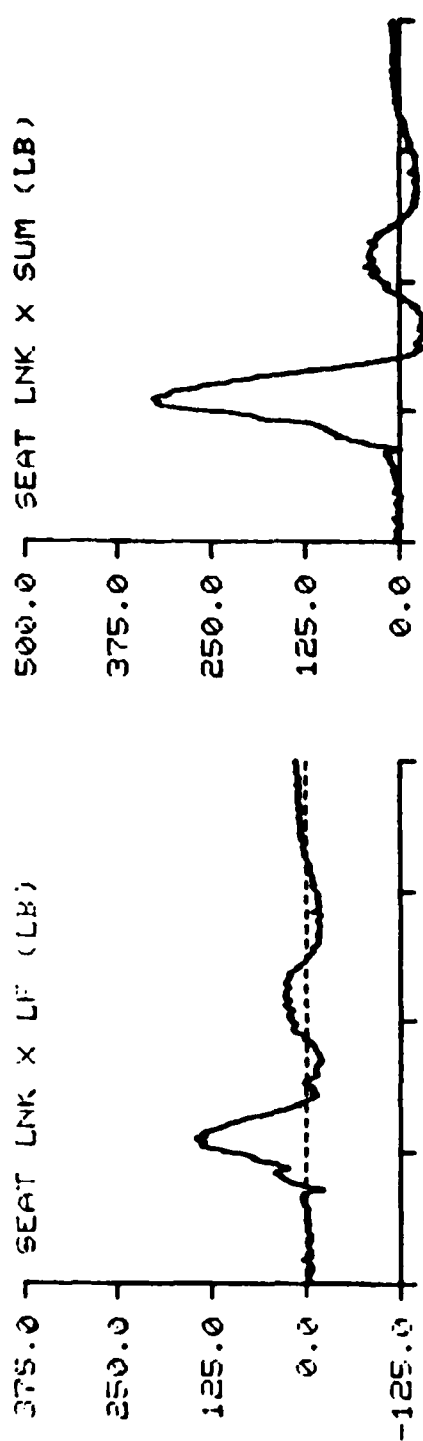
F-111 TEST NO: 265 SUBJECT ID: E-1



TIME IN MILLISECONDS



F-111 TEST NO: 265 SUBJECT ID: E-1

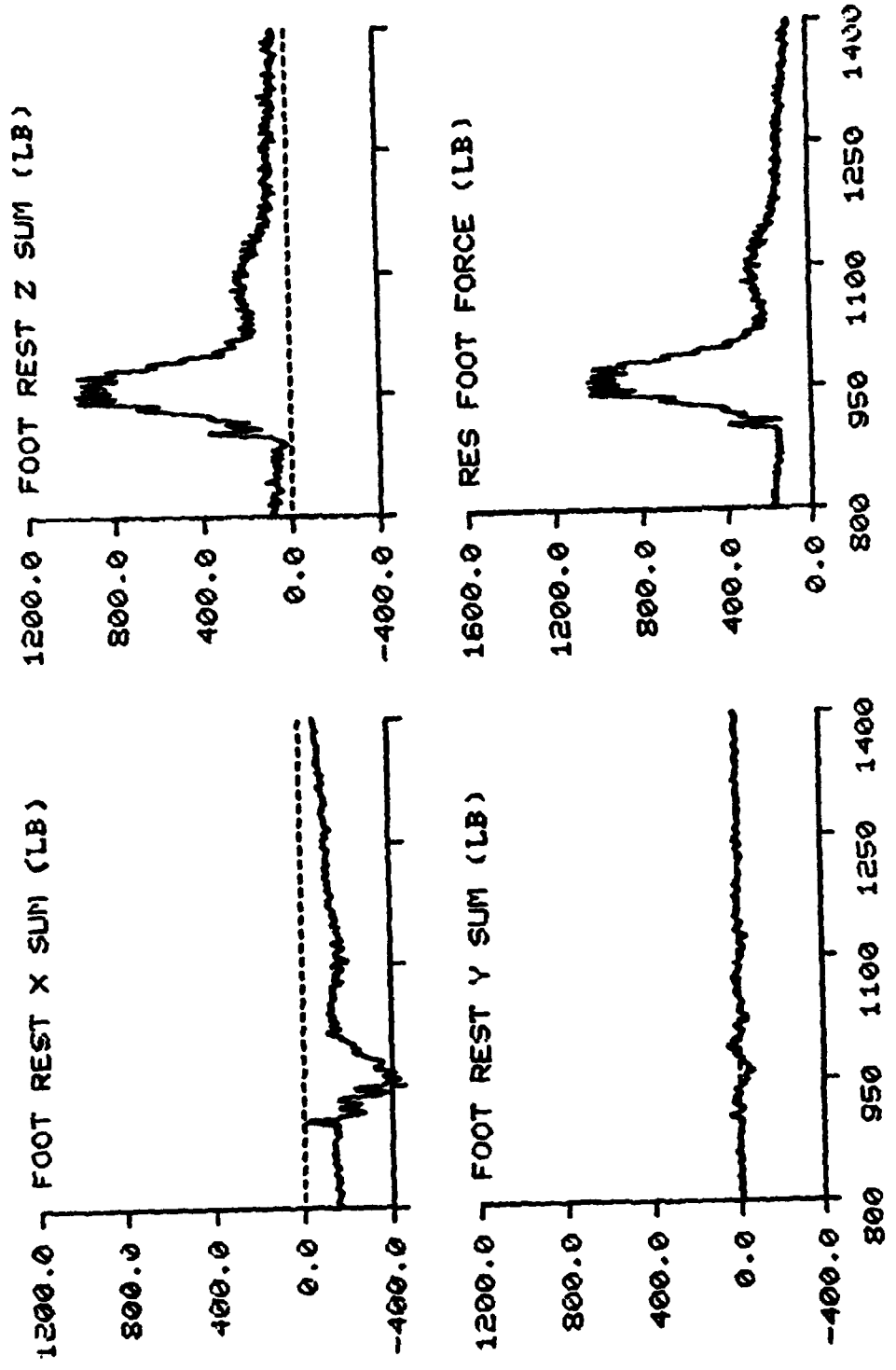


SEAT LNK X SUM (LB)

SEAT LNK Y (LB)

TIME IN MILLISECONDS

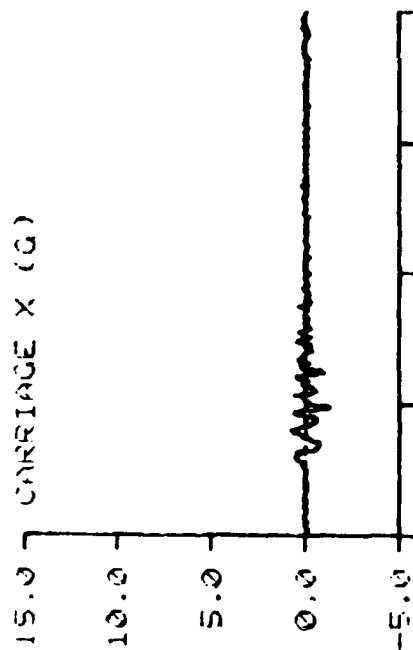
F-111      TEST NO: 265      SUBJECT ID: E-1



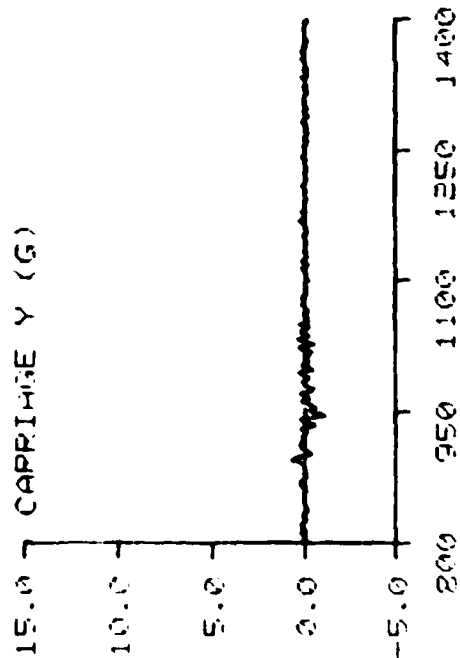
TIME IN MILLISECONDS

F-111 TEST NO: 270 SUBJECT ID: R-1

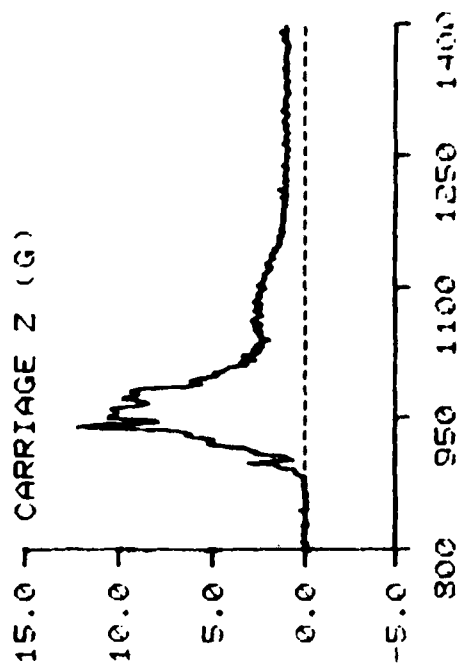
CARRIAGE X (G)



CARRIAGE Y (G)

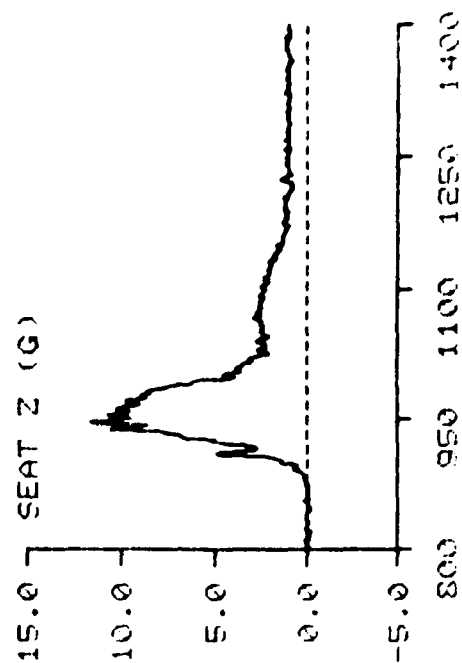
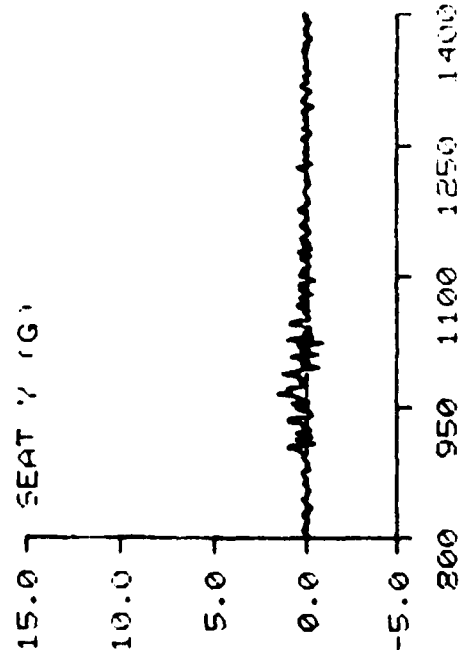
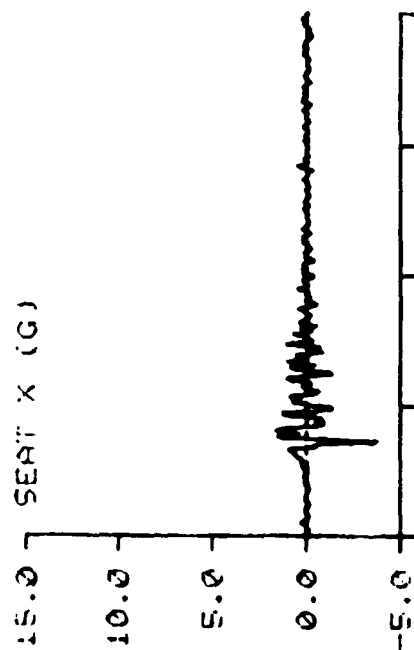


CARRIAGE Z (G)



TIME IN MILLISECONDS

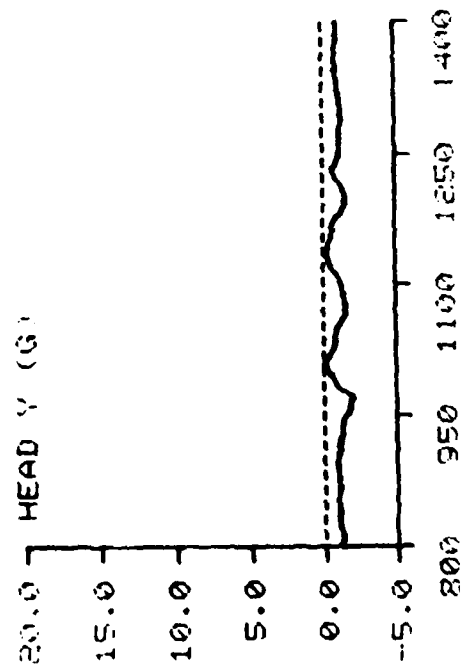
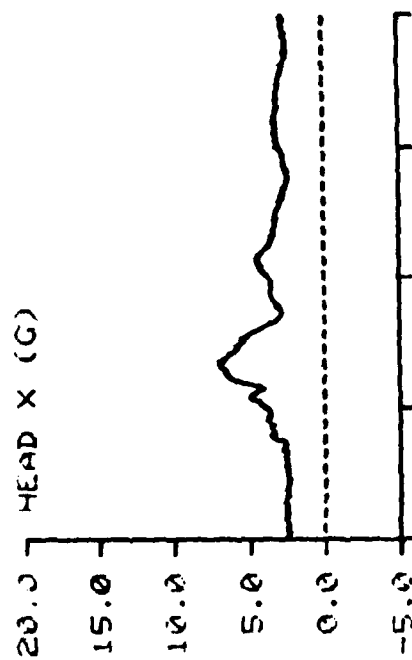
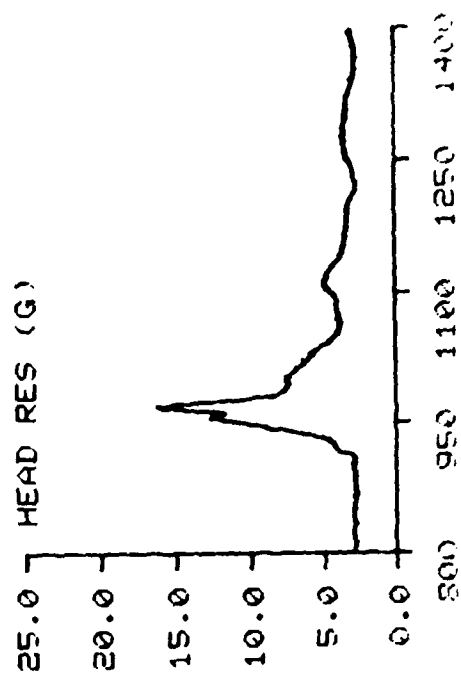
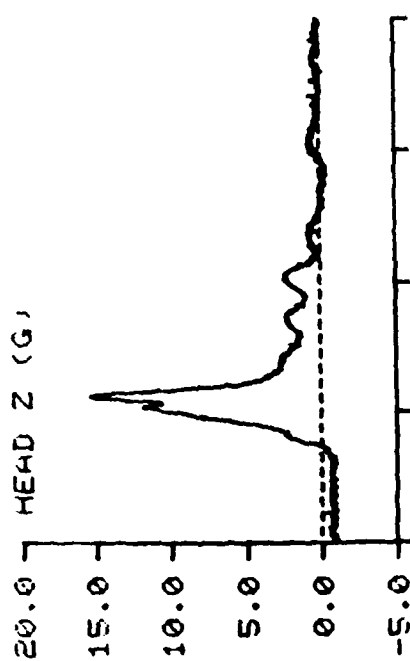
F-111 TEST NO: 270 SUBJECT ID: P-1



TIME IN MILLISECONDS

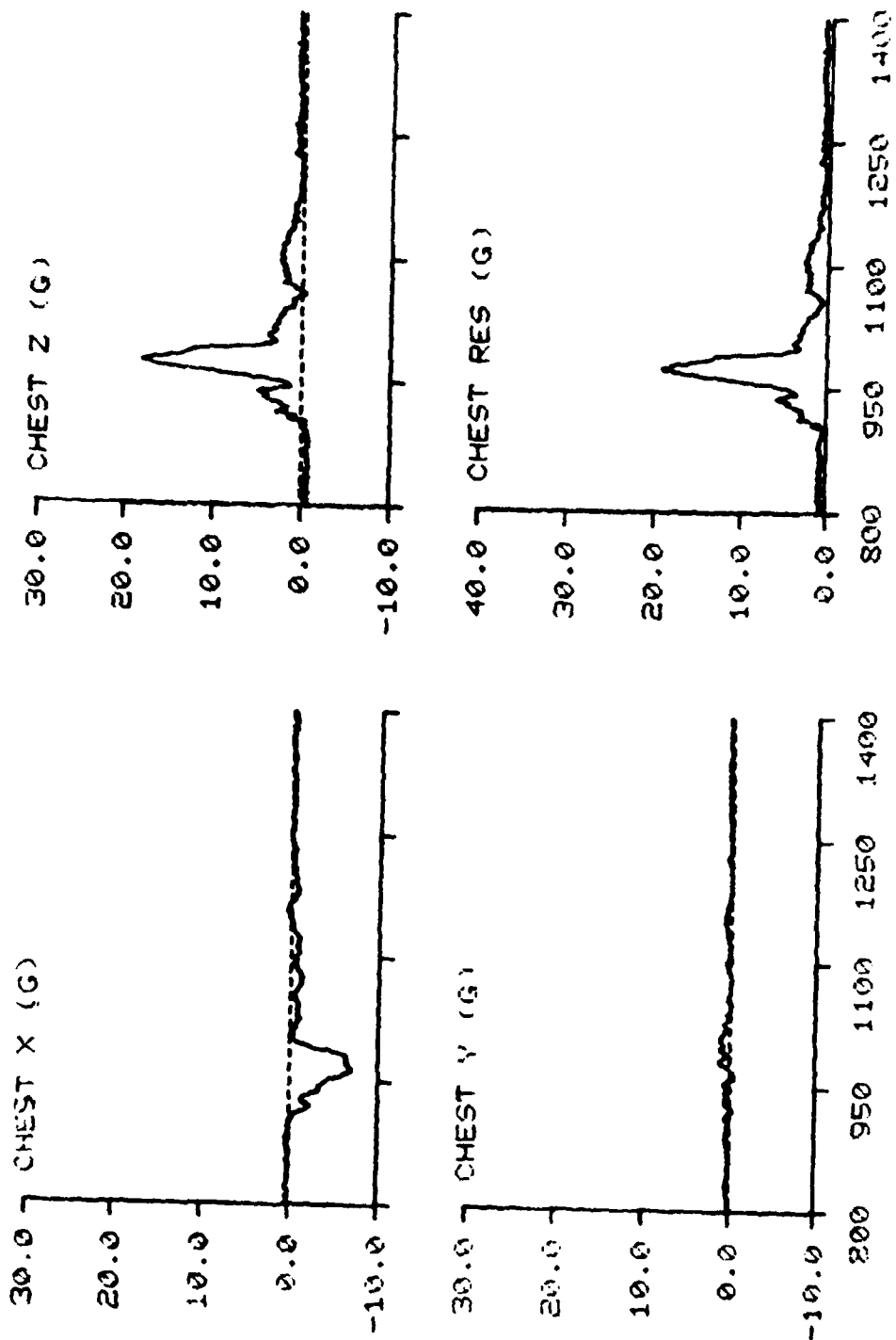
SUBJECT ID: R-1

F-111 TEST NO: 270



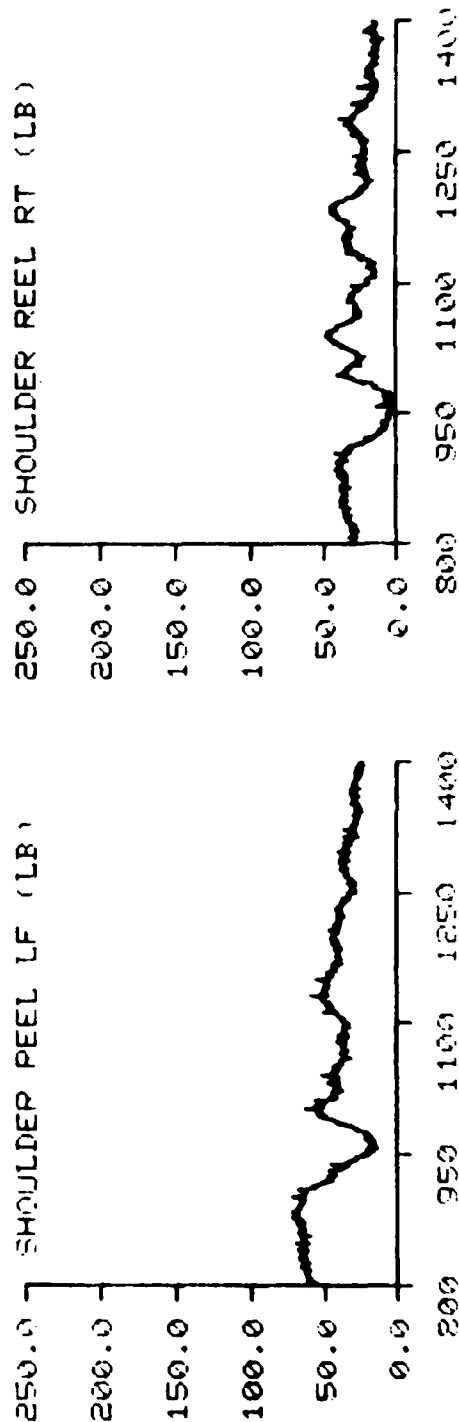
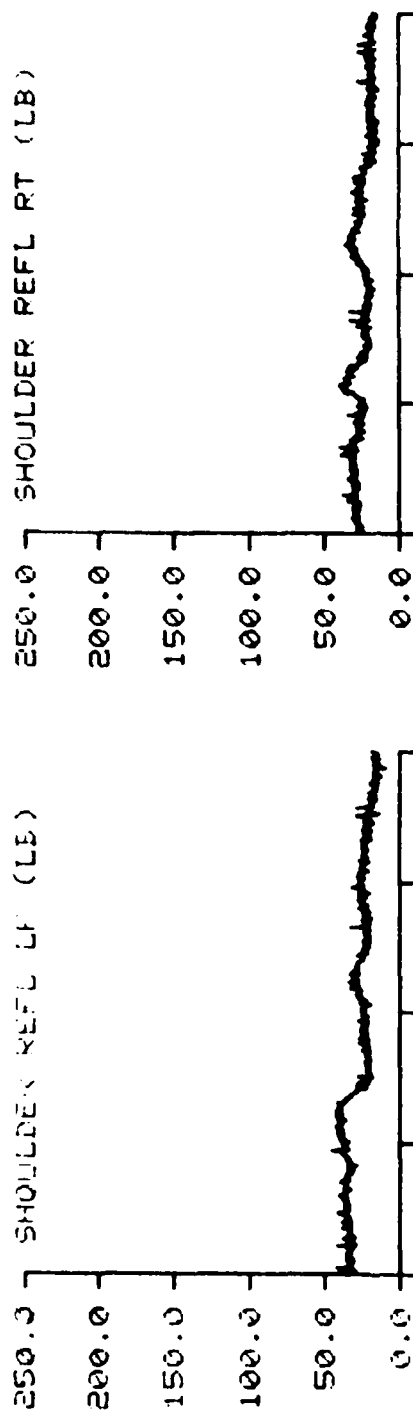
TIME IN MILLISECONDS

F-111 TEST NO: 270 SUBJECT ID: R-1



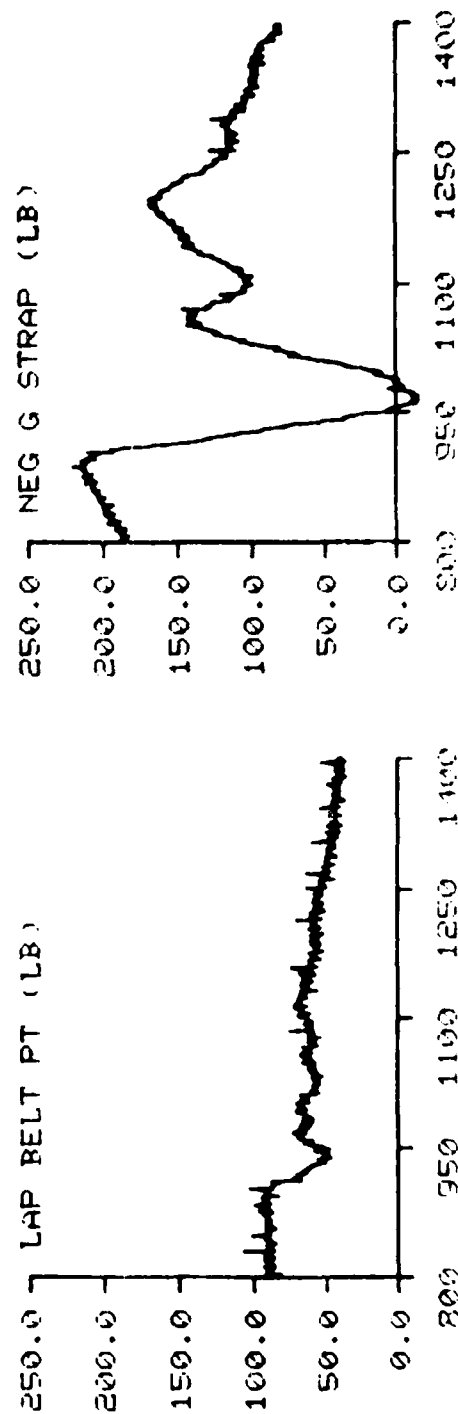
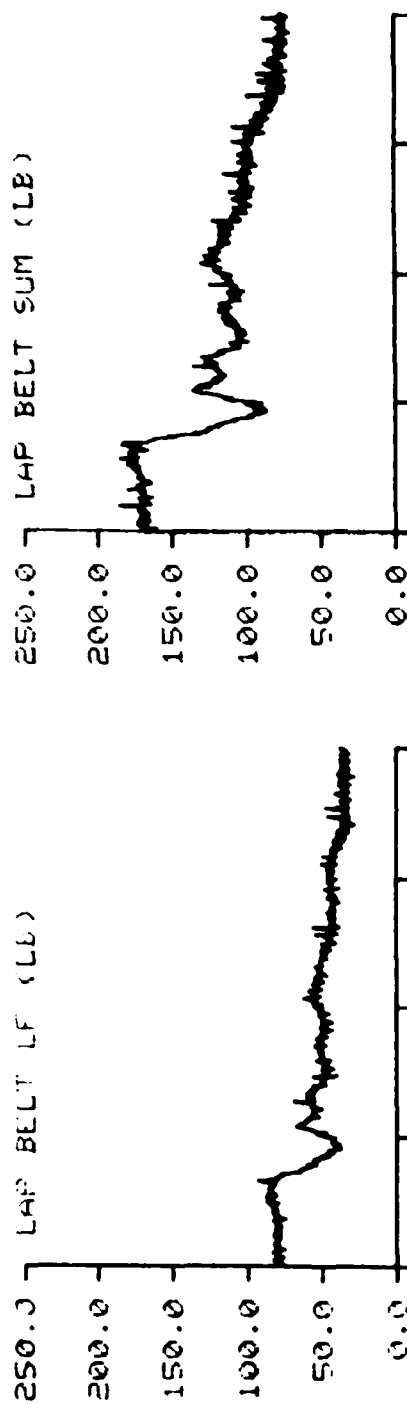
TIME IN MILLISECONDS

F-111 TEST NO: 270 SUBJECT ID: P-1



TIME IN MILLISECONDS

F-111 TEST NO: 270 SUBJECT ID: P-1



TIME IN MILLISECONDS



F-111 TEST NO: 270 SUBJECT ID: R-1

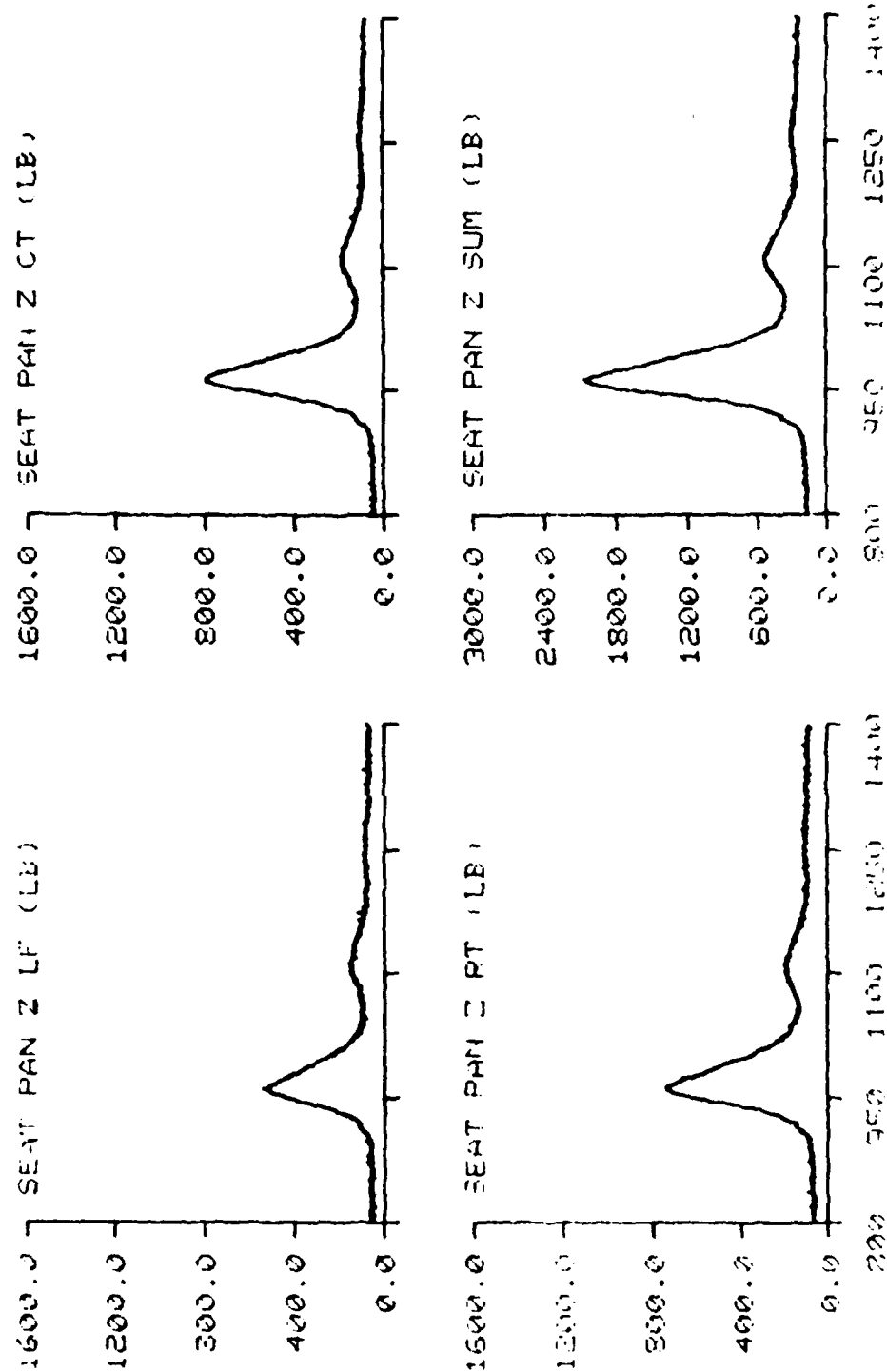
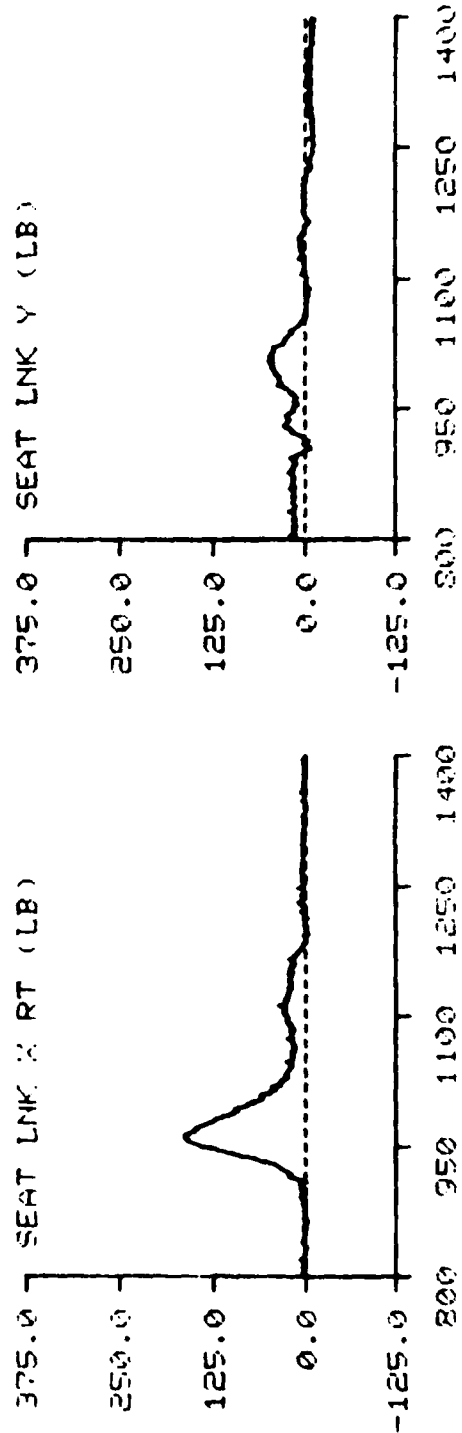
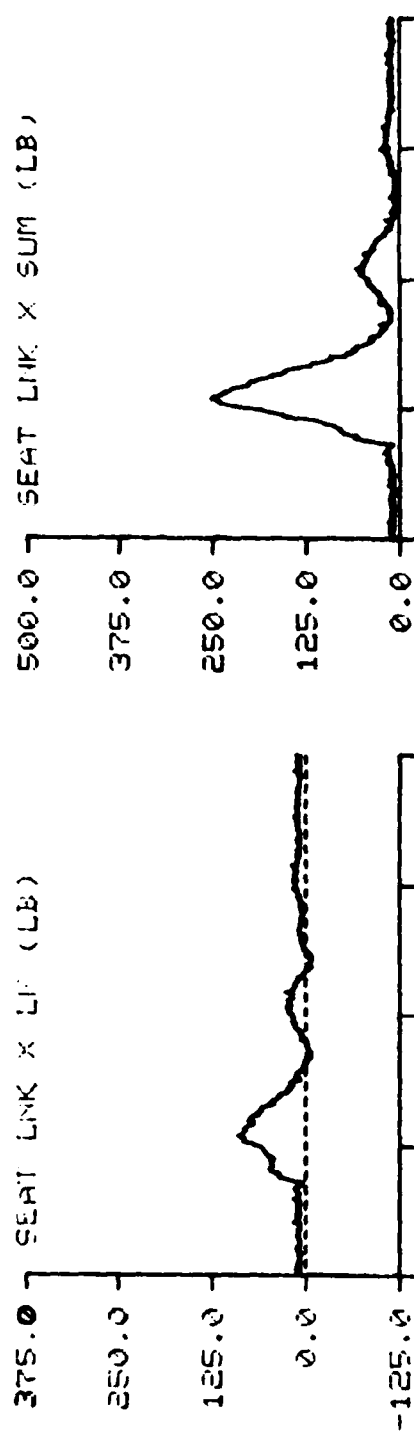
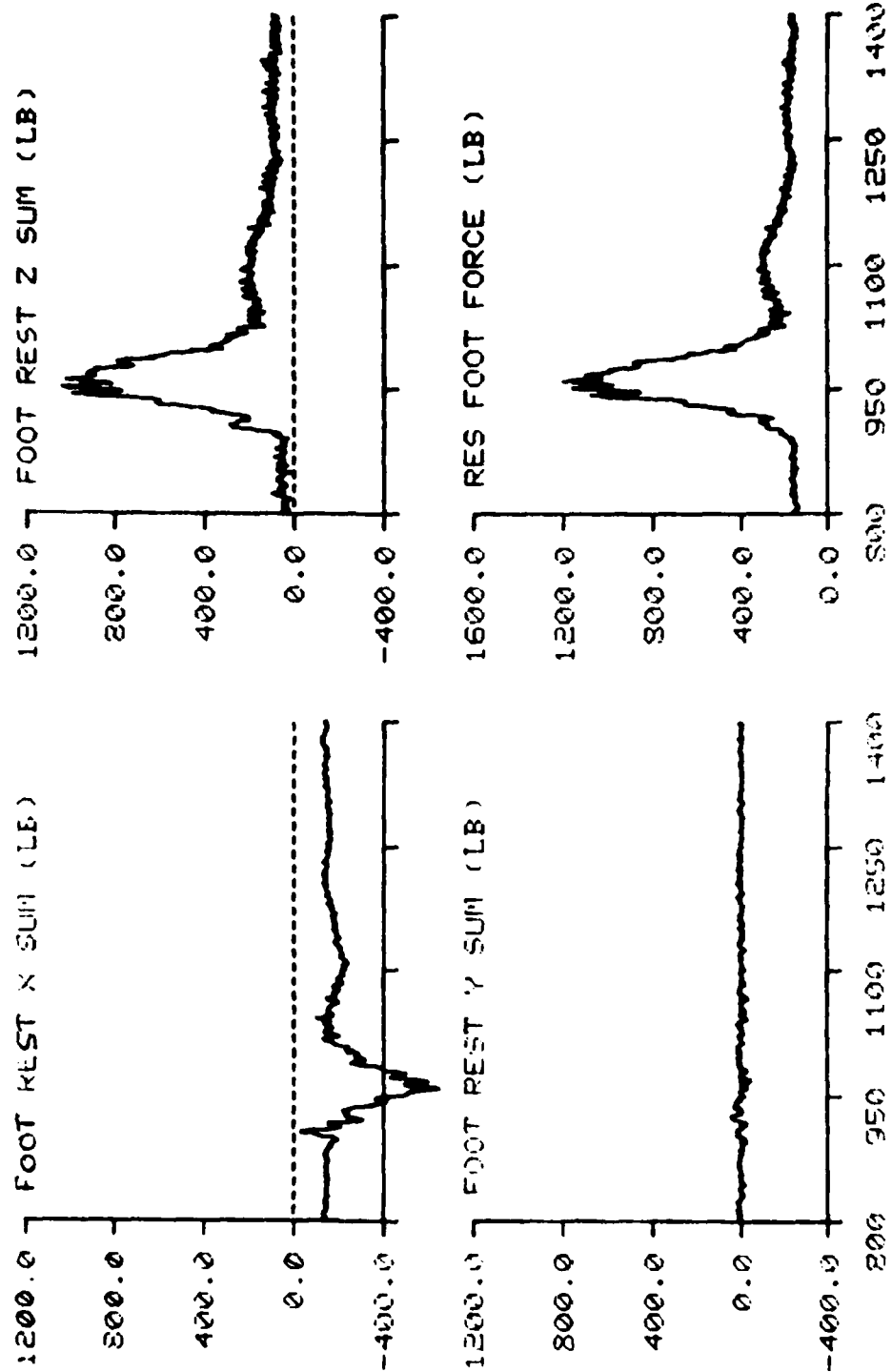


FIGURE 10 MILLISECONDS

F-111 TEST NO: 270 SUBJECT ID: P-1



F-111      TEST NO: 270      SUBJECT ID: R-1



TIME IN MILLISECONDS

## APPENDIX D

### SUMMARY OF LATERAL IMPACT TEST DATA

This appendix contains tables that list the maximum values of the measured forces, loads, accelerations, severity indices, and velocities measured during each lateral impact test with a volunteer subject. Also included is one set of data plots for each nine cells of the test matrix used in the +G<sub>y</sub> phase. The matrix is summarized as follows:

1. There were three test levels, four, six and eight G.
2. There were three test configurations. Each of the three configurations was used at each test level. The three configurations were:
  - a. Zero degree shoulder harness and 90 degree seat back.
  - b. Zero degree shoulder harness and 103 degree seat back.
  - c. Seat full down (which gave a maximum shoulder strap angle) and 103 degree seat back.

A complete data package has been submitted to ASD/AES and a complete data package will be maintained by AFAMRL/BBP until this work unit is retired. The experimental results will eventually be recorded within a permanent data bank at AFAMRL.

The sample data plots were selected based on the subject who had the most measured responses which fell within one-half standard deviation of the mean of the measured responses of all of the subjects.

F-111 4 G<sub>y</sub> TEST SUMMARY TABLE (CONFIGURATION 0/90)

TEST #	428	430	434	470	472	474	478	MEAN	STD DEV
Subject ID	R-1	J-1	G-1	P-2	M-2	H-2	M-7		
Subject Weight	200	160	186	160	162	175	135	168	21.0
Sh Strap Angle	.5	0	1.5	0	2.0	2.25	5	1.61	1.76
Seatback Angle	89	89.5	89	90	89.5	89.5	89	89.4	.378
Sled Y	4.34	2.53	4.06	4.21	4.60	4.44	4.04	4.03	.692
Sled Velocity	20.3	17.4	19.2	20.5	21.7	21.2	21.2	20.2	1.48
Seat Y	4.84	2.80	4.42	4.47	5.29	4.90	4.44	4.45	.794
Chest Res	9.50	3.14	6.14	9.48	6.57	6.29	8.12	7.03	2.24
Chest SI	13.8	1.34	5.63	7.24	6.67	6.73	5.22	6.66	3.71
Head Res	9.27	5.42	7.50	8.80	9.34	7.26	8.16	7.96	1.39
Head SI	18.1	7.86	13.9	16.3	30.0	15.5	18.4	17.2	6.68
Shoulder Sum	229	116	302	281	336	342	277	269	77.6
Sh Sum/Wt.	1.15	0.72	1.62	1.76	2.07	1.95	2.05	1.62	.508
Lap Belt Sum	413	132	299	326	179	302	310	280	94.6
Lap Sum/Wt.	2.07	.82	1.61	2.04	1.11	1.73	2.30	1.67	.538
Neg-G Strap									
Seat Lnk X Sum	-383	-34.2	-73.4	417	511	476	206	403	137
Seat Lnk Y	230	38.6	148	-77.5	-51.2	-154	-51.7	-118	123
Seat Pan Z Sum	802	320	520	150	190	161	158	154	58.5
Seat Z/Wt.	4.01	2.00	2.80	3.74	3.48	3.48	486	557	146
Res Seat Force	877	322	545	611	588	643	507	585	.682
Res Seat/Wt.	4.39	2.01	2.93	3.82	3.63	3.68	3.75	3.46	.768
Foot X Sum	-232	-473	-473	-144	-416	-184	-140	-295	153
Foot Y Sum	371	275	360	346	366	346	301	338	36.1
Foot Z Sum	152	231	235	105	207	140	108	168	55.7
Res Foot Force	452	550	607	368	579	370	330	465	113
Foot X Preload	-187	-431	-451	-111	-377	-167	-120	-263	150
Foot Y Preload	31.5	49.1	31.5	10.7	30.5	17.8	14.9	26.6	13.1
Foot Z Preload	100	207	196	65.2	171	106	55.7	129	62.1
Res Preload	214	477	482	129	415	199	133	293	159

F-111 4 G<sub>y</sub> TEST SUMMARY TABLE (CONFIGURATION 0/103)

TEST #	433	437	451	453	471	473	MEAN	STD DEV
Subject ID	0-1	E-1	F-2	M-9	S-3	G-2		
Subject Weight	173	189	156	166.5	166	123	162	22.1
Sh Strap Angle	2.5	1.25	0	-25	-5	5.25	1.38	2.21
Seatback Angle	102	102	102	102	102	102.5	102	.204
Sled Y	3.90	4.53	4.57	4.47	4.54	4.46	4.25	.410
Sled Velocity	18.7	21.1	21.7	21.7	21.5	21.5	21.0	1.16
Seat Y	4.38	5.37	5.29	5.26	5.07	5.25	5.10	.368
Chest Res	5.67	7.07	5.79	6.30	6.47	7.13	6.41	.617
Chest SI	4.29	8.70	5.36	6.55	6.21	6.96	6.35	1.50
Head Res	7.26	8.28	9.22	8.31	9.04	9.63	8.62	.851
Head SI	15.3	20.0	22.0	17.7	17.5	25.6	19.7	3.70
Shoulder Sum	233	343	267	322	243	220	271	50.3
Sh Sum/Wt.	1.35	1.81	1.71	1.93	1.47	1.79	1.68	.222
Lap Belt Sum	293	429	386	429	378	302	371	61.8
Lap Sum/Wt.	1.69	2.27	2.47	2.58	2.28	2.45	2.29	.317
Neg-6 Strap								
Seat Lnk X Sum	-50.3	-57.5	-54.5	-56.0	481	460	470	14.8
Seat Lnk Y	130	171	138	179	-61.8	58.6	-56.5	3.90
Seat Pan Z Sum	575	639	520	539	194	218	172	33.4
Seat Z/Wt.	3.33	3.38	3.34	3.24	580	462	553	60.3
Res Seat Force	584	654	533	562	3.50	3.76	3.43	.185
Res Seat/Wt.	3.38	3.46	3.42	3.38	607	505	574	53.2
Foot X Sum	-228	-260	-361	-380	-193	-166	-265	.285
Foot Y Sum	328	417	420	372	370	318	371	88.1
Foot Z Sum	148	183	172	169	111	117	150	42.8
Res Foot Force	378	492	547	528	414	336	449	30.2
Foot X Preload	-157	-206	-353	-353	-141	-92.4	-217	85.7
Foot Y Preload	43.2	33.5	36.8	7.84	41.0	60.6	37.2	111
Foot Z Preload	108	124	125	138	66.4	43.4	101	17.2
Res Preload	185	232	376	371	161	119	241	37.5

F-111 4 G<sub>y</sub> TEST SUMMARY TABLE (CONFIGURATION FD/103)

TEST #	449	450	461	466	467	475	477	MEAN	STD DEV
Subject ID	F-3	D-1	J-2	M-5	S-5	M-10	W-1		
Subject Weight	162	200	211	170	173	144	150	173	24.7
Sh Strap Angle	21	16	16	22	30	27	28	22.9	5.67
Seatback Angle	103	102.5	102	103	103	102	102.5	102.6	.450
Sled Y	4.23	4.05	4.51	4.26	4.43	4.37	4.27	4.30	.150
Sled Velocity	20.3	20.3	21.5	20.8	21.3	21.0	21.2	20.9	.474
Seat Y	4.78	4.60	5.02	4.60	5.23	5.07	4.95	4.89	.241
Chest Res	5.92	6.29	6.10	5.74	7.08	7.44	5.77	6.33	.668
Chest SI	5.71	7.63	7.15	4.93	7.69	5.84	4.91	6.27	1.21
Head Res	6.98	7.14	7.62	5.52	8.73	7.37	7.97	7.33	.991
Head SI	11.3	10.2	13.6	7.54	17.7	13.0	14.1	12.5	3.22
Shoulder Sum	345	379	407	281	276	275	291	322	54.7
Sh Sum/Wt.	2.13	1.90	1.93	1.65	1.60	1.91	1.94	1.87	.182
Lap Belt Sum	354	337	409	297	562	448	479	412	91.7
Lap Sum/Wt.	2.18	1.69	1.94	1.75	3.25	3.11	3.20	2.45	.712
Neg-G Strap			738	554	723	595	535	629	95.3
Seat Lnk X Sum	73.5	-45.8	74.8	179	117	71.0	71.9	77.3	67.3
Seat Lnk Y	151	166	243	170	219	226	155	190	38.0
Seat Pan Z Sum	405	550	663	497	700	633	440	555	114
Seat Z/Wt.	2.50	2.75	3.14	2.92	4.04	4.40	2.93	3.24	.705
Res Seat Force	430	570	699	540	729	666	462	585	117
Res Seat/Wt.	2.65	2.85	3.31	3.18	4.22	4.63	3.08	3.42	.731
Foot X Sum	-372	-325	-327	-622	-400	-74.4	-337	-351	160
Foot Y Sum	358	378	377	395	383	303	362	365	30.1
Foot Z Sum	182	163	244	189	224	83.6	205	184	51.9
Res Foot Force	510	483	497	727	486	305	511	503	123
Foot X Preload	-363	-275	-302	-584	-255	-47.0	-280	-361	123
Foot Y Preload	29.6	39.7	7.84	45.6	31.7	17.2	6.80	25.5	15.2
Foot Z Preload	148	137	177	149	133	47.0	121	130	40.7
Res Preload	386	298	343	595	278	68.7	305	325	156

F-111 6 G<sub>y</sub> TEST SUMMARY TABLE (CONFIGURATION 0/90)

TEST #	460	463	485	493	503	MEAN	STD DEV
Subject ID	G-1	J-1	P-2	H-2	M-2		
Subject Weight	183	164	161	175	161	169	9.81
Sh Strap Angle	1.5	3.0	1.25	1.25	1.25	1.65	.762
Seat Back Angle	89	90	90	90	90	89.8	.447
Sled Y	6.32	6.04	6.11	6.17	6.34	6.20	.131
Sled Velocity	26.0	25.6	26.3	25.5	25.6	25.8	.339
Seat Y	6.97	6.69	6.52	6.83	7.00	6.80	.200
Chest Res	10.9	11.3	9.92	8.68	9.72	10.1	1.03
Chest S.I.	16.1	14.8	14.1	13.6	14.5	14.6	.942
Head Res	10.4	13.0	9.40	11.2	10.7	10.9	1.33
Head S.I.	27.4	33.1	24.5	32.1	26.5	28.7	3.71
Shoulder Sum	386	403	298	421	507	403	74.9
Sh Sum/Wt.	2.11	2.46	1.85	2.40	3.15	2.39	.488
Lap Blt Sum	384	347	499	258	385	375	86.6
Lap Sum/Wt.	2.10	2.12	3.10	1.47	2.39	2.24	.589
Neg-6 Strap	524	545	327	547	523	423	93.6
Seat Lnk X Sum	-96.6	-72.1	-84.0	-58.3	-66.9	-75.6	15.0
Seat Lnk Y	247	304	200	265	291	261	40.9
Seat Pan Z Sum	851	724	730	660	651	723	80.0
Seat Z/Wt.	4.65	4.41	4.53	3.77	4.05	4.28	.364
Res Seat Force	887	773	755	709	705	766	73.8
Res Seat/Wt.	4.85	4.72	4.69	4.05	4.38	4.54	.323
Foot X Sum	-630	-588	-313	-707	-792	-606	181
Foot Y Sum	596	506	506	505	489	520	42.9
Foot Z Sum	297	243	191	272	331	267	53.3
Res Foot Force	815	759	613	867	961	803	130
Foot X Preload	-526	-556	-278	-659	-730	-550	172
Foot Y Preload	29.4	45.1	21.7	22.5	39.6	31.7	10.4
Foot Z Preload	208	206	131	207	291	209	56.6
Res Foot Preload	560	581	308	692	787	586	180



F-111 6 G<sub>y</sub> TEST SUMMARY TABLE (CONFIGURATION 0/103)

TEST #	459	464	465	494	495	496	MEAN	STD DEV
Subject ID	E-1	0-1	M-9	S-3	G-2	F-2		
Subject Weight	185	172	168	165	121	161	162	21.8
Sh Strap Angle	2.5	3.5	-25	.5	9.5	.75	2.75	3.58
Seat Back Angle	101	102.5	103	102.5	103.5	102.5	102.5	.837
Sled Y	6.33	6.39	6.77	6.21	6.12	6.32	6.36	.224
Sled Velocity	25.9	26.2	26.5	24.4	25.3	25.7	25.7	.745
Seat Y	7.12	6.99	7.23	7.03	7.43	7.44	7.21	.195
Chest Res	10.3	12.0	10.1	8.36	10.1	9.31	10.0	1.21
Chest SI	17.1	18.5	16.0	12.2	15.2	15.4	15.7	2.12
Head Res	11.6	13.0	10.4	10.2	11.5	9.97	11.1	1.15
Head SI	33.2	44.2	29.6	28.6	33.2	24.1	32.2	6.80
Shoulder Sum	499	437	414	340	331	297	386	76.4
Sh Sum/Wt.	2.70	2.54	2.47	2.06	2.74	1.84	2.39	.363
Lap Belt Sum	759	723	470	467	417	571	568	144
Lap Belt Sum/Wt.	4.10	4.21	2.80	2.83	3.45	3.55	3.49	.601
Neg-G Strap	730	704	742	654	628	651	685	46.9
Seat Lnk X Sum	106	-55.9	134	103	124	89.7	83.5	70.1
Seat Lnk Y	287	280	298	234	271	256	271	23.1
Seat Pan Z Sum	832	1014	674	674	519	631	724	174
Seat Z/Wt.	4.50	5.89	4.01	4.09	4.30	3.92	4.45	.735
Res Seat Force	868	1039	730.	703	585	678	767	162
Res Seat/Wt.	4.69	6.04	4.34	4.26	4.85	4.21	4.73	.689
Foot X Sum	-322	-211	-545	-567	-309	-563	-420	157
Foot Y Sum	556	560	552	481	481	539	528	37.2
Foot Z Sum	206	152	257	254	176	279	221	50.5
Res Foot Force	618	587	719	733	538	792	665	98.1
Foot X Preload	-262	-127	-482	-528	-215	-514	-355	174
Foot Y Preload	11.0	19.6	19.6	2.50	32.8	58.7	24.0	19.8
Foot Z Preload	141	74.8	185	207	96.3	243	158	65.4
Res Foot Preload	298	149	507	567	238	571	372	203

F-111 6 G<sub>y</sub> TEST SUMMARY TABLE (CONFIGURATION FD/103)

TEST #	468	482	483	486	490	498	504	MEAN	STD DEV
Subject ID	F-3	M-5	S-5	M-10	D-1	J-2	W-1		
Subject Weight	164	170.5	172	142	200	216	150	174	26.3
Sh Strap Angle	20.5	22.5	33	27	14.5	12.5	31.5	23.1	7.93
Seat Back Angle	103	102.5	102	102.5	102.5	103	102	103	.378
Sled Y	6.35	6.37	6.53	6.30	6.15	7.21	6.56	6.50	.344
Sled Velocity	25.9	26.0	26.1	25.9	25.9	27.0	26.3	26.2	.399
Seat Y	7.45	7.40	7.63	7.01	7.32	7.94	7.76	7.50	.306
Chest Res	12.1	11.0	13.8	14.4	9.31	14.5	9.91	12.1	2.15
Chest SI	16.9	17.4	24.6	17.3	15.5	26.9	15.8	19.2	4.58
Head Res	11.3	8.57	12.2	10.4	11.0	15.6	10.7	11.4	2.16
Head SI	34.2	22.9	34.6	25.9	28.5	49.4	30.4	32.3	8.65
Shoulder Sum	543	354	429	396	498	588	417	461	84.5
Sh Sum/Wt.	3.31	2.08	2.49	2.79	2.49	2.72	2.78	2.67	.377
Lap Belt Sum	473	660	7.32	624	583	1425	792	756	313
Lap Sum/Wt.	2.88	3.87	4.25	4.39	2.91	6.60	5.28	4.31	1.32
Neg-G Strap	992	824	1122	769	1012	1273	855	978	179
Seat Lnk X Sum	172	194	194	151	124	-110	138	123	106
Seat Lnk Y	266	265	234	292	274	245	227	258	23.2
Seat Pan Z Sum	560	719	790	768	808	1257	773	811	214
Seat Z/Wt.	3.66	4.22	4.59	5.41	4.04	5.82	5.16	4.70	.788
Res Seat Force	659	784	827	809	842	1271	792	855	193
Res Seat/Wt.	4.02	4.60	4.81	5.70	4.21	5.89	5.28	4.93	.720
Foot X Sum	-453	-667	664	-151	-814	-337	-479	-509	225
Foot Y Sum	550	527	546	469	492	585	483	522	42.0
Foot Z Sum	268	214	282	173	327	204	247	245	52.4
Res Foot Force	707	826	790	488	951	636	702	729	147
Foot X Preload	-403	-566	-525	-131	-695	-244	-368	-419	194
Foot Y Preload	39.3	27.4	35.5	15.9	38.4	19.4	10.0		
Foot Z Preload	147	150	218	73.0	250	122	179	163	59.2
Res Foot Preload	427	587	570	151	740	273	409	451	200

F-111 8 G<sub>y</sub> TEST SUMMARY TABLE (CONFIGURATION 0/90)

TEST #	458	492	507	508	520	MEAN	STD DEV
Subject ID	R-1	J-1	M-9	H-2	G-2		
Subject Weight	200	163	166	178	121	166	29.9
Sh Strap Angle	90	91	89	89	89	1.9	2.08
Seat Back Angle	9.13	7.85	8.57	8.80	8.14	89.6	.894
Sled Y	30.9	27.8	29.3	30.3	29.2	8.50	.511
Sled Velocity	9.49	8.37	8.97	8.85	8.91	29.5	1.19
Seat Y	15.1	11.9	12.3	13.7	13.1	8.92	.398
Chest Res	36.7	21.1	25.5	26.6	27.0	13.2	1.26
Chest SI	14.2	12.2	11.8	15.9	16.3	27.4	5.71
Head Res	39.1	36.2	35.2	57.0	62.3	14.1	2.06
Head SI	458	386	544	663	426	46.0	12.7
Shoulder Sum	2.29	2.37	3.28	3.72	3.52	495	110
Sh Sum/Wt.	803	584	455	503	456	3.04	.664
Lap Belt Sum	4.02	3.59	2.74	2.82	3.77	560	146
Lap Sum/Wt.	661	362	626	806	549	3.39	.576
Neg-G Strap	-206	-91.4	-134	-172	95.7	601	163
Seat Lnk X Sum	299	265	349	332	301	-102	118
Seat Lnk Y	1399	860	894	932	613	309	32.6
Seat Pan Z Sum	7.00	5.28	5.39	5.23	5.07	940	285
Seat Z/Wt.	1431	897	960	981	678	5.59	.794
Res Seat Force	7.16	5.50	5.78	5.51	5.60	989	275
Res Seat/Wt.	-535	-611	-529	-575	-514	5.91	.708
Foot X Sum	796	648	727	651	659	-553	39.6
Foot Y Sum	279	275	281	209	252	696	64.5
Foot Z Sum	888	875	879	781	814	259	30.4
Res Foot Force	-411	-603	-478	-448	-466	847	47.2
Foot X Preload	24.9	32.3	18.1	29.5	98.6	-481	72.8
Foot Y Preload	174	222	203	138	203	40.7	32.8
Foot Z Preload	447	644	519	469	518	188	32.6
Res Foot Preload						519	76.1

F-111 8 G<sub>y</sub> TEST SUMMARY TABLE (CONFIGURATION O/103)

TEST #	481	489	505	510	512	513	515	MEAN	STD DEV
Subject ID	M-9	E-1	R-1	F-3	F-2	G-2	S-3		
Subject Weight	165	186	200	167	153	122	168	166	24.7
Sh Strap Angle	-1	1.25	0.5	2	1.75	6.75	1	1.75	2.42
Seat Back Angle	102	103	103	102	102	102.5	102	102	.48
Sled Y	8.26	8.40	8.72	8.07	8.45	8.05	7.99	8.28	.264
Sled Velocity	29.0	29.3	30.3	29.4	30.0	29.2	29.1	29.3	.514
Seat Y	9.27	9.46	9.17	8.95	9.33	9.37	9.37	9.27	.169
Chest Res	12.3	13.7	14.7	11.1	11.4	12.4	11.7	12.5	1.30
Chest SI	24.9	29.1	27.8	23.0	23.5	22.6	20.4	24.5	3.04
Head Res	12.2	14.1	16.0	12.1	12.7	16.0	12.2	13.6	1.77
Head SI	41.2	48.8	45.5	41.5	41.3	59.0	35.4	44.7	7.58
Shoulder Sum	468	562	555	546	412	374	468	484	73.9
Sh Sum/Wt.	2.84	3.02	2.78	3.27	2.69	3.07	2.79	2.92	.204
Lap Belt Sum	598	855	1002	680	678	504	758	725	165
Lap Sum/Wt.	3.63	4.60	5.01	4.07	4.43	4.13	4.51	4.34	.442
Neg G Strap	762	931	1018	817	788	634	768	817	125
Seat Lnk X Sum	112	94.0	80.8	235	104	188	121	134	56.4
Seat Lnk Y	301	304	284	281	307	303	292	296	10.3
Seat Pan Z Sum	898	1122	1047	731	767	559	873	857	192
Seat Z/Wt.	5.45	6.03	5.23	4.38	5.01	4.58	5.20	5.13	.549
Res Seat Force	939	1144	1072	793	816	650	908	903	169
Res Seat/Wt.	5.69	6.15	5.36	4.75	5.34	5.33	5.41	5.43	.423
Foot X Sum	-541	-474	-681	-896	-634	-595	-651	-639	133
Foot Y Sum	684	697	724	637	690	606	654	670	40.2
Foot Z Sum	278	260	238	362	370	304	306	303	49.5
Res Foot Force	838	819	909	1039	938	833	908	898	77.1
Foot X Preload	-495	-376	-551	-754	-588	-553	-621	-563	116
Foot Y Preload	27.1	32.9	51.3	30.1	66.5	43.7	45.6	42.5	13.8
Foot Z Preload	187	211	190	280	254	247	263	233	36.9
Res Foot Preload	530	433	585	805	644	607	676	611	117

F-111 8 G<sub>y</sub> TEST SUMMARY TABLE (CONFIGURATION FD/103)

TEST #	480	488	506	511	516	518	519	521	MEAN	STD DEV
Subject ID	F-3	R-1	M-5	M-10	J-1	S-5	D-1	W-1		
Subject Wt.	164	200.5	170	141	162	172	202	150	170	21.7
Sh Strap Angle	22	23.5	19	28	26	33.5	14	30	24.5	6.25
Seat Back Angle	102	102.5	103	103	101	102	102	102.5	102	.65
Sled Y	8.78	8.31	8.48	7.81	8.05	7.88	8.00	8.16	8.18	.326
Sled Velocity	29.9	29.3	29.9	28.0	28.9	28.3	28.4	29.2	29.0	0.72
Seat Y	9.54	9.52	9.64	9.0	9.28	9.19	9.18	9.41	9.34	.221
Chest Res	12.3	12.9	13.78	12.2	13.2	18.5	12.3	12.9	13.5	2.08
Chest SI	28.0	29.6	28.78	24.3	28.4	36.1	26.5	24.3	28.3	3.74
Head Res	13.6	13.0	12.4	15.0	12.2	13.3	12.6	11.5	13.0	1.07
Head SI	48.9	38.9	48.7	49.0	34.4	42.9	38.4	34.6	42.0	6.31
Shoulder Sum	684	625	445	416	541	481	590	400	523	104
Shoulder Sum/Wt	4.17	3.12	2.62	2.95	3.34	2.80	2.92	2.67	3.07	.501
Lap Belt Sum	804	1004	592	785	693	987	720	1057	830	168
Lap Sum/Wt	4.90	5.01	3.48	5.57	4.28	5.74	3.56	7.05	4.95	1.19
Neg-6 Strap	1085	1039	983	874	878	1147	1329	908	1030	156
Seat Lnk X Sum	239	169	278	204	179	225	102	208	201	52.6
Seat Lnk Y	316	260	332	344	301	253	299	295	300	31.9
Seat Pan Z Sum	794	1126	882	900	694	893	986	888	895	127
Seat Z/Wt.	4.84	5.62	5.19	6.39	4.28	5.19	4.88	5.92	5.29	.668
Res Seat Force	866	1142	961	952	760	939	1013	929	945	110
Res Seat/Wt	5.28	5.70	5.66	6.75	4.69	5.46	5.02	6.20	5.60	.653
Foot X Sum	-700	-871	-1070	-215	-797	-1032	-838	-576	-762	274
Foot Y Sum	685	661	711	566	670	614	736	662	662	53.4
Foot Z Sum	328	309	290	196	307	354	337	317	305	48.1
Res Foot Force	887	998	1173	611	993	1171	1085	800	965	193
Foot X Preload	-492	-725	-896	-197	-734	-915	-777	-401	-642	254
Foot Y Preload	16.9	43.7	44.7	48.1	45.0	24.7	66.8	13.7	38.0	18.0
Foot Z Preload	193	230	198	105	226	304	263	196	214	58.4
Res Foot Preload	528	762	919	228	769	964	823	447	680	255

F-111      TEST NO: 474      SUBJECT ID: H-2

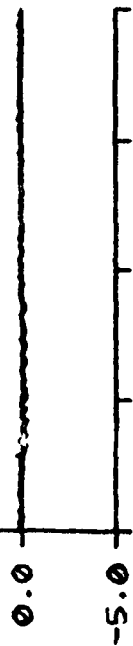
15.0 SLED X (G)

10.0

5.0

0.0

-5.0



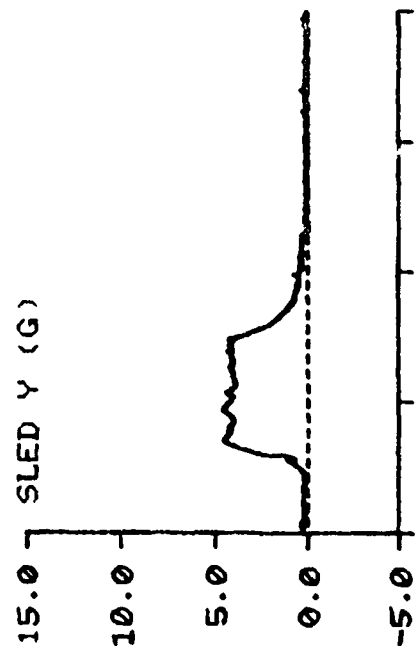
15.0 SLED Y (G)

10.0

5.0

0.0

-5.0



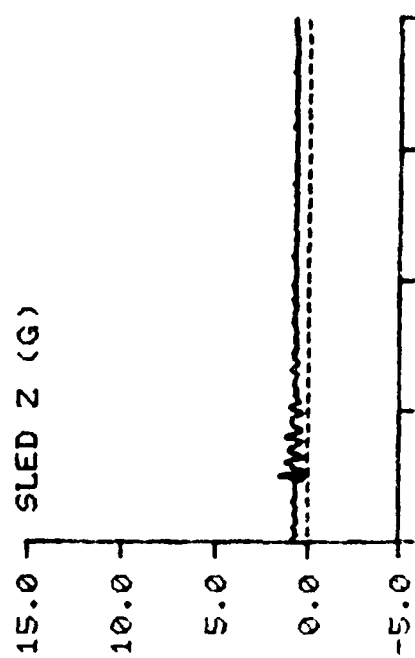
15.0 SLED Z (G)

10.0

5.0

0.0

-5.0

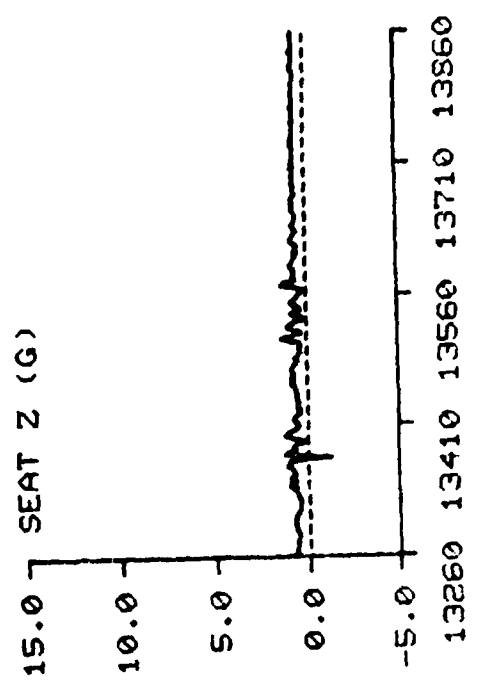
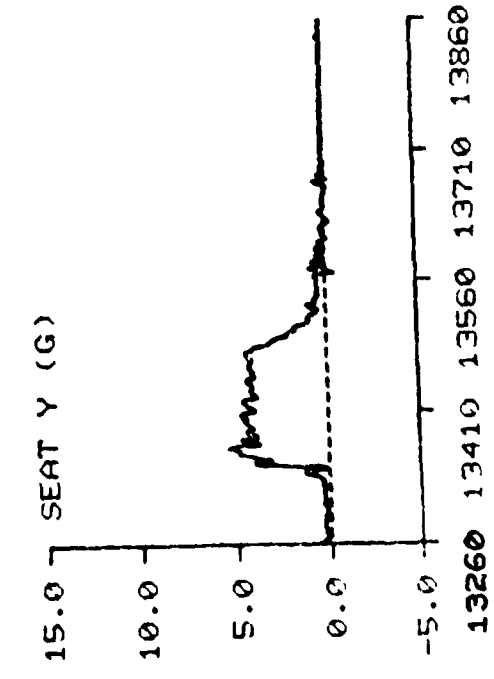
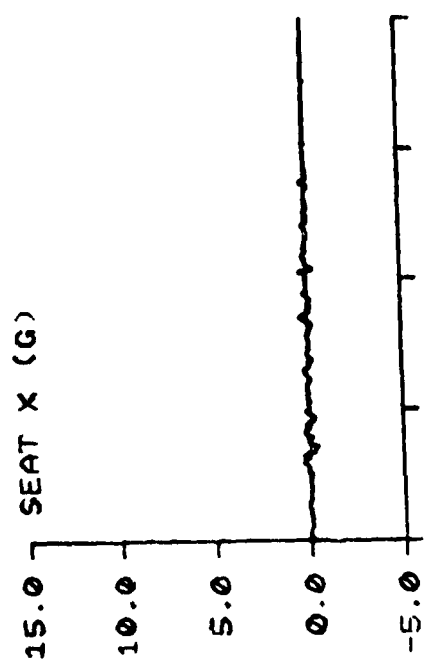


13260 13410 13560 13710 13860

TIME IN MILLISECONDS

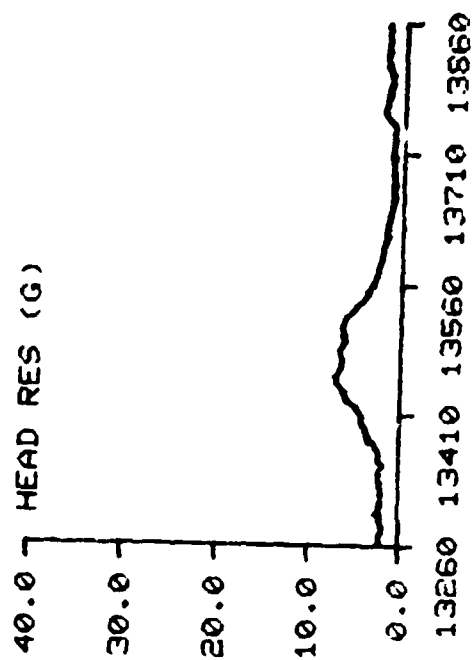
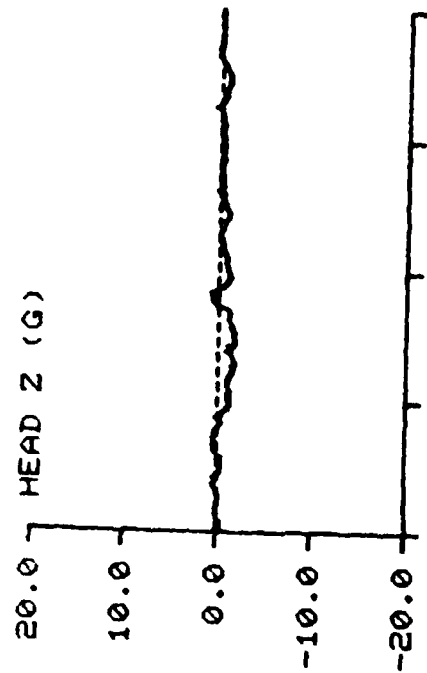
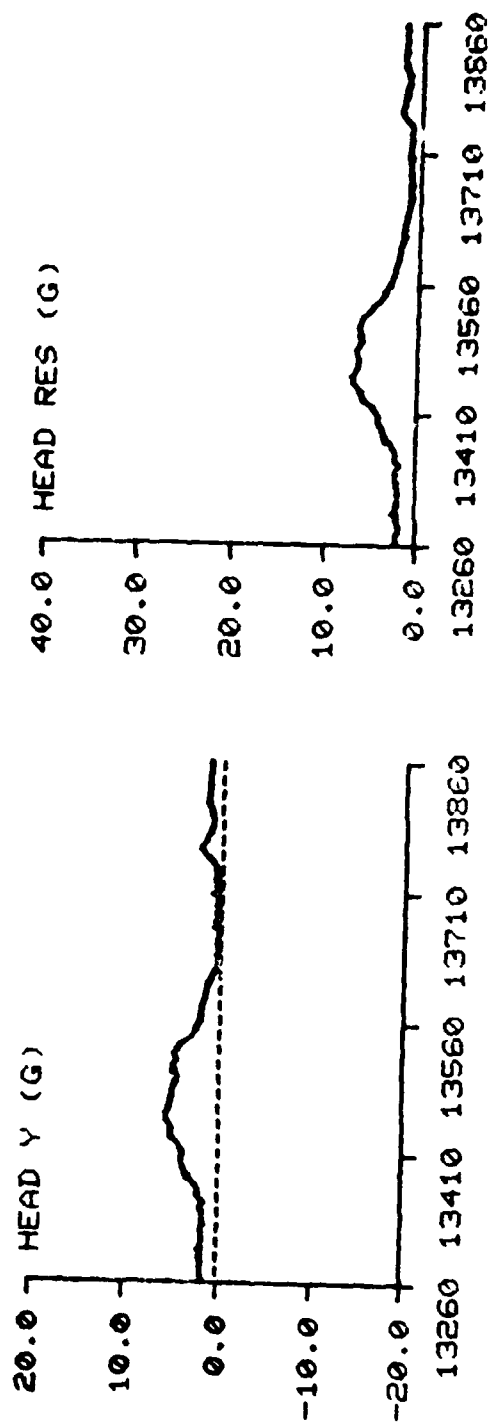
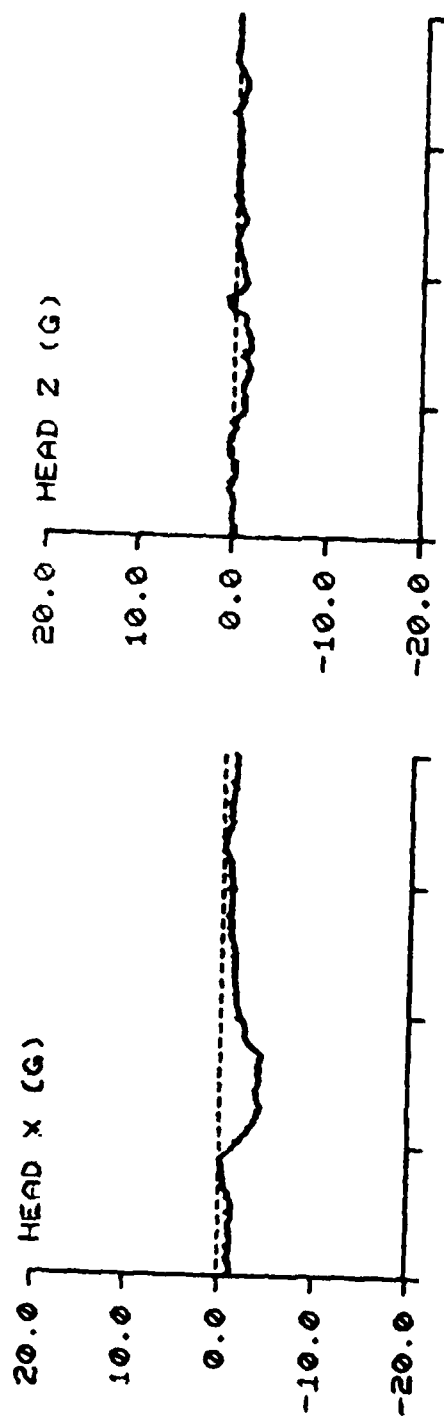
SUBJECT ID: H-2

F-111 TEST NO: 474



TIME IN MILLISECONDS

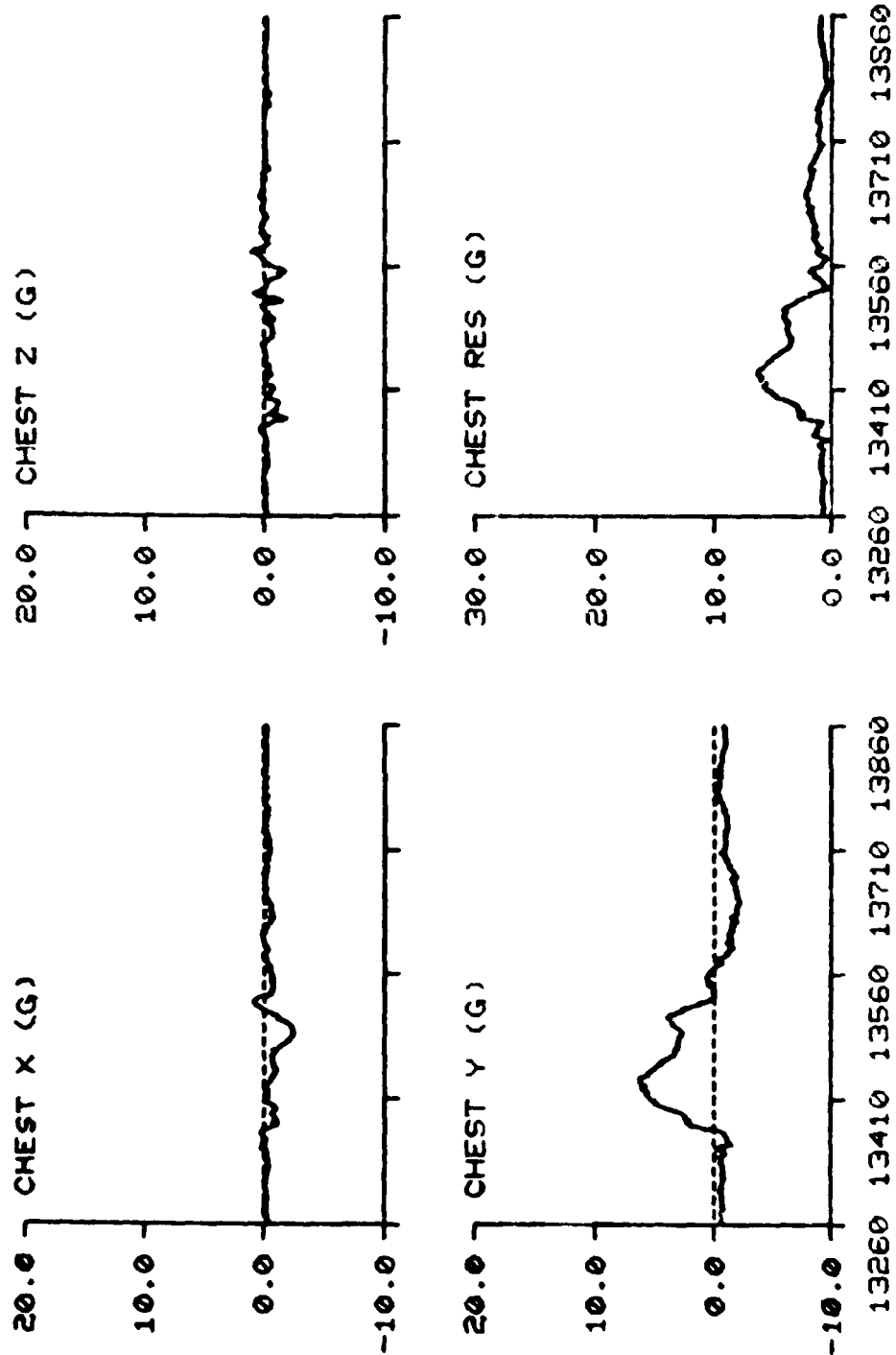
F-111      TEST NO: 474      SUBJECT ID: H-2



TIME IN MILLISECONDS

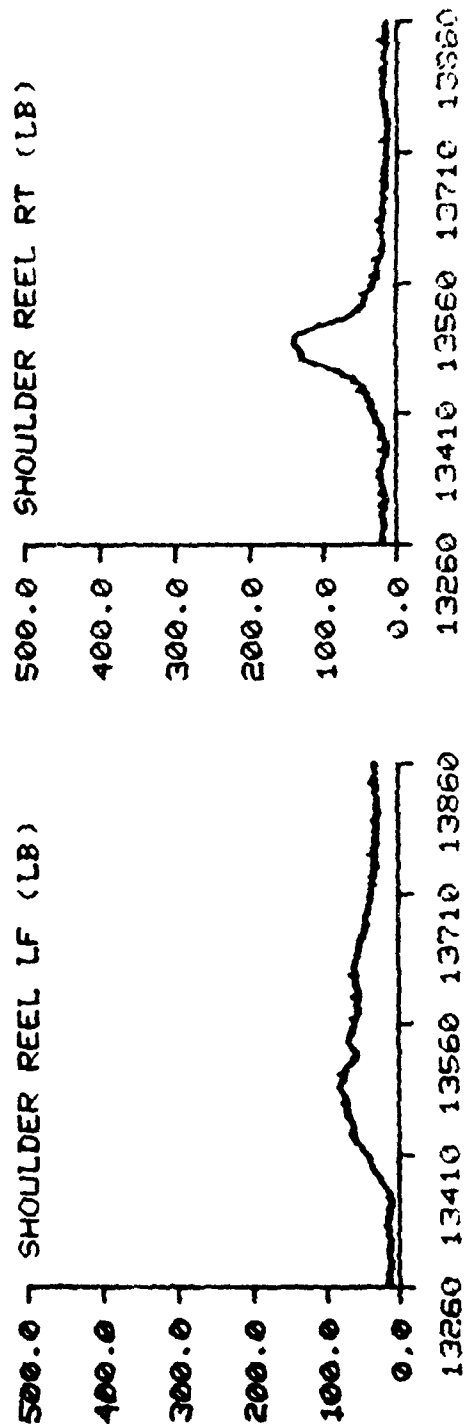
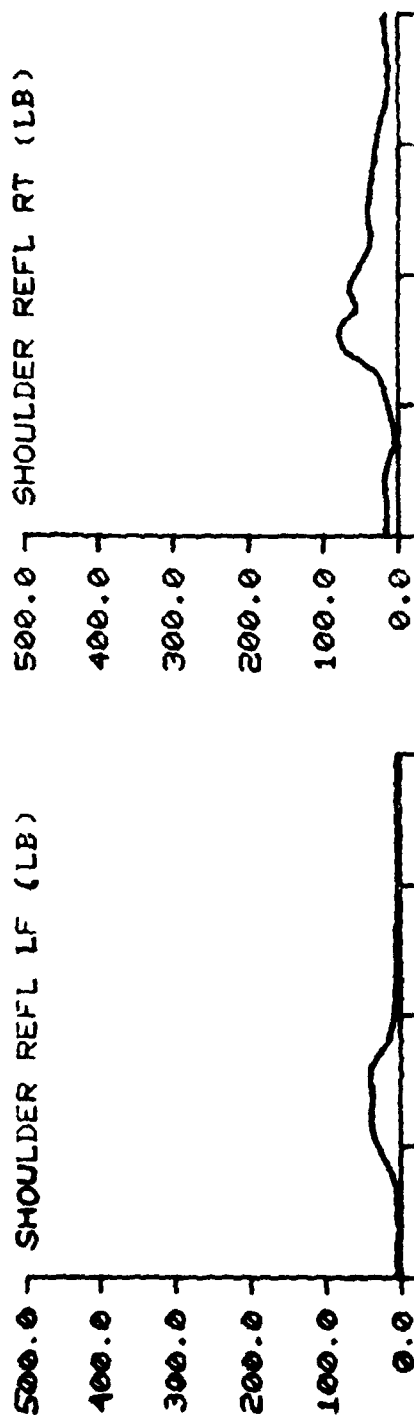


F-111 TEST NO: 474 SUBJECT ID: H-2



TIME IN MILLISECONDS

F-111 TEST NO: 474 SUBJECT ID: H-2

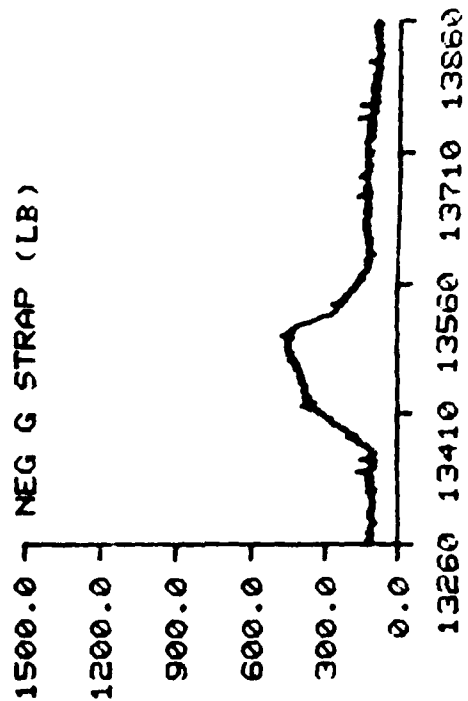
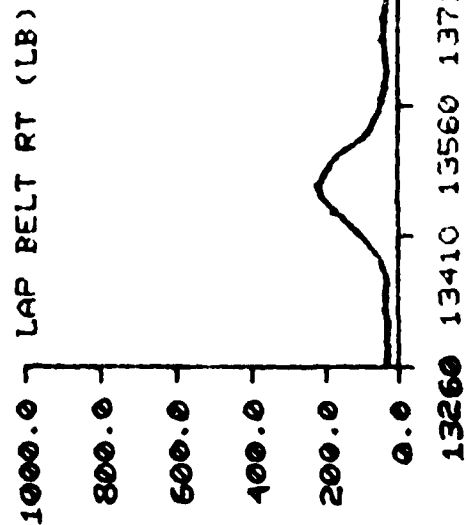
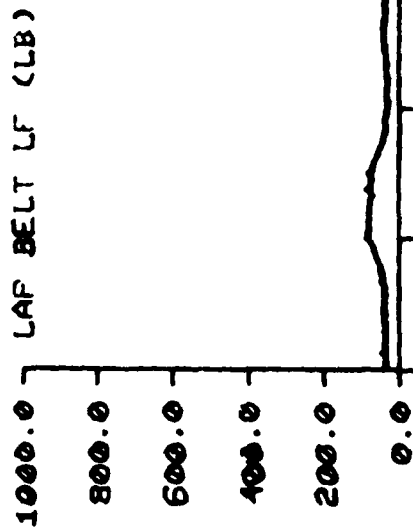


TIME IN MILLISECONDS

F-111

TEST NO: 474

SUBJECT ID: H-2

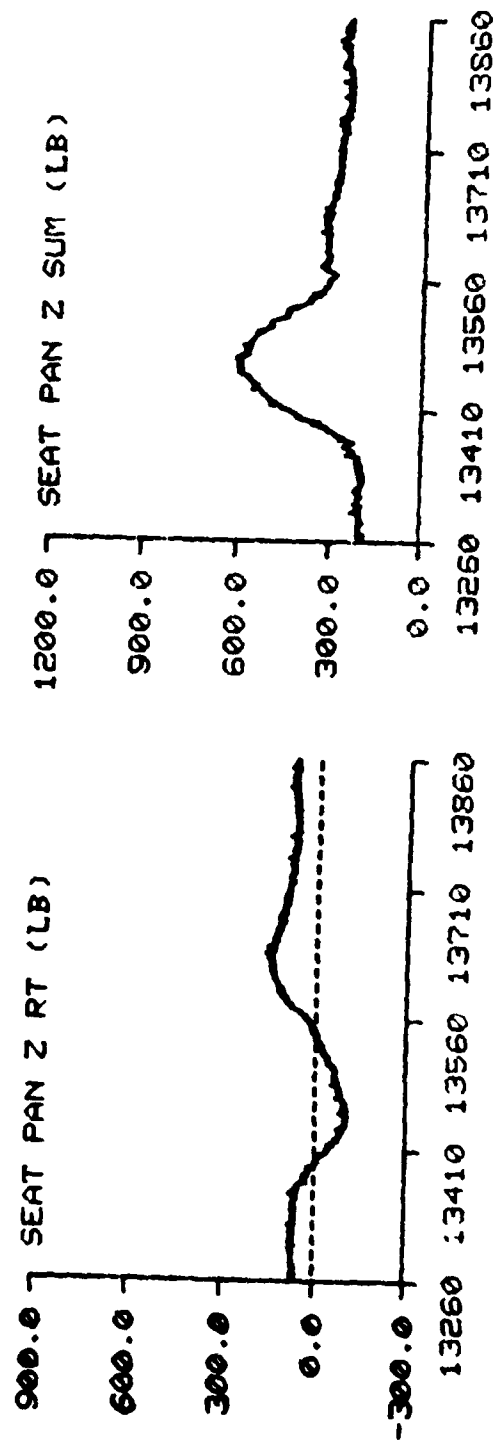
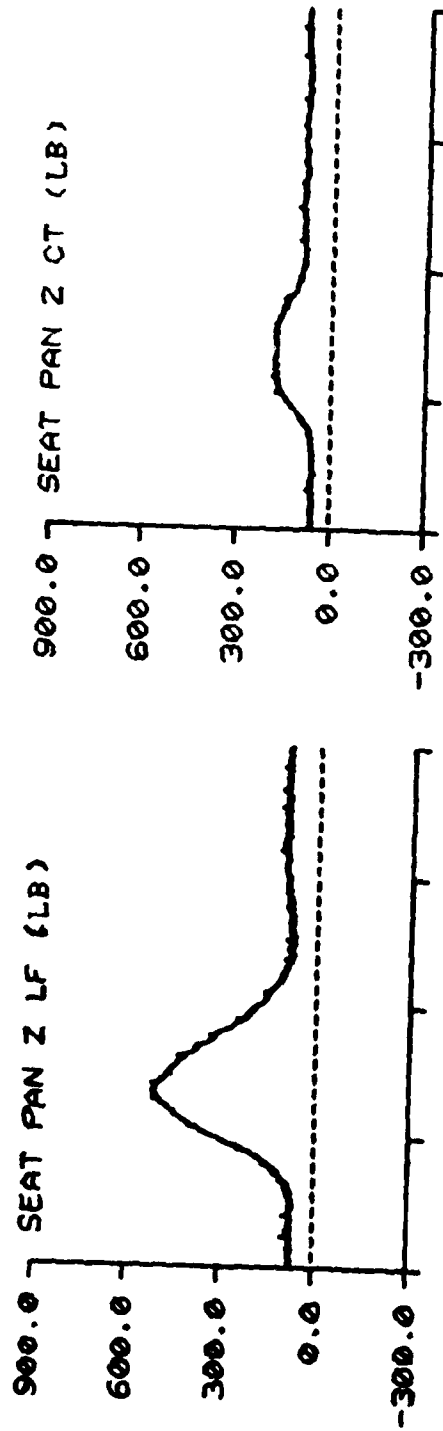


TIME IN MILLISECONDS

F-111

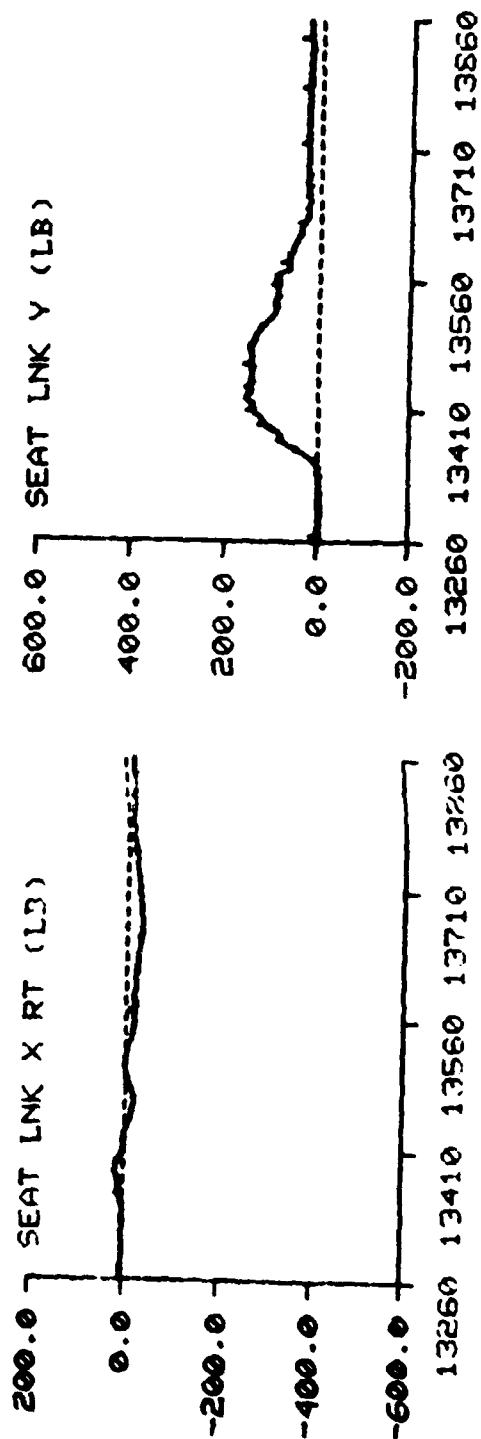
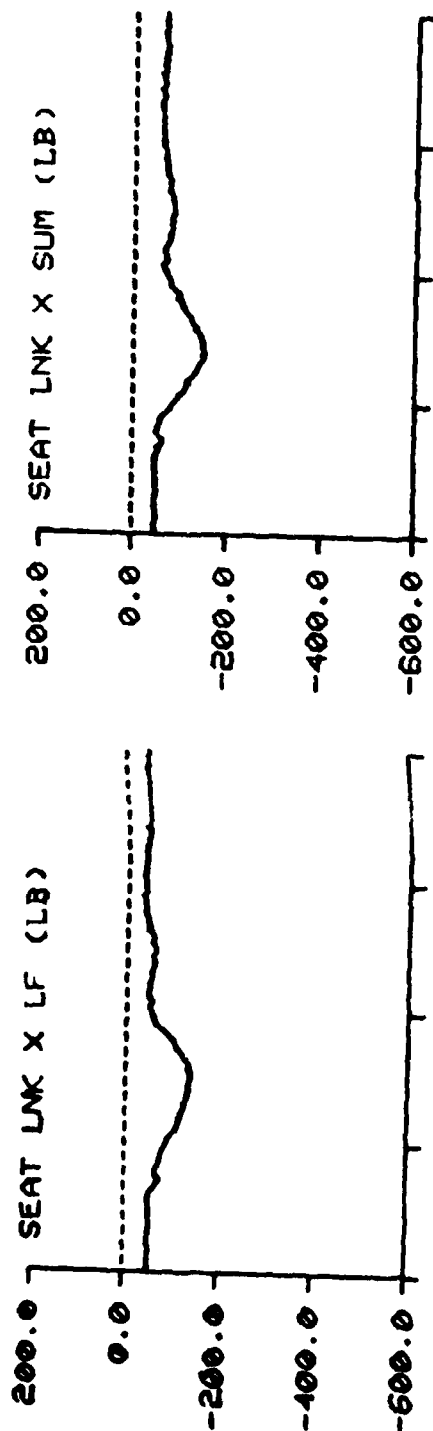
TEST NO: 474

SUBJECT ID: H-2



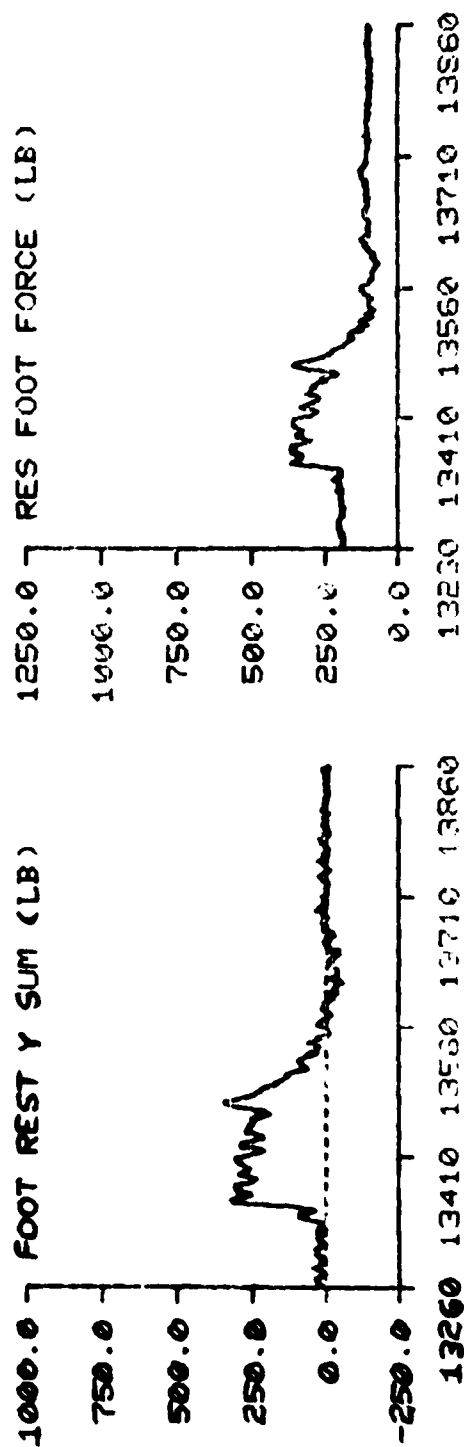
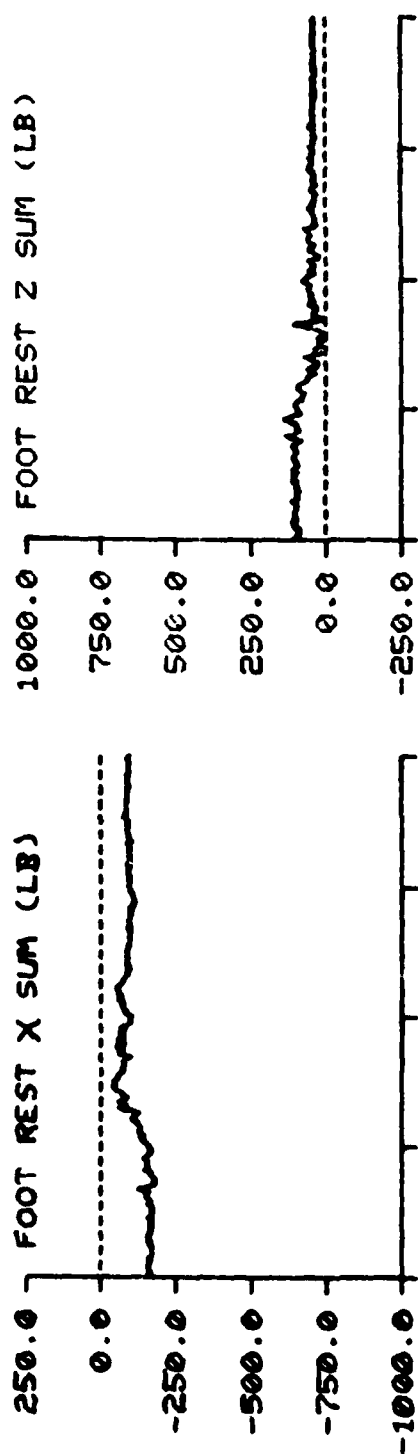
TIME IN MILLISECONDS

F-111 TEST NO: 474 SUBJECT ID: H-2



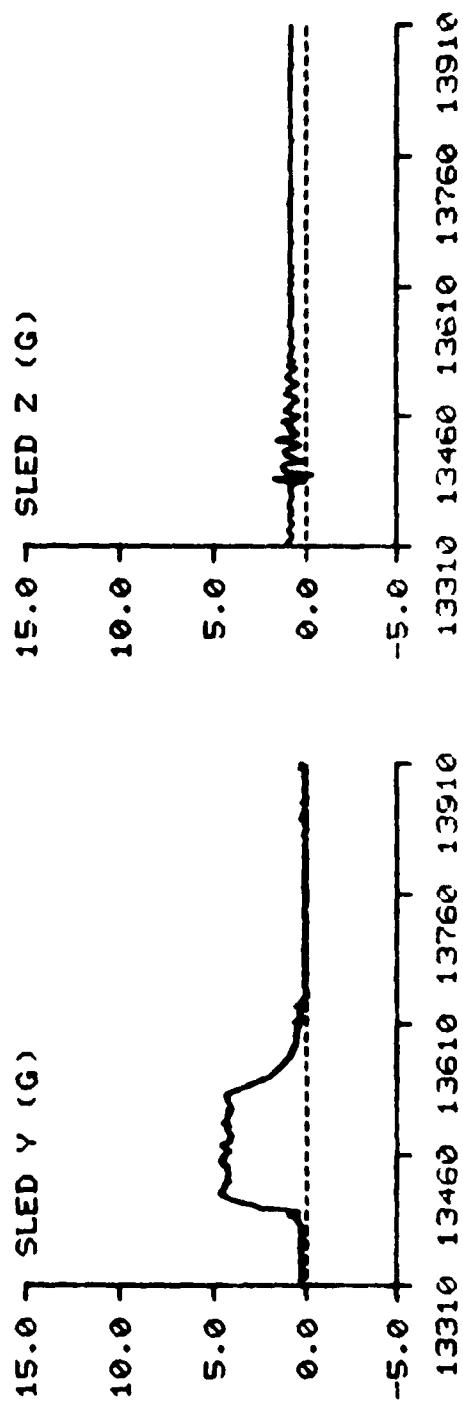
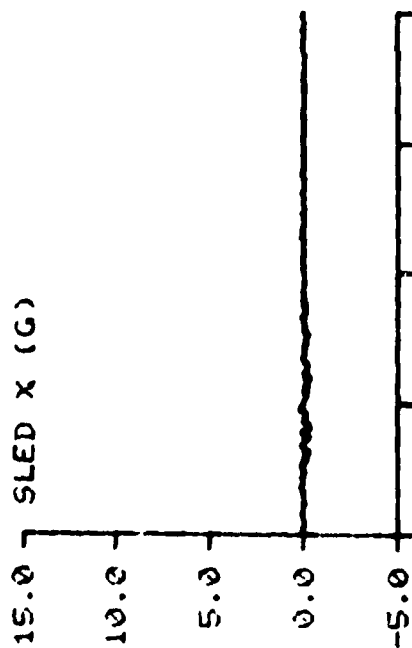
TIME IN MILLISECONDS

F-111 TEST NO: 474 SUBJECT ID: H-2



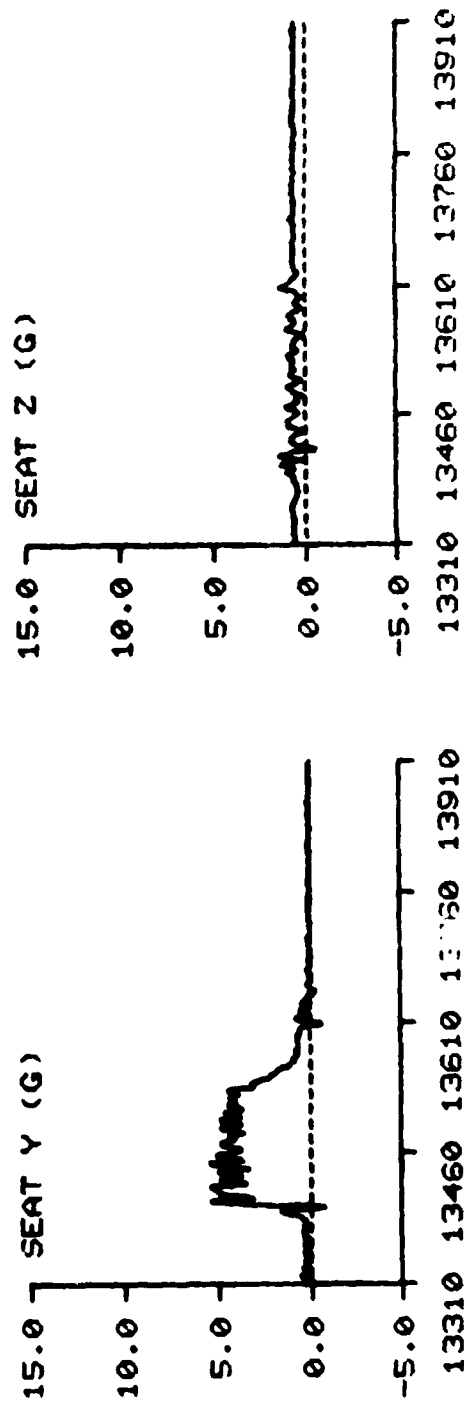
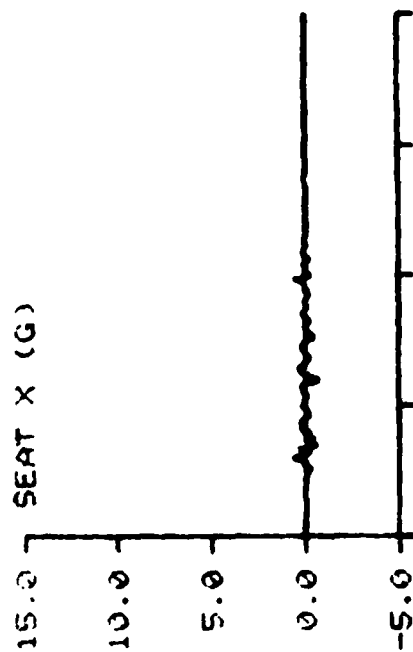
TIME IN MILLISECONDS

F-111 TEST NO: 471 SUBJECT ID: S-3



TIME IN MILLISECONDS

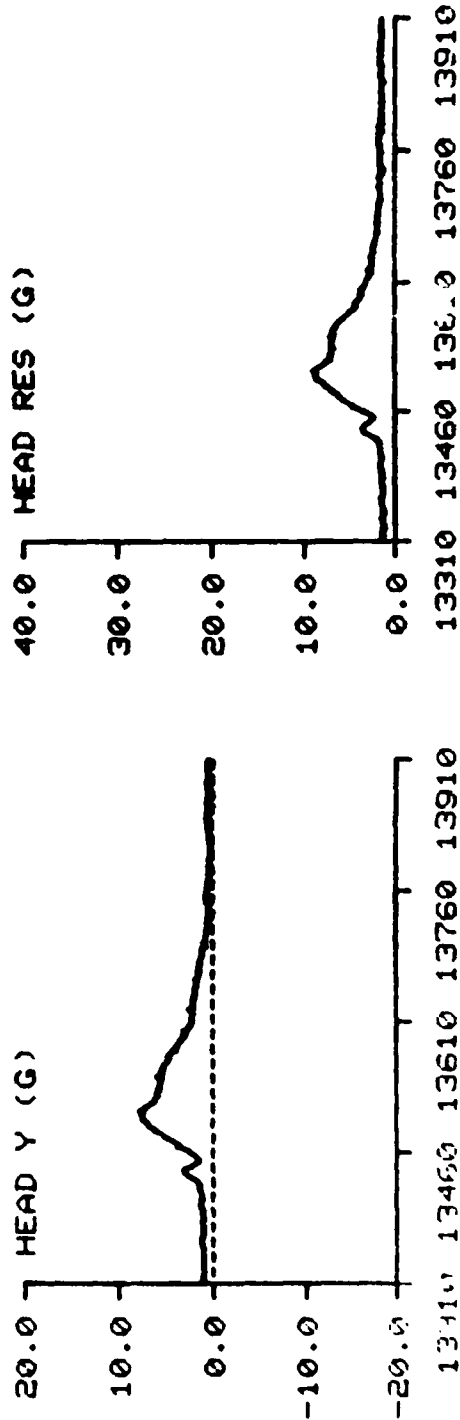
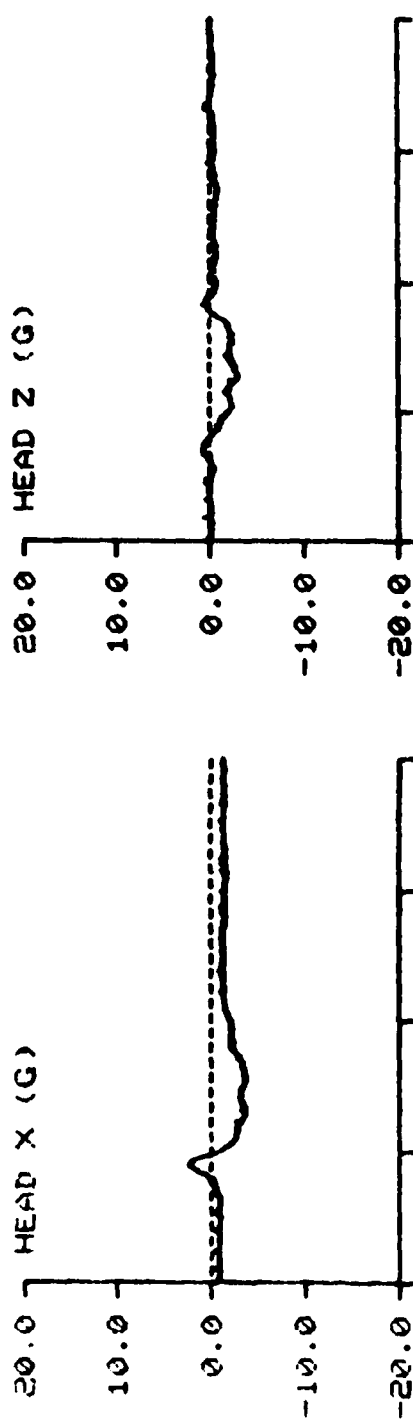
F-111      TEST NO: 471      SUBJECT: S-3



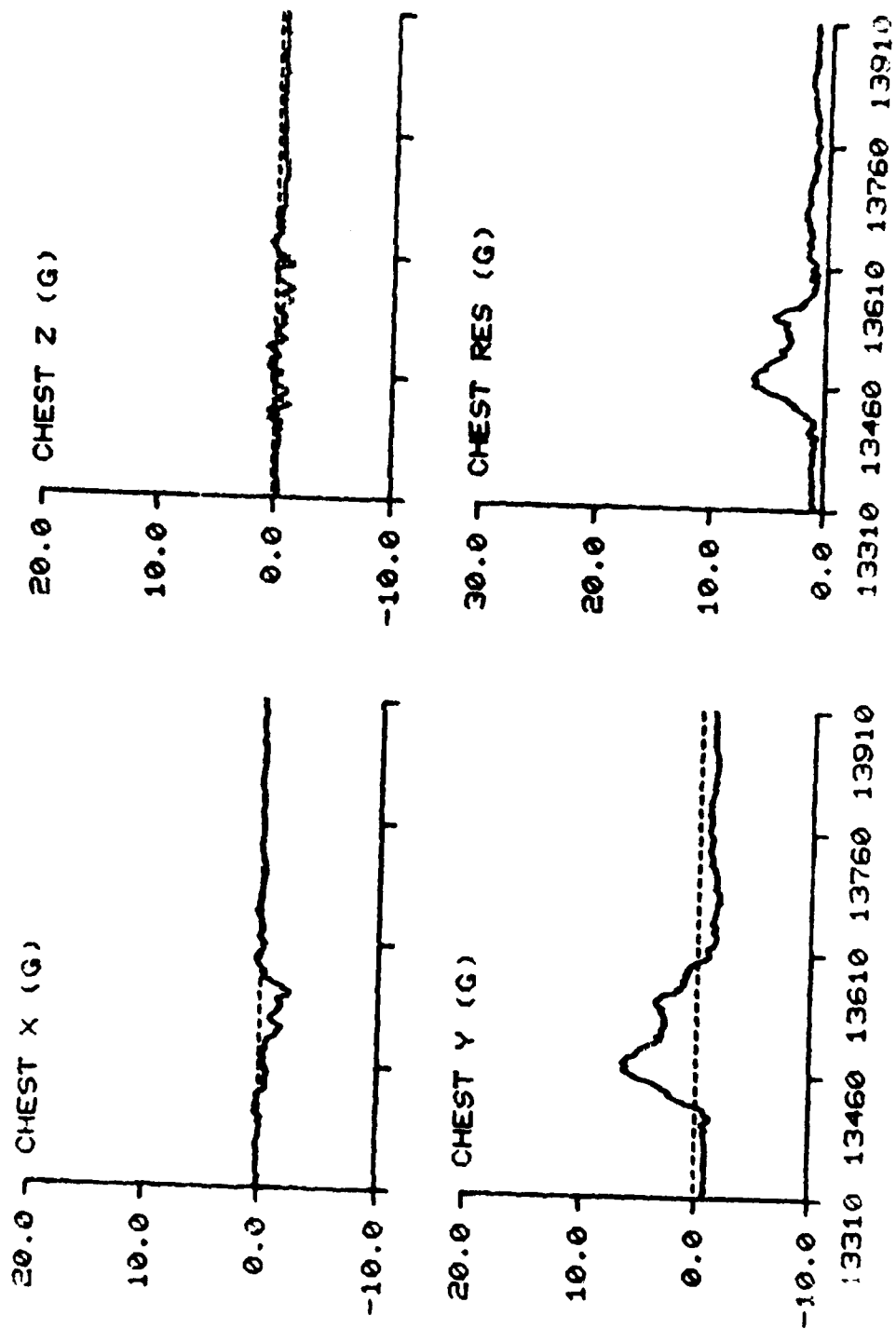
TIME IN MILLISECONDS



F-111 TEST NO: 471 SUBJECT ID: S-3

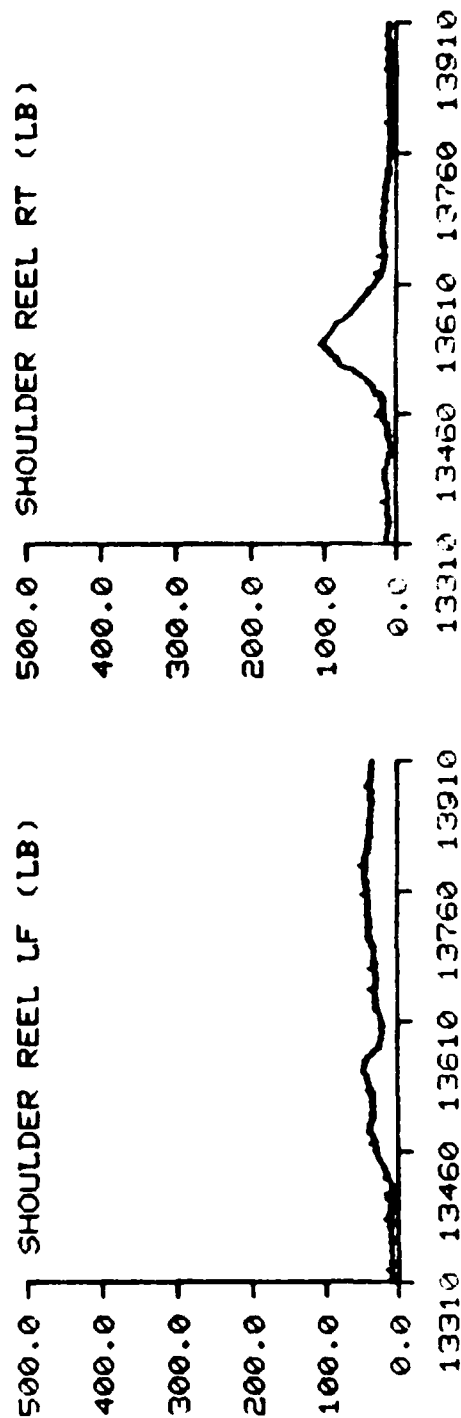
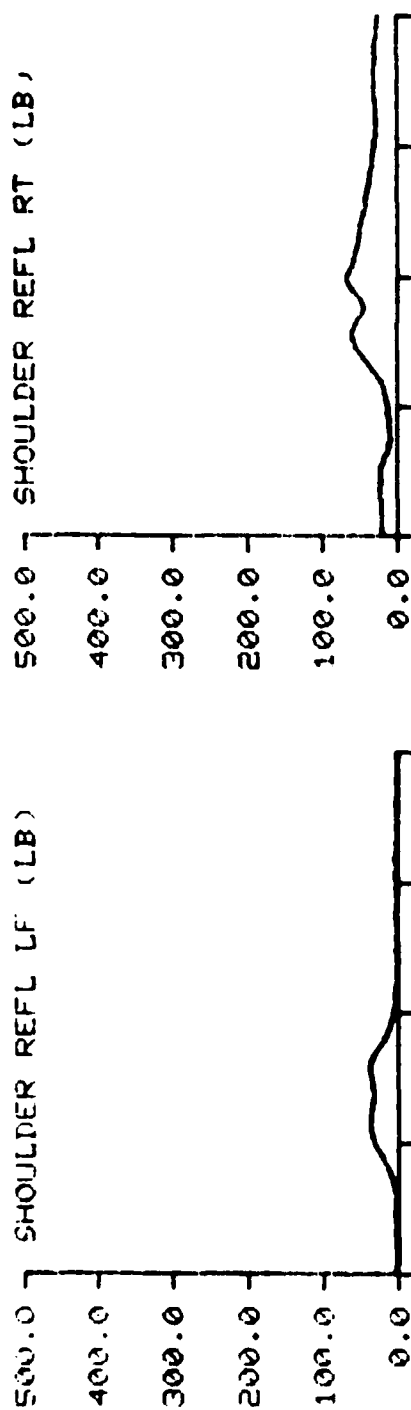


F-111 TEST NO. 471 SUBJECT ID: S-3



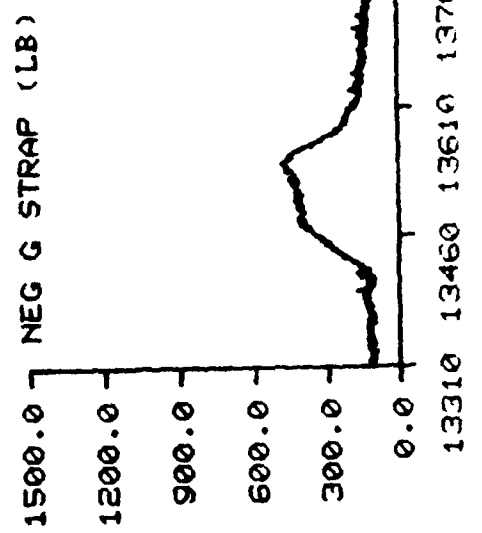
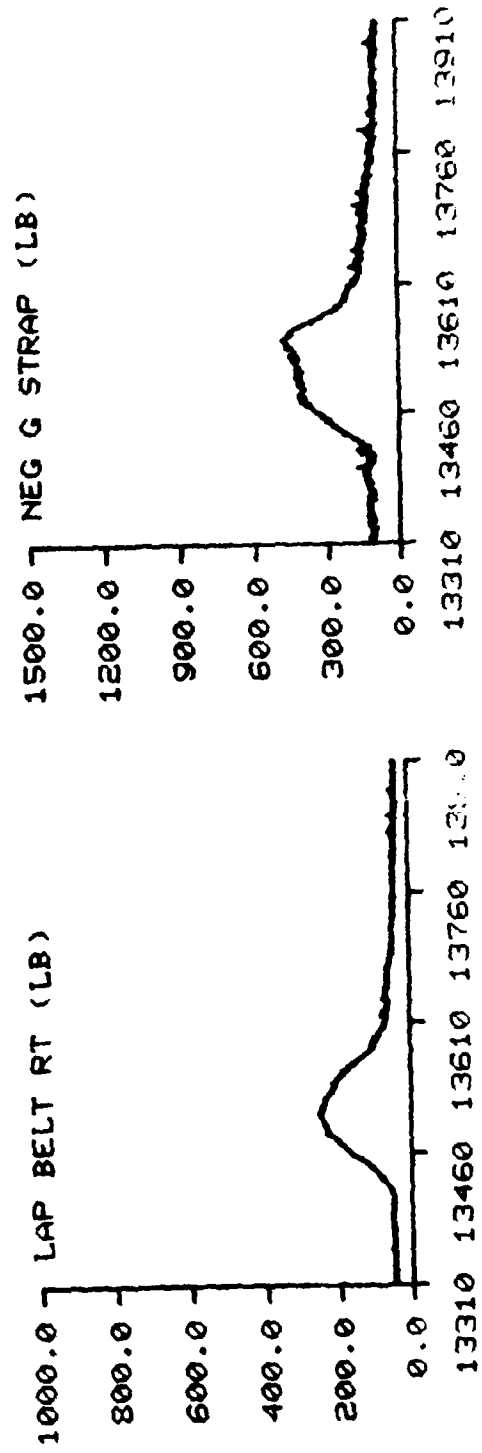
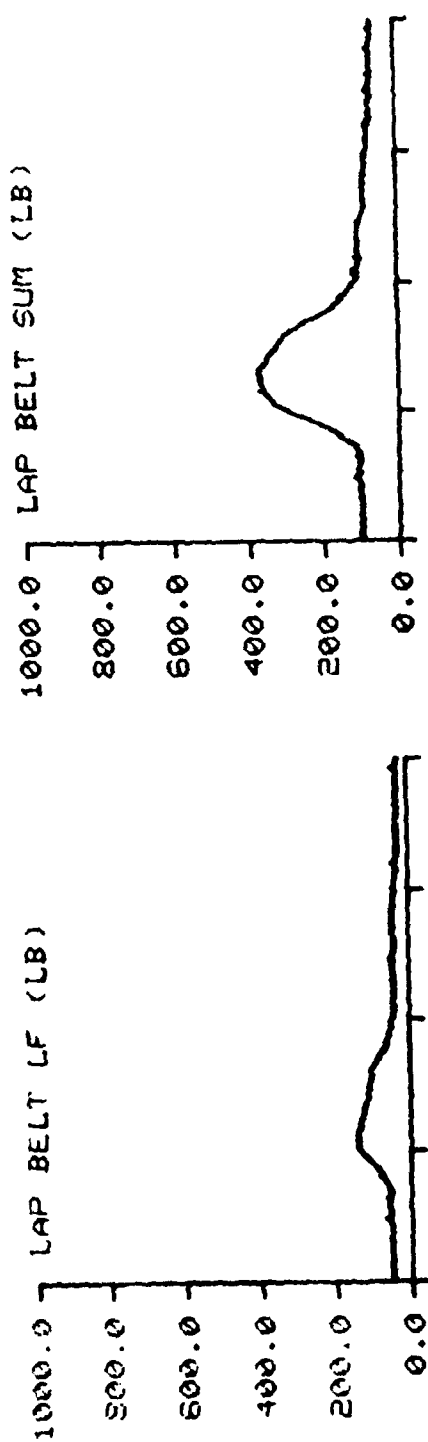
TIME IN MILLISECONDS

F-111 TEST NO: 471 SUBJECT ID: S-3



TIME IN MILLISECONDS

F-111 TEST NO: 471 SUBJECT ID: S-3

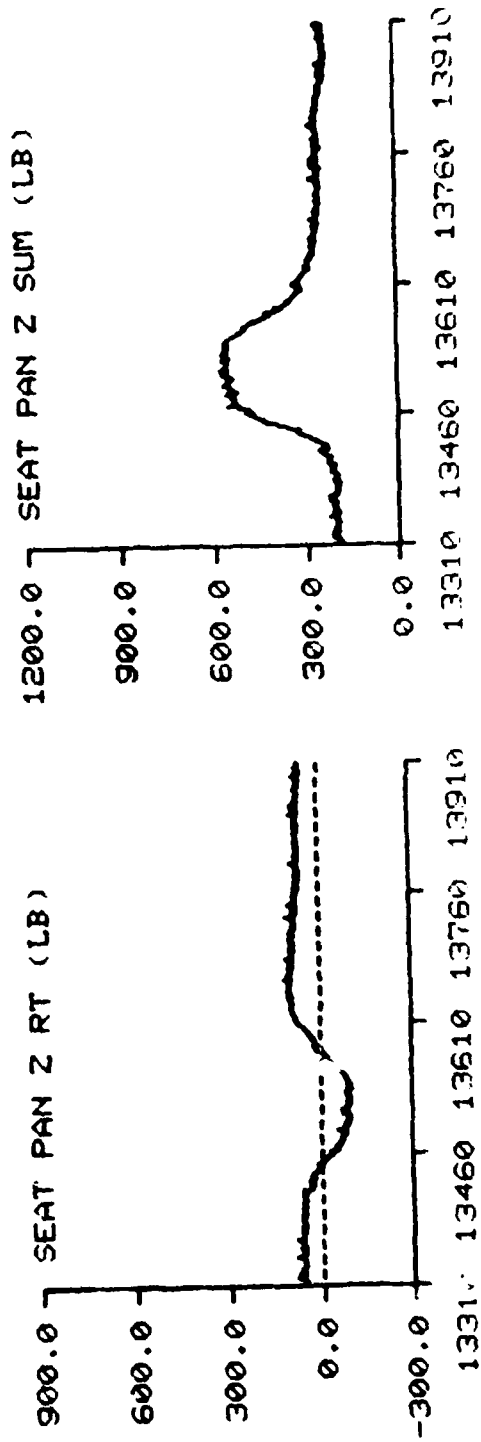
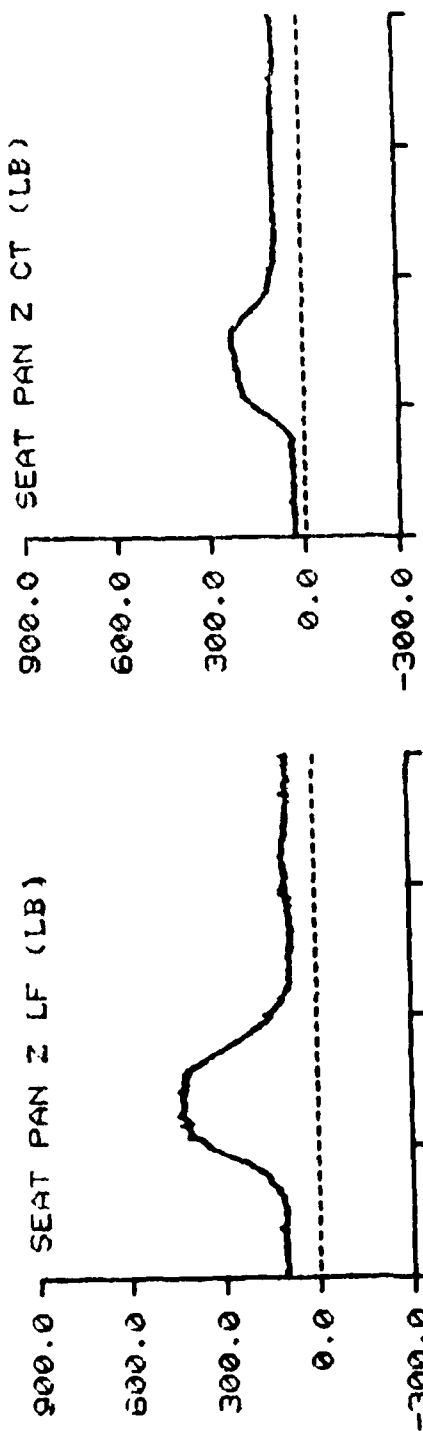


TIME IN MILLISECONDS

F-111

TEST NO: 473

SUBJECT ID: S-3

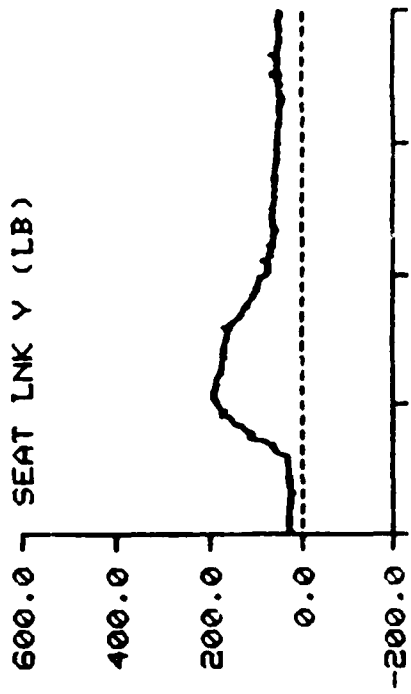
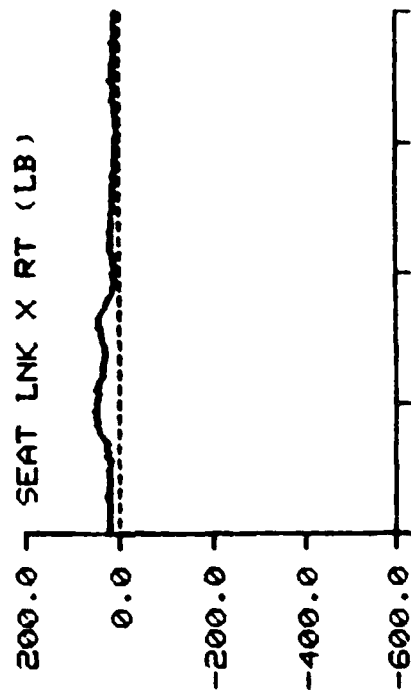
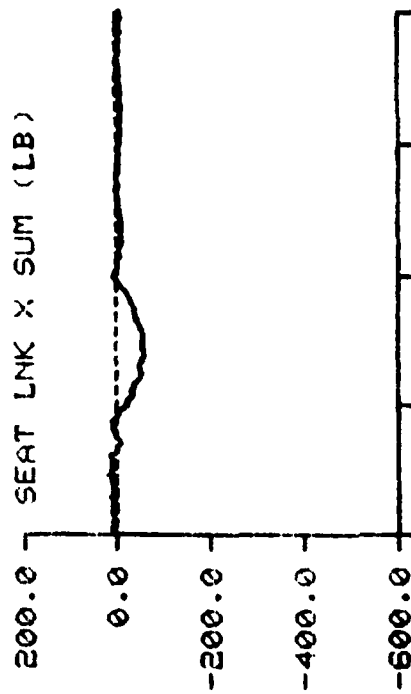
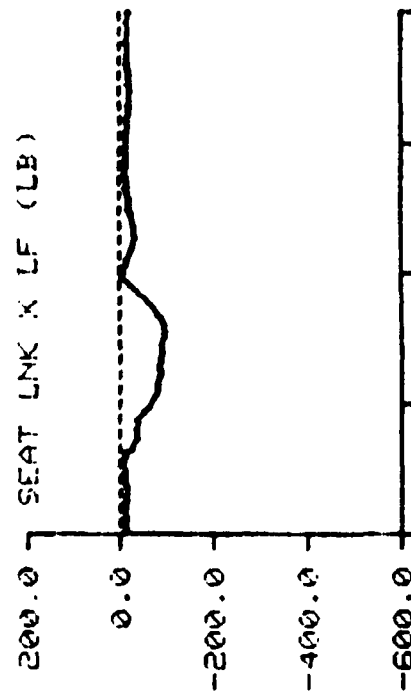


TIME IN MILLISECONDS

F-111

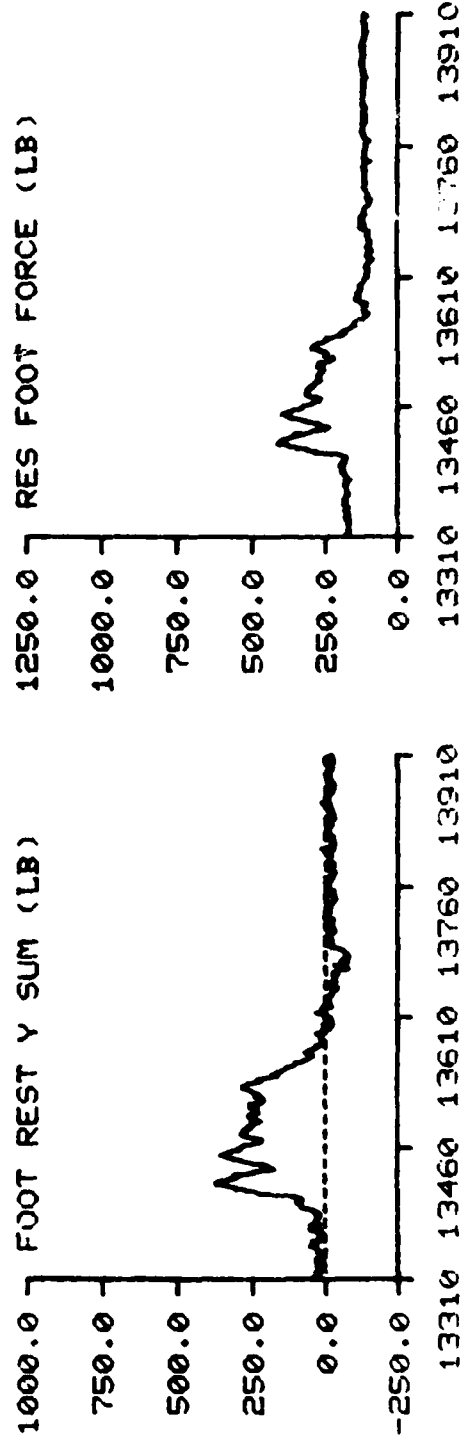
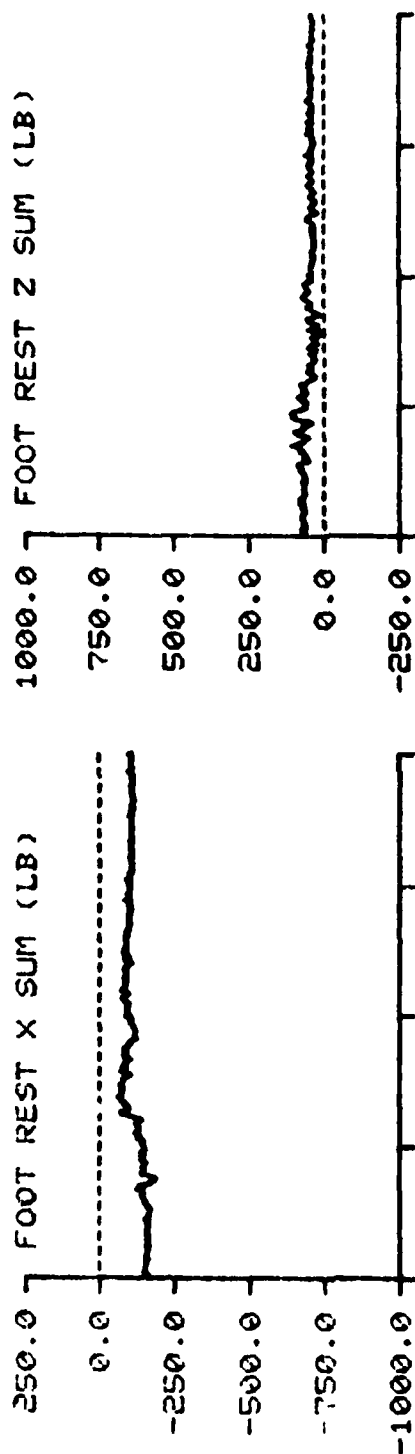
TEST NO: 471

SUBJECT ID: S-3



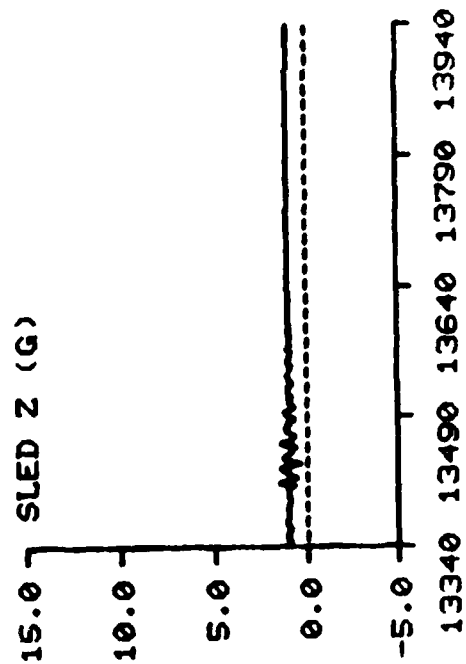
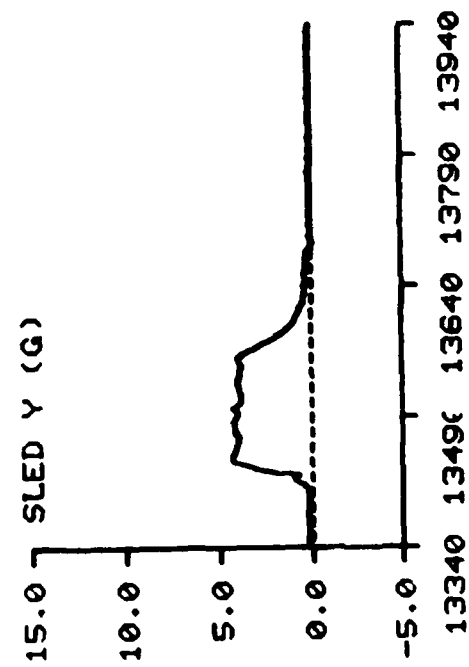
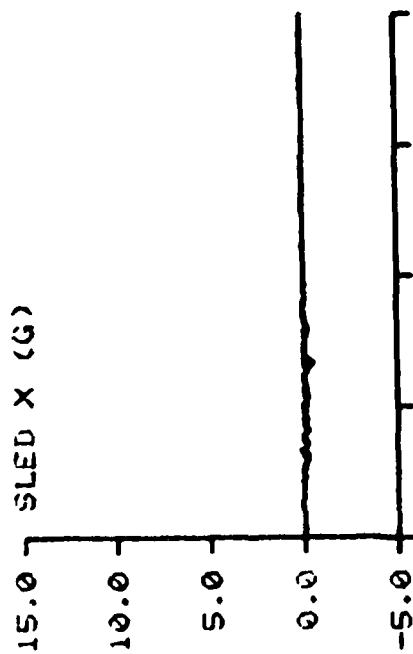
TIME IN MILLISECONDS

F-111 TEST NO: 471 SUBJECT ID: S-3



TIME IN MILLISECONDS

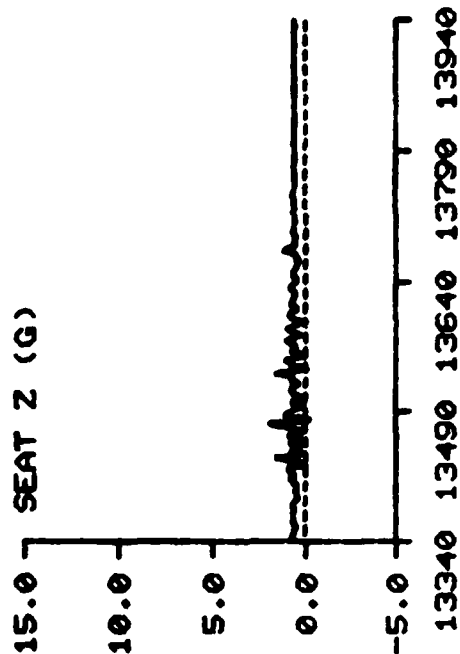
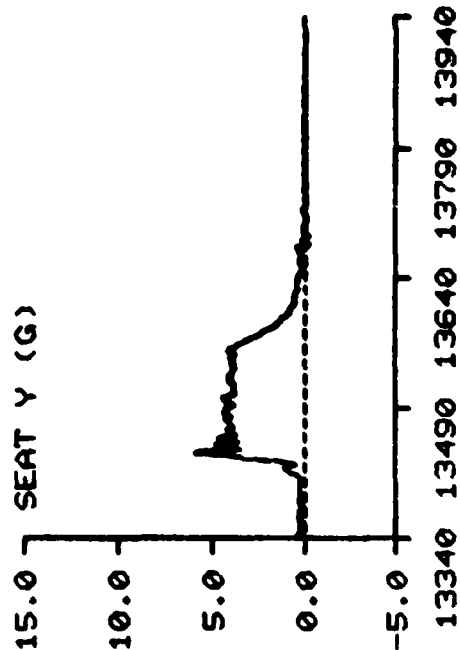
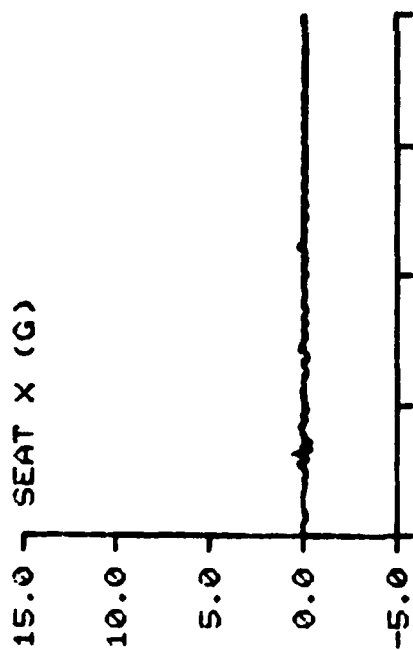
F-111 TEST NO: 477 SUBJECT ID: W-1



TIME IN MILLISECONDS



F-111 TEST NO: 477 SUBJECT ID: W-1

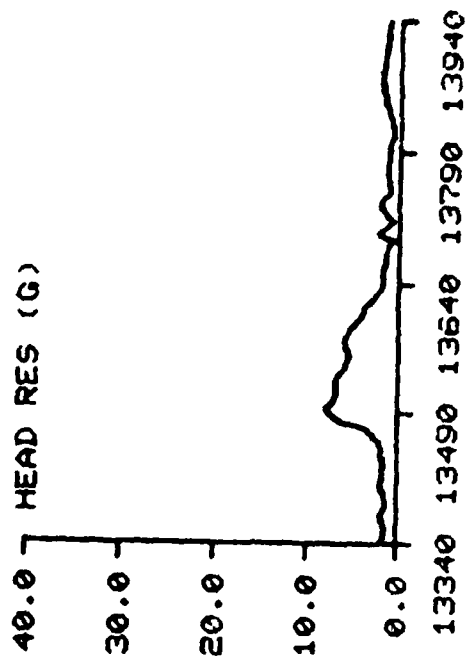
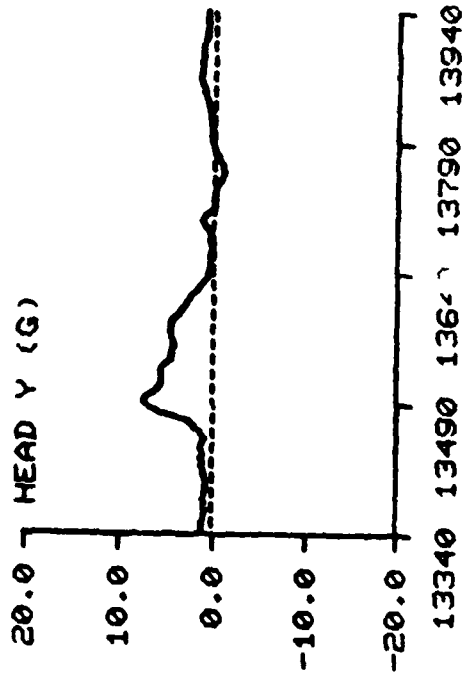
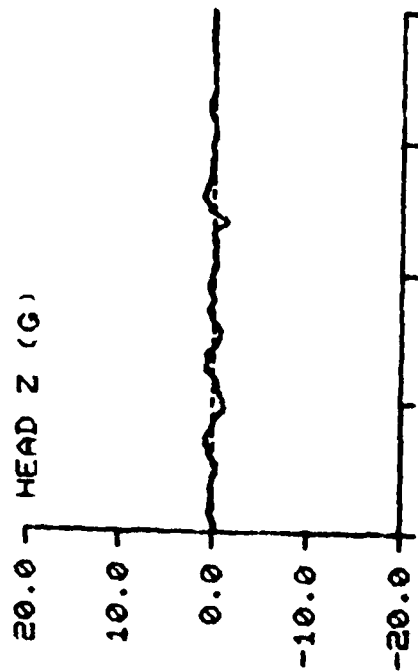
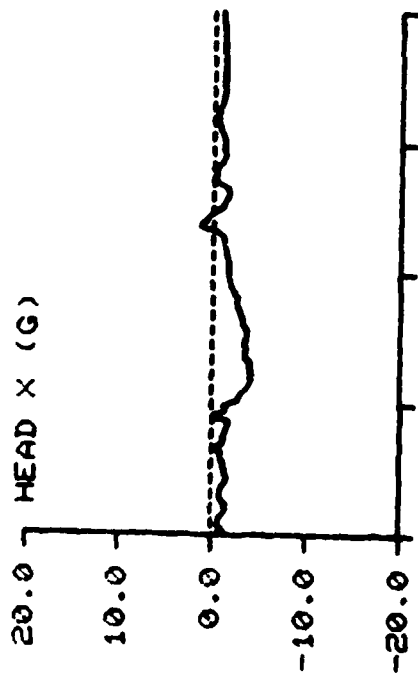


TIME IN MILLISECONDS

F-111

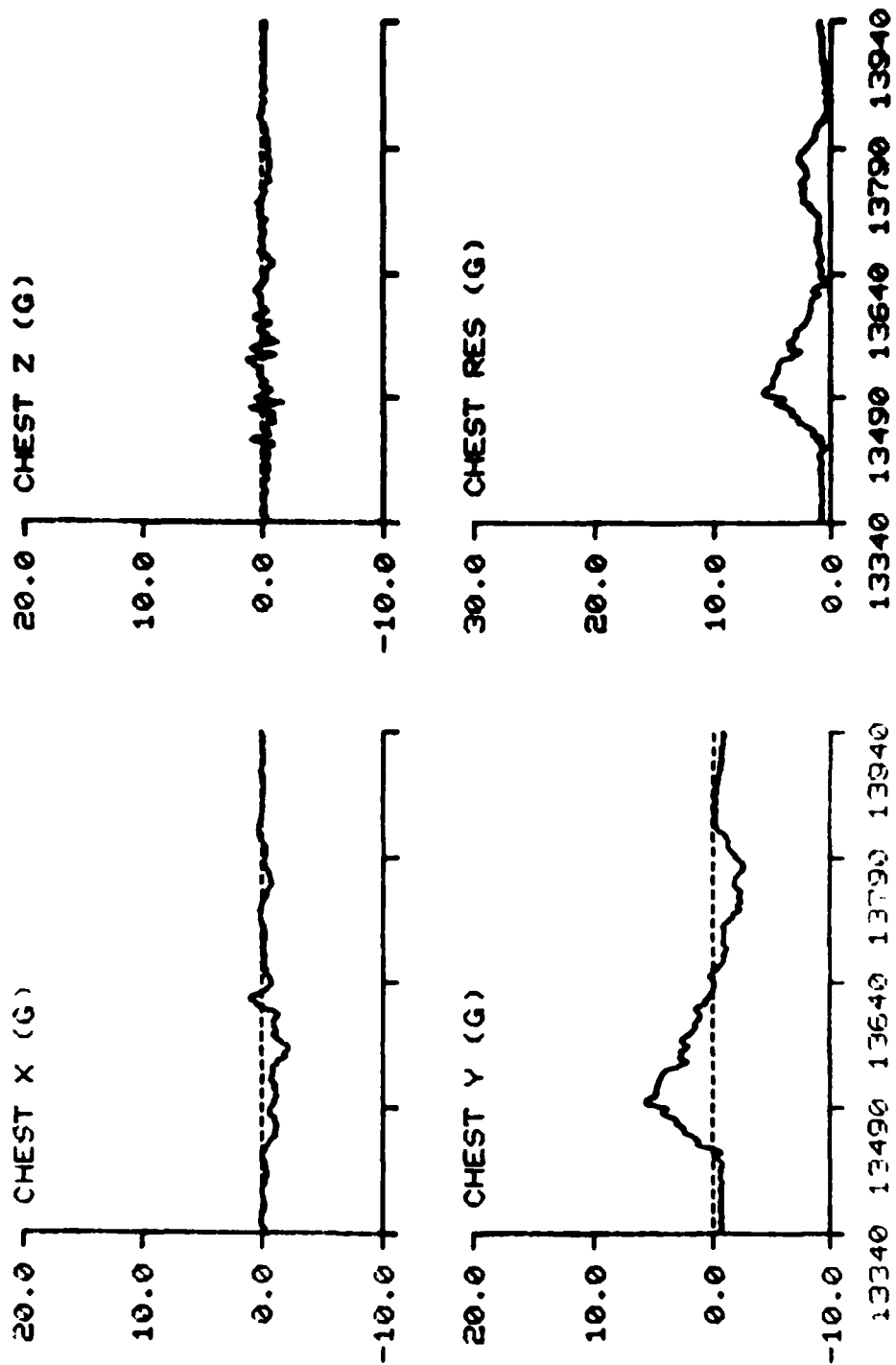
TEST NO: 477

SUBJECT ID: W-1



TIME IN MILLISECONDS

F-111, TEST NO: 477 SUBJECT ID: W-1

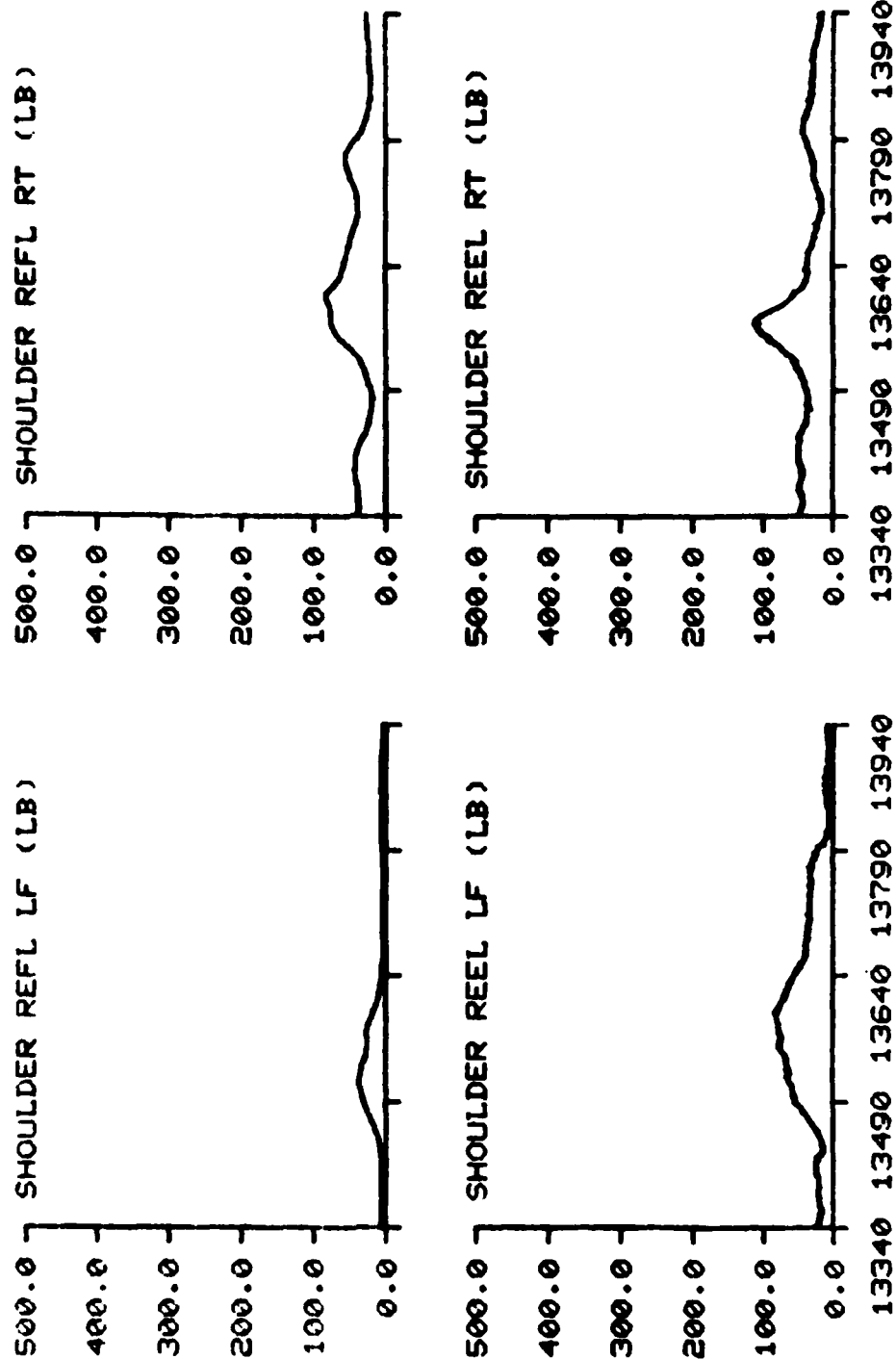


TIME IN MILLISECONDS

F-111

TEST NO: 477

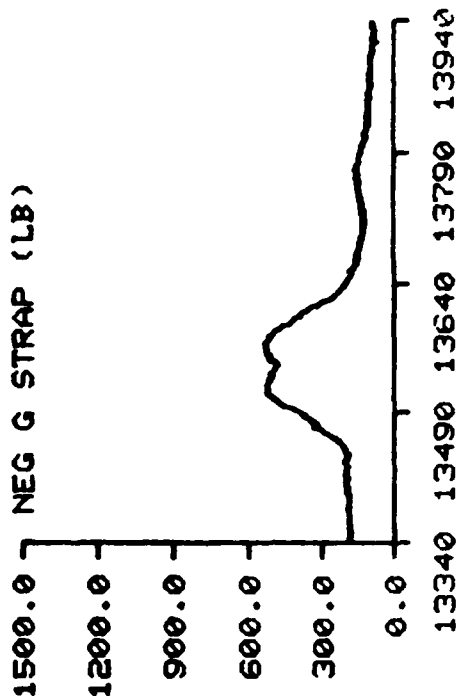
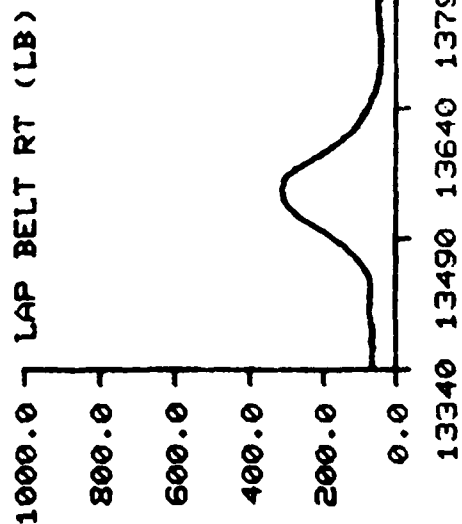
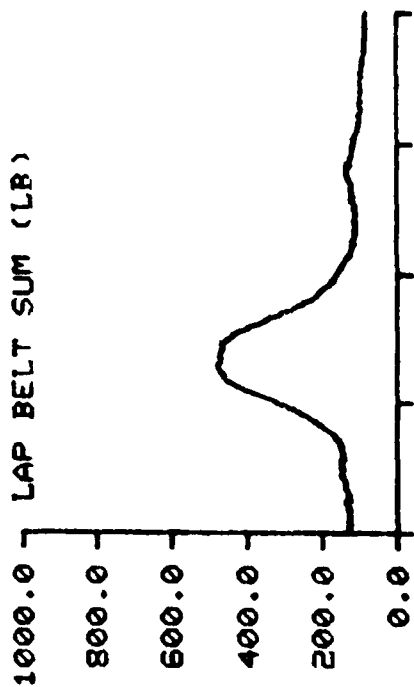
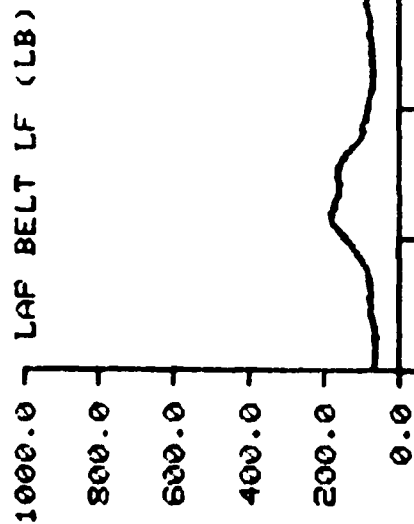
SUBJECT ID: W-1



F-111

TEST NO: 477

SUBJECT ID: W-1

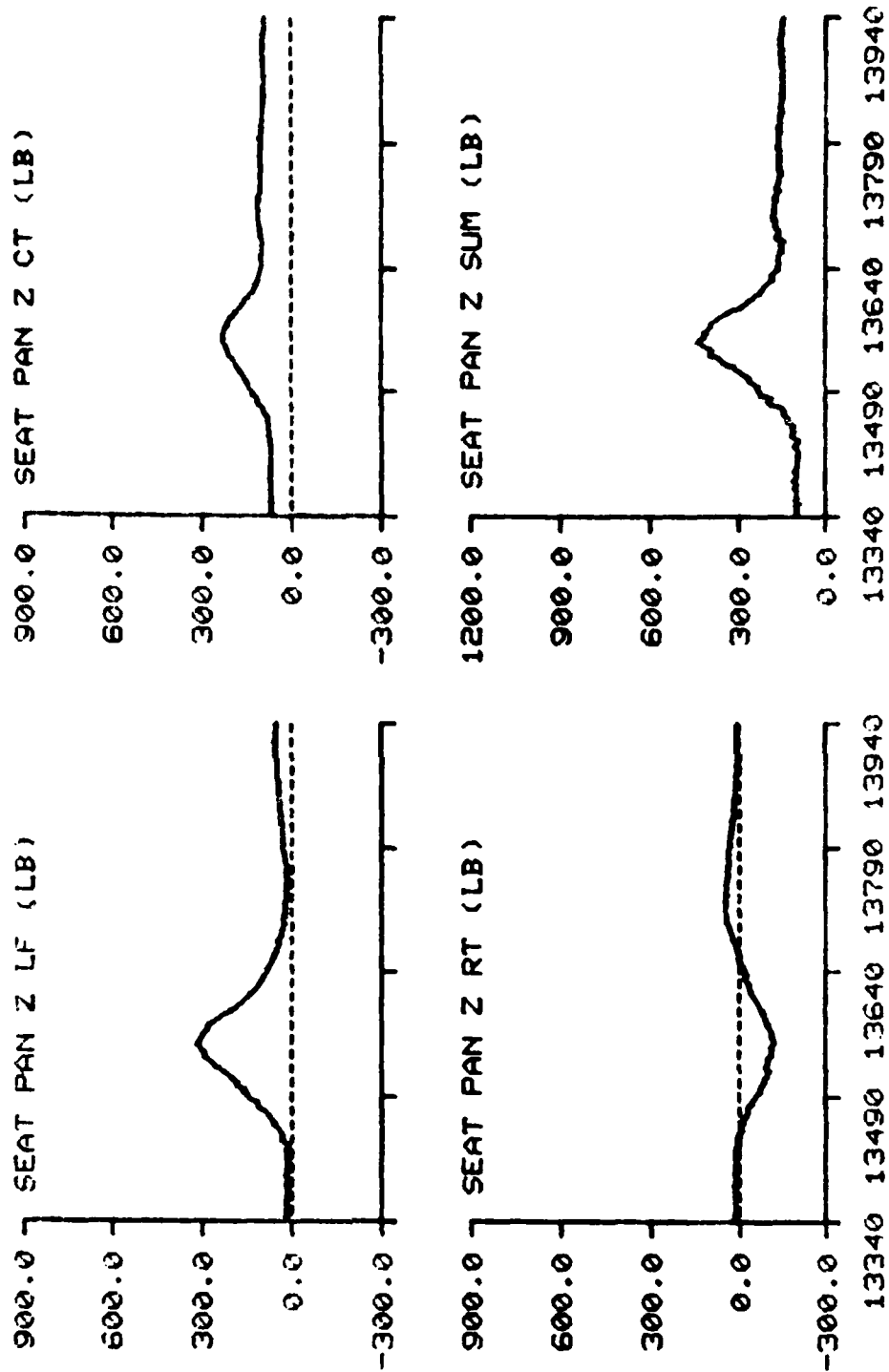


TIME IN MILLISECONDS

F-111

TEST NO: 477

SUBJECT ID: W-1

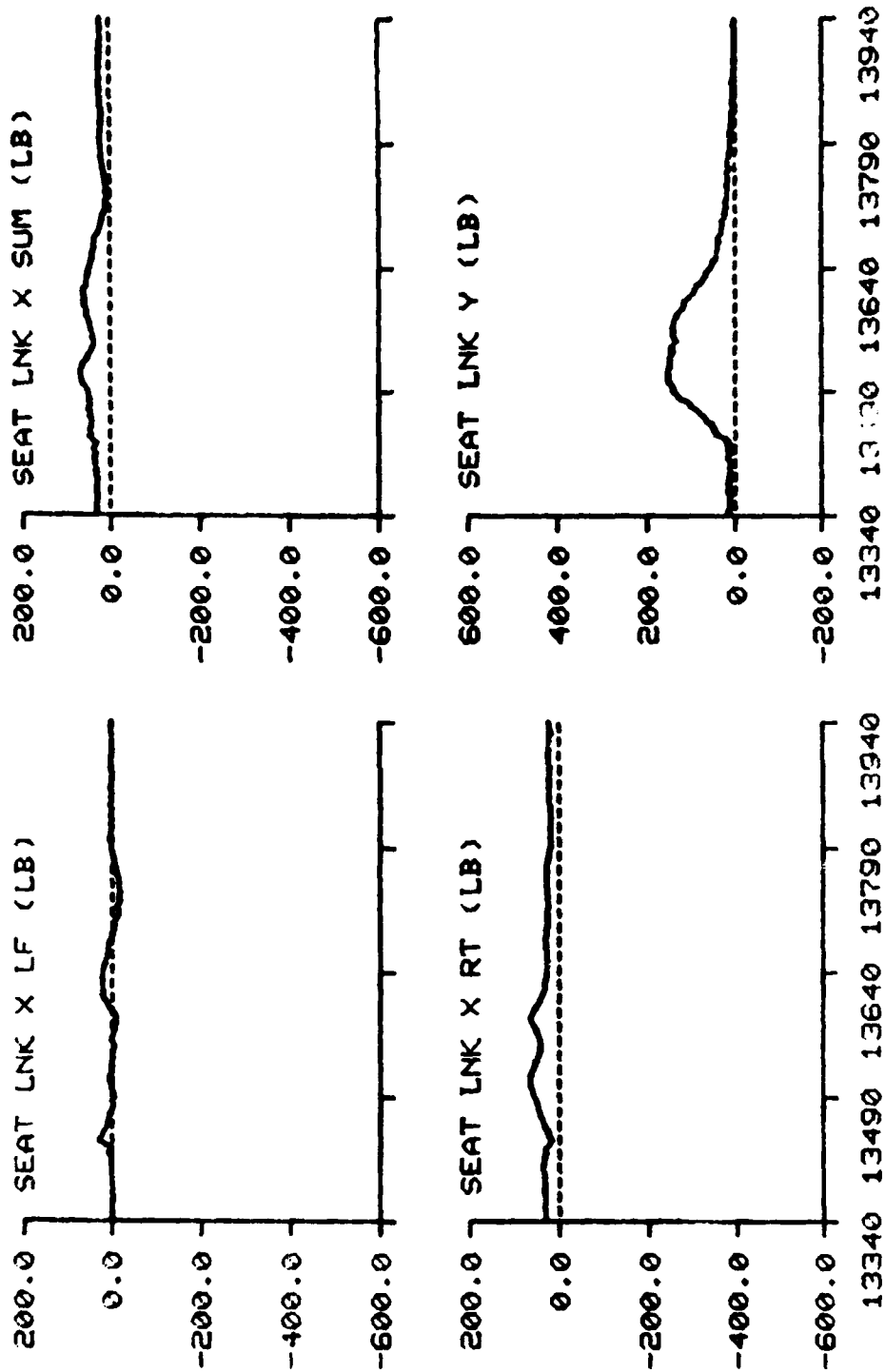


TIME IN MILLISECONDS

F-111

TEST NO: 477

SUBJECT ID: W-1

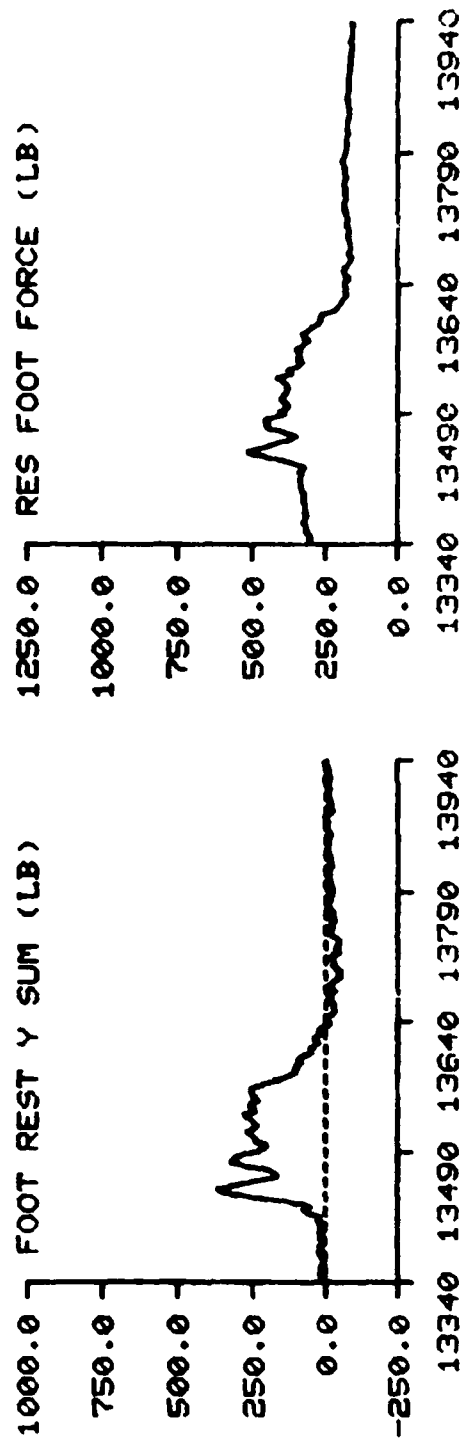
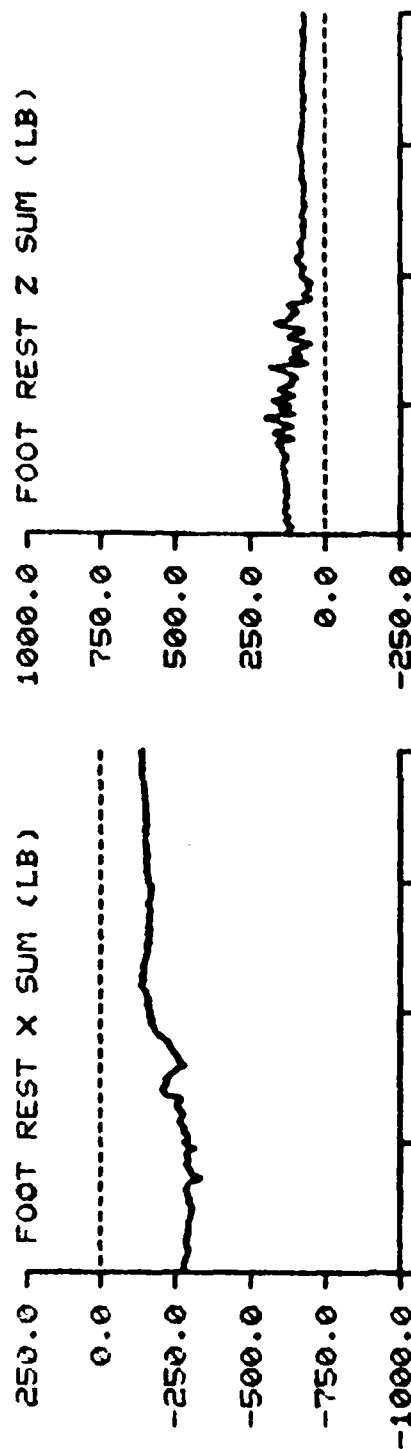


TIME IN MILLISECONDS

F-111

TEST NO: 477

SUBJECT ID: W-1



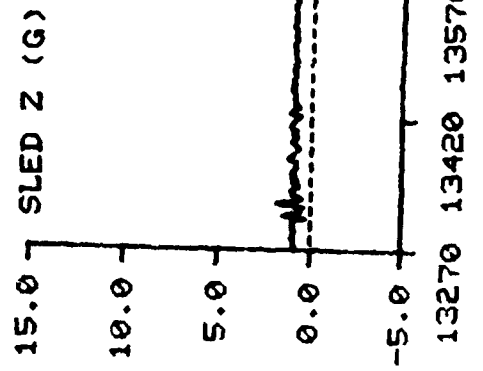
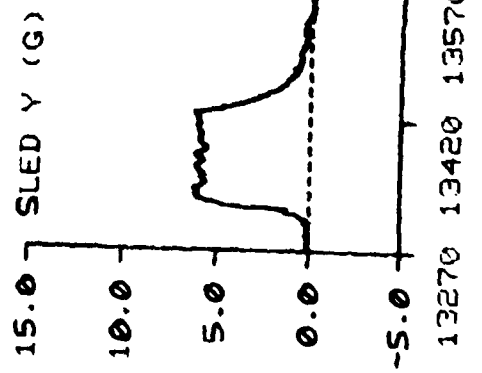
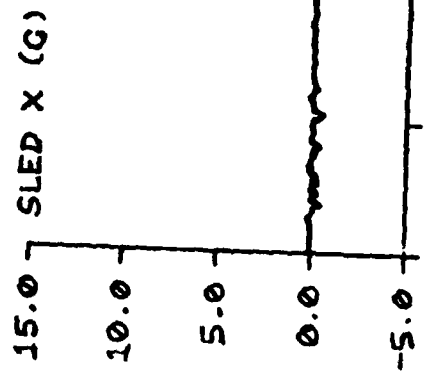
TIME IN MILLISECONDS



F-111

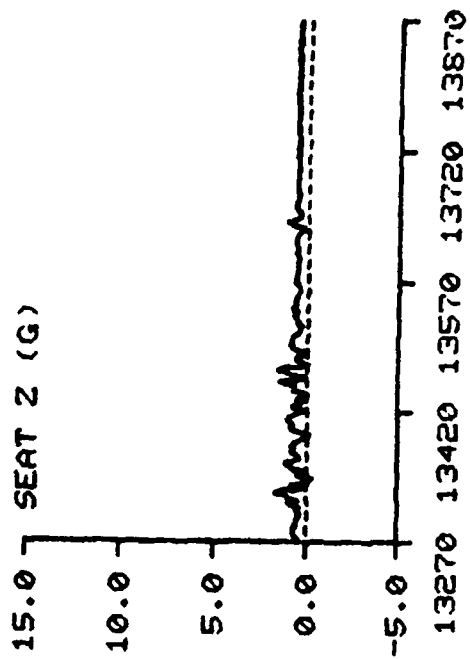
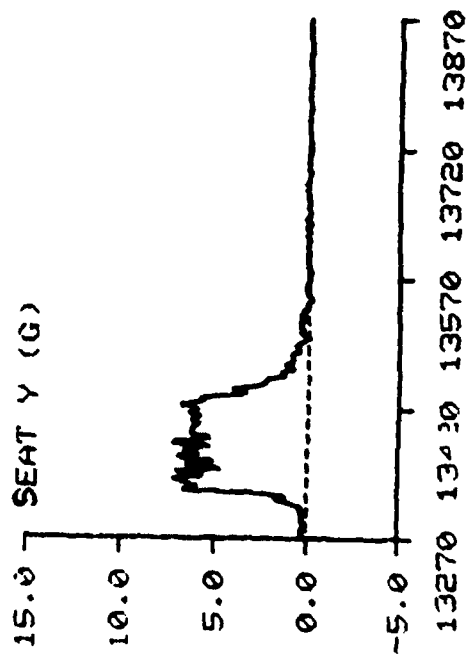
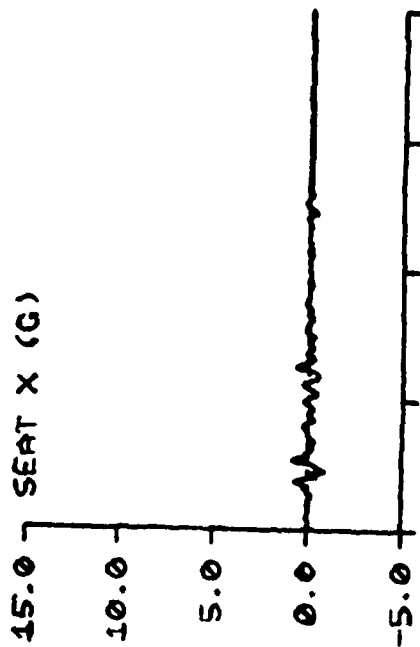
TEST NO: 463

SUBJECT ID: J-1



TIME IN MILLISEC. DS

F-111      TEST NO: 463      SUBJECT ID: J-1

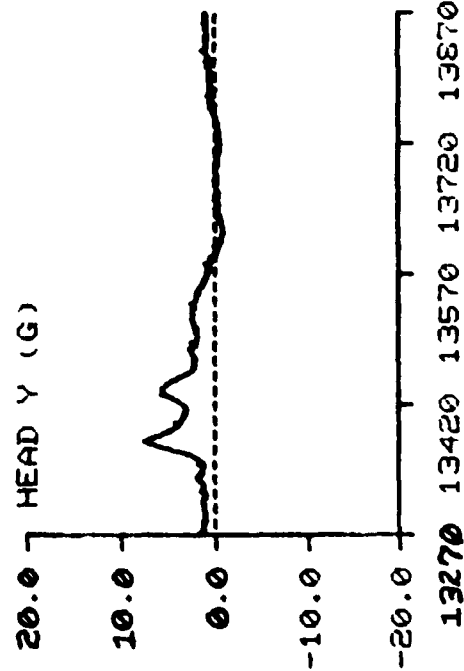
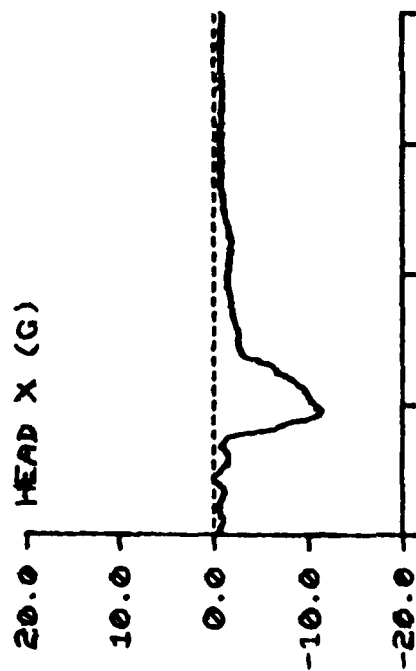
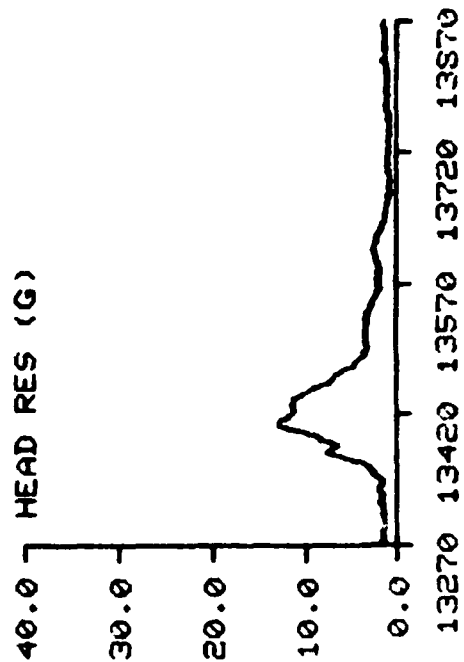
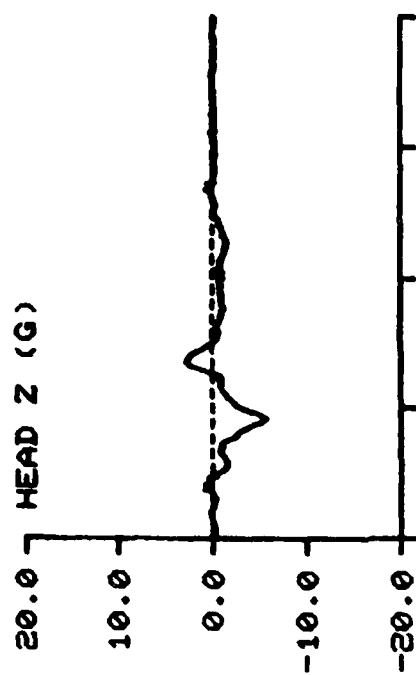


TIME IN MILLISECONDS

F-111

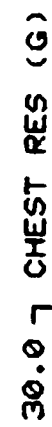
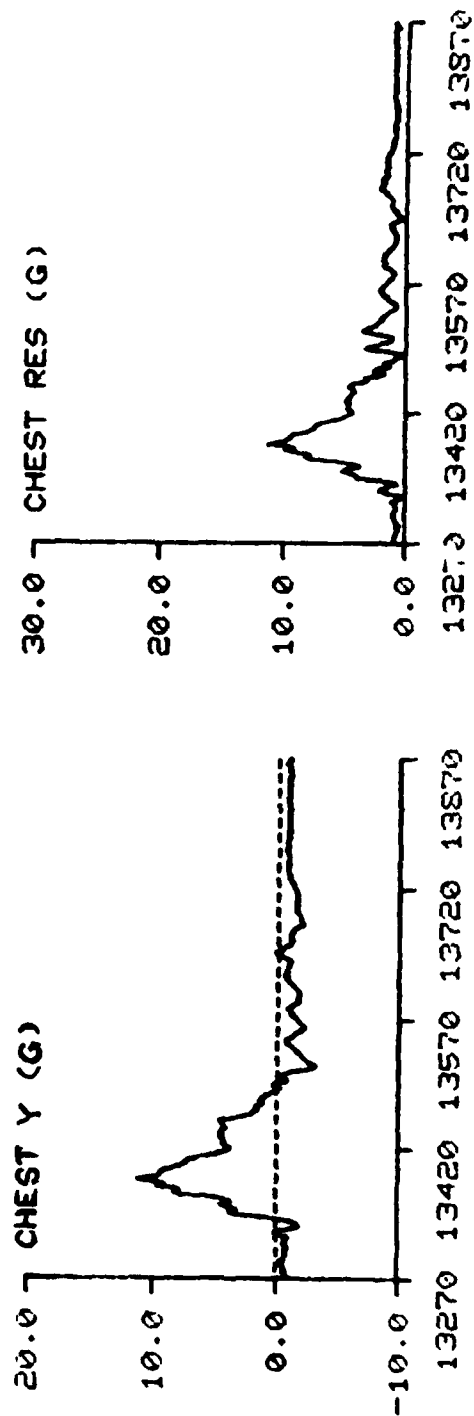
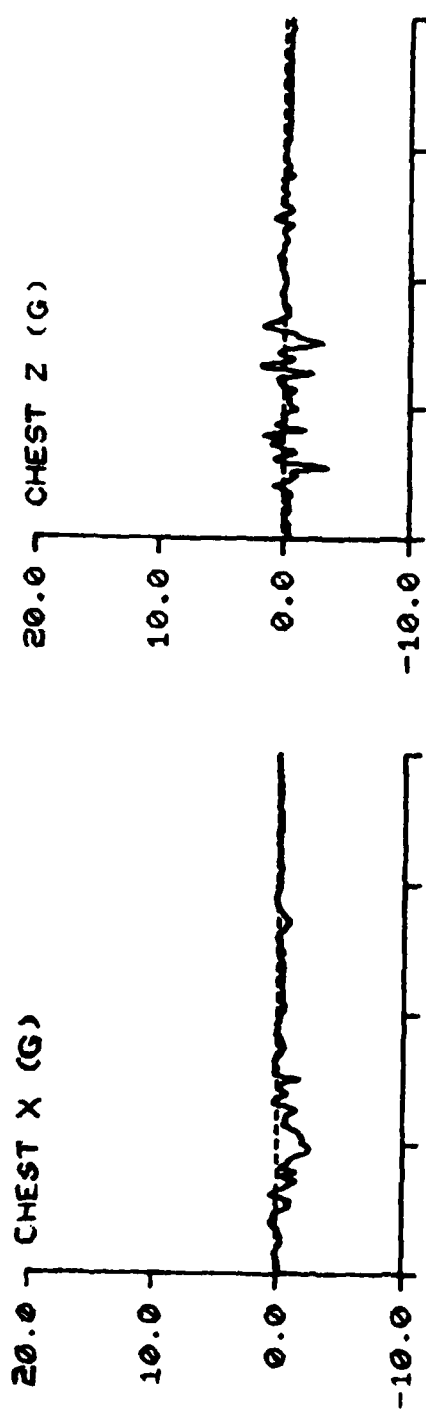
TEST NO: 463

SUBJECT ID: J-1



TIME IN MILLISECONDS

F-111 TEST NO: 453 SUBJECT ID: J-1



TIME IN MILLISECOND

F-111

TEST NO: 463

SUBJECT ID: J-1

500.0 SHOULDER REFL LF (LB)

400.0

300.0

200.0

100.0

0.0

500.0 SHOULDER REFL RT (LB)

400.0

300.0

200.0

100.0

0.0

500.0 SHOULDER REEL LF (LB)

400.0

300.0

200.0

100.0

0.0

500.0 SHOULDER REEL RT (LB)

400.0

300.0

200.0

100.0

0.0

13270 13420 13570 13720 13870

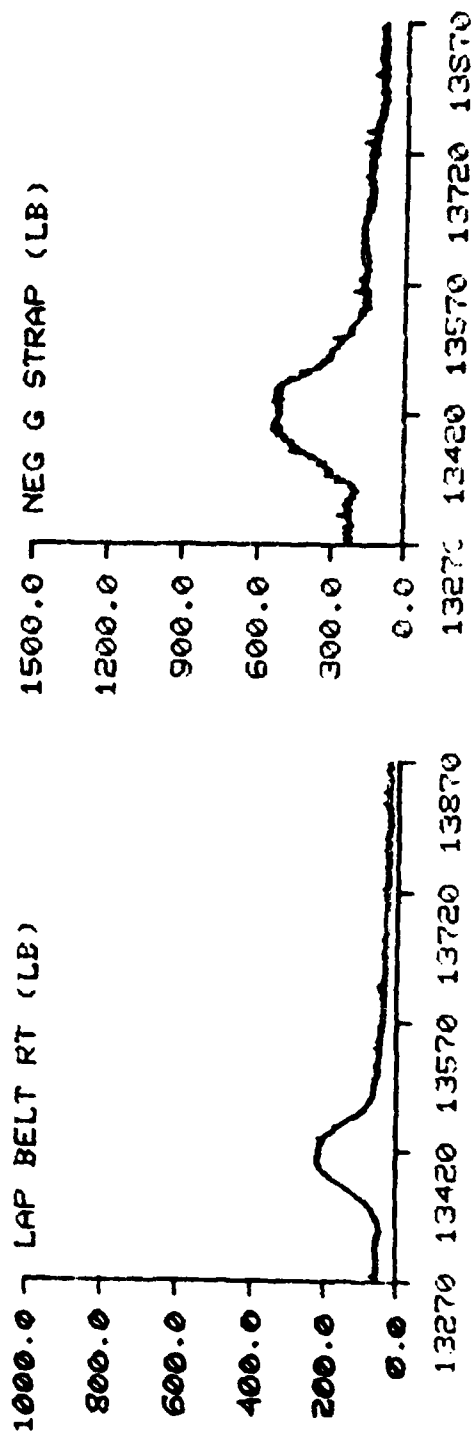
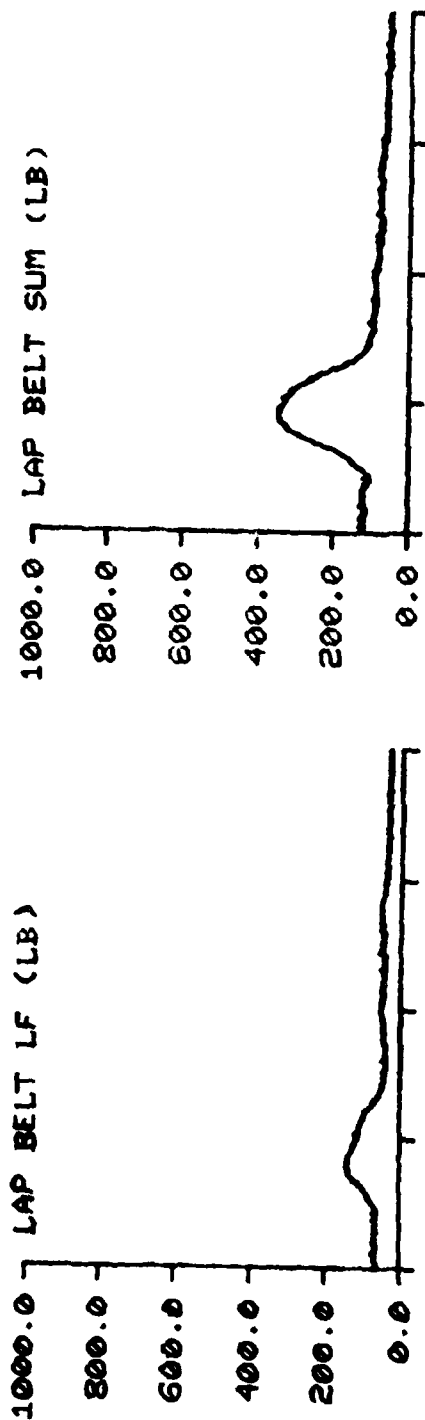
13270 13420 13570 13720 13870

TIME IN MILLISECONDS

F-111

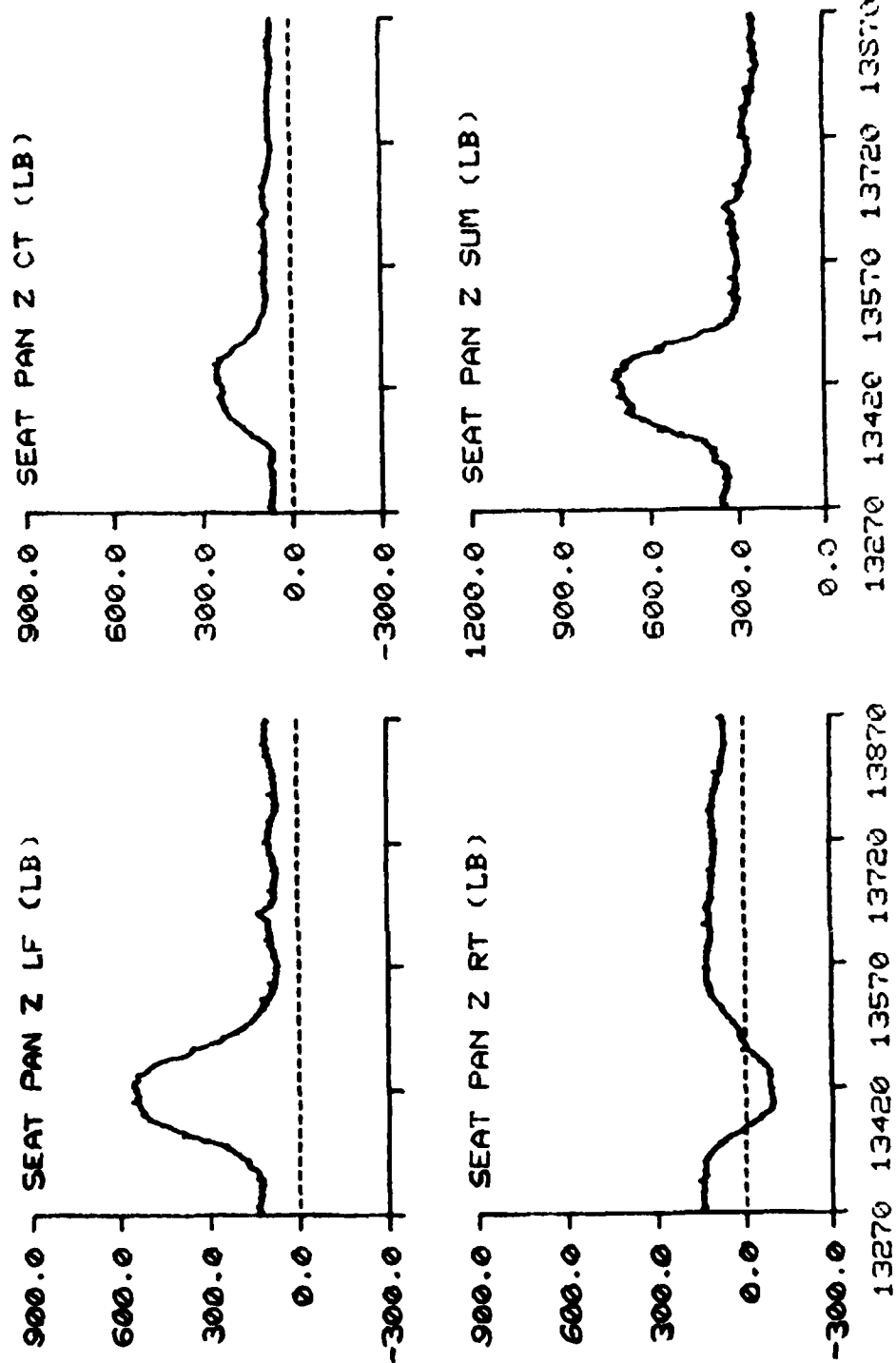
TEST NO: 453

SUBJECT ID: J-1



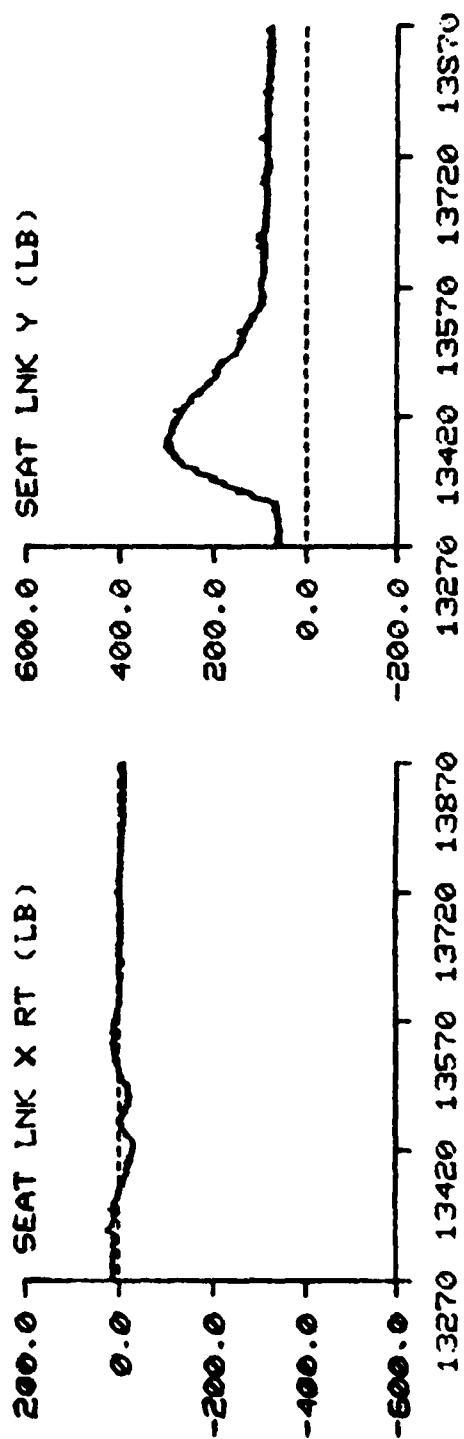
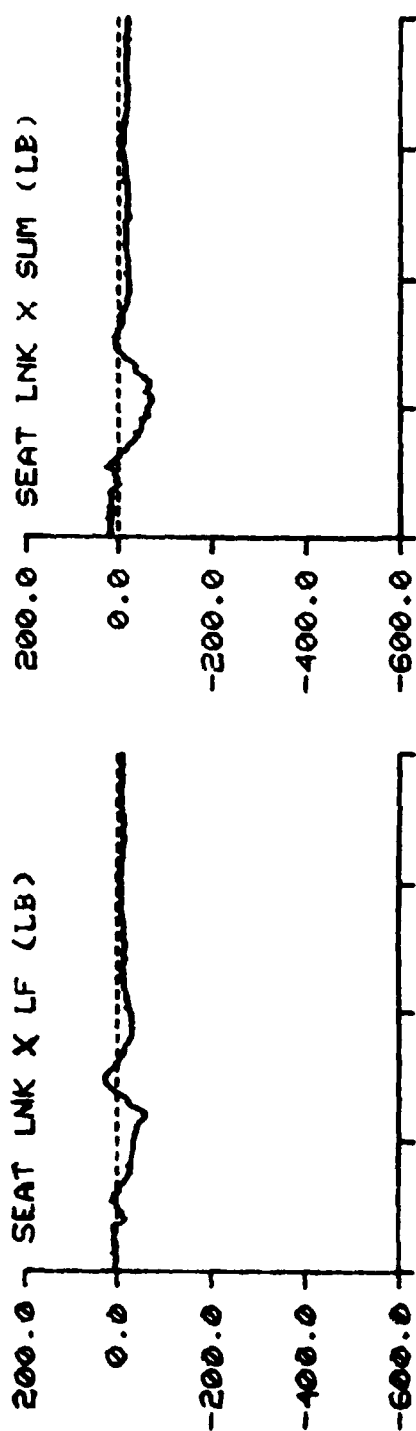
TIME IN MILLISECOND

F-111      TEST NO: 483      SUBJECT ID: J-1



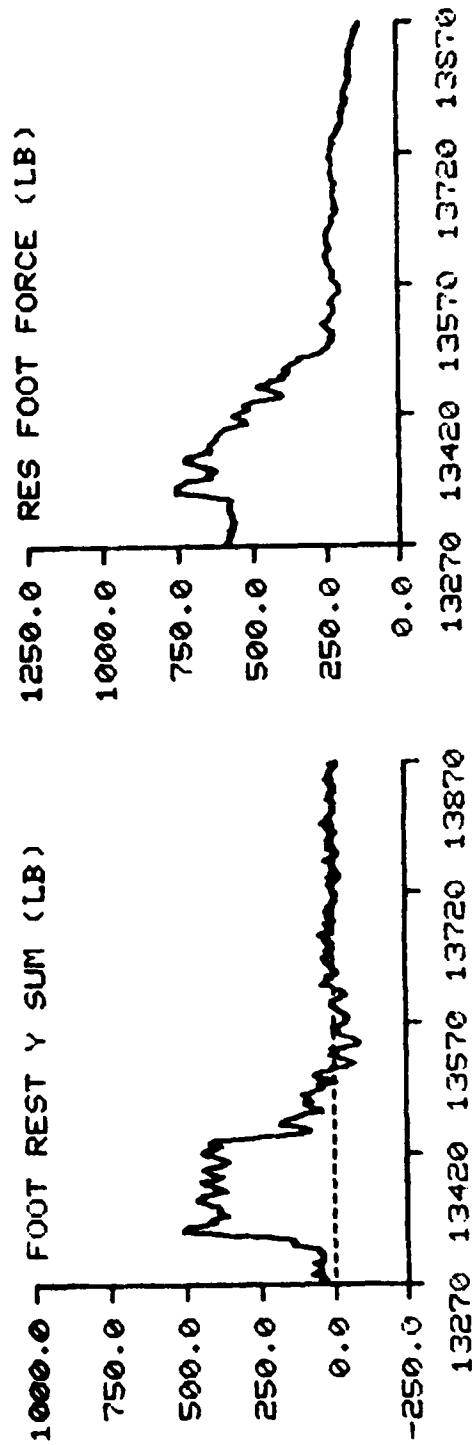
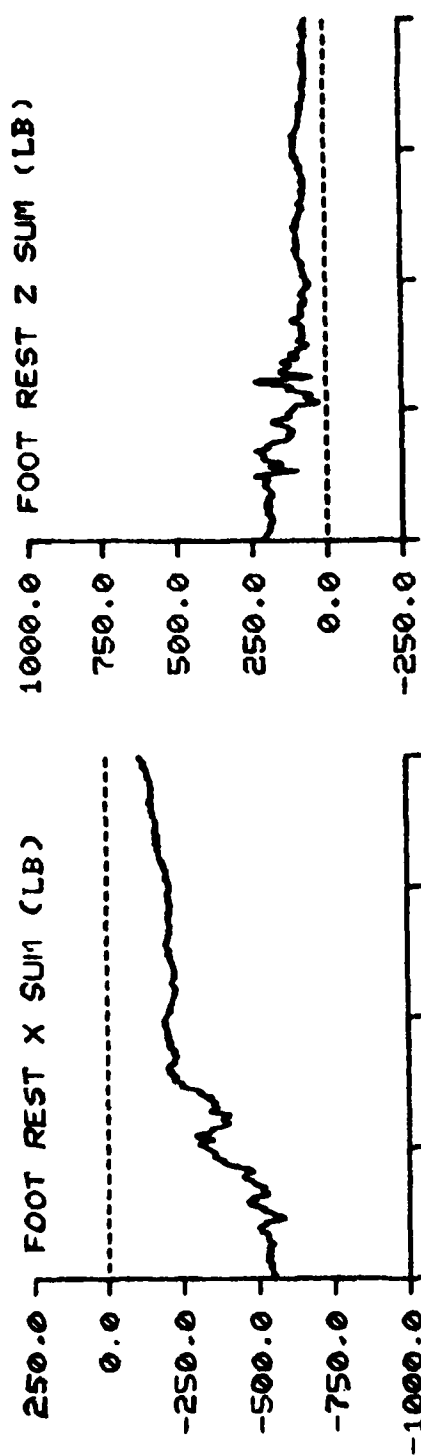
TIME IN MILLISECONDS

F-111 TEST NO: 463 SUBJECT ID: J-1





F-111 TEST NO: 463 SUBJECT ID: J-1



TIME IN MILLISECONDS

F-111 TEST NO: 459 SUBJECT ID: E-1

15.0 SLED X (G)

10.0

5.0

0.0

-5.0

15.0 SLED Y (G)

10.0

5.0

0.0

-5.0

15.0 SLED Z (G)

10.0

5.0

0.0

-5.0

13330 13480 13630 13780 13930

13330 13480 13630 1. '80 13930

TIME IN MILLISECONDS

F-111 TEST NO: 459 SUBJECT ID: E-1

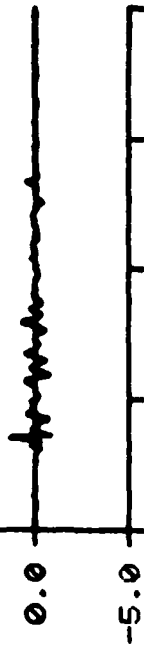
15.0 SEAT X (G)

10.0

5.0

0.0

-5.0



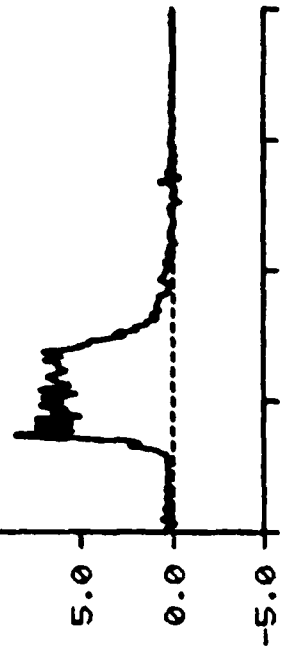
15.0 SEAT Y (G)

10.0

5.0

0.0

-5.0



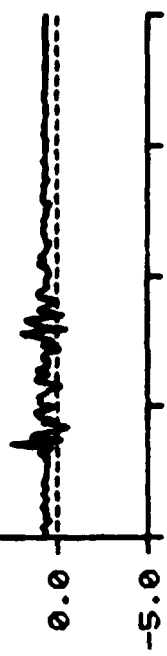
15.0 SEAT Z (G)

10.0

5.0

0.0

-5.0



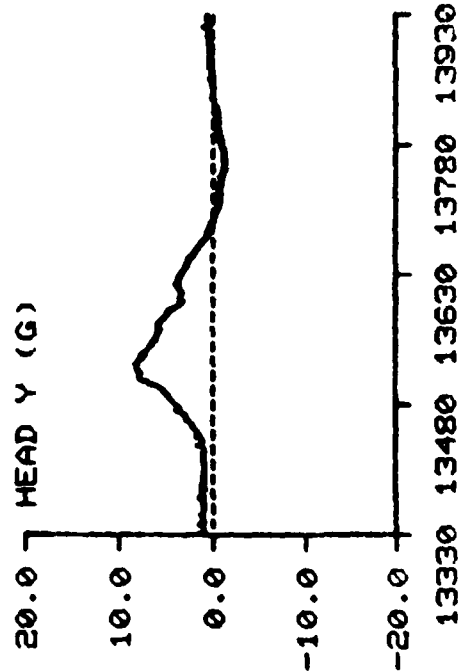
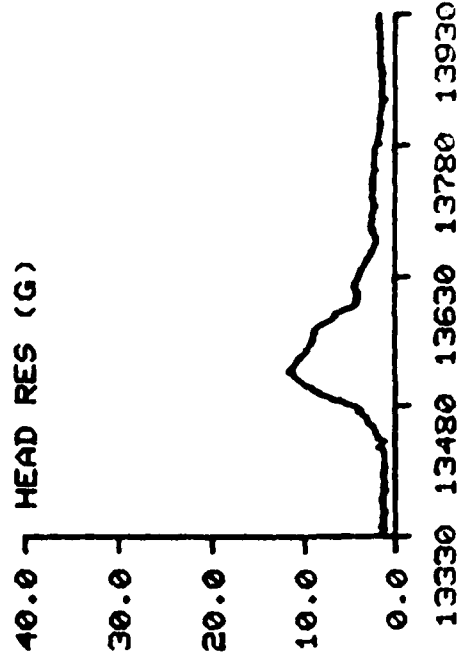
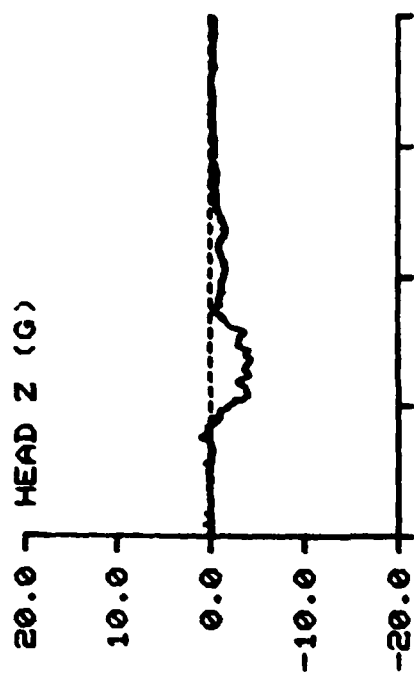
13330 13480 13630 13780 13930

TIME IN MILLISECONDS

F-111

TEST NO: 459

SUBJECT ID: E-1

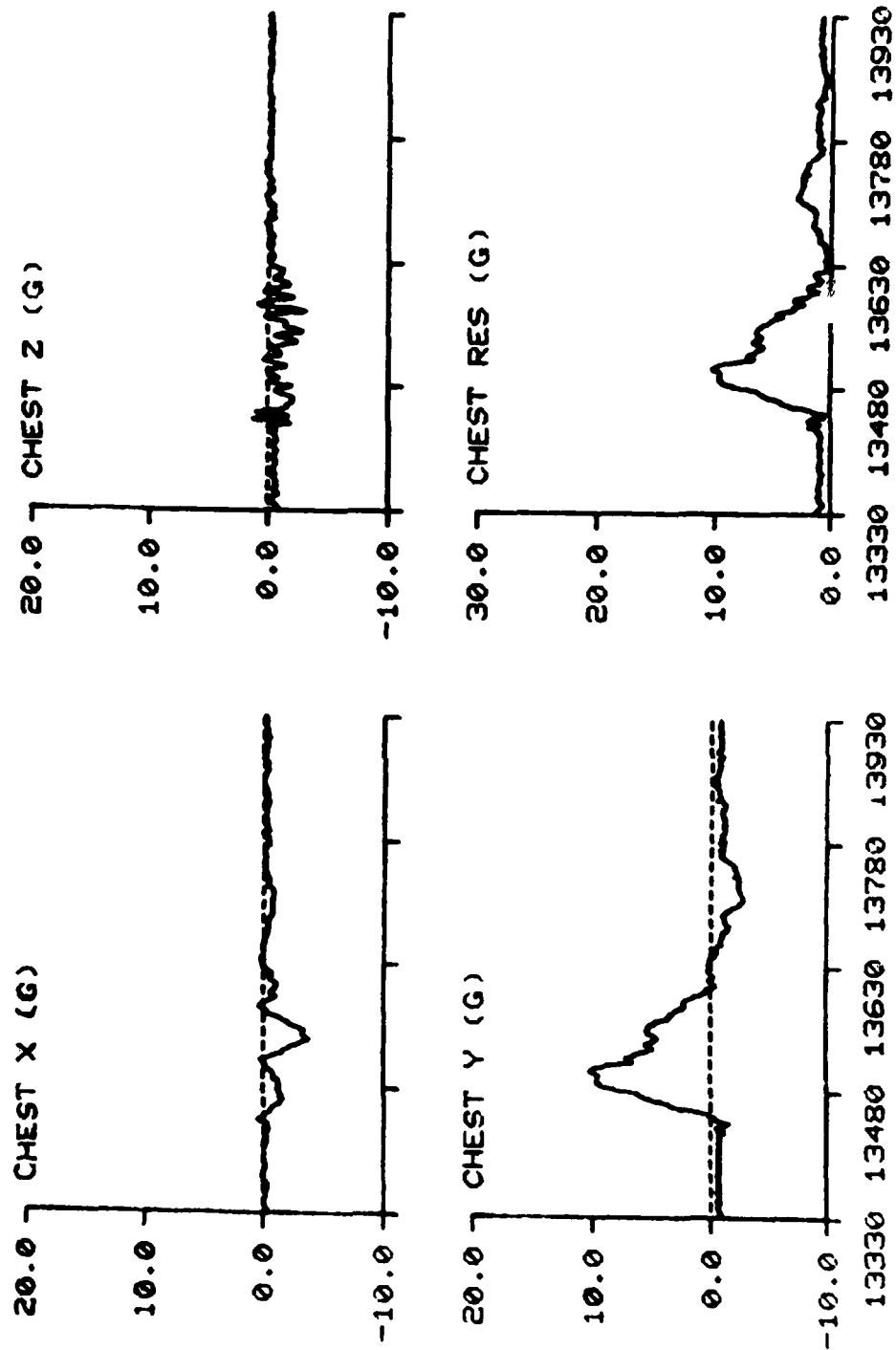


TIME IN MILLISECONDS

F-111

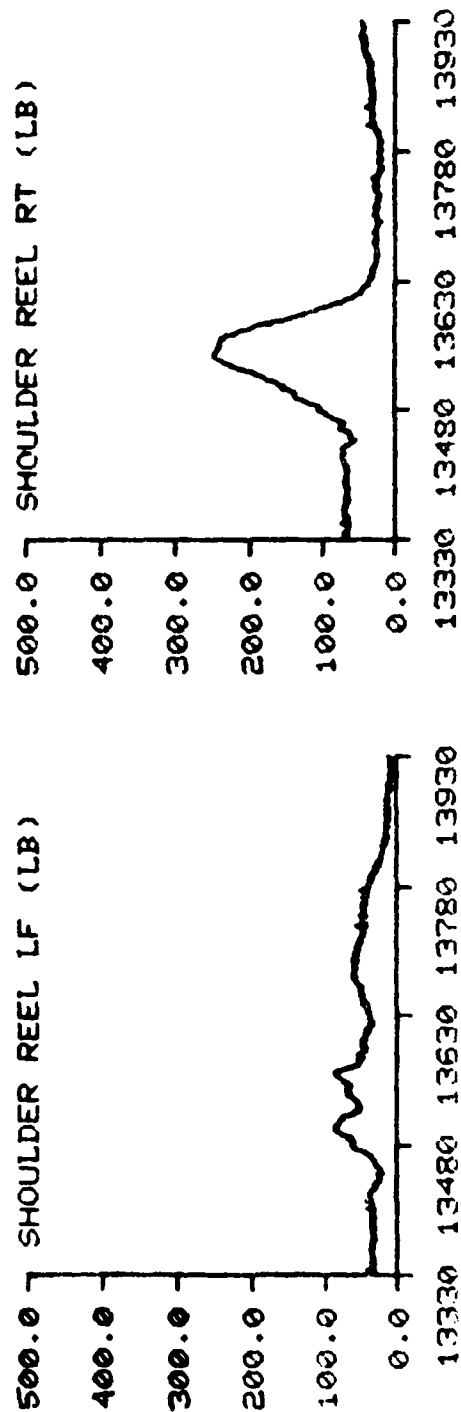
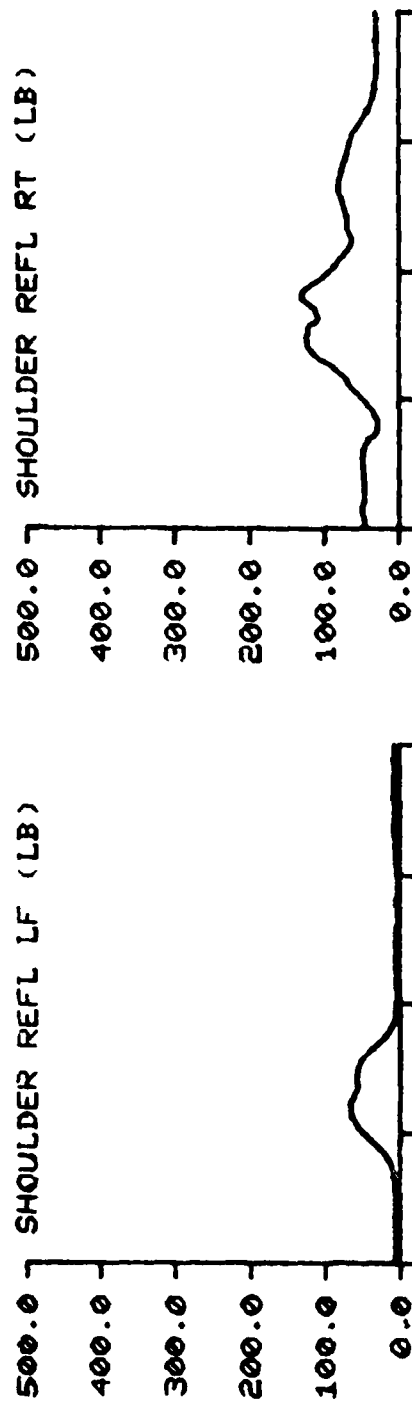
TEST NO: 459

SUBJECT ID: E-1



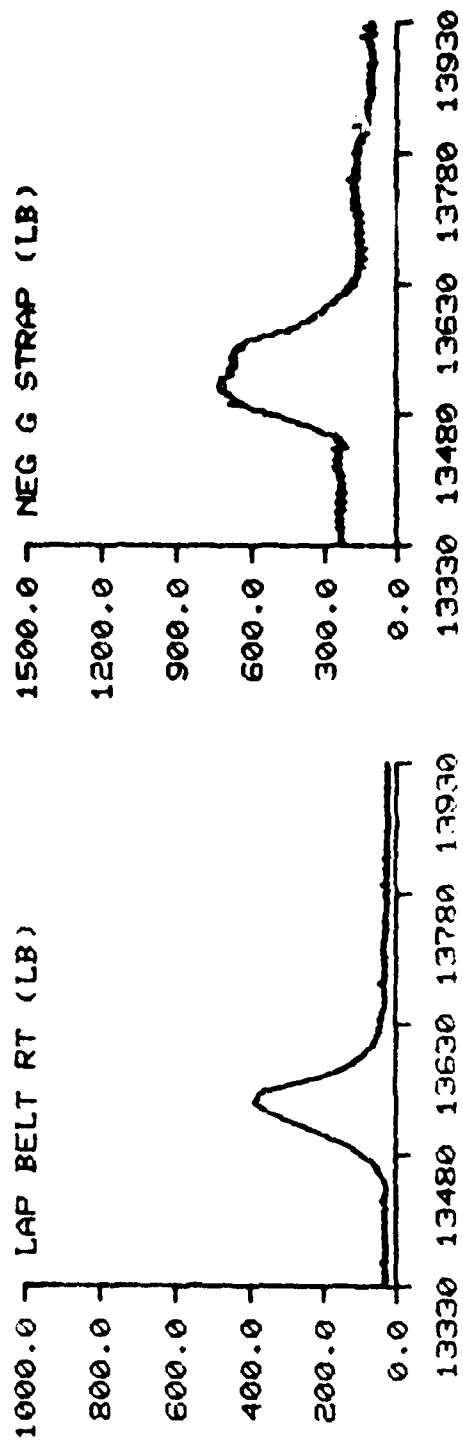
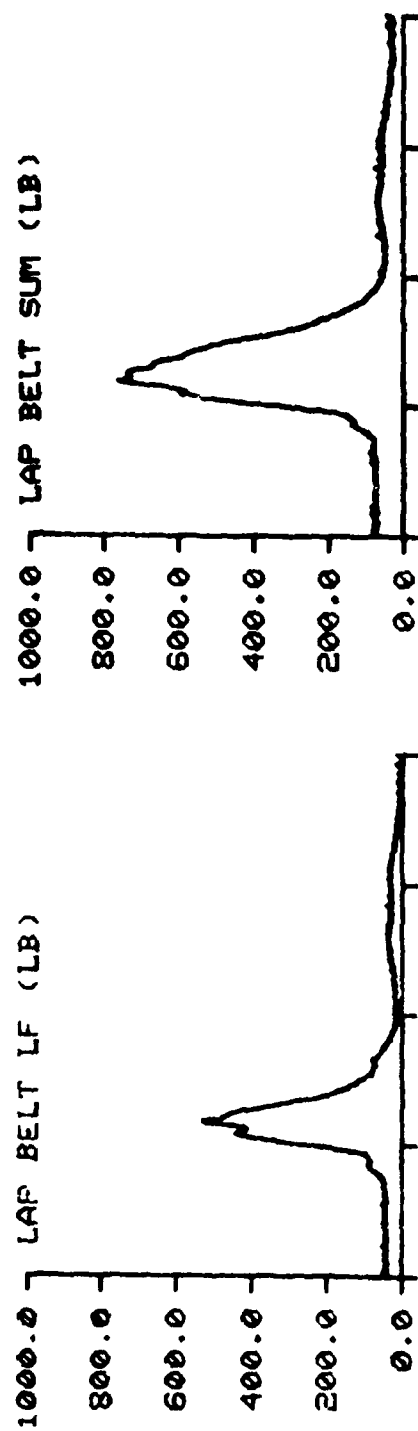
TIME IN MILLISECONDS

F-111      TEST NO: 459      SUBJECT ID: E-1



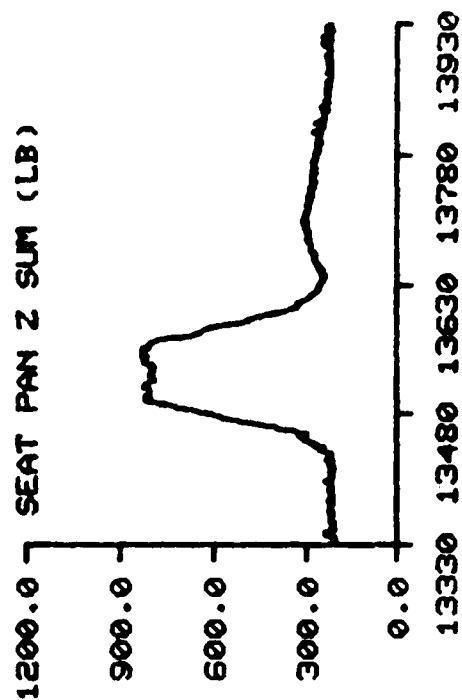
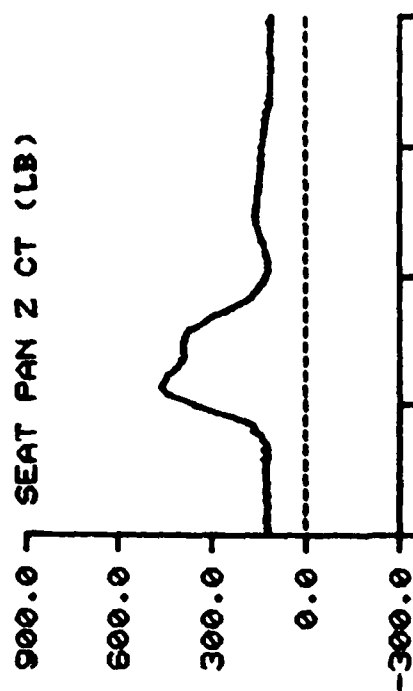
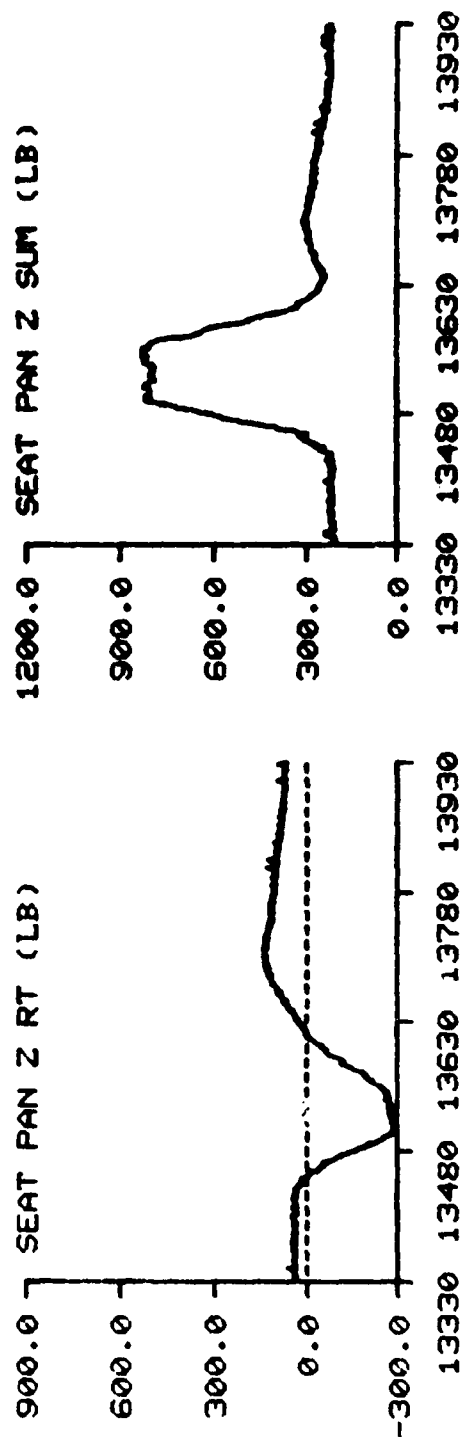
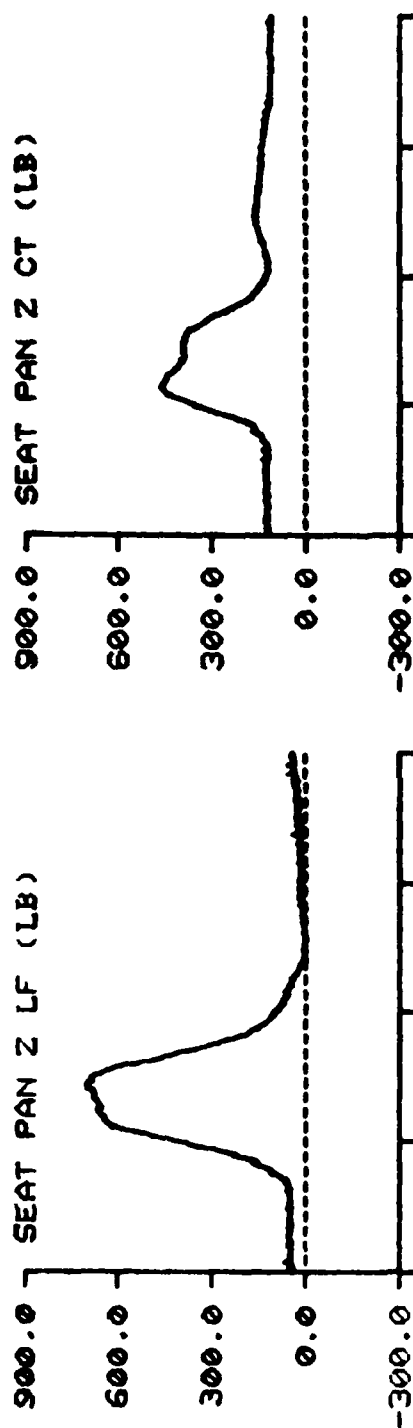
TIME IN MILLISECONDS

F-111      TEST NO: 459      SUBJECT ID: E-1



TIME IN MILLISECONDS

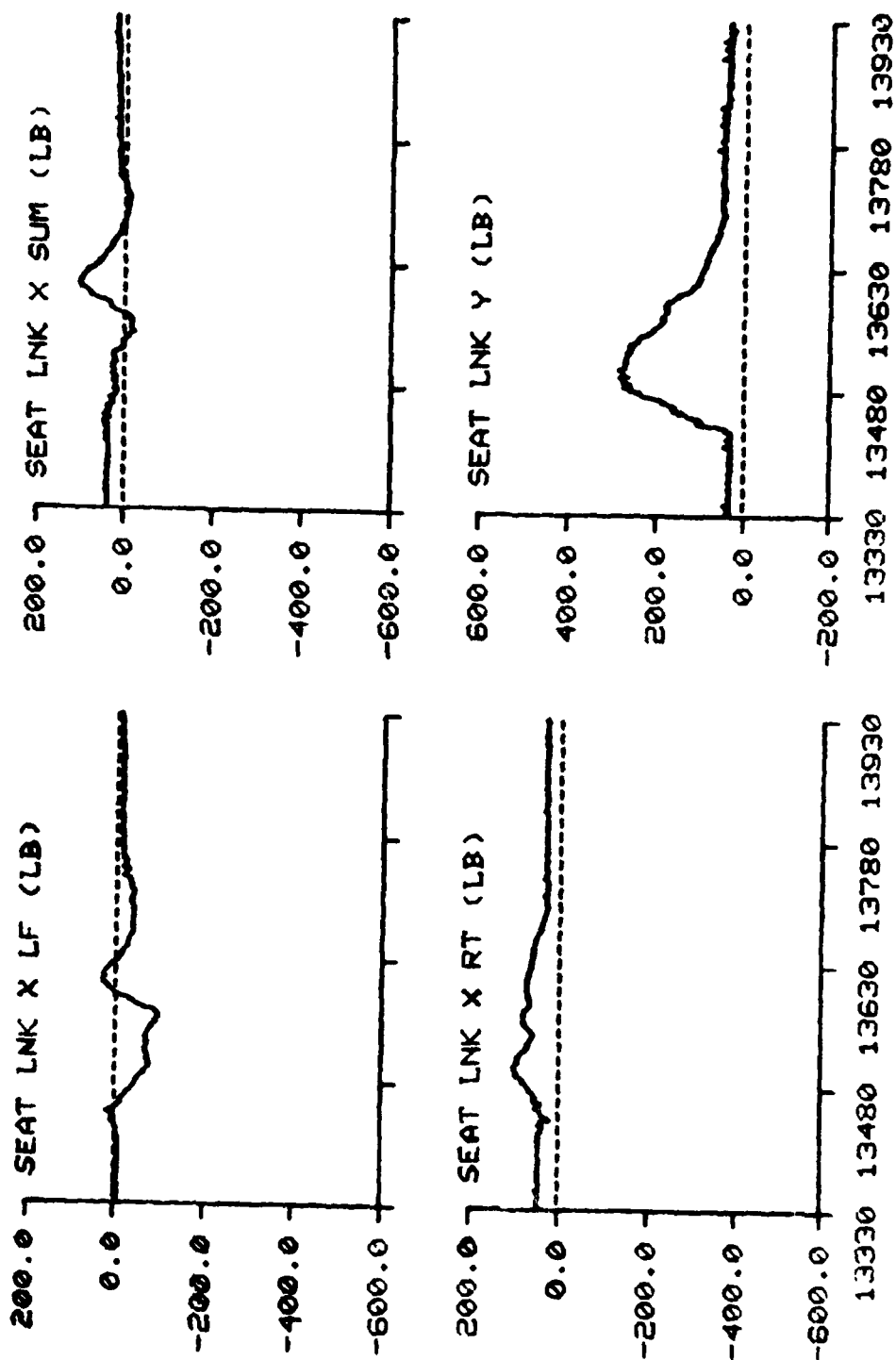
F-111 TEST NO: 459 SUBJECT ID: E-1



TIME IN MILLISECONDS

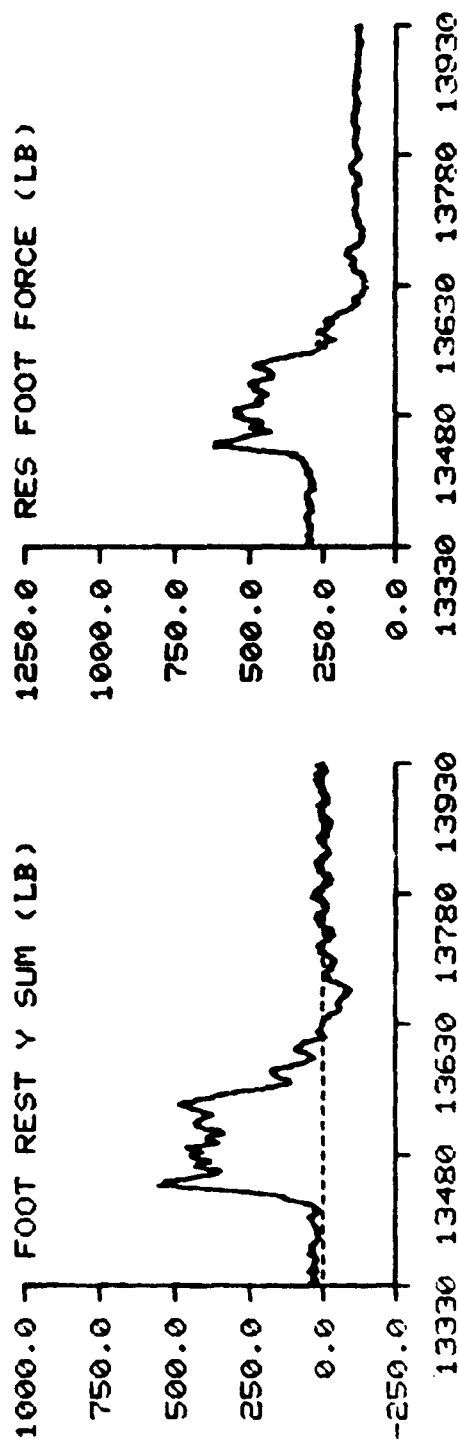
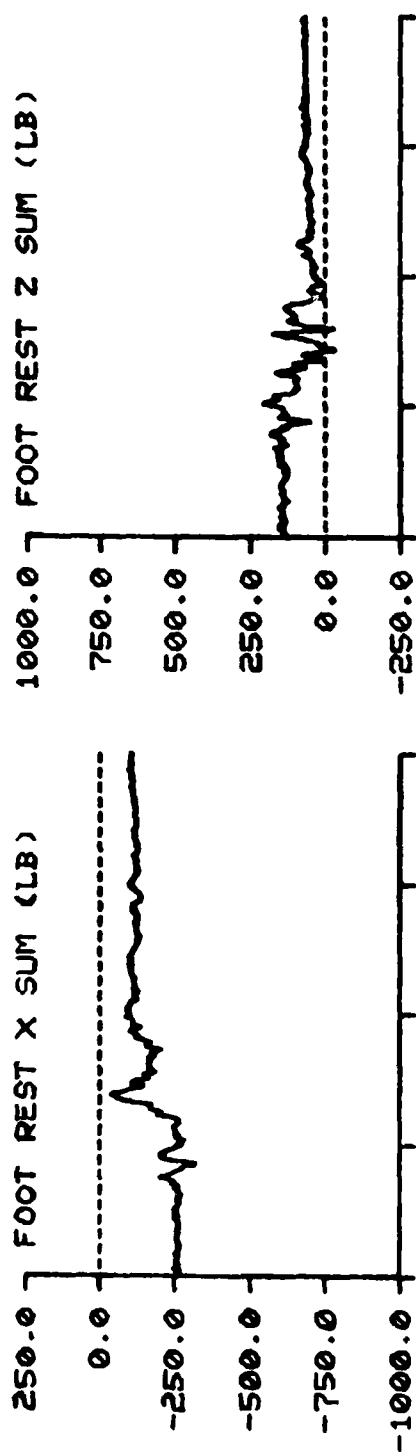


F-111 TEST NO: 459 SUBJECT ID: E-1



TIME IN MILLISECONDS

F-111 TEST NO: 459 SUBJECT ID: E-1

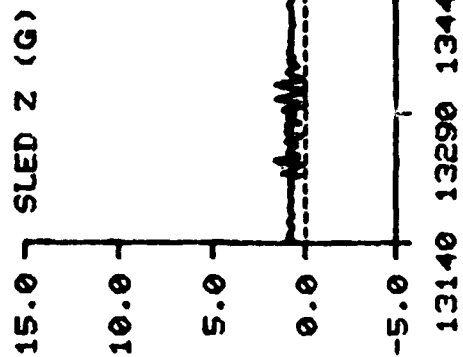
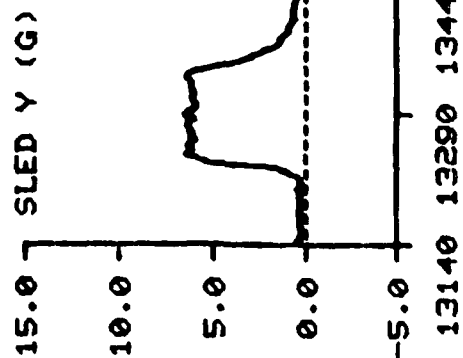
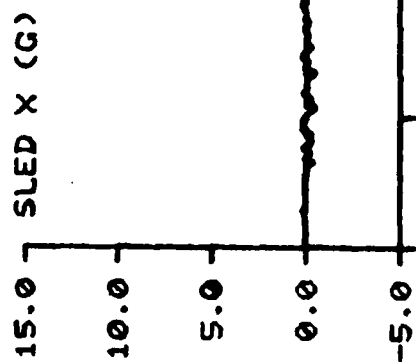


TIME IN MILLISECONDS

F-111

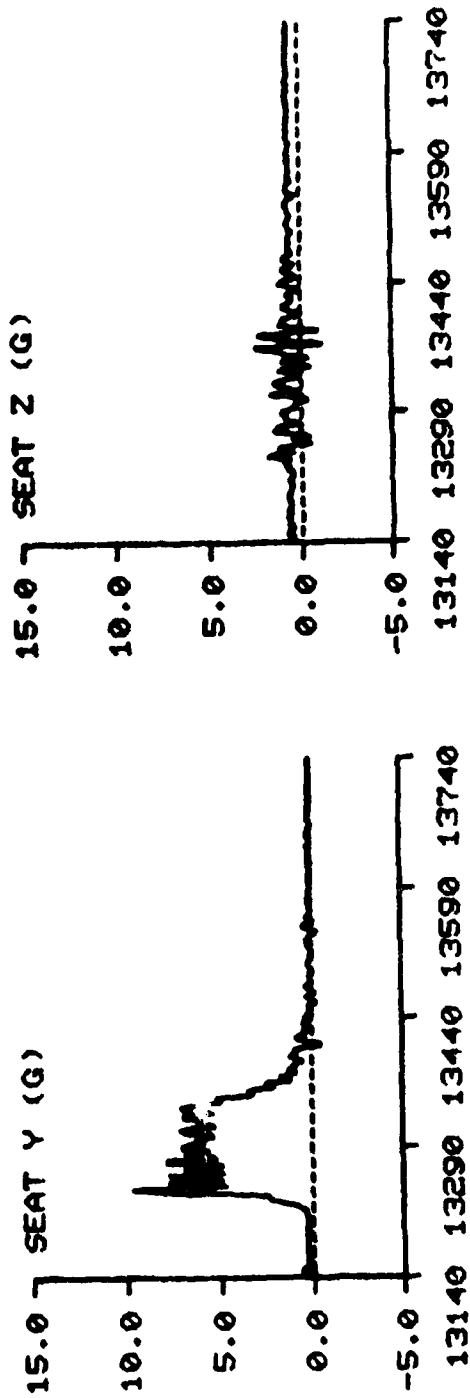
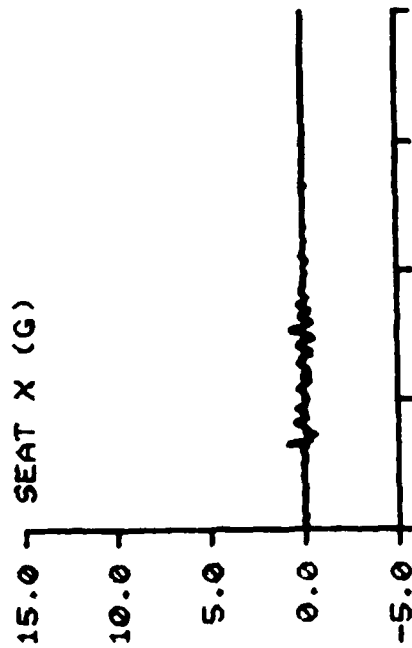
TEST NO: 468

SUBJECT ID: F-3



TIME IN MILLISECONDS

F-111      TEST NO: 468      SUBJECT ID: F-3

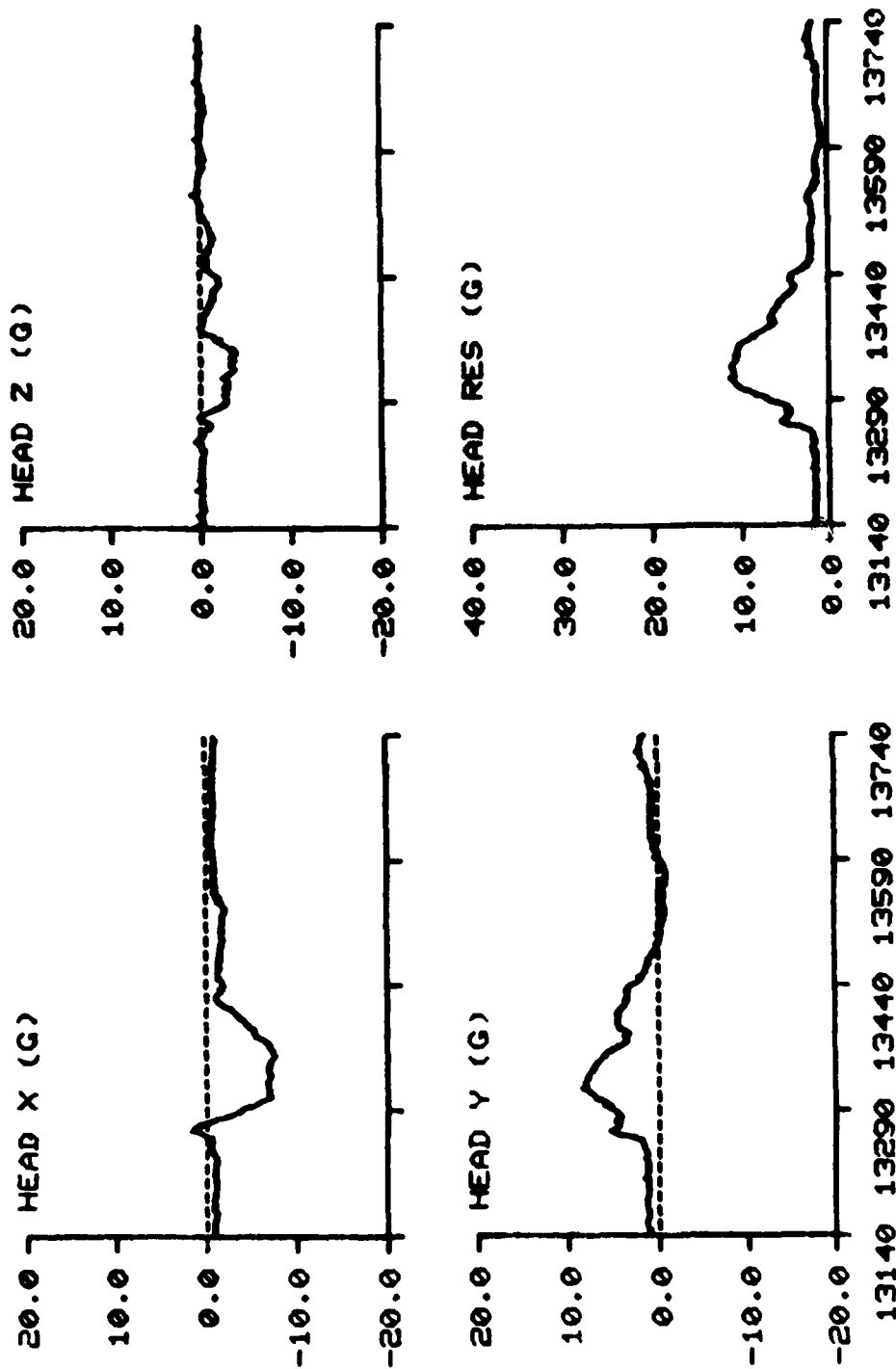


TIME IN MILLISECONDS

F-111

TEST NO: 468

SUBJECT ID: F-3



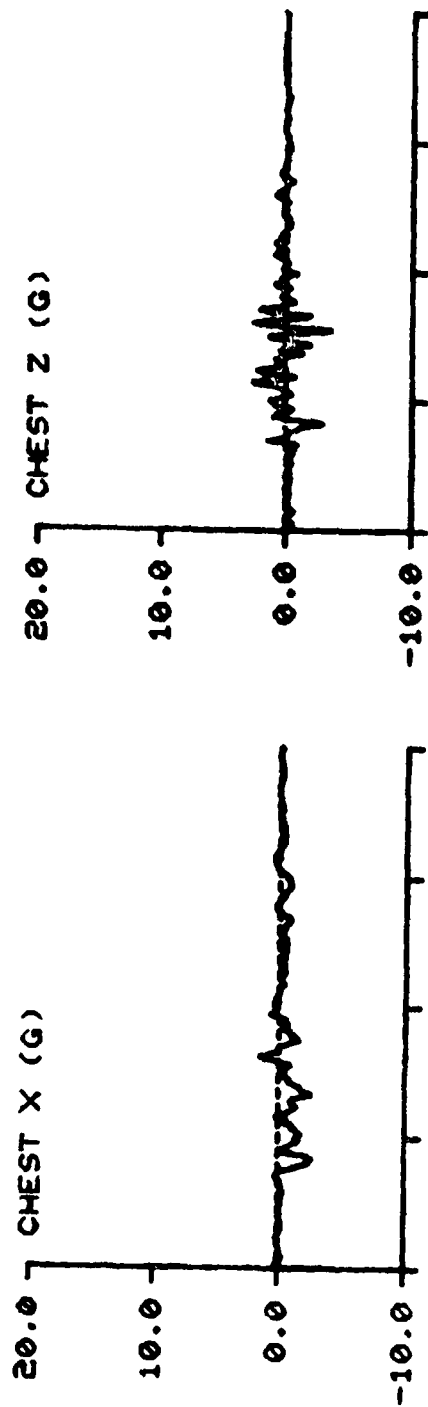
TIME IN MILLISECONDS

F-111

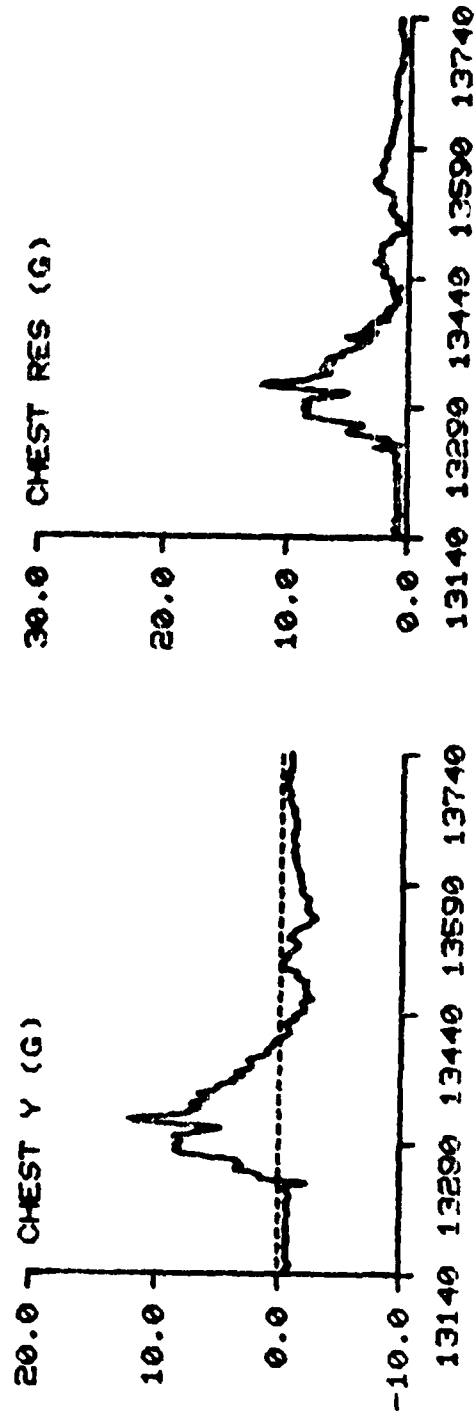
TEST NO: 468

SUBJECT ID: F-3

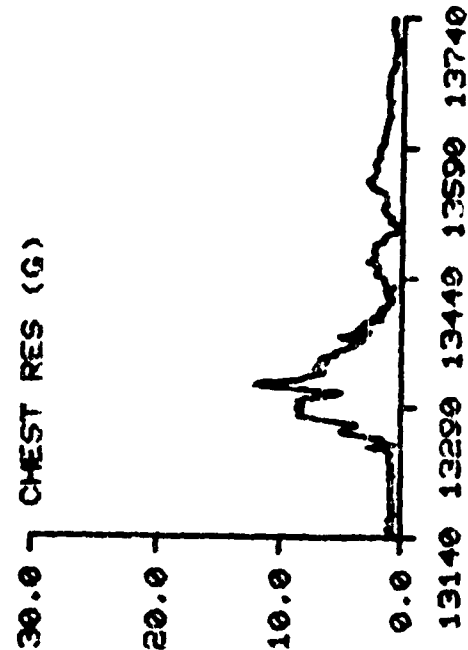
CHEST X (G)



CHEST Y (G)



CHEST RES (G)

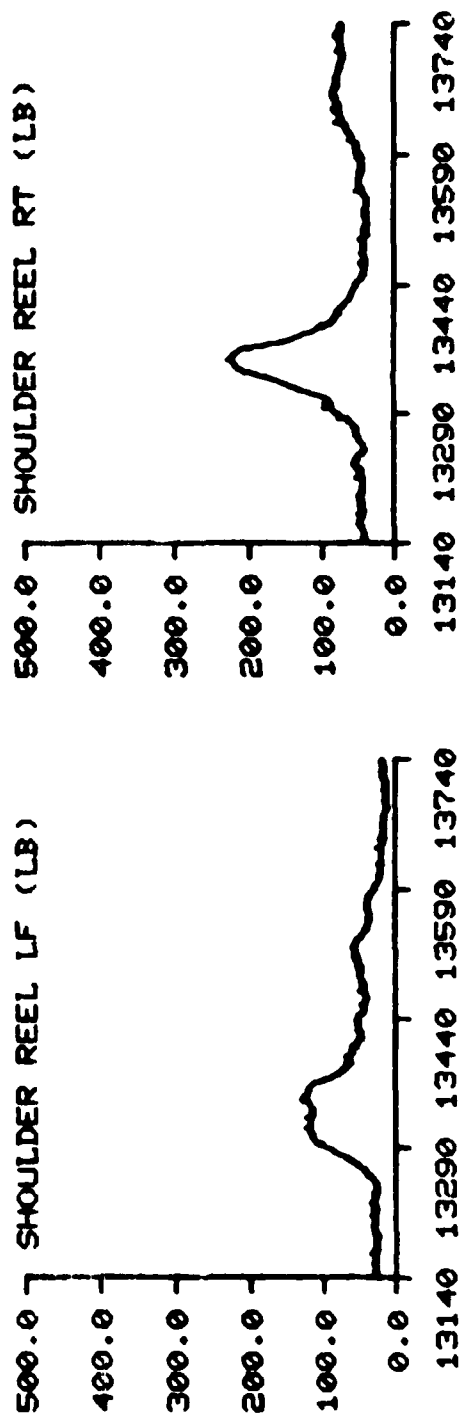
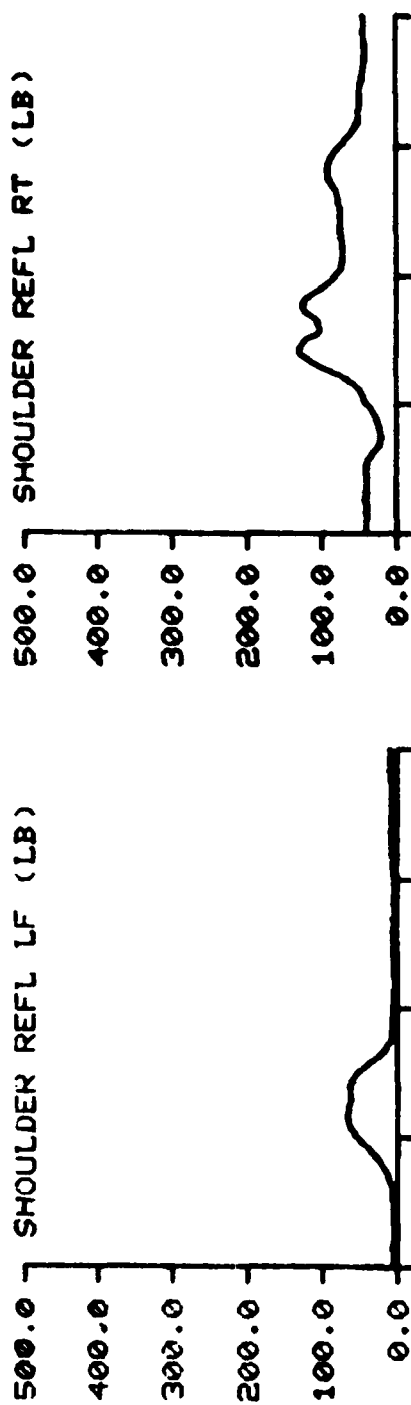


TIME IN MILLISECONDS

F-111

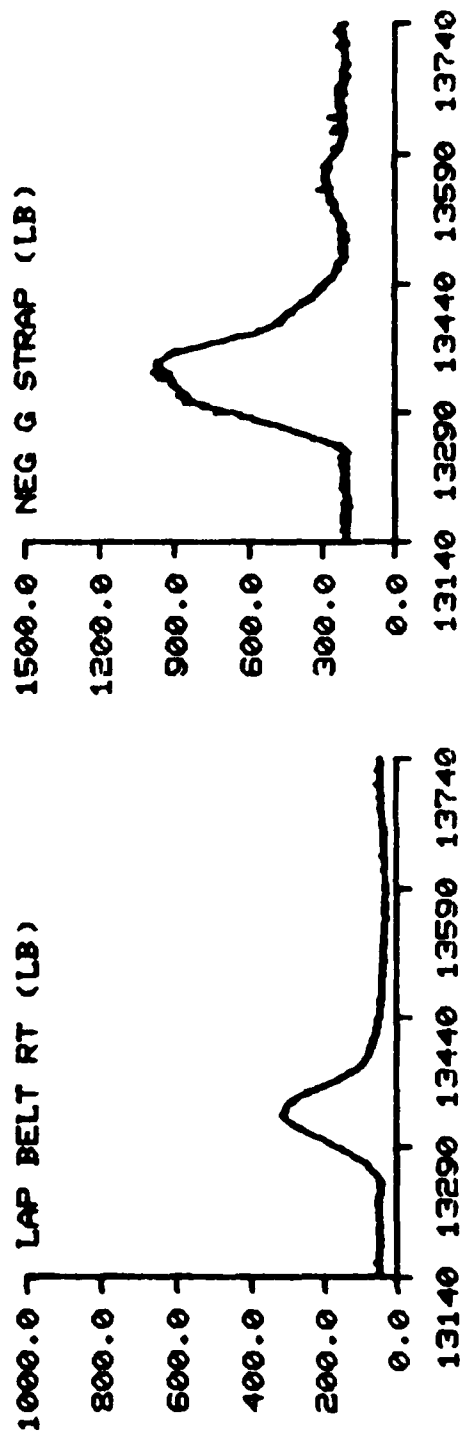
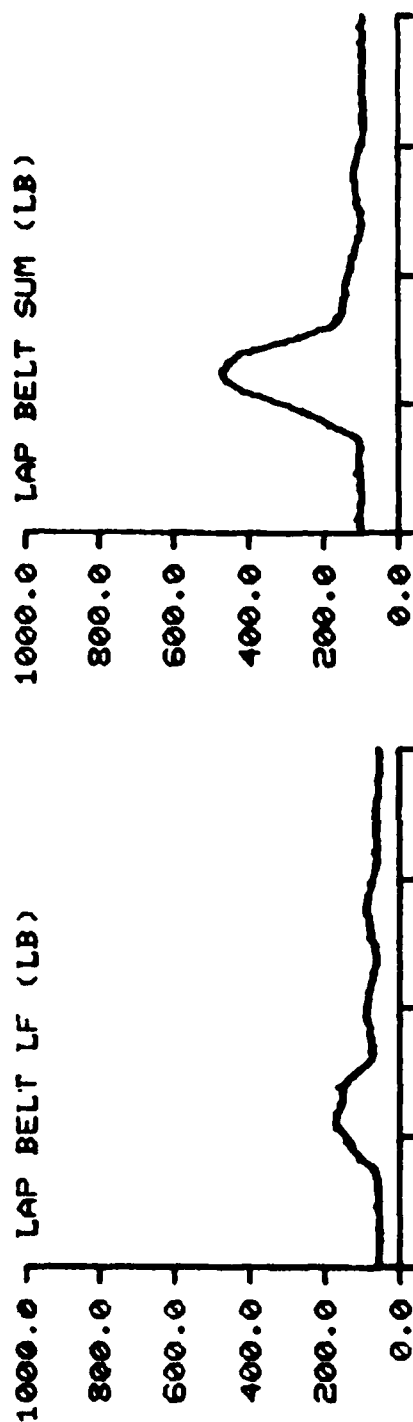
TEST NO: 468

SUBJECT ID: F-3



TIME IN MILLISECONDS

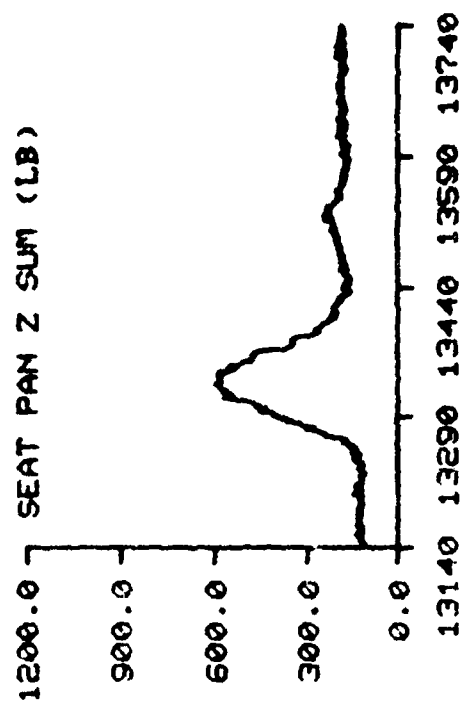
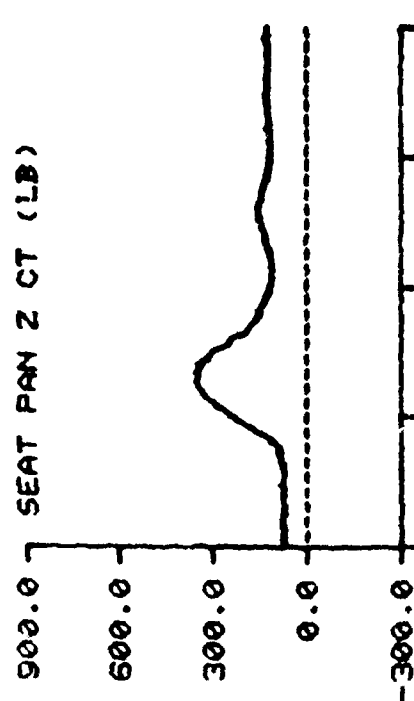
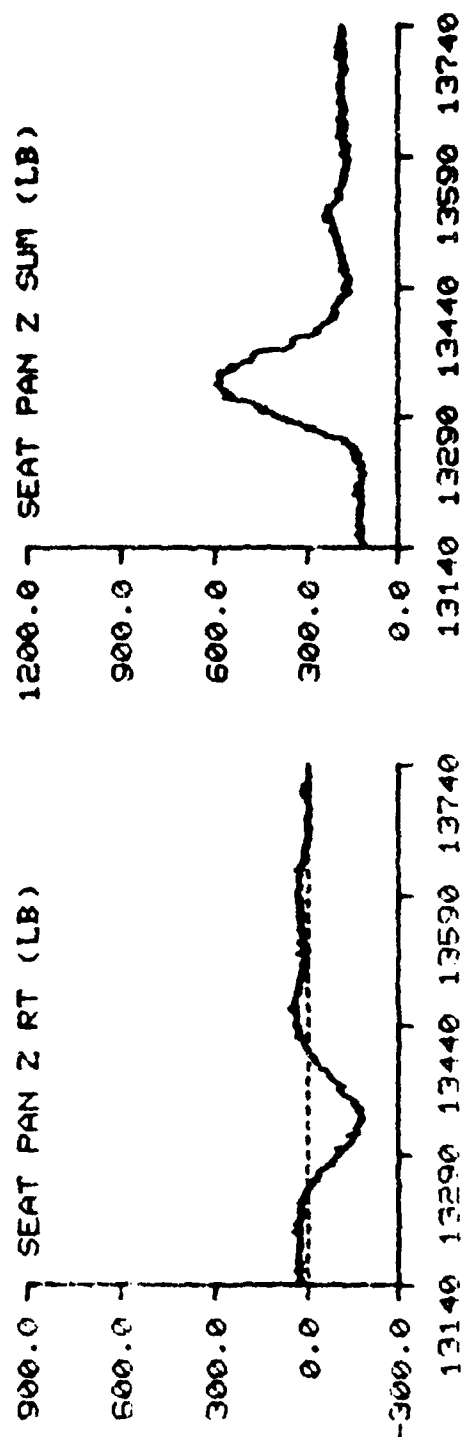
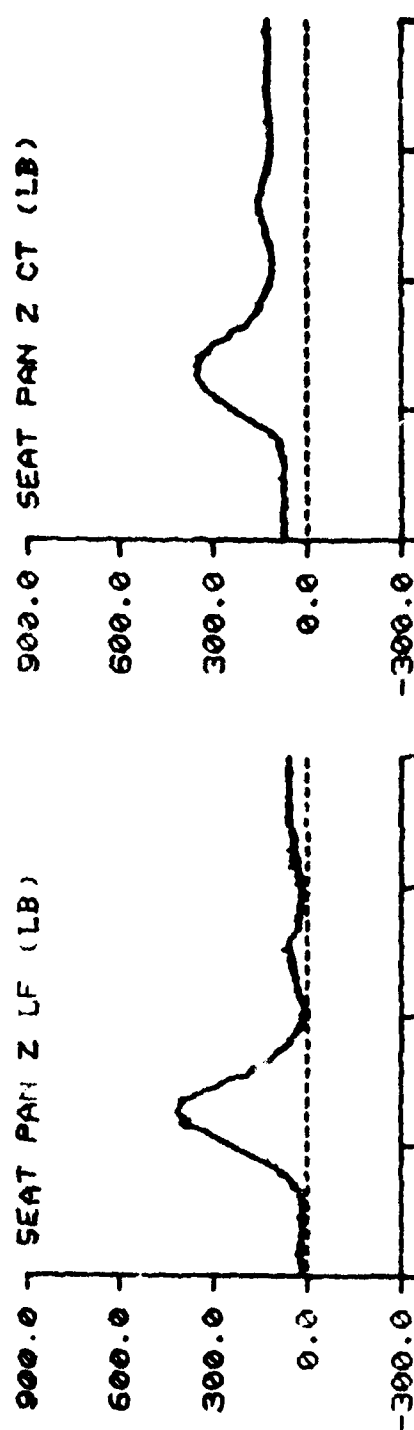
F-111      TEST NO: 468      SUBJECT ID: F-3



TIME IN MILLISECONDS

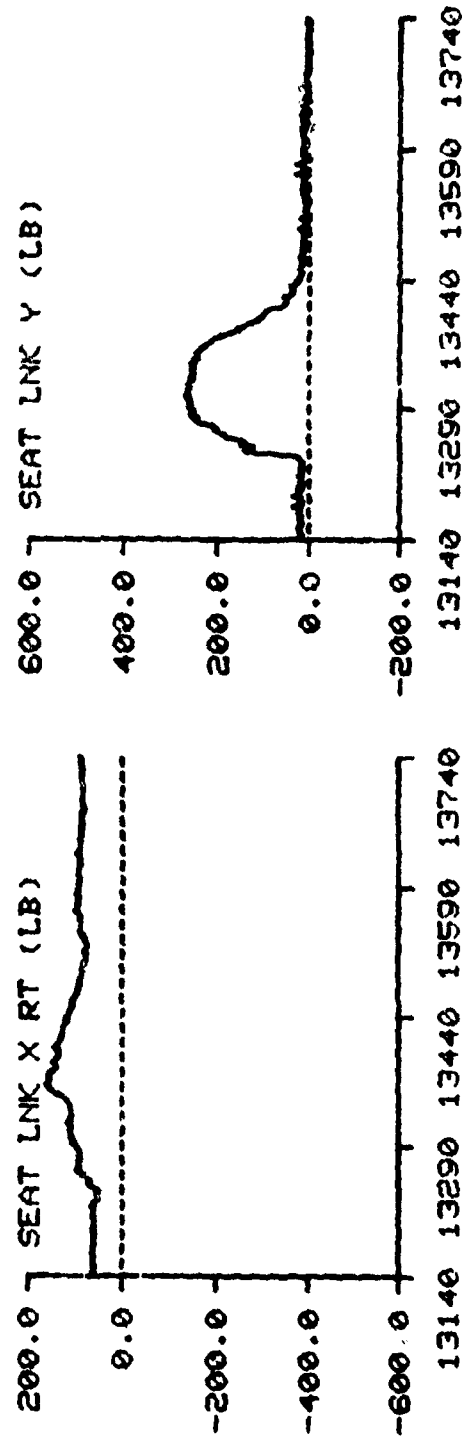
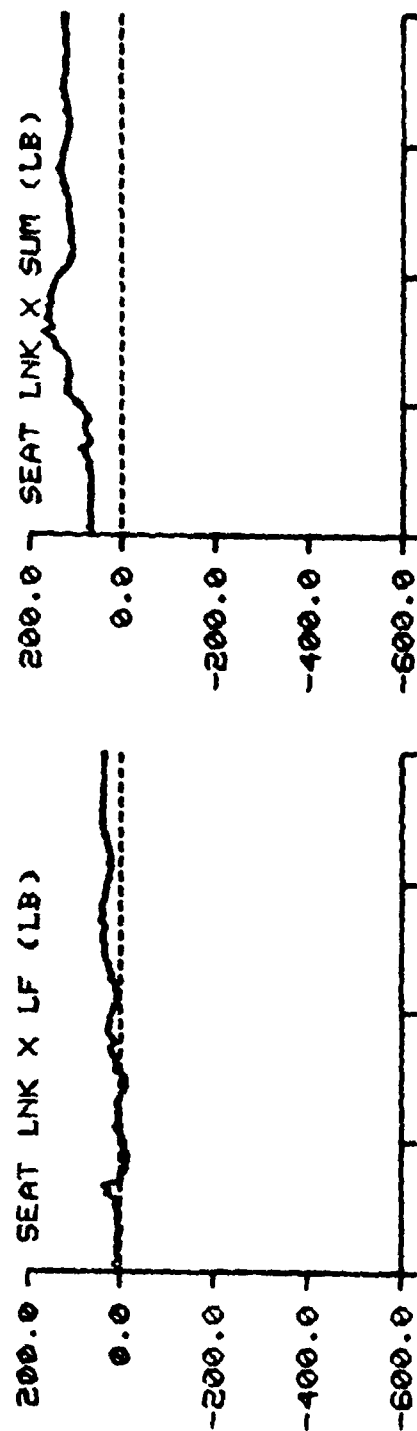


F-111      TEST NO: 468      SUBJECT ID: F-3



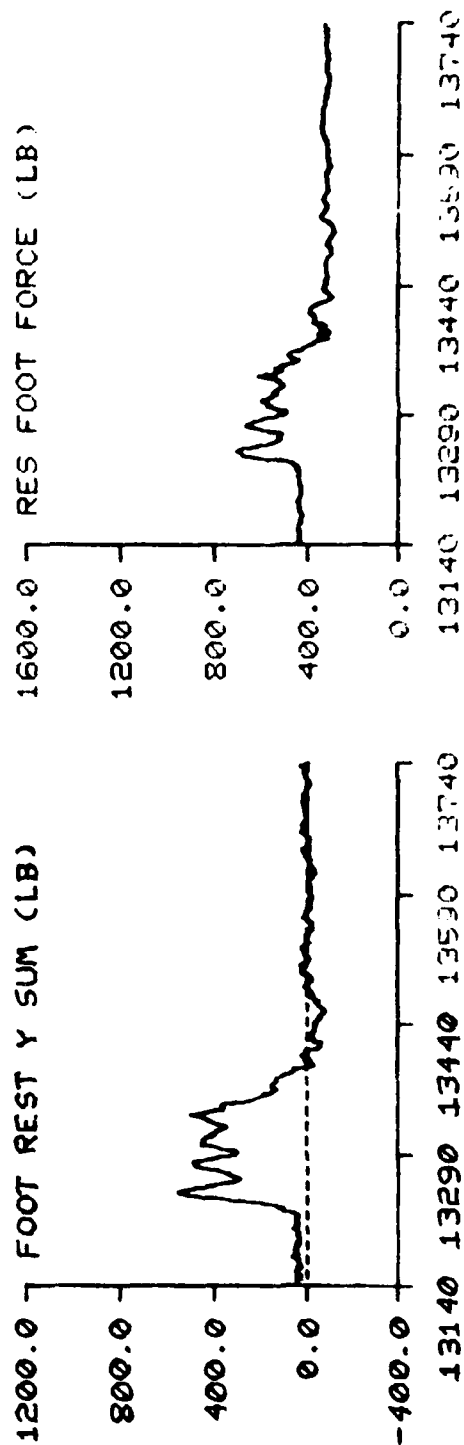
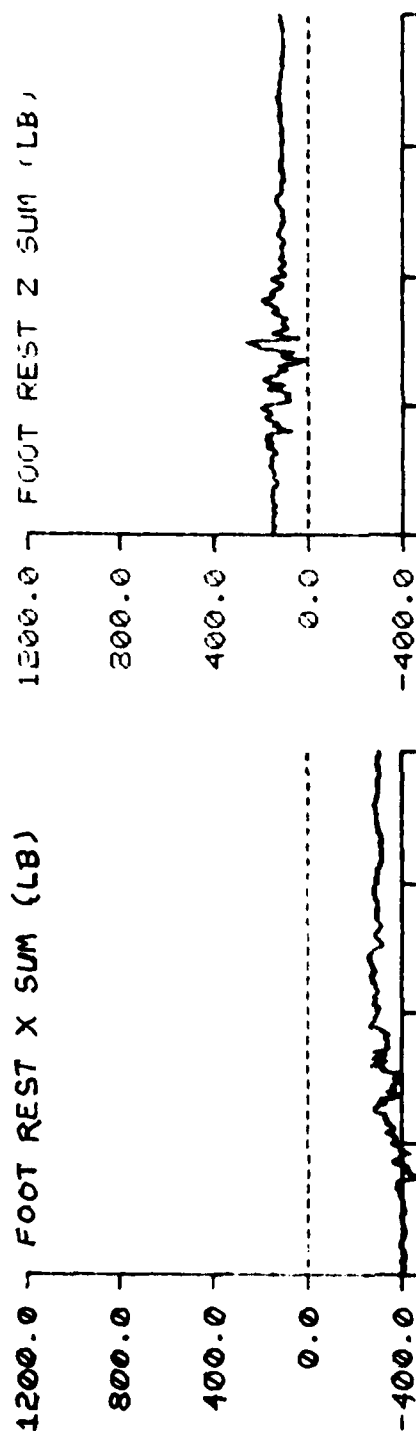
TIME IN MILLISECONDS

F-111 TEST NO: 468 SUBJECT ID: F-3



TIME IN MILLISECONDS

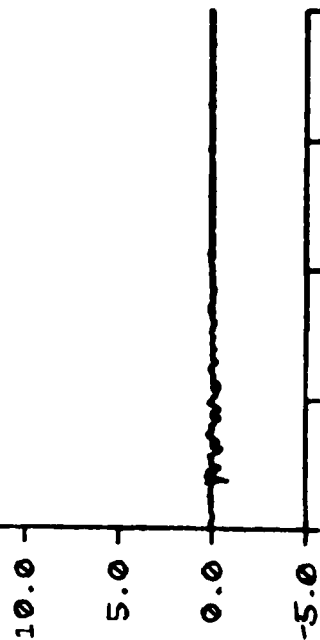
F-111 TEST NO: 468 SUBJECT ID: F-3



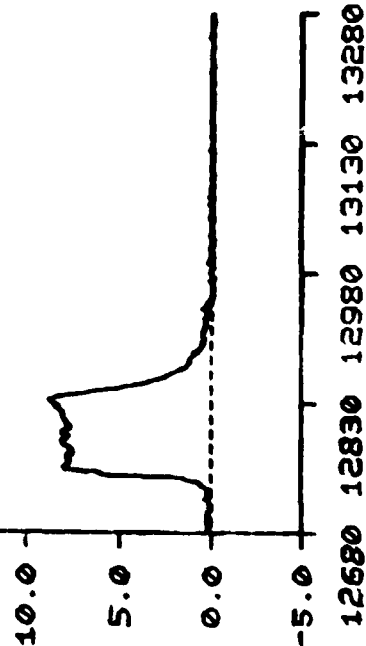
TIME IN MILLISECONDS

F-111      TEST NO: 507      SUBJECT ID: M-9

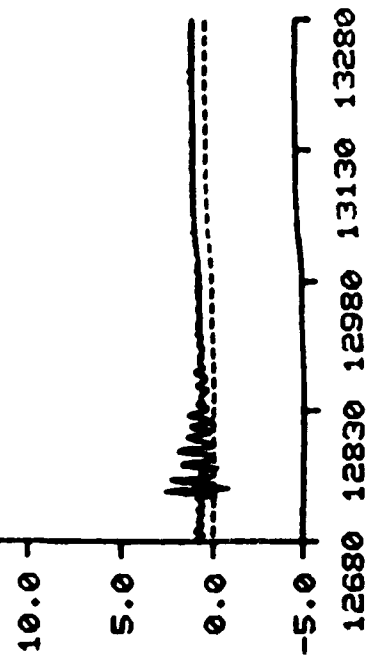
15.0 SLED X (G)



15.0 SLED Y (G)



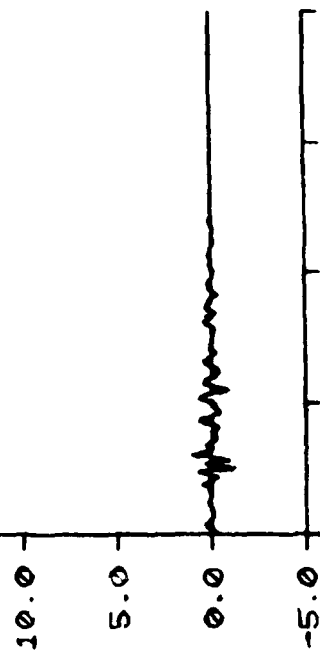
15.0 SLED Z (G)



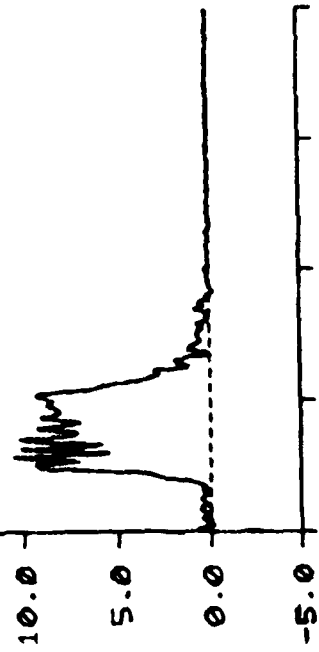
TIME IN MILLISECONDS

F-111      TEST NO: 507      SUBJECT ID: M-9

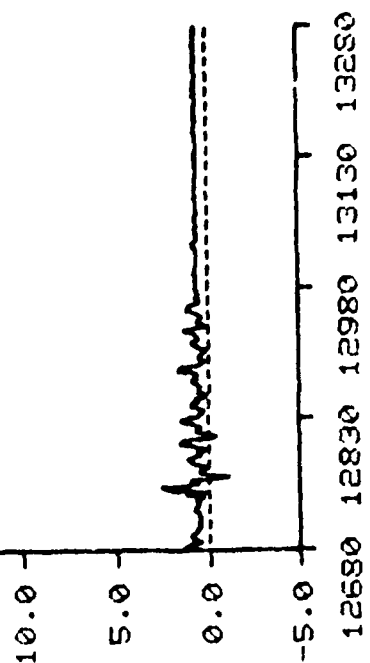
15.0 SEAT X (G)



15.0 SEAT Y (G)

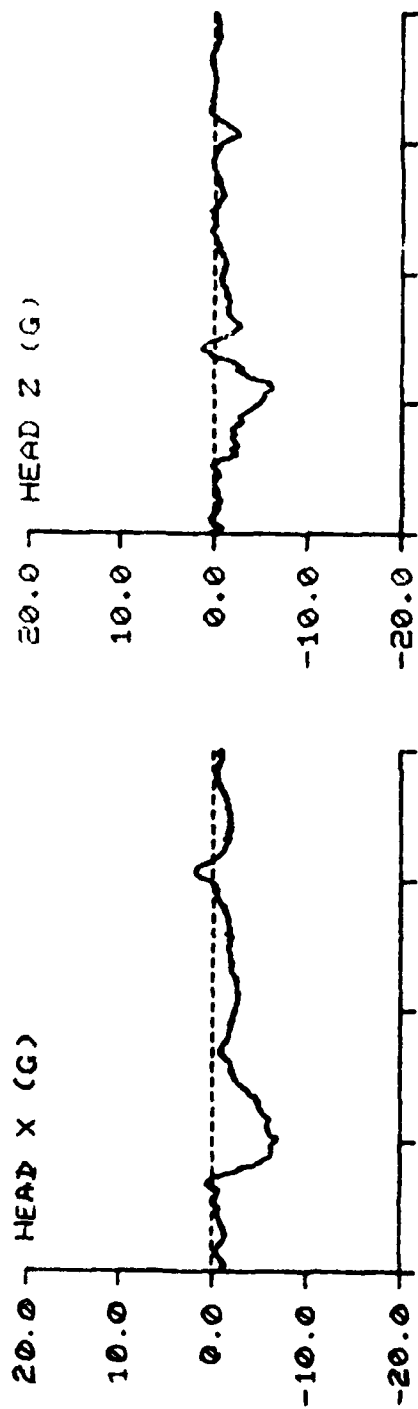


15.0 SEAT Z (G)



TIME IN MILLISECONDS

F-111 TEST NO: 507 SUBJECT ID: M-9

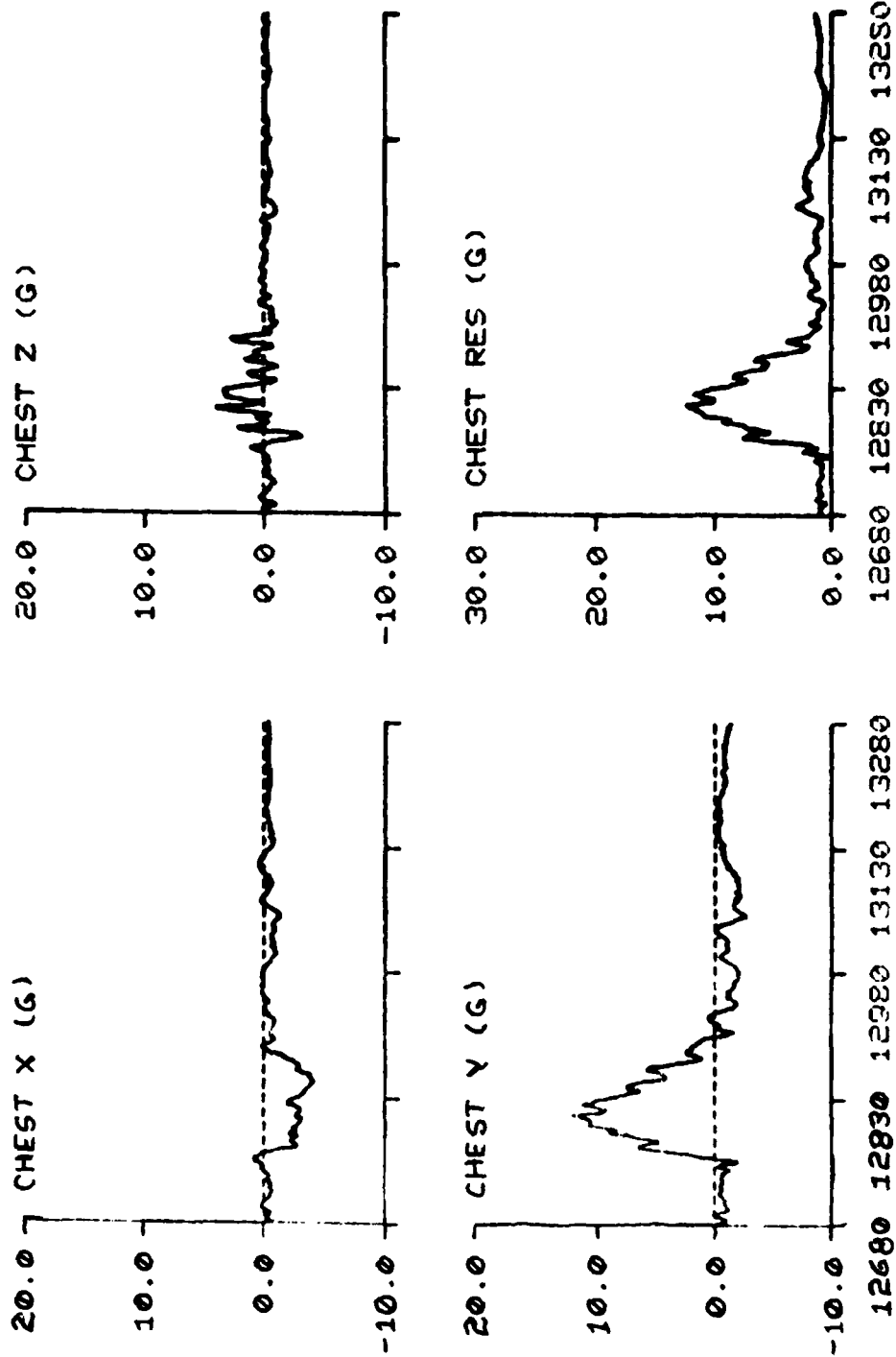


TIME IN MILLISECONDS

F-111

TEST NO: 507

SUBJECT ID: M-9

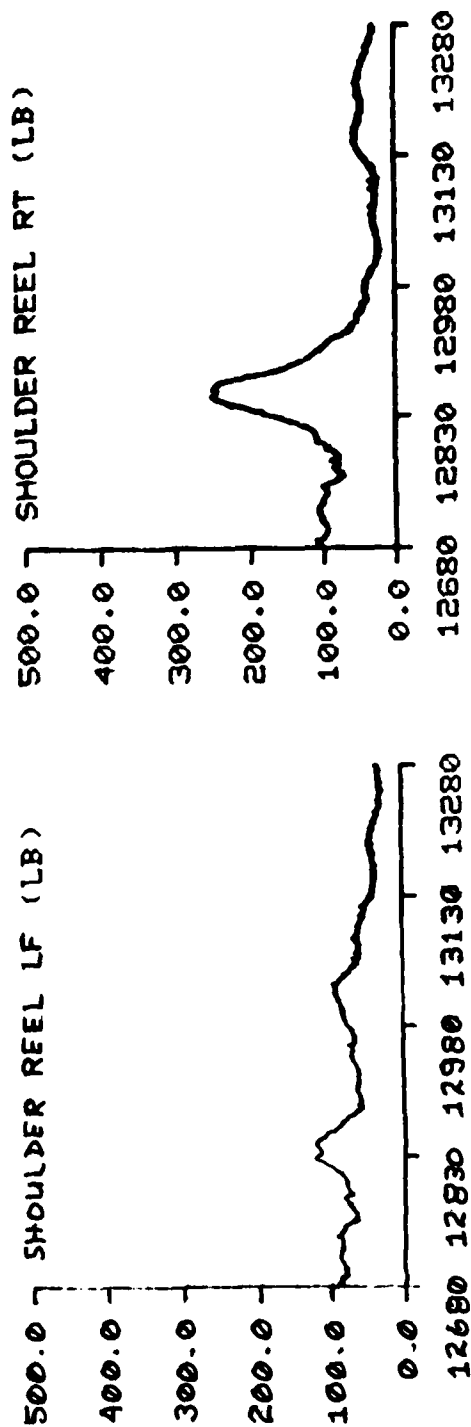
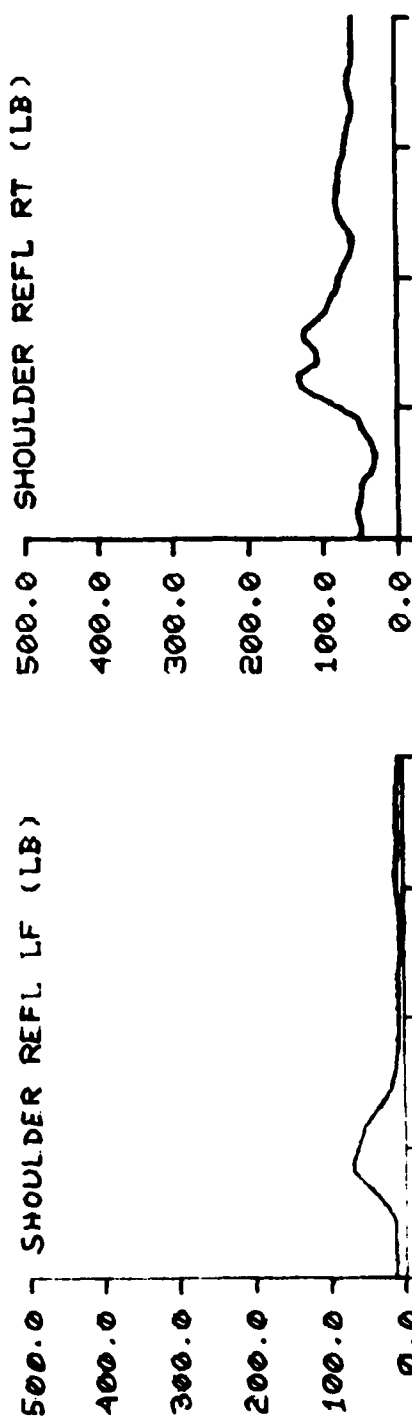


TIME IN MILLISECONDS

F-111

TEST NO: 507

SUBJECT ID: M-9



TIME IN MILLISECONDS



F-111

TEST No: 507

SUBJECT ID: M-9

LAP BELT LF (LB)

LAP BELT SUM (LB)

LAP BELT RT (LB)

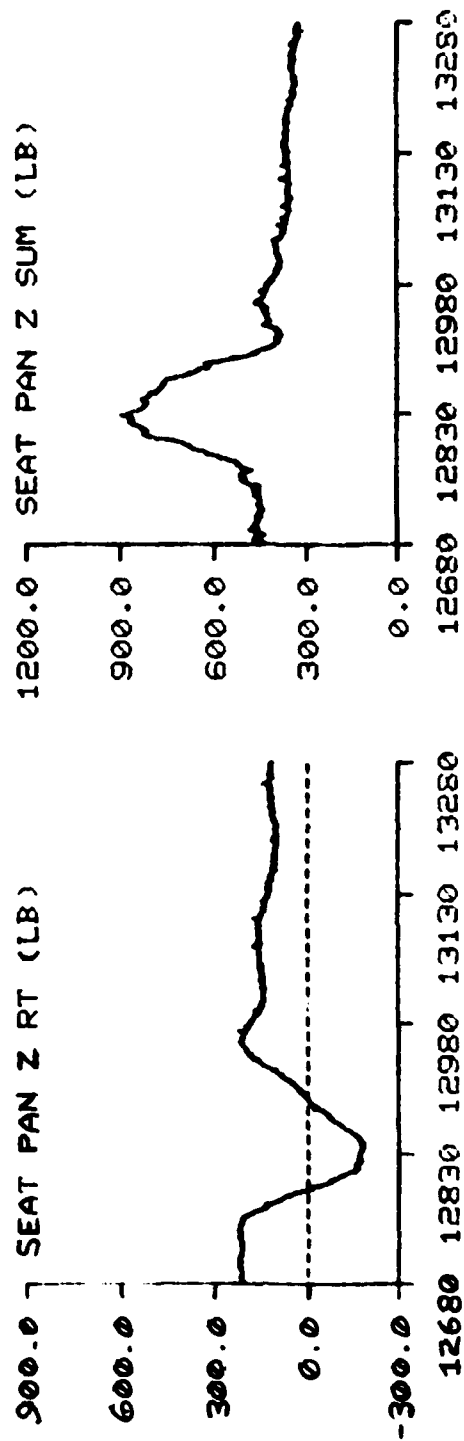
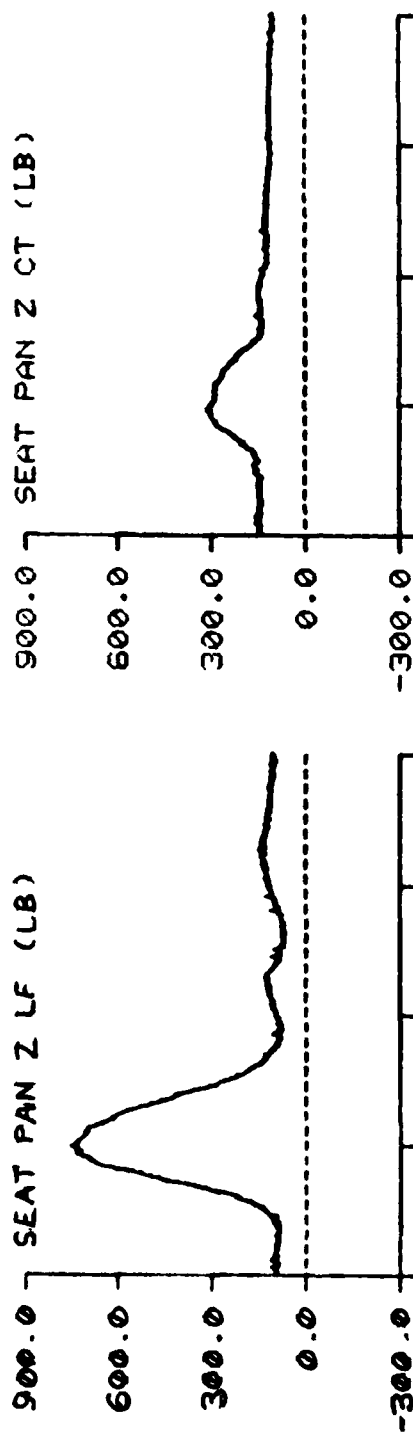
NEG G STRAP (LB)

TIME IN MILLISECONDS

F-111

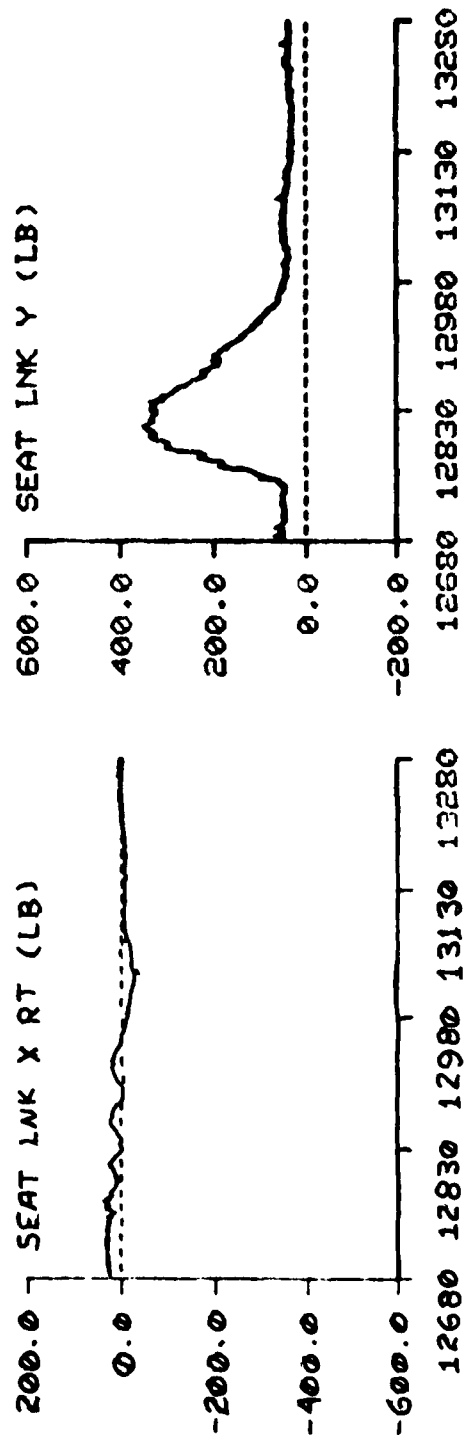
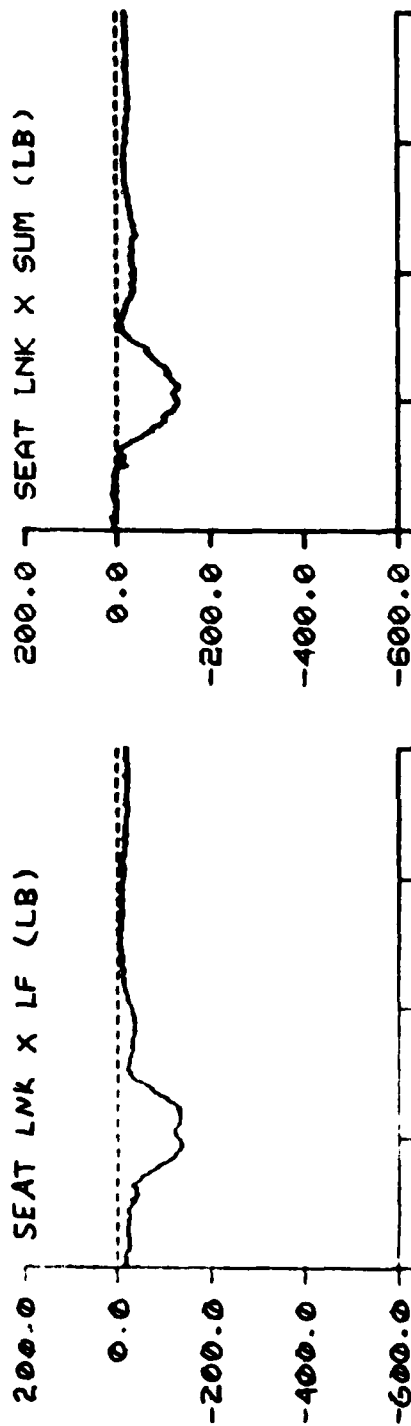
TEST NO: 507

SUBJECT ID: M-9



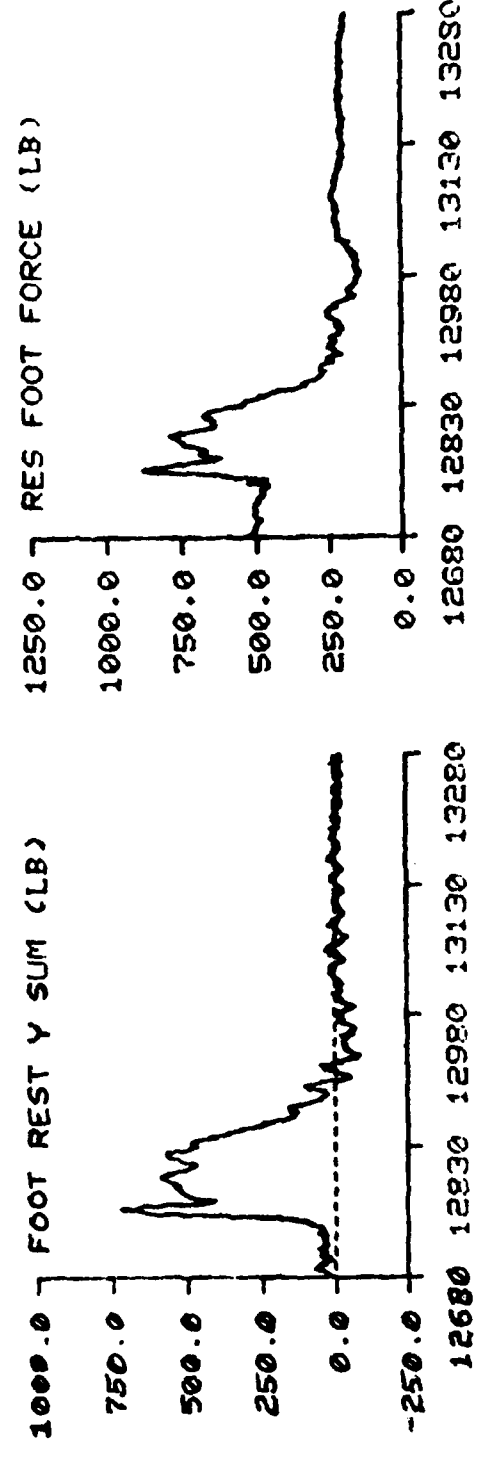
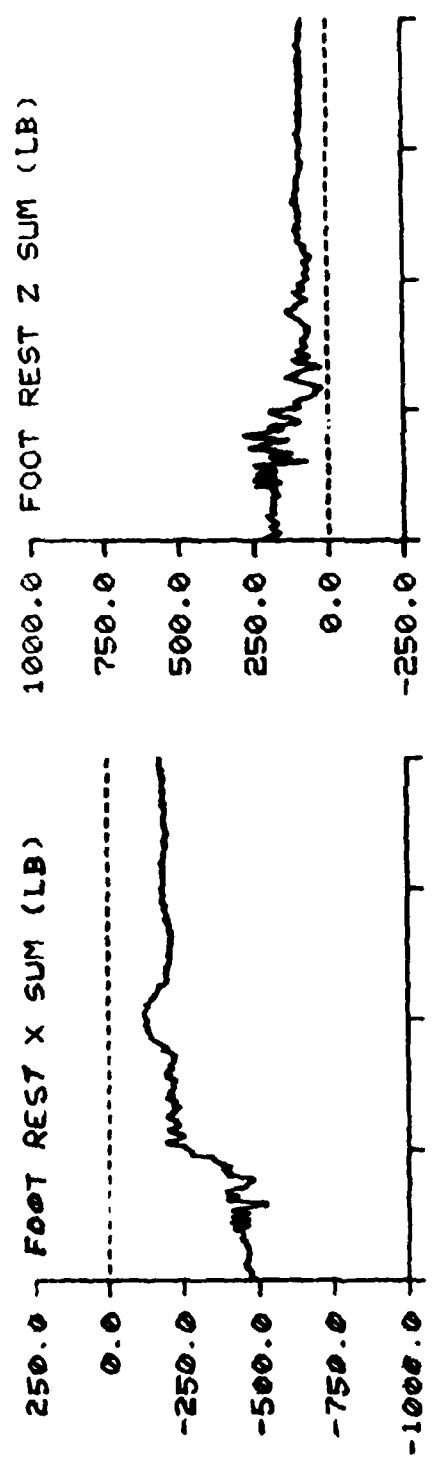
TIME IN MILLISECONDS

F-111 TEST NO: 507 SUBJECT ID: M-9



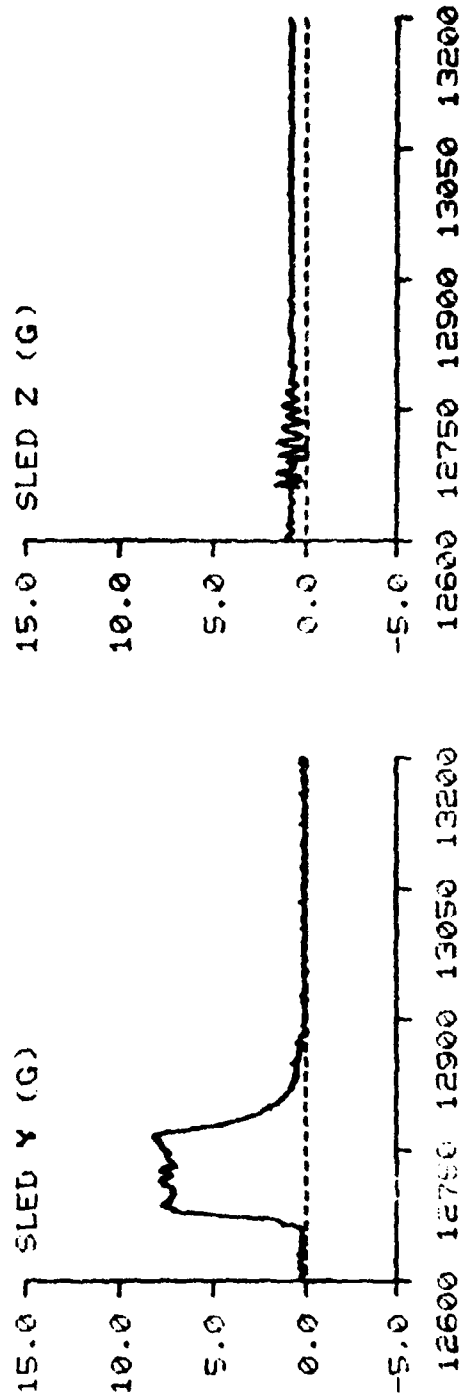
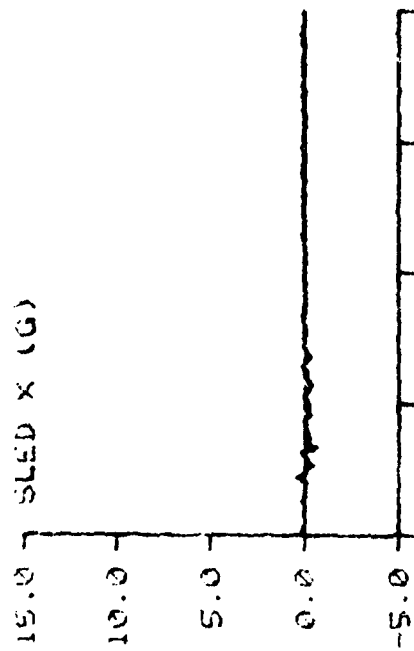
TIME IN MILLISECONDS

F-111 TEST NO: 507 SUBJECT ID: M-9



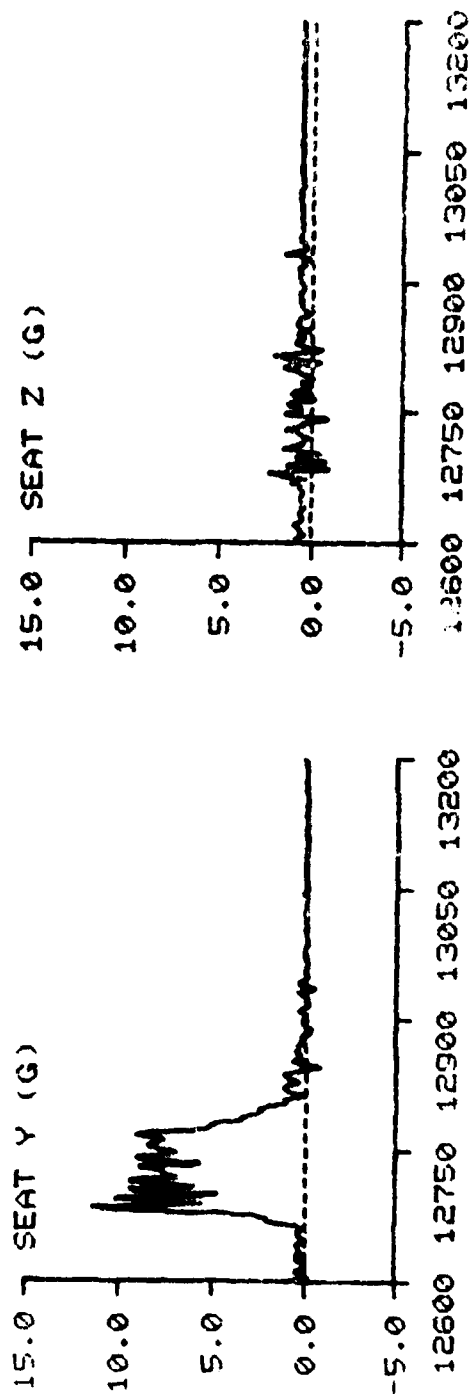
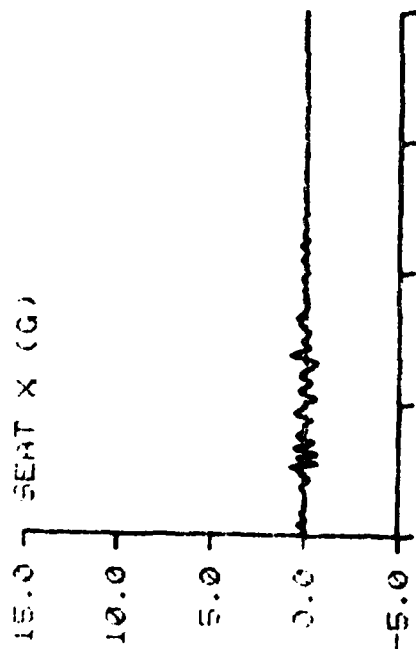
TIME IN MILLISECONDS

F-111 TEST NO: 515 SUBJECT ID: G-2



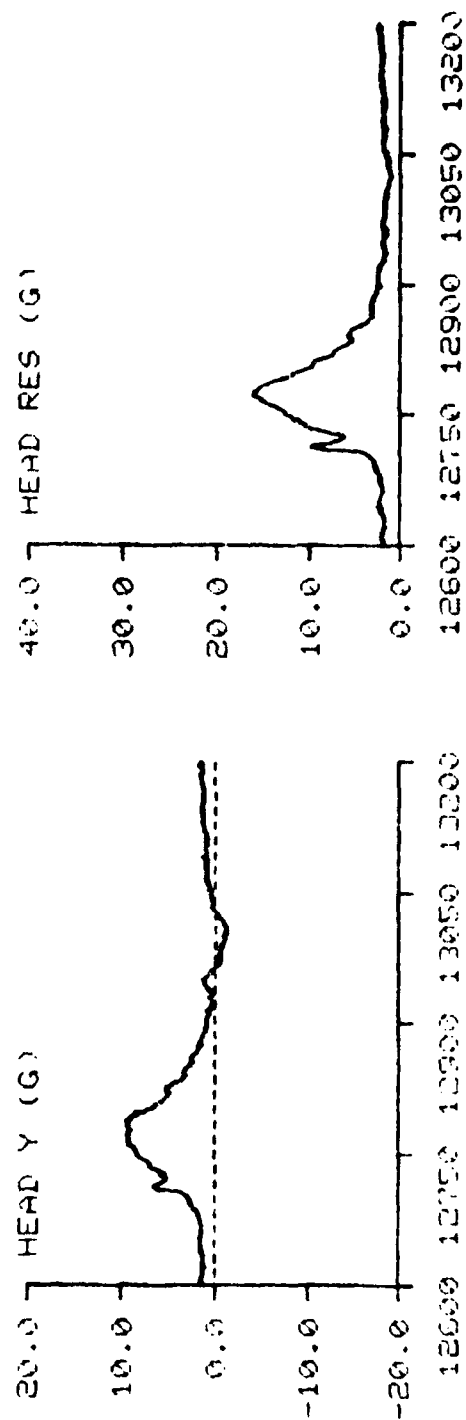
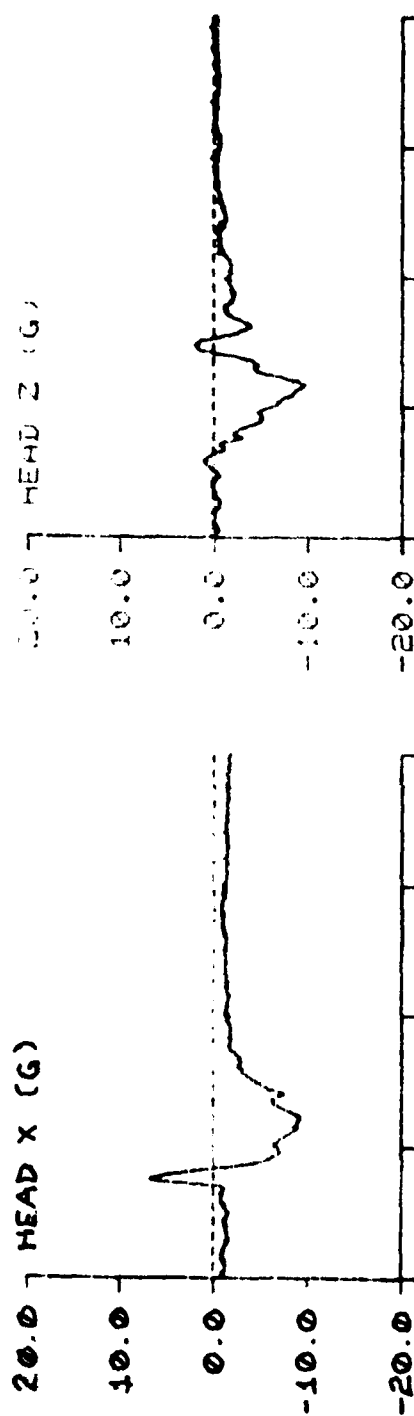
TIME IN MILLISECONDS

F-111 TEST NO: 513 SUBJECT ID: G-2



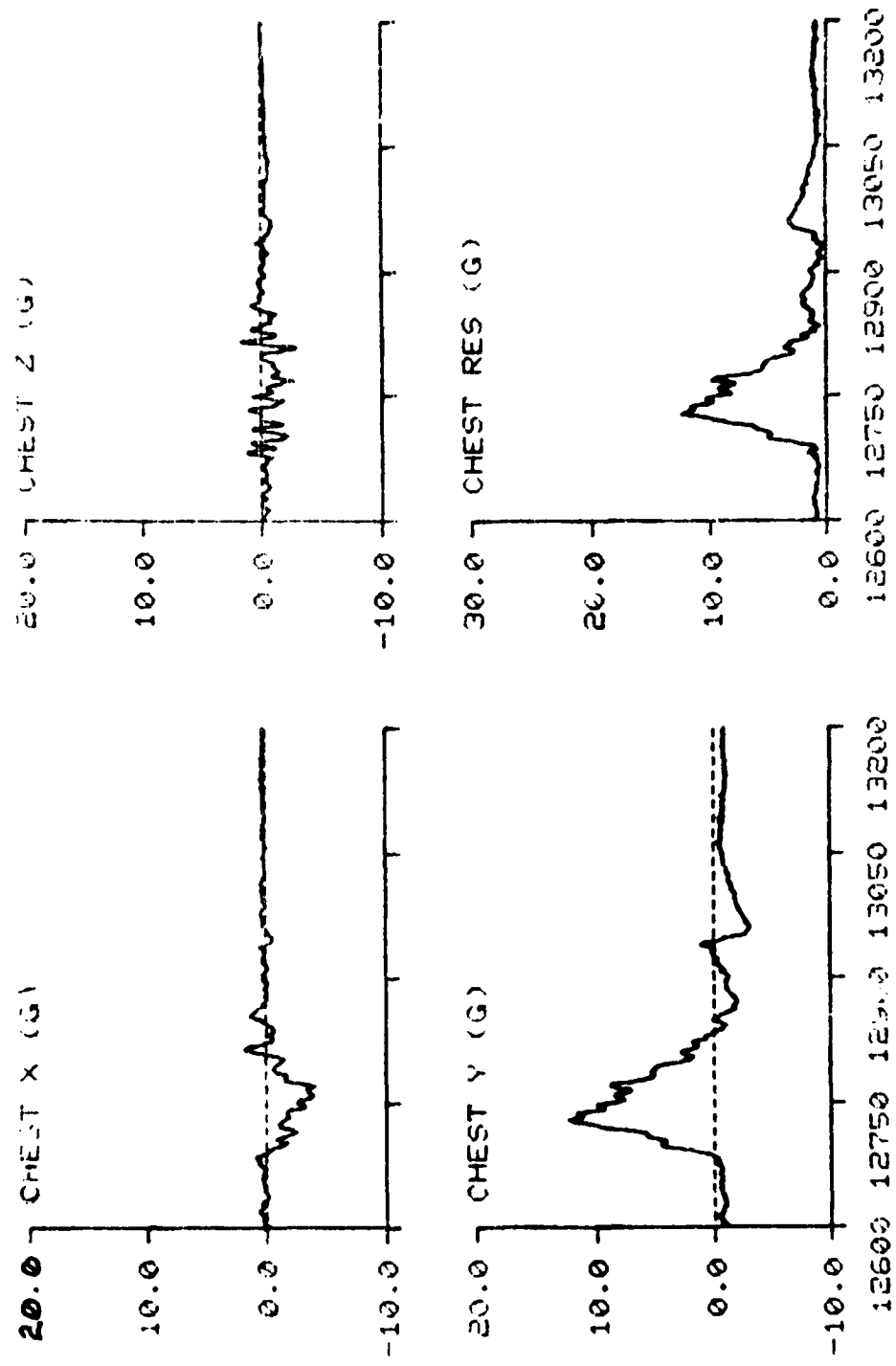
TIME IN MILLISECONDS

F-111 TEST NO: 513 SUBJECT ID: G-2



TIME IN MILLISECONDS

F-111      TEST NO: 513      SUF      CT ID: G-2



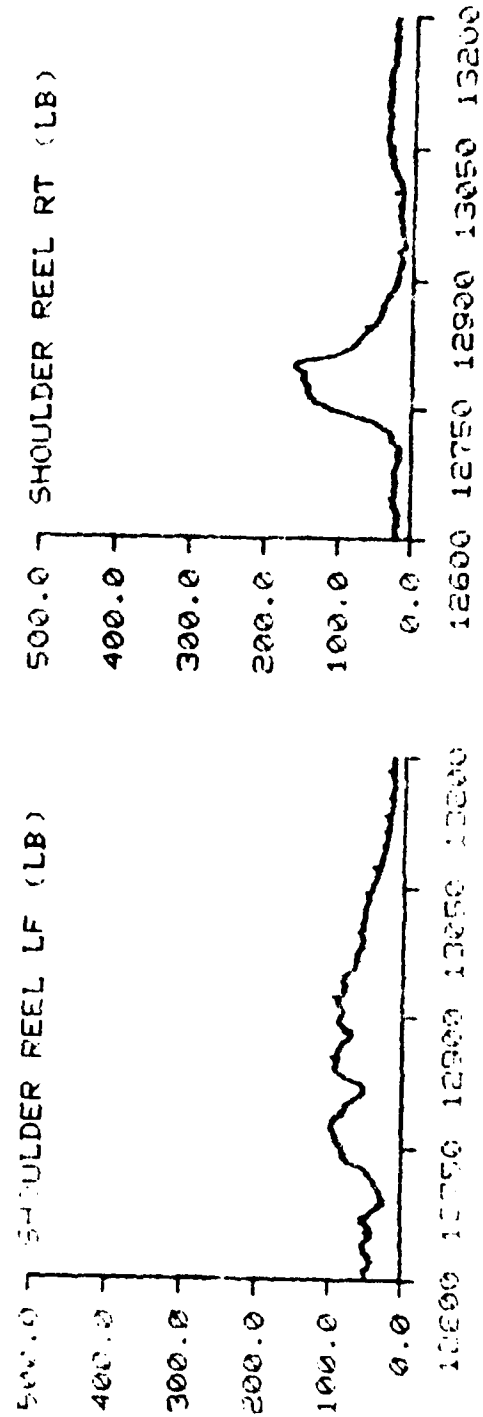
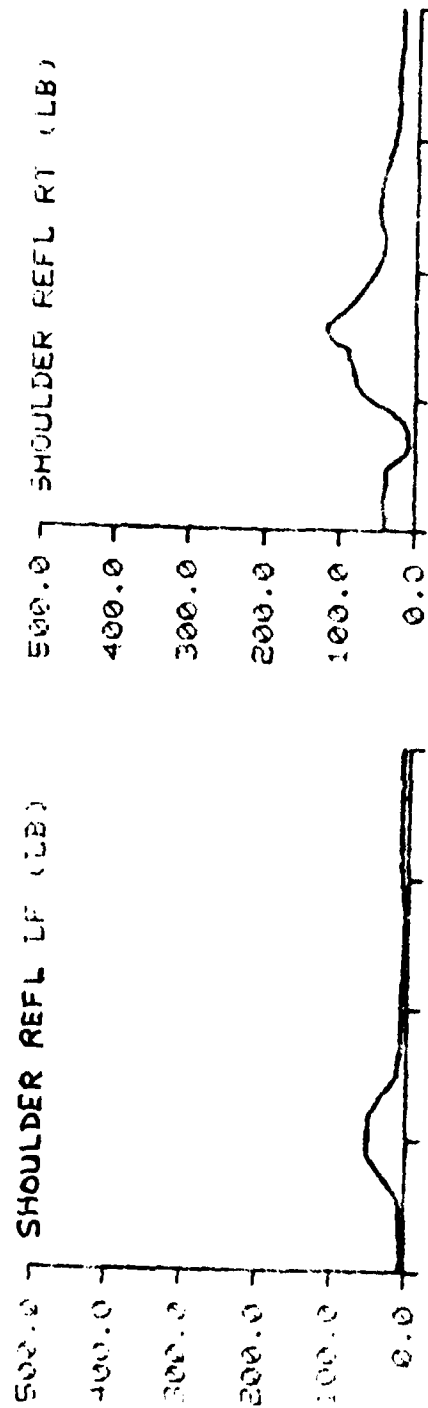
TIME IN MILLISECONDS



1-111

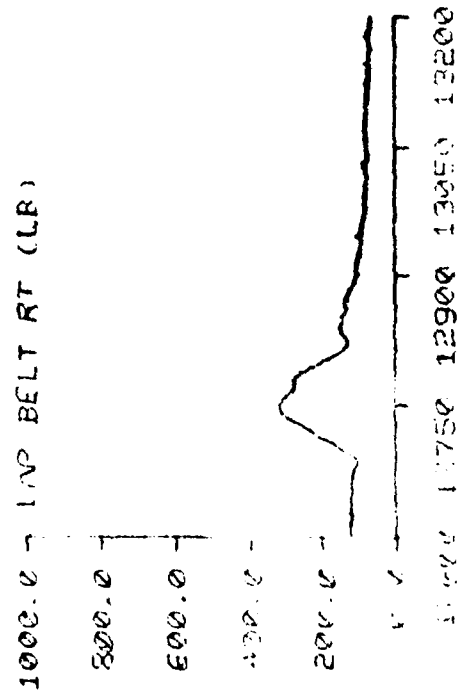
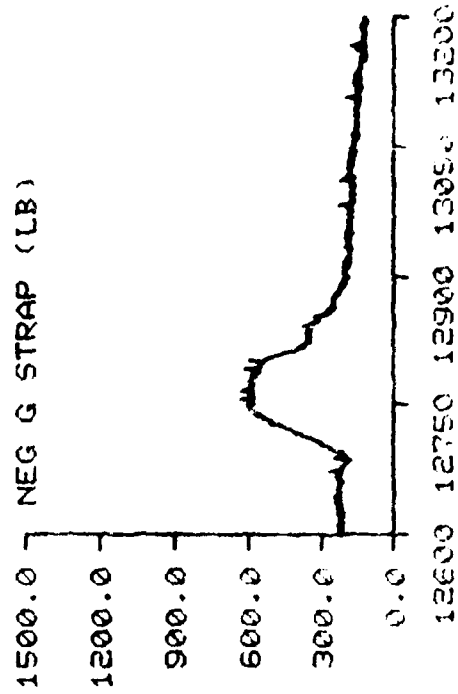
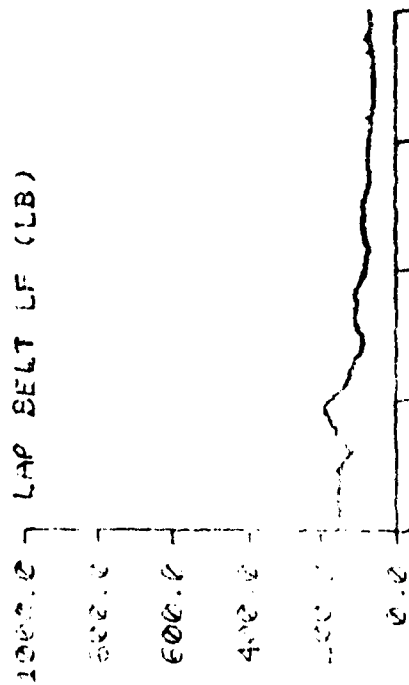
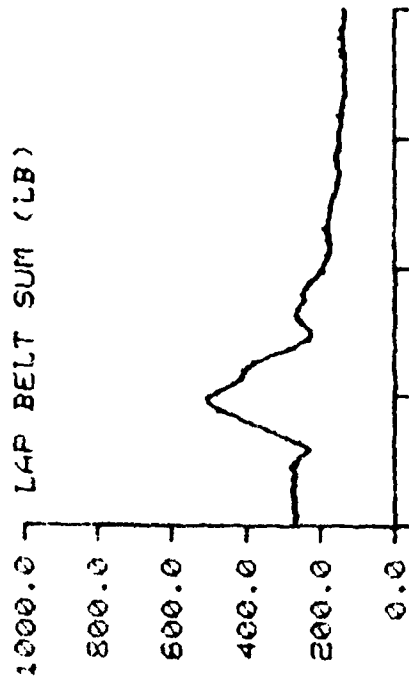
TEST NO: 513

SUBJECT ID: G-2



TIME IN MILLISECONDS

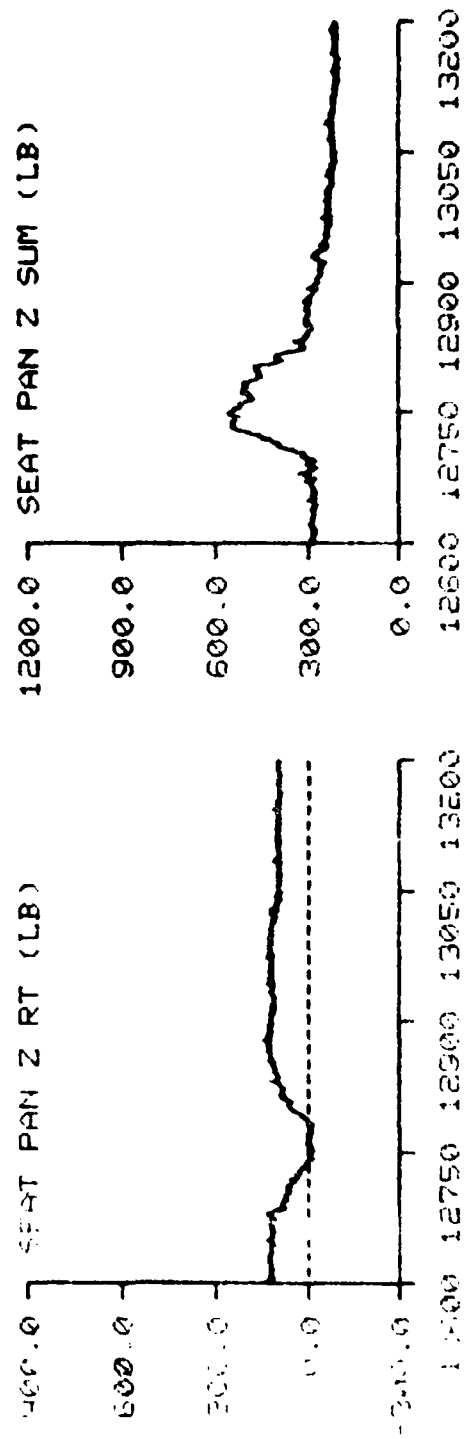
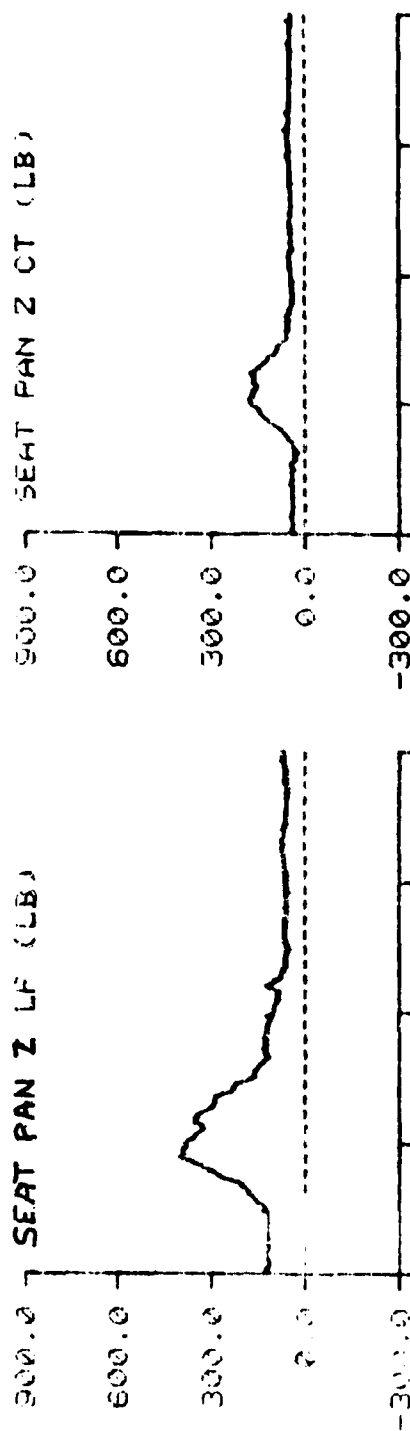
F-111 TEST NO: 513 SUBJECT ID: G-2



TIME IN MILLISECONDS

-11- TEST NO: 513

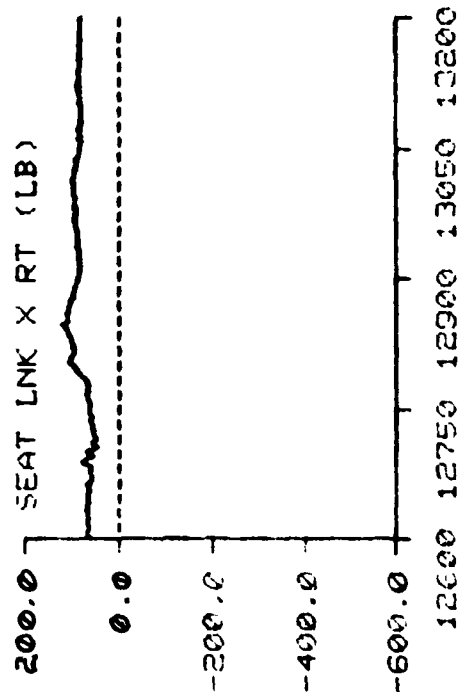
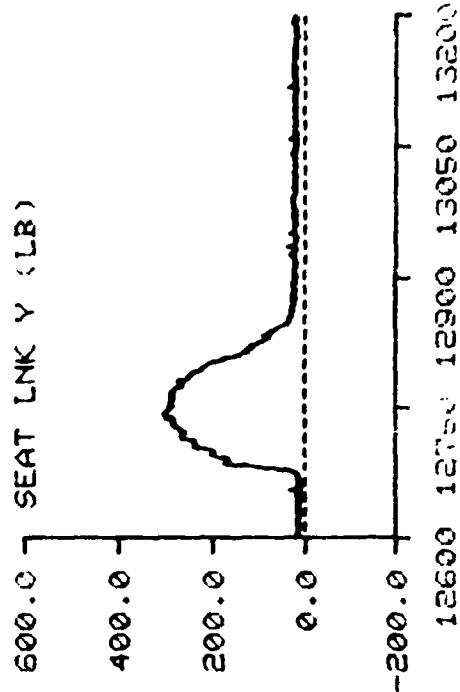
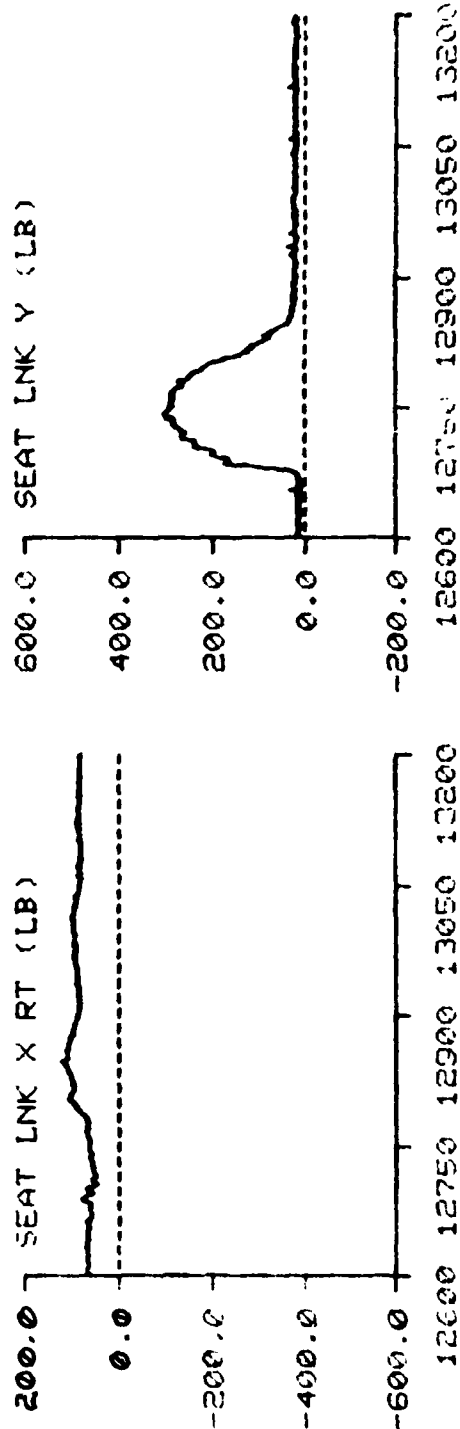
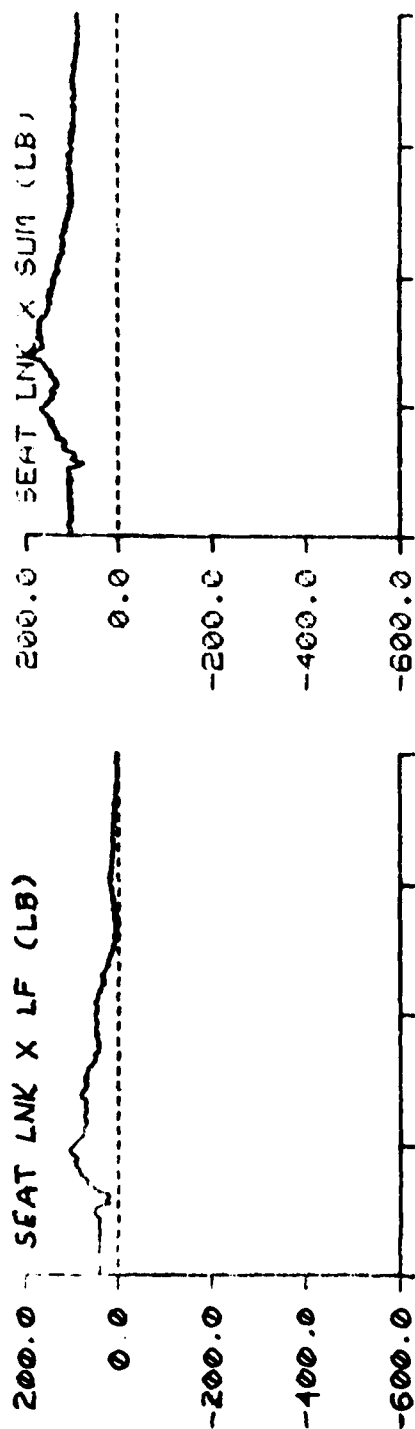
SUBJECT ID: G-2



TIME IN MILLISECONDS

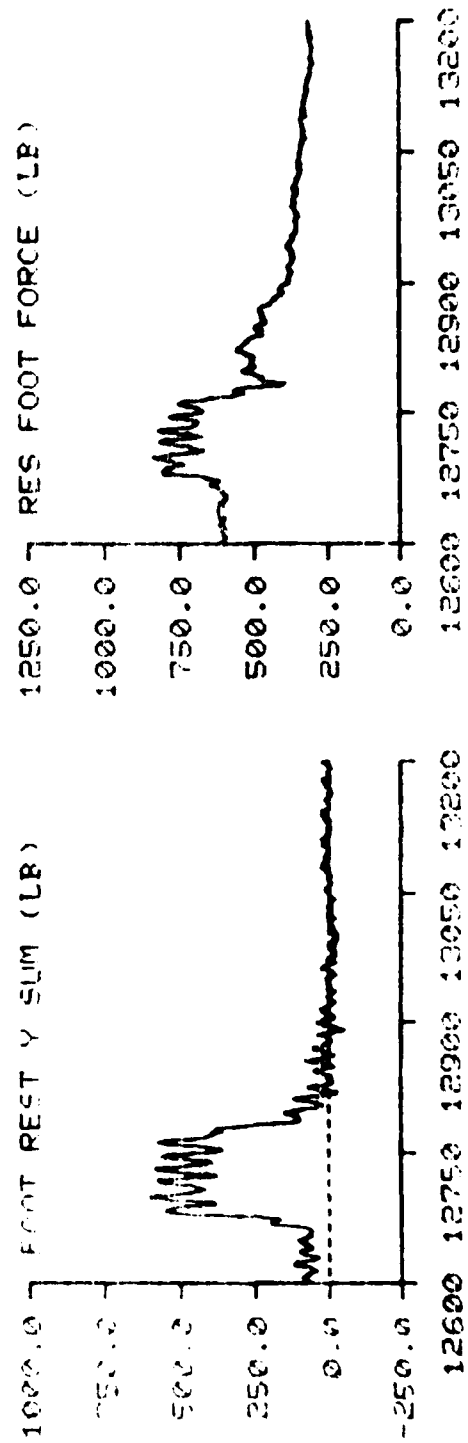
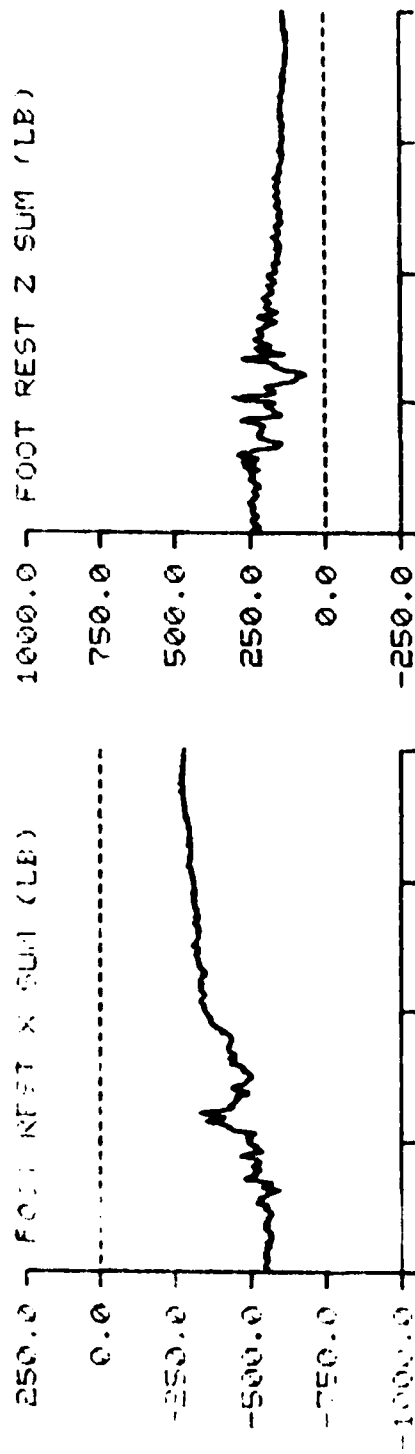
F-111 TEST NO: 513

SUBJECT ID: G-2



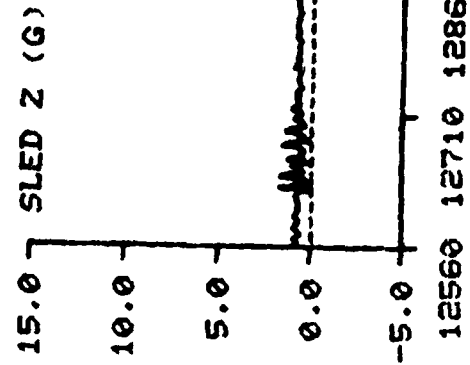
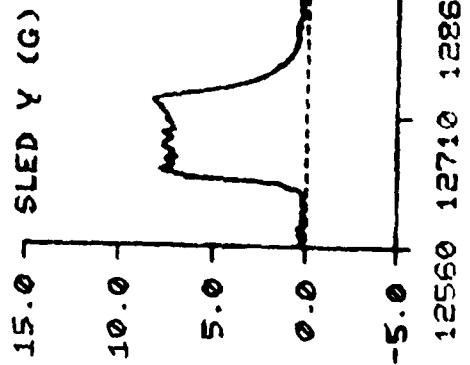
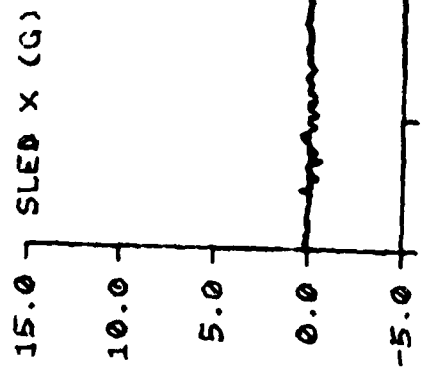
TIME IN MILLISECONDS

111 TEST NO: 513 SUBJECT ID: G-2



TIME IN MILLISECONDS

F-111      TEST NO: 516      SUBJECT ID: J-1

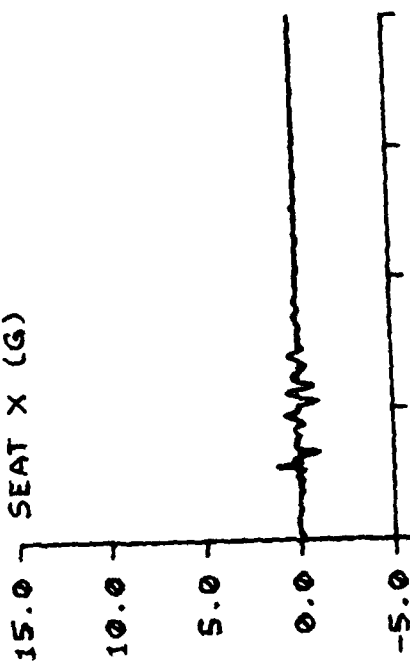


TIME IN MILLISECONDS

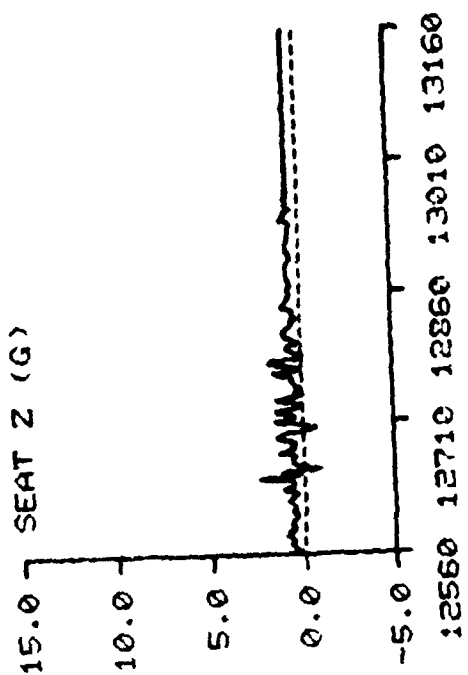
SUBJECT ID: J-1

F-111 TEST NO: 516

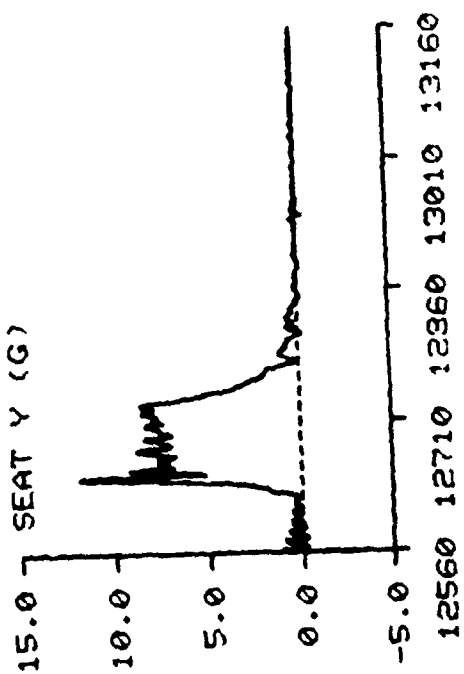
SEAT X (G)



SEAT Z (G)

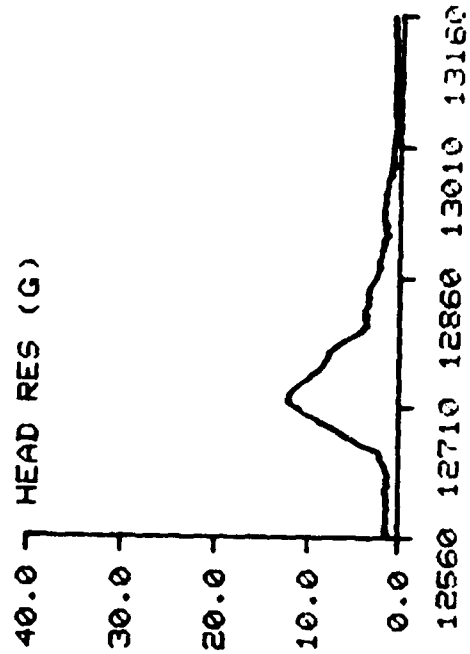
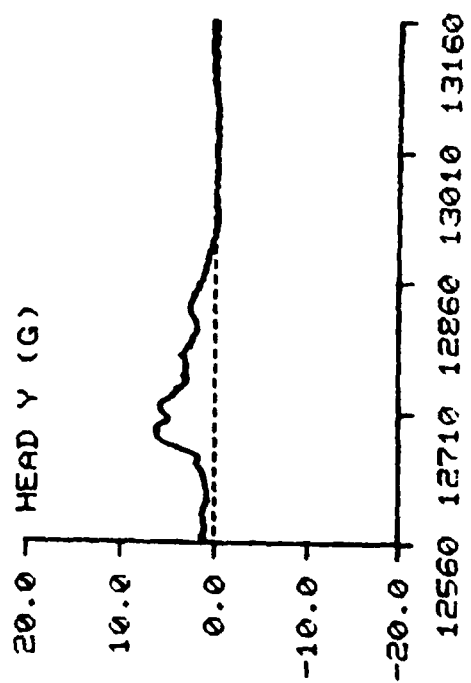
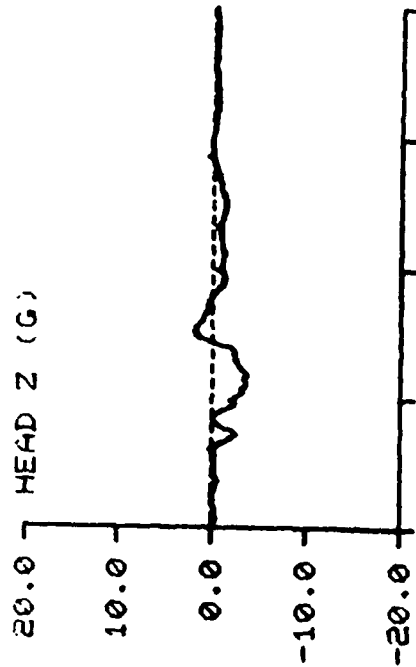
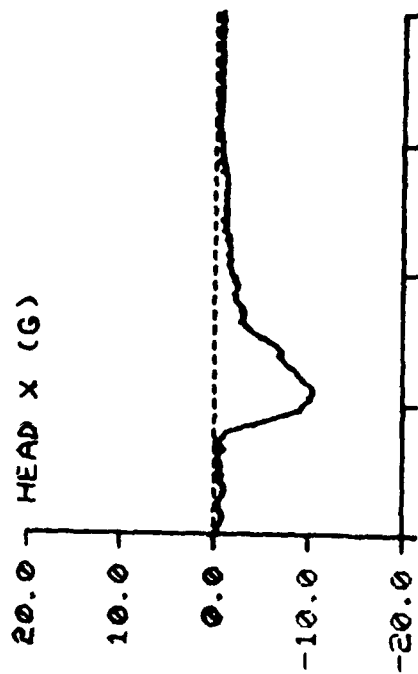


SEAT Y (G)



TIME IN HILISECONDS

F-111 TEST NO: 516 SUBJECT ID: J-1

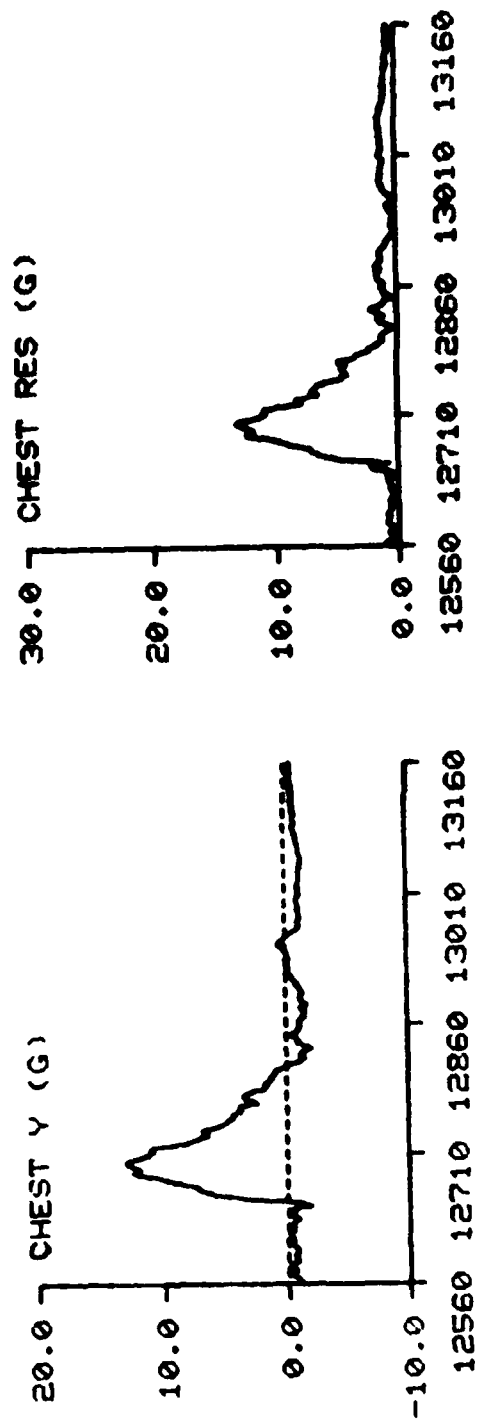
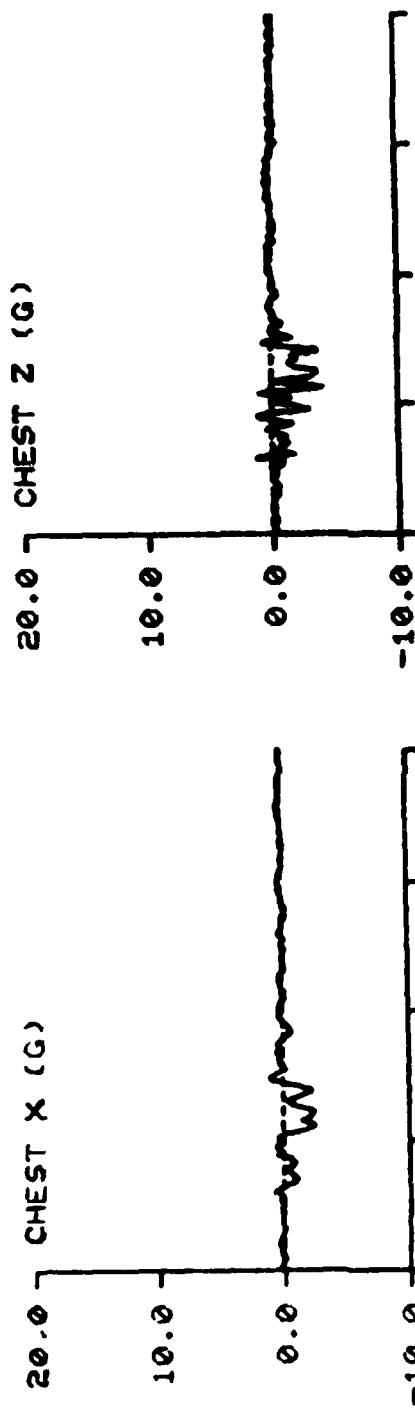


TIME IN MILLISECONDS



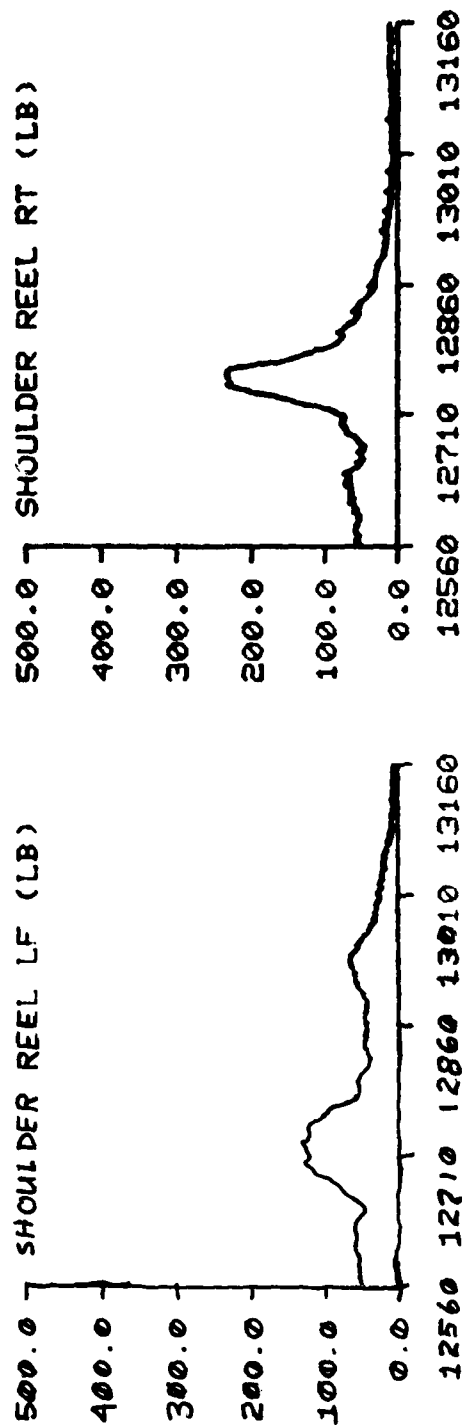
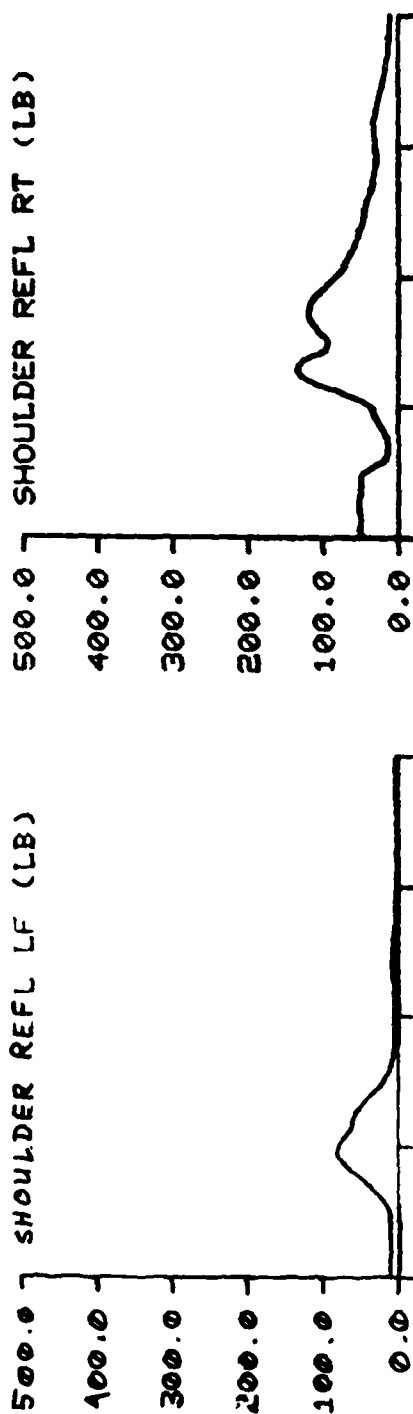
SUBJECT ID: J-1

TEST NO: 516



TIME IN MILLISECONDS

F-111      TEST NO: 516      SUBJECT ID: J-1

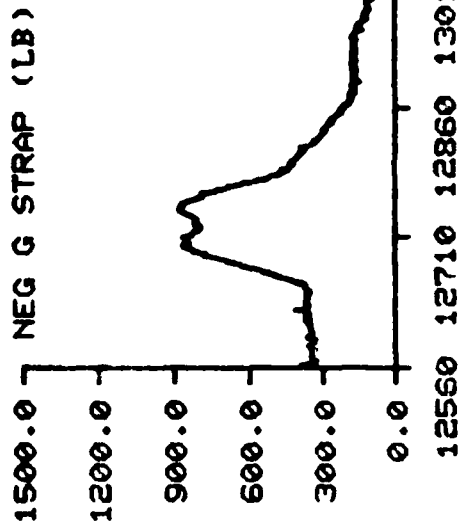
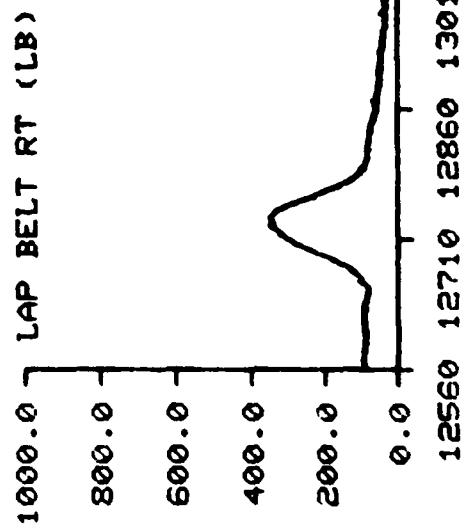
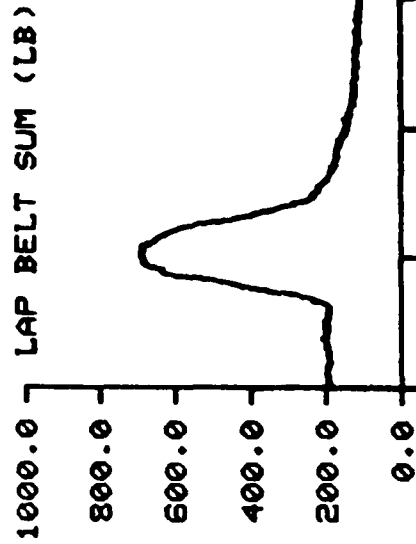
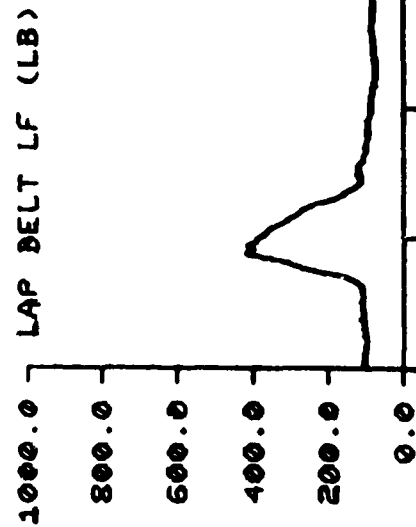


TIME IN MILLISECONDS

F-111

TEST NO: 516

SUBJECT ID: J-1

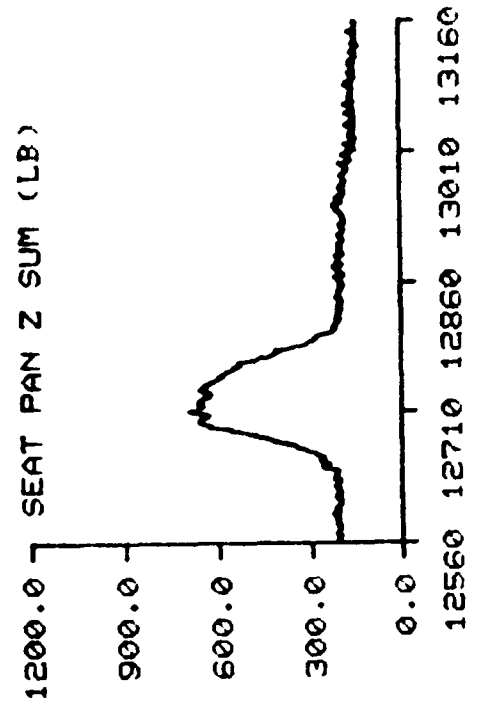
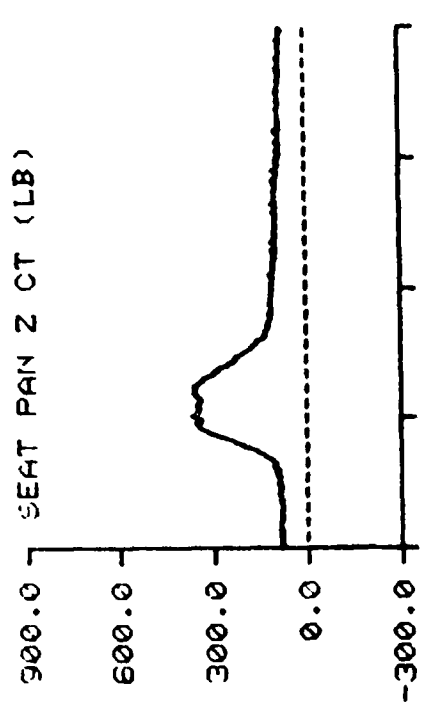
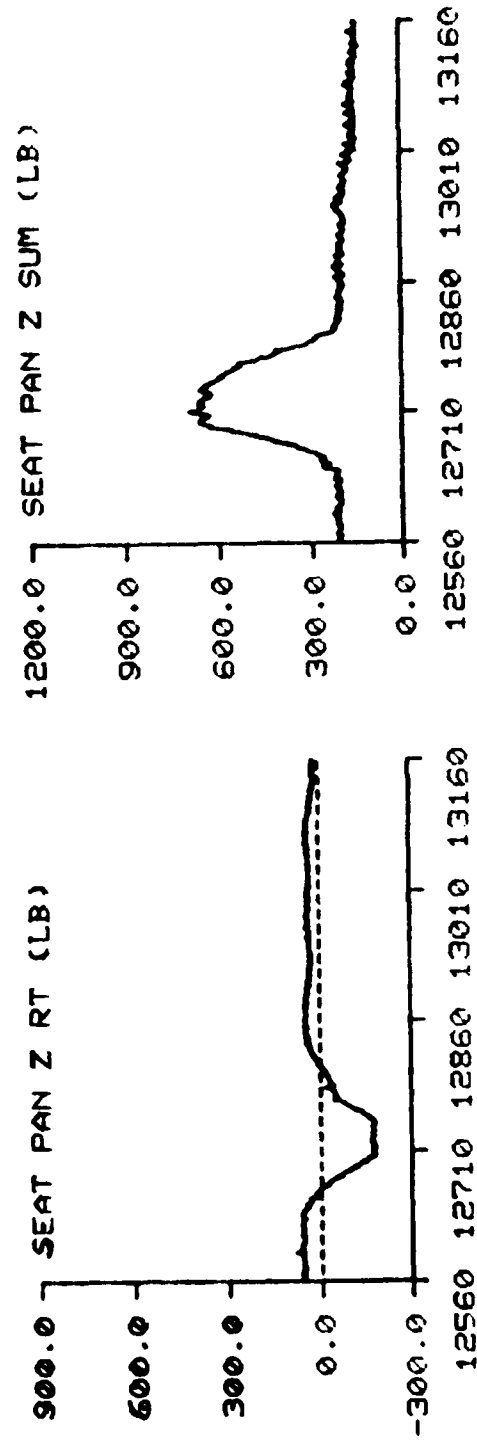
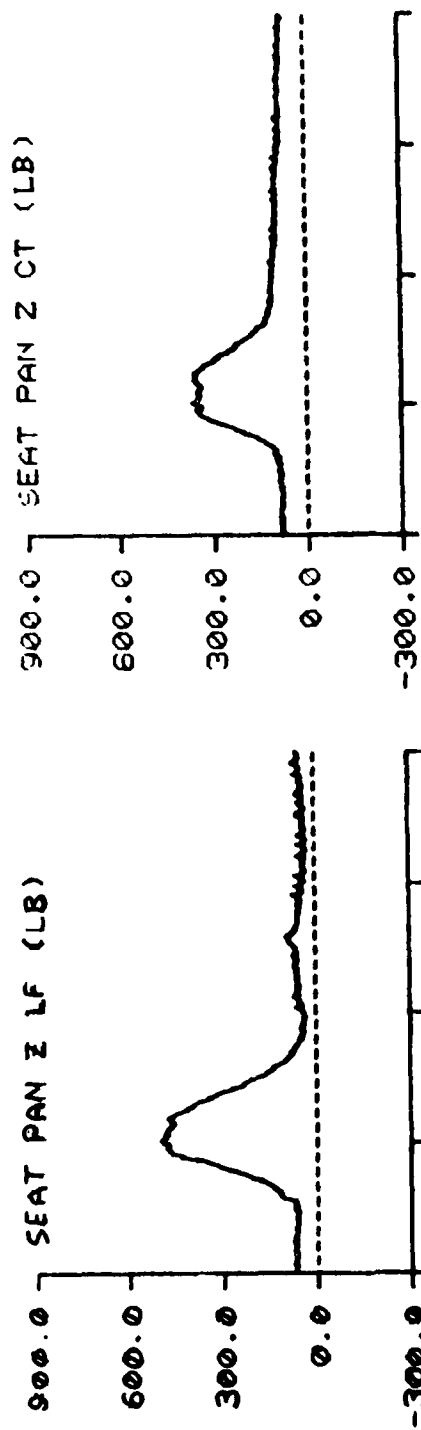


TIME IN MILLISECONDS

P-111

TEST NO: 516

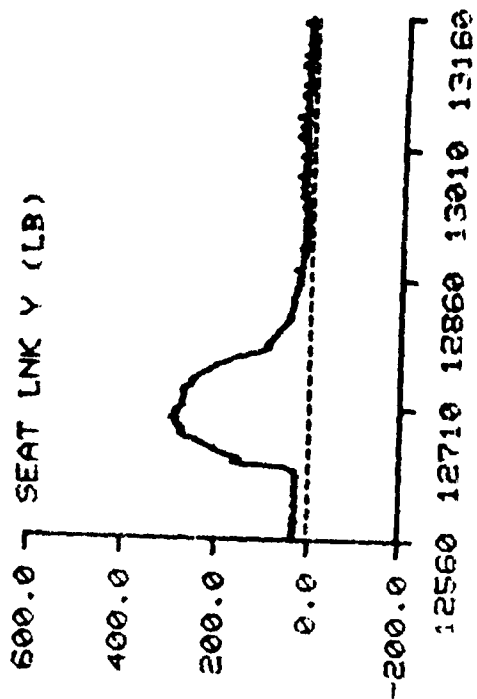
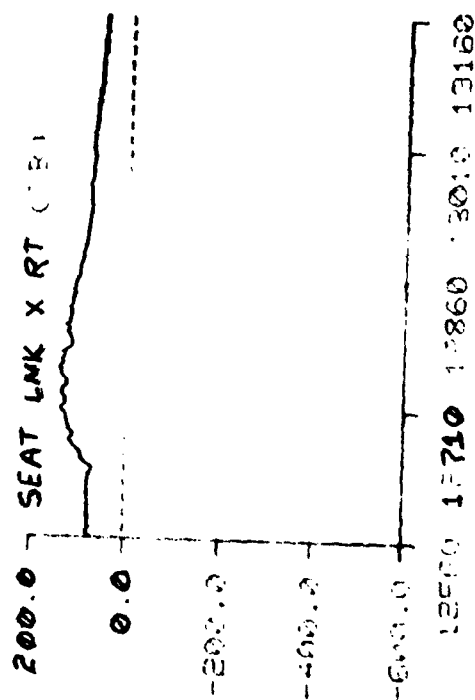
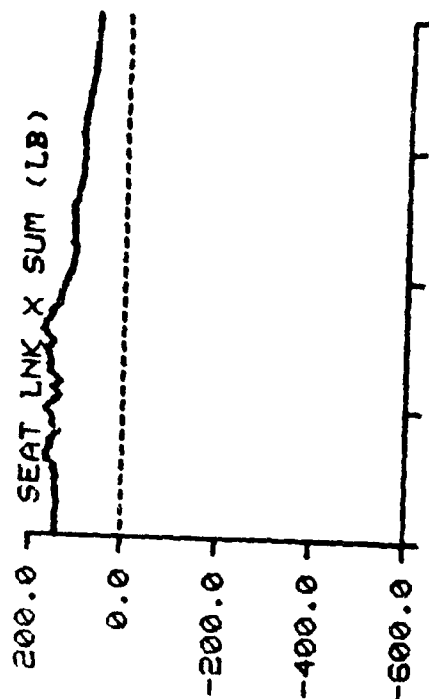
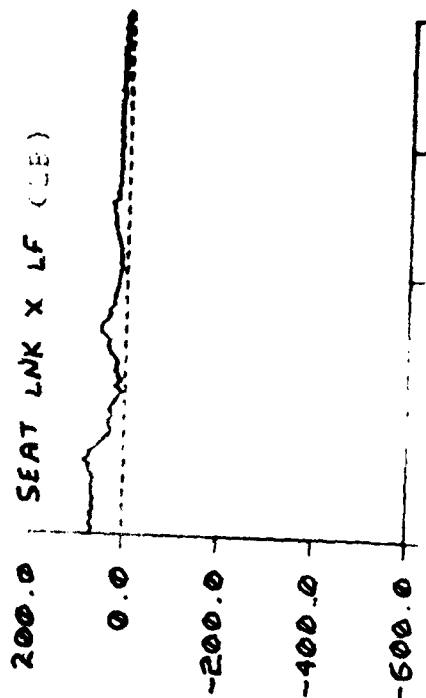
SUBJECT ID: J-1



TIME IN MILLISECONDS

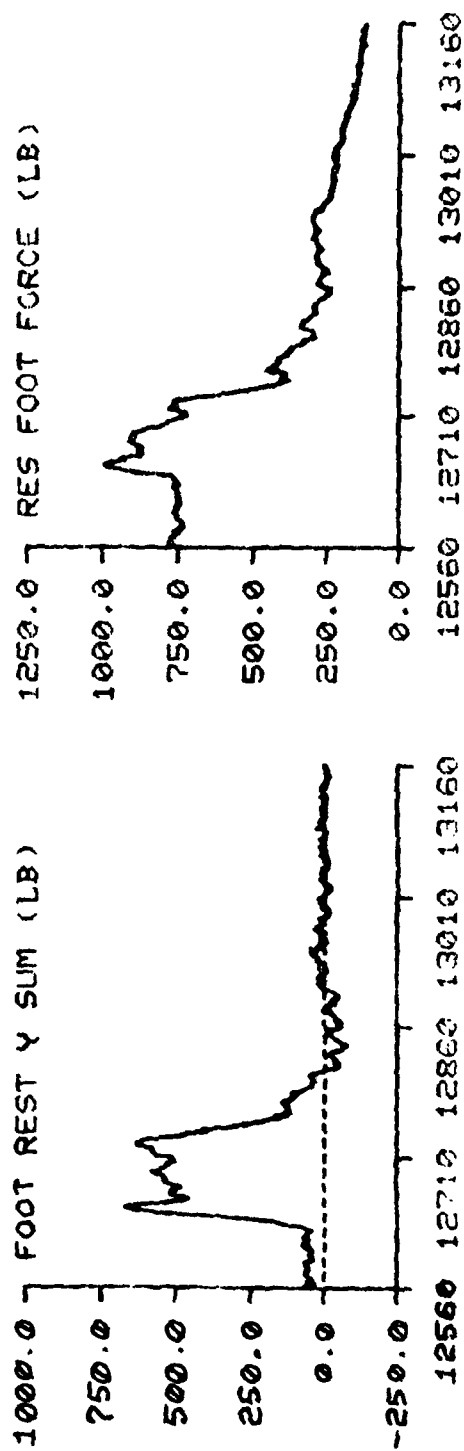
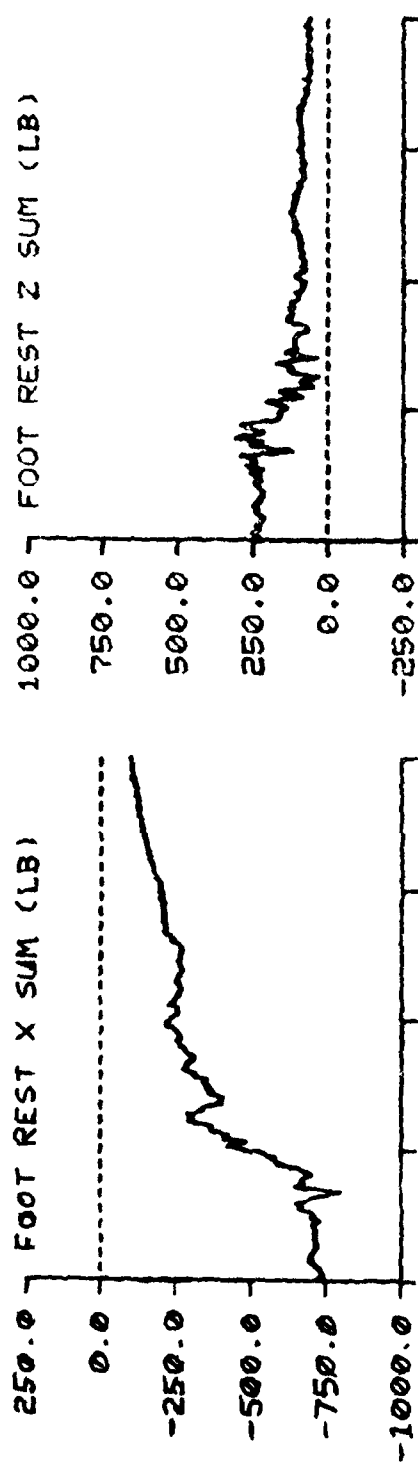
TEST NO: 516

SUBJECT ID: J-1



TIME IN MILLISECONDS

F-111      TEST NO: 516      SUBJECT ID: J-1



TIME IN MILLISECONDS

## APPENDIX E

### SUMMARY OF FORWARD FACING IMPACT TEST DATA

This appendix contains tables that list the maximum values of the measured forces, loads, accelerations, severity indexes, and velocities measured during each forward facing impact test with a volunteer subject. Also included is one set of data plots for each six cells of the test matrix used in the -G<sub>x</sub> phase. The matrix is summarized as follows:

1. 8G, 0° shoulder strap, 90° seat back angle.
2. 8G, 0° shoulder strap, 103° seat back angle.
3. 8G, (FD) maximum shoulder strap angle, 110° seat back angle.
4. 10G, 0° shoulder strap, 90° seat back angle.
5. 10G, 0° shoulder strap, 103° seat back angle.
6. 10G, (FD) maximum shoulder strap angle, 103° seat back angle.

A complete data package has been submitted to ASD/AES and a complete data package will be maintained by AFAMRL/BBP until this work unit is retired. The experimental results will eventually be recorded within a permanent data bank at AFAMRL.

The sample data plots were selected based on the subject who had the most measured responses which fell within one-half standard deviation of the mean of the measured responses of all of the subjects.

F-111 8G<sub>x</sub> TEST SUMMARY TABLE (CONFIGURATION 0/90)

TEST #	532	536	537	542	552	556	MEAN	STANDARD DEVIATION
Subject ID	R-1	M-9	G-2	F-2	E-1	M-2		
Subject Weight	199	168.5	121	157	188	163	166	27.2
SH Strap Angle	1.75	2.50	5.0	0	2.5	1.5	2.21	1.65
Seat Back Angle	88.5	89.5	89.5	90	88.5	90	89.3	0.68
Sled X	-8.74	-8.42	-7.59	-8.09	-7.91	-7.81	-8.09	0.42
Sled Velocity	31.2	31.0	28.5	29.6	29.1	29.4	29.8	1.08
Seat X	-10.4	-10.0	-10.2	-10.1	-9.82	-10.8	-10.2	0.34
Chest Res	12.4	14.0	11.9	13.0	11.6	13.1	12.7	0.88
Chest SI	20.7	26.3	19.5	23.8	21.6	22.3	22.4	2.41
Head Res	10.7	12.0	10.4	10.2	9.16	10.8	10.5	0.92
Head SI	23.9	33.8	28.5	26.4	20.9	28.2	27.0	4.41
Shoulder Sum	689	677	371	435	490	532	532	129
Shoulder Sum/Wt	3.46	4.02	3.07	2.77	2.60	3.27	3.20	0.51
Lap Belt Sum	588	457	567	608	647	517	564	67.9
Lap Sum/Wt	2.95	2.71	4.69	3.88	3.44	3.17	3.47	0.72
Neg -G Strap	342	426	257	324	394	166	318	94.7
Seat Link X Sum	-342	-244	-193	-306	-335	-239	-277	60.0
Seat Link Y	46.4	66.4	28.2	44.7	46.0	73.6	50.9	16.5
Seat Pan Z Sum	808	670	459	620	597	522	613	121
Seat Z/Wt	4.06	3.98	3.79	3.95	3.18	3.20	3.69	0.40
Res Seat Force	873	707	469	673	683	549	659	139
Res Seat/Wt	4.39	4.20	3.87	4.29	3.63	3.37	3.96	0.40
Foot X Sum	-1310	-1604	-1024	-1164	-1221	-1264	-1265	193
Foot Y Sum	69.9	72.5	82.2	-70.2	-115	-87.1	-7.95	91.9
Foot Z Sum	470	547	383	498	497	500	483	54.7
Res Foot Force	1345	1644	1048	1203	1271	1312	1304	197
Foot X Preload	-567	-747	-395	-459	-421	-587	-529	132
Foot Y Preload	12.5	-2.6	18.2	-6.2	4.5	-15.2	1.87	12.4
Foot Z Preload	258	270	166	189	182	261	221	46.8
Res Preload	623	794	429	496	459	642	574	138



P-111 8G TEST SUMMARY TABLE (CONFIGURATION 0/103)

TEST #	534	535	538	539	543	544	MEAN	STANDARD DEVIATION
Subject ID	W-1	M-5	D-1	M-7	F-3	M-10		
Subject Weight	157	168	200	135	164.5	145	162	22.5
SH Strap Angle	0.25	2.50	102.5	4.50	0	1.00	1.63	1.67
Seat Back Angle	102.5	102.5	102.5	102.5	102.5	102.5	102.5	0
Sled X	-8.31	-7.91	-7.85	-7.57	-7.58	-7.49	-7.79	0.31
Sled Velocity	29.7	29.3	28.7	28.6	28.8	28.5	28.9	0.47
Seat X	-10.6	-10.3	-9.95	-9.91	-9.59	-9.85	-10.0	0.36
Chest Res	11.2	10.7	10.3	10.4	9.60	11.2	10.6	0.61
Chest SI	24.1	23.3	19.9	21.0	18.3	20.7	21.2	2.15
Head Res	9.60	9.63	12.2	12.8	12.1	11.5	11.3	1.37
Head SI	21.4	20.8	30.7	33.8	28.9	26.3	27.0	5.17
Shoulder Sum	546	629	671		516	561	585	63.6
Shoulder Sum/Wt	3.48	3.74	3.36		3.14	3.87	3.52	0.29
Lap Belt Sum	521	462	674	602	490	727	579	106
Lap Sum/Wt	3.32	2.75	3.37	4.46	2.98	5.01	3.65	0.89
Neg -G Strap	271	389	579	155	327	172	316	157
Seat Link X Sum	-276	-179	-294	-290	-260	-396	-283	69.8
Seat Link Y	31.0	65.5	44.3	-25.4	40.1	-30.0	20.9	39.4
Seat Pan Z Sum	678	625	857	615	556	726	676	106
Seat Z/Wt	4.32	3.72	4.29	4.55	3.38	5.01	4.21	0.58
Res Seat Force	721	649	903	658	610	827	728	114
Res Seat/Wt	4.59	3.86	4.52	4.87	3.71	5.70	4.54	0.72
Foot X Sum	-1212	-1362	-1336	-704	-1030	-690	-1056	302
Foot Y Sum	-96.1	-88.6	-67.8	-58.8	66.9	71.3	-28.9	77.1
Foot Z Sum	397	447	434	309	435	339	394	57.2
Res Foot Force	1235	1384	1373	718	1064	696	1078	310
Foot X Preload	-504	-562	-472	-90.7	-376	-95.1	-350	208
Foot Y Preload	-39.3	-31.3	-1.2	5.6	10.0	-5.6	-10.3	20.2
Foot Z Preload	159	212	174	67.0	158	45.6	136	65.1
Res Preload	529	602	505	113	408	106	377	216

F-111 8G TEST SUMMARY TABLE (CONFIGURATION FD/110)

TEST #	553	573	MEAN	STANDARD DEVIATION
Subject ID	P-2	O-1		
Subject Weight	160	175	167.5	10.6
SH Strap Angle	29	23	26.0	4.24
Seat Back Angle	109.5	110	109.8	0.35
Sled X	-7.52	-7.87	-7.70	0.25
Sled Velocity	28.4	29.4	28.9	0.71
Seat X	-9.92	-10.5	-10.2	0.41
Chest Res	9.21	9.91	9.56	0.49
Chest SI	16.3	19.5	17.9	2.26
Head Res	10.8	6.61	8.71	2.96
Head SI	23.1	9.87	16.5	9.36
Shoulder Sum	601	374	488	161
SH Sum/Wt	3.75	2.14	2.95	1.14
Lap Belt Sum	827	707	767	84.9
Lap Sum/Wt	5.17	4.04	4.61	0.80
Neg -G Strap	403	412	408	6.36
Seat Link X Sum	-289	-304	-297	10.6
Seat Link Y	28.2	52.0	40.1	16.8
Seat Pan Z Sum	676	600	638	53.7
Seat Z/Wt	4.23	3.43	3.83	0.57
Res Seat Force	732	670	701	43.8
Res Seat/Wt	4.57	3.83	4.20	0.52
Foot X Sum	-959	-1295	-1127	238
Foot Y Sum	-107	-81.4	-94.2	18.1
Foot Z Sum	438	581	510	101
Res Foot Force	1031	1372	1202	241
Foot X Preload	-303	-661	-482	253
Foot Y Preload	-9.8	-1.6	-5.70	5.80
Foot Z Preload	138	374	256	167
Res Preload	333	760	547	302

F-111 LOG<sub>x</sub> TEST SUMMARY TABLE (CONFIGURATION 0/90)

TEST #	541	549	557	561	567	572	598	599	601	MEAN	STANDARD DEVIATION
Subject ID	R-1	G-2	M-9	F-2	S-3	M-2	M-7	M-5	M-1		
Subject Wt	200	121	166	157	166	164	138	170	159	160	21.8
Sh Strap Angle	1.25	5	2.5	1.0	1.25	1.0	3.0	0.25	-0.75	1.61	1.68
Seat Back Angle	90	89	90	90	90	90	90	91	90	90	0.50
Sled X	-9.53	-9.14	-9.19	-8.98	-9.43	-9.24	-8.88	-9.11	-8.65	-9.13	0.27
Sled Velocity	31.8	31.9	31.2	31.2	31.5	31.6	31.1	31.4	30.8	31.4	0.35
Seat X	-11.1	-10.8	-10.3	-11.0	-11.0	-11.5	-10.7	-11.0	-10.0	-10.8	0.45
Chest Res	12.1	13.0	14.0	13.2	13.3	16.2	14.2	14.5	11.3	13.5	1.42
Chest SI	24.9	27.4	29.4	28.7	28.9	31.9	30.2	29.7	25.7	28.5	2.21
Head Res	13.2	12.3	9.44	9.48	10.3	11.0	10.5	9.39	9.18	10.5	1.41
Head SI	35.8	30.5	16.2	17.9	21.0	23.0	24.8	20.4	26.7	24.0	6.23
Shoulder Sum	713	451	724	491		694	537	639	584	604	105
Sh Sum/Wt	3.57	3.74	4.36	3.13		4.23	3.89	3.76	3.68	3.80	0.38
Lap Belt Sum	611	502	551	693	484	552	525	286	382	510	120
Lap Sum/Wt	3.06	4.17	3.32	4.42	2.91	3.37	3.80	1.68	2.41	3.24	0.86
Neg -G Strap	255	317	364	289	354	243	154	441	181	289	91.5
Seat Lnk X Sum	341	-258	-241	-290	-364	-234	-384	-217	-352	-298	63.3
Seat Lnk Y	36.3	47.5	39.7	63.3	42.4	86.2	65.0	17.6	51.0	49.9	19.8
Seat Pan Z Sum	685	400	732	652	586	600	575	571	502	589	98.5
Seat Z Wt	3.43	3.32	4.41	4.15	3.53	3.66	4.17	3.36	3.16	3.69	0.44
Res Seat Force	760	456	761	698	670	637	684	594	574	648	96.8
Res Seat/Wt	3.81	3.78	4.59	4.44	4.04	3.88	4.95	3.49	3.61	4.07	0.49
Foot X Sum	-1483	-1046	-1553	1293	-1353	-1424	-925	-1725	-1432	-1359	247
Foot Y Sum	68.1	104	95.2	74.1	85.8	96.8	118	98.9	75.4	90.7	16.2
Foot Z Sum	534	423	596	550	594	571	379	538	478	518	76.1
Res Foot Force	1526	1079	1620	1341	1440	1471	941	1755	1456	1403	254
Foot X Preload	-652	-357	-773	-520	-619	-664	-162	-887	-740	-596	221
Foot Y Preload	9.0	12.2	5.3	-7.3	-8.0	7.0	2.3	-09.2	-25.5	-1.58	12.0
Foot Z Preload	286	142	281	262	283	287	77.4	236	275	237	75.4
Res Preload	713	384	823	582	680	723	180	909	790	643	230

F-111 LOG<sub>x</sub> TEST SUMMARY TABLE (CONFIGURATION 0/103)

TEST #	548	550	554	555	565	571	576	581	582	583	588	592
Subject ID	W-1	M-7	M-5	D-1	F-3	M-10	S-3	M-2	E-1	G-2	F-2	M-9
Subject Weight	154	135	169	200	168	135	165	164	189	119.5	158	170
SH Strap Angle	2.5	13.5	102	0.75	1.0	3.0	2.50	2.50	1.50	9.0	1.0	-25
Seatback Angle	102.5	102.5	102	102	102.5	102	102	102	102.5	103.5	102	102.5
Sled X	-9.78	-9.07	-9.53	-9.80	-8.53	-9.40	-8.79	-8.93	-9.41	-9.16	-9.51	-9.43
Sled Velocity	31.7	31.0	31.9	32.4	30.4	31.7	31.0	31.2	31.6	31.4	31.9	31.7
Seat X	-11.2	-9.85	-11.1	-10.2	-10.2	-10.5	-11.2	-10.8	-10.7	-11.2	-10.2	-10.7
Chest Res	12.8	12.9	11.2	12.2	11.1	13.9	11.7	11.2	11.6	11.3	12.5	11.9
Chest SI	27.8	26.5	31.3	32.7	26.4	30.7	23.7	26.5	27.1	25.8	33.6	31.1
Head Res	11.0	10.4	10.8	15.5	12.2	10.23	8.70	10.8	11.0	12.0	10.4	9.18
Head SI	28.8	21.9	24.4	46.3	25.4	26.8	14.1	25.0	28.7	24.7	18.8	16.4
Shoulder Sum	690	572	666	887	635	662	618	614	585	457	537	703
SH Sum/Wt	4.48	4.24	3.94	4.44	3.78	4.90	3.74	3.74	3.10	3.83	3.40	4.13
Lap Belt Sum	551	795	603	867	566	901	471	503	872	548	596	463
Lap Sum/Wt	3.58	5.89	3.57	4.33	3.37	6.67	2.85	3.07	4.62	4.58	3.77	2.73
Neg -G Strap	271	235	390	459	346	205	533	371	434	350	448	586
Seat Lnk X Sum	-325	-366	-222	-487	-351	-443	-314	-188	-419	-208	-455	-321
Seat Lnk Y	40.7	33.2	91.8	55.5	44.7	59.1	60.7	54.9	62.5	48.5	90.3	103
Seat Pan Z Sum	796	743	569	1035	686	859	617	674	774	488	619	678
Seat Z/Wt	5.17	5.50	3.36	5.18	4.08	6.37	3.74	4.11	4.10	4.09	3.92	3.99
Res Seat Force	858	821	613	1140	759	964	691	698	879	530	767	751
Res Seat/Wt	5.57	6.08	3.63	5.70	4.52	7.14	4.19	4.26	4.65	4.44	4.86	4.42
Foot X Sum	-1218	-853	-1741	-1442	-1175	-854	-1325	-1307	-1374	-1110	-1303	-1568
Foot Y Sum	-109	84.5	-137	-106	75.4	111	-88.8	-75.1	-67.9	112	121	101
Foot Z Sum	391	397	591	513	473	440	519	563	578	419	580	595
Res Foot Force	1229	877	1803	1511	1213	893	1385	1376	1442	1136	1345	1638
Foot X Preload	-469	-147	-839	-437	-371	-165	-686	-653	-542	-409	-474	-827
Foot Y Preload	-19.3	-4.4	-28.5	-5.4	6.1	5.9	-10.2	-7.7	2.0	16.5	8.0	7.3
Foot Z Preload	160	49.8	277	146	158	75.2	293	282	279	155	235	310
Res Preload	496	155	884	460	404	182	746	711	610	438	529	884

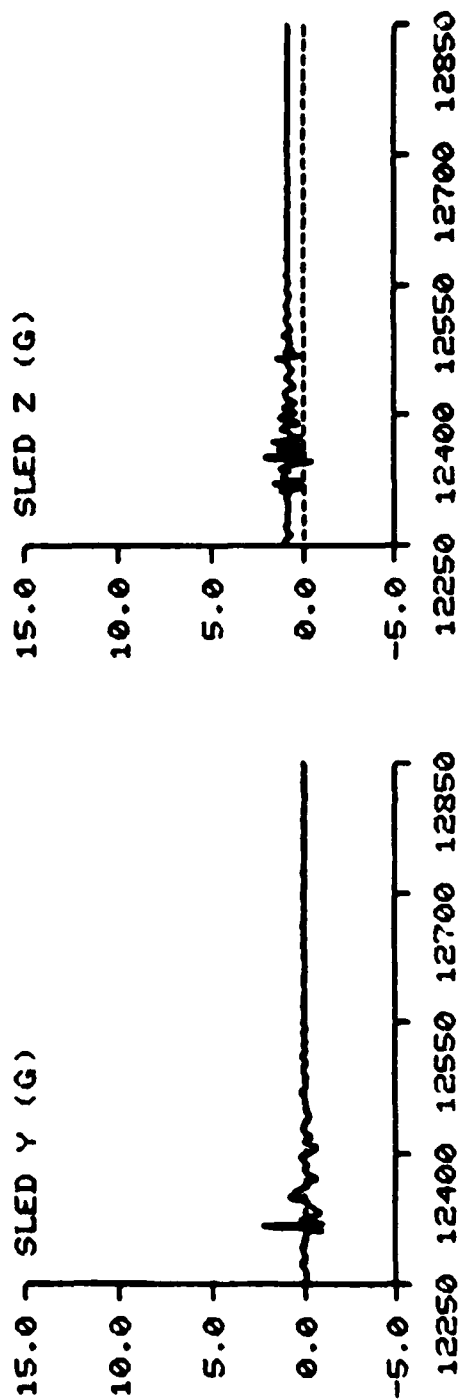
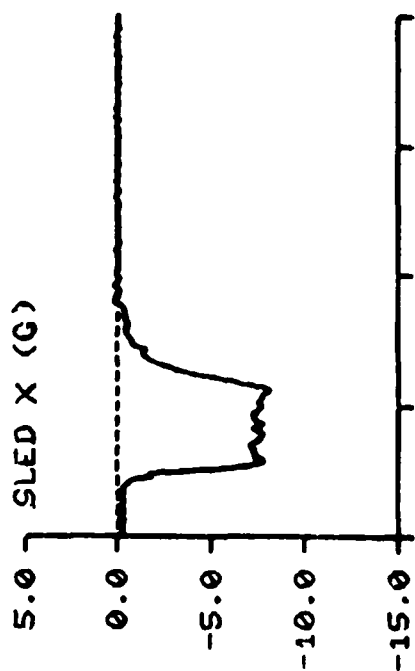
103<sub>x</sub> 0/103 CONTINUATION

TEST #	594	597	603	Mean	Std Dev
Subject ID	R-1	O-1	J-1		
Subject Weight	196	181	162	164	22.5
SH Strap Angle	1.25	0.75	0.50	2.67	3.70
Seatback Angle	102.5	102	102.5	102	0.41
Sled X	-9.16	-8.65	-8.91	-9.21	0.39
Sled Velocity	31.1	30.7	31.2	31.4	0.52
Seat X	-10.9	-11.2	-10.9	-10.7	0.44
Chest Res	9.96	10.9	12.3	11.8	0.97
Chest SI	22.9	27.0	27.0	28.0	3.17
Head Res	12.5	9.79	11.5	11.1	1.62
Head SI	29.0	20.7	26.9	25.2	7.39
Shoulder Sum	768	702	602	647	101
SH Sum/Wt	3.92	3.88	3.71	3.95	0.44
Lap Belt Sum	566	437	411	610	166
Lap Sum/Wt	2.89	2.42	2.54	3.79	1.24
Neg -G Strap	694	491	348	411	131
Seat Lnk X Sum	-470	-229	-222	-335	104
Seat Lnk Y	51.2	59.6	46.6	60.2	19.9
Seat Pan Z Sum	848	559	523	698	147
Seat Z/Wt	4.33	3.09	3.23	4.28	0.91
Res Seat Force	969	594	551	772	171
Res Seat/Wt	4.94	3.28	3.40	4.74	1.04
Foot X Sum	-1439	-1636	-1415	-1317	252
Foot Y Sum	118	131	149	37.0	105
Foot Z Sum	505	769	609	529	99.6
Res Foot Force	1482	1722	1520	1371	269
Foot X Preload	-592	-816	-562	-533	215
Foot Y Preload	15.2	-6.0	22.9	0.16	13.77
Foot Z Preload	222	377	221	216	90.9
Res Preload	633	899	605	576	231

F-111 LOG TEST SUMMARY TABLE (CONFIGURATION FD/103)

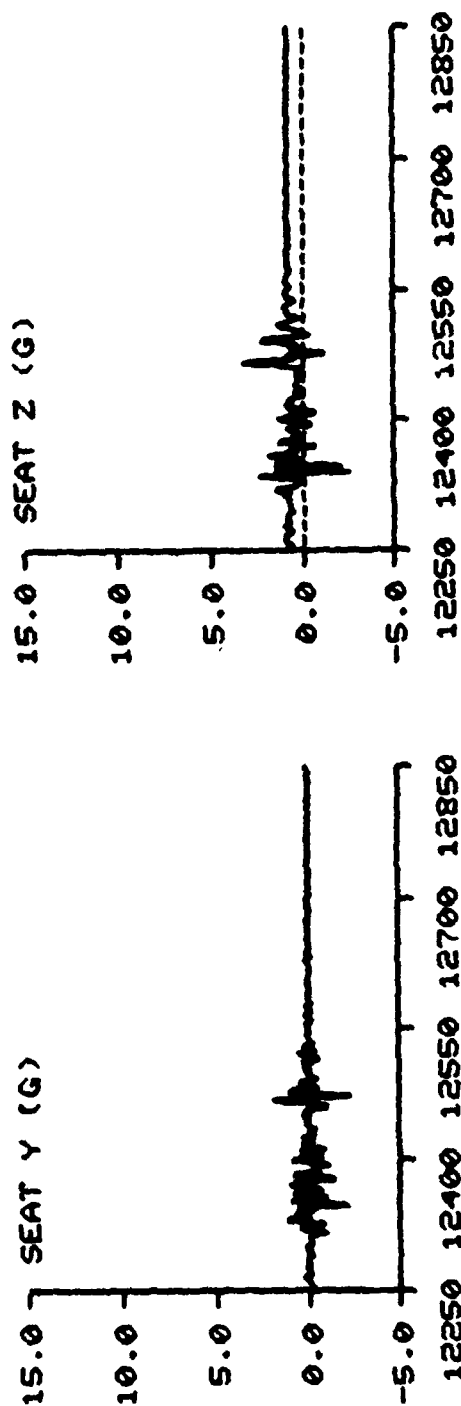
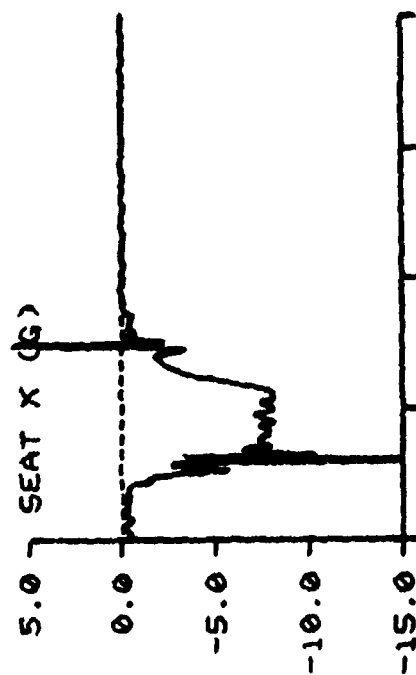
TEST #	560	575	577	578	586	587	589	590	591	600	602	Mean	STD	DEV
Subject ID	W-1	J-1	M-5	O-1	P-2	M-10	M-7	D-1	F-3	F-2	M-2			
Subject Weight	158	159	170	175	160	143	138	205	167.5	156	166	163	17.6	
Sh Strap Angle	29	28.5	22.5	23	26.5	28.5	37	18	27.75	30	32.75	27.6	5.15	
Seatback Angle	102.5	102.5	102	102	103	102.5	102.5	102.5	102.5	102.5	102.5	102	0.27	
Sled X	-9.95	-9.56	-9.07	-9.23	-8.97	-8.91	-9.52	-9.36	-9.23	-9.06	-9.00	-9.26	0.32	
Sled Velocity	32.1	31.9	31.2	31.4	31.2	31.1	31.8	31.4	31.5	31.3	31.2	31.5	0.33	
Seat X	-11.4	-11.3	-10.5	-11.1	-10.8	-10.8	-10.4	-10.8	-10.7	-10.6	-10.78	-10.8	0.31	
Chest Res	11.5	12.7	11.7	11.6	11.5	12.4	14.0	11.2	11.1	11.4	10.3	11.8	0.97	
Chest SI	28.8	27.9	27.0	26.0	23.5	26.4	29.7	26.9	24.7	26.8	26.6	26.8	1.73	
Head Res	9.38	12.0	8.59	8.39	10.7	8.42	12.4	10.4	9.92	9.18	11.7	10.1	1.46	
Head SI	18.6	26.5	15.7	16.0	27.1	16.4	27.0	21.6	21.9	22.6	34.5	22.5	5.86	
Shoulder Sum	752	668	643	704	690	670	743	875	746	597	788	716	76.2	
SH Sum/Wt	4.78	4.20	3.78	4.03	4.31	4.69	5.38	4.27	4.46	3.83	4.75	4.41	0.47	
Lap Belt Sum	667	466	415	581	892	779	873	711	530	456	525	627	169	
Lap Sum/Wt	4.24	2.93	2.44	3.32	5.57	5.45	6.33	3.47	3.17	2.93	3.16	3.91	1.30	
Neg -G Strap	389	588	579	562	408	321	286	847	556	556	626	520	160	
Seat Lnk X Sum	-228	-86.8	-82.5	-203	-329	-346	-358	-449	-293	-254	-284	-265	112	
Seat Lnk Y	57.1	-41.2	42.2	77.0	46.3	65.8	68.0	84.3	48.1	-37.6	76.4	44.2	43.5	
Seat Pan Z Sum	677	499	486	579	660	521	574	1031	501	432	532	590	164	
Seat Z/Wt	4.30	3.14	2.86	3.31	4.13	3.64	4.16	5.03	3.00	2.77	3.21	3.60	0.72	
Res Seat Force	714	500	491	595	737	622	674	1123	577	500	603	649	178	
Res Seat/Wt	4.53	3.15	2.89	3.40	4.61	4.35	4.88	5.48	3.45	3.20	3.63	3.96	0.84	
Foot X Sum	-1272	-1657	-1730	-1544	-1193	-961	-894	-1392	-1290	-1454	-1203	-1326	264	
Foot Y Sum	-84.0	84.5	-82.7	60.8	-80.8	108	84.1	74.2	109	110	115	45.3	83.8	
Foot Z Sum	423	587	526	599	438	420	388	401	528	611	502	493	83.2	
Res Foot Force	1301	1724	1753	1597	1221	989	920	1405	1322	1513	1221	1361	273	
Foot X Preload	-511	-833	-972	-698	-364	-249	-185	-475	-464	-700	-476	-539	241	
Foot Y Preload	-26.2	25.7	-3.3	-6.8	-14.3	14.0	6.40	-7.7	9.6	-5.7	-6.2	-1.32	14.3	
Foot Z Preload	161	270	290	295	135	150	84.2	138	203	269	188	198	72.4	
Res Preload	536	876	1015	758	388	291	204	494	506	750	512	575	249	

F-111      TEST NQ: 552      SUBJECT ID: E-1



TIME IN MILLISECONDS

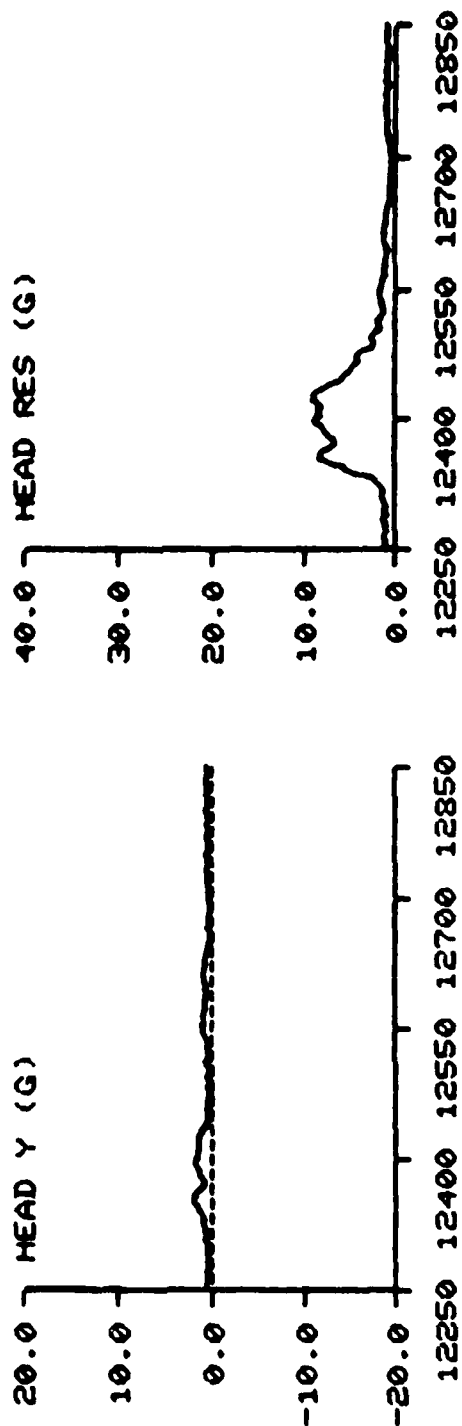
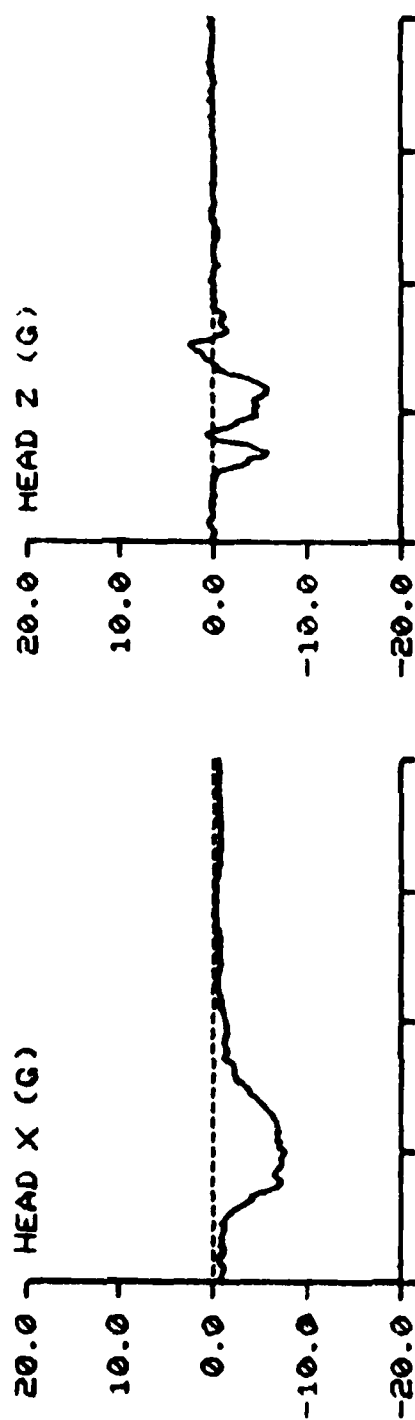
F-111 TEST NO: 552 SUBJECT ID: E-1



TIME IN MILLISECONDS

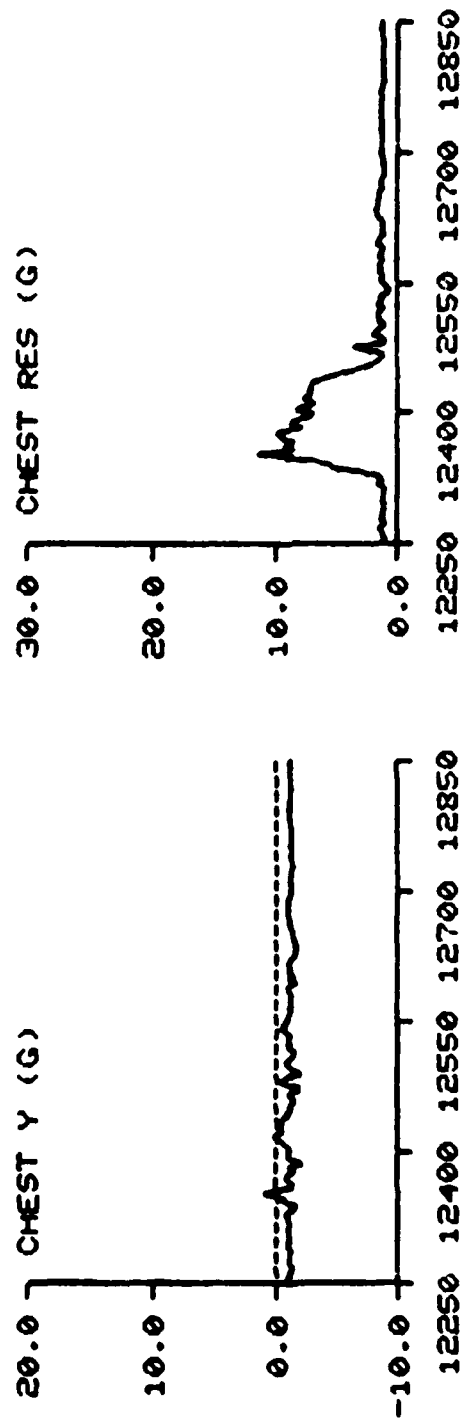
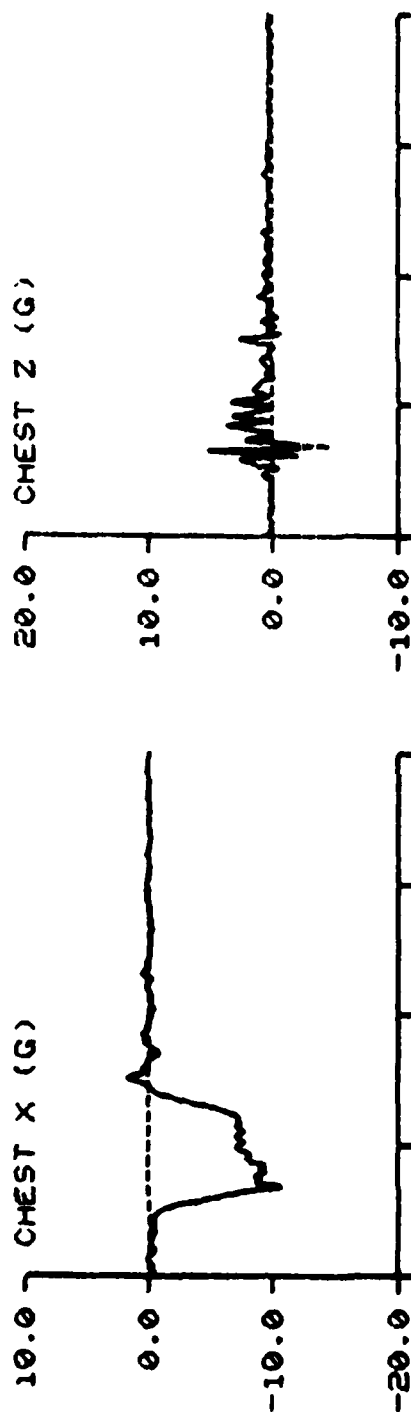


F-111 TEST NO: 552 SUBJECT ID: E-1



TIME IN MILLISECONDS

F-111      TEST NO: 552      SUBJECT ID: E-1

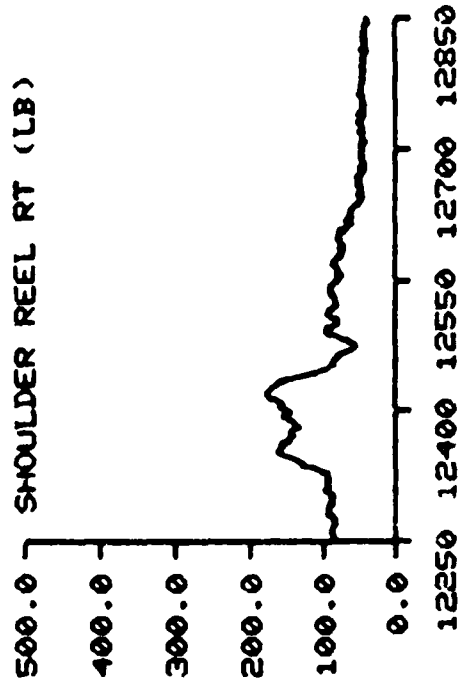
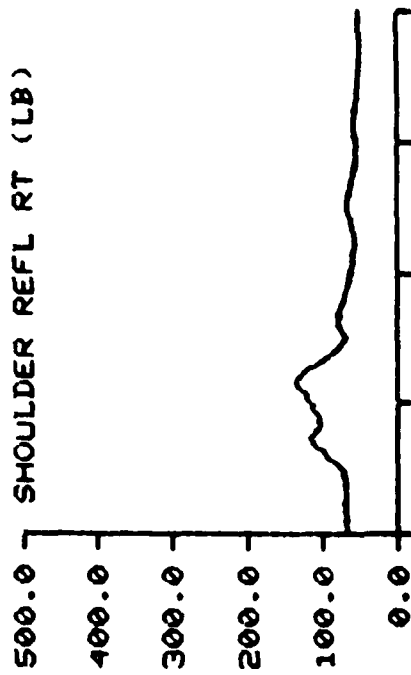
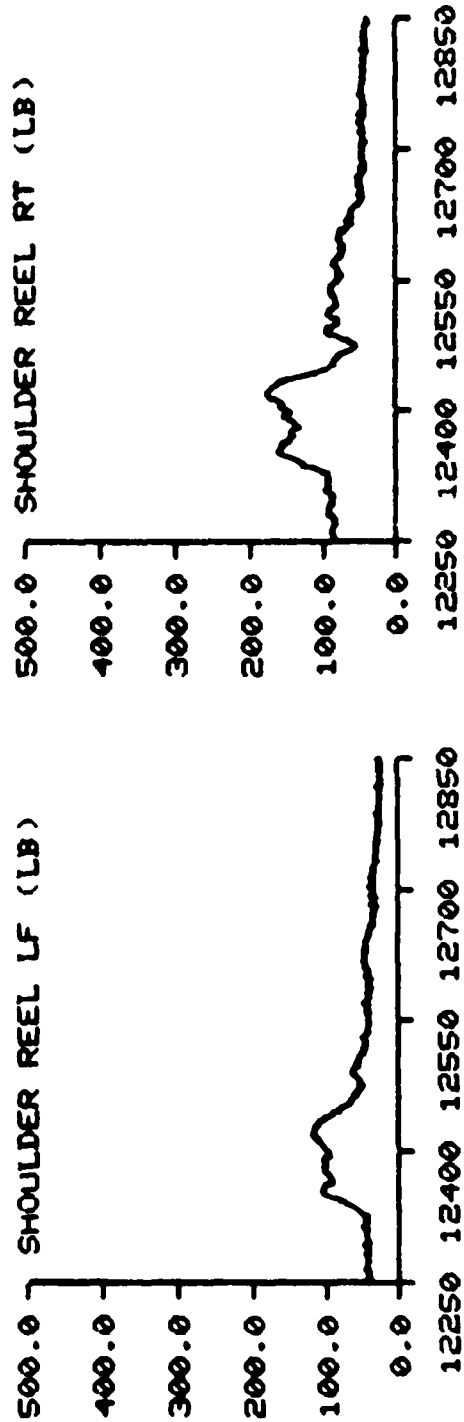
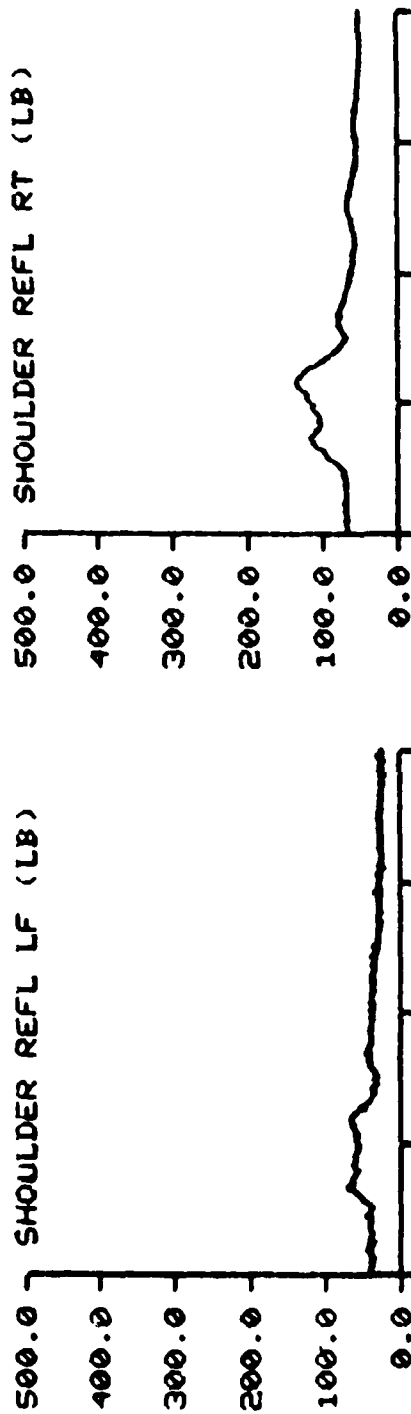


TIME IN MILLISECONDS

F-111

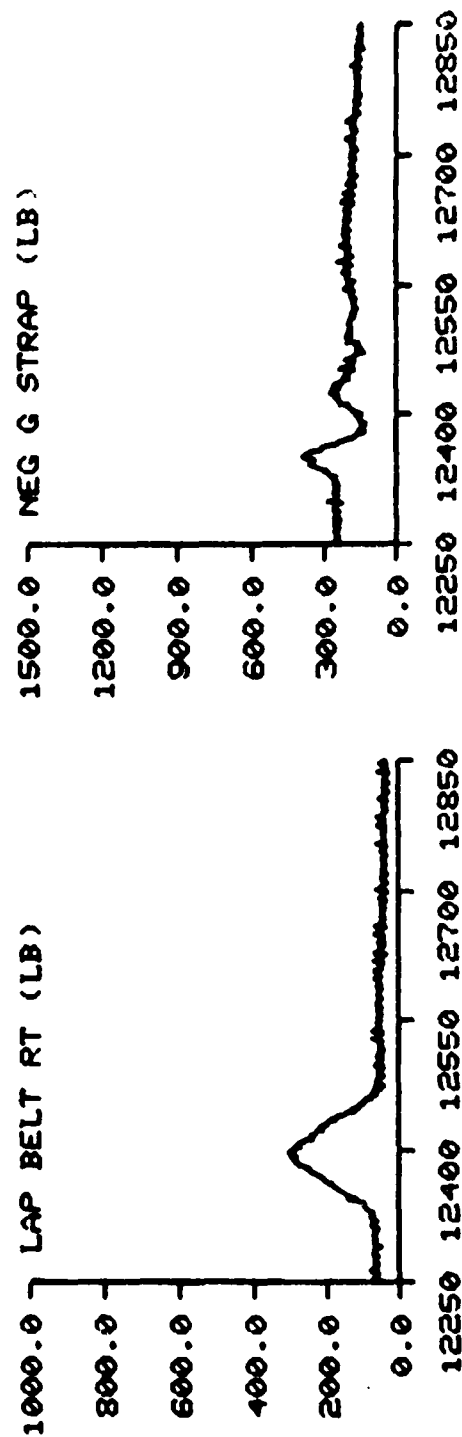
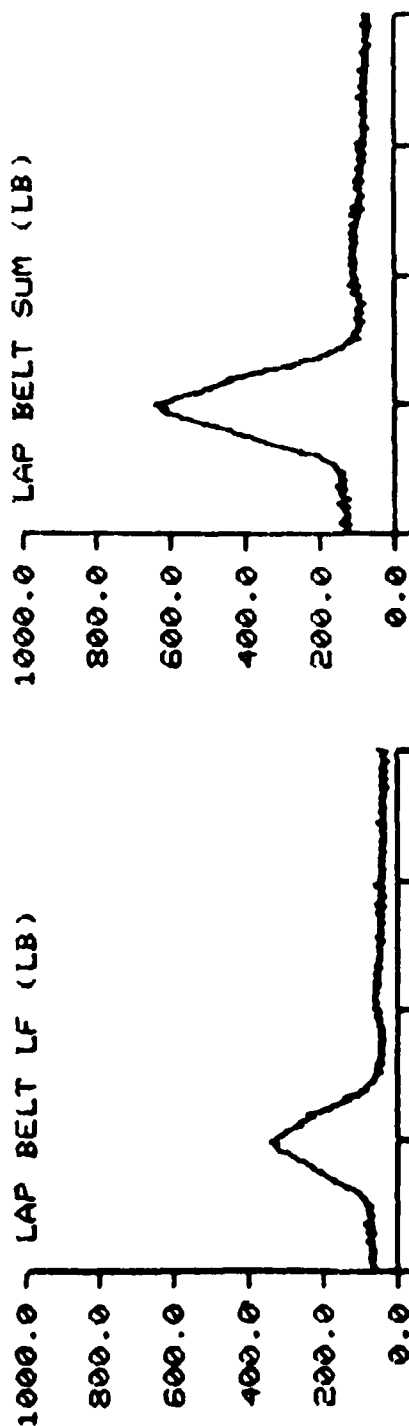
TEST NO: 552

SUBJECT ID: E-1



TIME IN MILLISECONDS

F-111 TEST NO: 552 SUBJECT ID: E-1

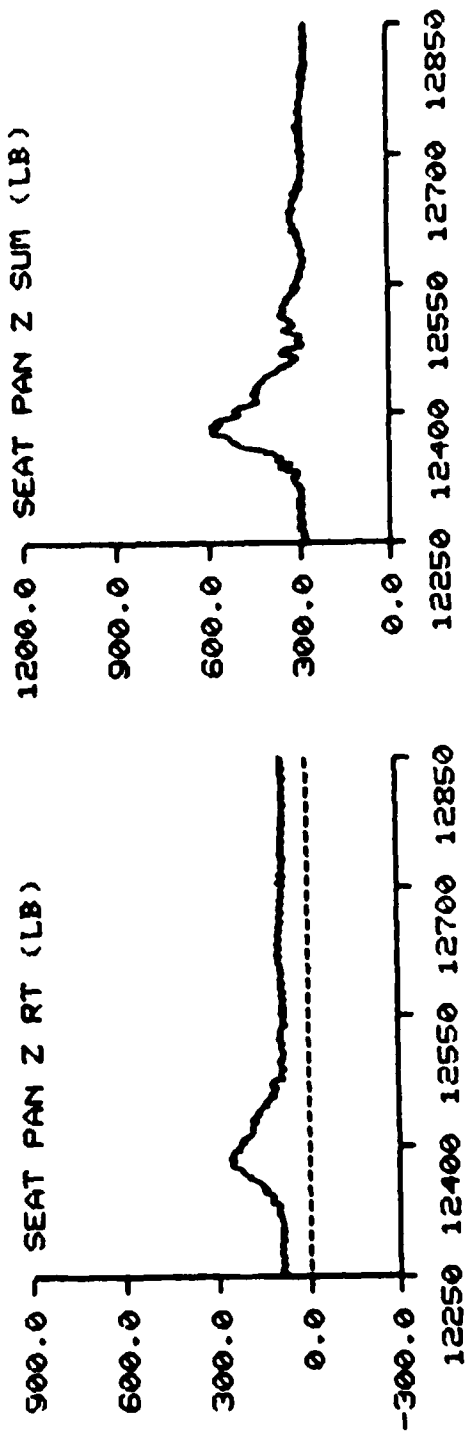
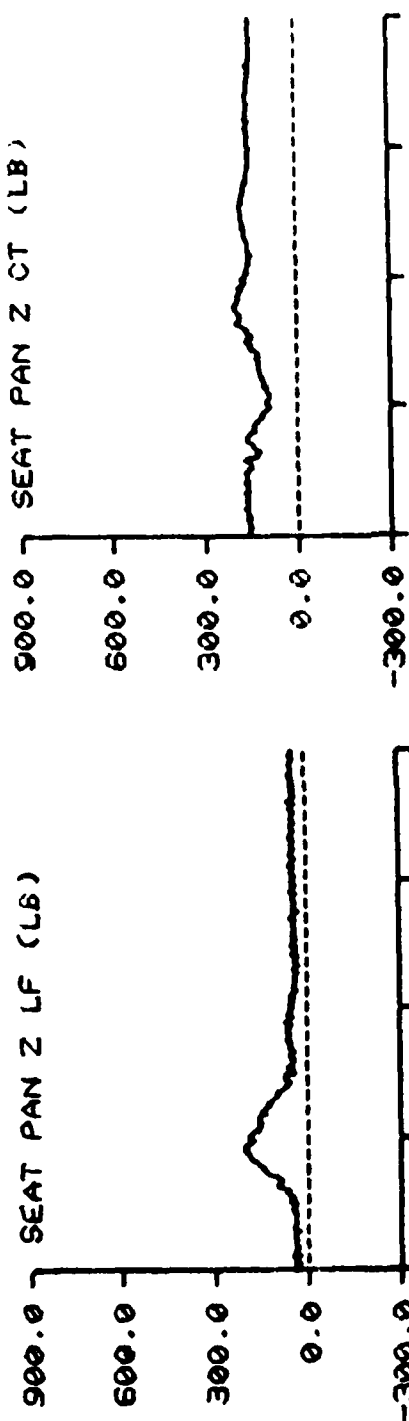


TIME IN MILLISECONDS

F-111

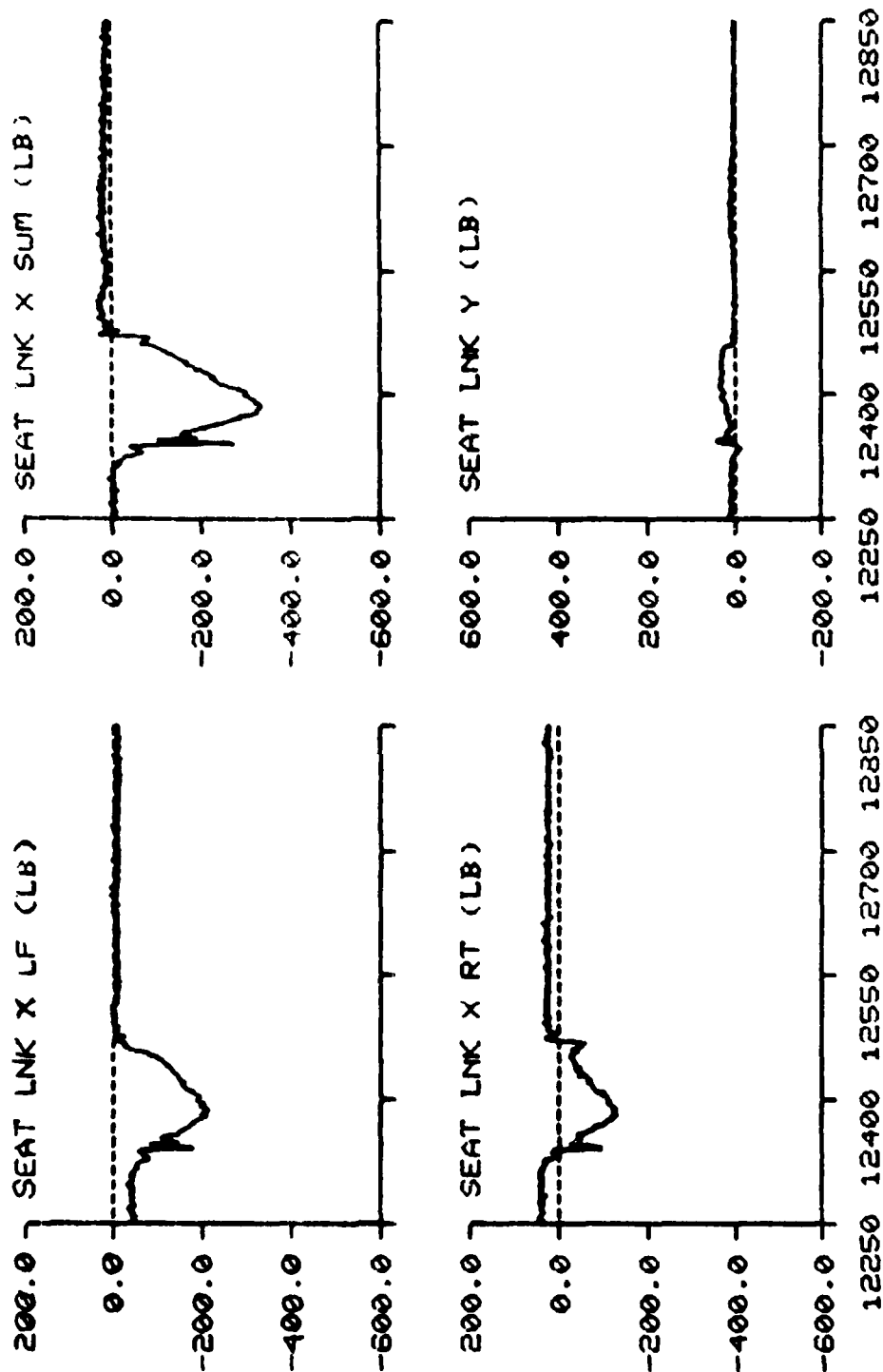
TEST NO: 552

SUBJECT ID: E-1



TIME IN MILLISECONDS

F-111 TEST NO: 552 SUBJECT ID: E-1

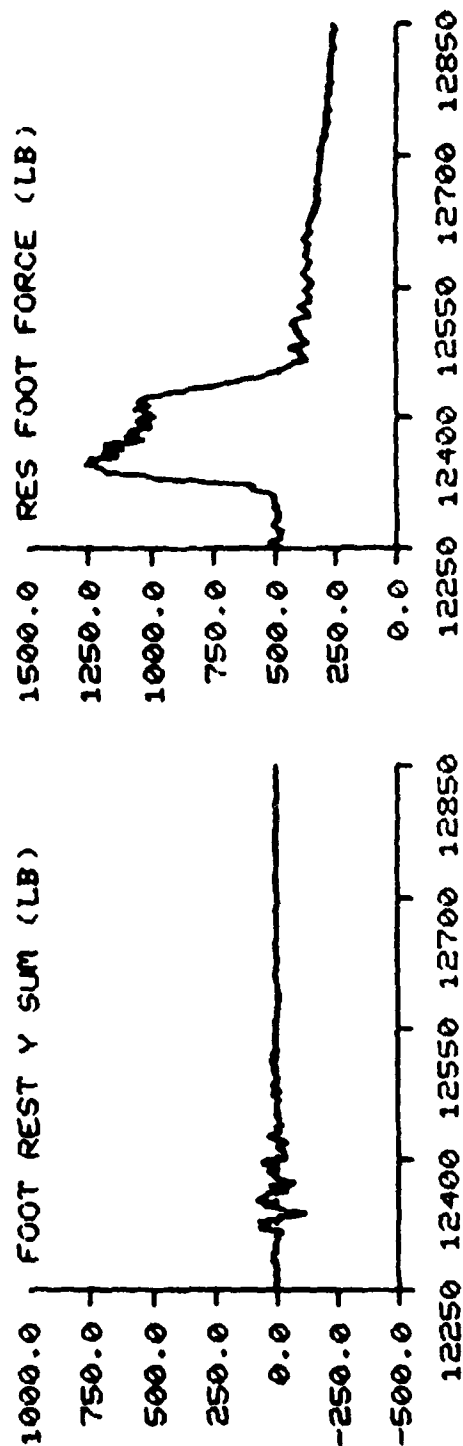
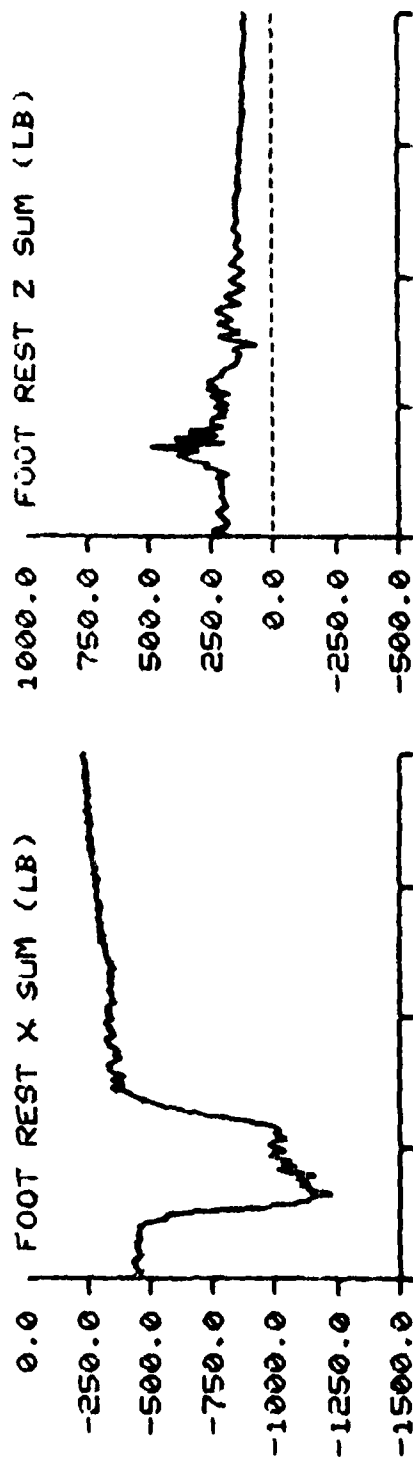


TIME IN MILLISECONDS

F-111

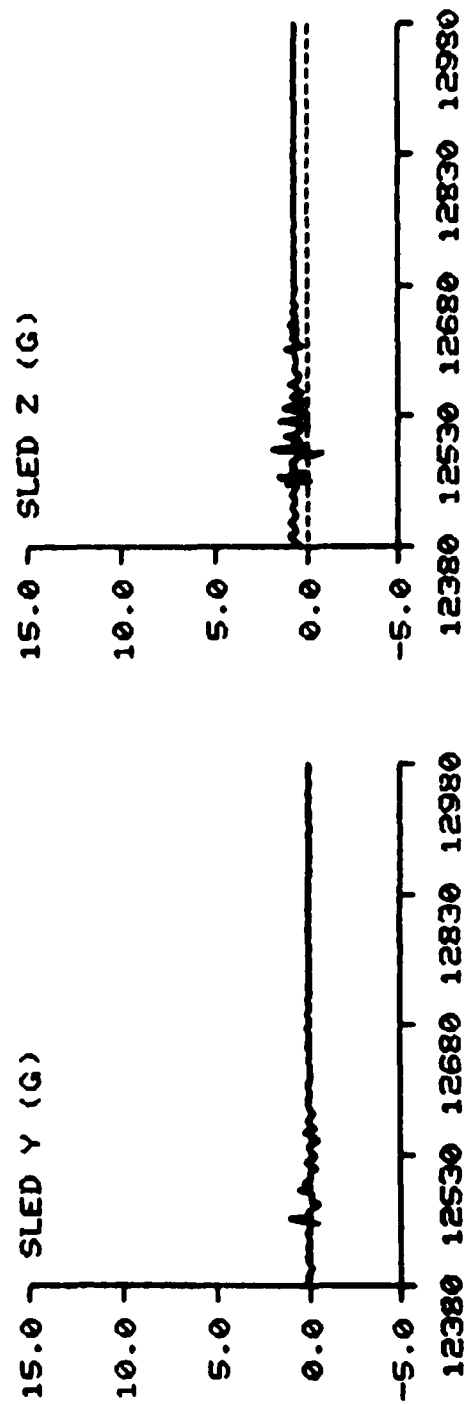
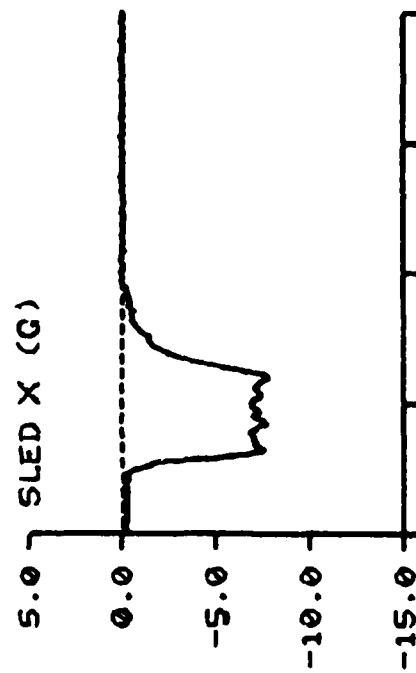
TEST NO: 552

SUBJECT ID: E-1



TIME IN MILLISECONDS

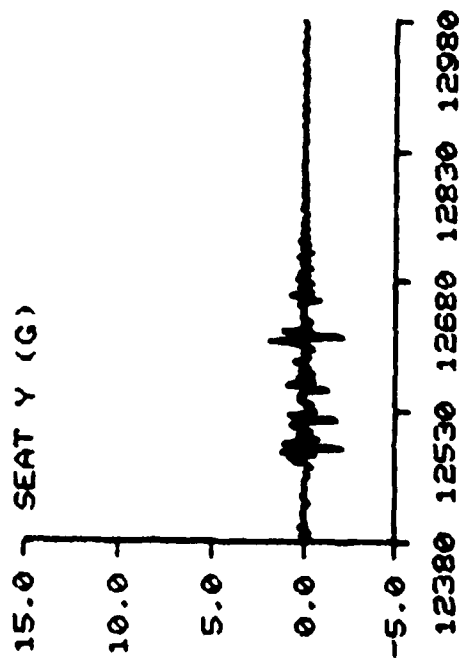
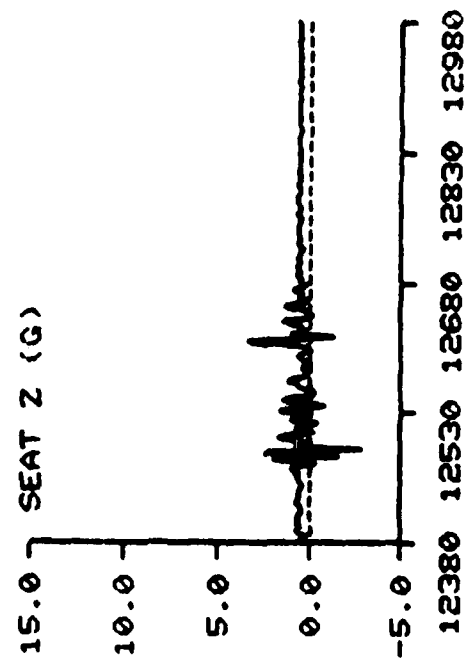
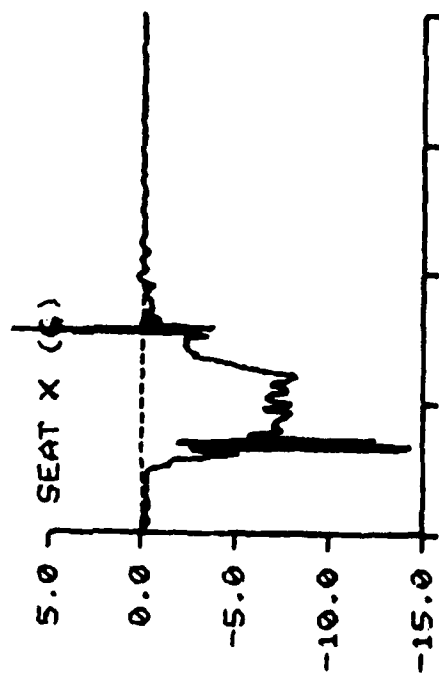
F-111      TEST NO: 543      SUBJECT ID: F-3



TIME IN MILLISECONDS

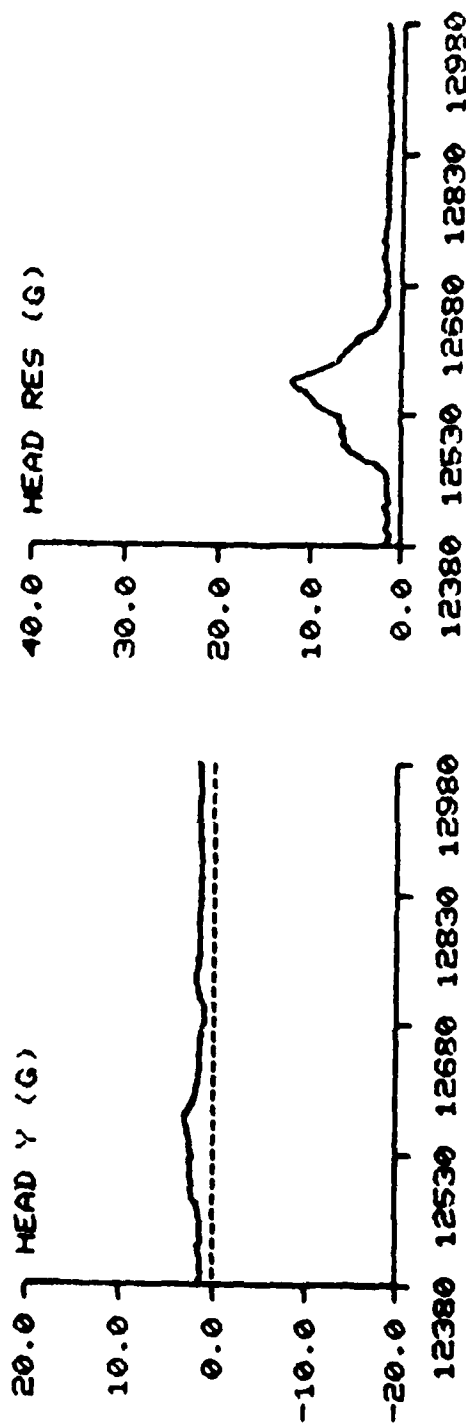
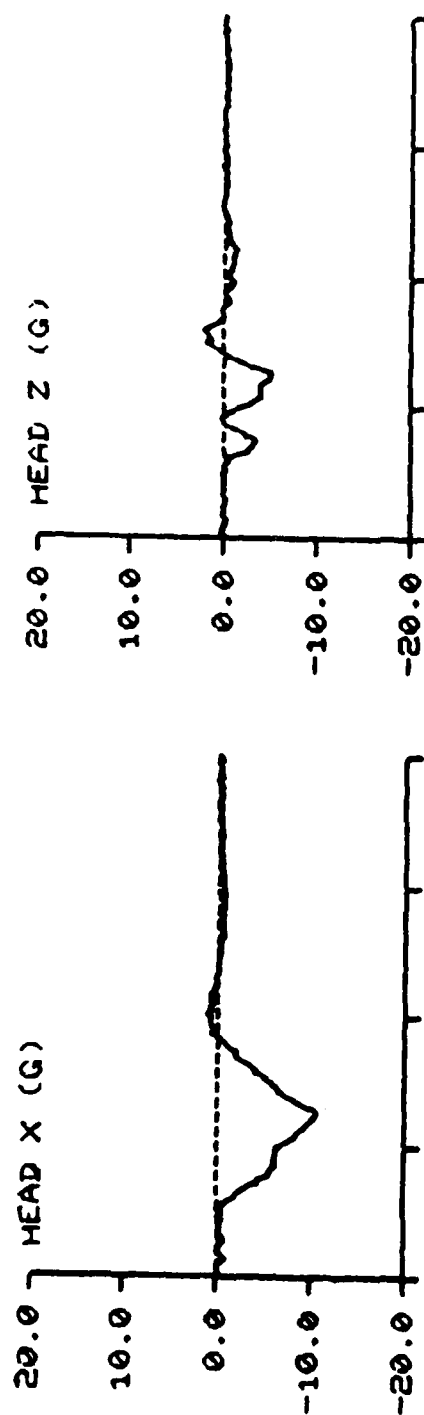


F-111 TEST NO: 543 SUBJECT ID: F-3



TIME IN MILLISECONDS

F-111 TEST NO: 543 SUBJECT ID: F-3

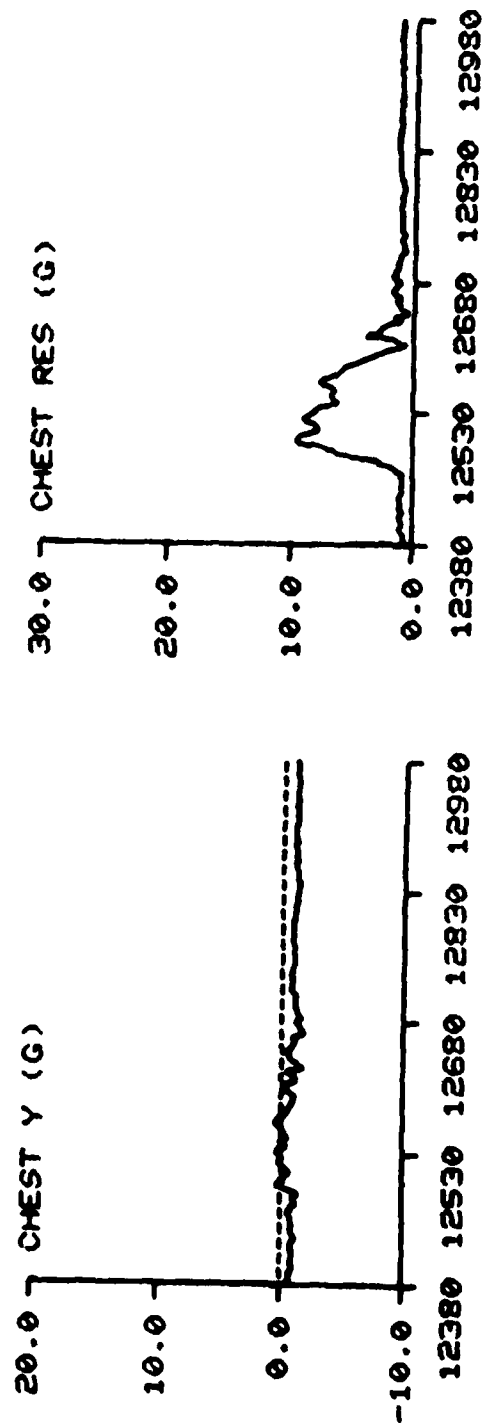
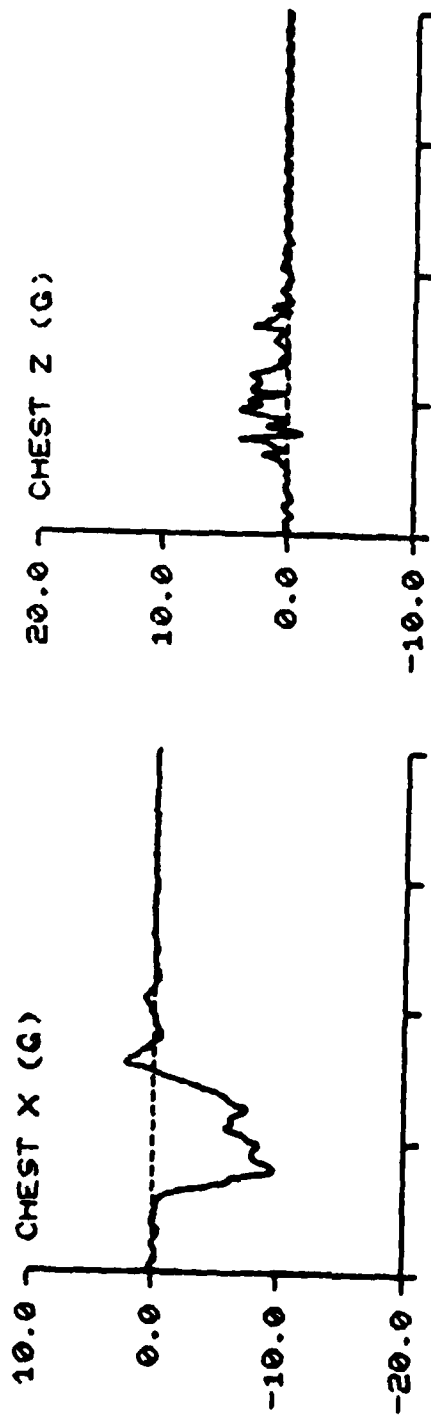


HEAD Z (G)

HEAD RES (G)

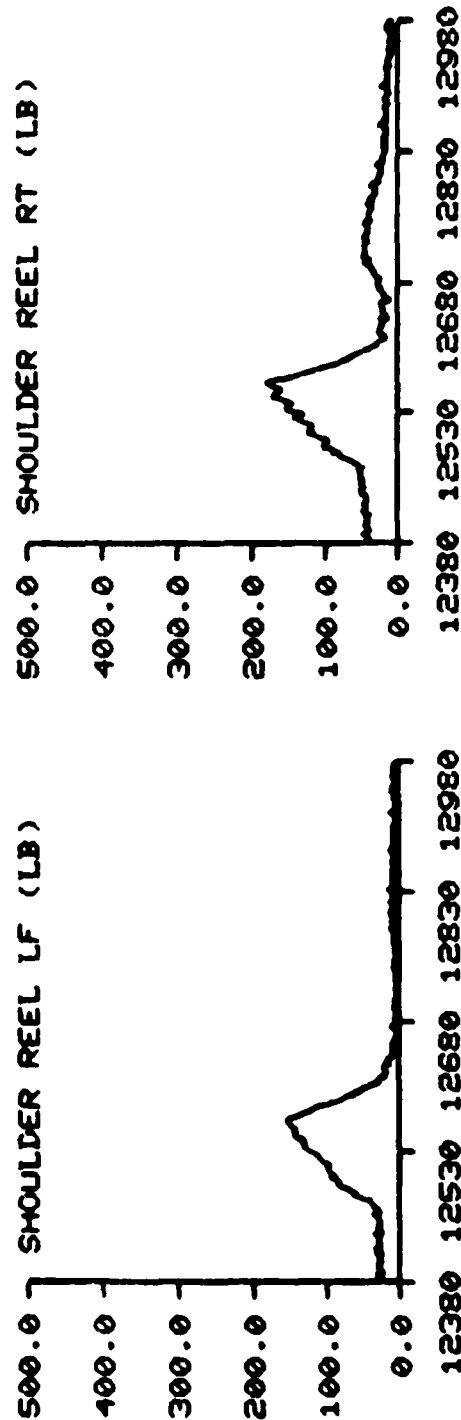
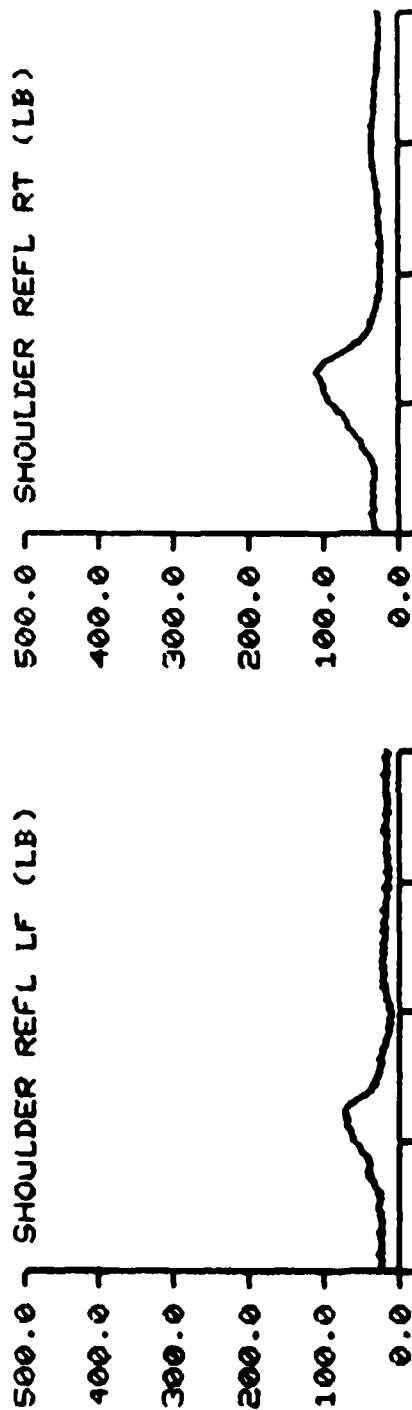
TIME IN MILLISECONDS

F-111 TEST NO: 543 SUBJECT ID: F-3



TIME IN MILLISECONDS

F-111 TEST NO: 543 SUBJECT ID: F-3

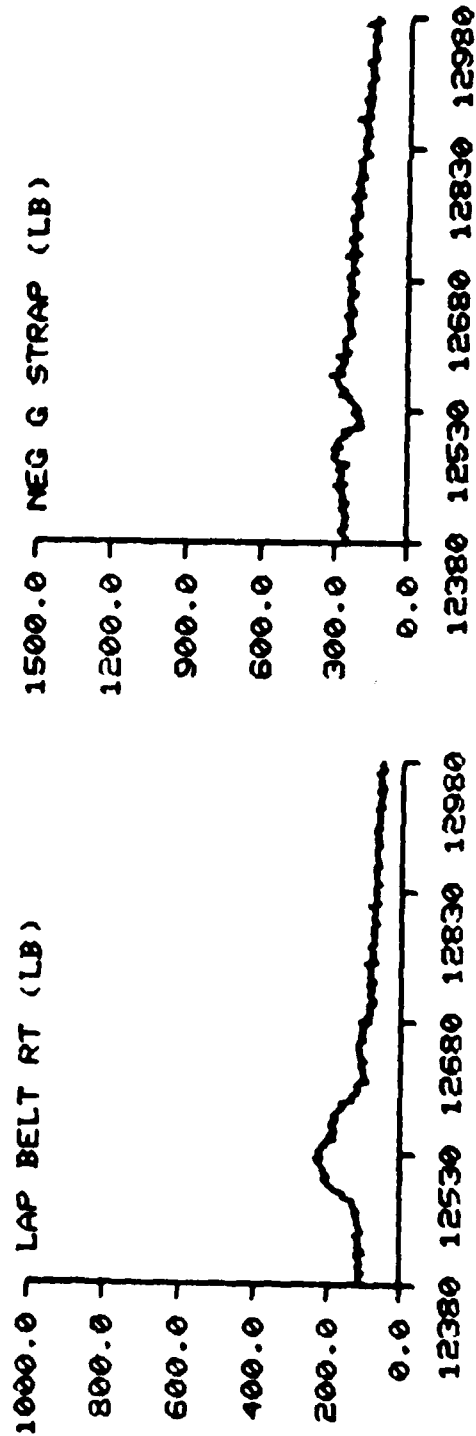
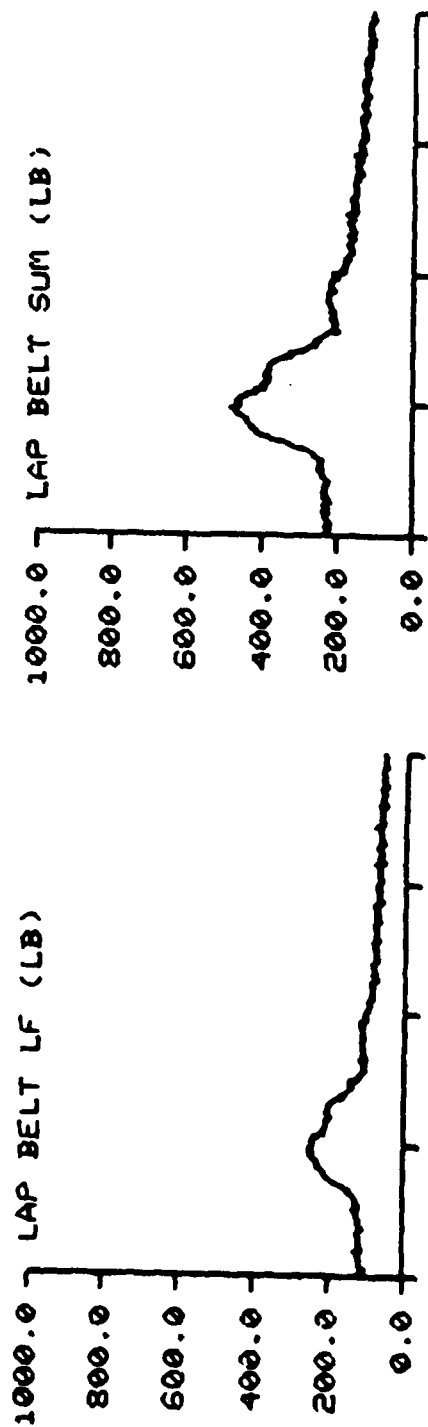


TIME IN MILLISECONDS

F-111

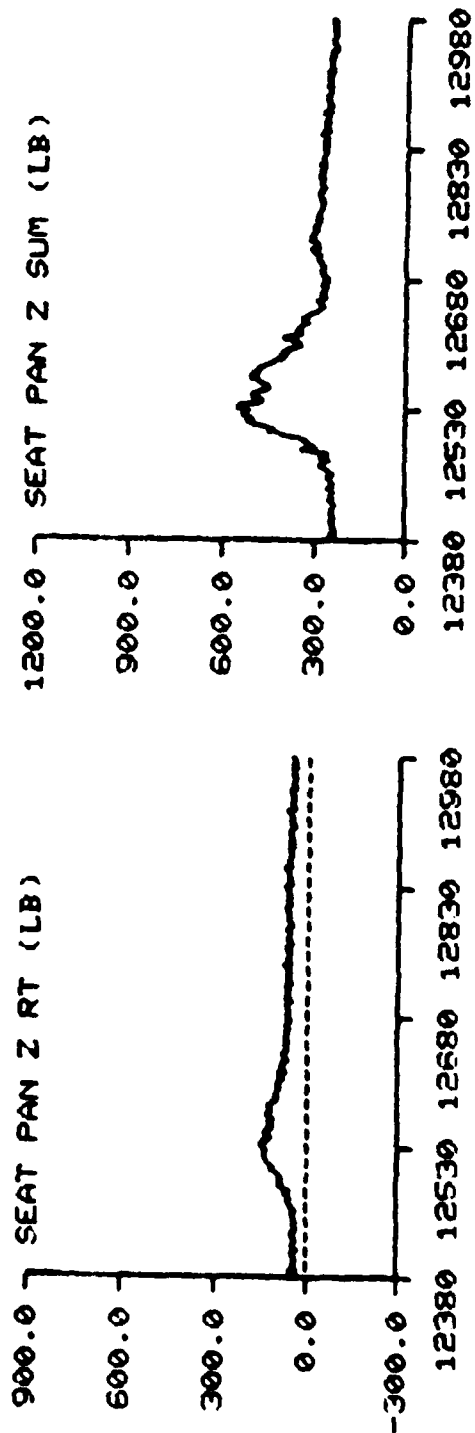
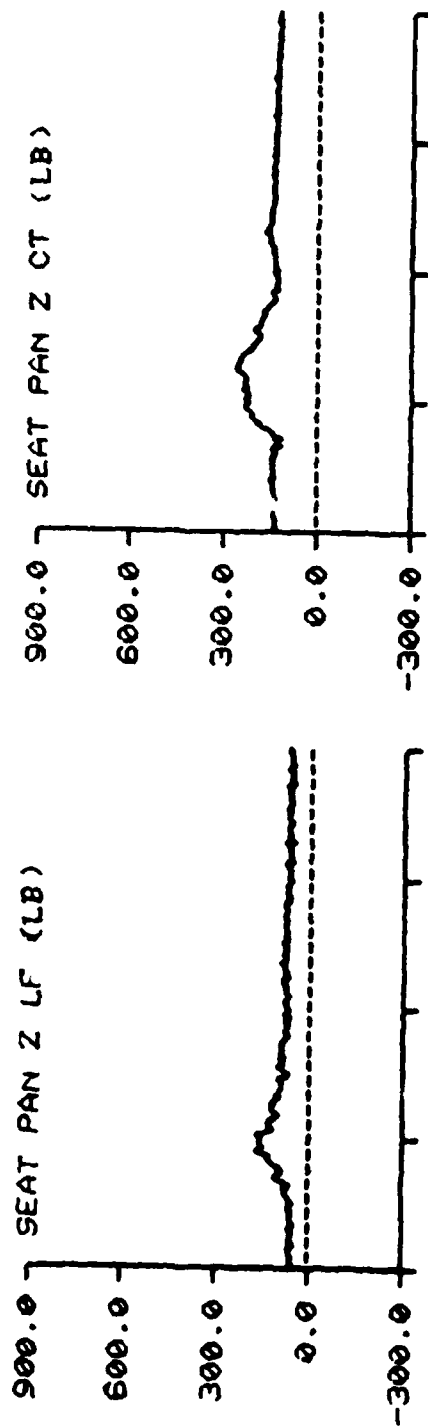
TEST NO: 543

SUBJECT ID: F-3



TIME IN MILLISECONDS

F-111 TEST NO: 543 SUBJECT ID: F-3

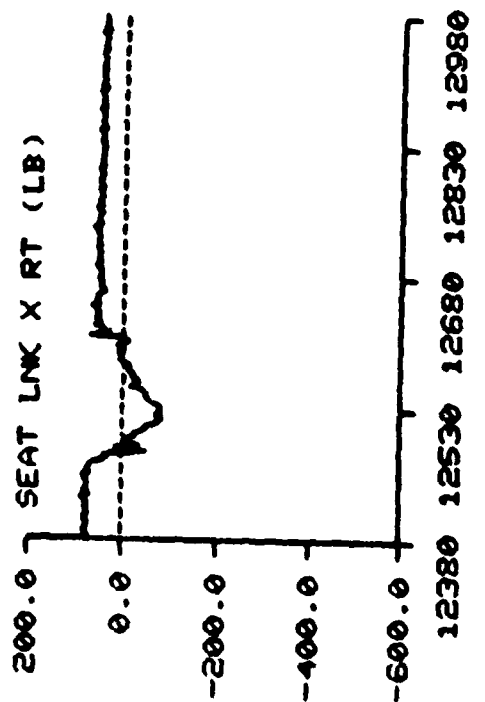
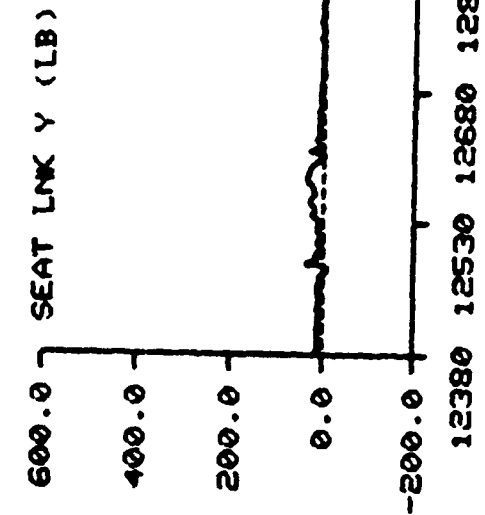
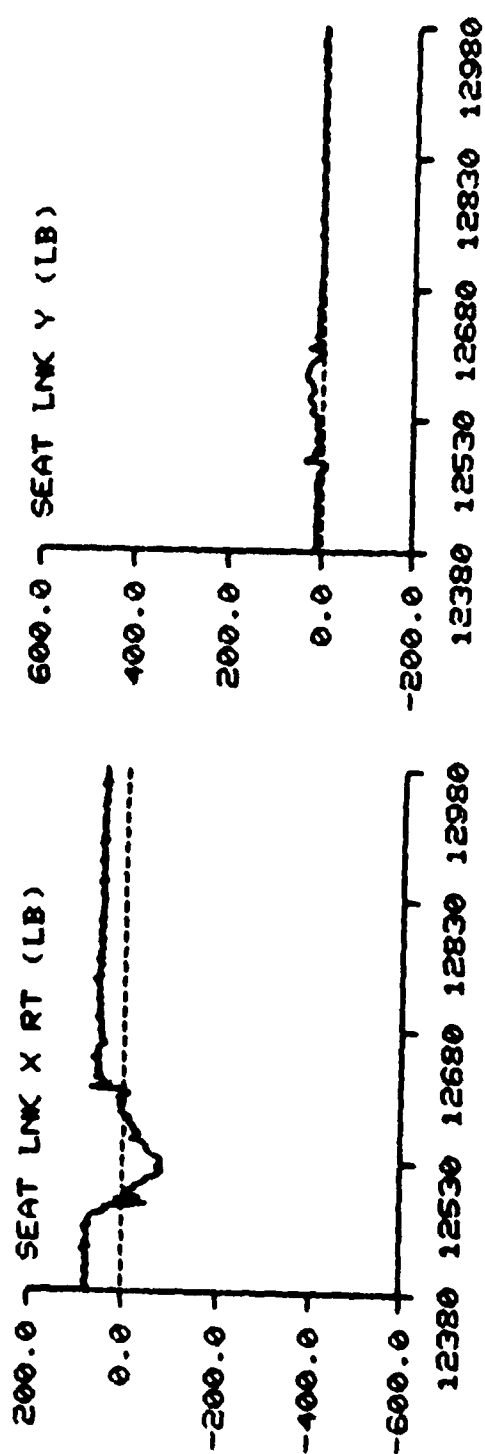
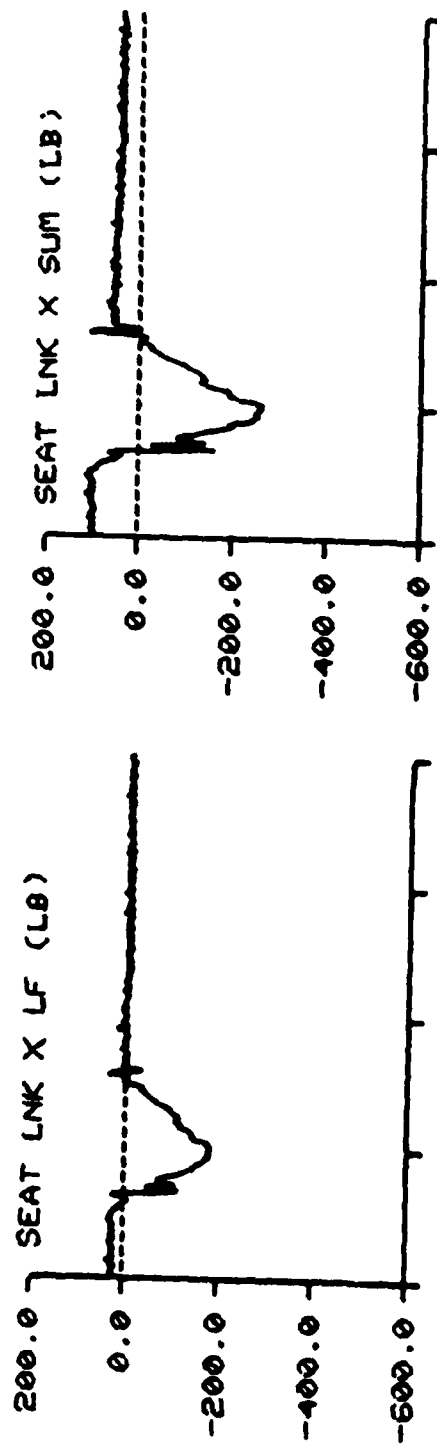


TIME IN MILLISECONDS

F-111

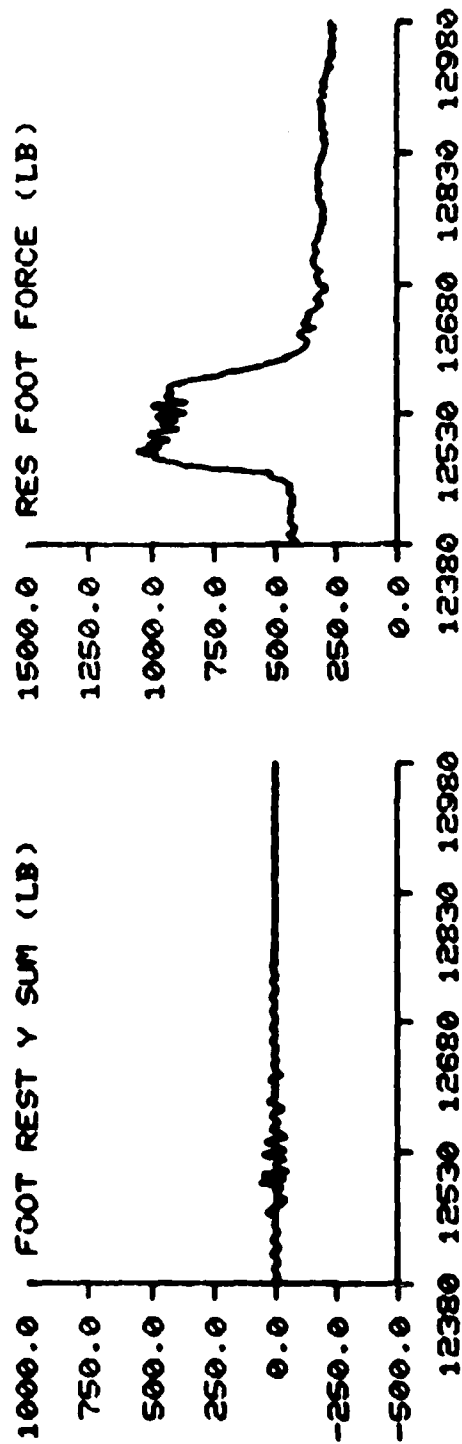
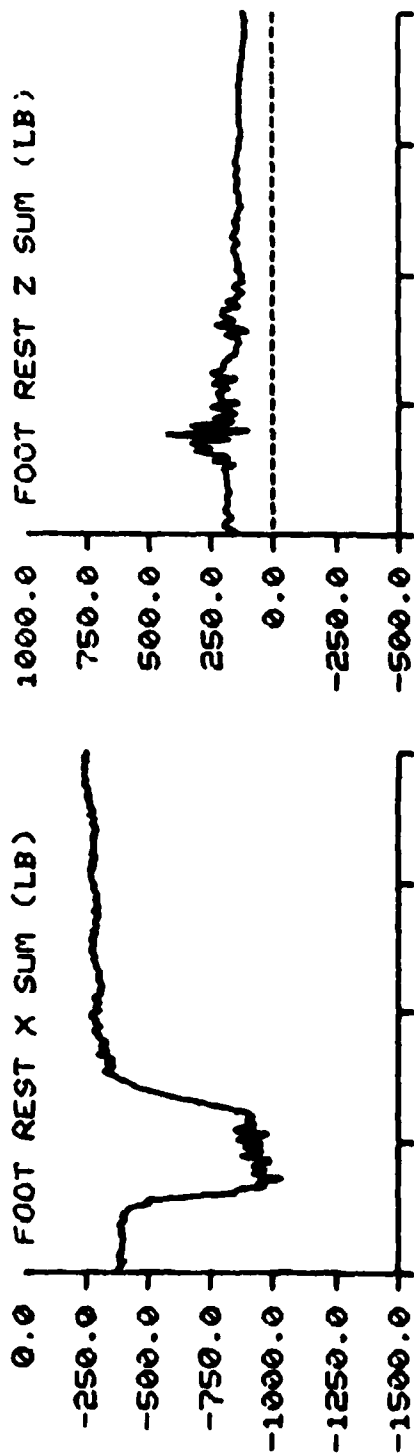
TEST NO: 543

SUBJECT ID: F-3

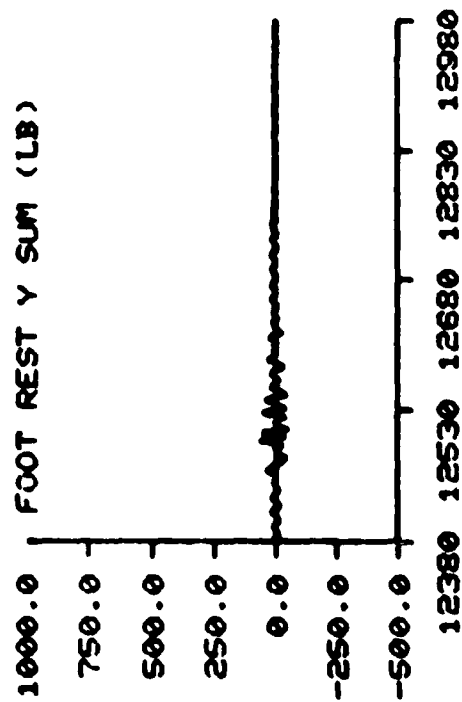


TIME IN MILLISECONDS

F-111 TEST NO: 543 SUBJECT ID: F-3



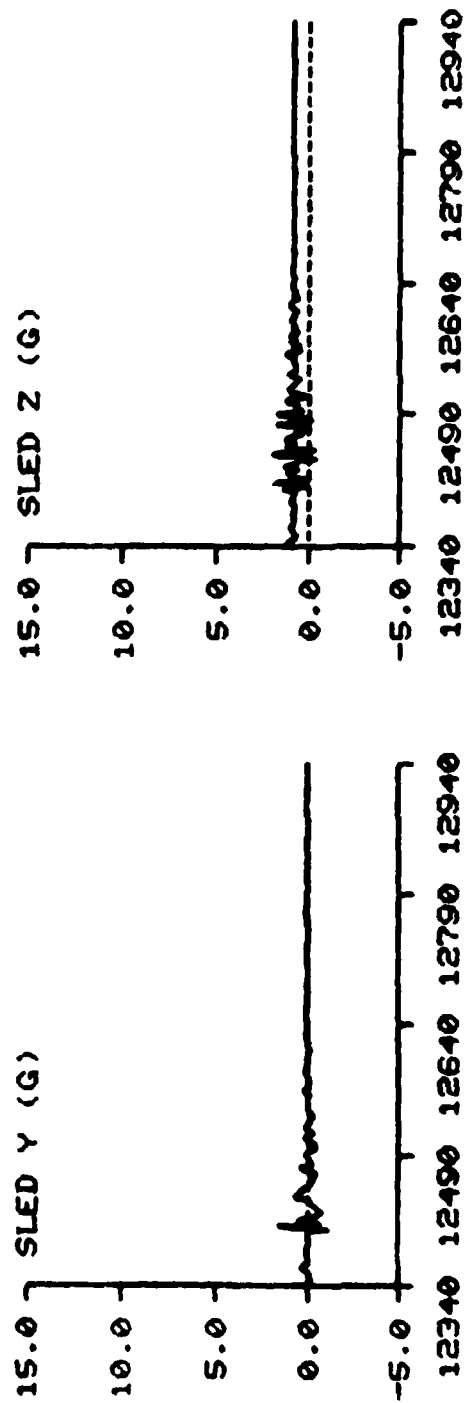
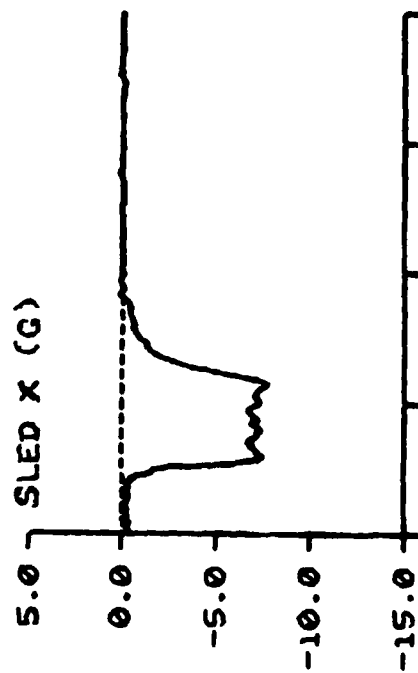
RES FOOT FORCE (LB)



TIME IN MILLISECONDS

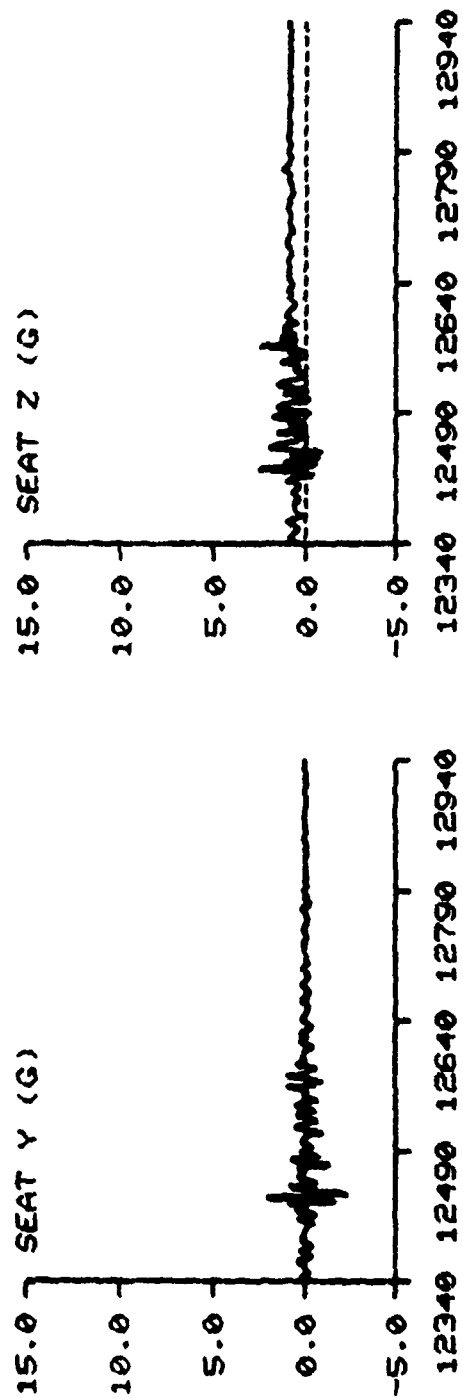
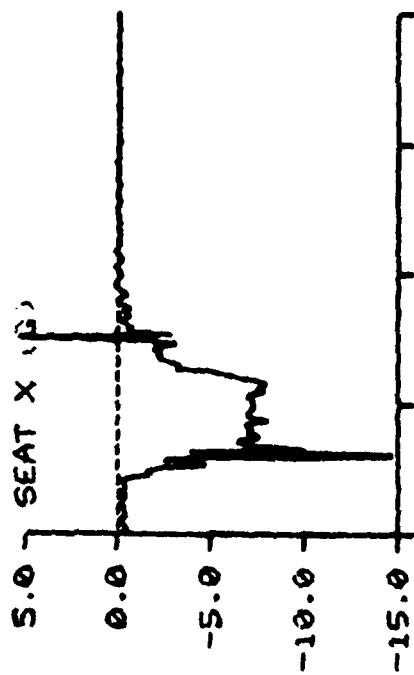


F-111      TEST NO: 553      SUBJECT ID: P-2



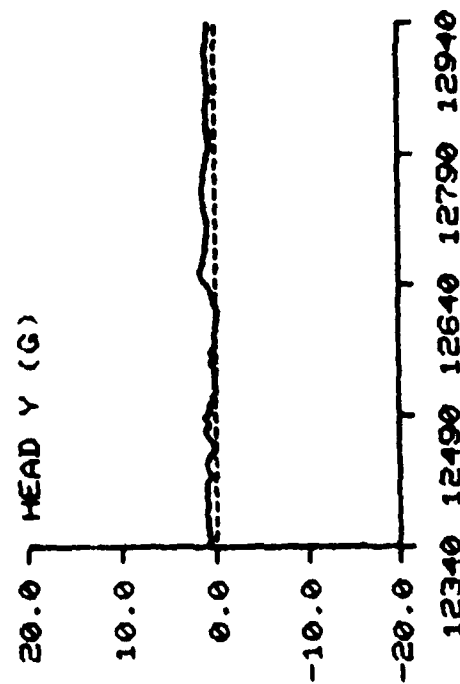
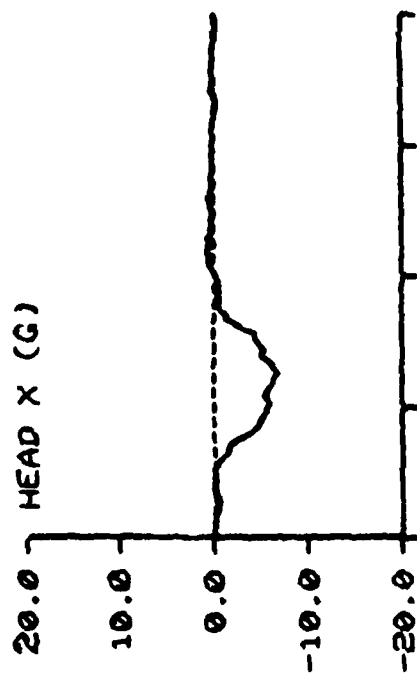
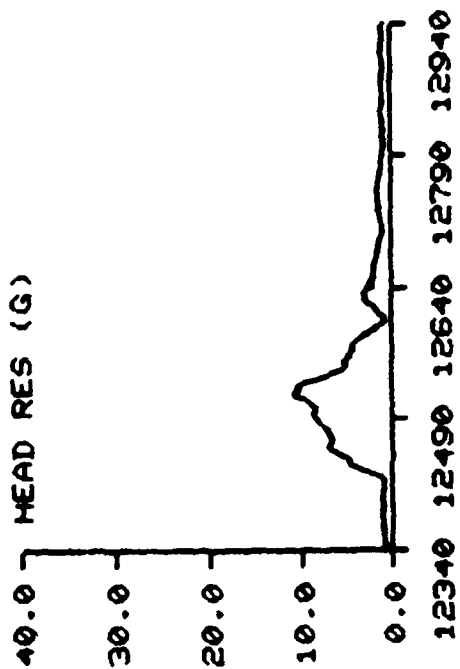
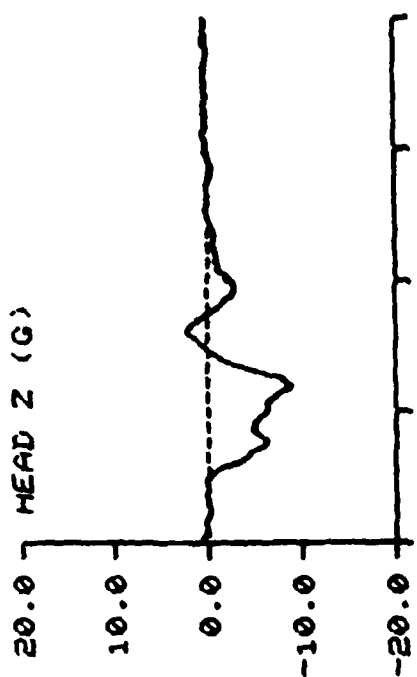
TIME IN MILLISECONDS

F-111 TEST NO: 553 SUBJECT ID: P-2



TIME IN MILLISECONDS

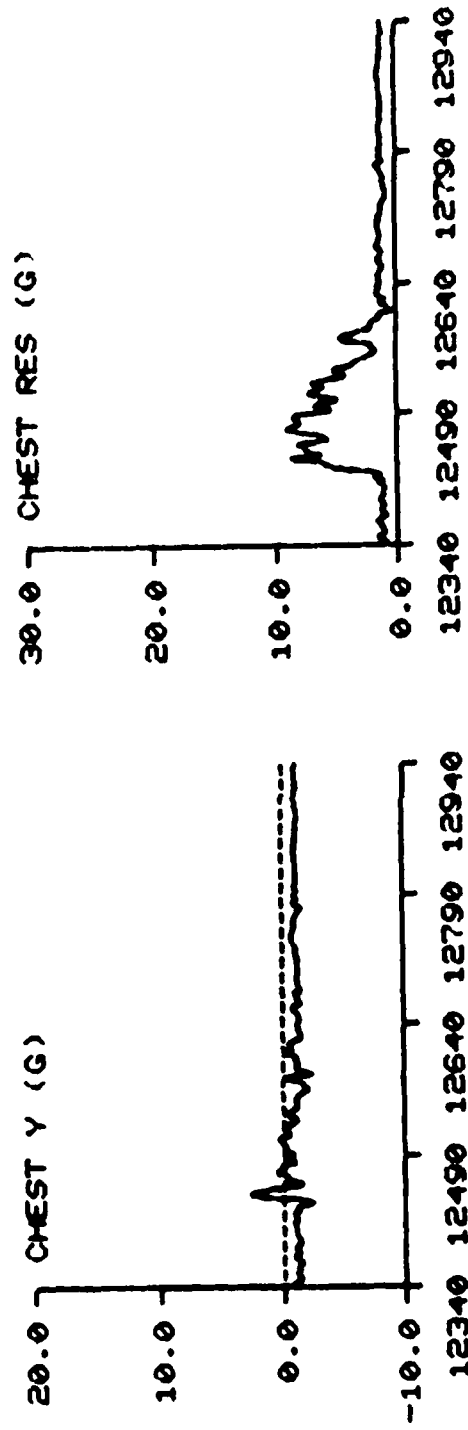
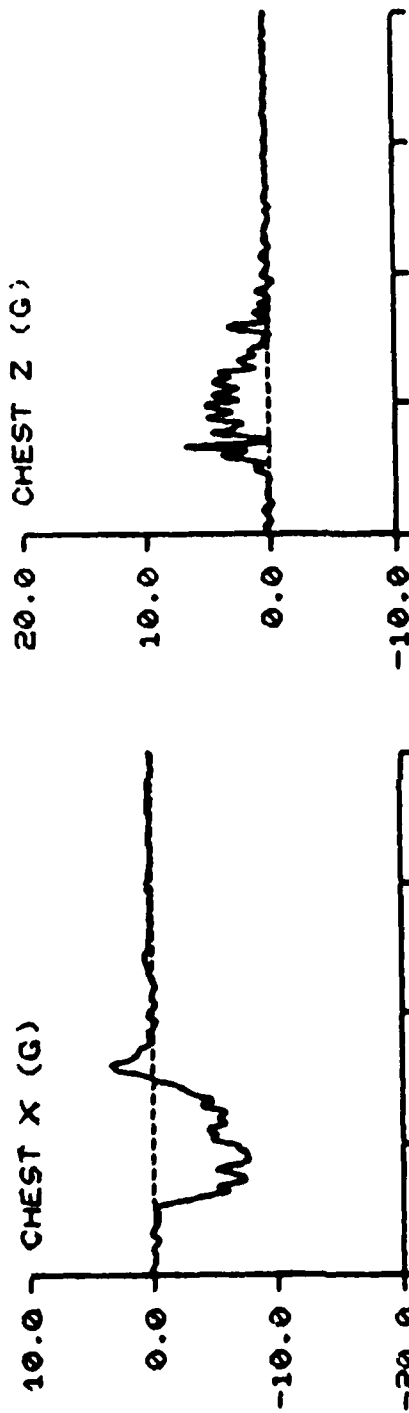
F-111      TEST NO: 553      SUBJECT ID: P-2



TIME IN MILLISECONDS

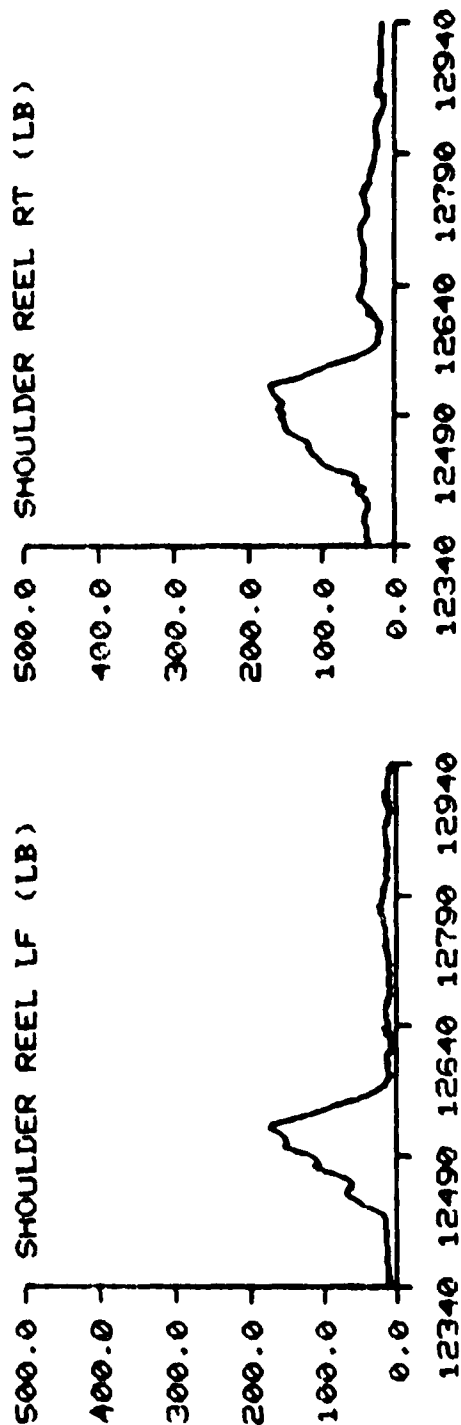
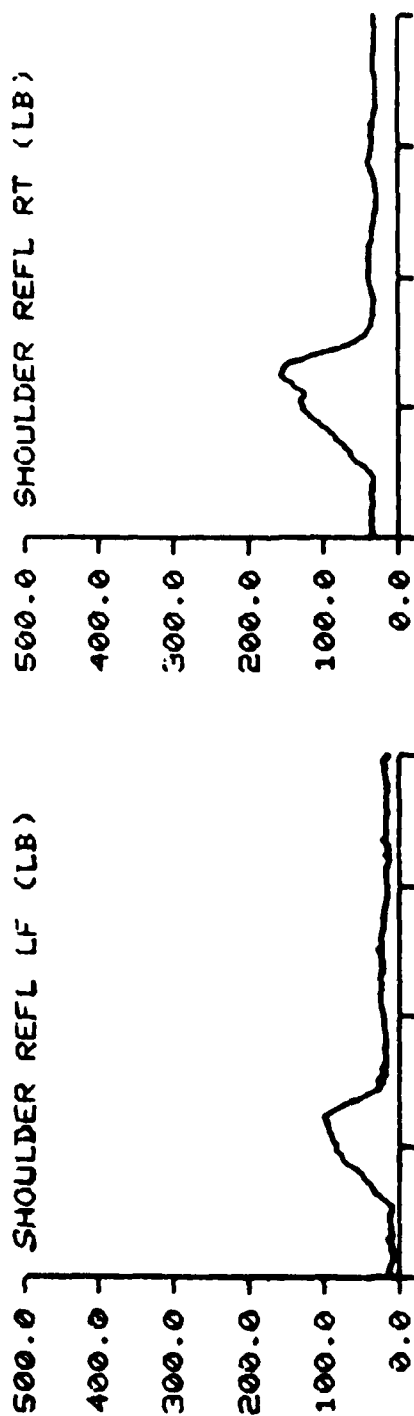
SUBJECT ID: P-2

F-111 TEST NO: 553



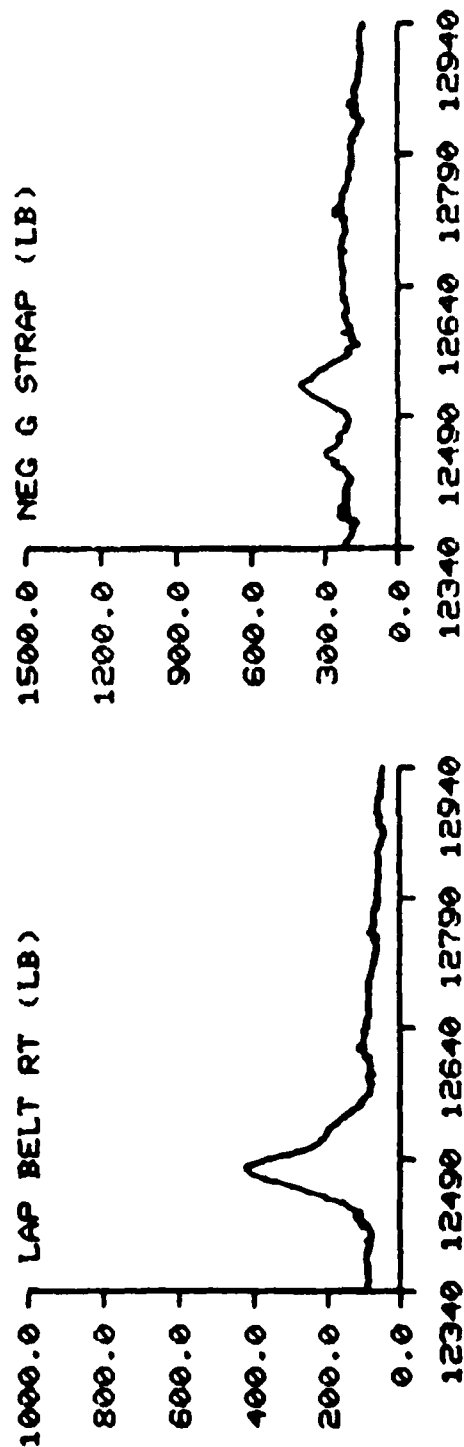
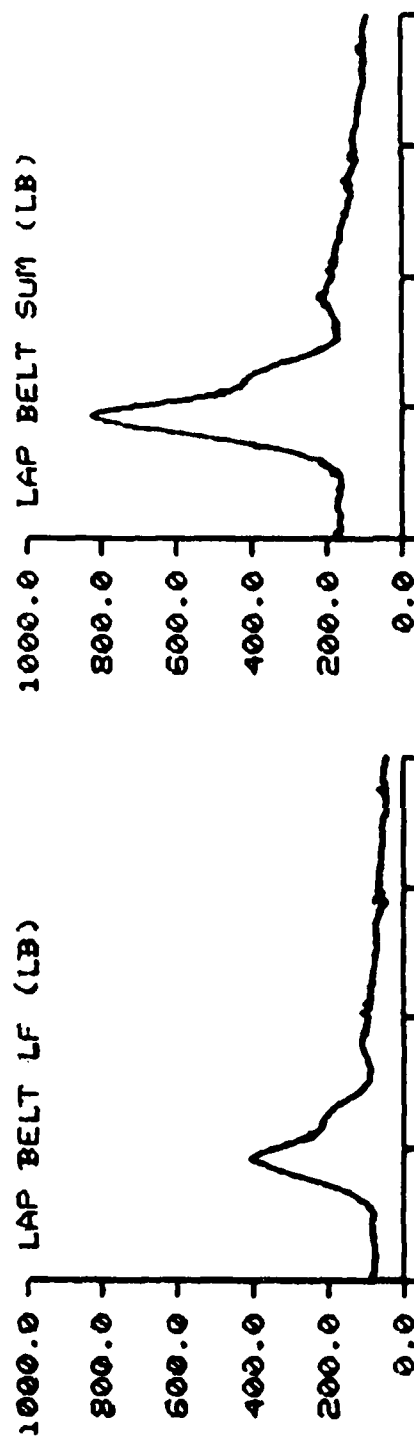
TIME IN MILLISECONDS

F-111      TEST NO: 553      SUBJECT ID: P-2



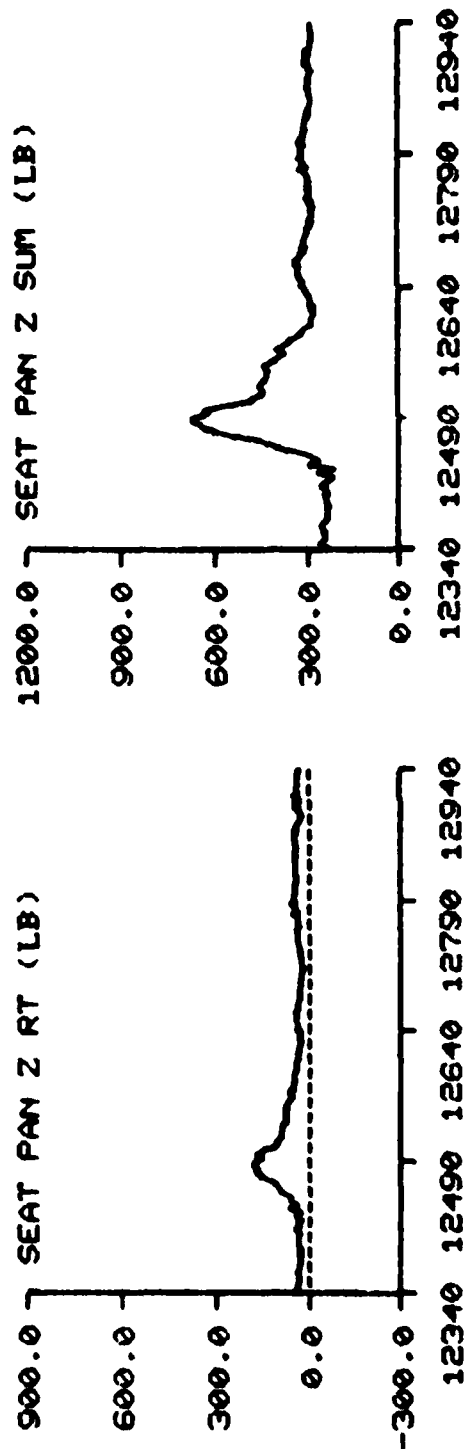
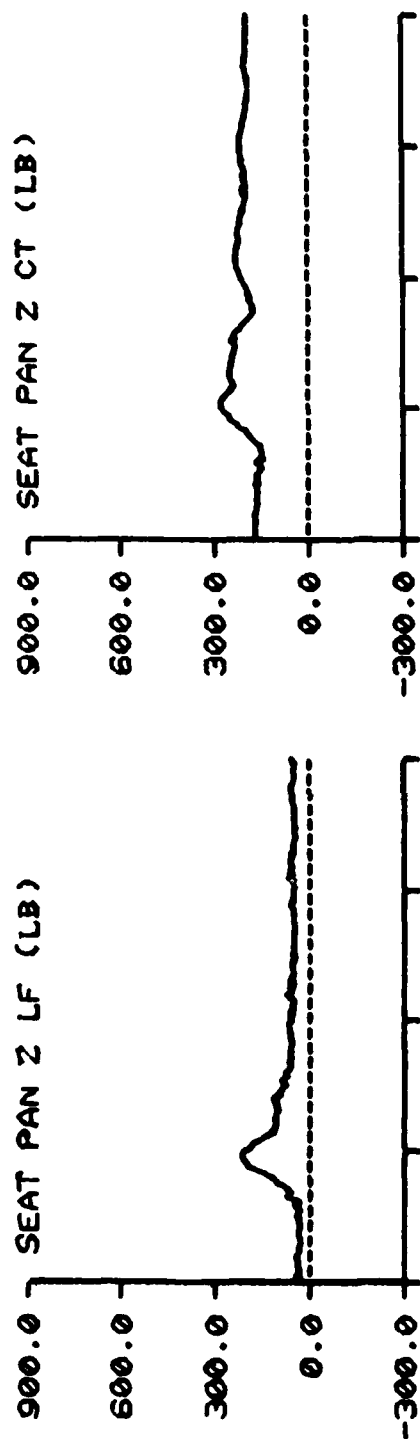
TIME IN MILLISECONDS

F-111 TEST NO: 553 SUBJECT ID: P-2

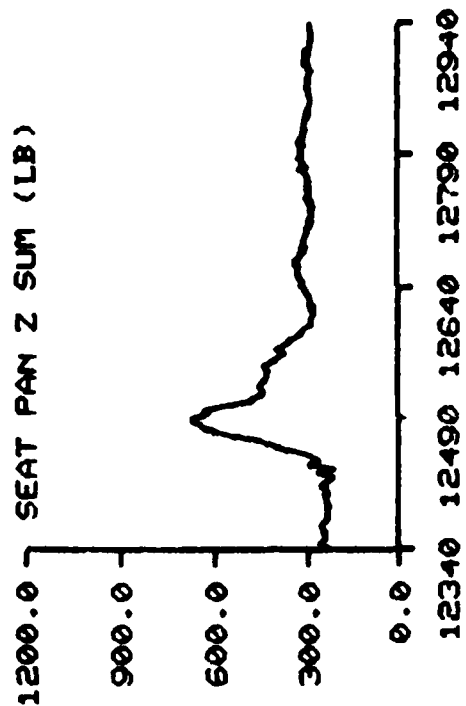


TIME IN MILLISECONDS

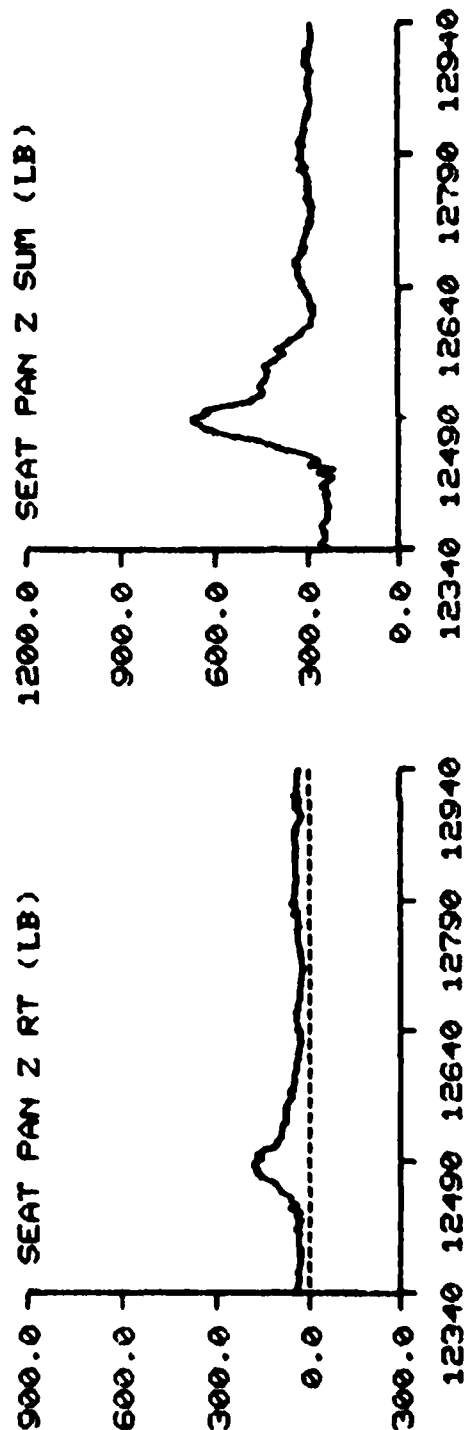
F-111 TEST NO: 553 SUBJECT ID: P-2



SEAT PAN Z CT (LB)

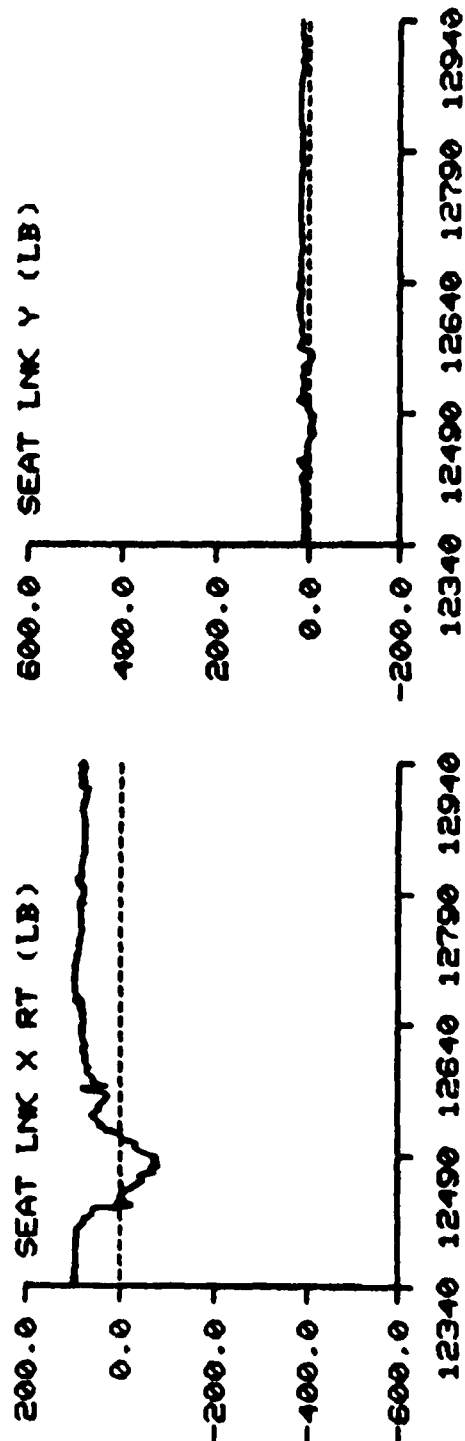
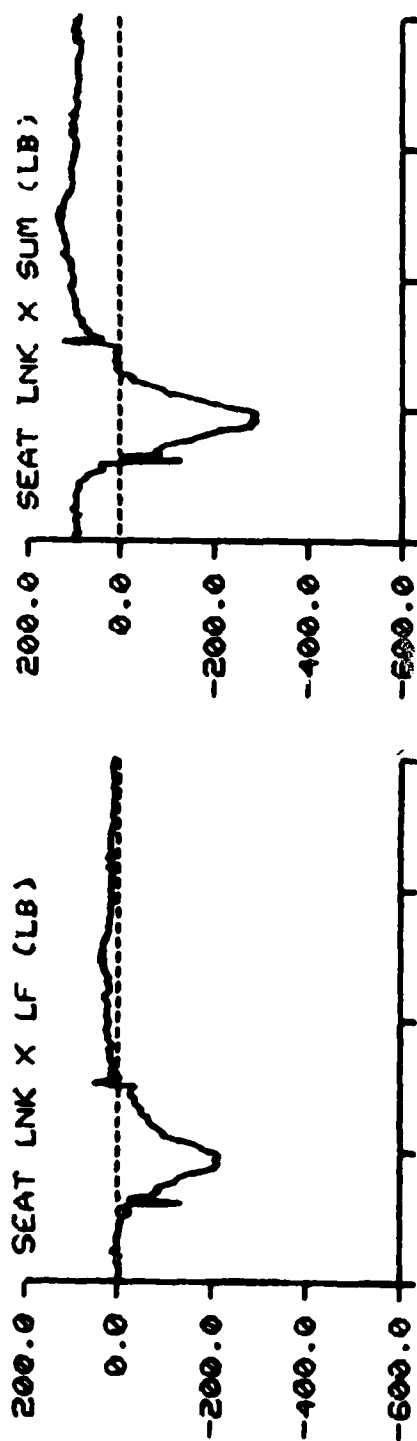


SEAT PAN Z SUM (LB)



TIME IN MILLISECONDS

F-111 TEST NO: 553 SUBJECT ID: P-2



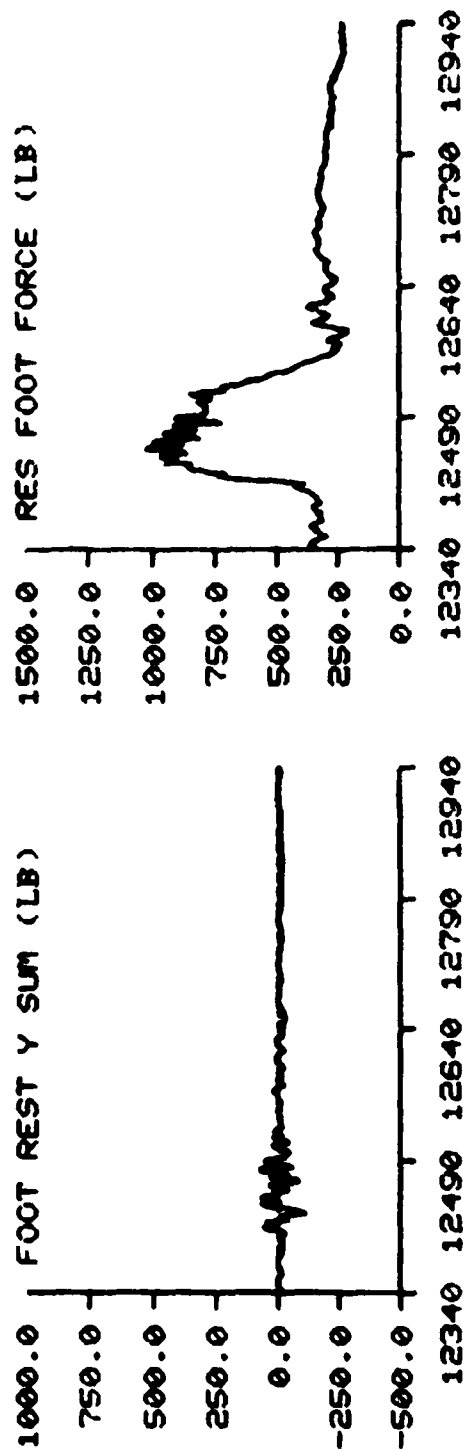
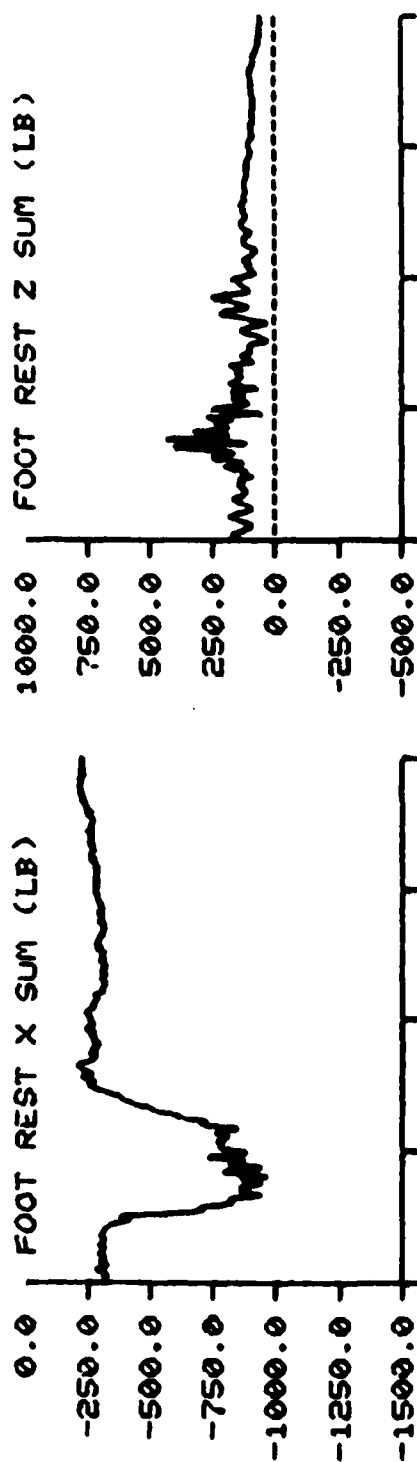
SEAT LNK Y (LB)

SEAT LNK X SUM (LB)

TIME IN MILLISECONDS

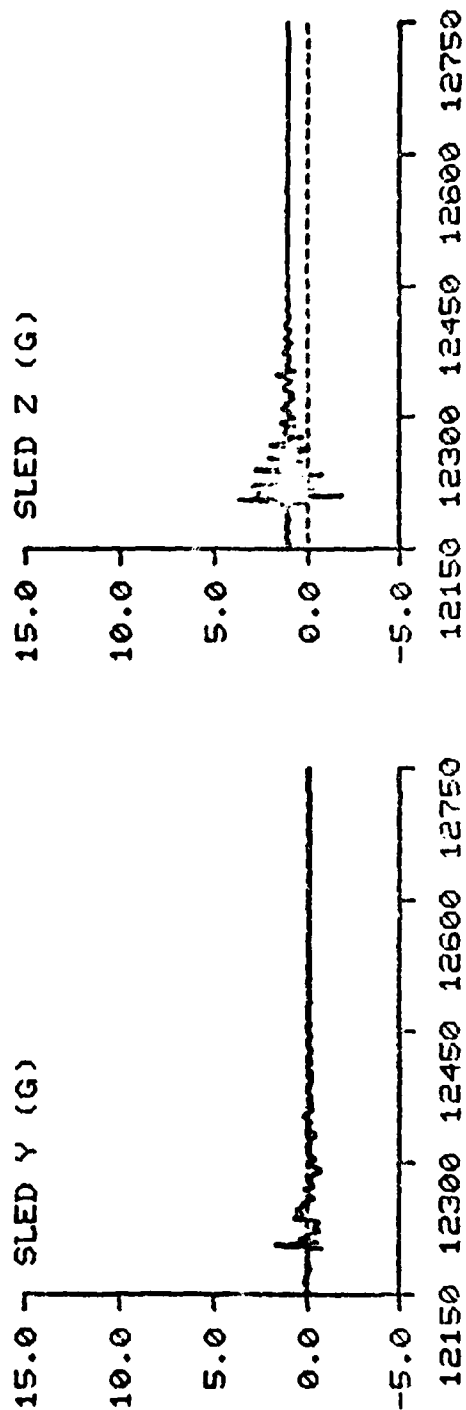
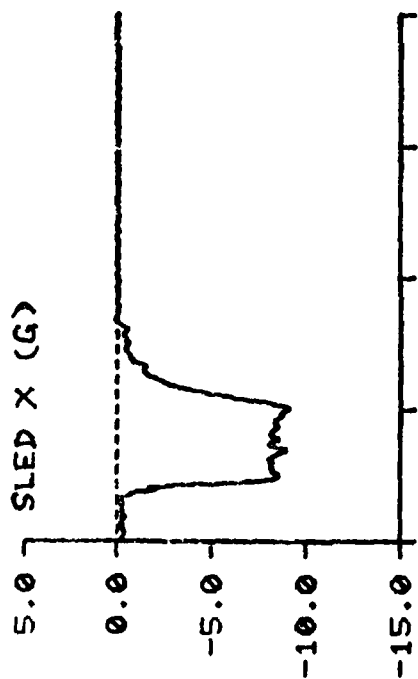


F-111 TEST NO: 553 SUBJECT ID: P-2



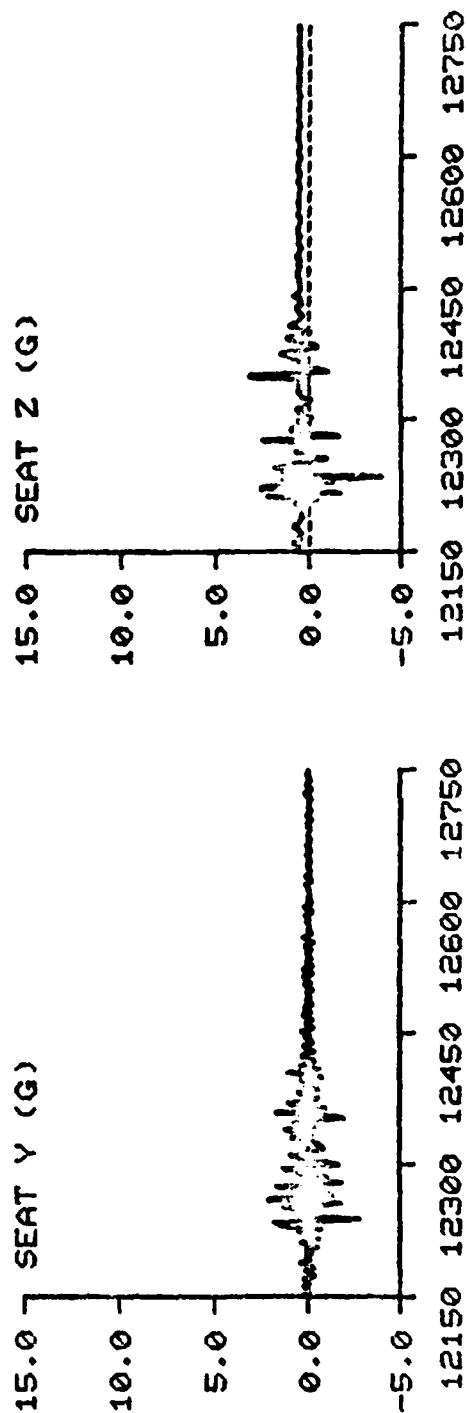
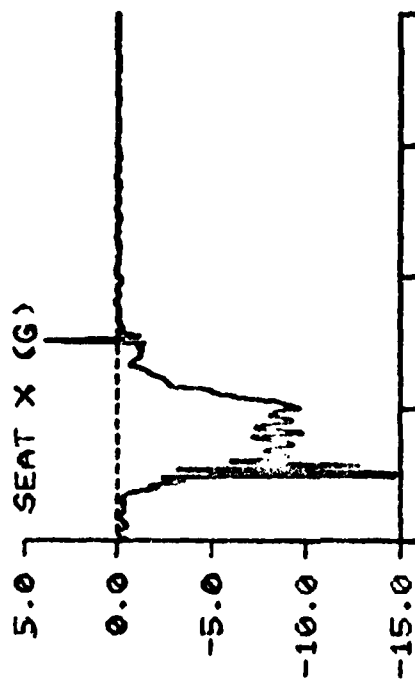
TIME IN MILLISECONDS

F-111 TEST NO: 598 SUBJECT ID: M-7



TIME IN MILLISECONDS

F-111 TEST NO: 598 SUBJECT ID: M-7



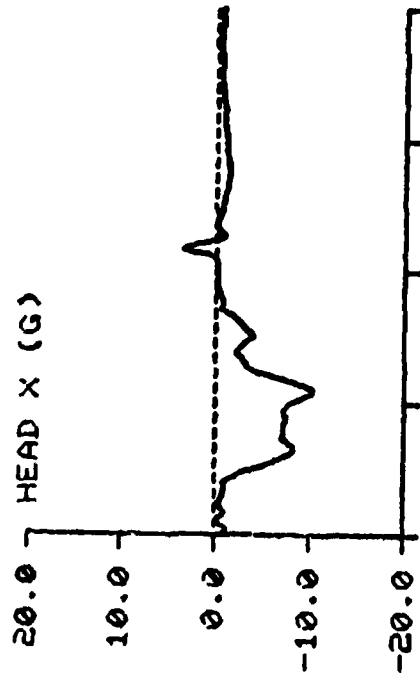
TIME IN MILLISECONDS

F-111

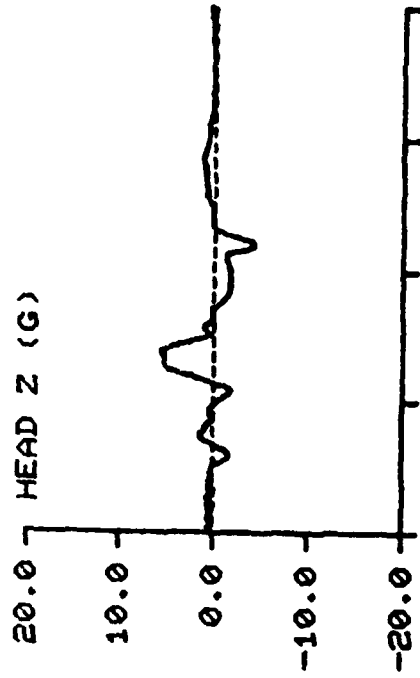
TEST NO: 598

SUBJECT ID: M-7

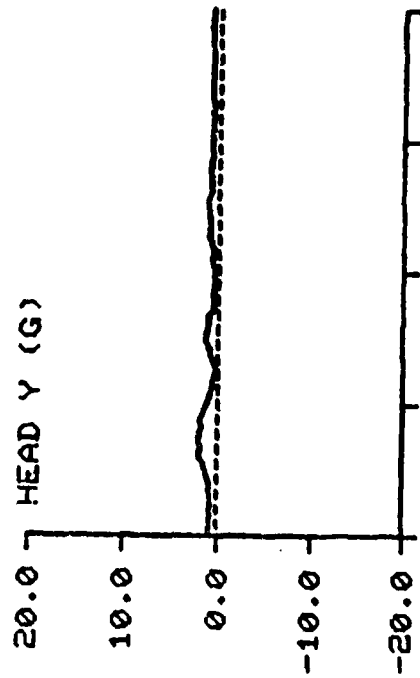
HEAD X (G)



HEAD Z (G)



HEAD Y (G)



HEAD RES (G)

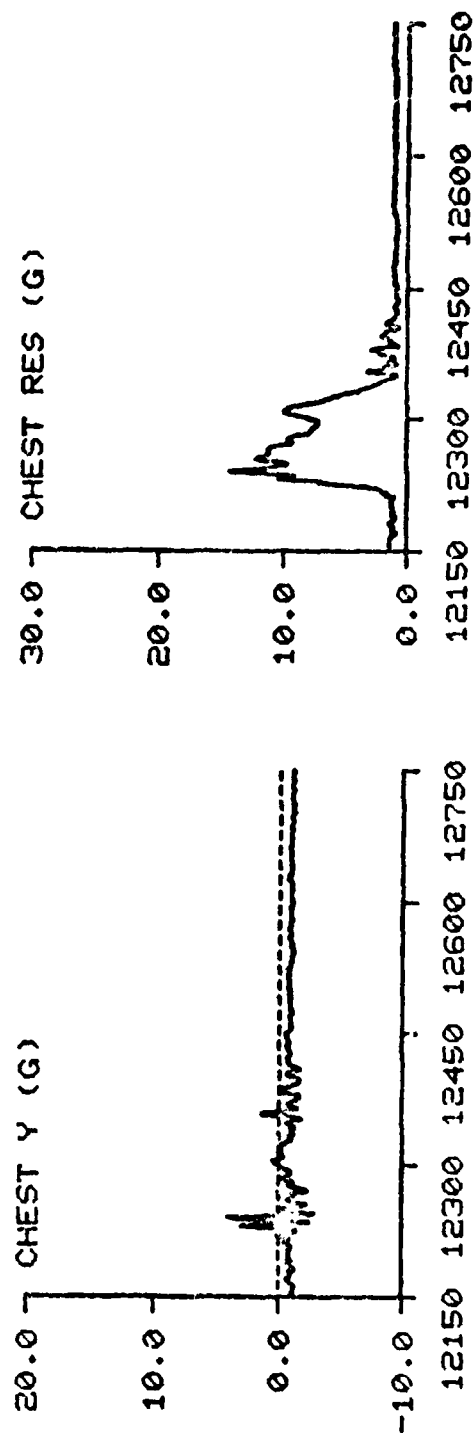
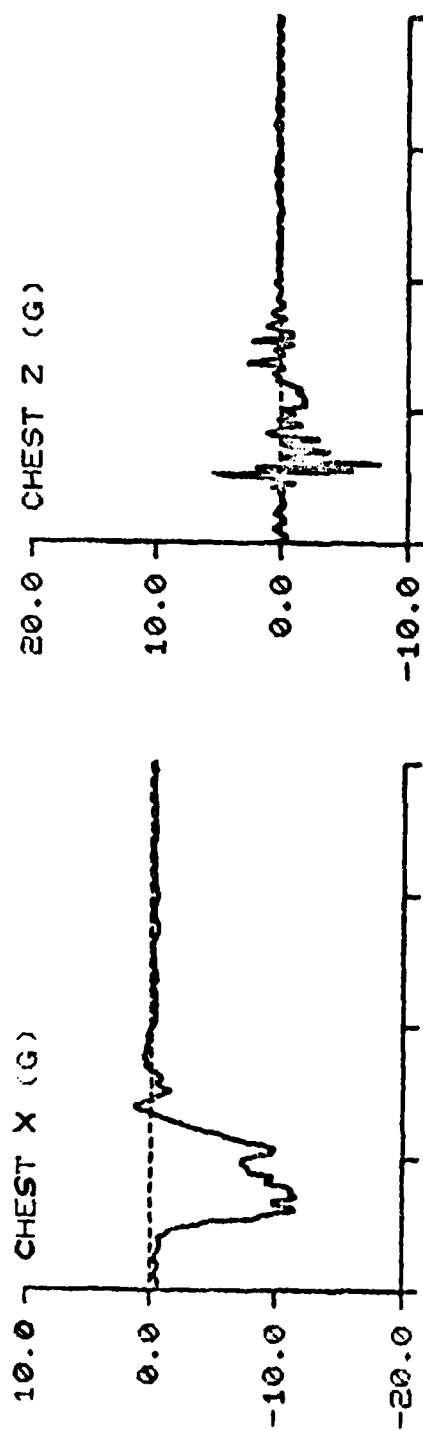


12150 12300 12450 12600 12750

12150 12300 12450 12600 12750

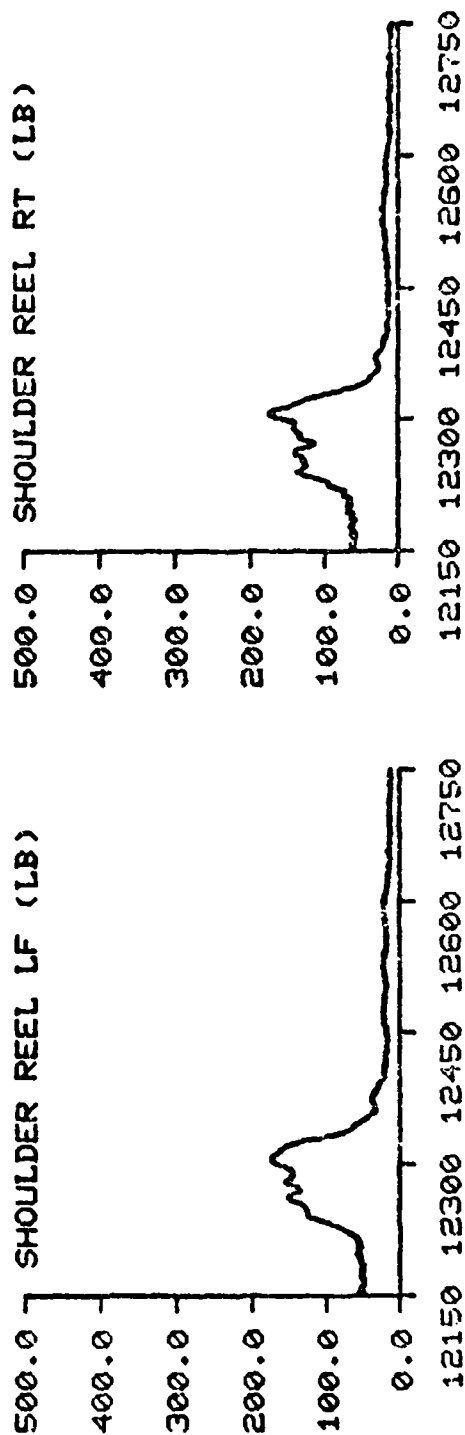
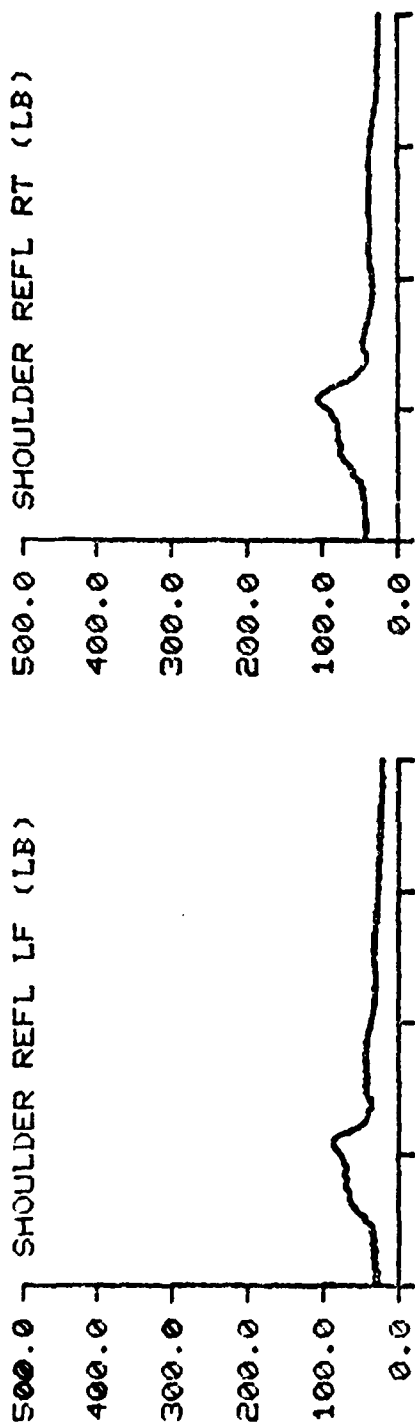
TIME IN MILLISECONDS

F-111 TEST NO: 598 SUBJECT ID: M-7



TIME IN MILLISECONDS

F-111      TEST NO: 598      SUBJECT ID: M-7

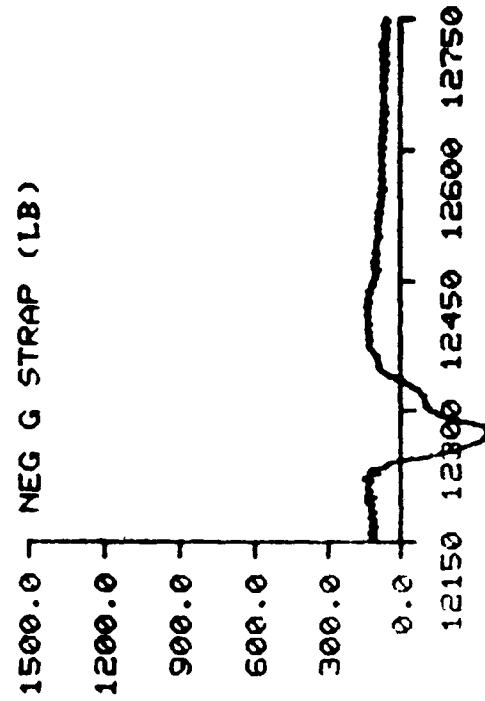
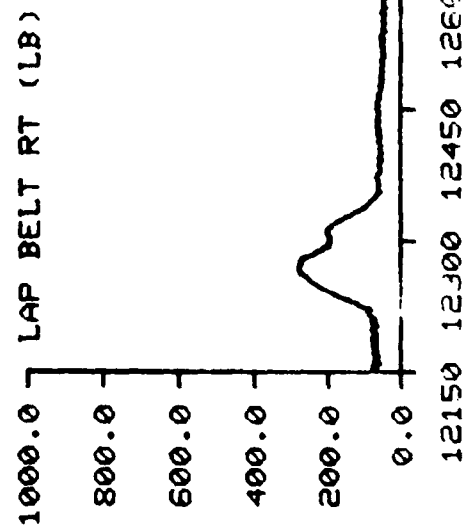
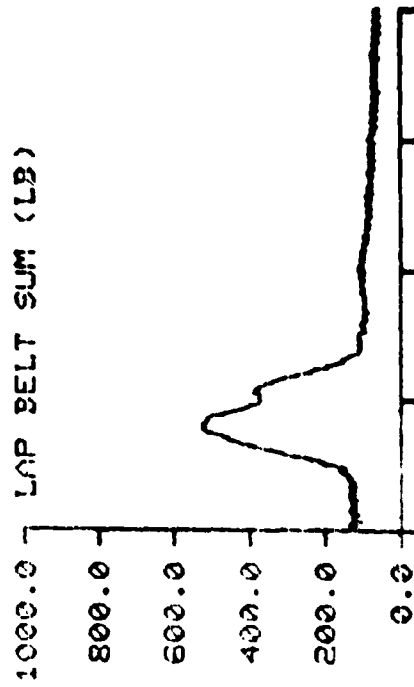
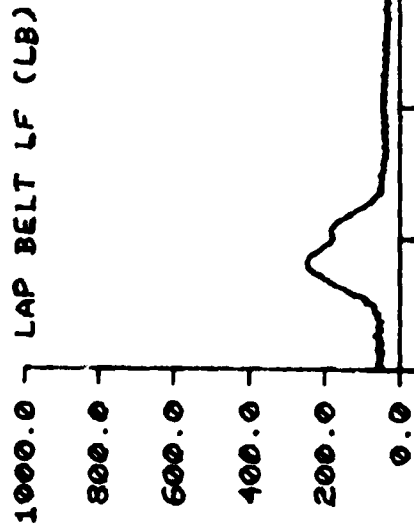


TIME IN MILLISECONDS

F-111

TEST NO: 598

SUBJECT ID: M-7

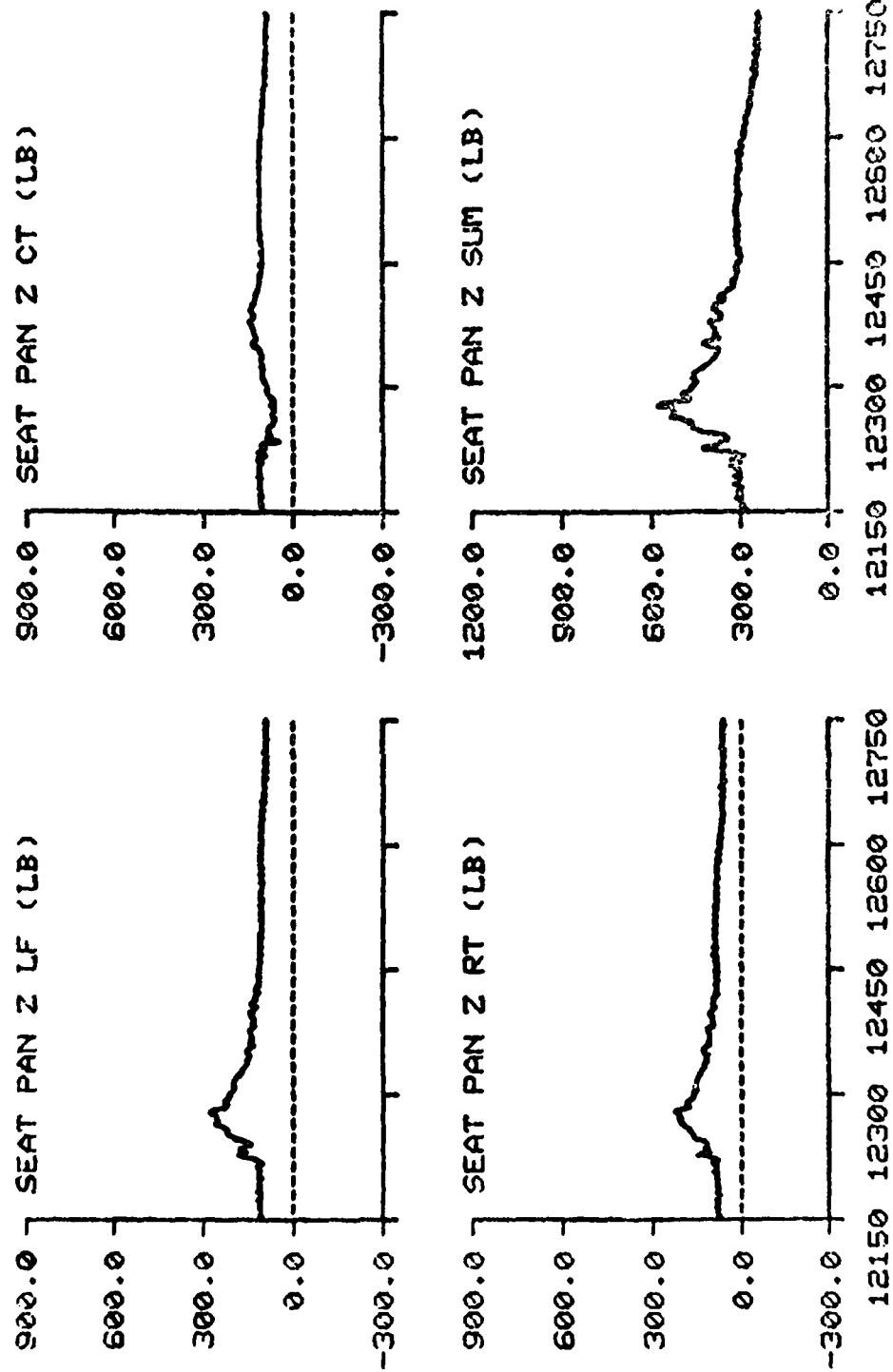


TIME IN MILLISECONDS

F-111

TEST NO: 598

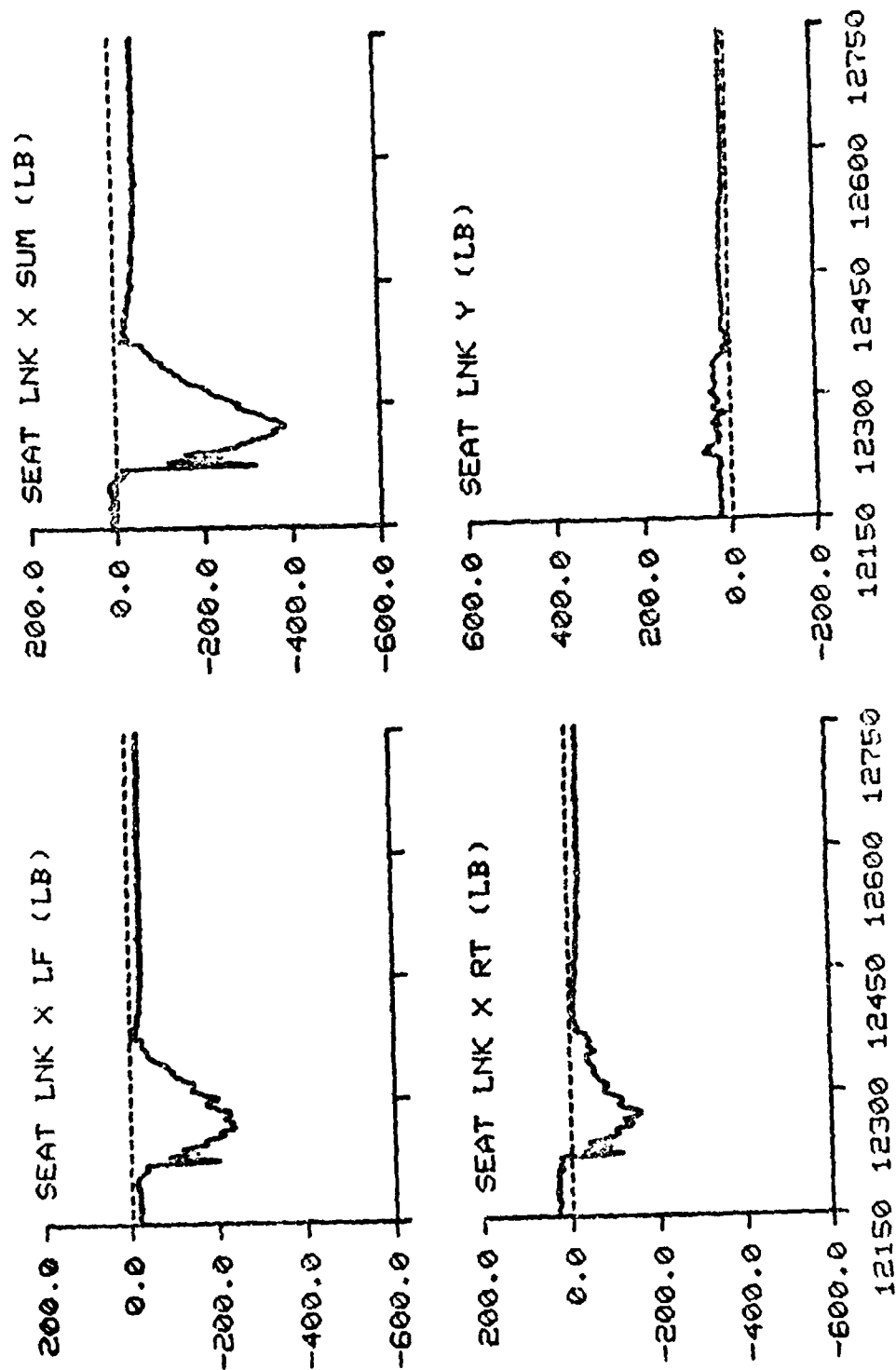
SUBJECT ID: M-7



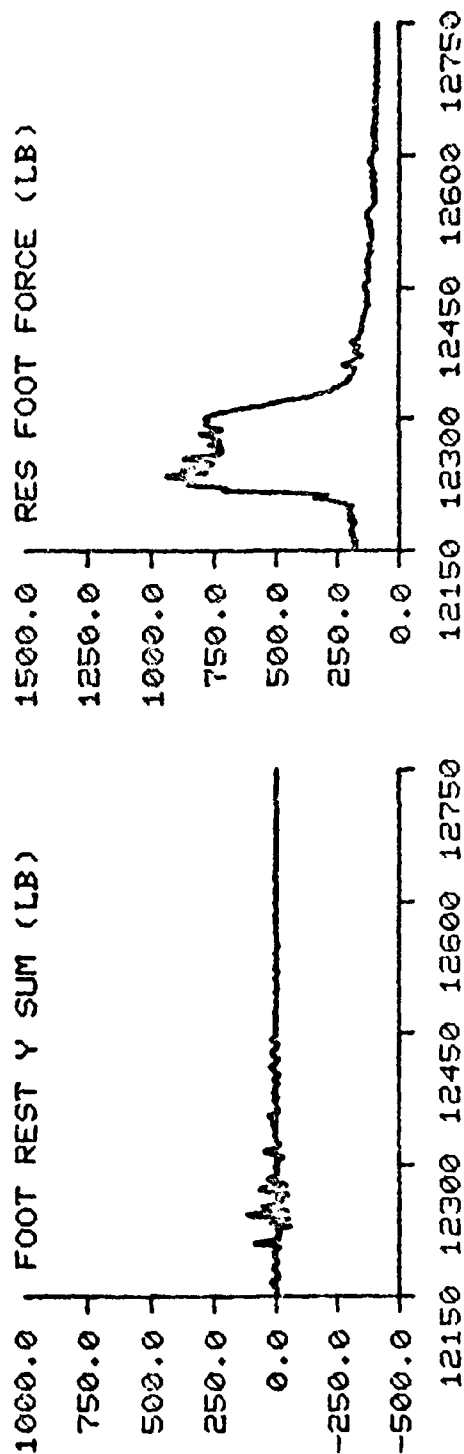
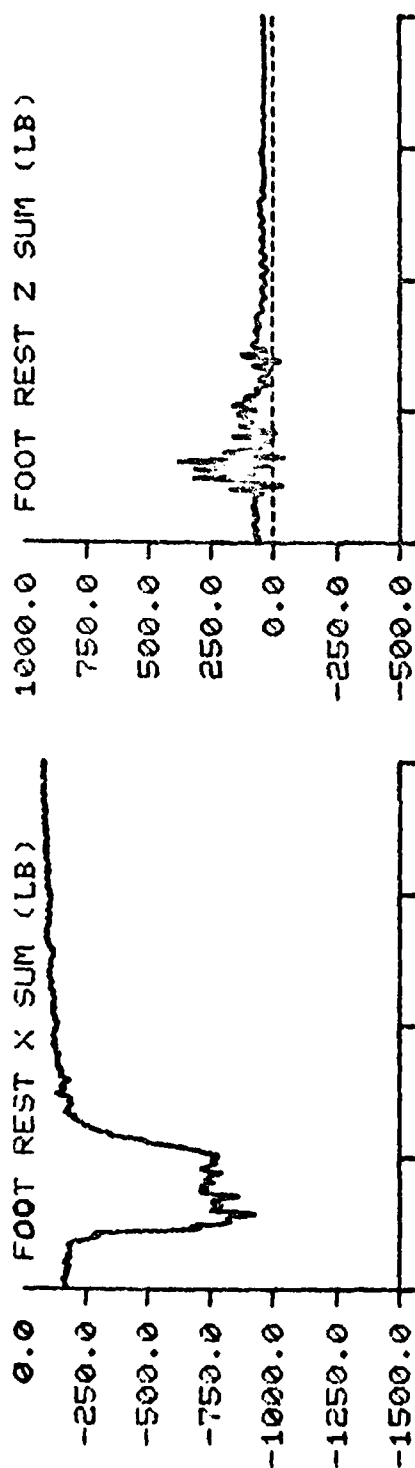
TIME IN MILLISECONDS



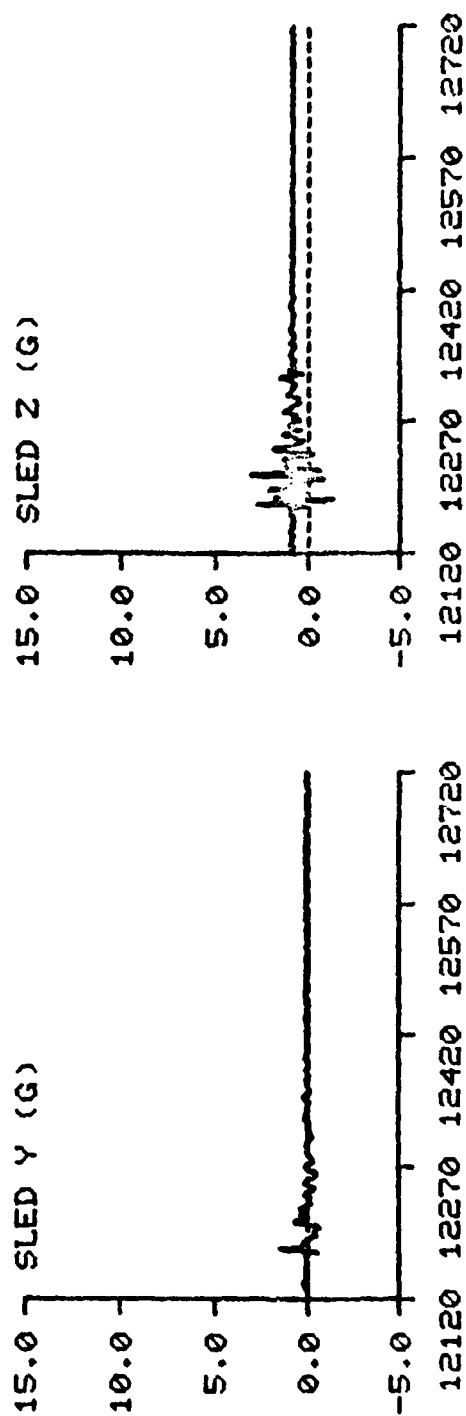
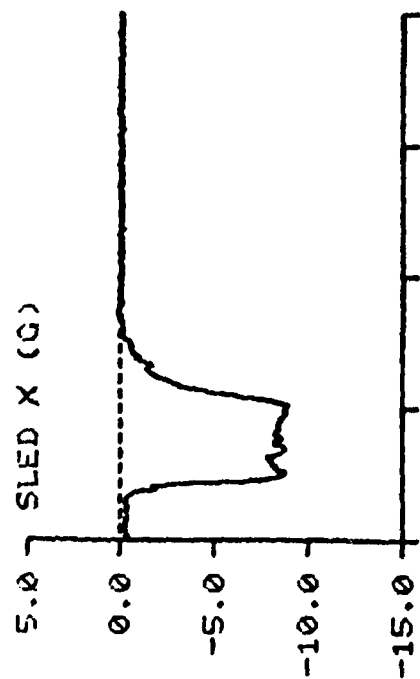
F-111      TEST NO: 598      SUBJECT ID: M-7



F-111 TEST NO: 598 SUBJECT ID: M-7

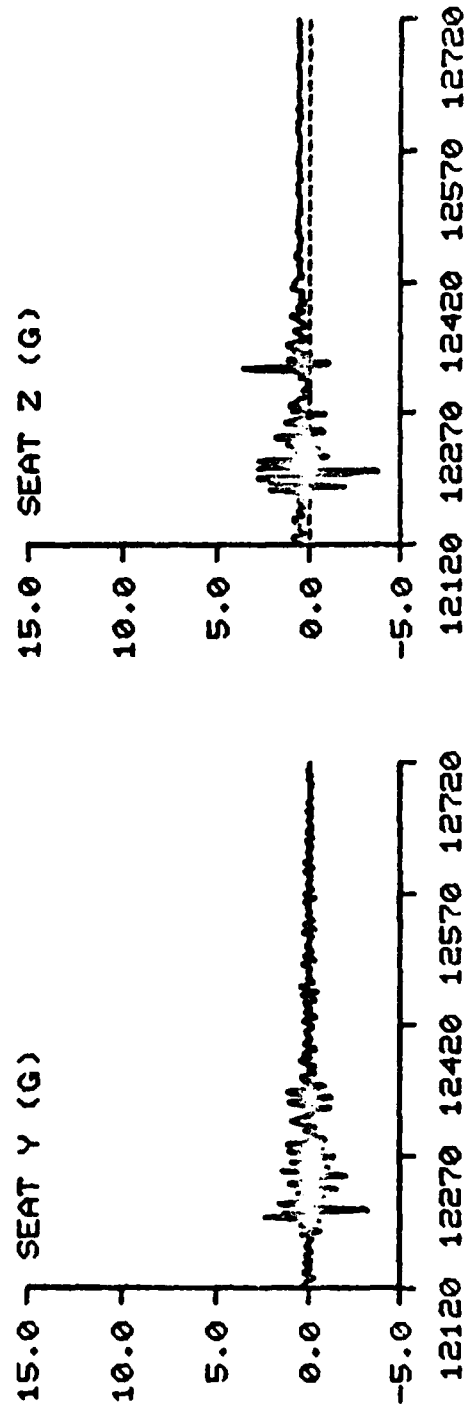
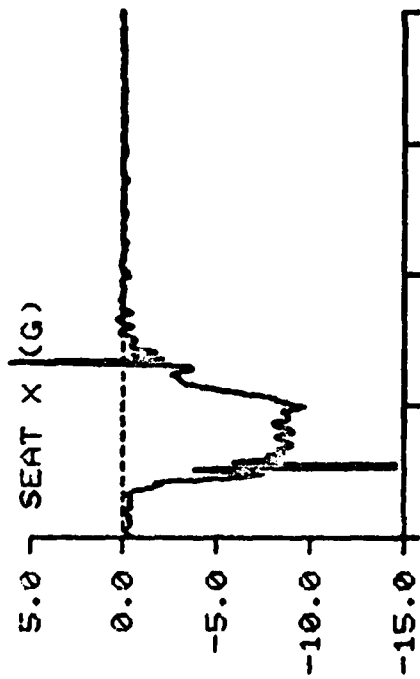


F-111 TEST NO: 576 SUBJECT ID: S-3



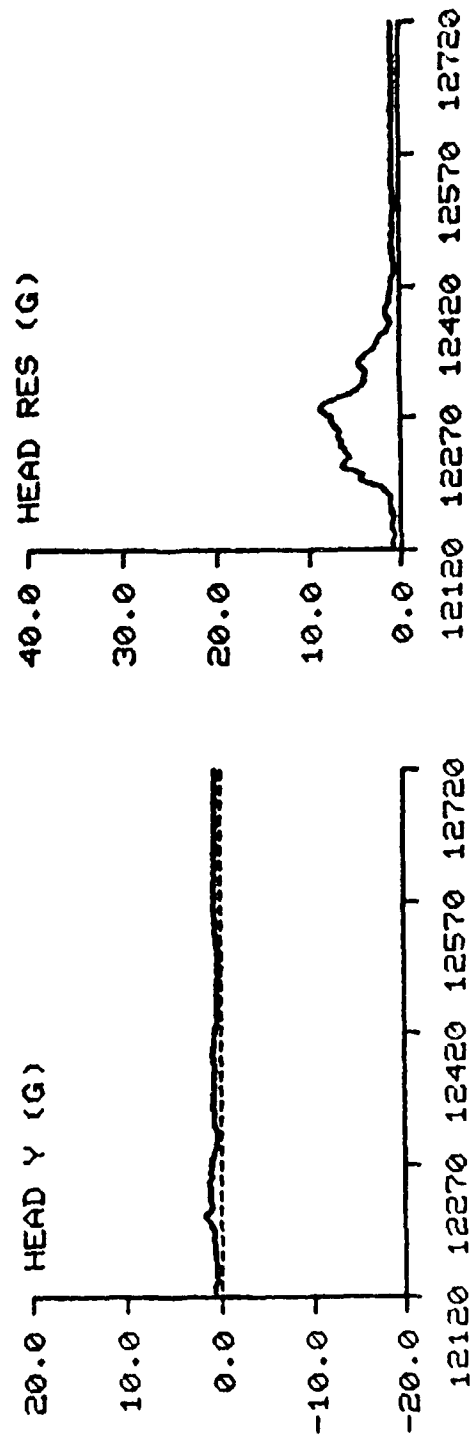
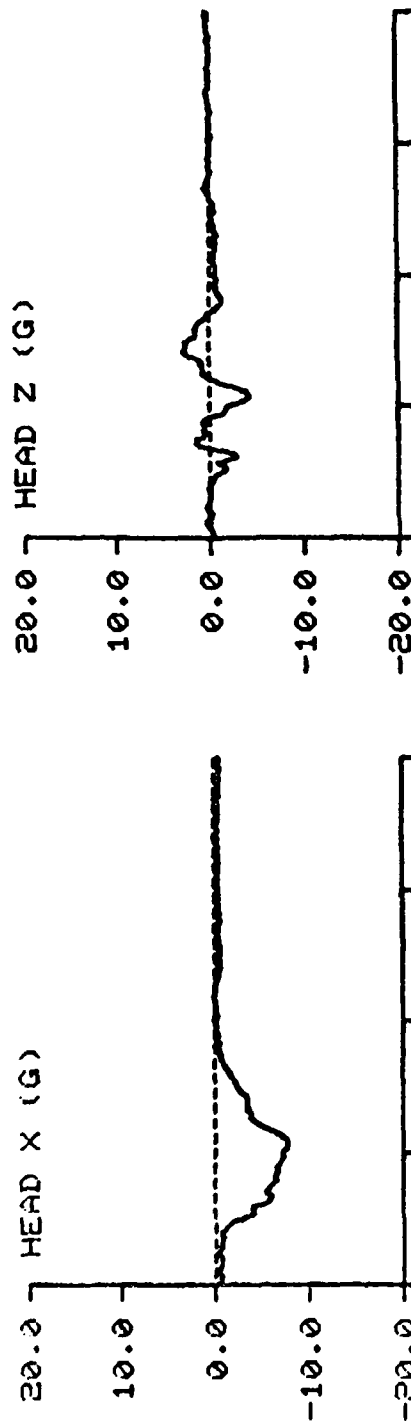
TIME IN MILLISECONDS

F-111 TEST NO: 576 SUBJECT ID: 9-3



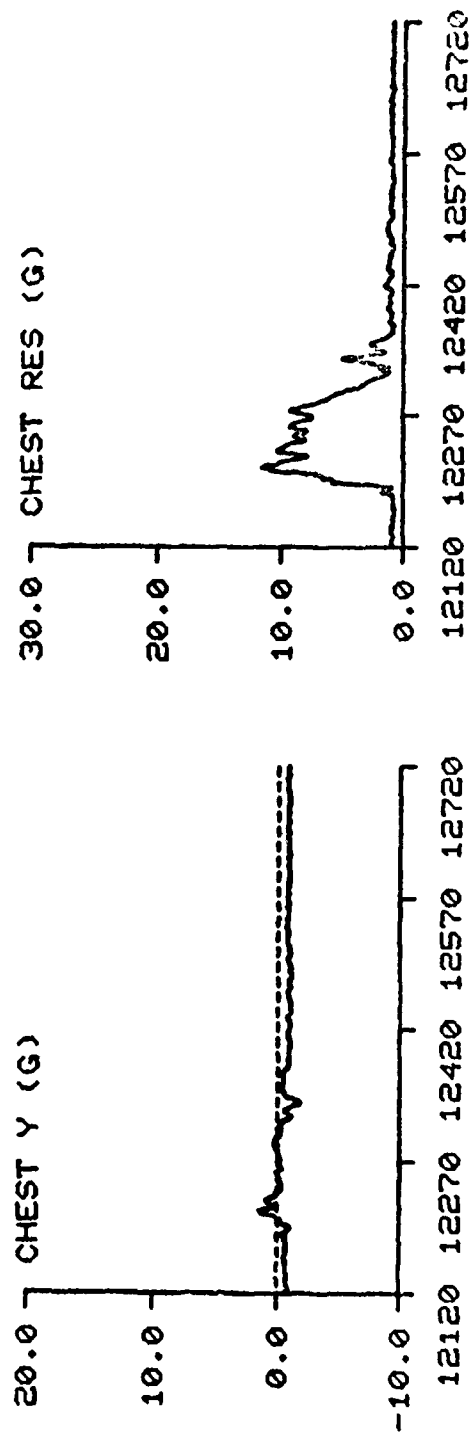
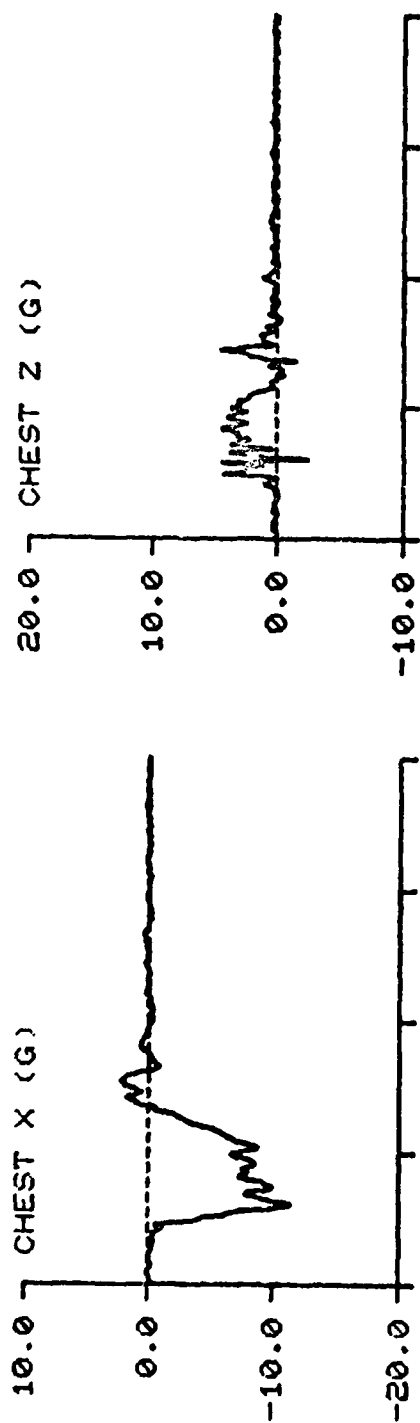
TIME IN MILLISECONDS

F-111 TEST NO: 576 SUBJECT ID: S-3

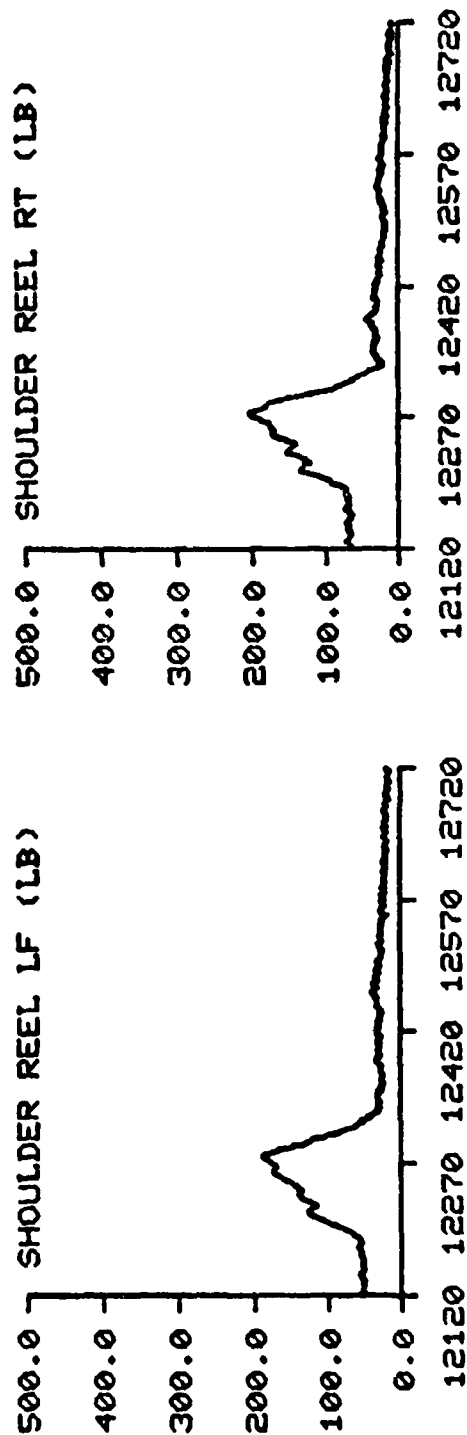
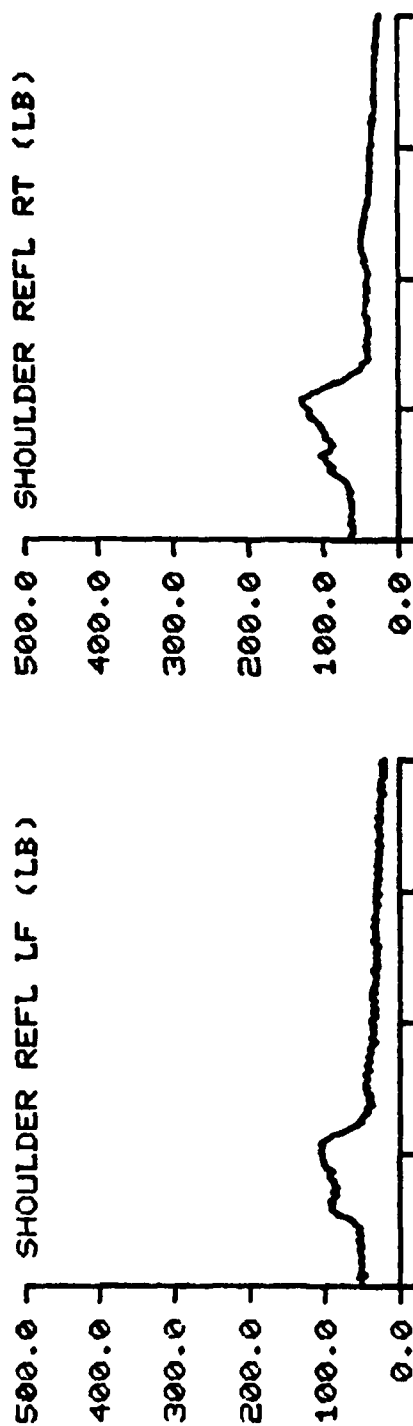


TIME IN MILLISECONDS

F-111      TEST NO: 576      SUBJECT ID: S-3



F-111      TEST NO: 576      SUBJECT ID: 9-3

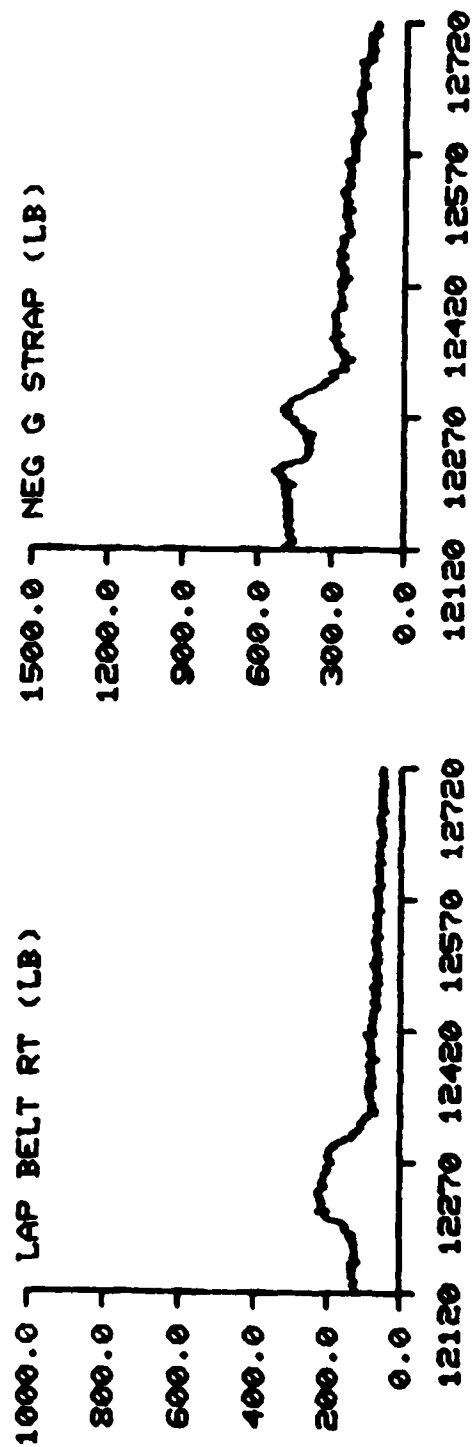
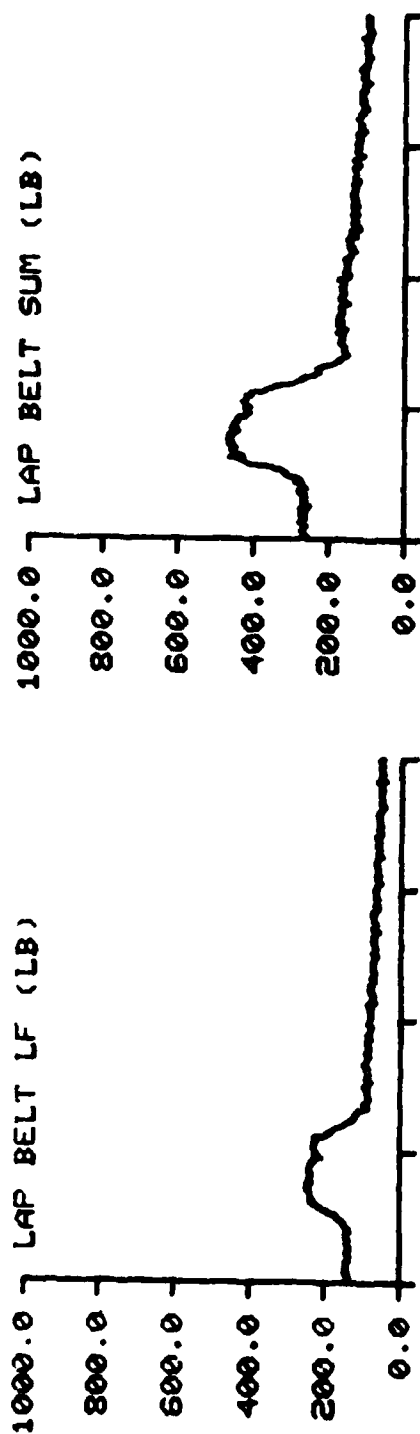


TIME IN MILLISECONDS

F-111

TEST NO: 576

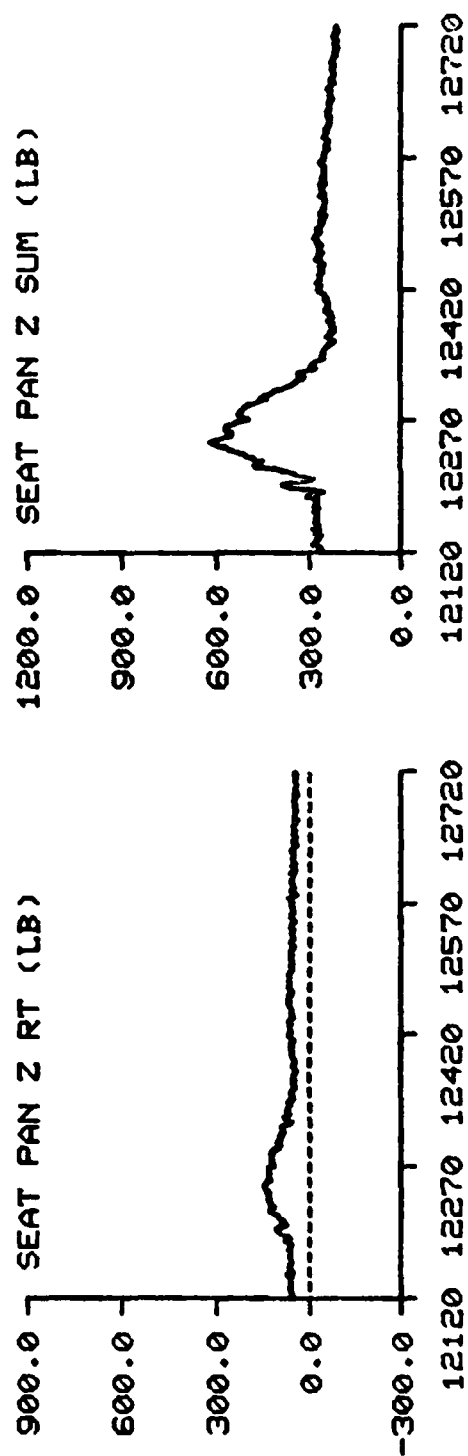
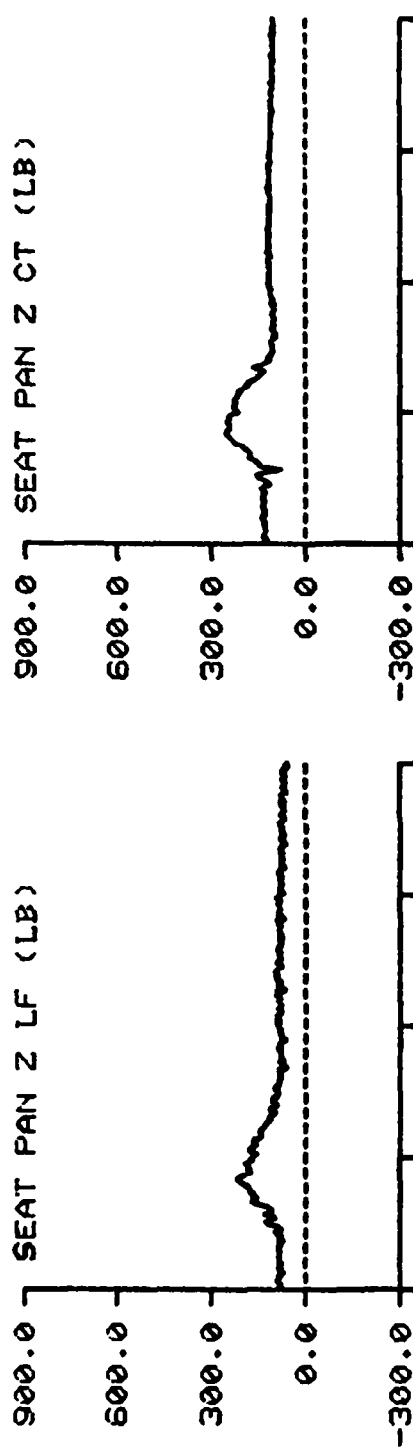
SUBJECT ID: S-3



TIME IN MILLISECONDS



F-111      TEST NO: 576      SUBJECT ID: S-3

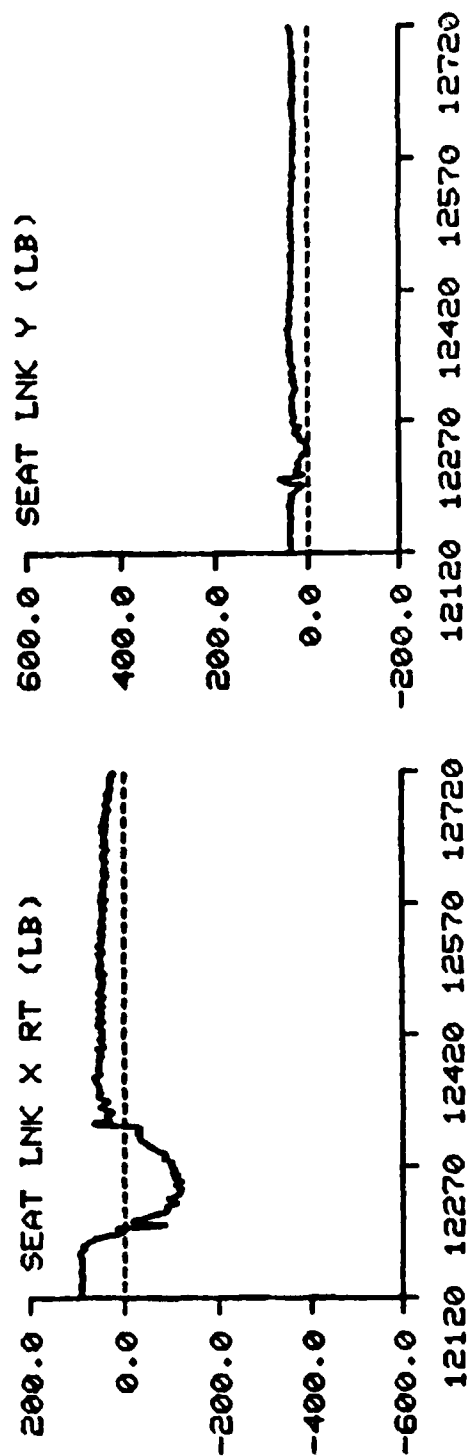
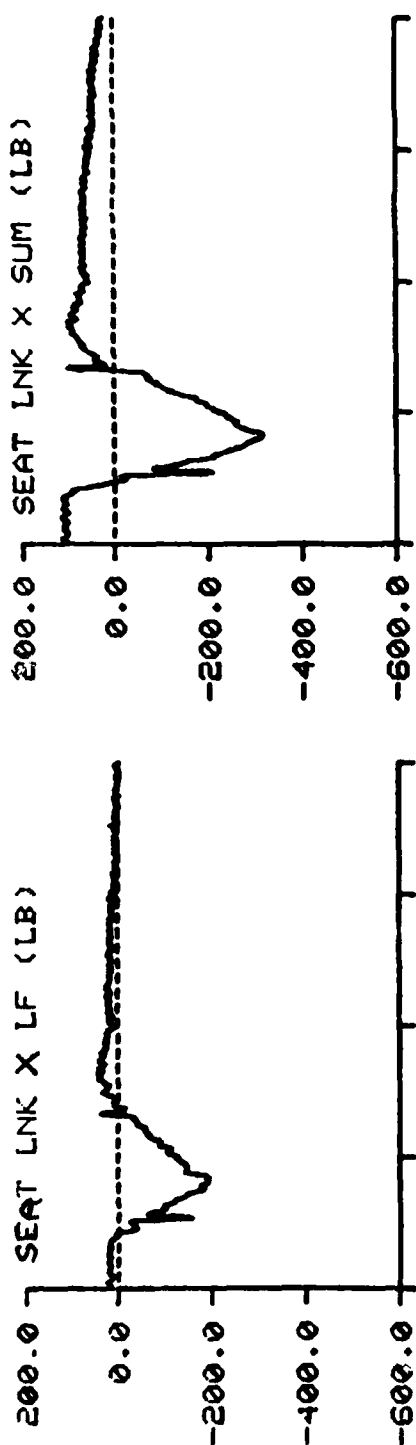


SEAT PAN Z CT (LB)

SEAT PAN Z SUM (LB)

TIME IN MILLISECONDS

F-111 TEST NO: 576 SUBJECT ID: S-3



SEAT LNK Y (LB)

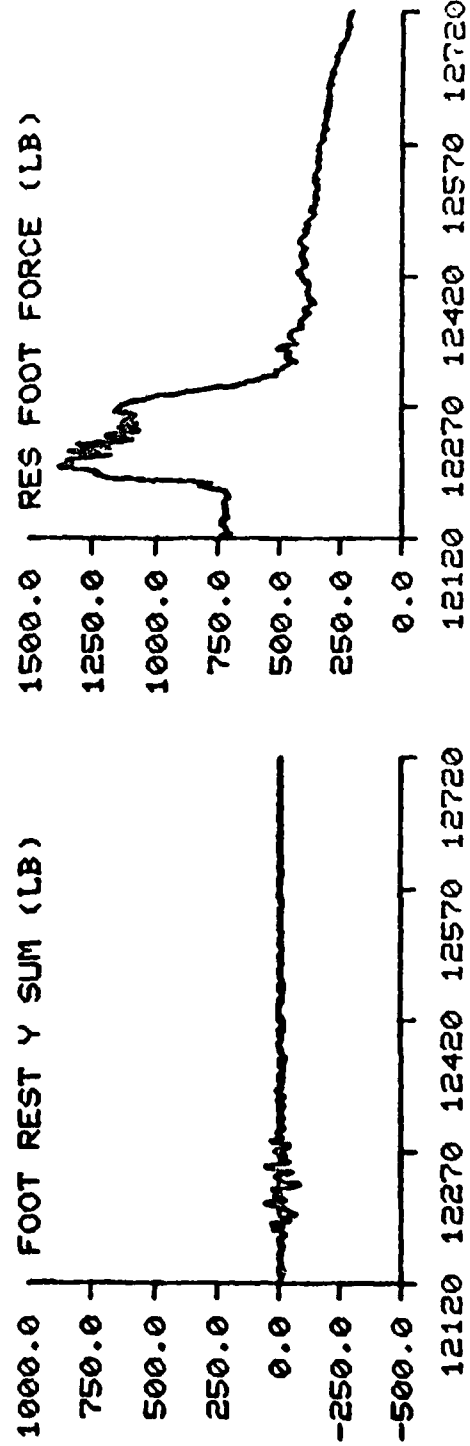
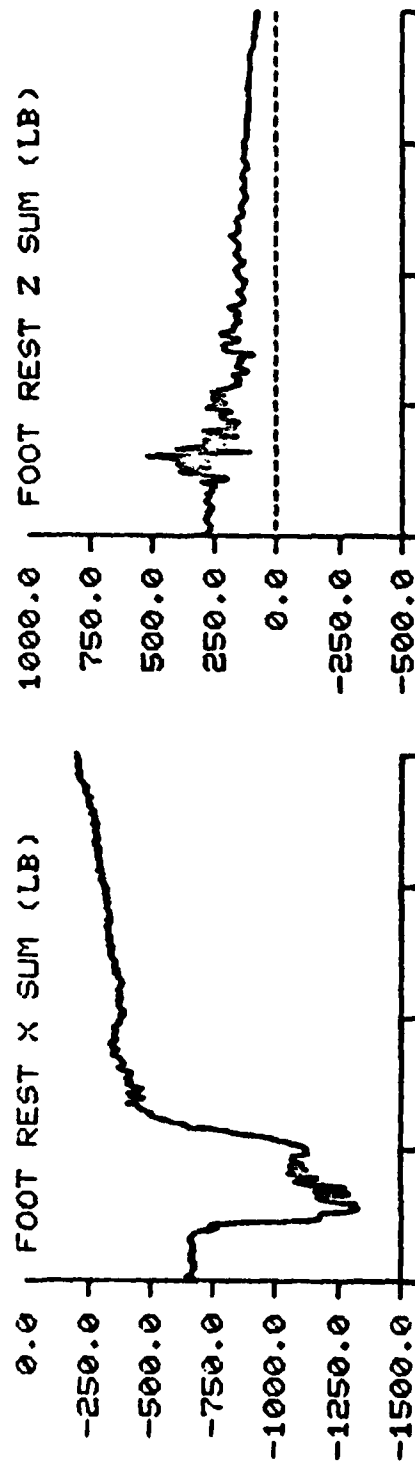
SEAT LNK X RT (LB)

TIME IN MILLISECONDS

F-111

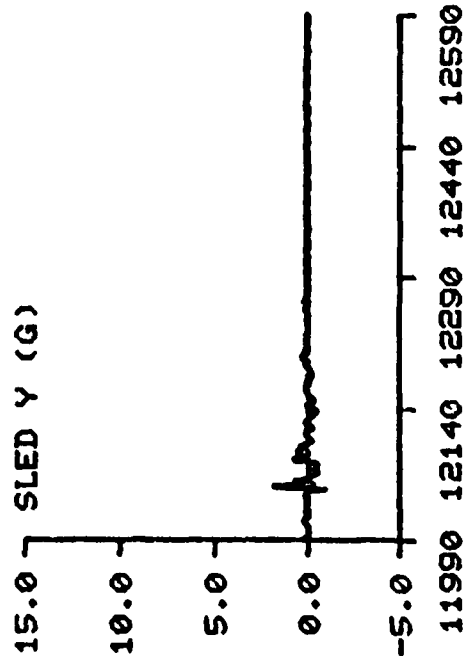
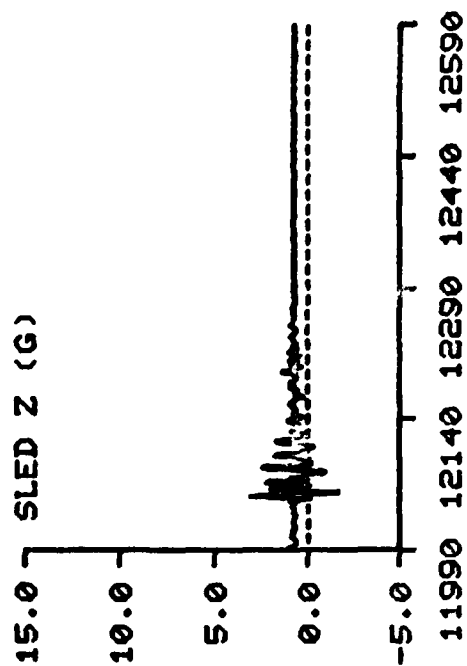
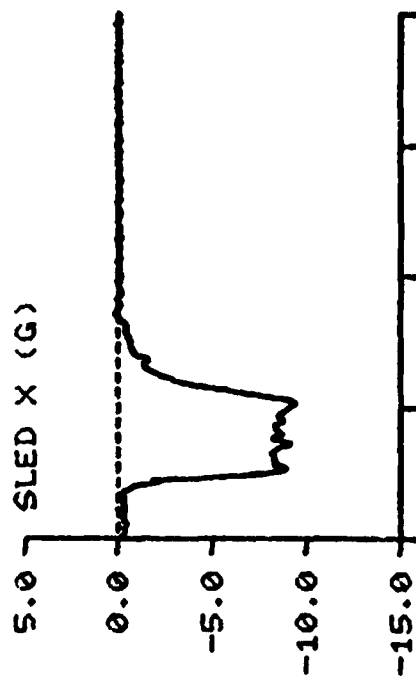
TEST NO: 576

SUBJECT ID: S-3



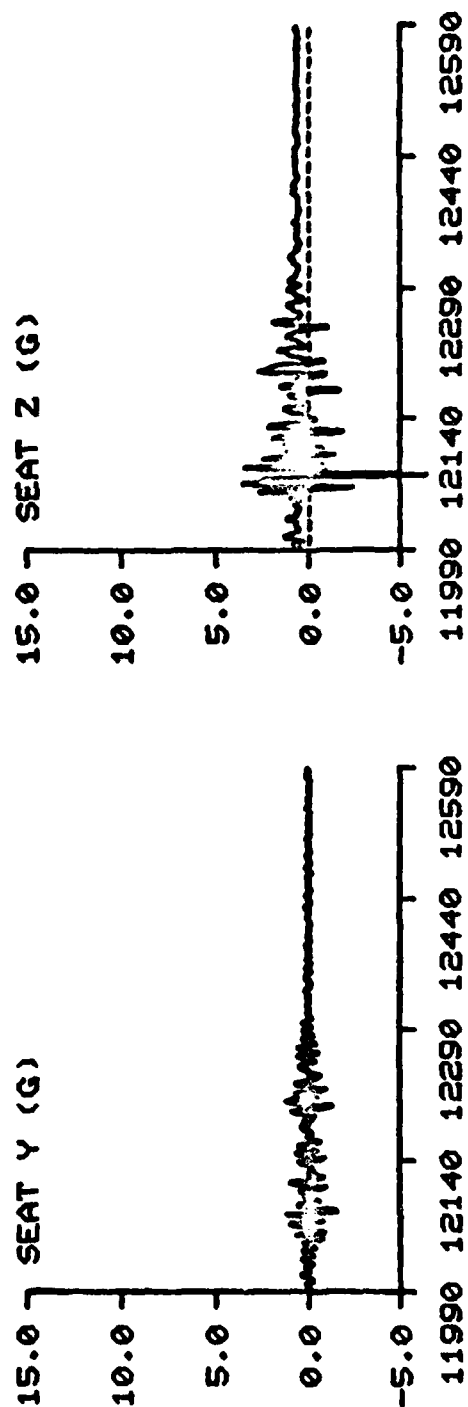
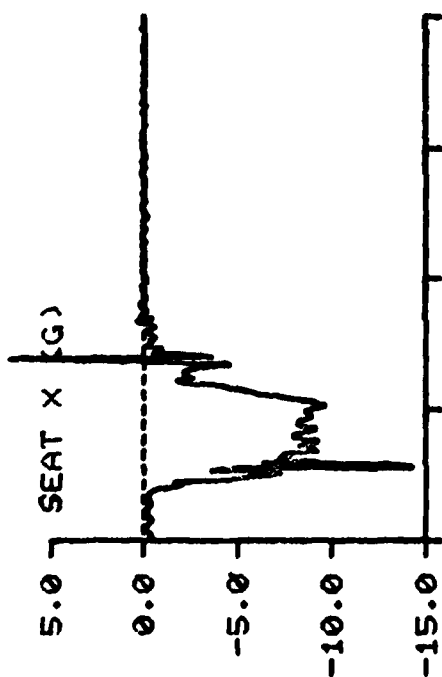
TIME IN MILLISECONDS

F-111 TEST NO: 591 SUBJECT ID: F-3



TIME IN MILLISECONDS

F-111 TEST NO: 591 SUBJECT ID: F-3

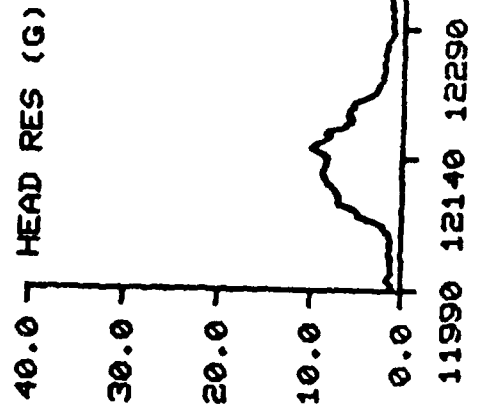
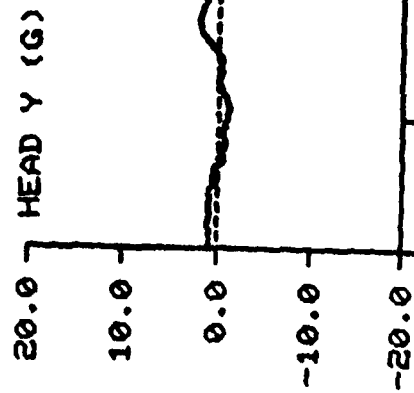
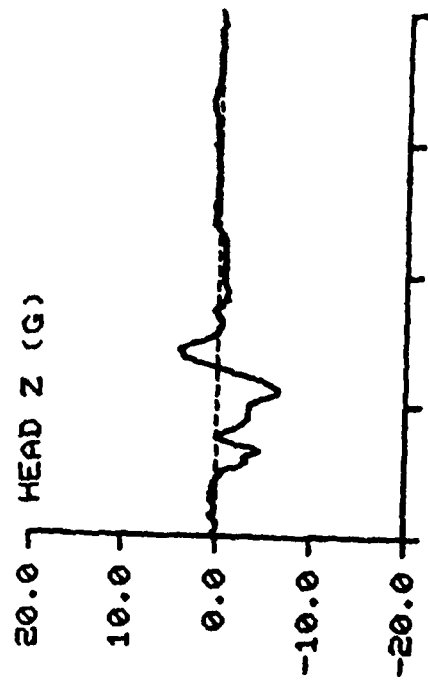
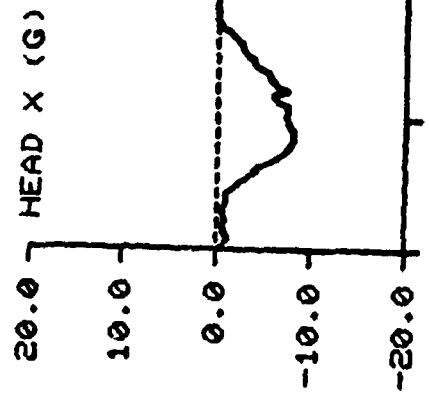


TIME IN MILLISECONDS

F-111

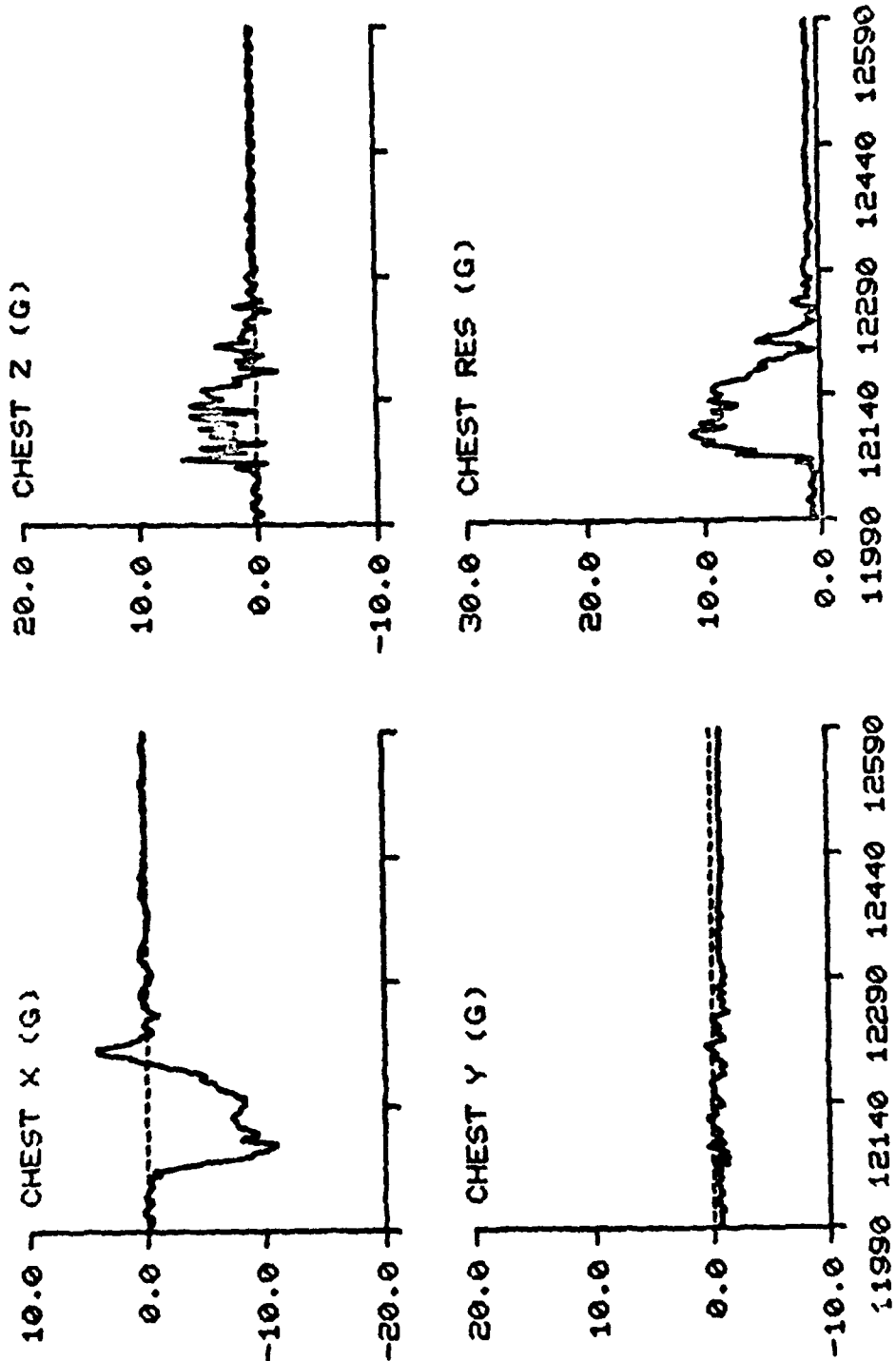
TEST NO: 591

SUBJECT ID: F-3



TIME IN MILLISECONDS

F-111 TEST NO: 591 SUBJECT ID: F-3

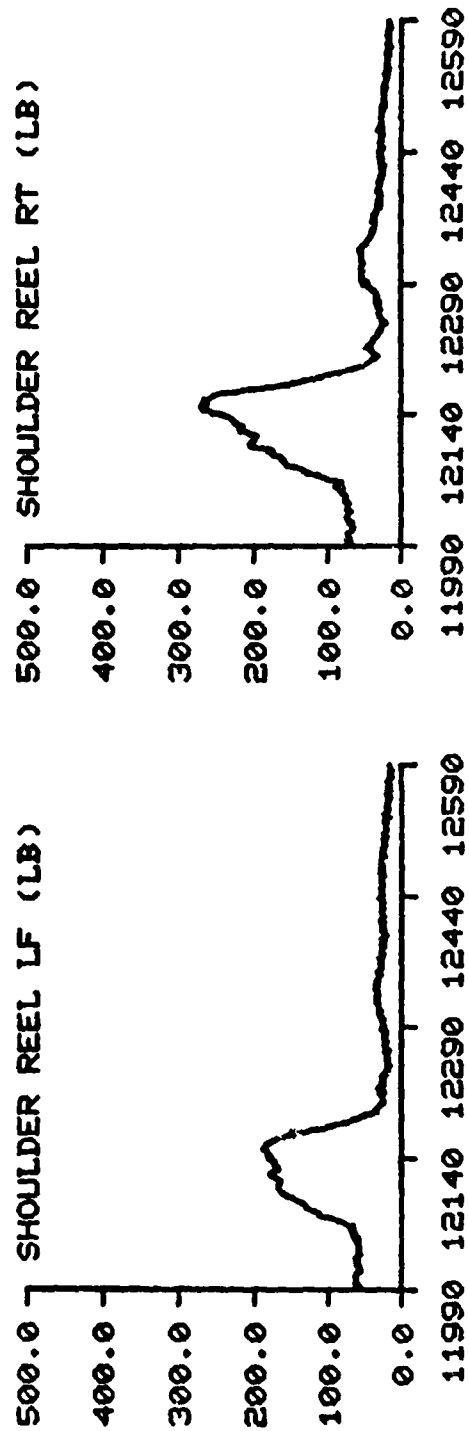
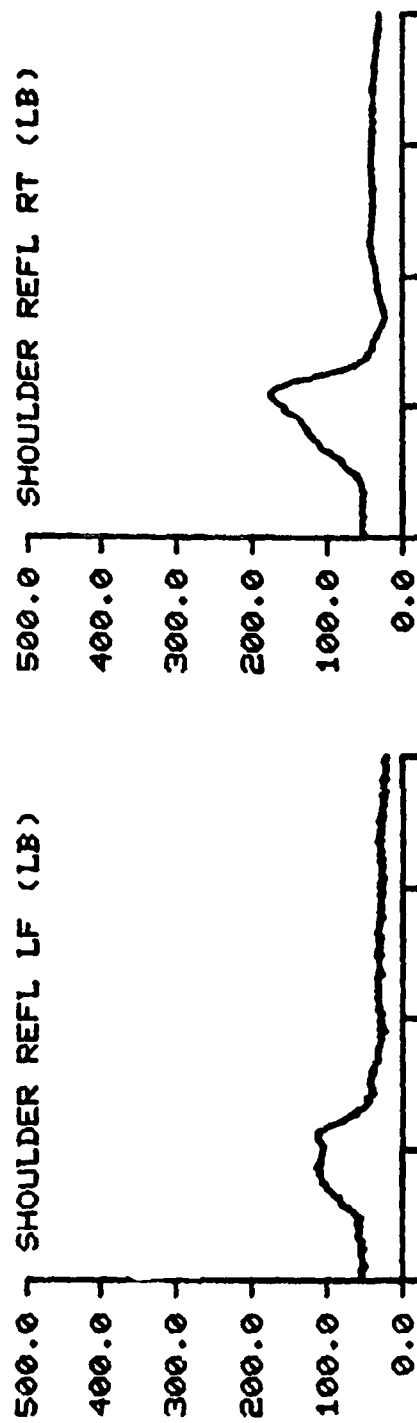


TIME IN MILLISECONDS

F-111

TEST NO: 591

SUBJECT ID: F-3



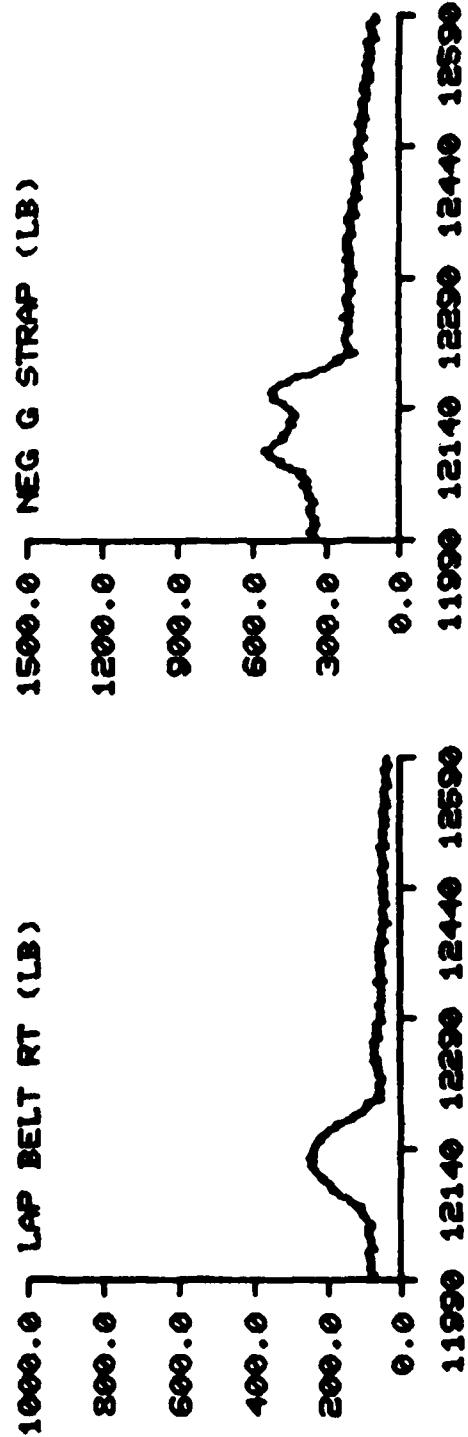
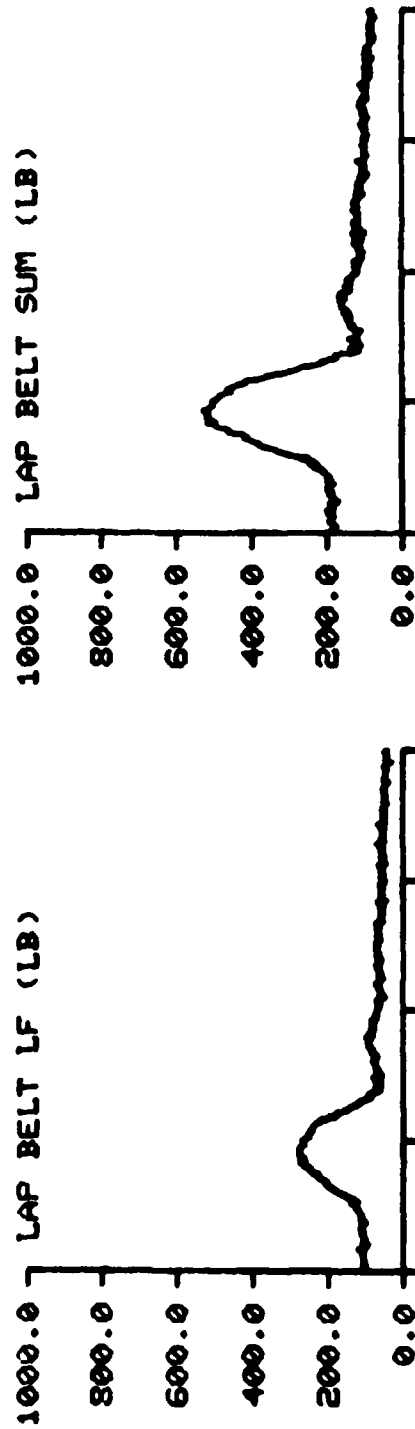
TIME IN MILLISECONDS



F-111

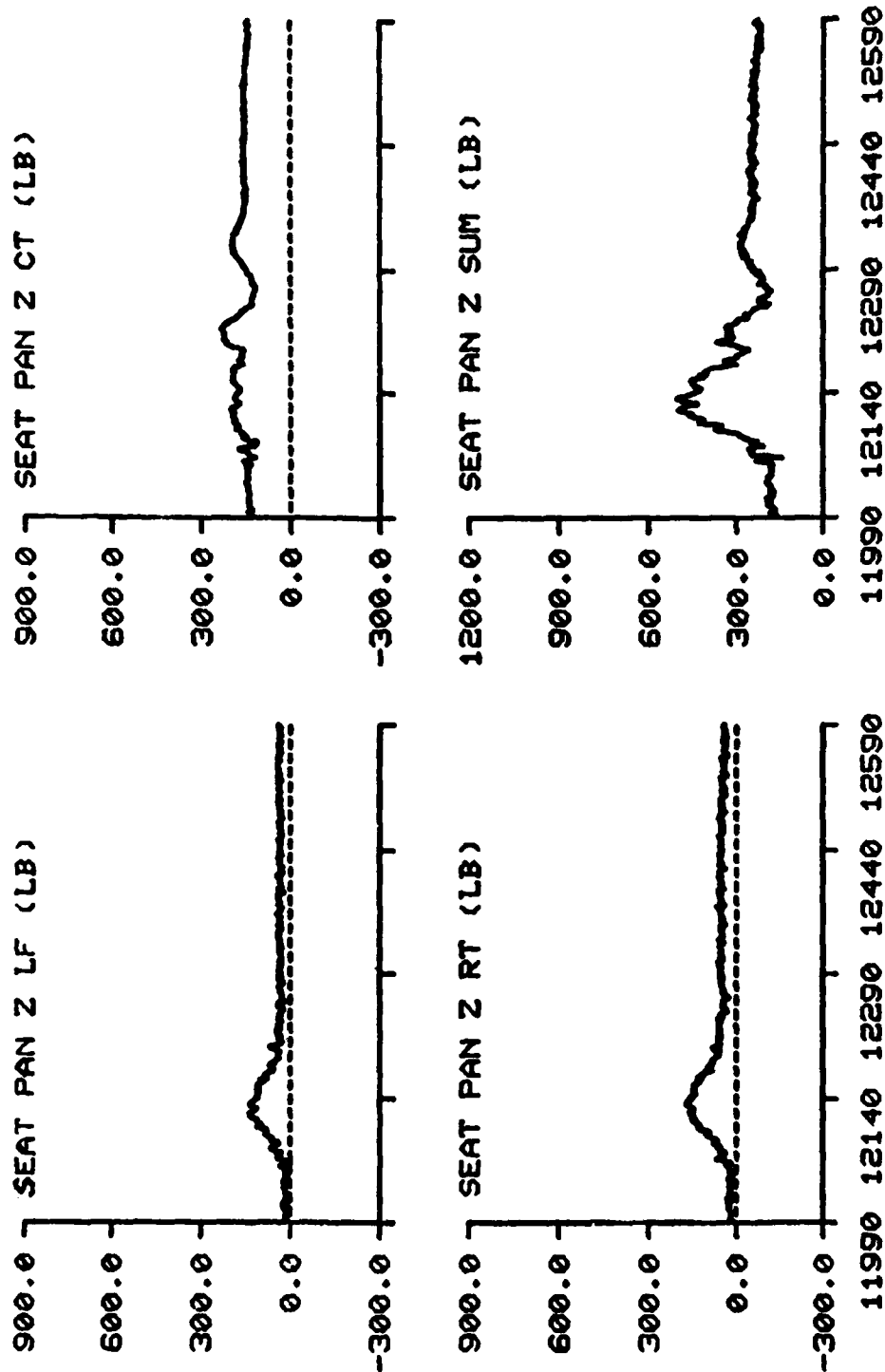
TEST NO: 591

SUBJECT ID: F-3



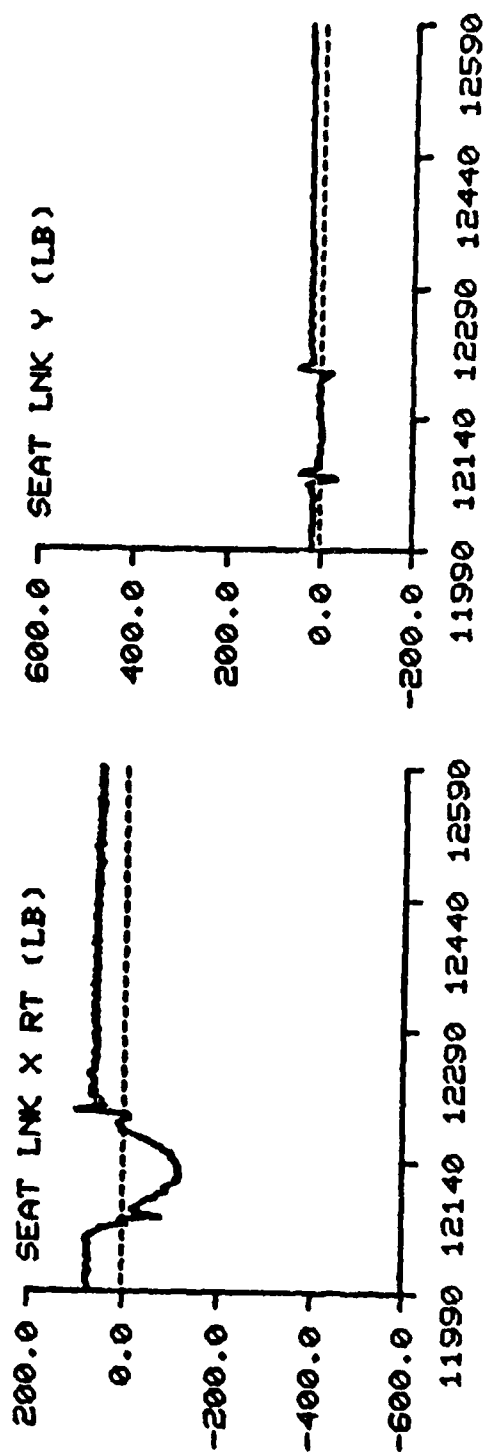
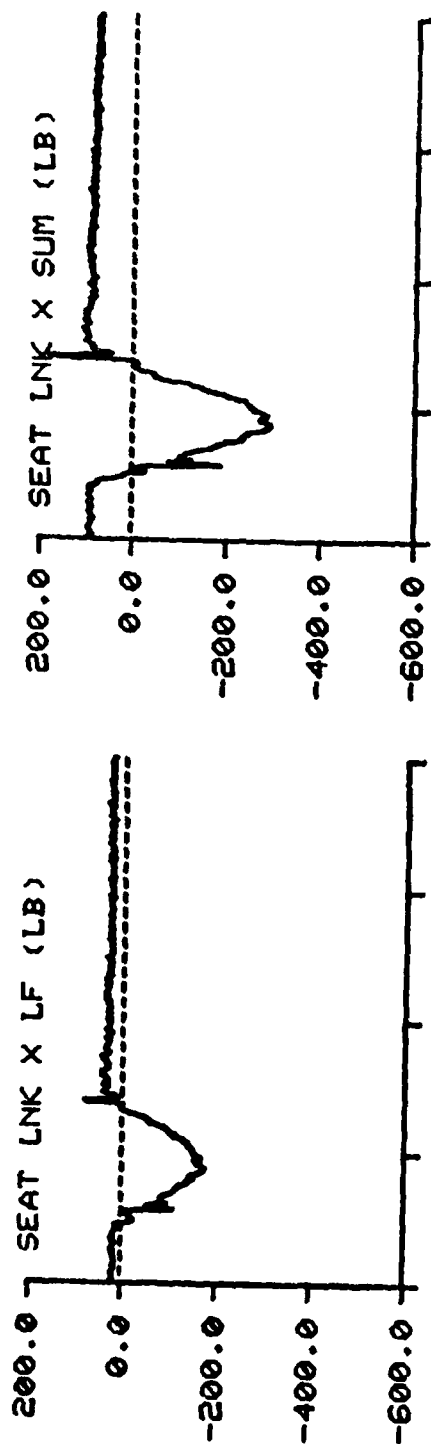
TIME IN MILLISECONDS

F-111      TEST NO: 591      SUBJECT ID: F-3



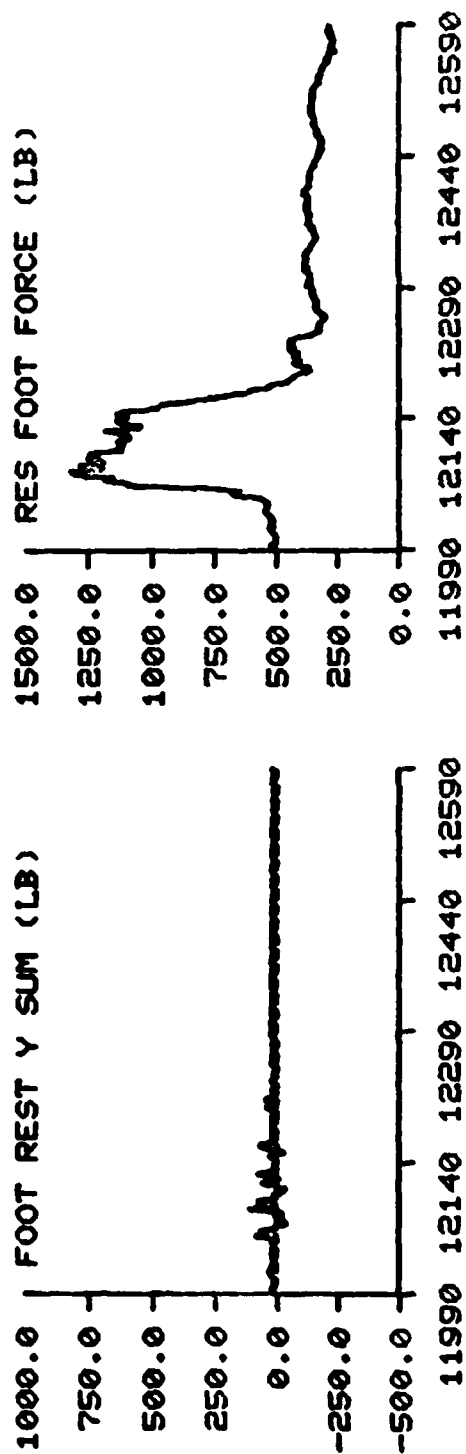
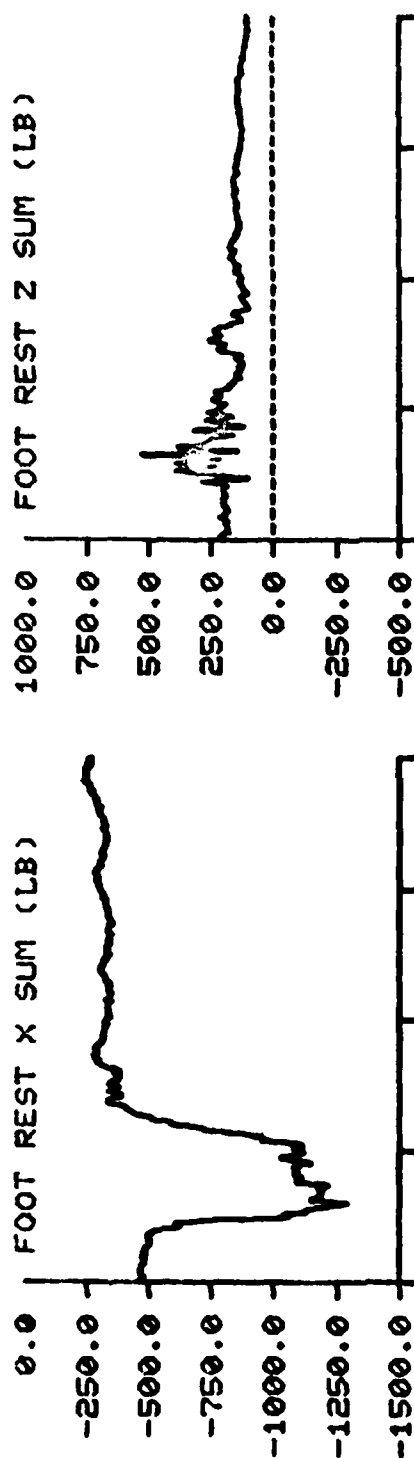
TIME IN MILLISECONDS

F-111      TEST NO: 591      SUBJECT ID: F-3



TIME IN MILLISECONDS

F-111      TEST NO: 591      SUBJECT ID: F-3



TIME IN MILLISECONDS

#### REFERENCES

Aerospace Medical Research Laboratory Regulation 127-1, 9 November 1976, AMRL Accident Prevention Program Plan.

Air Force Regulation 169-3, 12 February 1979, Use of Human Subjects in Research Development, Test and Evaluation.

ASD TWX No. 131630Z, June 1978, to Sacramento ALC.

Atkins, R. L., The F-111 Crew Module, 25 July 1971, Report No. FZM-12-4094D, General Dynamics, Fort Worth Division, Fort Worth, Texas.

Brinkley, J. W. and J. T. Shaffer, December 1971, "Dynamic Simulation Techniques for the Design of Escape Systems: Current Applications and Future Air Force Requirements", Symposium of Biodynamic Models and Their Applications, AMRL-TR-71-29 (AD 739501), Aerospace Medical Research Laboratory, Wright-Patterson AFB, Ohio.

Carney, C. T. and R. T. Melvin, 23 March 1966, Test Results Static Ejection and Sled Test Program, F-111 Recovery Group Qualification Test PTP 5 Static Ejection Test, Report No. B772, McDonnell Aircraft Corporation, St. Louis, Missouri.

Feagin, J., 1979, "The Syndrome of the Torn Anterior Cruciate Ligament", Orthopedic Clinics of North America, 10(1):81-90.

Federal Motor Vehicle Safety Standard No. 208, U.S. Department of Transportation, May 1972.

"Film Analysis Guides for Dynamic Studies of Test Subjects, Recommended Practice", March 1980, SAE J138, VSMF Industry Standards, Issue 9-1.

Final Report, TAC Project 79G-019T, QOT&E of the F-111 Improved Crew Restraint System, 13 August 1979, HQ TAWC, Eglin AFB, Florida.

Fricker, G. F., 1 December 1966, Model F-111 A/B Crew Module Attenuation Group Qualification Landing Simulation Test Results. Report No. B758, Revision B, McDonnell, St. Louis, Missouri.

Gadd, C. W., 1966, "Use of Weighted Impulse Criterion for Estimating Injury Hazard", in 10th Stapp Car Crash Conference, Society of Automotive Engineers, Inc., New York.

Gossick, L. F. and G. C. Mohr, 8 January 1968, F-111 Escape Capsule Review for DDR&E and SAF-RD.

Graf, P. A., H. T. Mohlman, and R. C. Reboulet, October 1978, Photometric Methods for the Analysis of Human Kinematic Responses to Impact Environments, AMRL-TR-78-94 (A-062006), Aerospace Medical Research Laboratory, Wright-Patterson Air Force Base, Ohio.

- Good, E., F. Noyes and D. Butler, 1978, Knee Flail Design Limits: Background, Experimentation, and Design Criteria, AMRL-TR-78-58 (A-062384), Aerospace Medical Research Laboratory, Wright-Patterson AFB, Ohio.
- Hatcher, J. L., 10 June 1966, Test Results Static Ejection and Sled Test Program, F-111 Recovery Group Qualification Test PTP 6 Static Ejection Test, Report No. B772-7, McDonnell Aircraft Corporation, St. Louis, Missouri
- Hefti, N. B., 21 April 1967, Test Results Static Ejection and Sled Test Program, F-111 Escape System Qualification Test PTP 2 270 KEAS Test, Report No. B773-5, McDonnell Aircraft Corporation, St. Louis, Missouri.
- Juhasz, P. R. and R. P. Parsons, May 1980, "Computer Velocity Control of a Sled Used in Impact Studies", Proceedings of the 26th International Instrumentation Symposium, Instrument Society of American, Seattle, Washington.
- Kazarian, L. E., October 1977, F/FB-111 Escape Injury Mechanism Assessment, AMRL-TR-77-60 (A-052337), Aerospace Medical Research Laboratory, Wright-Patterson AFB, Ohio.
- Kennedy, K. W., AFAMRL/HEG Letter to AFAMRL/BB, dated 3 October 1979, F-111 Crew Restraint Program.
- Kennedy, J., R. Hawkins, and R. Willis, 1977, "Strain Gauge Analysis of Knee Ligaments", Clin Orthopedics, 129:225-229.
- Kennedy, J., H. Weinberg, and A. Wilson, 1974, "The Anatomy and Function of the Anterior Cruciate Ligament", J Bone and Joint Surg, 56-A(2):223-235.
- Military Specification, MIL-C-25969B (USAF), 4 March 1970, "General Requirement for Capsule Emergency Escape Systems.
- Moss, R. E., April 1968, Escape System - Crew Restraint Hardware Daisy Track (HAFB) Testing, Report No. FGT-5351, Fort Worth Division, Fort Worth, Texas.
- McCauley, D. E., 17 June 1966, Test Results Static Ejection and Sled Test Program, F-111 Recovery Group Qualification Test PTP 7 800 KEAS, Report No. B772-6, McDonnell Aircraft Corporation, St. Louis, Missouri.
- McCauley, D. E. and R. T. Melvin, 20 January 1966, Test Results Static Launch and Sled Test Program, F-111 Recovery Group Qualification Test PTP 5 600 KEAS Bi-Nozzle Rocket Sled Test, Report No. B772-3, McDonnell Aircraft Corporation, St. Louis, Missouri.
- McMaster, J., C. Weinert, and P. Scranton, 1974, "Diagnosis and Management of Anterior Cruciate Ligament Tears", J Trauma, 14(3):230-235.
- Pope, M., R. Johnson, D. Brown, and C. Tighe, 1979, "The Role of the Musculature in Injuries to the Medial Collateral Ligament", J Bone and Joint Surg, 61-A(3):398-402.

Reader, D. C., 1967, The Restraint Afforded by the USAF and Proposed RAF IAM Seat Harnesses for the F-111 Under High Forward and Lateral Decelerations, IAM Report No. 421, RAF Institute of Aviation Medicine, Farnborough Hants, England.

Shaffer, A. C., 3 April 1979, F-111 Module Restraint Harness Roller Support Assembly with the 12K271 Machined from Solid Plate, Static Structural Test Report, Report No. FGT-5946, General Dynamics, Fort Worth Division, Fort Worth, Texas.

Subsystem/Engineering Development Report Feasibility of Concept and Preliminary Design Analysis of F-111 Crew Module Restraint Harness, Headrest and Seat to Significantly Reduce Back Injury, 13 February 1978, Report No. FZM-12-13984, General Dynamics, Fort Worth Division, Fort Worth, Texas.

Whitney, R. F., 30 April 1979, Testing Conducted on GD/FW AKO 3802-30 Inertia Reel Assembly, Powered (PSCO P/N 0103157-75) GD/FW Headrest Support Assembly, Report No. 836, Pacific Scientific Kin-Tech Division, Anaheim, California.

Whitney, R. F. and P. A. Hass, 30 July 1970, Qualification Test Firings 0103157-75 Inertia Reel-Powered (GD/FW ZKO 3802-30) British Harness Modification, Report No. 740, Pacific Scientific Company Aerospace Division, Anaheim, California.

Wilcoxon, F. and R. A. Wilcox, 1964, Some Rapid Approximate Statistical Procedures, Lederle Laboratories, New York.